OXYGEN ISOTOPE AND ELEMENTAL GEOCHEMISTRY OF ARCHEAN ROCKS

THE OXYGEN ISOTOPE AND ELEMENTAL GEOCHEMISTRY OF ARCHEAN ROCKS FROM NORTHERN ONTARIO

By

FREDERICK JOHN LONGSTAFFE, B.Sc. (Windsor)

A Thesis

Submitted to the School of Graduate Studies

in Partial Fulfilment of the Requirements

for the Degree

Doctor of Philosophy

McMaster University

November, 1977

© FREDERICK JOHN LONGSTAFFE 1978

DOCTOR OF PHILOSOPHY (1977)
(Geology)

McMASTER UNIVERSITY
Hamilton, Ontario

TITLE: The oxygen isotope and elemental geochemistry of Archean rocks from northern Ontario

AUTHOR: Frederick John Longstaffe, B.Sc.
(University of Windsor)

SUPERVISORS: Dr. R.H. McNutt

Dr. H.P. Schwarcz

NUMBER OF PAGES: xxvi, 564

ABSTRACT

The oxygen isotope and chemical compositions (including rare earth elements) of Archean rocks from northern Ontario have been interpreted in terms of various magmatic, sedimentary, metamorphic and/or alteration processes that have occurred during the history of these samples.

The greenschist facies clastic metasedimentary rocks from the Wabigoon, Abitibi, and Uchi granite-greenstone belts have chemical compositions that indicate derivation from dominantly felsic source terrains. Their $\delta^{18}O$ values range from 8.0 to 13.3 °/₀₀, about 2 to 3 °/₀₀ lower than Phanerozoic clastics, a result of the immature nature of the Archean metasediments. The most immature samples analyzed show no recognizable chemical or isotopic effects of residence in a sedimentary environment. More mature samples, however, have $\delta^{18}O$ values (>9 °/₀₀), and chemical discriminant function values that indicate chemical and isotopic modification during sedimentary processes. These characteristics are useful in the recognition of clastic sedimentary protoliths in Archean gneisses.

The felsic metavolcanic rocks, also from the granite-greenstone belts, have $\delta^{18}O$ values of 7.5 to 13.0 °/₀₀. The higher values are probably due to low temperature alteration.

Because of the overlap in $\delta^{18}O$ values between the clastic metasedimentary rocks and the felsic metavolcanic rocks, oxygen isotope compositions cannot be used to distinguish between the two rock types.

The $\delta^{18}O$ values of metabasalts (4.4 to 9.2 °/₀₀) suggest that isotopic alteration has accompanied their metamorphism, but no consistent relationships between $\delta^{18}O$ and usually mobile elements such as K, Rb, Sr and Ba were observed. The chemical composition of least-altered mafic metavolcanic rocks from the Burditt Lake - Lake Despair area is compatible with the formation of these rocks in an island-arc type environment.

Least-altered felsic metavolcanic rocks interlayered with the Burditt Lake - Lake Despair metabasalts have rare earth element compositions consistent with formation by moderate degrees of melting of quartz eclogite. Other samples of felsic metavolcanic rocks from the area have been chemically and isotopically altered by magmatic fluids accompanying the intrusion of the Burditt Lake granodiorite.

The Jackfish Lake Complex (diorite, quartz monzodiorite and monzodiorite, leucodiorite and leuco quartz diorite, granodiorite, and Na-syenite), which was intruded along the contact between the Burditt Lake - Lake Despair metavolcanics and the Footprint gneiss, differentiated along a 'gabbro-trondhjemite' trend (Na-enrichment). The most abundant rock type, diorite, has a chemical composition compatible with its formation by

partial melting of eclogite. The other rock types were probably differentiated from the dioritic magma along a path first controlled by the crystallization of hornblende, and then by the precipitation of feldspar, especially microcline. The $\delta^{18}O$ rock (6.4-9.2 °/₀₀) and mineral values of the Complex result from this differentiation, except for a few samples, which have been depleted in ^{18}O by low temperature interaction with meteoric water.

The Footprint gneiss also has a chemical composition that suggests that its protolith formed by partial melting of LREE-enriched quartz eclogite. Thus, most of the tonalitic to granodioritic rocks of the Burditt Lake - Lake Despair area are best interpreted as primitive additions to the Archean sialic crust derived from mantle depths.

The somewhat low average $\delta^{18}O$ value (7.5 °/₀₀) of many of the isotopically unaltered Archean meta-igneous gneisses and plutonic rocks also could be the result of formation from less differentiated, more mafic sources than Phanerozoic batholiths, which have $\delta^{18}O$ values of 8 to 10 °/₀₀.

The $\delta^{18}O$ values of ortho- and paragneisses (5.9-11.7 °/₀₀) from the English River gneiss belt, and the Wabigoon granite-greenstone belt, span the range observed for least-metamorphosed meta-igneous and metasedimentary rocks. Up to middle amphibolite facies, the oxygen isotope compositions of the rock usually reflect the protolith of the gneiss. During the

metamorphism, quartz-magnetite oxygen isotope temperatures are quenched at 500-600°C; quartz-biotite temperatures are lower (400°C) and reflect continued isotopic exchange, mostly of biotite. This process results in the formation of low ^{18}O biotites (<3 °/₀₀).

Above middle amphibolite facies, the oxygen isotope composition of Archean gneisses cannot be relied upon to reflect the isotopic nature of protolith rock types. Partial melting seems to encourage isotopic exchange of the gneisses with a low ^{18}O reservoir, probably basalt, and results in $\delta^{18}O$ values for the gneisses of 6 to 7 °/₀₀, regardless of their previous isotopic composition.

ACKNOWLEDGEMENTS

The work contained between these covers has been completed in spite of tennis, physical chemistry, wood ticks, and a crotchety mass spectrometer. Its completion would have taken much longer had it not been for the assistance of the following persons:

Dr. R.H. McNutt, who supervised much of the elemental geochemistry and provided the opportunity and the funds to attend many pertinent field trips and conferences;

Dr. H.P. Schwarcz, who introduced me to oxygen isotopes, supervised the stable isotope portion of the research, and provided the funds and the opportunity to attend many pertinent field trips and conferences;

Dr. W.B. Clarke, who acted as the non-departmental member of my Ph.D. supervisory committee;

Dr. A. Fallick, who led the way in the frequent resuscitations of the mass spectrometer when others had left it for dead;

Miss A. Dixon, who helped with some of the XRF pellet preparation, assisted with XRD and computing projects, and performed all of the LOI experiments;

Mr. F. Graef, who helped to keep the laboratory operative throughout many crises, often at night and on weekends;

Dr. D.M. Shaw, who provided invaluable training in the behaviour of trace elements, and in tennis;

Dr. J.H. Crocket, who provided access to, and assistance with, the neutron activation laboratory;

Dr. D.K. Paul, who unravelled the mysteries of peak stripping programme, SAMPO;

Ms. H. Elliott, who cheerfully and competently typed the manuscript;

Mr. G. Beakhouse, D. Birk, C. Gower, R. Hyde, J. Kwong, P. Teal, and C. Westerman for providing some samples and access to their unpublished data;

Mr. P. Fung, for AAS mineral analyses, and a thorough training in badminton;

Mr. C. Gower, for many useful and corrective discussions;

Mr. J. Whorwood, who provided invaluable assistance in photography;

The National Research Council of Canada, for a 1967 Science Scholarship, which provided most of my salary, and

Mrs. L. Longstaffe, who drew many of the diagrams, and always kept dinner warm.

TABLE OF CONTENTS

ABSTRACT iii

ACKNOWLEDGEMENTS vii

CHAPTER I THE ARCHEAN - THE PROBLEM AND THE PROPOSAL

I-1 An introduction to the aims and objectives 1

I-2 Archean crustal evolution: facts and speculations 4

CHAPTER II THE GEOCHEMISTRY OF ARCHEAN CLASTIC METASEDIMENTARY ROCKS

II-1 Introduction 20

II-2 The concept of chemical maturity 21

II-3 The geology and sedimentology of Archean clastic metasedimentary rocks 25

Upper Manitou Lake 27

Kirkland Lake 31

Abram Lake 36

Pakwash Lake 39

II-4 Chemical classification of Archean clastic metasedimentary rocks and estimates of chemical maturity. 39

II-5 The chemistry of greywackes: variation with geological time 46

II-6 The chemistry of clastic metasedimentary rocks of northern Ontario 49

Provenance 49

Chemical modification during sedimentary processes 72

II-7 The oxygen isotope geochemistry of Archean clastic metasedimentary rocks from northern Ontario 77

$\delta^{18}O$ results 78

Interpretation 78

$\delta^{18}O$ in felsic metavolcanic rocks and the problem of alteration 89

$\delta^{18}O$ quartz results for the Upper Manitou Lake area 93

Chemical and isotopic correlations in Archean clastic metasedimentary rocks 98

$\delta^{18}O$ results for altered clastic metasedimentary rocks from Pakwash Lake 104

II-8 General conclusions 106

CHAPTER III THE GEOCHEMISTRY OF THE BURDITT LAKE - LAKE DESPAIR AREA, NORTHWESTERN ONTARIO

III-1 Introduction 109

III-2 Geological background 109

III-3 Comparative geochemistry 125

III-4 Isotopic and chemical alteration of basalt - general considerations 127

Seawater alteration of basalt, effect on oxygen isotopes 127

Seawater alteration of basalt, effect on chemistry 128

Prograde metamorphism, effect on oxygen isotopes 130

Prograde metamorphism, effect on chemistry 130

Retrograde metamorphism 132

III-5 Oxygen isotope geochemistry of the Burditt Lake - Lake Despair mafic metavolcanic rocks and enclaves 133

III-6 Elemental geochemistry of the mafic metavolcanic rocks 142

Trace elements and tectonic setting 148

REE modelling and basalt petrogenesis 159

Evolution of the metabasalts 165

III-7 Geochemistry of the felsic metavolcanic rocks and the Burditt Lake pluton 168

General geochemistry 168

Oxygen isotope rock results, felsic metavolcanic rocks 171

The oxygen isotope geochemistry of the Burditt Lake stock and associated felsic country rocks 173

Oxygen isotope mineral results, Manomin Lake felsic schists 180

The origin of Archean 'tonalites' - general considerations 186

Rare earth geochemistry and the origin of the felsic metavolcanic rocks 191

III-8 The geochemistry of the Jackfish Lake Complex 202

Introduction 202

The Jackfish Lake Complex and its trondhjemitic affinities 203

The Jackfish Lake Complex meta-diorites, mafic enclaves, and the possibility of hybridization 209

Low temperature alteration processes affecting the Jackfish Lake Complex 214

Chemical variation, JLC rock suites 227

REE partial melting models for the Jackfish Lake Complex diorite 237

Origin of the Jackfish Lake Complex monzodiorites, leucodiorites, granodiorites and Na-syenites 252

The effect of differentiation upon the oxygen isotope geochemistry of the Jackfish Lake Complex 274

Some comments on the oxygen isotopic composition of eclogite 278

The petrogenesis of the Jackfish Lake Complex - a summary 281

III-9 The geochemistry of the Footprint gneiss 283

Chemical effects of metamorphism on the Footprint gneiss 284

REEs and the origin of the Footprint gneiss 291

Possible sedimentary origin for the Footprint gneiss 297

Conclusions and speculations 300

CHAPTER IV THE OXYGEN ISOTOPE GEOCHEMISTRY OF ARCHEAN GNEISSES

IV-1 Introduction 304

IV-2 Oxygen isotope results for Archean granitoids - a review of the literature 306

IV-3 Oxygen isotope results for Archean gneisses from northwestern Ontario 313

IV-4a Isotopic exchange with meteoric water 319

IV-4b The isotopic composition of the Archean oceans 323

IV-4c Isotopic exchange with seawater 326

IV-5 The effect of regional metamorphism upon the oxygen isotopic composition of siliceous rocks - a review of the literature 327

Dimensions of oxygen isotope equilibrium 329

Nature of the isotopic exchange medium 330

Nature of the oxygen isotope reservoirs 332

IV-6 The oxygen isotope geochemistry of the Footprint gneiss 333

Low ^{18}O Footprint gneiss samples and open system isotopic exchange during migmatization 349

IV-7 The oxygen isotope geochemistry of the Kenora area: the Melick gneiss and related granitoids 353

IV-8 Oxygen isotope geochemistry of the Cedar Lake - Clay Lake area 365

IV-9 The oxygen isotope geochemistry of the Pakwash gneiss 375

IV-10 Summary and conclusions 392

CHAPTER V CONCLUSIONS 396

REFERENCES 404

APPENDIX I Oxygen isotope accuracy and precision, and geothermometry 444

APPENDIX II Operation of the bromine pentafluoride line 465

APPENDIX III Petrography of the Burditt Lake - Lake Despair area 485

APPENDIX IV X-ray fluorescence spectrography: technique, precision and accuracy, and results 527

APPENDIX V Instrumental non-destructive neutron activation analysis 560

LIST OF FIGURES

2-1a	Granite-greenstone and gneiss belts of the Superior Province	28
2-1b	Locations of study areas	28
2-2a	Geology of the Upper Manitou Lake area	29
2-2b	Generalized stratigraphy of the Upper Manitou Lake area	29
2-3a	Geology of the Kirkland Lake area	32
2-3b	Generalized facies distribution map, Kirkland Lake area	32
2-4	Geology of the Kakagi Lake area	37
2-5	Na_2O-$Fe_2O_3^t$+MgO-K_2O diagram for the Archean clastic metasedimentary rocks	41
2-6	Log (SiO_2/Al_2O_3) versus log (Na_2O/K_2O) diagram for the Archean clastic metasedimentary rocks	41
2-7a	Normalized Si versus Al/Fe diagram for Archean clastic metasedimentary rocks	45
2-7b	Normalized Si versus Al/Fe diagram for the Jackfish Lake Complex igneous rocks	45
2-8	Average chemical compositions of greywackes throughout geological time	50
2-9	Major and minor element variations observed for Archean clastic metasedimentary rocks	59
2-10	AFM diagrams for Archean metagreywackes	60
2-11	SiO_2 versus FeO^t+MgO for the metavolcanic and clastic metasedimentary rocks from the Upper Manitou Lake area	62
2-12	Trace element variations observed for the Upper Manitou Lake area metagreywackes	63

2-13	Ni versus Rb diagram for the Archean clastic metasedimentary rocks	66
2-14a	K/Rb versus K diagram for the Archean clastic metasedimentary rocks	67
2-14b	Ca/Sr versus Ca diagram for the Archean clastic metasedimentary rocks	67
2-15	K_2O versus Na_2O diagram for the Archean clastic metasedimentary rocks	73
2-16	Na_2O-CaO-K_2O diagram for the Archean clastic metasedimentary rocks	75
2-17	Whole rock oxygen isotope results for the Archean clastic metasedimentary and felsic metavolcanic rocks	83
2-18	Whole rock oxygen isotope results for the Upper Manitou Lake area	87
2-19	Oxygen isotope results for quartz from the Upper Manitou Lake area	94
2-20	$\delta^{18}O$ rock versus Al/Fe diagram for the Archean clastic metasedimentary rocks	100
2-21	Discriminant Function (D.F.) versus $\delta^{18}O$ diagram for the Archean clastic metasedimentary rocks	100
2-22	$\delta^{18}O$ versus CaO/Na_2O diagram for rocks from the Upper Manitou Lake area	103

3-1	Location map for the Burditt Lake - Lake Despair areas	110
3-2	General geology of the Burditt Lake area	112
3-3	General geology of the Lake Despair area	113
3-4	Normative quartz-plagioclase-orthoclase-feldspathoids diagram for the Burditt Lake-Lake Despair area	126

3-5	$\delta^{18}O$ rock results for mafic and ultramafic rocks from the Burditt Lake - Lake Despair area	137
3-6	AFM diagram for the Burditt Lake - Lake Despair metavolcanic rocks	143
3-7	Ti-Zr-Y diagram for the Burditt Lake - Lake Despair mafic metavolcanic rocks	151
3-8	Ti-Zr diagram for the Burditt Lake - Lake Despair mafic metavolcanic rocks	151
3-9	Ti-Zr-Sr diagram for the Burditt Lake - Lake Despair mafic metavolcanic rocks	152
3-10	TiO_2-K_2O-P_2O_5 diagram for the Burditt Lake - Lake Despair mafic metavolcanic rocks	152
3-11	Chondrite normalized rare earth element results for the Burditt Lake - Lake Despair mafic metavolcanic rocks	163
3-12	Chondrite normalized rare earth element model results for the Burditt Lake - Lake Despair mafic metavolcanic rocks	163
3-13	Chondrite normalized rare earth element model results for the Jackfish Lake Complex mafic enclave D4	163
3-14	$\delta^{18}O$ rock results for felsic metavolcanic rocks from the Burditt Lake and Manomin Lake areas, and for the Burditt Lake granodiorite	172
3-15	$\delta^{18}O$ rock results for the northwest-southeast traverse across the Burditt Lake stock and its felsic metavolcanic country rocks	175
3-16	A model for magmatic water movement, Burditt Lake stock	178
3-17	Chemical variation along the northwest-southeast traverse across the Burditt Lake stock and the associated felsic metavolcanic country rocks	181

3-18	$\delta^{18}O$ versus Na_2O diagram for the altered felsic metavolcanic rocks	182
3-19	Chondrite normalized rare earth element results for the Manomin Lake felsic schists	193
3-20	Chondrite normalized rare earth element modelling for the Manomin Lake felsic schists	195
3-21a	LIL element model for the Manomin Lake felsic schists	199
3-21b	Comparison of LIL element models for the Manomin Lake felsic schists	200
3-22	Sketch map of the Jackfish Lake Complex	206
3-23	AFM diagram for the Jackfish Lake Complex	207
3-24	Na_2O-K_2O-CaO diagram for the Jackfish Lake complex	208
3-25a,b	Chemical variation of the Jackfish Lake Complex granodiorite along a north-south traverse from the southern portion of Lake Despair to the Northwest Bay Fault	218
3-26	REE patterns for altered granodiorite F37	220
3-27	Oxygen isotope results for Archean granitic rocks	221
3-28	Oxygen isotope results for rocks and minerals from the Jackfish Lake Complex altered granodiorites	223
3-29	Modified Larsen Index diagrams for the Jackfish Lake Complex	229
3-30	Ca versus Sr diagram for the Jackfish Lake Complex	231
3-31	K versus Rb diagram for the Jackfish Complex	231

3-32	Ba versus Sr diagram for the Jackfish Lake Complex	236
3-33	Chondrite normalized rare earth element results for the dioritic rocks from the Jackfish Lake Complex	240
3-34	Chondrite normalized rare earth element melting model results for the Jackfish Lake Complex diorite F146	244
3-35	LIL element enrichment factors for the Jackfish Lake Complex diorite F146	251
3-36	Chondrite normalized rare earth element patterns for the Jackfish Lake Complex granodiorites and Na-syenite	254
3-37a	Chondrite normalized rare-earth element partial melting models for the Jackfish Lake Complex (quartz) monzodiorite, quartz diorite and leuco quartz diorite	256
3-37b	Chondrite normalized rare earth element melting model for the Jackfish Lake Complex granodiorites	256
3-38	LIL element enrichment factor diagrams for the Jackfish Lake Complex leucodiorites, granodiorites and Na-syenite	256
3-39	Modal hornblende content versus heavy rare-earth element contents of the Jackfish Lake Complex rocks	256
3-40	CaO versus Y diagram for the Jackfish Lake Complex	259
3-41	Ce versus SiO_2 diagram for the Jackfish Lake Complex	259
3-42	K-feldspar triclinicity versus plagioclase structural state for coexisting feldspar pairs from the Jackfish Lake Complex	265

3-43	K-feldspar triclinicity versus K-feldspar-hornblende oxygen isotope fractionations for some Jackfish Lake Complex rock types	265
3-44	Rb, Tl and Ba content of microcline versus microcline triclinicity for some Jackfish Lake Complex rock types	268
3-45	$\delta^{18}O$ versus SI diagram for the Jackfish Lake Complex rocks	275
3-46	Oxygen isotope concordancy diagrams for the Jackfish Lake Complex	279
3-47a	K versus Ba diagram for the Footprint gneiss and migmatite	290
3-47b	K versus Rb diagram for the Footprint gneiss and migmatite	290
3-48	TiO_2 versus Zr diagram for the Footprint gneiss and migmatite	292
3-49	Chondrite normalized rare-earth element patterns for the Footprint gneiss and migmatite	293
3-50	REE models for the Footprint gneiss and migmatite	293
3-51	Normalized Si versus Al/Fe diagram for the Footprint and Pakwash gneisses	298

4-1	Oxygen isotope results taken from the literature for Archean granitic and gneissic rocks	312
4-2	Oxygen isotope results for Archean gneisses analyzed during this study	312
4-3	$\delta^{18}O$ mineral and rock results for the Footprint gneiss and migmatite	336
4-4	Oxygen isotope concordancy diagram for the mineral phases from the Footprint gneiss and migmatite	337

4-5	Trace element content of microcline from the Footprint gneiss versus the Modified Larsen Index for the host rock	342
4-6	Oxygen isotope mineral fractionations for the Footprint gneiss and migmatite that involve epidote	342
4-7	Oxygen isotope results for biotite	345
4-8	$\delta^{18}O_{H_2O_i}$ versus W/R diagram for the Footprint and Pakwash gneisses	352
4-9	K_2O-Na_2O-CaO diagram for the Kenora area gneisses and related rocks	356
4-10	$\delta^{18}O$ results for the Kenora area gneisses and related rocks	361
4-11	Oxygen isotope geothermometry for the Kenora area gneisses and related rocks	361
4-12	K_2O-Na_2O-CaO diagram for the Cedar Lake - Clay Lake area	367
4-13	Normalized Si versus Al/Fe diagram for some Archean gneisses	369
4-14	Discriminant Function (D.F.) versus $\delta^{18}O$ diagram for some Archean gneisses	369
4-15	$\delta^{18}O$ rock values for gneisses from the Cedar Lake - Clay Lake area	372
4-16	Mesonorm plot for the Pakwash gneiss and greenschist facies metagreywackes	381
4-17	Oxygen isotope results for the Pakwash gneiss and associated pegmatoids	386
4-18	Oxygen isotope concordancy diagram for the Pakwash gneiss and associated pegmatoids	387
4-19	$\delta^{18}O_{H_2O_i}$ versus W/R diagram for the Pakwash and Footprint gneisses	390

A2-1	Schematic of the BrF_5 line	482
A2-2	BrF_5 gas calibration graph	483
A2-3	Manometer calibration graph for CO_2 gas	483
A3-1	Quartz-alkali feldspar-plagioclase diagram for rocks from the Burditt Lake - Lake Despair areas	513
A3-2	Quartz-feldspar-mafics diagram for rocks from the Burditt Lake - Lake Despair areas	513

PHOTOGRAPHS	Burditt Lake - Lake Despair metaigneous rocks	121

LIST OF TABLES

2-1	Modal data for some metagreywackes	34
2-2	Average greywacke compositions throughout geological time	51
2-3	Chemical analyses for greywackes derived from felsic rocks	53
2-4	Chemical analyses for greywackes derived from mafic rocks	56
2-5	U, Th and K in greywacke	69
2-6	Trace element comparison: Kakagi Lake and Upper Manitou Lake areas	71
2-7	Oxygen isotope whole rock results for Archean clastic metasedimentary and metavolcanic rocks	79
2-8	Oxygen isotope mineral data, Upper Manitou Lake area	95
2-9	Oxygen isotope results for the Pakwash Lake metasedimentary rocks	95

3-1	Selected geochronology, District of Rainy River and related areas	119
3-2	Comparison of $\delta^{18}O$ whole rock and LIL element abundances in the mafic metavolcanic rocks	134
3-3	$\delta^{18}O$ mineral results, mafic amphibolites	136
3-4	Chemical comparison of Archean metatholeiites	145
3-5	LIL element geochemistry for Archean mafic metavolcanics and modern island arc tholeiites	149
3-6	Selected analyses: mafic metavolcanic rocks	156

3-7	Average chemical results for the siliceous rock types	169
3-8	$\delta^{18}O$ results, Burditt Lake stock	174
3-9	Selected felsic metavolcanic rock analyses	184
3-10	$\delta^{18}O$ mineral results, felsic schists	186
3-11	Major element compositions, quartz eclogite mineral phases (hypothetical)	197
3-12	Average chemical compositions for the Jackfish Lake Complex and similar rock types from the Vermilion District	204
3-13	Hybridization model for the Jackfish Lake Complex diorites	213
3-14a	Mineral analyses, altered granodiorite F37	215
3-14b	Chemical comparison of altered and unaltered mineral phases from the Jackfish Lake Complex granodiorites	216
3-15	Oxygen isotope results, Jackfish Lake Complex	222
3-16	$\delta^{18}O$ mineral data, unaltered Jackfish Lake Complex rocks	225
3-17	Oxygen isotope results, Northwest Bay Complex	227
3-18	Mineral analyses, diorite suite	232
3-19	Mineral analyses, granodiorite suite	233
3-20	Selected analyses, diorite suite	239
3-21	Chemical comparison of Jackfish Lake Complex diorite and modern andesite	241
3-22	Eclogite melting models for the Jackfish Lake Complex diorite F146	247

3-23	Selected analyses, granodiorite suite	253
3-24	Feldspar structural states	262
3-25	Chemical comparison of the Footprint gneiss with other Precambrian siliceous rock types	285
3-26	Selected analyses, Footprint gneiss and the Northwest Bay Complex	289
3-27	Chemical comparison, Footprint gneiss and some Archean metagreywackes	299

4-1	Oxygen isotope mineral data for the In Ouzzal granulites	308
4-2	$\delta^{18}O$ rock results for Archean gneisses from Northwestern Ontario	314
4-3	Oxygen isotope mineral results for the Footprint gneiss	335
4-4	Footprint gneiss microcline triclinicity and Rb/Tl geothermometry	339
4-5	Mineral analyses for the Footprint gneiss	340
4-6	Oxygen isotope composition of biotite in siliceous rocks	346
4-7	Oxygen isotope mineral results, Kenora area	360
4-8	Trace element contents of the Pakwash gneiss metagreywacke layers and related rock types	377
4-9	Major element composition, Pakwash gneiss	380
4-10	Oxygen isotope mineral results for the Pakwash gneiss and associated pegmatoids	385

A1-1a	Accuracy and precision of $\delta^{18}O$ results	448
A1-1b	Precision on duplicate analyses of unknowns	449
A1-2a	$\delta^{18}O$ results for standards	450
A1-2b	Duplicate differences of unknowns	452
A1-3a	Comparison of quartz-magnetite oxygen isotope geothermometers	458
A1-3b	Comparison of quartz-muscovite oxygen isotope geothermometers	460
A1-3c	Comparison of plagioclase-magnetite oxygen isotope geothermometers	461
A1-4a	Oxygen isotope geothermometry for the Lake Despair area	462
A1-4b	Oxygen isotope geothermometry for the Pakwash Lake and Kenora areas	464
A2-1	Temperature calibration of furnaces	484
A3-1	Modal analyses for the Lake Despair area rocks	514
A4-1	Rb-Sr analytical methods	530
A4-2	Ba-Ce analytical methods	530
A4-3	Rb-Sr-Y-Zr-Nb analytical methods	531
A4-4	U-Rb-Th-Pb-Zn-Ni analytical methods	531
A4-5	Accuracy and reproducibility of major and minor elements in standard rocks	536

A4-6	Results for replicate fusion pellets for the same sample (major and minor elements)	540
A4-7	1σ error for reproducibility of duplicate pellets	540
A4-8a	Standard results for Rb	541
A4-8b	Standard results for Sr	542
A4-8c	Standard results for Ba	543
A4-8d	Standard results for Ce	543
A4-8e	Standard results for Zr	544
A4-8f	Standard results for Y	544
A4-8g	Standard results for Nb	544
A4-8h	Standard results for Th	545
A4-8i	Standard results for Pb	545
A4-8j	Standard results for Zn	546
A4-8k	Standard results for Ni	546
A4-9	Results for reproducibility of replicate powder pellets (trace elements)	547
A4-10	Individual XRF major, minor and trace element results for the samples analyzed during this study	548
A5-1	Instrumental non-destructive neutron activation analyses (INNA) for standard rock GSP-1	562
A5-2	Distribution coefficients used in model calculations	564

CHAPTER I

THE ARCHEAN - THE PROBLEM AND THE PROPOSAL

I-1 AN INTRODUCTION TO OUR AIMS AND OBJECTIVES

> "Oh now comes that bitter word - BUT
> Which makes all nothing that was said before,
> That smooths and wounds, that strikes and dashes more
> Than flat denial, or a plain disgrace."
>
> Daniel

The first objective of this study is to determine and interpret the oxygen isotope geochemistry of selected rock types from Archean granite-greenstones and gneiss belts located within the Superior Province, northern Ontario. The pursuit of such a goal requires a full understanding of the geochemistry and geology of the isotopically analyzed samples. Therefore, the second major objective of this thesis is the determination of the effects of magmatic, sedimentary, metamorphic and alteration processes upon the major and trace element chemistry of the selected silicate rock types.

The elemental geochemical portion of this study is similar to others (e.g. Arth and Hanson, 1975) which formulate geochemical models for Archean crustal evolution in a particular

area. In our case, however, equal attention is given to geochemical patterns that arise from post-magmatic processes. The oxygen isotope study, on the other hand, represents an attempt to provide an isotopic data base for Archean silicate rocks and then to relate these results to the magmatic, metamorphic, sedimentary and metasomatic processes inferred from the geological and geochemical information. The ultimate purpose of this portion of our investigation is to test the usefulness of oxygen isotopes as a petrogenetic indicator in Archean rocks.

The study is divided into three parts:

1. the major and trace element and oxygen isotope chemistry of greenschist facies, Archean clastic metasedimentary and related felsic metavolcanic rocks (Chapter II);
2. the major and trace element and oxygen isotope chemistry of the metavolcanic, plutonic and gneissic rocks of the Burditt Lake-Lake Despair area, Wabigoon granite-greenstone belt (Chapter III);
3. the oxygen isotope geochemistry of middle amphibolite to granulite facies meta-igneous and metasedimentary gneisses from the English River gneiss belt (Chapter IV).

The respective controls of provenance, sedimentary processes, metamorphism and alteration upon the oxygen isotope and elemental geochemistry of Archean clastic metasedimentary rocks, and, to a lesser extent, felsic metavolcanic rocks, are discussed in Chapter II. An attempt is then made to identify those chemical and isotopic characteristics of these low grade

rocks that could be useful in the recognition of such protoliths in high grade gneiss terrains.

The oxygen isotopic and chemical nature of a reasonably typical meta-igneous portion of an Archean granite-greenstone belt is described in Chapter III. The variation of oxygen isotope values in the mafic metavolcanic rocks is compared with that observed for the 'mobile' elements (K, Rb, Sr, Ba) and discussed as a possible index of alteration. The chemistry of least altered mafic metavolcanic samples is then interpreted in terms of possible models of tectonic setting and magma source. The felsic metavolcanic, plutonic and gneissic rocks from the area are also discussed in terms of partial melting and/or fractional crystallization processes and incorporated into a geochemical model of crustal evolution for the Burditt Lake-Lake Despair area. Equally important, however, are the chemical and isotopic manifestations of contact metamorphism, autometasomatism, meteoric water interaction, regional metamorphism and migmatization that occur in various members of the tonalitic to granodioritic rocks located in this portion of the Wabigoon granite-greenstone belt.

Chapter IV concentrates upon the relative contributions of magmatic, sedimentary, metamorphic, migmatitic and alteration processes to the range of oxygen isotope values observed in Archean gneisses from the English River Gneiss Belt. Much of this study is facilitated by the isotopic and chemical data

presented in Chapters II and III for the metasedimentary, metavolcanic and plutonic rocks, all of which are possible protoliths for Archean gneisses.

Chapter V is a summary of the main conclusions.

I-2 ARCHEAN CRUSTAL EVOLUTION: FACTS AND SPECULATIONS

Some of the general problems associated with Archean crustal evolution studies are presented here as a clothground for the present geochemical and isotopic crewel-work. For example, before one can understand why it would be useful to know if oxygen isotopes reflect their protolith compositions in high grade gneiss terrains, the controversy concerning the origin of Archean gneisses must first be outlined. Proper understanding of that problem in turn requires knowledge of many other facets of the early history of the earth. This type of information is summarized here.

Lithologies

Two main types of Archean terrain are exposed at the earth's surface, low grade greenstone belts and associated rocks, and high grade gneiss belts.

The granite-greenstone belts contain a lowermost ultramafic group (dunites, peridotites, and komatiites) interlayered

with tholeiites, minor pyroclastics, and chemical sediments, a greenstone group consisting of cyclic sequences of tholeiite, andesite, dacite and rhyolite (together with increasing abundances of clastic metasediments, pyroclastics, and iron-formation near the top of the cycle), and an upper metasedimentary group of turbidites, fluvial metasedimentary rocks, iron-formation, chert, and sometimes shallow marine carbonates (Anhaeusser et al., 1969; Anhaeusser, 1973). Large synkinematic plutonic and gneissic complexes are located at the margins of the greenstones; the greenstones are also intruded by smaller late to post-kinematic diorite to granite plutons.

The greenstones form linear belts that can extend for many hundreds of kilometers. In many localities, however, they are of more limited extent, and frequently have an arcuate shape.

The gneiss belts are composed of remetamorphosed granitic and gneissic rocks, layered igneous complexes (dominated by calcic anorthosite), and supracrustal sequences containing amphibolite, felsic metavolcanic and metasedimentary rocks (Bridgwater et al., 1973). Severe deformation accompanying multi-stage metamorphism has resulted in the formation of complex fold patterns and the production of basin and dome structures in some areas (Windley, 1973).

Models for the evolution of these granite-greenstone and gneiss belts must incorporate many factors, the more important

of which include:

1. the composition of the primordial crust and the Archean mantle;
2. the geothermal gradient and the thickness of the Archean crust;
3. the age relationships and genetic relationships between the gneiss belts and granite-greenstone belts;
4. the applicability of horizontal versus vertical tectonics during the Archean - the feasibility of Archean plate tectonics.

The Primordial Crust

The debate concerning the composition of the primordial crust is most vigorous, perhaps in part because it is unlikely that any remnants have been preserved to interfere with speculation. Recent models include: anorthosite (Shaw, 1976); basalt produced during mantle outgassing by partial melting of pyrolite (Barker and Peterman, 1974); basic to ultrabasic rocks, resembling modern ocean rise tholeiites (Glikson, 1972; Anhaeusser, 1973); ultramafic to mafic metavolcanics produced by meteorite impact (Green, 1972; Glikson, 1976b; Goodwin, 1976b); tonalite (Anhaeusser et al., 1969); and granite (Fyfe, 1973).

In his arguments against a primordial sialic crust, Glikson (1972) notes that lowermost Archean ultrabasic assemblages

do not conformably overly granitic or metasedimentary rocks. He also points out that Sr and Pb isotopic data for many Archean gneisses reflect derivation from mantle-like materials not much earlier than 3.0 b.y. However, Bridgwater and Fyfe (1974) suggest that the depletion of Rb and U from sialic crustal rocks affected by higher Archean geothermal gradients would cause Archean granitoids to have isotopic ratios close to theoretical mantle curves, regardless of the original source(s) of the magma.

The nature of the primordial crust and the question of the age relationship between Archean granite-greenstone and gneiss belts are difficult to resolve into completely separate arguments. One school (Goodwin, 1968; Anhaeusser et al., 1969; Glikson, 1971; White et al., 1971) maintains that the oldest rocks are to be found in the granite-greenstone belts. Another suggests that the gneiss belts are the paradigm of antiquity (Windley, 1973). The oldest dated rocks are granitic gneisses (Bridgwater et al., 1973; Hurst et al., 1975; Barton, 1975; Goldich and Hedge, 1974; Wilson et al., 1974; O.I.G.L. and McGregor, 1971). However, the fact that sialic crustal material existed at 3.8 b.y. does not necessarily imply the presence of primordial granitic crust. Nevertheless, the very old gneisses may give some indication of the nature of the earliest crust prior to its stabilization and complete differentiation (Anhaeusser et al., 1969; Bridgwater et al., 1973).

Archean Crustal Thickness

Proponents of thin Archean crusts base much of their argument upon the following details:

1. the paucity of substantial shelf-type sedimentary facies (Goodwin, 1974) - the result of crustal instability;
2. the very rare occurrences of basal unconformities (Goodwin, 1974);
3. the general absence of kyanite, eclogite, and blue-schist facies metamorphic terrains (Anhauesser et al., 1969; Bridgwater and Fyfe, 1974);
4. the abundance of sillimanite, andalusite and cordierite assemblages in the gneisses, such as would be favoured by thinner, more radioactive crust (Bridgwater and Fyfe, 1974; Windley, 1973);
5. higher Archean radioactivity levels (5 times present values) (Windley, 1973), causing granitic crust over ten kilometers thick to melt (Fyfe, 1973).

Many of these arguments can be questioned. The Moodies group of South Africa has recently been interpreted as a shelf deposit (Eriksson, 1977); Sutton (1976) has noted that more stable shelf type orthoquartzite and limestone deposits, accompanied by basic and ultrabasic activity (but not the intrusion of acid plutonics), are now being recognized in Archean terrains. Baragar and McGlynn (1976) have compiled

a list of at least six undisputed basal unconformities. Archean rocks containing high pressure mineral assemblages are also not as uncommon as previously supposed. Kyanite-talc and hypersthene-kyanite-quartz bearing rocks have been reported by Condie (1973) and Windley and Smith (1976); Lambert (1976) notes that Russian geologists have reported extensive kyanite-sillimanite bearing gneisses in the Siberian shield. According to Lambert (op. cit.), the seemingly ubiquitous development of low pressure mineral assemblages in Archean rocks may be connected to the later (synkinematic) plutonism, which has obscured the original regional metamorphic grade of the rocks. Burke et al. (1976) obviate the presumption that greater radioactive thermal energy in the Archean would cause melting of granitic crust greater than ten kilometers in thickness by suggesting that the extra thermal energy was manifested instead by longer spreading zones and/or faster spreading rates. They go as far as to suggest that Archean oceanic crust was somewhat thicker than its modern analogue.

The geochemistry of Archean metavolcanic rocks has been compared reasonably successfully to the rock types observed in modern island arcs (Jahn et al., 1974; Condie and Baragar, 1974; Hart et al., 1970; Baragar and Goodwin, 1969; Jakes and White, 1970; White et al., 1971). The relationship observed between crustal thickness and K_2O (Condie and Potts, 1969; Condie, 1973) in continental margin and island arc settings,

when applied to Archean greenstones, yields estimates of 15 (Hart et al., 1970) to 25 km (Condie, 1973). However, changes in upper mantle chemistry, variations in thermal regimes, and the possibility that such parameters may only reflect ease of access to mantle material tend to cast a cloud upon the significance of such calculations (Shackleton, 1973; Bridgwater and Fyfe, 1974).

Archean Thermal Regimes

Most investigators agree that the rate of radiogenic heat production was higher during the Archean (Dickinson and Luth, 1971; Ray, 1970; Fyfe, 1973; Bridgwater and Fyfe, 1974; Burke et al., 1976; Lambert et al., 1976); the nature of the geothermal gradient is less certain.

Saggerson and Owen (1969) suggested a reduction in geothermal gradient from 75°C/km to 10°C/km since 3.0 b.y. Shackleton (1973) also proposed thermal gradients several times modern rates at 3.0 b.y. and at least twice modern values by 2.7 b.y. The formation of Archean granulite facies rocks, accompanied by the concentration of U, Th, Rb, and K from the granulites into the upper crust at an early stage in the crust's evolution (Heier, 1973; Lambert and Heier, 1967; Heier and Thoresen, 1971; Lewis and Spooner, 1973; Robertson, 1973), suggested Archean thermal gradients of 100°C/km to Fyfe (1973) and Bridgwater and Fyfe (1974). Engel et al. (1974) and

and D.H. Green (1974) noted that the juxtaposition of ultramafic magmas and protocontinental material would require extremely steep geothermal gradients.

There are a few dissenting, but not generally accepted opinions on the nature of Archean geothermal gradients. Burke et al. (1976) believe the gradients to be similar to modern values. Talbot (1968) proposed that geothermal gradients were lower during the Archean, a proposal, however, that has been challenged (Bliss, 1969).

The Archean Mantle

The chemical composition of the Archean mantle has an important control upon the geochemistry of Archean rocks. For example, studies of trace elements (including rare earths) indicate a mantle origin for almost all of the meta-igneous rocks from the Vermilion District (Arth, 1976b). Likewise, Moorbath (1976), Windley (1976) and Tarney et al. (1976) believe that Sr and Pb isotopic characteristics of several Archean granite-greenstone and gneiss belts indicate upper mantle sources. Much of the present continental crust seems, therefore, to have formed from the upper mantle by 2.5 b.y. (Burke et al., 1976; Arth, 1976b). Removal of this material would irreversibly deplete the primitive upper mantle in elements such as K, Rb, Ba and the light rare-earths (Condie, 1976), especially as continental crust, once formed, appears

to be "non-geodegradible" (Dietz's phrase, from Burke et al., 1976). Lambert et al. (1976) have concluded that the Archean mantle was less depleted in incompatible elements, less fractionated and more hydrous than the modern mantle; they suggest the existence of a K-rich zone extending to 100 km as one characteristic of the Archean mantle.

Models for Archean Crustal Evolution

The results of rare earth element studies were interpreted by Arth and Hanson (1972) to imply that most Archean tonalitic rocks formed by partial melting of amphibolite or eclogite of basaltic composition at depths of greater than 30 km, leaving behind a residue of garnet and clinopyroxene. Subsequent investigators (Barker and Arth, 1976; Arth and Barker, 1976) stress the importance of hornblende and amphibolite (rather than higher pressure garnet bearing parent rocks) in the formation of Archean tonalitic rocks. This particular controversy will be further discussed in Chapter III. Our immediate problem is the logistics of placing Archean basalt into the pressure and temperature regimes of the lower crust or upper mantle, as well as the production of the observed distributions of Archean granite-greenstone and gneiss belts. The suggested mechanisms can be divided into two categories, those which accept the operation of Archean plate tectonics, and those which do not.

Some of the evidence and/or speculations used to deny the operation of Archean plate tectonic processes include:

1. thin crust could not retain sufficient rigidity for subduction (Lambert, 1976).
2. measured Archean pole wandering curves do not suggest large cratonic movements (McElhinny et al., 1968);
3. intraplate sutures that should result from collision orogenies are not recognized (Shackleton, 1973);
4. the symmetrical nature of Archean basins appears to preclude extensive continental drift (Windley, 1973);
5. blueschists are absent in the Archean (Talbot, 1973; Lambert, 1976);
6. many Proterozoic fold belts appear to have formed on pre-existing continental crust, and older structures can be traced through them; in some localities, uninterrupted cover sequences from Proterozoic mobile belts extend onto Archean cratons (Cahen and Snelling, 1966; Mason, 1973);
7. very steep Archean geothermal gradients would cause basaltic rocks to encounter the stability field of garnet granulite (rather than eclogite) and thus the metabasaltic material would remain gravitationally stable relative to underlying upper mantle peridotite (D.H. Green, 1974).

A plethora (Gower's term) of non-plate tectonic crustal evolution models have been developed; the more important of these are summarized below:

Eskola (1948) - Macgregor (1951) - Ramberg (1967) - Anhaeusser et al. (1969)

Mafic volcanic rocks were erupted through and onto a tonalitic gneissic basement along fundamental crustal fractures, and subsequently sank into the underlying lighter, more mobile rocks. This process forced the gneisses to the surface as domes and ridges. Rapid erosion of these re-emergent granitic rocks contributed abundant immature clastics into the subsiding trough. The structure and metamorphism of the greenstones resulted from the upwelling of the granitic rocks and the concomitant downsagging of the dense volcanic-sedimentary pile.

Glikson (1972)

Primordial basaltic crust developed from partial melting of the upper mantle at depths of less than 15 km. Subsequent crustal megarippling caused partial melting of the subsiding zones, and the production of sodic granodiorites and related extrusives. The plutonic rocks formed island continents which then progressively began to exert control upon the configuration of the intervening volcanic-sedimentary troughs during the aggregation of granitic crust.

D.H. Green (1972) - Goodwin (1976b)- Glikson (1976b)

The distinctive character of the ultramafic and mafic bodies of some Archean greenstone belts suggests catastrophic magmatism triggered by meteorite impact. The age of such greenstone belts may therefore be similar to the impacting events responsible for the lunar maria (greater than 3.5 b.y.); other processes only began to dominate crustal evolution after the magnitude and frequency of the large impacts diminished.

Recently, more investigators have begun to believe that some modified form of plate tectonic activity did occur during the Archean. One of the strongest motivations to apply plate tectonic theory to Archean rocks is that their geochemistry can be readily interpreted in terms of such models.

The geochemical evidence favouring island arc models has already been briefly discussed. Some aspects of geochemistry and metallogeny are also suggestive of extensional environments: Au-Ag, telluride and Cu-Zn deposits associated with greenstone belts are, in many ways, comparable to those found in more modern areas of high heat flow, such as the Basin and Range Province (Windley, 1973); Zr, Y, Ni, SiO_2/K_2O and Fe^3/Fe^2 of mid-ocean ridge tholeiites are similar to those measured in some Archean mafic metavolcanic rocks. Recently, the focus of geochemical comparisons has shifted to the ubiquitous

Archean tonalitic rocks. These have chemical characteristics such as fractionated, light rare earth enriched patterns that are similar to rocks produced in modern island arcs and Andean-type continental margins. Such rocks are located at plate margins, but derived from mantle sources (Windley, 1976; Windley and Smith, 1976; Tarney et al., 1976; Langford and Morin, 1976).

Recent structural re-interpretations also suggest the importance of horizontal rather than vertical tectonics in the Archean. Wrench faults found in Archean terrains have been compared to modern transform faults (Shackleton, 1973), although Mason (1973) and Coward et al. (1973) preferred to produce such structures by cratonic rotation. Burke et al. (1976) state quite bluntly that models involving vertical tectonics in Archean rocks are incorrect, citing Ramsay's (1963) study of the Barberton granite-greenstone belt as one example where the presumed control of granitic batholiths upon the deformation of greenstone belts was disproven. Burke et al. (op. cit.) instead suggest that greenstone deformation is due to crustal shortening during microcontinental collisions. Windley (1976) and Windley and Smith (1976) say that thrust structures are far more important in the tectonic development of greenstone belts than previously believed. Westerman (1975, 1977) earlier suggested the importance of thrusting in portions of the English River Gneiss Belt of Ontario.

My opinion is that plate tectonic mechanisms did operate during the Archean; the exact nature of the processes is less certain. Some of the more popular plate tectonic models are described below; the last cited is perhaps the most compatible with the existing facts.

Windley (1973)

Archean granitic crust underwent incipient separation of crustal plates during the formation of graben-like rifted zones. Intense volcanism in the rifts was then followed by molasse and turbidity type sedimentation from nearby continental areas. Subsidence of the volcanic-sedimentary pile gave rise to down-sagging basins with vertical stretching and upright folds. During such deformation, the gneisses contacting the greenstones were remobilized to form the large batholiths associated with the margins of greenstone belts.

Talbot (1973)

The first sialic crust consisted of small independently accreted micro-continents concentrated by plate tectonic processes behind subduction zones. Greenstones, for the most part, represent vestiges of oceanic crust trapped between continental nuclei. By the end of the Archean sialic concentrations were sufficiently extensive to survive ocean closure without significant remobilization.

Goodwin (1973)

Individual Archean basins represent spreading centers driven by mantle thermal plumes. Ocean floor basalts develop at the center of the basin and are subducted at the rim with the resulting development of arc-type volcanics. The basins were then tectonically modified by the intrusion of the granitic batholiths.

Windley (1976) - Windley and Smith (1976) - Tarney et al. (1976)

Greenstone belts represent ancient crustal equivalents of margin basins, such as the Mesozoic 'Rocas Verdes' basin of southern Chile, and are evolved in extensional back arc environments. They develop coevally with the adjacent high grade Archean gneisses. The gneisses are equivalent to the batholiths located along the west coast of North America and along the Andes. This paired development causes Archean clastic metasediments to be of a mixed (mafic) volcanic and sialic nature. The Archean gneisses, according to this model, should be largely meta-igneous. The chemistry of these Archean tonalites, however, is not expected to be identical to that of the Mesozoic granitic rocks, given the formation of the former group of rocks from more primitive and less fractionated lower crust and upper mantle than the Mesozoic analogues. The anorthosite-ultramafic layered igneous complexes common to both the Archean gneisses

and the younger analogues are considered to be the hydrous residue from the formation of basaltic rocks.

The Archean arcs would be sites of high heat flow and subsequent granulite facies metamorphism. Some thrusting activity would be expected, and could cause tectonic interleaving of arc gneisses with marginal basin supracrustals. Major Archean nappes, such as proposed for the Dalradian of Scotland, would represent the final stages of tectonic activity at a continental margin.

Concluding Remark

It is not expected that this oxygen isotope and chemical study will provide the panacea for these general problems. However, a proper understanding of Archean crustal evolution will only be obtained when specialized studies such as this one have been incorporated into a geological and geochemical panoply that can be donned for the comprehensive assault upon the nature of the early history of the earth.

CHAPTER II

THE GEOCHEMISTRY OF ARCHEAN CLASTIC METASEDIMENTARY ROCKS

"Praise the sea, but keep on land."

G. Herbert

II-1 INTRODUCTION

Geochemical and oxygen isotope results for Archean greenschist facies clastic metasedimentary and spatially associated felsic metavolcanic rocks (from which some of the detritus in the metasedimentary rocks may have been derived) are presented in this chapter. Some possible applications of such information include:

1. the determination of the average composition of the portion of the Archean crust from which the metasedimentary rocks were derived, as well as the relative contributions of basic and acidic rocks to the detritus;
2. the recognition of chemical and/or isotopic characteristics of Archean clastic metasedimentary rocks that distinguish them from Archean (felsic) metavolcanic or meta-igneous

rocks, and that may be useful in the identification of highly metamorphosed metasedimentary sequences within Archean gneiss terrains;

3. the estimation of the chemical maturity of these metasedimentary rocks, and its implications for the tectonic style during sedimentary processes;
4. the establishment of an average chemical composition of Archean greywacke useful in models for the anatectic production of Archean granitic rocks;
5. the detection of overall chemical and isotopic characteristics peculiar to Archean clastic metasedimentary rocks that may reflect somewhat unique chemical processes during the early history of the earth.

II-2 THE CONCEPT OF CHEMICAL MATURITY

The final chemical and isotopic composition of greenschist facies clastic metasedimentary rocks is a function of three main processes:

1. the chemical and isotopic composition of the provenance;
2. the degree of chemical and isotopic modification that occurs during weathering, erosion, transport, sedimentation and diagenesis of the detritus;

3. the chemical and isotopic changes that occur during greenschist facies metamorphism and alteration.

Most altered samples can be eliminated by careful sampling; the geochemical effects of greenschist facies metamorphism are more difficult to evaluate, but most investigators have concluded that prograde greenschist facies metamorphism occurs quasi-isochemically (Winkler, 1976; see Chapter III-4).

The evaluation of (1) and (2) represent a chemical attempt to determine what is commonly denoted as "sediment maturity". Sediment maturity has been defined as "the extent to which a clastic sediment texturally and compositionally approaches the ultimate end product to which it is driven by the formative processes that operate upon it" (Gary et al., 1972, p.435; Pettijohn, 1957). Textural maturity is measured by the uniformity of particle size and the perfectness of rounding; mineralogic maturity is often characterized by the quartz + chert/feldspar + rock fragment ratio, the most mature sandstone being composed of pure quartz. Chemical maturity is much more difficult to quantitatively express because of the varied consequences of 'formative processes' such as physical abrasion, sorting during sediment transport, weathering, diagenesis and halmyrolysis. The effects of such processes have been discussed by Pettijohn et al. (1973), from which most of the following summary is drawn.

Surficial weathering causes feldspars to alter to clays (kaolinite) and mafic minerals to chemically decompose as many of their components enter solution. Some minerals, such as quartz, however, resist surface weathering and are transported in a chemically unmodified form. SiO_2, nevertheless, is more soluble than Al_2O_3 under normal surface water pH and temperature conditions; this results in a progressive decrease of the SiO_2/Al_2O_3 ratio in the residual weathering rind, as the weathering process proceeds.

The chemistry of a sedimentary rock can also be greatly modified by physical abrasion during transport. Softer minerals or rock fragments are reduced in size as distance or vigor of transport is increased; the changes in hydraulic properties attendant to such diminuation causes the concentration of these particles in silts and muds. Some detritus which achieves colloidal dimensions then becomes especially sensitive to the effects of adsorption. Physically harder minerals such as quartz are not as affected by abrasion, and therefore tend to concentrate in coarser grained sediment fractions, resulting in SiO_2 enhancement in sandstones relative to finer grained clastic sedimentary rocks.

Diagenesis (all transformations undergone by a sediment after reaching the final resting place during the current depositional cycle, except surface weathering and metamorphism; AGI Glossary, 1972, p.192) can cause significant modification

of the chemistry of a sediment. Most important are the Si and/or Ca enrichments attendant to cementation and the redistribution of alkali and alkaline-earth elements that occurs during the formation and alteration of clay minerals. The very different chemical composition of pore fluid brines in equilibrium with deep-seated sedimentary rocks from that of fresh or seawater emphasizes the importance of post-depositional chemical reactions (Pettijohn et al., 1973).

Studies of the diagenetic alteration of deeply buried volcanogenic sandstones resulted in the recognition of the zeolite facies (Coombs et al., 1959), a paragenesis in geological limbo somewhere between diagenesis and metamorphism. The devitrification of volcanic glass provides many of the components necessary for the formation of authigenic clays, zeolites, feldspar and quartz during the lower and higher grade diagenesis of clastics rich in volcanic rock fragments.

The geochemical reaction of sediment and seawater (halmyrolysis) can also cause significant modification of the chemistry of a sediment. It is characterized by the formation of glauconite from feldspars and mica and the degradation of volcanic ash to phillipsite and palagonite.

Finally, the effects of sediment recycling must be considered. The superposition of the collective chemical effects of multi-stage sedimentary processes upon the already complex geochemical system can thoroughly confuse any attempt to determine

sediment provenance from chemical data. Our discussion will attempt to focus upon those chemical and isotopic traits that are representative of provenance; nevertheless, we cannot expect to avoid all of the chemical and/or isotopic effects that may result from the myriad of weathering, diagenesis and metamorphism that could have affected Archean clastic metasedimentary rocks.

II-3 THE GEOLOGY AND SEDIMENTOLOGY OF ARCHEAN CLASTIC METASEDIMENTARY ROCKS

The metasedimentary rock types found within Archean granite-greenstone belts include metagreywacke, meta-argillite, metaconglomerate, chert, iron-formation, and pyroclastic material (Anhaeusser, 1971). The volume of these rocks increases upward in the stratigraphic succession in any particular volcanic-sedimentary cycle, and several cycles may occur within a given granite-greenstone belt (Talbot, 1973; Anhaeusser, 1971). Some sedimentary sequences have been derived mostly from granitic terranes (Pettijohn, 1943; Walker and Pettijohn, 1971; Turner and Walker, 1973); others are composed mostly of volcanic rock fragments (Ayres, 1969; Ojakangas, 1972; Teal and Walker, 1977; Hyde and Walker, 1977); still others represent a mixed volcanic-granitic source area (Henderson, 1972; Teal and Walker, 1977; Turner and Walker, 1973).

The application of sedimentological techniques to Archean metasedimentary rocks, as pioneered by Walker and his coworkers, has provided constraints upon possible depositional environments in Archean granite-greenstone belts. Two general facies associations have been defined in these Archean clastic metasedimentary rocks, the 'resedimented association', which includes turbidites, resedimented conglomerates, pebbly mudstone and argillite, and the 'continental association' (or 'non-marine association' of Hyde and Walker, 1977), which is composed of all facies deposited inland or at the shoreline (Turner and Walker, 1973). The preservation of turbidites (resedimented association) implies deposition in a quiet, deep (below storm wave base) basin, located near shallow water areas. Examples of such metasedimentary Archean rocks occur in the Minnitaki Group (Walker and Pettijohn, 1971), the Mosher Bay unit (Teal and Walker, 1977), and portions of the Timiskaming Group (Hyde and Walker, 1977). The non-marine association includes alluvial fan and braided river (fluvial) deposits such as those recognized in the Uphill Lake unit (Teal and Walker, 1977), portions of the Timiskaming Group (Hyde and Walker, 1977), and parts of the Ament Bay Formation (Turner and Walker, 1973).

Because the sedimentary rocks formed in any one of these environments may differ in provenance, and will differ in the amount of reworking and mineralogical modification that occurs during transport, their chemical and isotopic compositions are

expected to vary. Accordingly, clastic metasedimentary rocks from each of these differing sedimentary facies and associations have been analyzed.

The areas of study are the Timiskaming Group, near Kirkland Lake, Ontario, Abitibi granite-greenstone belt, and the Kakagi Lake and Upper Manitou Lake areas, both within the Wabigoon granite-greenstone belt, Ontario (Figure 2-1a,b). A few samples have also been analyzed from the Abram Lake area, Wabigoon granite-greenstone belt, and the Pakwash Lake area, Uchi granite-greenstone belt (Figure 2-1a,b).

All samples are of low metamorphic grade, ranging from prehnite-pumpellyite facies in the Kirkland Lake area (Jolly, 1974) to greenschist facies in the Wabigoon granite-greenstone belt. Typically, the rocks contain plagioclase, quartz, biotite and/or chlorite, muscovite and/or sericite, minor calcite, and, in a few samples, some microcline. A chlorite-rich matrix is present in almost every sample.

Upper Manitou Lake area

A generalized geological map of the Upper Manitou Lake area, containing sample locations, is shown in Figure 2-2 (from Teal and Walker, 1977). The geology of the area has been described by Blackburn (1976b,c,d) and the sedimentology and detailed stratigraphy by Teal and Walker (1977); these works

FIGURE 2-1a Granite-greenstone and gneiss belts of the Superior Province

1. Sachigo Volcanic Belt
2. Berens Plutonic Belt
3. Uchi Volcanic Belt
4. English River Gneiss Belt
5. Wabigoon Volcanic Belt
6. Quetico Gneiss Belt
7. Wawa Belt
8. Abitibi Volcanic Belt
9. Opatica Belt
10. Ungava Belt

FIGURE 2-1b Location of study areas:

1. Lake Despair
2. Kakagi Lake
3. Upper Manitou Lake
4. Abram Lake
5. Kirkland Lake
6. Cedar Lake - Clay Lake
7. Pakwash Lake
8. Kenora area

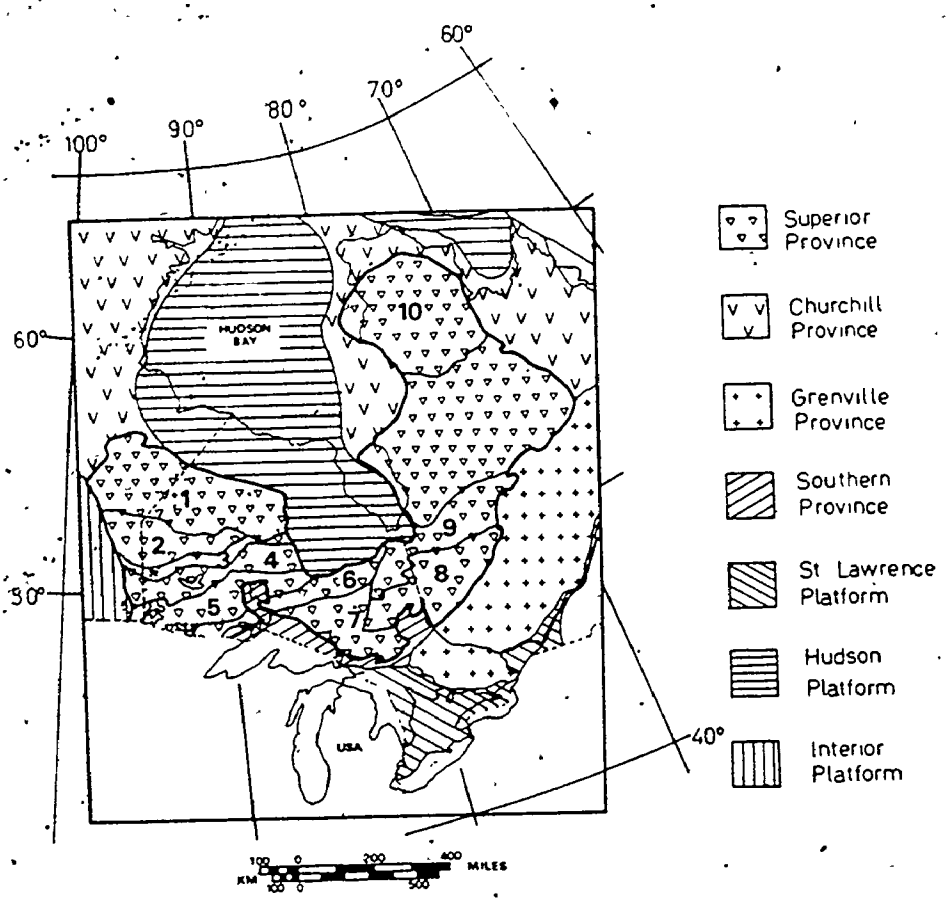
60°
70°
80°
90°
100°
60°
50°
40°
HUDSON BAY
USA
1
2
3
4
5
6
7
8
9
10
Superior Province
Churchill Province
Grenville Province
Southern Province
St Lawrence Platform
Hudson Platform
Interior Platform
KM
MILES

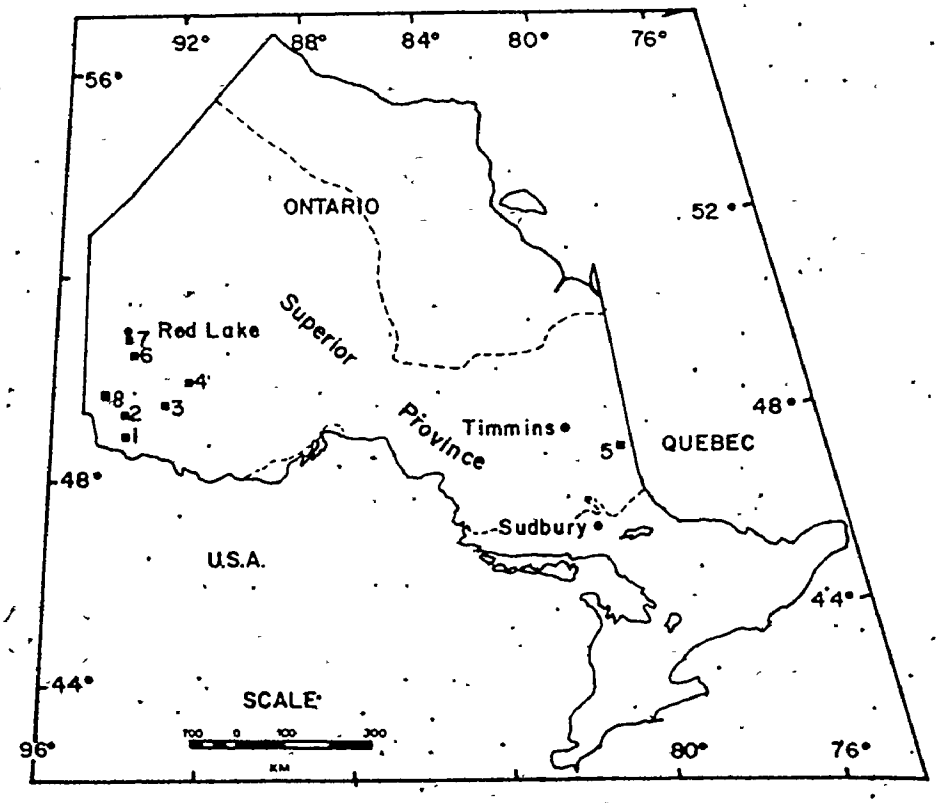
92°
88°
84°
80°
76°
56°
52°
48°
44°
ONTARIO
QUEBEC
Red Lake
Superior Province
Timmins
Sudbury
U.S.A.
SCALE
KM

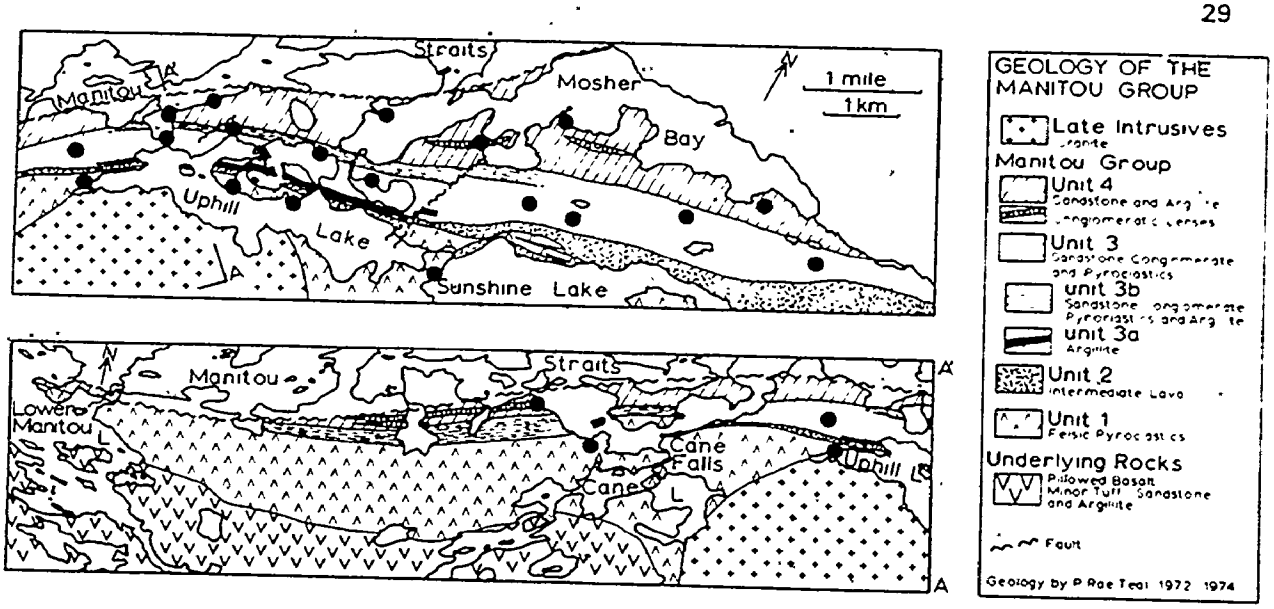

FIGURE 2-2a Geology of the Upper Manitou Lake area

● indicates sampling locality; drawing from Teal and Walker (1977)

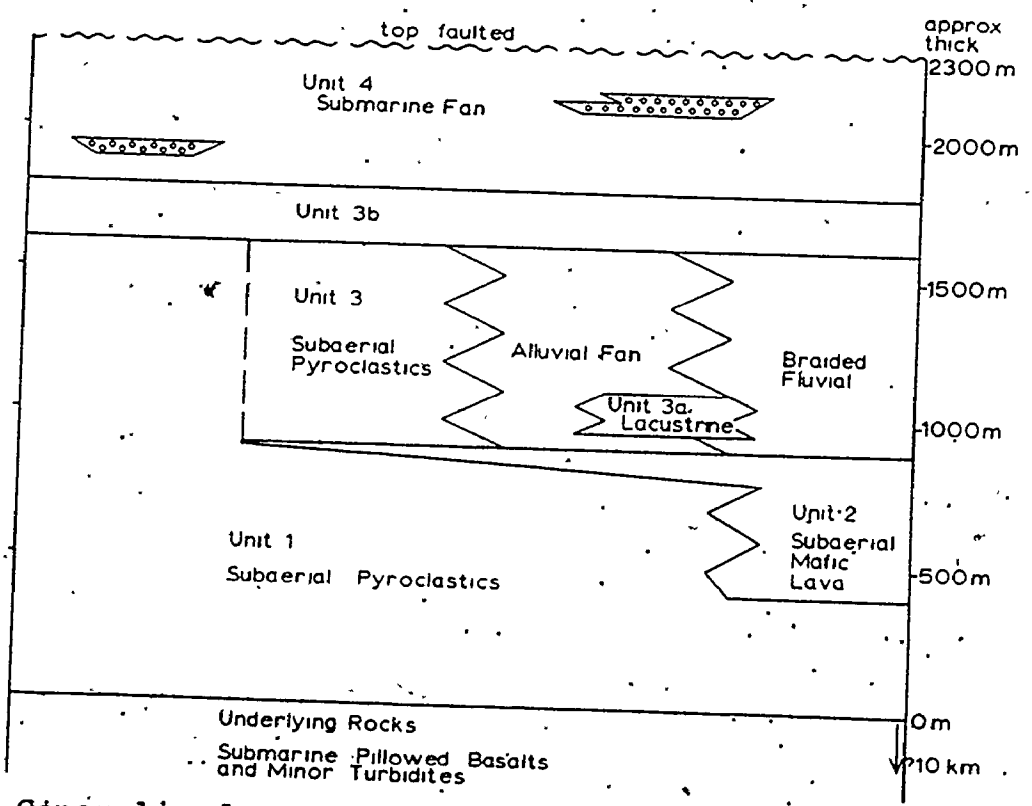

FIGURE 2-2b Generalized stratigraphic section of the Upper Manitou Lake area; drawing from Teal and Walker (1977)

are briefly summarized below.

The stratigraphically lowermost Cane Lake unit (unit 1) is composed of coarse, dacitic pyroclastic rocks. To the east, in the vicinity of Sunshine Lake, intermediate, somewhat alkalic lava flows (unit 2) separate unit 1 from the overlying Uphill Lake unit (unit 3). The Uphill Lake unit contains a dacitic pyroclastic facies, an alluvial fan facies (composed of clastics eroded from a presumably nearby dacitic volcanic vent), and a braided river facies, predominantly of pyroclastic derivation, but containing some granitic debris, especially in conglomeratic units. The first appearance of free quartz occurs in the braided river facies, but felsic and some mafic metavolcanic rock fragments are still the most important framework component of these metagreywackes. The alluvial fan facies contains little or no free quartz, only occasional cross-bedding (10 to 50 cm sets) and is coarse grained. The metasandstones of this facies occur in lenses, interbedded with abundant conglomerate which is wholly composed of volcanic debris.

The Rush Bay sub-unit (unit 3b) is transitional between the Uphill Lake unit and the overlying metasedimentary rocks, the Mosher Bay unit (unit 4). The Rush Bay unit is interpreted by Teal (pers. comm.) to represent the transition between the "continental" and "marine" associations. The Mosher Bay unit is composed of metasandstones, meta-argillites and metaconglomerates, and is a turbidite facies. The metasandstones of this

unit contain larger amounts of free quartz and a smaller percentage of rock fragments than the underlying fluvial facies (Table 2-1).

Kirkland Lake area

A generalized geological map of the Kirkland Lake area (Hyde and Walker, 1977), showing sample locations for the Timiskaming Group, is presented in Figure 2-3. The Timiskaming Group is composed of metasedimentary and alkaline metavolcanic rocks which overlie the predominantly mafic metavolcanic rocks of the Abitibi granite-greenstone belt. The area has been studied by many investigators (Thomson, 1946; Hewitt, 1963; Cooke and Moorhouse, 1969; Ridler, 1970, 1976; Jolly, 1974, 1975; Hyde and Walker, 1977). Hyde and Walker (1977) described the sedimentology of the area; their work is briefly summarized below.

All of the metasandstones examined in this study belong to the 'non-marine association', and have been interpreted as braided river deposits. The association is dominated by polymictic metaconglomerates and medium to coarse grained metasandstones, and contains only a small amount of meta-argillite. The metasandstones are volcanic litharenites, sandstones with greater than 25% recognizable volcanic rock fragments (Hyde, pers. comm.). They contain free quartz (2-36%), plagioclase

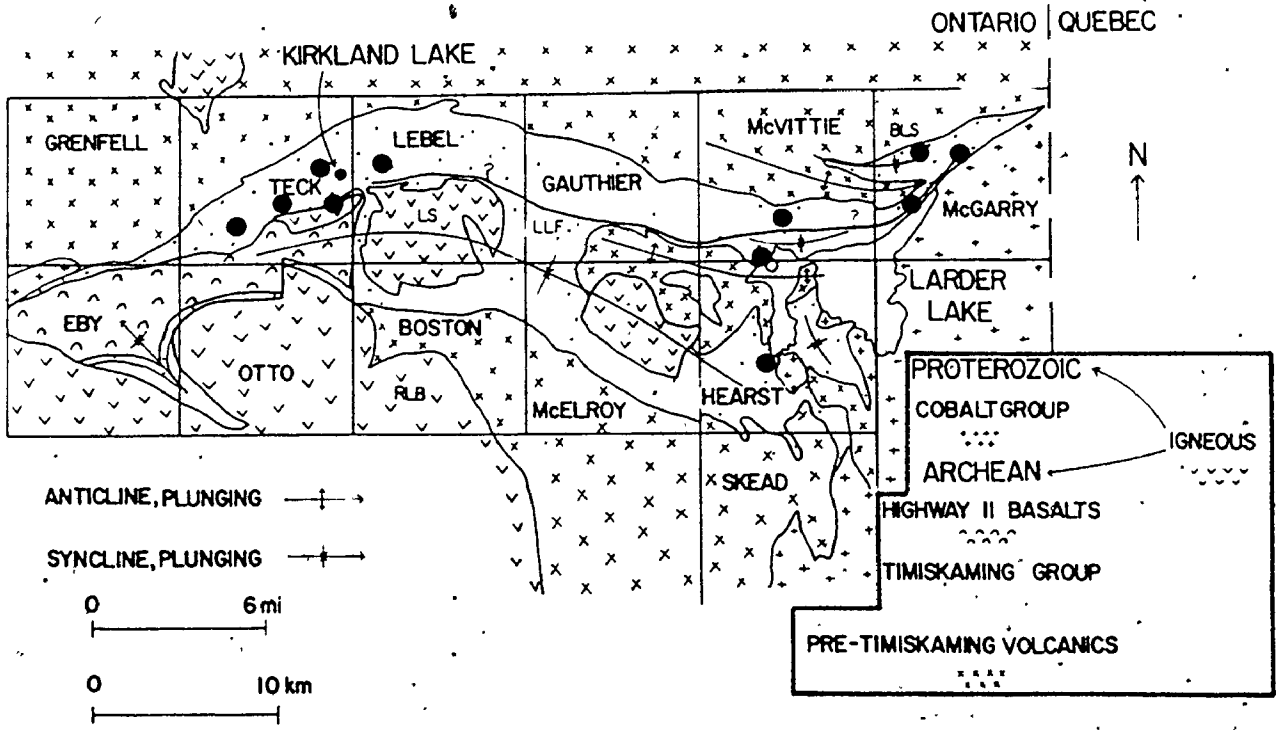

FIGURE 2-3a Geology of the Kirkland Lake area.

● indicates sampling locality; drawing from Hyde and Walker (1977). The field shown for Pre-Timiskaming metavolcanic rocks includes metatholeiites, calc-alkaline intermediate to felsic metavolcanics, and some alkaline metabasalts.

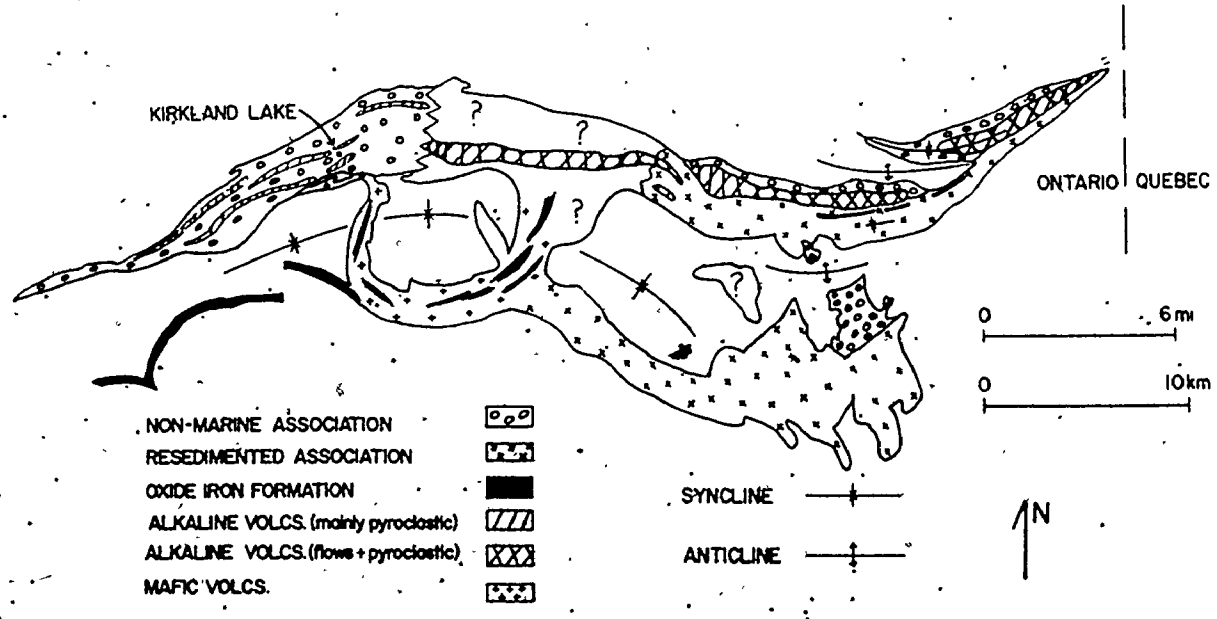

FIGURE 2-3b Generalized facies distribution map, Kirkland Lake area; drawing from Hyde and Walker (1977)

(4-19%), and rock fragments (43-82%) in a chlorite plus (minor) carbonate matrix (10-16%). Small amounts of chert have been observed, but potassium feldspar is absent (Table 2-1).

The analyzed samples are representative of discrete metasandstone bodies which Hyde (pers. comm.) feels have somewhat differing provenances. All have been derived from a predominantly metavolcanic terrain, but the relative contribution of mafic to felsic metavolcanic rocks appears to vary; some plutonic contribution is indicated by the presence of granodioritic and trondhjemitic boulders in the metaconglomerates. The source of the mafic metavolcanic fragments is not certain; Jolly (1975) proposed that the metasedimentary rocks were derived largely from the underlying mafic metavolcanic rocks. Hyde (pers. comm.) suspects that some of the mafic detritus may have been cannibalized from the Timiskaming alkali metavolcanic rocks.

A few turbidite facies meta-argillite samples, and one sample of mafic metatuff (DU-3), from the 'resedimented association', have also been analyzed. This association is dominated by turbidites and interbedded conglomerates, but also contains interstratified iron-formation, graphitic rocks and magnesite-carbonate rocks. Petrographic studies (Hyde and Walker, 1977; Hewitt, 1963) suggest a largely volcanic origin for the clastic metasedimentary rocks of this facies.

Table 2-1 Modal data for some metagreywackes examined in this study

UPPER MANITOU LAKE*	pyroclastics		sandstones							
			alluvial fan	braided river				turbidites		
	T25	T214	T10	T9	T109	OT6	T32	S2	S5	T42
quartz			0.6	1.0	2.2	10.2		11.6	11.4	17.4
K-feldspar				8.8			0.6		0.6	0.4
plagioclase	18.4	20.8	0.6	17.6	3.6	10.4	9.2	18.8	8.4	12.0
volcanic RF	34.8		76.2	31.2	74.8	39.6	72.4	24.2	27.4	8.2
plutonic RF						2.0		1.2	1.2	2.8
sedimentary RF										0.6
chert						1.8	0.6			
matrix	46.8	79.2	22.6	41.4	18.6	36.0	17.2	44.2	51.0	57.8

KIRKLAND LAKE**	sandstones							
	CH7	EL3	RP4	CK2	LS1	LL8	IL3	ME2
quartz	8.0	5.7	3.5	2.5	13.2	7.3	15.3	35.5
K-feldspar								
plagioclase	16.0	9.0	19.3	5.0	14.1	11.2	15.3	4.5
felsic RF	20.0	20.7	33.8	27.0	25.3	51.0	25.0	19.8
mafic RF	40.0	51.0	22.4	53.0	34.5	12.5	26.5	20.0
chert	0.2	0.7	1.5	1.5	1.2	7.5	0.5	2.5
matrix	13.5	10.5	16.0	9.7	10.7	9.8	14.8	13.7
cement	2.3	2.4	3.5	1.3	1.0	0.7	2.8	4.0
nature of matrix	chl & cal	chl & cal	chl	chl	chl & cal	chl	chl & cal	chl, cal & qtz

Table 2-1/continued

ABRAM LAKE***	sandstones			pyroclastic
	AR12	GW19	AR30	C12
quartz	40	22	26	6
feldspar	20	28	17	38
RF	18	12	17	
matrix	20	38	40	56

* analyses by P.R. Teal; matrix composed of chlorite and minor carbonate

** analyses by R.S. Hyde, renormalized to 100% chl - chlorite; cal - calcite; qtz - quartz

*** analyses by Turner (1972)

Kakagi Lake area

The general geology of the Kakagi Lake area, Wabigoon granite-greenstone belt, is shown in Figure 2-4 (from Kwong, 1975, after Kaye, 1974). The geology of this area has been described by Burwash (1933), Fraser (1943), Goodwin (1965), Davies and Morin (1972), Ridler (1965), Cuddy (1971), Smith et al. (1972), Wilson (1973) and Kaye (1974). Unfortunately a detailed sedimentological study of this area has not been made.

Interbedded clastic metasedimentary and felsic metavolcanic rocks (largely of pyroclastic origin) overlie a thick sequence of basic metavolcanics and associated gabbroic material. The metasedimentary rocks include well-banded chert, siltstone, greywacke, and laminated, water-laid, somewhat reworked felsic tuff. Graphitic argillite also occurs within the now metamorphosed sedimentary pile. Poor sorting and angularity of the grains in the coarse clastics probably resulted from rapid erosion of the contemporaneous felsic metavolcanic rocks (Kwong, 1975).

Abram Lake area

Only a few samples from the Abram Lake area, Wabigoon granite-greenstone belt, have been analyzed. The geological details and sample locations are given in Turner (1972). The

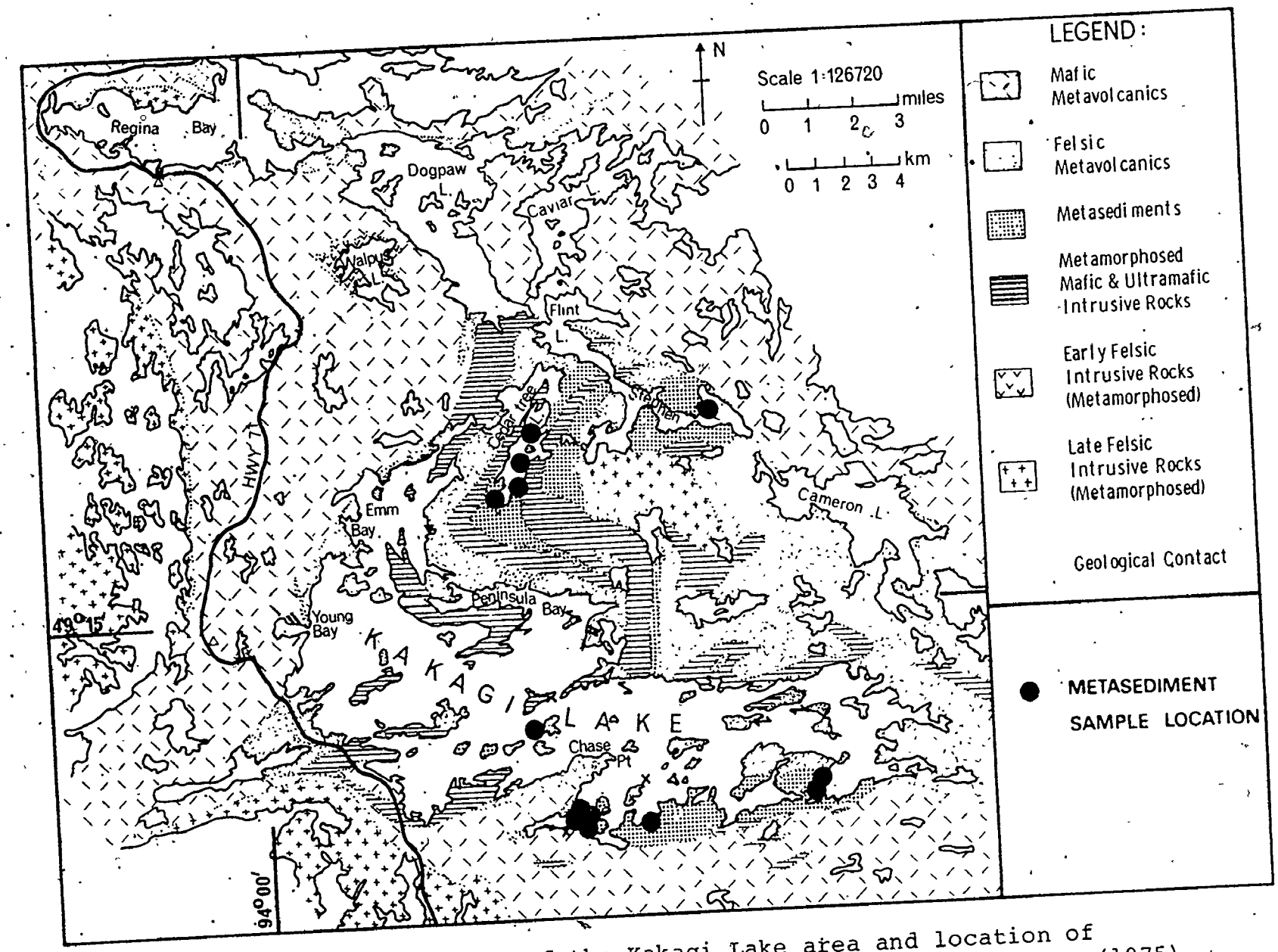

FIGURE 2-4 Geology of the Kakagi Lake area and location of analyzed samples. Diagram modified from Kwong (1975)

stratigraphy and sedimentology have been described by Turner and Walker (1973), from which the following is summarized.

The Ament Bay Formation unconformably overlies a thick sequence of metavolcanic rocks, and is composed of conglomerates and arkoses; these have been interpreted as alluvial fan deposits. Petrographic study suggested a granodioritic provenance for these metasedimentary rocks (Table 2-1; Ar12). A meta-arkose (Ar12), a meta-argillite (Ag27), and a granodiorite clast (Cl 8) from the metaconglomerate have been analyzed. Chemical analyses for these samples were also reported by Turner (1972).

The Daredevil Formation, composed of felsic (Cl2) and mafic (Ar17) metatuffs as well as turbidites (metagreywacke GW19) derived mostly from the underlying metavolcanics, conformably overlies the Ament Bay Formation. The Daredevil Formation, in turn, is overlain by the Little Vermilion Formation, which is composed of turbidites probably derived from the metasedimentary rocks of the underlying formations, as well as some volcanic and granodioritic material. One metagreywacke (Ar30) and one meta-argillite (Ag24) from this unit have been analyzed.

Pakwash Lake area

The geology of this portion of the Uchi granite-greenstone belt has been discussed by Beakhouse (1974b). The clastic metasedimentary rocks are interbedded metaconglomerates, metasandstones, metasiltstones, and meta-argillites, and are probably turbidity deposits. Only two samples of these rocks were analyzed, both of which were metasandstones located near a major tectonic break, the Sydney Lake fault. Clast types within the conglomeratic units include mafic to felsic metavolcanic rocks, as well as granodiorite, thus reflecting a mixed provenance for these rocks.

II-4 CHEMICAL CLASSIFICATIONS OF ARCHEAN CLASTIC METASEDIMENTARY ROCKS AND ESTIMATIONS OF CHEMICAL MATURITY

The major and trace element results for over 50 Archean clastic metasedimentary rocks are given in Appendix IV. The purpose of this section is to determine the control of provenance upon the major element chemistry of these rocks.

Blatt et al. (1972) identified $Fe_2O_3^t$ + MgO, K_2O and Na_2O as chemical components that can be used to relate the chemical composition of sandstones to their tectonic setting, and, therefore, to their source rocks (Figure 2-5). These chemical parameters are related to three major tectonic environments:

1. taphrogeosynclinal, containing sandstones (mostly arkoses) which are deposited in continental fault-bounded basins and derived from predominantly granitic rocks;
2. exogeosynclinal, comprised of clastic sediments (usually lithic sandstones which still include a significant proportion of non-volcanic rock fragments) accumulated at a cratonic margin adjacent to an uplifted orthogeosynclinal belt, and
3. eugeosynclinal, composed of clastic sediments (volcanic lithic sandstones - greywackes) associated with volcanic activity located away from major cratons (island arc type sedimentation).

This latter group of sediments are usually quartz-poor, as opposed to the more quartz-rich varieties derived mostly from plutonic or sedimentary sources.

Almost all of the Archean metasandstones analyzed in this study plot within the eugeosynclinal field (Figure 2-5). The meta-argillites are also shown, but only for comparison. Their finer grain size makes the chemical factors used in this diagram less appropriate to tectonic setting, and more indicative of possible alteration during sedimentary processes. Indeed, the meta-argillites are more potassium rich than the metasandstones.

A eugeosynclinal environment for Archean greywackes is compatible with the generally accepted models of granite-greenstone

FIGURE 2-5 Na_2O-$Fe_2O_3{}^t$+MgO-K_2O plot for the Archean clastic metasedimentary rocks analyzed during this study. Fields are shown for:

1. taphrogeosynclinal environment
2. exogeosynclinal environment
3. eugeosynclinal environment

as outlined in Blatt et al. (1972)

FIGURE 2-6 Log (SiO_2/Al_2O_3) versus log (Na_2O/K_2O) diagram for the Archean clastic metasedimentary rocks analyzed during this study

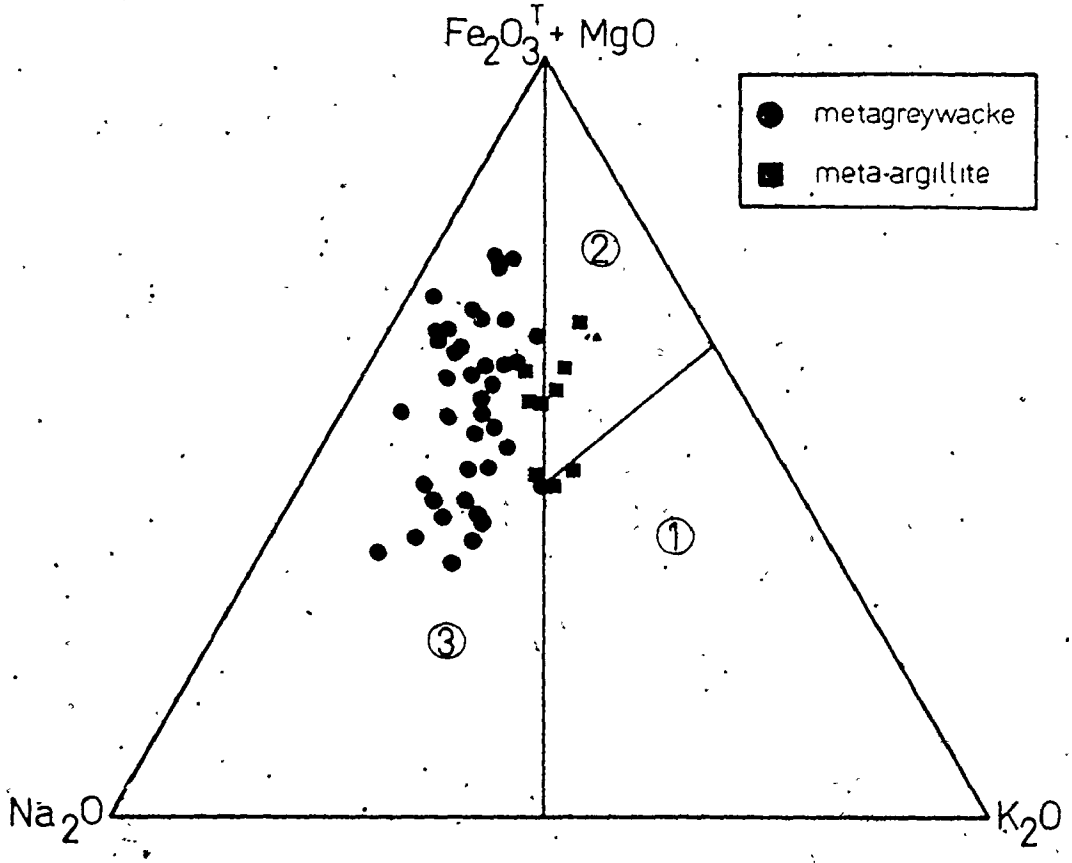
$Fe_2O_3^T + MgO$
metagreywacke
meta-argillite
①
②
③
Na_2O
K_2O

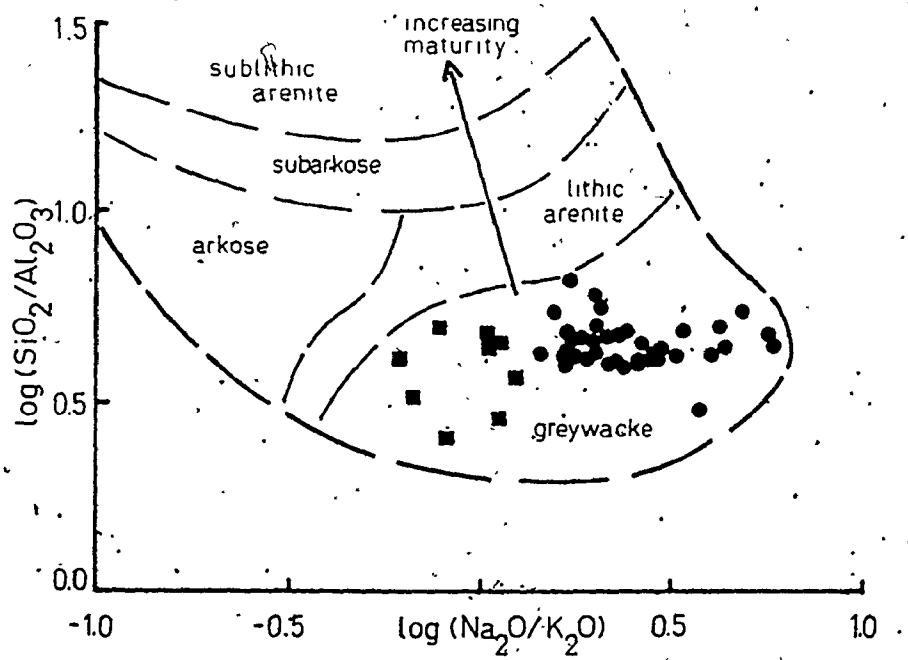
increasing maturity
sublithic arenite
subarkose
arkose
lithic arenite
greywacke
1.5
1.0
0.5
0.0
-1.0
-0.5
0.5
1.0
$\log(SiO_2/Al_2O_3)$
$\log(Na_2O/K_2O)$

belt evolution that require rapid erosion of volcanic piles and coevally emplaced Na-rich plutonic rocks to produce the clastic metasediments. If the chemical components used in Blatt et al.'s (op. cit.) scheme still accurately reflect protolith chemistry, then K-rich source rocks such as granites were not important contributors of detritus. The absence of potassium feldspar in the analyzed clastic metasedimentary rocks, unlike some other Archean metagreywackes (Wyoming: Condie, 1967; South Africa: Condie et al., 1970) also fits such an interpretation. Detrital contribution from quartz diorites and tonalites, however, is certainly not ruled out.

Sedimentary rocks formed in unstable tectonic regimes are generally texturally and compositionally immature. Pettijohn et al. (1973) developed a somewhat comparable chemical classification of sandstones that is related both to provenance and to maturity. The scheme is based upon the ratio of major framework elements, SiO_2/Al_2O_3, which is high in mature, quartz-rich sandstones, and low in immature arkoses and greywackes, and the ratio of Na_2O/K_2O, which is higher in greywackes than in arkoses, probably because of variations in provenance chemistry (but see section II-7) (Figure 2-6). All of the analyzed samples plot within the greywacke field, and all of the metasandstones have $Na_2O > K_2O$; the potassic nature of the meta-argillites is again apparent.

Other chemical indices also indicate that the analyzed clastic metasedimentary rocks are immature. Pettijohn (1957) proposed Al_2O_3/Na_2O as an index of chemical maturity related to the intensity of surface weathering. Values greater than 10 are observed in mature sandstones. Unaltered volcanic rocks have values of 3-4. The samples analyzed in this study have an average value of 4.6 and no values are higher than 6.5. The metasedimentary rocks from the Upper Manitou Lake area, for example, have low Al_2O_3/Na_2O (3.1-5.2), similar to the contemporaneous felsic metavolcanic rocks (average of 4.1). Other Archean greywackes also have low Al_2O_3/Na_2O ratios; those from Wyoming range from 3.8-4.6 (Condie, 1967); those from the Yellowknife Supergroup average about 5 (Henderson, 1975), and those from the Sheba and Belvue Road Formations of South Africa average 5.7 and 4.6, respectively (Condie et al., 1970).

An index that combines aspects of both of the previous examples has been proposed by Pettijohn et al. (1973). According to this latter scheme, immature clastic rocks have values of log $(SiO_2 + Al_2O_3/K_2O + Na_2O)$ (in wt. %) of less than 1.5. All of the samples analyzed in this study lie between 0.8 and 1.4.

A chemical maturity index that does not depend upon the alkali or alkaline-earth elements (which are particularly susceptible to alteration unrelated to sedimentary processes) has been proposed by Moore and Dennen (1970) and Dennen and Moore (1971). They found, from a statistical analysis of a large

number of analyses, that mature clastic sedimentary rocks have Al/Fe of 1.9±0.4. This empirical observation has yet to be explained. Recycling of the detritus causes the Si content to vary, due to hydraulic sorting processes during transport, but the Al/Fe ratio remains relatively constant until supermature products such as ferruginous quartz sandstones (Al/Fe < 1.5; Si > 90) or aluminous shales (Al/Fe > 2.4; Si < 70) are formed.

Since supermature clastic metasedimentary rocks have not been sampled in our study, deviations from Al/Fe of 1.9±0.4 probably reflect chemical immaturity. The most mature samples examined are the turbidite facies metasandstones and meta-argillites from the Upper Manitou Lake area, and the fluvial metasandstones and marine meta-argillites from the Kirkland Lake area (Figure 2-7a). The alluvial fan facies and braided river facies metasandstones from the Upper Manitou Lake area, and the Kakagi Lake metasandstones plot along the igneous trend observed for the Uphill Lake and Cane Lake metavolcanics (Figure 2-7a), as well as for the plutonic Jackfish Lake Complex, which includes a variety of igneous rocks (Figure 2-7b). Since normal chemical weathering produces a constant Al/Fe ratio rather rapidly, even in first cycle sediments, regardless of source rock composition (Moore and Dennen, 1970), the metasedimentary rocks which follow igneous trends such as shown by the Jackfish Lake Complex are probably chemically immature.

Given their textural and mineralogical immaturity, it is

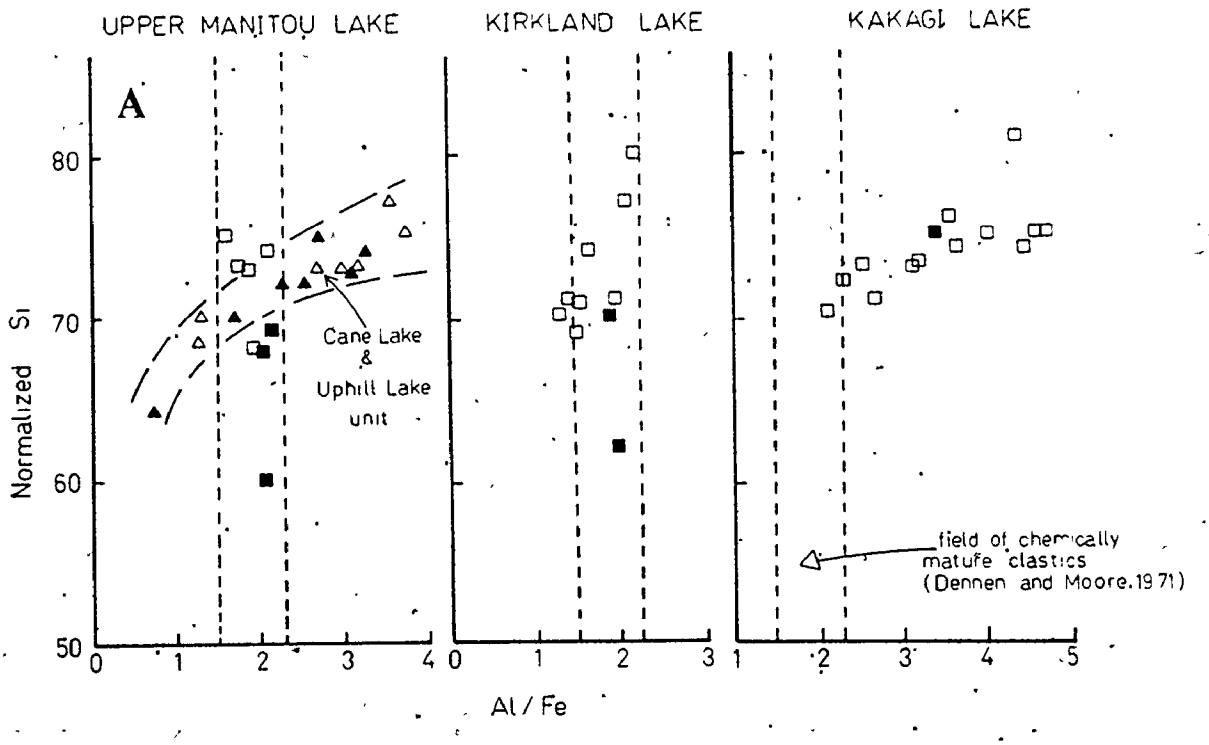

FIGURE 2-7a Normalized Si versus Al/Fe diagram for Archean clastic metasedimentary rocks analyzed during this study. Normalized Si = 100 [Si/(Si+Al+Fe)]

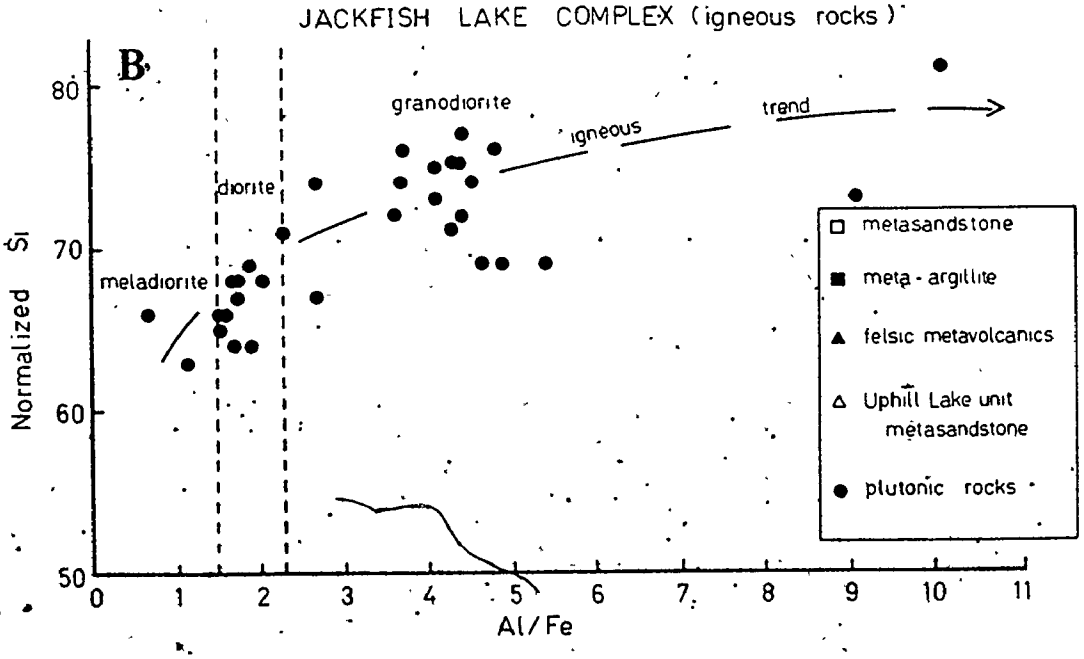

FIGURE 2-7b Normalized Si versus Al/Fe diagram for the Jackfish Lake Complex igneous rocks

not surprising that by most chemical tests, many metagreywackes appear to be immature. Provenance chemistry is probably the most important factor in determining the final chemical composition of many such metagreywackes. Such a conclusion has also been reached by Ronov (1972) and Condie et al. (1970) from their considerations of ancient clastic metasedimentary rocks. However, as the Dennen and Moore index has shown us for the Upper Manitou Lake area turbidites and the Timiskaming fluvial and marine metasediments, chemical modifications during sedimentary processes, even in Archean metagreywackes, cannot be completely ignored.

II-5 THE CHEMISTRY OF GREYWACKES: VARIATION WITH GEOLOGICAL TIME.

If the geochemistry of greywacke is largely a function of source rock composition, any variations that occur throughout geologic time may provide information about the composition and/or abundances of the source rock(s).

A number of evolutionary trends have been observed for clastic rocks as a group (Engel et al., 1974; Veizer, 1973; Ronov, 1972). These include:

1. a decrease in the abundance of Na-rich volcanogenic sedimentary rocks, and corresponding increase in the amount of preserved mature sedimentary rocks.

2. an increase in the K/Na ratio of clastic sedimentary rocks from about 0.7 in the Archean to 2.0 in the Proterozoic, followed by a decline to somewhat lower values in the late Mesozoic and Cenozoic;
3. a significant increase in the abundance of carbonates, which are generally rare in Archean terrains.

A combination of the effects of provenance and crustal instability can account for the observed variations in Na and K. Tectonically unstable conditions during the Archean (and also during the late Mesozoic) prevented large scale preservation of stable shelf type deposits which may have been enriched in K. Engel et al. (1974) note that the abundance of amphibolite and granulite facies rocks in Archean terrains may reflect a period of large scale erosion in which such shelf type deposits may have been lost. Some of the old (>3 b.y.) gneisses from Greenland and Labrador are rich in K (see Table 3-25, #8, 9, 10, 11) and could have been eroded to produce K-rich detritus. However, such source rocks do not form the bulk of the early Archean continental crust; most of the early plutonic rocks were quartz diorites, tonalites and trondhjemites, all of which have Na-affinities. It is therefore unlikely that large amounts of K-rich sediments could have been generated until more K-rich granitic rocks were emplaced, later in the Archean.

Another cause of the time dependent increase in K/Na is

sediment recycling. Crustal stabilization encourages sediment recycling. During such activity, Na is gradually leached from the detritus and carried to the oceans (Ronov, 1972). During halmyrolysis, K may be preferentially absorbed by sediment from seawater (Garrels and Mackenzie, 1969, 1971; Garrels et al., 1971). The operation of this process during recycling would also cause an increase in the K/Na ratio.

Thus the nature of the K/Na ratio appears related to the degree of crustal stability; the major continental breakup in the late Mesozoic and the major period of continental formation during the Archean are marked by low K/Na; the major period of crustal stabilization in the Proterozoic is reflected in high K/Na.

The paucity of Archean carbonates may also be related to crustal stability. Cameron and Baumann (1971) propose that, while Ca was available from the erosion of Archean rocks (in spite of very rapid erosion and deposition), the stable sea margins necessary for shallow marine carbonate formation were absent; they further suggest that carbonate was deposited in deep water, and subsequently subducted.

But has the chemical composition of greywacke changed with geological time? Some average greywacke analyses, taken from the literature, are given in Table 2-2; these show no consistent age-dependent chemical variations. Pettijohn et al. (1973) and Bell and Jolly (1975) also reached this conclusion, although

the latter authors suggest that Fe may be somewhat more abundant in post-Archean greywackes. To properly evaluate chemical variation in greywackes of differing age, those derived from similar types of source rocks should be examined. Figure 2-8 summarizes some of the results of such a compilation for greywackes of predominantly felsic (Table 2-3) and mafic (Table 2-4) origin. At least on this crude level of subdivision, no consistent time dependent variations are observed.

It appears, therefore, that while the relative volume of greywacke preserved in the sedimentary column has decreased through time, the average chemical composition has not changed recognizably.

II-6 THE CHEMISTRY OF CLASTIC METASEDIMENTARY ROCKS FROM NORTHERN ONTARIO

Provenance

The geochemistry of the clastic metasedimentary rocks from the Kakagi Lake, Upper Manitou Lake and Kirkland Lake areas are considered in this section in terms of their provenance.

Some major and minor element results are summarized in Figure 2-9; complete analyses are available in Appendix IV. A striking pattern emerges from most of these results; progressively higher Al_2O_3 and lower $Fe_2O_3{}^t$, MgO, and TiO_2 contents have been

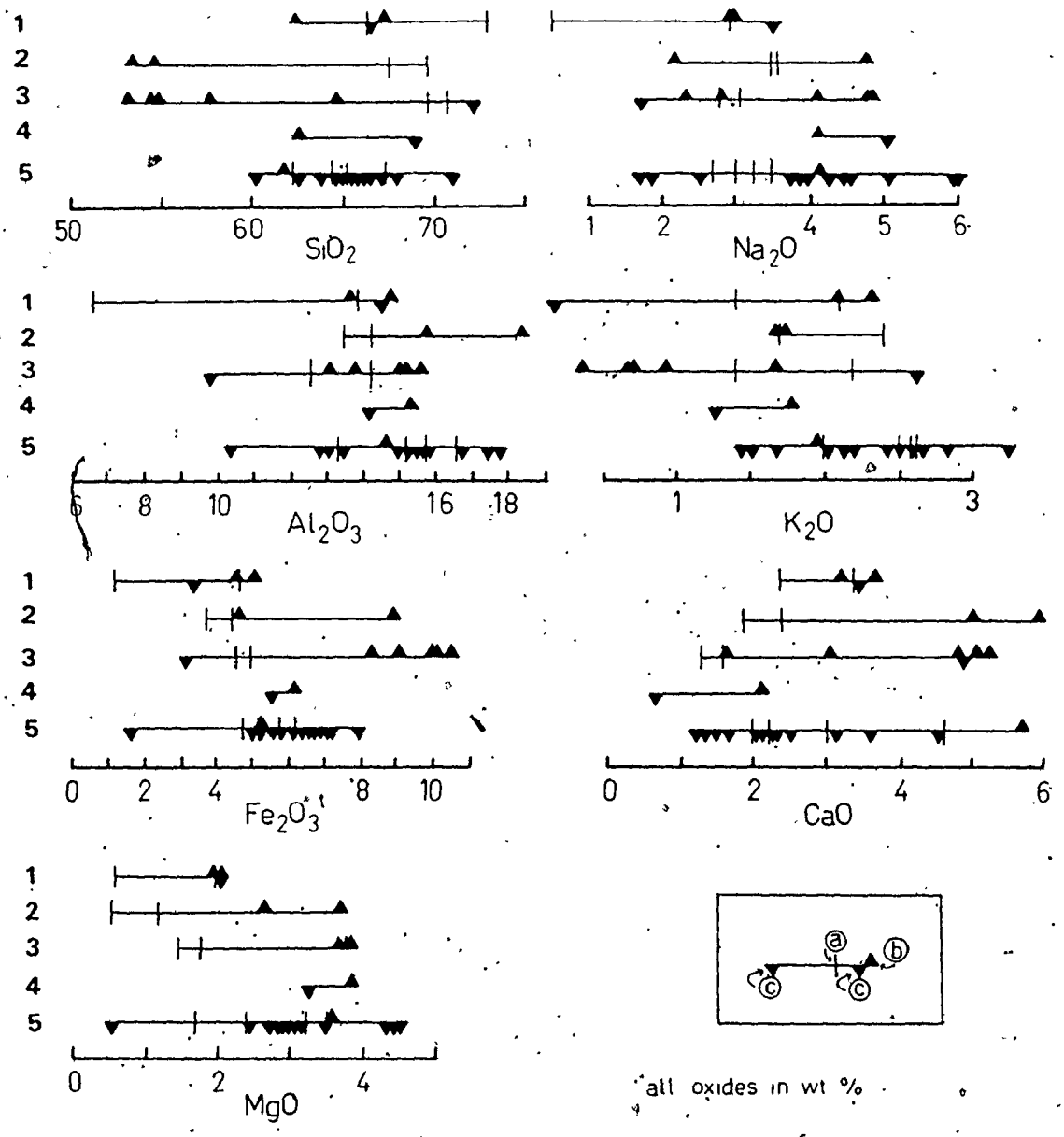

FIGURE 2-8 Average chemical compositions of greywacke throughout geological time

1. Cenozoic
2. Mesozoic
3. Paleozoic
4. Proterozoic
5. Archean

a. Average greywacke (Table 2-2)
b. Average analyses for greywackes of mafic origin (Table 2-4)
c. Average analyses for greywackes of felsic origin (Table 2-3)

Table 2-2 Average greywacke compositions throughout geologic time

	1	2	3	4	5	6	7
SiO_2	77.1	66.75	69.0	66.5	72.90	69.7	67.5
TiO_2	0.3	0.63		0.8	0.20	0.6	0.5
Al_2O_3	8.7	13.54	13.0	13.9	6.59	14.3	13.5
FeO	0.7	3.54					
Fe_2O_3	1.5	1.60	5.4[t]	4.7[t]	1.15[t]	3.8[t]	4.5[t]
MgO	0.5	2.15	2.5	2.0	0.55	1.2	2.2
CaO	2.7	2.54	4.4	3.4	2.36	1.9	2.4
K_2O	2.8	1.99	2.0	2.1	1.41	2.4	1.7
Na_2O	1.5	2.93	3.2	2.9	0.51	3.5	3.6
MnO	0.2	0.12		0.1	0.06		
P_2O_5	0.1	0.16			0.05		
No. of samples	32	61	41	68	216		

	8	9	10	11	12	13	14
SiO_2	69.7	70.6	64.67	65.2	67.47	62.40	65.2
TiO_2	0.5	0.64	0.57	0.51	0.49	0.50	0.57
Al_2O_3	14.3	12.6	13.41	16.6	15.70	15.20	15.8
FeO			4.53	4.0	6.10[t]	4.61	3.4
Fe_2O_3	4.6[t]	4.97[t]	1.23	0.8		0.57	1.2
MgO	1.8	1.51	3.23	2.4	1.70	3.52	2.2
CaO	1.3	1.61	3.04	2.2	1.98	4.59	3.3
K_2O	1.4	2.19	2.02	2.5	2.59	2.57	3.23
Na_2O	3.1	2.76	2.99	3.5	3.23	2.68	3.7
MnO			0.13	0.07	0.09		0.09
P_2O_5			0.14	0.12			0.17
No. of samples			12	16			

t: total Fe

Notes for Table 2-2 Average greywacke compositions throughout geological time

1. Pettijohn (1963): average arkose
2. Pettijohn (1963): average greywacke
3. Middleton (1960): average eugeosynclinal sandstone
4. Whetten et al. (1969): average Columbia River sand, excluding the Grand Coulee reservoir
5. Vine and Tourtelot (1973): average Lower Eocene sandstone, Rocky Mountain region, U.S.A.
6. Reed (1957): average lower Mesozoic greywacke, New Zealand (from Condie et al., 1970)
7. Bailey et al. (1964): average Franciscan greywacke, Jurassic (from Condie et al., 1970)
8. Mattiat (1960): average Harz Mountain greywacke, Paleozoic (from Condie et al., 1970)
9. Ondrick and Griffiths (1969): average Rensselaer greywacke, Paleozoic (from Condie et al., 1970)
10. Pettijohn (1963): average Precambrian greywacke
11. Goodwin (1972): average Archean greywacke from the Superior Province
12. Goodwin (1976a): average metasediment from Wabigoon granite-greenstone belt
13. Goodwin (1976a): average metasediment, Shebandowan granite-greenstone belt
14. Eade and Fahrig (1971): average composition, Canadian Shield

Table 2-3 Chemical analyses for greywackes derived from felsic rocks

	1	2	3a	3b	4a	4b	4c	5
SiO_2	67.50	64.43	66.07	63.66	63.41	65.62	66.78	65.9
TiO_2	0.52	0.62	0.64	0.57	0.66	0.66	0.62	0.7
Al_2O_3	14.50	15.48	15.24	14.85	15.19	16.68	15.72	15.3
FeO			4.52	4.67				4.7
Fe_2O_3	5.29[t]	6.45[t]	0.70	1.01	7.29[t]	6.75[t]	6.14[t]	1.2
MgO	2.77	3.12	2.73	2.99	2.94	2.73	2.42	2.8
CaO	3.30	2.22	1.70	2.63	3.62	1.32	2.38	1.5
K_2O	1.75	2.44	1.91	2.30	2.30	2.66	1.88	2.0
Na_2O	4.11	3.74	3.10	3.14	4.28	3.37	3.84	2.9
MnO	0.08	0.07	0.06	0.11	0.09	0.07	0.08	0.1
P_2O_5	0.12		0.12	0.14	0.19	0.12	0.12	
No. of samples	32	23	3	20	5	7	5	4

	6	7	8	9	10	11	12	13
SiO_2	62.40	67.80	64.57	66.20	59.80	69.03	72.20	66.2
TiO_2	0.50	0.25	0.48	0.52	0.55	0.54	0.49	0.7
Al_2O_3	15.20	17.40	12.76	10.20	12.90	14.05	9.60	14.4
FeO	4.61	1.30				3.56		
Fe_2O_3	0.57	0.20	8.01[t]	7.01[t]	6.56[t]	1.78	3.06[t]	3.3[t]
MgO	3.52	0.50	2.69	4.50	4.44	3.25		2.1
CaO	4.59	2.20	1.18	1.97	3.18	0.62	4.92	3.5
K_2O	2.57	2.10	1.95	1.58	2.23	1.51	1.41	2.1
Na_2O	2.68	6.00	1.65	1.80	2.83	5.07	1.66	3.5
MnO		0.02	0.02	0.10	0.09	0.05	0.04	0.1
P_2O_5		0.09	0.05					
No. of samples	1	1	1	17	7	7	7	12

t:

Notes for Table 2-3 Some chemical analyses for greywackes derived from felsic rocks

1. Average of 32 metagreywackes analyzed in this study from Upper Manitou Lake, Kirkland Lake, and Kakagi Lake; predominantly of felsic metavolcanic origin; normalized anhydrous to 100%

2. Condie (1967): Early Precambrian greywackes from Wyoming; source area of quartz-rich metasedimentary rocks and lesser amounts of granitic material; minor mafic component

3a. Henderson (1975): Archean greywackes of the Burwash Formation, Slave Province; derived mostly from silicic volcanics and some granodiorite

3b. Henderson (1975): average Archean greywacke of the Slave Province

4. Peeling (1974): as described in 3a, but further subdivided: 4a. Lower Burwash Formation, basic to intermediate volcanic source plus granitic debris; 4b. Middle Burwash Formation, intermediate to felsic volcanic debris and increasing abundance of granitic material; 4c. Upper Burwash Formation, abundant granitic debris plus acid to intermediate volcanics

5. Ramsay (1973): as in 3a, but from the Prosperous Lake area, Northwest Territories

6. Ojakangas (1972): Archean Vermilion District greywackes analyzed by Grout (1933); composed mostly of felsic volcanic debris plus minor granitic material

7. Donaldson and Jackson (1965): Archean North Spirit Lake area, northwestern Ontario; arkose derived from pre-existing sedimentary and granitic rocks

8. Nance and Taylor (1977): Archean greywacke from the Kalgoorlie area, Western Australia; contains abundant felsic porphyry clasts

9. Condie et al. (1970): Archean greywackes of the Fig Tree Group, South Africa, Sheba Formation; dominantly granitic source area, but some mafic and ultramafic contribution

Notes for Table 2-3/continued

10. Condie et al. (1970): as in 9, but for the overlying Belvue Road Formation; contains larger percentage of granitic rock fragments than the Sheba Formation

11. Young (1969): Early Proterozoic tillite matrix, Bruce Mines - Blind River area, Ontario; primarily granodioritic source area

12. Condie and Snansieng (1971): Ordovician Duzel Formation greywackes, Northern California; derived from a dominantly plutonic-metamorphic source area

13. Whetten et al. (1969): Upper Columbia River sediment; derived largely from plutonic and metasedimentary rocks of granodioritic composition

Table 2-4 Some chemical analyses for greywackes derived from mafic rocks

	1	2	3a	3b	3c	4a	4b	5	6	7	8
SiO_2	61.86	62.43	64.4	52.8	57.7	54.63	54.89	67.4	62.3	54.63	53.30
TiO_2	0.40	0.65	0.62	1.14	0.82	1.11	1.15	0.8	1.1	1.11	0.84
Al_2O_3	14.61	15.27	13.1	15.1	13.7	15.69	15.62	13.6	14.9	15.69	18.33
FeO		3.83				7.30				7.30	2.36
Fe_2O_3	5.08[t]	2.38	10.68[t]	10.30[t]	8.32[t]	1.65	10.05[t]	5.1[t]	4.6[t]	1.65	2.41
MgO	3.58	3.82				3.70	3.82	2.0	2.1	3.70	2.62
CaO	5.74	2.15	1.56	4.81	3.05	5.01	5.29	3.3	3.7	5.01	5.88
K_2O	1.90	1.77	0.34	0.92	1.65	0.66	0.71	2.1	2.3	0.66	1.72
Na_2O	4.10	4.07	2.36	4.13	2.79	4.79	4.90	2.9	2.9	4.79	2.18
MnO	0.17	0.08	0.20	0.13	0.15	0.16	0.17	0.1	0.3	0.16	0.08
P_2O_5	0.50	0.18				0.23	0.22			0.23	0.28
No. of samples	10	9	2	4	3	10	7	47	9	1	1

t: total Fe

Notes for Table 2-4 Some chemical analyses for greywackes derived from mafic rocks

1. Naqvi and Hussain (1972): Archean Chitaldrug greywackes, India; derived from basic volcanic rocks with minor contribution of metasedimentary and granitic material

2. Young (1969): Early Proterozoic tillite matrix from the Cobalt-Gowganda area, Ontario; composed of volcanic and volcaniclastic Archean rocks, with a significant contribution of mafic volcanic rocks

3. Condie and Snansieng (1971): Silurian greywackes from the Gazelle Formation, Northern California: 3a - dominated by andesitic volcanics but diluted by quartz; 3b - dominated by andesitic volcanics, but also contains plutonic and metamorphic detritus of granodioritic composition; 3c - as in 3b but with a larger proportion of plutonic debris

4a. Chappell (1968): Upper Devonian greywackes from New South Wales; dominated by mafic volcanic debris

4b. Nance and Taylor (1977): as in 4a

5. Whetten et al. (1969): Lower Columbia River sediment; abundant andesitic detritus, progressively increasing in abundance downstream; some non-volcanic material included

6. Whetten et al. (1969): Snake River-Ice Harbour sediment; 50% andesite and 50% sedimentary and metamorphic rocks in the source area

7. Coombs (1954): Mesozoic albitic tuffaceous greywacke of mafic volcanic origin

8. Edwards (1950): Mesozoic Napere greywacke, Aure Trough, Papua; dominantly of andesitic origin.

measured as samples from, firstly, the Kakagi Lake area, then the Upper Manitou Lake area, and finally the Kirkland Lake area were considered.

Enrichments in Fe, Mg, Ti and Mn (Mn not shown in Figure 2-9) suggest a more mafic provenance, and this is borne out by the literature survey of greywacke compositions summarized in Tables 2-3 and 2-4. In keeping with the petrographic data of Kwong (1975), Teal (pers. comm.) and Hyde (pers. comm.), the chemical data therefore suggest that the Kakagi Lake suite is composed almost entirely of felsic debris, that the Upper Manitou Lake clastic metasedimentary rocks contain at least some component of mafic material, and that the Kirkland Lake rocks contain the largest component of mafic material observed in this study. Nevertheless, all of these metagreywackes have major and minor element compositions that most closely resemble other greywackes of dominantly felsic origin (Figure 2-8; Table 2-3).

The relative contributions of mafic and felsic source rocks to the Kakagi Lake, Upper Manitou Lake and Kirkland Lake metasediments can be inferred from AFM diagrams (Figure 2-10). The metasedimentary rock analyses for the Kakagi Lake area lie within the field of spatially related felsic metavolcanic rocks, which have been analyzed by Smith et al. (1973), Wolff (1977), and Kwong (1975). The more magnesium-rich clastic metasedimentary rocks of the Upper Manitou Lake area also have

FIGURE 2-9 Major and minor element variations observed for the Archean clastic metasedimentary rocks analyzed during this study (range and mean).

1. Kakagi Lake area (13 samples)
2. Upper Manitou Lake area (12 samples)
3. Kirkland Lake area (8 samples)

According to the "Students T test" for 95% confidence limits, there are significant differences between the Al_2O_3, MgO, and TiO_2 distributions for each of the three areas. There are no significant differences between 1, 2, and 3 for SiO_2, or between 2 and 3 for $Fe_2O_3{}^t$.

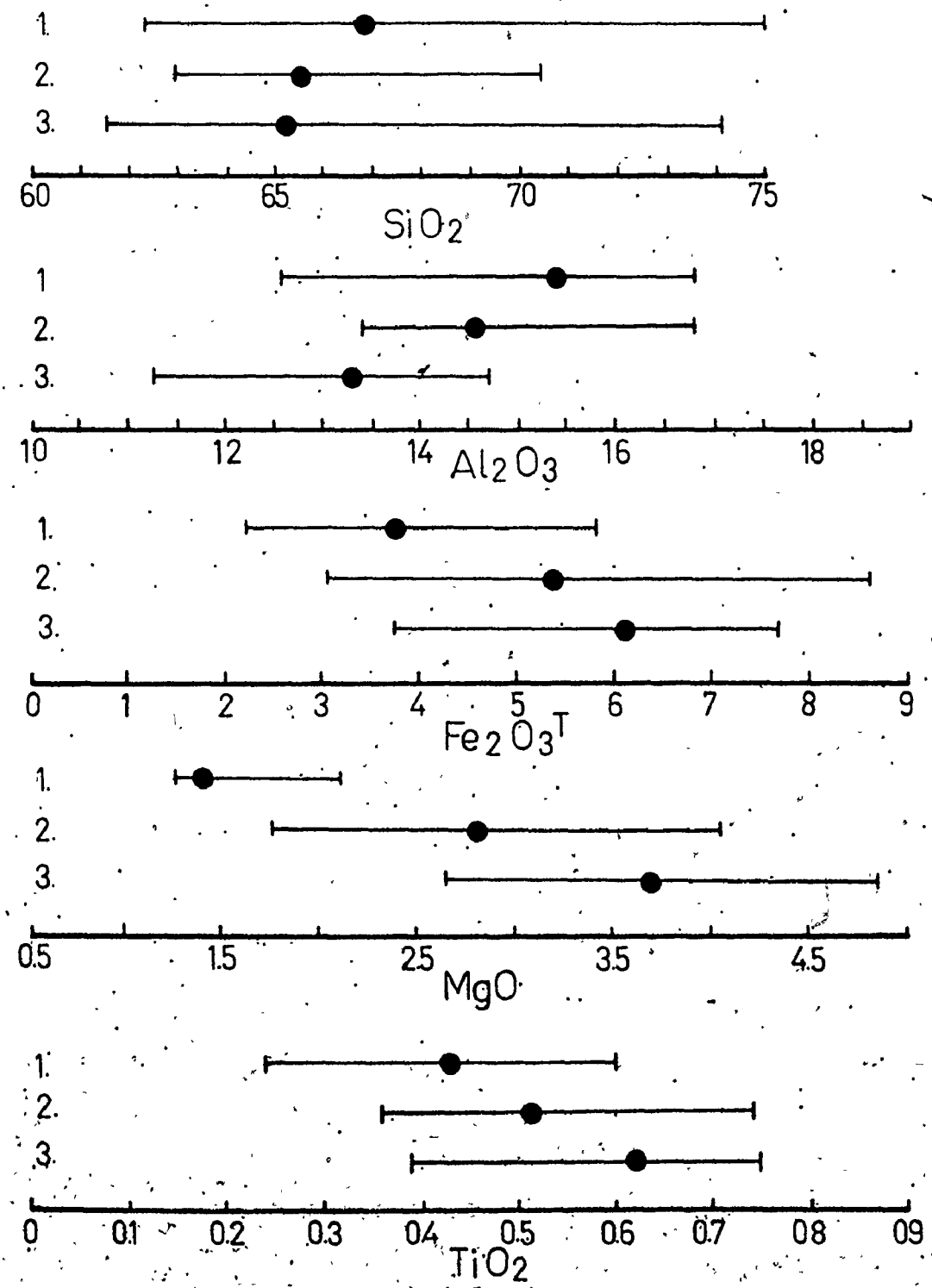

all oxides in wt.%

FIGURE 2-10 AFM diagram for metagreywackes analyzed during this study.

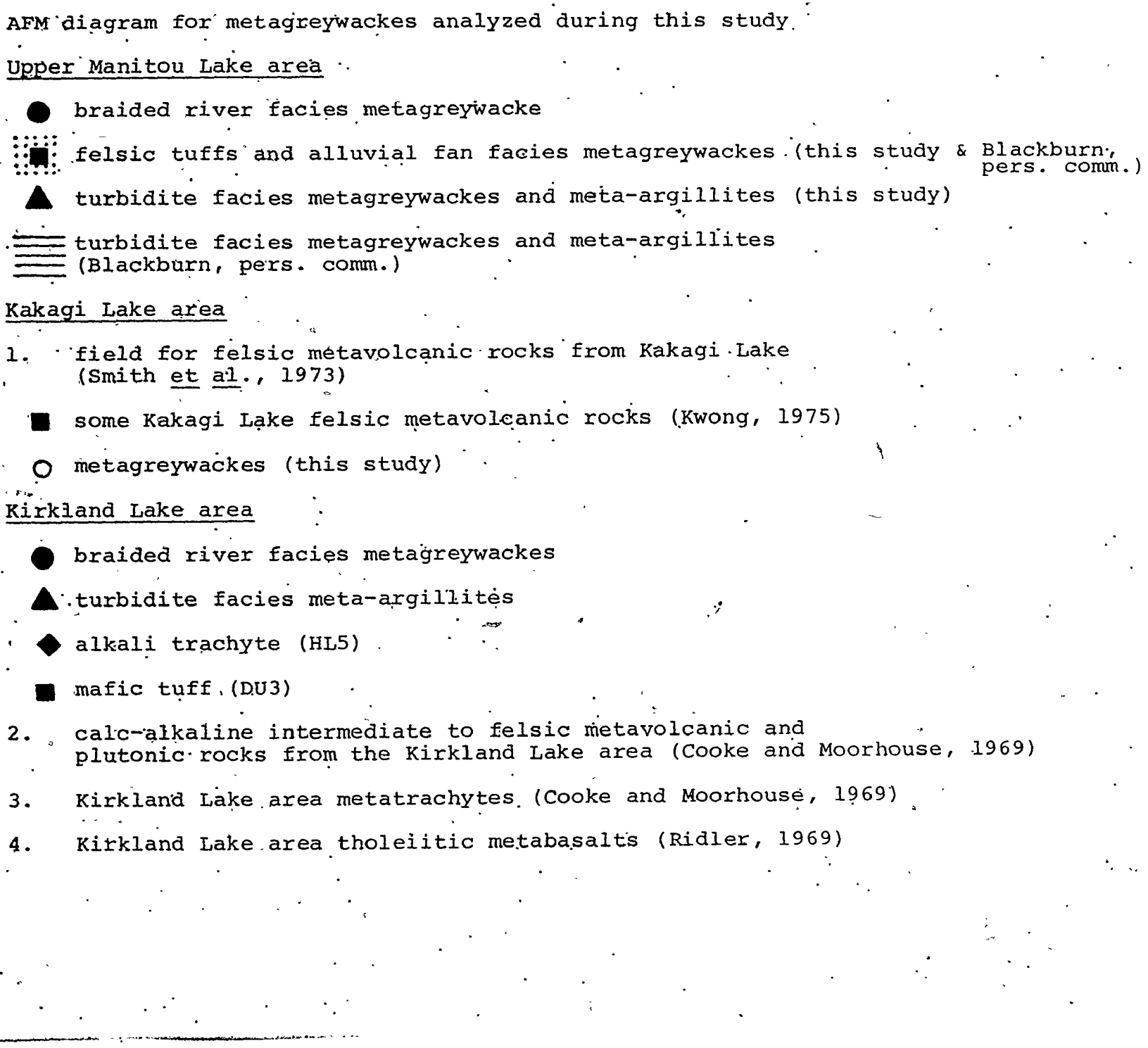

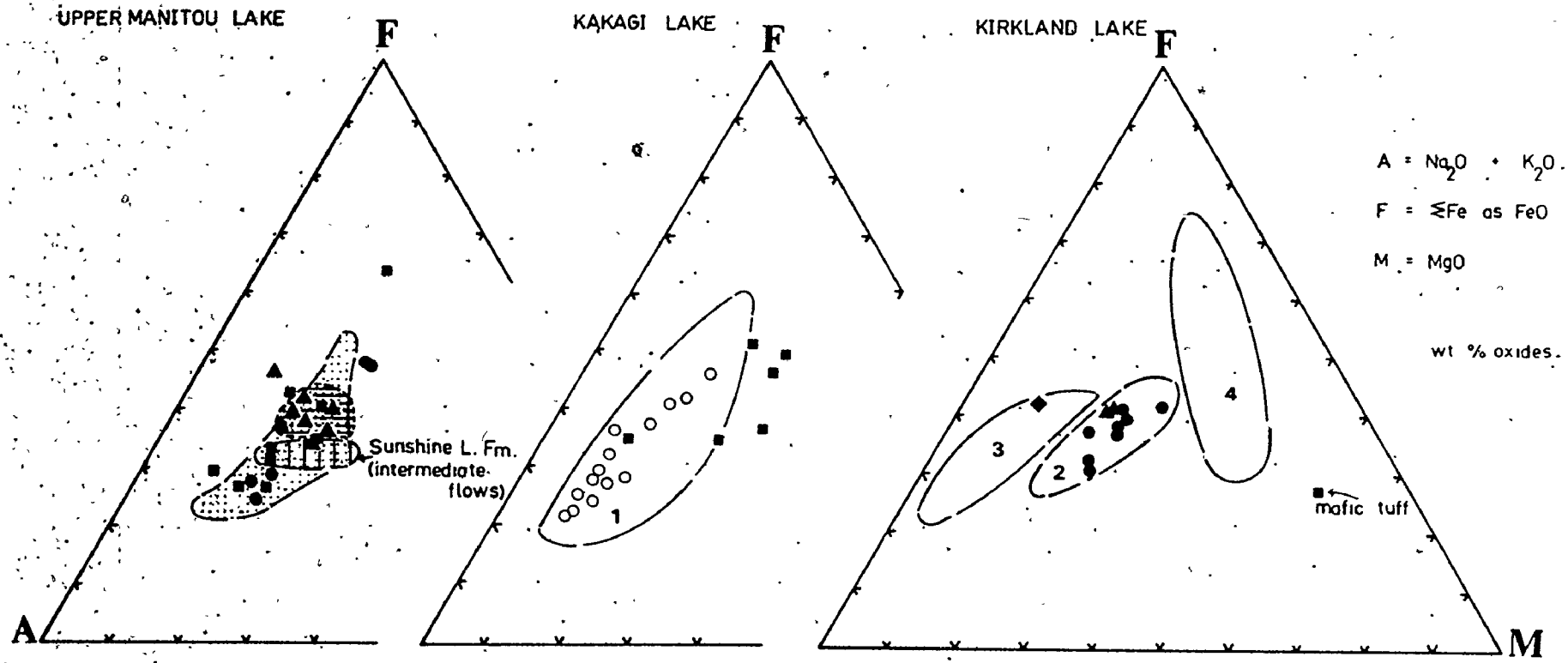
UPPER MANITOU LAKE
F
A
Sunshine L. Fm.
(intermediate
flows)
KAKAGI LAKE
F
1
KIRKLAND LAKE
F
M
3
2
4
mafic tuff
A = Na2O + K2O.
F = ΣFe as FeO
M = MgO
wt % oxides.

chemical compositions which coincide with those of the underlying and/or laterally equivalent felsic to intermediate metavolcanic rocks, some of which have been analyzed by Blackburn (1976b).

Figure 2-11 illustrates, in a somewhat different manner, how some of the chemical characteristics of the Upper Manitou Lake clastic metasedimentary rocks can be achieved by mixing various amounts of Cane Lake, Uphill Lake and Sunshine Lake metavolcanic rocks. The Mosher Bay turbidite facies metasandstones, however, have somewhat higher SiO_2 contents than expected for their FeO^t + MgO content. Enrichment in quartz and feldspar, as the result of winnowing during sediment recycling (these rocks are chemically mature; Figure 2-7a), as well as some change in provenance, are probably responsible for the high silica content. As the free quartz content in the metagreywackes increases, Rb, Sr, Ba and Ce contents decrease (Figure 2-12). If the increase in quartz content was alone due to the addition of granitic detritus, one might expect Rb, Sr, Ba and Ce contents to increase, as granitic rocks are enriched in most of these elements. However, if such plutonic detritus underwent abrasion and winnowing of fines during transport (during repeated recycling), the feldspar would be diminished in size and amount relative to the quartz, and the feldspar/quartz ratio of the sand-sized fraction reduced.

Choices of source rocks for the Kirkland Lake metagreywackes are more numerous. Three igneous fields are shown

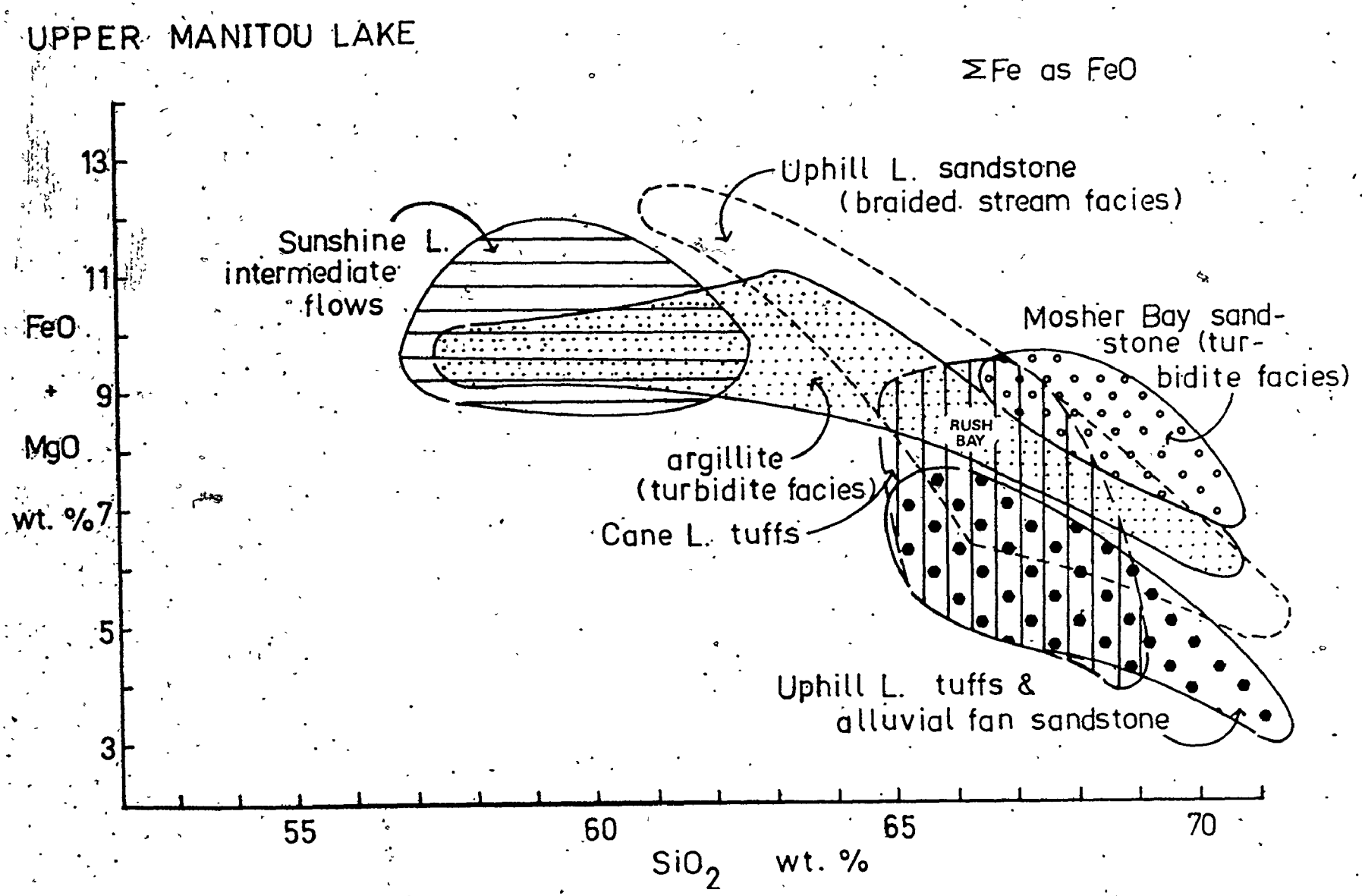

FIGURE 2-11 SiO_2 versus FeO+MgO for the metavolcanic and clastic metasedimentary rocks from the Upper Manitou Lake area. Total Fe expressed as FeO

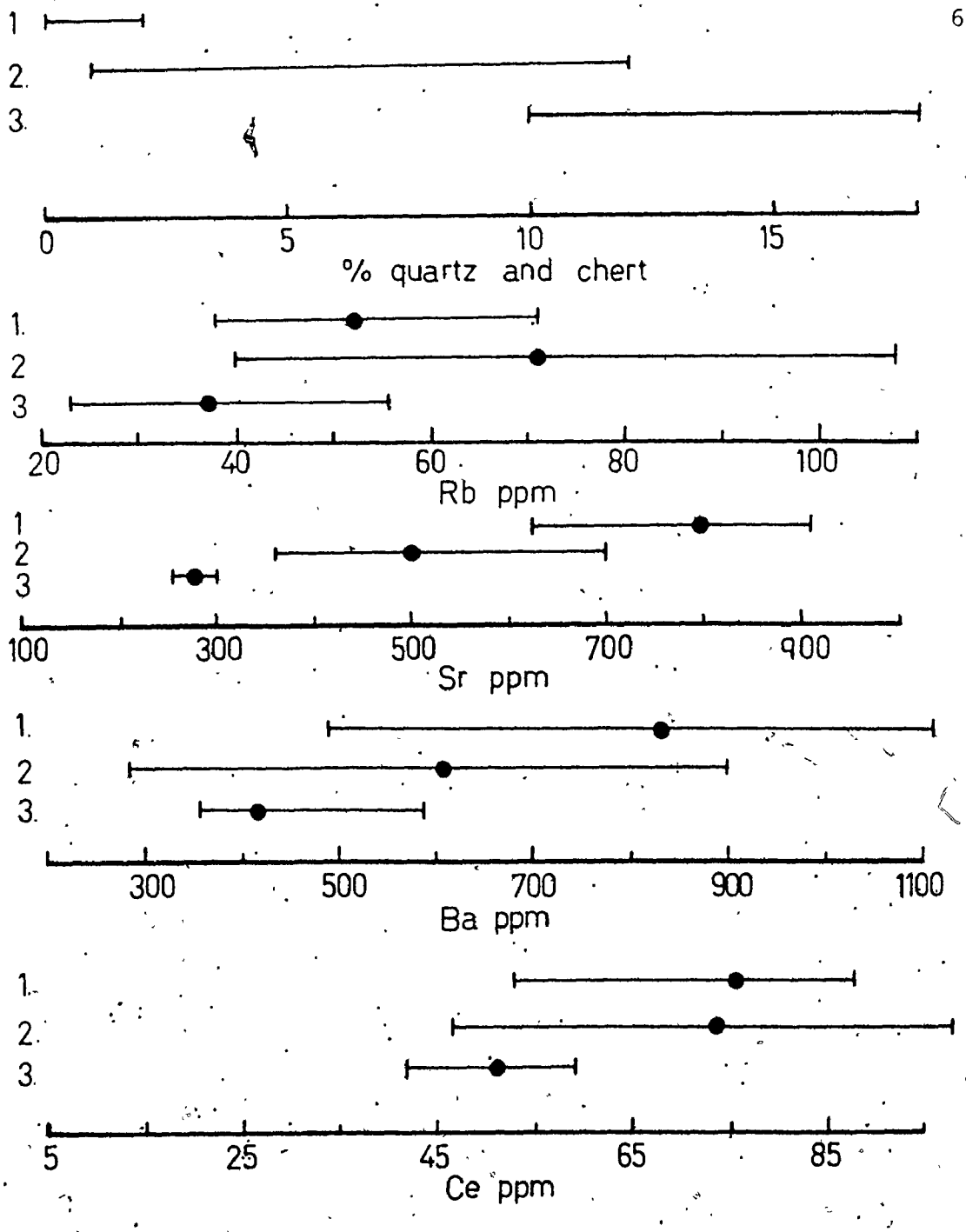

FIGURE 2-12 Trace element and modal quartz + chert variations observed for the Upper Manitou Lake metagreywackes (range and mean)

1. Alluvial fan facies (3 samples)
2. Braided river facies (4 samples)
3. Turbidite facies (5 samples)

Quartz + chert data from Teal (private comm., 1977)

(Figure 2-10); the tholeiitic metabasalts are the oldest meta-volcanic rocks in the area (Ridler, 1969); the calc-alkaline rocks, including dacite, andesite, porphyries and plutonic rocks (Cooke and Moorhouse, 1969), are generally younger than the tholeiites; the metatrachytes are the youngest meta-igneous rocks of consequence, and are roughly contemporaneous with the Timiskaming sedimentation (Cooke and Moorhouse, 1969). The chemical overlap of the metagreywacke field and the calc-alkaline field suggests that much of the detritus may have come from this group of meta-igneous rocks. Since the calc-alkaline suite stratigraphically overlies most of the metabasalts, it would undoubtedly have a much larger probability of being eroded.

Hyde (pers. comm.) suggested that some Timiskaming meta-trachyte may have been incorporated into the metasedimentary rocks of the area. However the K_2O of the Kirkland Lake meta-greywackes ranges from 0.84-2.31 wt. % (mean of 1.47 wt. %), far lower than the metatrachytes (4-8 wt. %; see Appendix IV, sa. # HL5; see also Cooke and Moorhouse, 1969; Ridler, 1969). Even the meta-argillites, which can concentrate potassium relative to metasandstones only have K_2O contents of 3.2%. Other chemical data also permit only limited contribution of trachytic debris; Rb, Sr, Ba, Th, Ce, Zr and Y contents are 2 to 7 times lower in the metagreywackes than in the meta-trachyte (see Appendix IV for data).

Other chemical variation diagrams also illustrate the effects of somewhat differing provenances upon the geochemistry of greywackes. The antipathetic relationship between Ni and Rb (Figure 2-13) reflects the presence of more mafic material in the Kirkland Lake metagreywackes than in the other areas examined. Condie et al. (1970) attributed a similar relationship found for the Archean Sheba Formation to the incorporation of small quantities of ultramafic debris. Komatiitic metavolcanic rocks are present in the Kirkland Lake area, and ultramafic clasts have been identified in the Timiskaming metasedimentary rocks (Hyde and Walker, 1977).

Other variation diagrams such as K/Rb versus K (Figure 2-14a) and Ca/Sr versus Ca (Figure 2-14b) confirm that the clastic metasedimentary rocks, including some chemically mature samples, more closely resemble felsic rather than mafic source rocks. Some samples, however, (especially the meta-argillites) do have lower Ca/Sr ratios than observed in felsic igneous rocks. This may result from the preferential loss of Ca during weathering (Cameron and Baumann, 1972), or some diagenetic effect (section II-7).

Th geochemistry in greywackes

Studies of U, Th, and K in greywackes (Rogers, 1966; Rogers et al., 1969; Rogers and Donnelly, 1966; Rogers and

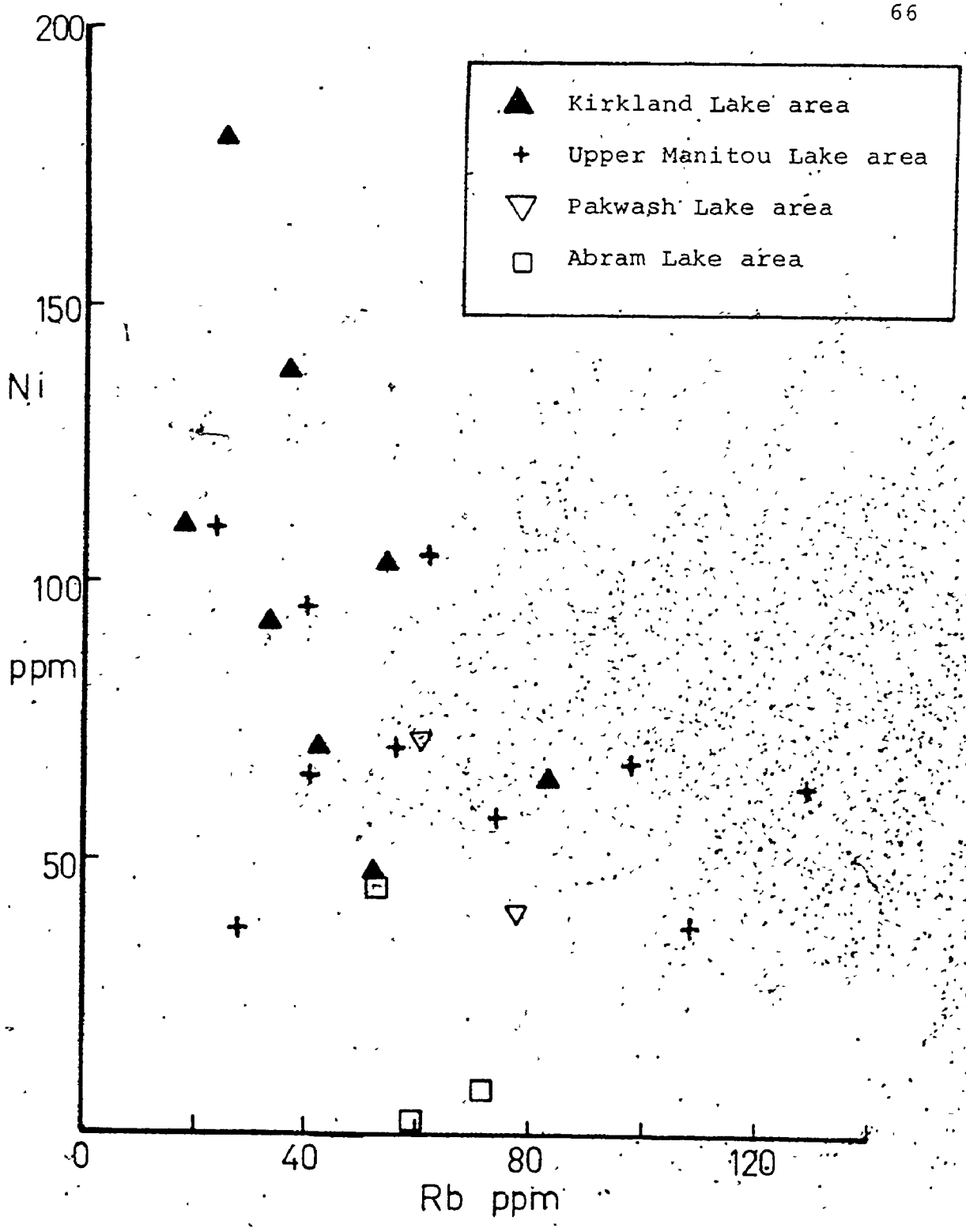

FIGURE 2-13 Ni.versus Rb diagram for the Archean clastic metasedimentary rocks analyzed during this study

FIGURE 2-14a K/Rb versus K diagram for the Archean clastic metasedimentary rocks analyzed during this study. Igneous rock fields from Condie et al. (1970)

Metagreywackes

X Kakagi Lake area

▲ Kirkland Lake area

\+ Upper Manitou Lake area

□ Abram Lake area

▽ Pakwash Lake area

● meta-argillites from all areas

FIGURE 2-14b Ca/Sr versus Ca diagram for the Archean clastic metasedimentary rocks analyzed during this study.

Note the low Ca/Sr ratio with respect to their Ca content of those samples which do not lie within the fields shown for igneous rocks (as taken from Condie et al., 1970). Symbols as in Figure 2-14a.

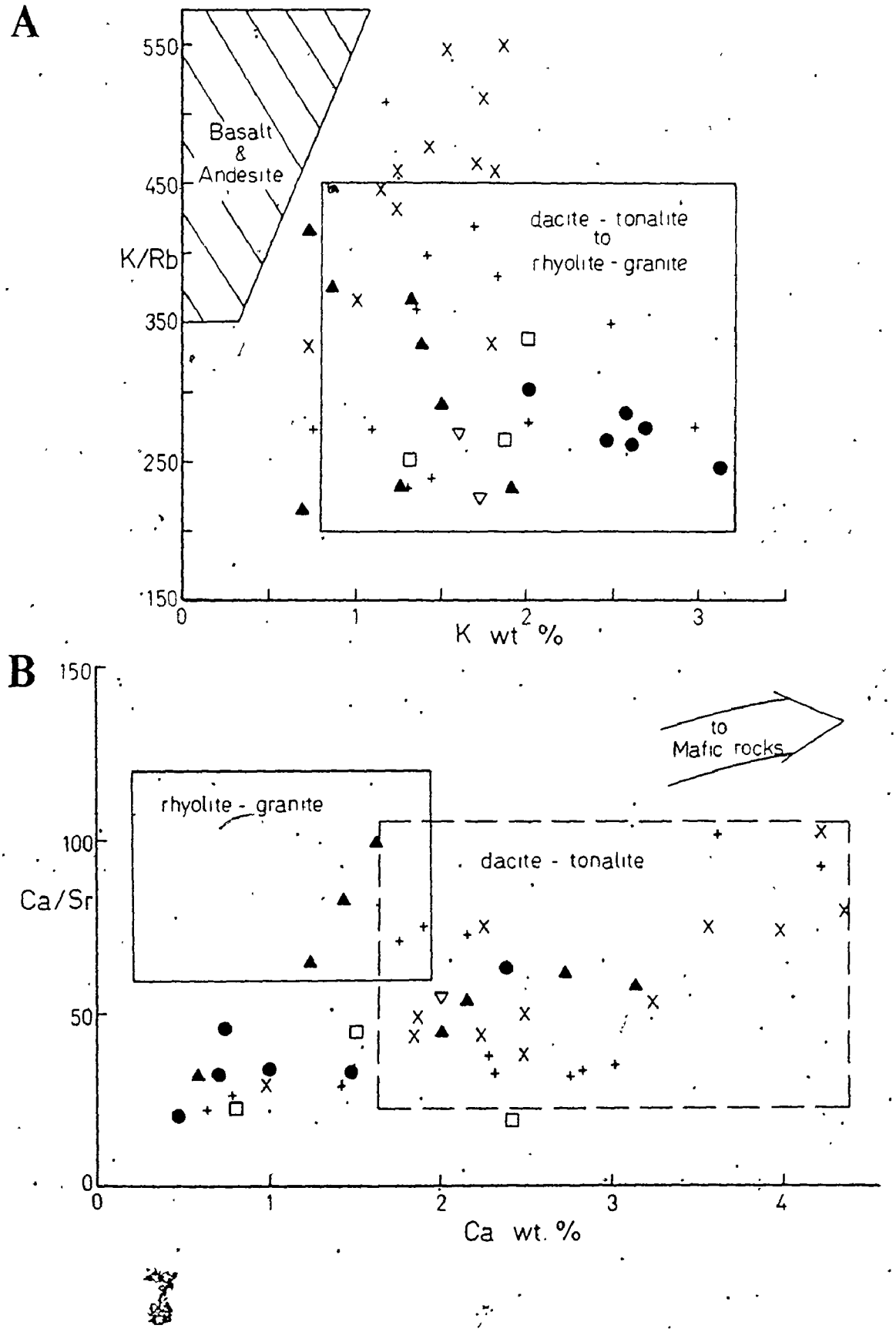
A
550
450
350
250
150
K/Rb
Basalt
&
Andesite
dacite - tonalite
to
rhyolite - granite
0
1
2
3
K wt %
B
150
100
50
0
Ca/Sr
to
Mafic rocks
rhyolite - granite
dacite - tonalite
0
1
2
3
4
Ca wt. %

Richardson, 1964; Wollenberg et al., 1967) showed that low concentrations of these elements occurred in greywackes formed from mafic detritus (Table 2-5; Umpqua, Caribbean and New South Wales examples); higher U, Th, and K abundances were found for clastic rocks derived from more felsic source rocks (Tyee and Franciscan examples; see Table 2-5). Very quartz-rich sandstones, however, were particularly low in Th, in spite of their felsic provenance (the Knife Lake lithic quartz-wackes, for example); the high content of quartz effectively diluted the Th content of the rock.

The observed Th values for the Upper Manitou Lake and Pakwash Lake clastic metasedimentary rocks range from 8-14 ppm, and vary little with grain size (Table 2-5). As in the Wyoming metagreywackes, these Th contents probably reflect a felsic provenance. Th results obtained for the Kirkland Lake metagreywackes are significantly lower (4-9 ppm). As the quartz content of the Kirkland Lake metagreywackes is similar to that of the Mosher Bay turbidite facies metagreywackes (which are about 4 ppm richer in Th), the slightly more mafic nature of the Kirkland Lake metagreywackes, already indicated by other data, is the probable cause of the lower Th values in the Kirkland Lake samples.

Table 2-5 U, Th and K in greywackes

Locality	Ref.	Description of clastic rock and age	K wt%	U ppm	Th ppm
Umpqua Fm. Oregon	1	greywacke: quartz, plagioclase, basic volcanic rock fragments and some quartz diorite fragments; clay and carbonate matrix (Tertiary)	0.96	1.3	2.8
Tyee Fm. Oregon	1	greywacke: quartz, plagioclase, biotite and quartz diorite fragments; clay matrix (Tertiary)	2.0	2.6	9.3
Caribbean	2	greywacke: quartz, plagioclase, basic rock fragments (Cretaceous to Tertiary)		0.5→1	1→2
California (Franciscan)	3	greywacke: quartz, plagioclase, felsic rock fragments (Tertiary)	1.3	2.0	7.0
New South Wales	4	greywacke: plagioclase, mafic rock fragments, chlorite matrix (Devonian)	0.59	0.45	1.2
Kalgoorlie	4	greywacke: quartz, plagioclase, abundant felsic porphyry clasts, chlorite matrix; abundant mafic clasts as well (Archean)	3.2	0.97	4.1
Wyoming	5	greywacke: quartz, biotite, plagioclase, no recognizable volcanic rock fragments (Archean)	1.9	1.6	9.1
Minnesota	5	(i) sandy and silty shales	2.3	1.7	8.2
		(ii) argillaceous quartz wackes; quartz, plagioclase, felsic rock fragments; clay matrix	1.2	1.8	8.7
		(iii) argillaceous sandstones	2.1	0.7	3.8
		(iv) lithic quartz wackes (Archean)	1.7	0.4	1.5

Table 2-5/continued

Locality	Ref.	Description of clastic rock and age	K wt%	U ppm	Th ppm
THIS STUDY					
Kirkland Lake		(i) metagreywacke	1.2	t	6
		(ii) meta-argillite	2.7	N.D.	N.D.
Abram Lake		metagreywacke and meta-arkose	1.7	t	6
Pakwash Lake		greywacke	1.7	t	11
Upper Manitou Lake		(i) alluvial fan facies metagreywacke	2.7	t	11
		(ii) braided river facies metagreywacke	1.9	t	12
		(iii) turbidite facies - metagreywacke	1.1	t	10
		- meta-argillite	2.6	t	10
Kakagi Lake		(i) metagreywacke	1.5	N.D.	N.D.
		(ii) meta-argillite	2.6	N.D.	N.D.

N.D.: not determined; t: trace

References

1. Rogers and Richardson (1964)
2. Rogers and Donnelly (1966)
3. Wollenberg et al., (1967)
4. Nance and Taylor (1977)
5. Rogers et al. (1969)

Summary, and a note of caution

The results presented in this section show that the geochemistry of the analyzed metagreywackes is useful in provenance determinations. However, it is important to remember that source rocks of similar petrographic and major element composition can vary considerably among themselves in their content of trace elements. For example, a comparison of Rb, Sr, Ba, Zr, and Y data for felsic metavolcanic rocks and associated metagreywackes from the Kakagi Lake and Upper Manitou Lake areas shows that Rb, Ba and Zr are markedly higher in the slightly more mafic metagreywackes of the Upper Manitou Lake area than they are in the Kakagi Lake clastic metasedimentary rocks (Table 2-6). However, the Rb, Ba and Zr contents of the felsic metavolcanic rocks from the Upper Manitou Lake area are correspondingly enriched in these elements relative to their Kakagi Lake analogues.

Table 2-6 Trace element comparison: Kakagi Lake and Upper Manitou Lake areas

	Kakagi Lake		Upper Manitou Lake	
	felsic metavolcanics*	meta-greywacke	felsic metavolcanics	meta-greywacke
Rb ppm	35	32	67	52
Sr	612	465	608	483
Ba	500	389	837	632
Y	8	7	12	11
Zr	110	97	139	136

*Kakagi Lake felsic metavolcanic analyses from Wolff (1977)

Chemical modification during sedimentary processes

Some of the chemical changes caused by sedimentary processes during the formation of the analyzed Archean clastic metasedimentary rocks are discussed in this section.

Al/Fe and Si

The variation in these elements and their relationship to sediment maturity have been discussed in section II-4; a brief summary is repeated here for the sake of completeness. The turbidite facies clastic metasedimentary rocks of the Upper Manitou Lake area and the fluvial metagreywackes of the Kirkland Lake area have Al/Fe ratios within the range of chemically mature clastic sediments (Dennen and Moore, 1971); the interaction of sedimentary processes that results in Al/Fe of 1.9±0.4 are not understood. The accompanying variation in Si between fine grained and coarser grained clastic metasedimentary rocks can, however, be attributed to hydraulic sorting during transport.

Na_2O, K_2O and Na_2O/K_2O

High Na_2O and Na_2O/K_2O ratios are characteristic of greywackes and those analyzed in this study are no exception (Figure 2-15) (Bastin, 1909; Engel and Engel, 1953; Pettijohn and Bastron, 1959; Middleton, 1960, 1972; Rogers, 1966; Condie, 1967; Young, 1969; Pettijohn et al., 1973). In fact, some of

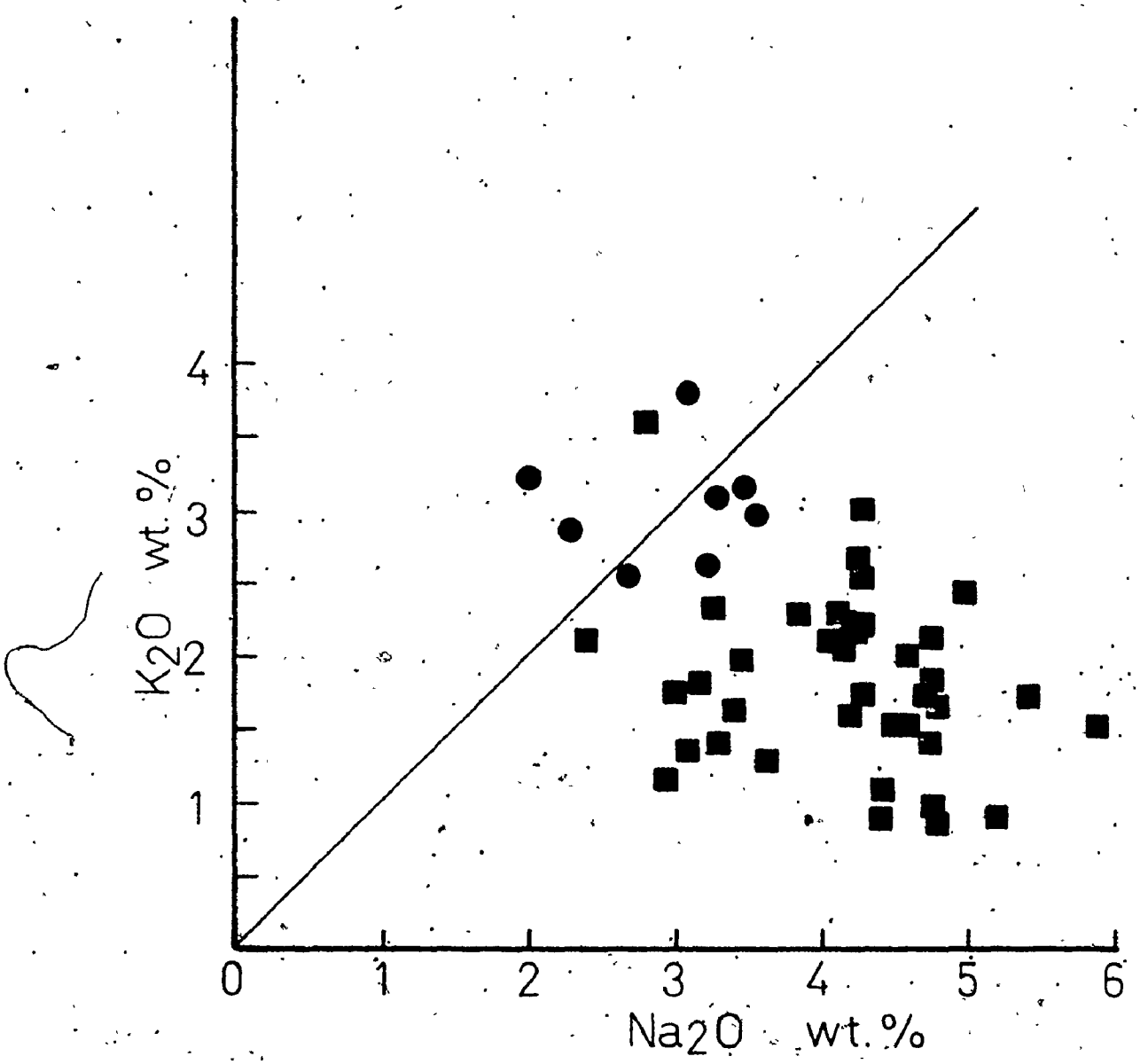

FIGURE 2-15 K_2O versus Na_2O diagram for the Archean clastic metasedimentary rocks analyzed during this study.

■ metagreywacke

● meta-argillite

the metagreywackes analyzed have Na_2O contents in excess of those which can be reasonably attributed to likely provenance rock types (Figure 2-16). The finer grained meta-argillites, on the other hand, are enriched in K_2O relative to the metagreywackes, and have K_2O/Na_2O near to or greater than unity (Figure 2-15). They also cluster within or near the fields of granite and granodiorite (Figure 2-16), whereas tonalite is a much more likely source rock.

The high Na content of greywacke reflects the abundance of albitic plagioclase (Blatt et al., 1972). However, opinions on its origin differ. One group suggests that the high Na contents reflect the abundance of Na-rich volcanic detritus in greywackes (Rogers, 1966; Pettijohn et al., 1973). Other investigators, however, invoke sodium metasomatism, largely involving plagioclase. Coombs et al. (1959) suggested that the reaction of calcic plagioclase during diagenesis and zeolite facies metamorphism yielded calcite, zeolites and sodic plagioclase. Garrels et al. (1971) indicated that the high K_2O/Na_2O of shales interlayered with the greywackes resulted from the growth of illite, which involved Na transfer from the shales to the sandstones and the complementary migration of K in the opposite direction. Gluskoter (1964) concluded that the absence of potassium feldspar in Franciscan greywackes resulted from post-depositional solution. Middleton (1972) proposed that much of the untwinned sodic plagioclase present in the Charney

FIGURE 2-16 Na_2O-CaO-K_2O diagram for the Archean clastic metasedimentary rocks analyzed during this study.

Note the relative Na_2O enrichment of some of the metasedimentary rocks relative to the fields shown for igneous rocks. Fields for igneous rocks from Condie (1967).

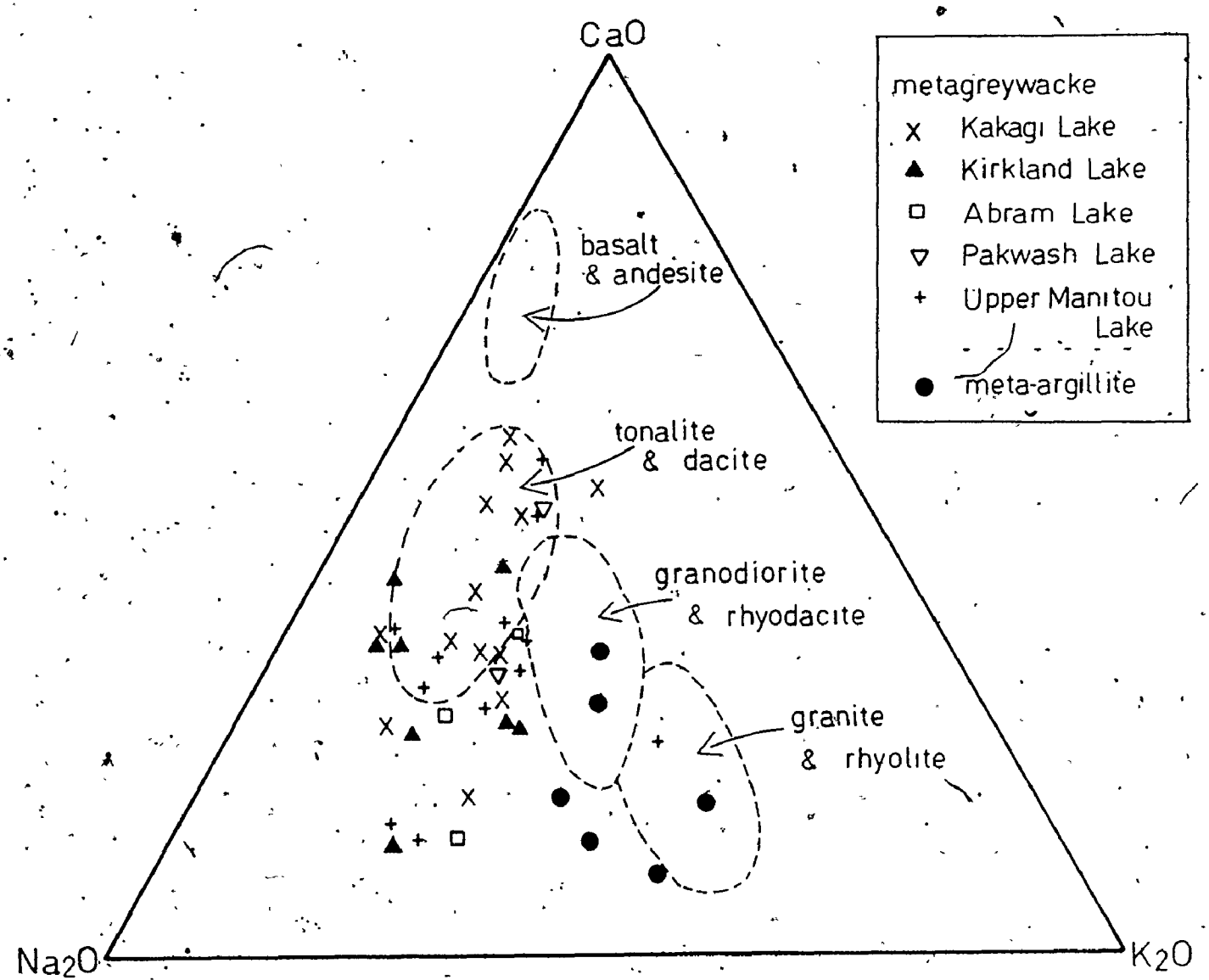
CaO
Na2O
K2O
basalt
& andesite
tonalite
& dacite
granodiorite
& rhyodacite
granite
& rhyolite
metagreywacke
Kakagi Lake
Kirkland Lake
Abram Lake
Pakwash Lake
Upper Manitou Lake
meta-argillite

Formation sandstones resulted from the diagenetic alteration of detrital perthite or potassium feldspar by seawater held in pores or argillaceous rocks. It is possible, therefore, that any or all of these processes may be responsible for at least part of the variation in Na_2O/K_2O observed in the analyzed samples.

CaO and Ca/Sr

Most of the analyzed meta-argillites contain less CaO than the coarser grained metagreywackes (Figure 2-14b; 2-16). CaO contents of the meta-argillites range from 0.8 to 3.3%, similar to that reported by Nanz (1953) and Cameron and Baumann (1972) for Archean and younger shales.

Most of the meta-argillites, as well as a few metasandstones, have Ca/Sr ratios that are lower than normal for their proposed provenance rock types (Figure 2-14b); this is a direct result of the low CaO contents mentioned above. Condie (1967) suggested that such behaviour resulted from the reaction of clastic plagioclase with Na^+ ions (derived from interstitial fluids or seawater) during diagenesis. According to his model, Ca^{+2} was preferentially released into solution during such a reaction.

At least for the fluvial metagreywackes analyzed in this study, the Na source cannot be seawater. Also, it is not clear why Sr^{2+} is not also removed into solution, unless its solubility is much lower than that of Ca^{2+} under such conditions.

The low Ca/Sr ratios of the analyzed meta-argillites are particularly difficult to explain, especially as other Archean meta-argillites are depleted in both Ca and Sr to equal extents (Reimer, 1972). Also Na, Ca, and Sr should enter solution during weathering of fine grained material more rapidly than for coarser grained detritus.

In summary, sedimentary processes have had an effect upon the Ca/Sr distributions in some of the analyzed clastic metasedimentary rocks, but the nature of the processes cannot be determined from the available data.

II-7 THE OXYGEN ISOTOPE GEOCHEMISTRY OF ARCHEAN CLASTIC METASEDIMENTARY ROCKS FROM NORTHERN ONTARIO

Introduction

The purpose of this section is to determine and then interpret the oxygen isotope geochemistry of Archean clastic metasedimentary rocks in terms of their provenance composition, sedimentary processes, and metamorphism. Much of the information presented here has been reported by Longstaffe and Schwarcz (1977).

Only a few oxygen isotope analyses of Archean clastic metasedimentary rocks have been previously published. Viswanathan (1974a,b) estimated (from quartz analyses) a range of 9.5-11.0°/₀₀

for five metasedimentary rocks from northeastern Minnesota. Shieh and Schwarcz (1977) report 9.2°/oo for an Archean clastic metasediment composite, prepared by Reilly and Shaw (1967) from 464 individual samples collected from the Superior Province of the Canadian shield in Ontario.

Results ($\delta^{18}O$ rock)

The $\delta^{18}O$ values of the clastic metasedimentary rocks and associated felsic metavolcanics analyzed in this study are given in Table 2-7 and shown in Figure 2-17. The metasedimentary rocks range in $\delta^{18}O$ from 8.0-13.3°/oo, (average 10.6°/oo), with the exception of sample L33 (Pakwash Lake), for which $\delta^{18}O$ = 5.2°/oo. This sample is located near a major shear zone and had probably been subjected to alteration subsequent to the regional metamorphism which affected the other rocks. Some aspects of this alteration are discussed below. The felsic metavolcanic rocks range from $\delta^{18}O$ = 7.5°/oo to 13.0°/oo, largely overlapping that of the metasedimentary rocks.

Interpretation

Clastic sedimentary rocks are usually derived from mixtures of detritus eroded from older plutonic, volcanic and sedimentary terranes fine-grained mineral components (chiefly clays) formed at low temperatures near the earth's surface, and, in many cases,

Table 2-7 Oxygen isotope whole rock results, metasedimentary and metavolcanic rocks

Locality[1]	$\delta^{18}O$ °/₀₀	Rock type[2]
ABRAM LAKE		
Ar12	10.34±0.07 (2)	arkosic sandstone
GW19	10.81	greywacke
AR30	9.24±0.13 (2)	greywacke
Ag27	11.90	argillite
Ag24	9.70	argillite
C18	11.02	granodiorite clast
C12	12.99	felsic tuff
Ar17	9.39	mafic tuff
UPPER MANITOU LAKE		
1. Cane Lake unit		
T25	8.47	felsic tuff
T10	8.79	felsic tuff breccia
OT17	9.45	felsic tuff
T214	10.58	felsic crystal tuff
T119	10.10	felsic tuff breccia
2. Uphill Lake unit		
OT21	8.29	felsic tuff
T9	8.03	alluvial fan: water laid tuff
OT4	7.96	alluvial fan: laminated siltstone
OT2	10.56±0.05 (2)	alluvial fan: bedded sandstone
T32	9.94	braided river: crossbedded litharenite
OT25	10.87	braided river: volcanogenic sandstone
T109	9.22±0.31	braided river: volcanogenic lithic sandstone
OT6	9.80	braided river: volcanogenic sandstone

Table 2-7 /continued

Locality[1]	$\delta^{18}O$ °/₀₀	Rock type[2]
3. Rush Bay sub unit		
T220	7.89	felsic tuff
T222	12.01	thinly bedded argillite
4. Mosher Bay unit		
OT5	10.90	turbidite facies: volcanic lithwacke
S2	10.71	turbidite facies: volcanic lithwacke
S5	11.64	turbidite facies: volcanic lithwacke
T42	12.79	turbidite facies: felspathic lithwacke
T152	11.55	turbidite facies: argillite
T38	10.78	turbidite facies: argillite
T104	11.19	turbidite facies: laminated argillite and siltstone
PAKWASH LAKE		
L30	8.63	laminated sandstone
L33	5.19	sheared sandstone matrix to conglomerate
KIRKLAND LAKE		
EL3	9.85	volcanic litharenite
RP4	11.90±0.28 (2)	volcanic litharenite
CH7	11.64	volcanic litharenite
LL8	9.57	volcanic litharenite
LS1	10.09	volcanic litharenite
CK2	10.74	volcanic litharenite
ME2	10.23	volcanic litharenite
IL3	10.06	volcanic litharenite

Table 2-7 /continued

Locality[1]	$\delta^{18}O$ °/₀₀	Rock type[2]
LL4	11.33	argillite
BC	10.49	argillite
DU3	9.01	mafic tuff (?)
LAKE DESPAIR		
F123	7.27	felsic metavolcanic, amphibolite facies
F124	8.88±0.10 (2)	felsic metavolcanic, amphibolite facies
F45	9.21	felsic metavolcanic, amphibolite facies
F119	9.37	felsic metavolcanic, amphibolite facies
424-2	9.42	felsic tuff
434-1	7.87	felsic tuff
G89	9.59	felsic tuff
B9	7.92	felsic tuff
B10	10.01	felsic tuff
B11	11.39	felsic tuff
B12	11.32	felsic tuff
KAKAGI LAKE		
JK4	9.98	tuffwacke
JK5	13.34	tuffwacke
JK6	11.02	tuffwacke
JK8	9.07	tuffwacke
JK28	9.58	tuffwacke
JK29A	12.87	tuffwacke
JK169	12.07	tuffwacke
JK173	11.06	tuffwacke
JK176	9.39	tuffwacke
JK178	10.88	tuffwacke

Table 2-7 /continued

Locality[1]	$\delta^{18}O$ °/₀₀	Rock type[2]
JK196	9.40	tuffwacke
JK252	8.70	tuffwacke
JK238	10.73	tuffwacke
JK76B	11.08	finely banded argillite

[1] The following persons kindly donated samples:

Abram Lake - C. Turner and D.M. Shaw;
Upper Manitou Lake - P.R. Teal;
Kirkland Lake - R.S. Hyde;
Kakagi Lake - Y-T. J. Kwong, J.H. Crocket;
Three samples from the Lake Despair area were provided by D. Birk.

[2] Donors' rock names are used; for the purposes of this discussion, all are considered as 'greywackes' as defined by Folk (1968), and indicated as sandstones on Figure 2-17.

FIGURE 2-17 Whole rock oxygen isotope results for the Archean clastic metasedimentary and felsic metavolcanic rocks analyzed during this study.

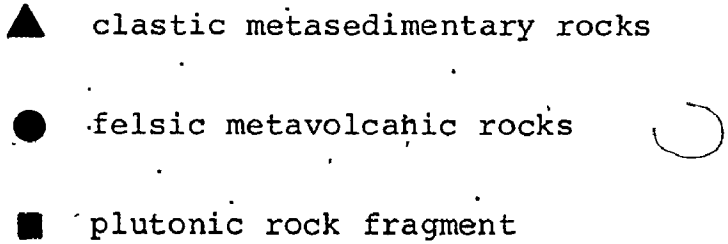

Lake Despair

felsic metavolcanics

high grade felsic metavolcanics

Abram Lake

metasandstone

meta-argillite

granodiorite clast

felsic metavolcanics

Upper Manitou Lake

felsic metavolcanics

metasandstone

meta-argillite

Kirkland Lake

metasandstone

meta-argillite

Kakagi Lake

metasandstone

meta-argillite

Pakwash Lake

metasandstone

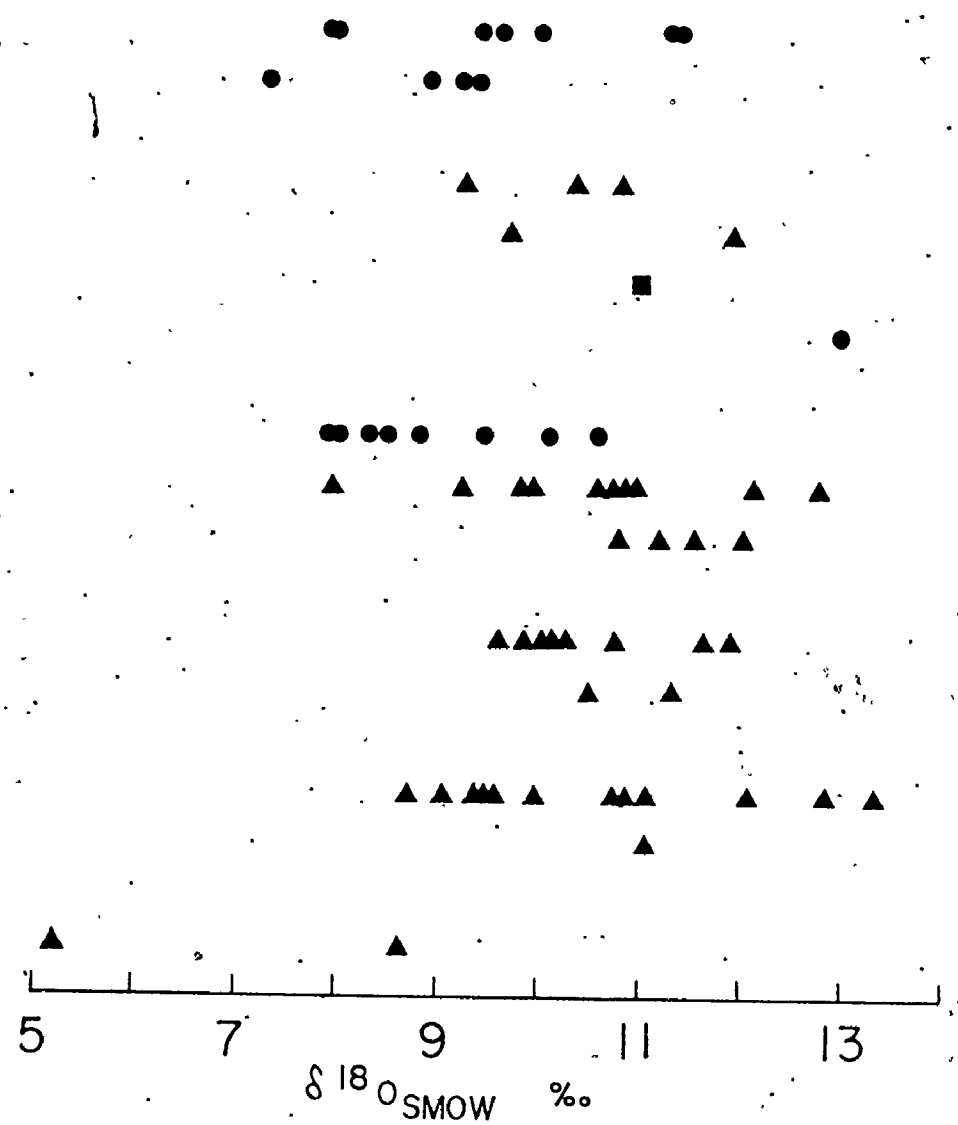

coarse-grained cement formed during early diagenesis. Consequently these rocks commonly have oxygen isotopic compositions intermediate between those of clay minerals (15-30°/$_{oo}$; Savin and Epstein, 1970) and igneous rocks (5-10°/$_{oo}$; Taylor, 1968). When metamorphosed to low and intermediate grades, the resulting metamorphic rocks usually retain the oxygen isotopic composition of the protolith sediments, although shifts towards slightly more ^{18}O-poor values have sometimes been observed (Garlick and Epstein, 1967; Eslinger and Savin, 1973).

Since the metasediments from our study are only slightly metamorphosed, it is unlikely that their bulk isotopic compositions markedly differ from those of their protoliths. However, the $\delta^{18}O$ values are lower than typical of geologically younger mixtures of sand, silt and clay sized detritus. For example, Magaritz and Taylor (1976a) reported somewhat higher values (10-15°/$_{oo}$) for Franciscan greywackes of similar metamorphic grade. Whole rock $\delta^{18}O$ values estimated from the compositions of separated quartz, potassium feldspar and biotite for low- and high-grade meta-arkoses of the French Valley Formation, Southern California fall in the range 13-15°/$_{oo}$ (Taylor and Epstein, 1962; Schwarcz, 1966).

The lower $\delta^{18}O$ of these Archean metasediments probably reflects the overall immaturity of the clastic material, as indicated by the high content of volcanic rock fragments, and by the chemical similarity to the nearby felsic metavolcanic

rocks from which they may have been largely derived.

Abram Lake area

The few samples analyzed from the Abram Lake area provide an insight into one possible relationship between the $\delta^{18}O$ of source rock and the derived sediment. Ament Bay Formation meta-arkose (Ar12) and meta-argillite (Ag27), as well as Daredevil Formation metagreywacke were largely derived from felsic metavolcanic and granodioritic source rocks (such unaltered source rocks have $\delta^{18}O$ = 7-9‰); these clastic metasedimentary rocks have $\delta^{18}O$ = 10.3-11.9‰. Metagreywacke (Ar30) and meta-argillite (Ag24), from the Little Vermilion Formation, contain much more mafic detritus than the other clastic metasedimentary rocks, and have lower $\delta^{18}O$ values (9.2-9.7‰), in keeping with the lower $\delta^{18}O$ values generally observed for unaltered mafic rocks (6‰).

Thus, the relative $\delta^{18}O$ values of these clastic metasedimentary rocks seem to reflect their different provenance. However, the processes involved in forming the actual $\delta^{18}O$ values are less clear. The $\delta^{18}O$ of felsic metavolcanic (C 12; 12.99‰) and mafic metavolcanic rocks (Ar17; 9.39‰) from the area imply that the sediments could have attained their present oxygen isotope compositions directly from the altered volcanic material, with little change in $\delta^{18}O$ during sedimentary processes. Further discussion, however, requires more data

than available for the Abram Lake area.

Upper Manitou Lake area

The detailed sedimentological data available for the Upper Manitou Lake area permitted a more detailed investigation of the isotopic variation between felsic metavolcanic rocks and related chemically immature and mature clastic metasedimentary rocks.

The oxygen isotopic compositions of rocks from the Upper Manitou Lake area are shown in Figure 2-18. A small but progressive enrichment in $\delta^{18}O$ from a mean of 8.0°/$_{oo}$ in the felsic pyroclastics of the Uphill Lake unit (including the Rush Bay sub-unit) to 10.0°/$_{oo}$ in the braided river facies to an average of 11.5°/$_{oo}$ in the turbidite facies can be observed.

The increasing $\delta^{18}O$ probably reflects the effects of the formation of clay minerals at low temperature, hydration and weathering of rock fragments, an increase in the abundance of detrital quartz, and low temperature overgrowth of silica on detrital quartz grains. Small amounts of chert in both the turbidites and the fluvial metasediments may also have contributed somewhat to their higher $\delta^{18}O$, as unaltered cherts typically have $\delta^{18}O$ values of 17-38°/$_{oo}$ (Knauth and Epstein, 1976).

It is unlikely that this variation in $\delta^{18}O$ resulted from metamorphism. Magaritz and Taylor (1976a) found little difference between metamorphosed and unmetamorphosed greywackes.

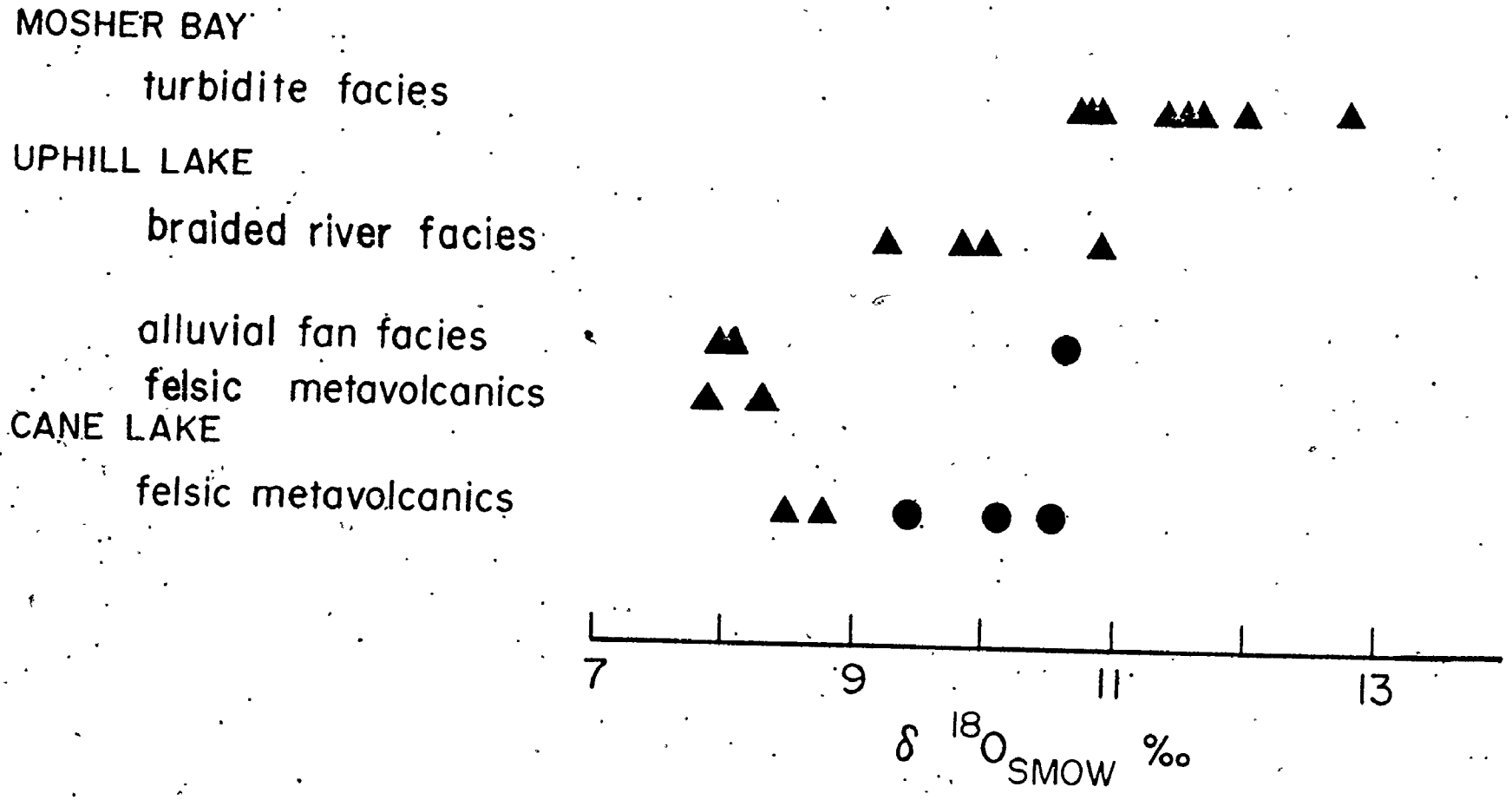

FIGURE 2-18. Whole rock oxygen isotope distribution for the Upper Manitou Lake area

● indicates possibly altered samples mentioned in the text (Cane Lake felsic metavolcanic rocks OT17, T214, T119 and Uphill Lake alluvial fan facies metasandstone OT2).

Eslinger and Savin (1973) and Yeh and Savin (1977) demonstrated that the whole rock $\delta^{18}O$ values of metamorphosed shale are in general not correlated with metamorphic grade. In any event, there appears to have been no regional metamorphic gradient within the Upper Manitou Lake area that could have affected the isotopic results.

Although some plutonic (granitic) detritus may have been mixed with the volcanogenic clasts, this probably did not have a large effect upon the initial isotopic composition of the sediment. Most Archean plutonic granitoids have $\delta^{18}O$ values of 7-9°/$_{oo}$ (Chapter III; Longstaffe et al., 1977a,b,c; Barker et al., 1976a; Taylor and Magaritz, 1975; Shieh and Schwarcz, 1977; Viswanathan, 1974a,b); gneissic rocks often have still lower $\delta^{18}O$ values. One granodiorite clast from an Abram Lake conglomerate (C18) has a $\delta^{18}O$ of 11.0°/$_{oo}$; it may have become enriched in ^{18}O during weathering and sedimentation. Incorporation of material derived from paragneiss bodies, such as the Pakwash paragneiss, would result in enrichment of ^{18}O in the sediment. However, it seems unlikely that greenstone belts contain large amounts of material eroded from pre-existing metasedimentary sequences.

The percentage of unaltered rock fragments within volcanogenic metasediments is a good index of sediment maturity. Since enrichment in ^{18}O during sedimentary processes depends upon the residence time of the detritus in such a wet, low temperature

environment, and hence upon the sediment maturity, a decrease in the abundance of unaltered rock fragments in volcanogenic sediments should accompany enrichment in ^{18}O.

The percentage of recognizable volcanic rock fragments within the various units of the Upper Manitou Lake area varies enormously, but averages 95-100% in the near vent alluvial fan facies, 70-80% in the more distal fluvial facies and 20-50% in the most distal turbidite facies (Teal, written comm.). The turbidites contain the highest abundances of free quartz. Therefore, increasing $\delta^{18}O$ does seem to correlate in these rocks with decreasing rock fragment content and increasing chemical maturity (Figure 2-7a). Excepting sample OT2, the alluvial fan facies metasedimentary rocks (95-100% rock fragments) are isotopically indistinguishable from the felsic metavolcanic rocks of the Uphill Lake unit. An alternative origin for the alluvial fan facies rocks, that they are metavolcanic breccias, cannot be ruled out by the isotopic data. Their extreme chemical immaturity has already been pointed out (Figure 2-7a).

$\delta^{18}O$ in felsic metavolcanic rocks, and the problem of alteration

Although the $\delta^{18}O$ range of clastic metasedimentary rocks analyzed in this study is identical to that of the felsic metavolcanic rocks from which the metasediments were presumably largely derived, some felsic metavolcanic samples (C12, B10, B11, B12, OT17, T214, T119) are more ^{18}O-rich than the range

normally observed for unaltered felsic volcanic rocks (6-9°/$_{oo}$; Taylor, 1968). Similar isotopic alteration of mafic metavolcanic rocks from the Lake Despair area is discussed in Chapter III. Enrichment in ^{18}O of felsic and mafic volcanic rocks is well documented (Taylor, 1968; Garlick and Dymong, 1970; Stuckless and O'Neil, 1973; Cerling et al., 1975; Muehlenbachs and Clayton, 1972), and accompanies low temperature hydration, devitrification, weathering and other alteration processes, all of which may have affected the samples analyzed in this study. The Cane Lake metavolcanic rocks, for example, have higher $\delta^{18}O$ values than the overlying Uphill Lake metavolcanic rocks; the highest values occur in samples located within 400 meters of a granitoid stock, and decrease with increasing distance from the stock. Alteration of $^{18}O/^{16}O$ ratios (generally lowering, however) of sedimentary or metasedimentary country rock (of initially higher $\delta^{18}O$) in the vicinity of granitic intrusions has been amply demonstrated (Shieh and Taylor, 1969; Turi and Taylor, 1971a,b). Further pursuit of such ideas, including the correlation of mineralogical, chemical and isotopic evidence of alteration, requires more detailed sampling; the results of such a study for the Burditt Lake stock and the surrounding felsic metavolcanic country rocks are given in Chapter III.

Another explanation, at least for some of the high isotopic values observed in 'felsic metavolcanic' rocks is that metamorphosed Archean clastic rocks have been mistaken for their

volcanic parents, a common error in poorly exposed Archean terrains.

Summary

Although the low $\delta^{18}O$ values of the Archean clastic metasediments relative to younger equivalents can largely be attributed to the immaturity of the Archean metasediments, other factors may have contributed:

1. interaction with meteoric water subsequent to diagenesis and metamorphism;
2. lower $\delta^{18}O$ values of Archean seawater (Perry and Tan, 1972; Becker and Clayton, 1976).

It is very unlikely that meteoric water interaction has affected all of the samples examined from geographically widespread localities throughout Ontario, and even more unlikely that the intensity of the meteoric water-rock interaction would correlate with the sedimentary facies found in the Upper Manitou Lake area. The importance of possible isotopic differences between the Archean and modern hydrosphere is difficult to evaluate on the basis of the limited data now available.

Our initial conclusions, therefore, are:

1. Archean clastic metasedimentary rocks analysed in this study have a mean $\delta^{18}O$ of 10.6°/$_{oo}$, lower than geologically younger greywackes, such as the Franciscan Formation (Magaritz and Taylor, 1976a), that have been analyzed. The lower range of $\delta^{18}O$ values probably reflects the high proportion of volcanic rock fragments in these rocks. One might expect modern greywackes derived very rapidly from a predominantly felsic volcanic source to have isotopic compositions similar to their Archean analogues.

2. Archean felsic metavolcanic rocks exhibit a range of isotopic values similar to that of Archean clastic metasedimentary rocks. Many samples have $\delta^{18}O$ values within the range of unaltered felsic volcanic rocks (6-9°/$_{oo}$; Taylor, 1968), but the range extends to higher $\delta^{18}O$ values presumably because of ^{18}O enrichment of some samples during low temperature alteration. Misclassification of some clastic metasedimentary rocks as metavolcanics could also explain some of the high values.

3. $\delta^{18}O$ values tend to increase with increasing sediment maturity, at least for the metagreywackes and meta-argillites examined. However, chemically immature metagreywackes can attain high $\delta^{18}O$ values if derived from previously ^{18}O-enriched metavolcanics.

$\delta^{18}O$ quartz results from Upper Manitou Lake

Quartz from the Upper Manitou Lake metagreywackes was analyzed to determine any isotopic changes that may have accompanied the fluvial to marine facies transition. Savin and Epstein (1970b) previously concluded that isotopic exchange affecting detrital quartz during weathering, transport, sedimentation and diagenesis was minimal.

The $\delta^{18}O$ quartz data (Figure 2-19; Table 2-8) define a roughly parallel trend to the $\delta^{18}O$ rock values. This trend, as well as the generally high isotopic values, may have resulted from:

1. progressive introduction of high $\delta^{18}O$ quartz from a different source than the metavolcanic rocks;
2. low temperature (authigenic) silica growth on detrital quartz cores;
3. diagenetic and low grade metamorphic reactions involving clays that produced fine grained, secondary quartz;
4. isotopic re-equilibration during greenschist facies metamorphism.

The relative importance of these factors cannot be determined from our data. Only the following suggestions can be made:

FIGURE 2-19 · $\delta^{18}O$ quartz results for the Upper Manitou Lake area.

Note that sample OT2 was treated with cold hydrofluoric acid prior to analysis, unlike any of the other samples. The acid stripping experiment was performed to determine if the quartz grains were isotopically zoned, perhaps because of secondary silica overgrowths which may have formed in a sedimentary environment.

■ quartz

● rock

▼ plagioclase

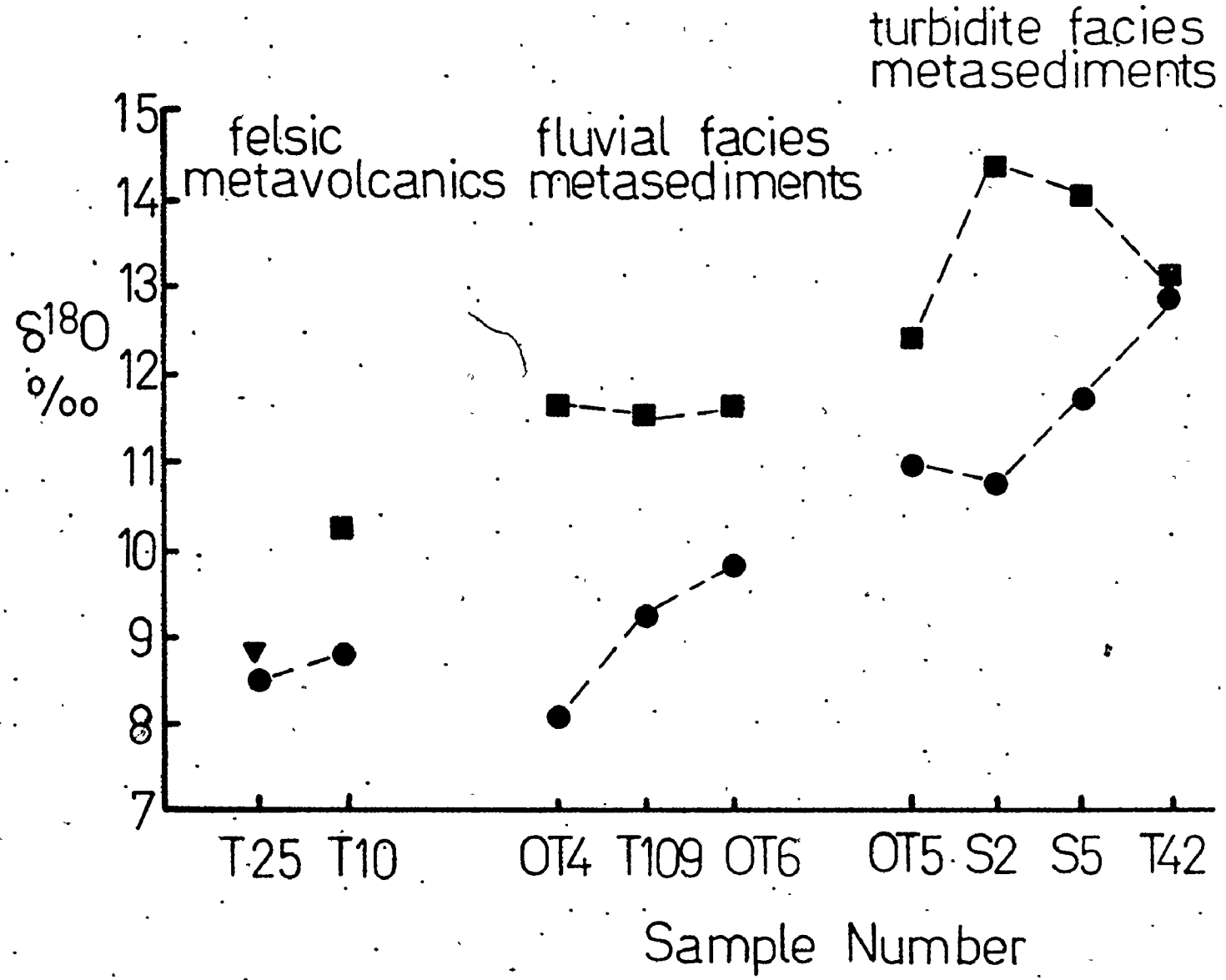
turbidite facies
metasediments
felsic
metavolcanics
fluvial facies
metasediments
15
14
13
12
11
10
9
8
7
δ18O
‰
T25
T10
OT4
T109
OT6
OT5
S2
S5
T42
Sample Number

Table 2-8 $\delta^{18}O$ mineral data, Upper Manitou Lake (°/oo)

	Quartz	Feldspar	Rock
Uphill Lake unit			
1. pyroclastic rocks			
T25		8.78±0.10 (2)	8.47
T10	10.19	-	8.79
2. alluvial fan facies			
OT4	11.64±0.00 (2)		7.96
3. braided river facies			
T109	11.44±0.10 (2)	-	9.22
OT6	11.60±0.03 (2)	-	9.80
Mosher Bay unit			
turbidite facies			
OT5*	12.30±0.08 (2)	-	10.90
S2	14.36±0.30 (2)	-	10.71
S5	13.95±0.28 (2)	-	11.64
T42	13.00	-	12.79

* Treated in cold HF; value in parentheses indicates number of analyses

Table 2-9 $\delta^{18}O$ results for the Pakwash Lake metasedimentary rocks (°/oo)

	Quartz	Plagioclase	Biotite	Rock
L30	10.34±0.00 (2)	-	5.11±0.18 (2)	8.63
L33	9.14±0.02 (2)	6.64±0.16 (2)	2.30±0.10 (2)	5.19

Value in parentheses indicates number of analyses

1. The $\delta^{18}O$ values of quartz from the braided river and alluvial fan facies are identical (11.5°/$_{oo}$; Table 2-8), and higher than for quartz from the Uphill Lake felsic metavolcanic sample (10.2°/$_{oo}$); Teal and Walker (1977) noted the presence of granitic pebbles within the braided river facies, and suggest such a source for the additional quartz there found. Such an origin is compatible with the oxygen isotope data; volcanic quartz can be ruled out, but only if our few analyses truly represent original source values. It also follows that the alluvial fan facies quartz be derived from the same granitic source rock.
2. The turbidite facies metagreywackes, which contain the most quartz, have the highest $\delta^{18}O$ values, and the greatest spread of results (13.0 to 14.4°/$_{oo}$). The analytical error for these samples is also greater than normally obtained for quartz (±0.1°/$_{oo}$), and greater than measured for quartz from the fluvial metagreywackes. Only sample OT5, which was treated in cold hydrofluoric acid (resulting in a 6% weight loss), gave results within normal reproducibility; its value, however, was lower than the other turbidite facies quartz samples. These results suggest that the turbidite facies quartz is isotopically inhomogeneous. This may be caused by (i) low temperature, high $\delta^{18}O$ overgrowths of authigenic

silica on detrital quartz cores; Yeh and Savin (1977) report that the diagenetic conversion of smectite to illite, as well as the decomposition of mica and feldspar, can produce the silica necessary for such activity; or (ii) the production of a discrete, fine-grained quartz during mineral reactions involving clays (H.P. Schwarcz, private comm.). Our data is insufficient to choose between these alternatives.

3. The apparent isotopic homogeneity of the fluvial quartz may be a result of (i) the chemical immaturity of the fluvial facies metagreywackes (insufficient clay development or feldspar and mica breakdown to permit notable release of silica), or (ii) a coincidental identity in the isotopic composition of the fine-grained and/or authigenic quartz with the detrital quartz; the fluvial secondary quartz might have lower $\delta^{18}O$ than the secondary marine quartz because the former equilibrated with meteoric waters, which are generally more ^{18}O-poor than seawater.
4. The isotopic re-equilibration accompanying greenschist facies metamorphism cannot be ignored (Schwarcz et al., 1970). Of the minerals stable under greenschist facies conditions, quartz would probably have the highest $\delta^{18}O$. The relative change in the oxygen isotopic composition of quartz during the metamorphism is more difficult to

predict. The meta-igneous (detrital) portion would probably be enriched in ^{18}O; any authigenic or metamorphic-diagenetic quartz would probably re-equilibrate to a lower $\delta^{18}O$ value. Isotopic studies on carefully separated mineral phases are required before any comment on the extent of re-equilibration can be made; Schwarcz et al. (1970) did find, however, a close approach to isotopic equilibrium in some greenschist facies metasedimentary rocks that they examined.

Chemical and isotopic correlations in Archean clastic metasedimentary rocks

The purpose of this section is to point out some chemical and isotopic correlations observed for the analyzed clastic metasedimentary rocks. Numerous possible parameters were tested (including normative corundum, (Na+K)/(Na+K+Ca), normative (Ab+Or)/(Ab+Or+An), and individual major and trace elements); perhaps the first comment that should be made is that chemical and isotopic correlations are conspicuous by their absence. However, a few useful results were obtained.

1. $\delta^{18}O$ and Al/Fe

Figure 2-20 shows that, except for the group B samples, those clastic metasedimentary rocks within the field of

chemically mature sediments have the highest $\delta^{18}O$ values. Thus, the sedimentary processes which drive Al/Fe towards 1.9±0.4 are also probably responsible, in part, for the enrichment in ^{18}O.

The group B samples (most of which are located at Kakagi Lake), do not fit this pattern. While chemically immature (Al/Fe = 2.5), they have $\delta^{18}O$ values as high as 13.3°/$_{oo}$. Three explanations can be offered for these results:

i. oxygen isotope compositions are affected more rapidly than chemical compositions during sedimentary processes;

ii. the rocks were derived from isotopically altered source rocks;

iii. the rocks were isotopically altered after the cessation of sedimentary processes.

The latter possibility should be further investigated as four of the six group B Kakagi Lake samples are located in the vicinity of post-sedimentation mafic and ultramafic intrusions (Figure 2-4). These samples are also richer in calcite than the other metasedimentary rocks from the area.

In spite of such difficulties, the $\delta^{18}O$-Al/Fe diagram has potential as a protolith indicator for gneisses.

FIGURE 2-20 $\delta^{18}O$ rock versus Al/Fe diagram for the Archean clastic metasedimentary rocks analyzed during this study. Field for chemically mature sediments from Dennen and Moore (1971). Group B samples have much higher $\delta^{18}O$ values than would be predicted from their chemical immaturity.

X Kakagi Lake area

\+ Upper Manitou Lake area

▲ Kirkland Lake area

▽ Pakwash Lake area

□ Abram Lake area

FIGURE 2-21 Discriminant Function (D.F.) versus $\delta^{18}O$ (rock) diagram for the Archean clastic metasedimentary rocks analysed during this study.

$$D.F. = 10.44 - 0.21\ SiO_2 - 0.32\ Fe_2O_3{}^t - 0.98\ MgO + 0.55\ CaO + 1.46\ Na_2O + 0.54\ K_2O$$ (Shaw, 1972).

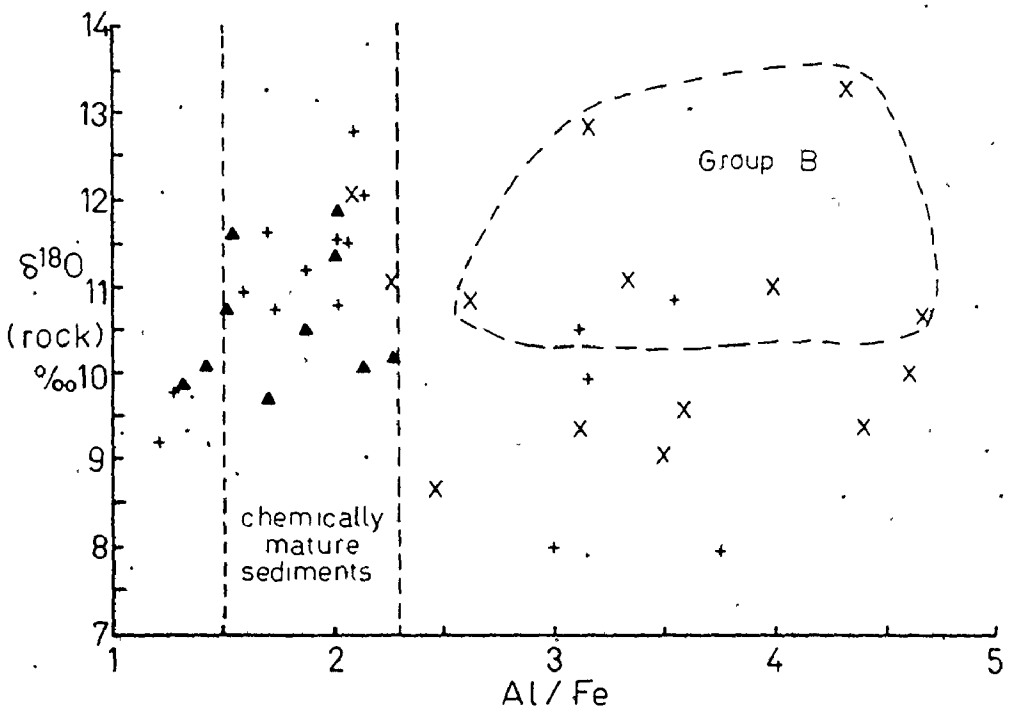
14
13
12
11
10
9
8
7
δ18O (rock) ‰
Group B
chemically mature sediments
1
2
3
4
5
Al / Fe

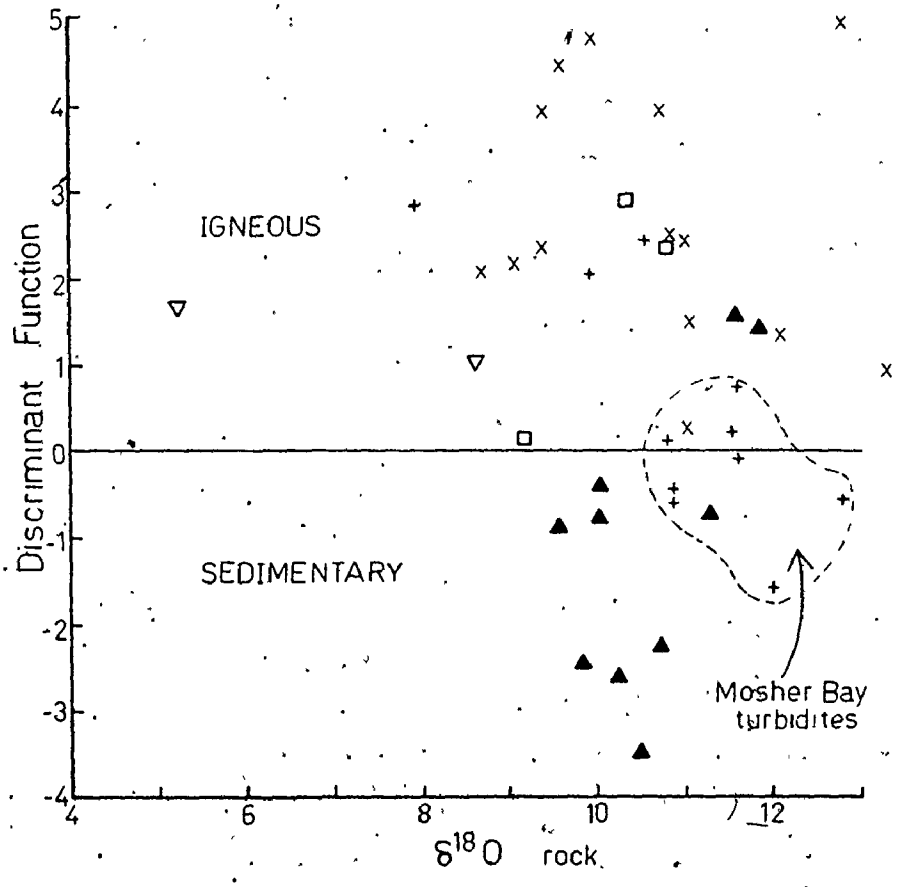
5
4
3
2
1
0
-1
-2
-3
-4
Discriminant Function
IGNEOUS
SEDIMENTARY
Mosher Bay turbidites
4
6
8
10
12
δ18O rock

2. $\delta^{18}O$ and the Discriminant Function

Shaw (1972) devised a major element discriminant function (D.F. = 10.44 - 0.21 SiO_2 - 0.32 $Fe_2O_3^t$ - 0.98 MgO + 0.55 CaO + 1.46 Na_2O + 0.54 K_2O) to distinguish sedimentary and igneous protoliths of quartzo-feldspathic gneisses. Discriminant function values for the analyzed clastic metasedimentary rocks are plotted against $\delta^{18}O$ (rock) after the fashion of Shieh et al. (1976) (Figure 2-21). Most of the Upper Manitou Lake turbidites and Kirkland Lake clastic metasedimentary rocks, which can be classified as chemically mature (Dennen and Moore, 1971), have D.F. values of near to or less than 0 (within the sedimentary field); other samples, which are classified as immature by their Al/Fe ratios, fall in the igneous field using the discriminant function of Shaw. However, if a D.F. value of 1.5 was used to separate the igneous and sedimentary fields, the two most ^{18}O-rich Kirkland Lake samples, and four out of five of the most ^{18}O-rich Kakagi Lake samples would then fall in the field of sedimentary rocks.

This plot may therefore be useful in protolith determinations in gneisses, providing that isotopic and chemical characteristics are preserved during metamorphism, and that D.F. values of 0 to 1.5 are interpreted somewhat more liberally than Shaw (1972) had intended.

3. $\delta^{18}O$ and CaO/Na_2O

A plot of $\delta^{18}O$ (rock) versus CaO/Na_2O (Figure 2-22) for the Upper Manitou Lake felsic metavolcanic and associated metasedimentary rocks, shows an inverse correlation not observed for the other metasedimentary suites analyzed. The Kakagi Lake suite, for example, shows a weak positive correlation between these two parameters, perhaps a function of calcite content, and the fluvial metasedimentary rocks from Kirkland Lake show no systematic correlation.

That some sort of correlation between $\delta^{18}O$ and CaO/Na_2O would exist, is not surprising, as exchange of Na for Ca could open up the feldspar structure to oxygen isotopic exchange. It is therefore interesting that the marine turbidite facies clastic metasedimentary rocks of the Upper Manitou Lake area, which, unlike fluvial facies metasediments, have presumably been exposed to Na-rich seawater, have the lowest CaO/Na_2O and the highest $\delta^{18}O$. It is likely, therefore, that isotopic exchange during halmyrolysis has at least in part controlled the ultimate isotopic composition of these marine metasedimentary rocks.

FIGURE 2-22 $\delta^{18}O$ (rock) versus CaO/Na_2O diagram for clastic metasedimentary and felsic metavolcanic rocks from the Upper Manitou Lake area

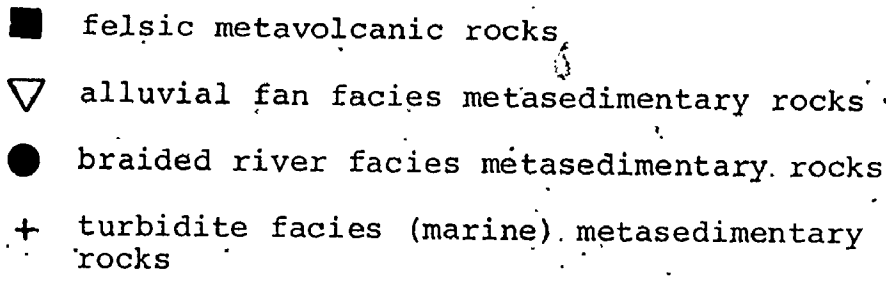

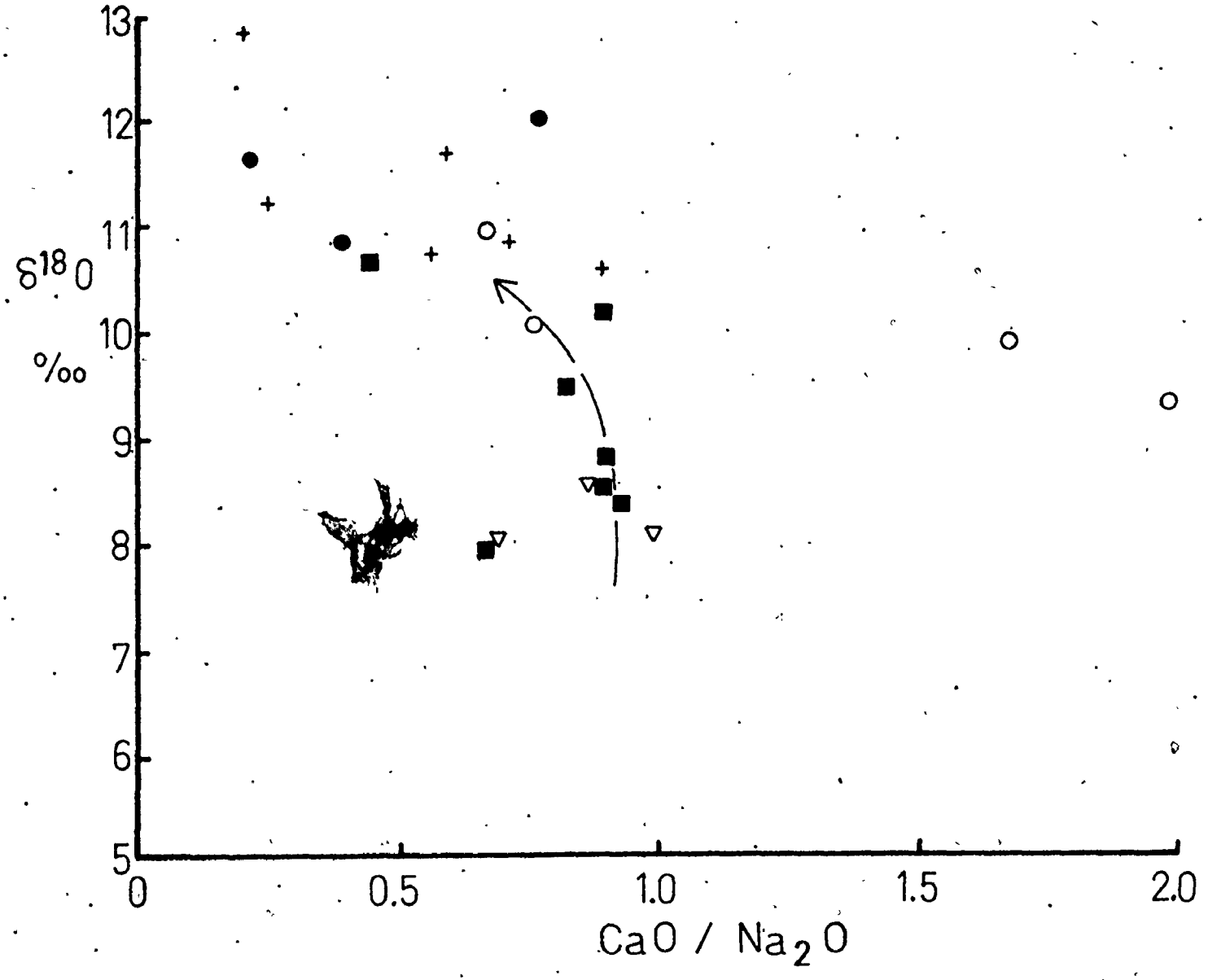
13
12
11
10
9
8
7
6
5
$\delta^{18}O$
‰
0
0.5
1.0
1.5
2.0
CaO / Na_2O

$\delta^{18}O$ results for altered clastic metasedimentary rocks from Pakwash Lake

The purpose of this section is to describe the effect of shearing upon the $\delta^{18}O$ composition of the Pakwash Lake metagreywackes; these data emphasize the importance of avoiding such tectonized localities if isotopic results indicative of provenance and sedimentary processes are to be obtained.

Two samples of Pakwash Lake metagreywacke were analyzed. L30 is located about one kilometer from a shear zone associated with the Sydney Lake Fault, a cataclastic zone which separates the Uchi granite-greenstone and the English River gneiss belts. The rock is an undeformed greenschist facies shaley metasandstone. L33 is the sand-sized matrix of a sheared metaconglomerate, located within the shear zone. Unlike L30, it contains garnet, and its feldspar is severely saussuritized.

L33 is more calcareous and less siliceous than L30, and contains higher abundances of Fe, Mn, Ti, Zn and Ni (see Appendix IV). These chemical differences may reflect differing provenance; the metaconglomerate (L33) contains numerous andesite clasts, while a more dacitic origin has been postulated for the metasandstone (Beakhouse, 1974b). However, at least some of the differences probably were caused by alteration associated with the shearing.

Oxygen isotope results

The $\delta^{18}O$ mineral and rock results are given in Table 2-9 (p. 95). The low $\delta^{18}O$ (rock) value of L33 (5.2°/$_{oo}$) probably reflects isotopic exchange with fluids that accompanied the shearing, and caused the alteration of the feldspar. The mineral phases of L33 are also depleted in ^{18}O; relative to L30, the $\delta^{18}O$ values of quartz and biotite are, respectively, 1.2 and 2.8°/$_{oo}$ lower.

Somewhat discordant quartz-biotite (431°C) and plagioclase-biotite (511°C) isotopic temperatures are preserved in L33. Since both biotite and plagioclase isotopically re-equilibrate more readily than quartz, the latter temperature probably reflects, more accurately, the temperature during alteration and shearing. This temperature is similar to that of L30 (quartz-biotite temperature of 522°C), which has probably preserved a regional metamorphic temperature minimum.

If the plagioclase and biotite did completely re-equilibrate with shear zone related fluids at about 500-520°C, and if (a) the fluids were mostly water, and (b) the total volume of oxygen in the fluid greatly exceeded the volume contained in the shear zone rocks, then the isotopic composition of the fluid can be estimated from the plagioclase-H_2O curve of O'Neil and Taylor (1967) to be about 5.7°/$_{oo}$. The final assumption, at least, can be supported by the severe feldspar alteration.

Both magmatic and metamorphic waters have isotopic compositions compatible with this calculation (4-8°/$_{oo}$; Taylor, 1974); neither can the mixing of some meteoric water with magmatic-metamorphic water be ruled out. Nevertheless, it is tempting to speculate that the Sydney Lake cataclastic zone was lubricated, and perhaps triggered, by magmatic-metamorphic waters related to the migmatization and anatexis of the Pakwash gneisses located south of the fault; some of these gneisses are also isotopically depleted in ^{18}O (Chapter IV).

II-8 GENERAL CONCLUSIONS

Possible applications of a geochemical and isotopic study of Archean clastic metasedimentary rocks are listed in II-1. Some general conclusions pertinent to these preliminary remarks are summarized below.

1. The chemical compositions of the analyzed metasedimentary rocks imply derivation from a dominantly felsic source area (dacite-tonalite). However, the presence of a mafic component of varying importance is also indicated for some of the study localities.
2. All of the analyzed metasedimentary rocks plot within the greywacke field, as chemically defined by Pettijohn et al. (1973), and most have chemical compositions that

suggest a eugeosynclinal (island arc) environment (Blatt et al., 1972). All have low Al_2O_3/Na_2O, a sign of chemical immaturity in so far as surface weathering is concerned. Some samples, however, have Al/Fe, D.F. values, Na_2O/K_2O, CaO/Na_2O, and oxygen isotopic compositions that indicate chemical and isotopic modification during sedimentary processes; these are designated as chemically mature clastic metasedimentary rocks. Other samples have little or no chemical characteristics that reflect residence in a sedimentary environment. Thus, their sedimentary residence time must have been very short. This latter group of samples is designated as chemically immature. Such rocks may have higher $\delta^{18}O$ values than their protoliths, and this may be the only geochemical clue to their sedimentary nature. However, high $\delta^{18}O$ values can be attained in other ways, and must be used cautiously as sedimentary indicators when unsupported by other evidence.

3. The chemically mature and isotopically enriched metasedimentary rocks should be recognizable in high grade gneiss terrains, if only by the chemical and isotopic criteria listed above, providing that high grade metamorphism has not altered these parameters. There is little hope of distinguishing chemically immature metasedimentary protoliths from felsic metavolcanic or

plutonic protoliths of a gneiss by the same techniques.

4. The chemical composition of Archean clastic metasedimentary rocks is not unlike that of modern 'eugeosynclinal' sedimentary rocks. The overall range in oxygen isotopic composition will also probably be found to be similar once some younger greywackes of volcanogenic origin are analyzed.

CHAPTER III

THE GEOCHEMISTRY OF THE BURDITT LAKE - LAKE DESPAIR AREA

III-1 INTRODUCTION

The geochemistry of a small portion of the Wabigoon granite-greenstone belt is examined in this chapter. The objective is to determine the relative effects of magmatic, metamorphic and metasomatic processes upon the isotopic and chemical composition of the greenschist facies metavolcanic and relatively unmetamorphosed dioritic to granodioritic plutonic rocks. The spatially associated amphibolite facies Footprint gneiss will also be considered.

III-2 GEOLOGICAL BACKGROUND

The Lake Despair and Burditt Lake areas occupy about 450 square kilometers in the southern portion of the Wabigoon granitoid-greenstone belt (latitude N 48°55'; longitude W 93°40'; NTS ref.: 52C/12, 52C/13), and are located about 40 kilometers northwest of Fort Frances, Ontario (Figure 2-1a,b; 3-1).

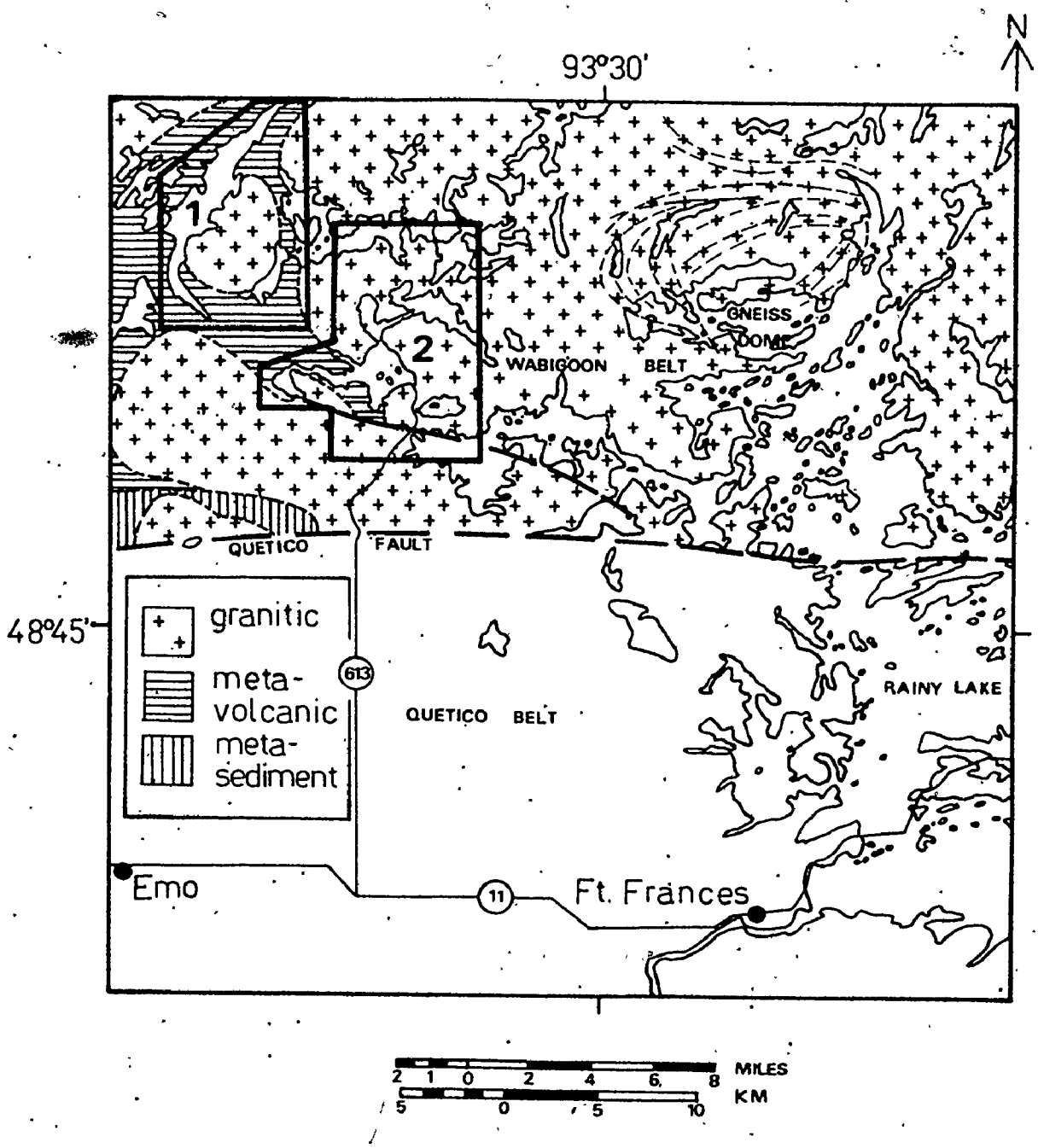

FIGURE 3-1 Location map, Burditt Lake and Lake Despair areas, Wabigoon granite-greenstone belt

1. Burditt Lake area
2. Lake Despair area

Previous geological investigations include those by Lawson (1888) and Blackburn (1976a), the latter work providing much of the geological background for this study. The Ontario Division of Mines is continuing mapping investigations in the area (Edwards and Lorsong, 1976; Edwards and Sutcliffe, 1977).

Rocks exposed in the study area can be divided into five major categories (Figure 3-2, 3-3):

1. interlayered mafic and felsic metavolcanic rocks;
2. the Footprint gneiss;
3. the Northwest Bay Complex;
4. the Jackfish Lake Complex;
5. the Burditt Lake granodiorite.

The detailed petrography of these units, except the Burditt Lake granodiorite, is described in Appendix III. Petrographic details of the Burditt Lake body are given in Birk (Ph.D. in prep.) and Birk and McNutt (1976, 1977).

Mafic metavolcanic rocks

The mafic metavolcanic rocks increase in metamorphic grade from greenschist facies in the vicinity of Burditt Lake (Figure 3-2) to amphibolite facies near the contact with the Jackfish Lake Complex (Photo A). Metadunites, now composed almost entirely of serpentine pseudomorphs after olivine,

FIGURE 3-2 General geology of the Burditt Lake area.

The locations of analyzed samples are also shown. The dashed line traces the northeast-southwest traverse across the Burditt Lake stock and associated felsic metavolcanic country rocks discussed in the text.

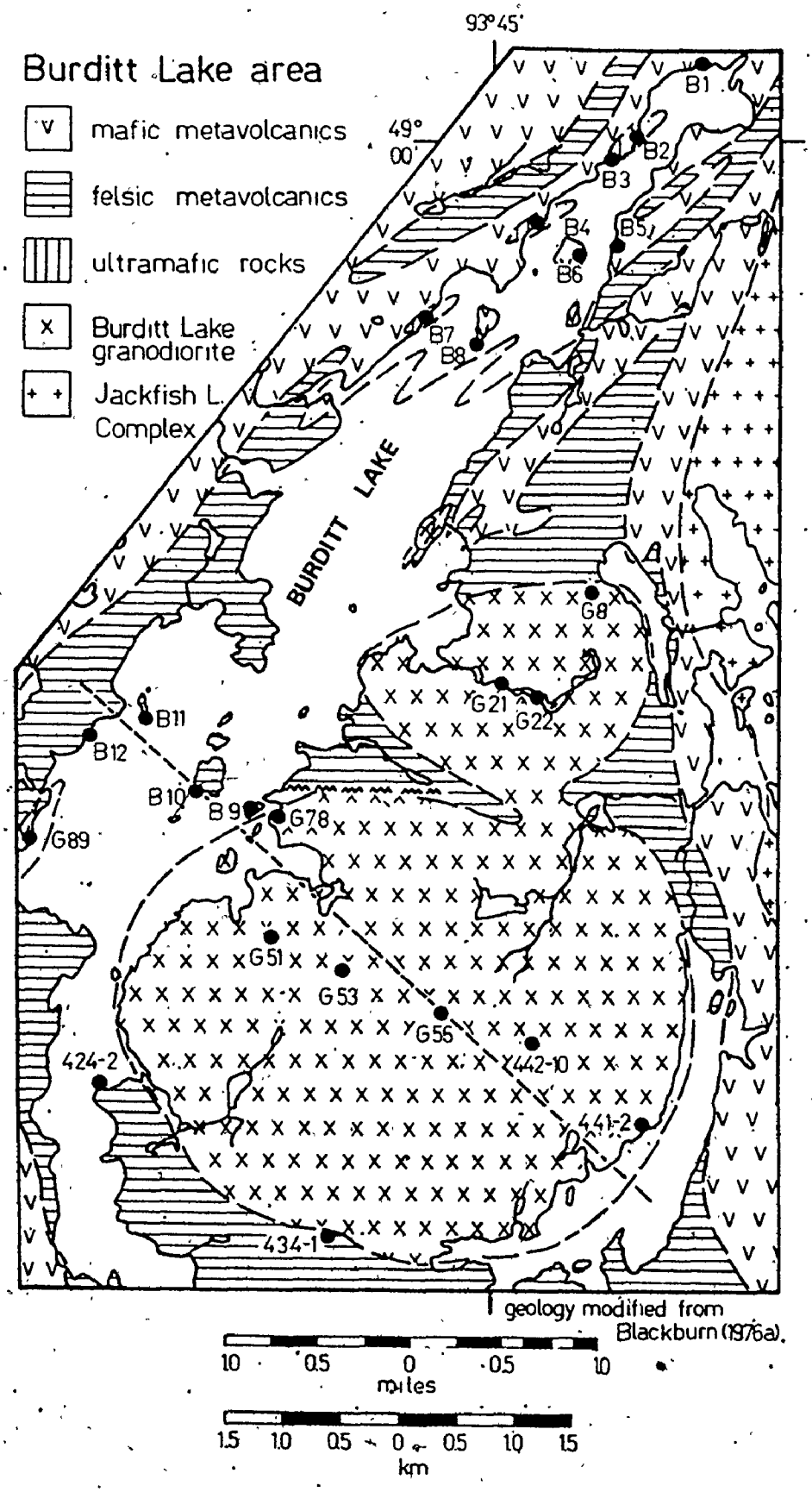
Burditt Lake area
mafic metavolcanics
felsic metavolcanics
ultramafic rocks
Burditt Lake granodiorite
Jackfish L. Complex
93°45'
49° 00'
BURDITT LAKE
B1
B2
B3
B4
B5
B6
B7
B8
B9
B10
B11
B12
G8
G21
G22
G78
G89
G51
G53
G55
424-2
442-10
441-2
434-1
geology modified from Blackburn (1976a).
10 0.5 0 0.5 10
miles
1.5 1.0 0.5 0 0.5 1.0 1.5
km

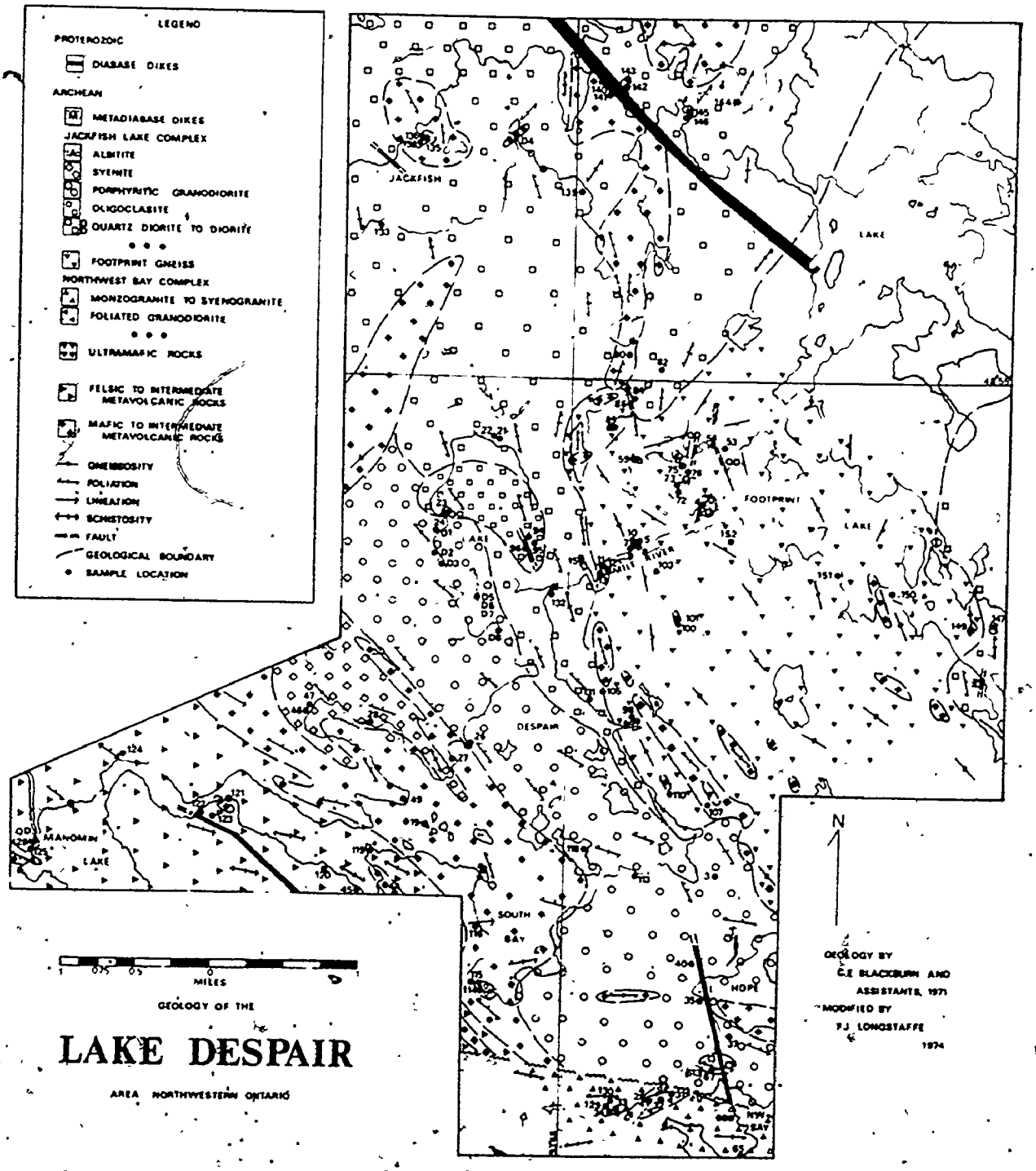

FIGURE 3-3 General geology of the Lake Despair area, including sample locations

occur in bodies elongated parallel to the regional foliation within the mafic metavolcanic pile (Figure 3-2, 3-3).

Felsic metavolcanic rocks

Greenschist facies felsic pyroclastic rocks located in the vicinity of Burditt Lake (Figure 3-2) grade along strike into quartz-feldspar-mica ± garnet schists, as both the Jackfish Lake Complex to the east and the Northwest Bay fault to the southeast are approached (Figure 3-3).

Footprint gneiss

The Footprint gneiss is a fine to medium grained, banded biotite trondhjemitic to granodioritic gneiss and migmatite. Essential mineralogy is quartz (18-28%), oligoclase (51-71%), microcline (1-16%) and biotite (4-12%). Concordant and discordant pegmatoidal material is ubiquitous (Photos J, K, L, M). Numerous migmatized and strongly lineated amphibolite enclaves, many greater than one kilometer in length, as well as some enclaves composed almost entirely of hornblende, have been observed within the gneiss (Photos E, F, G).

Recent mapping by the Ontario Division of Mines (Edwards and Lorsong, 1976; Edwards and Sutcliffe, 1977) has shown that such trondhjemitic to granodioritic gneiss is characteristic of much of the Rainy Lake Dome.

Northwest Bay Complex

The Northwest Bay Complex, a marginal phase of the Rainy Lake batholith, occurs southernmost within the study area and is separated from the other rock types by the Northwest Bay Fault, a probable offshoot of the Quetico Fault, which is located about three kilometers to the south (Blackburn, 1976a). Lithology varies from massive to strongly foliated biotite granodiorite (Photos N, O); highly sheared muscovite-biotite granite is also found near the fault (Photo P).

Jackfish Lake Complex

The Jackfish Lake Complex is bounded on the west by amphibolite facies mafic to intermediate metavolcanic rocks, some of which have been migmatized by the intrusion of the Complex (Photo A). To the east, the Complex is bounded by the Footprint gneiss, and, to the south, by the Northwest Bay Fault. The Complex widens from about one kilometer near the south end of Lake Despair to ten kilometers north of Jackfish Lake; the unit then swings eastward as it continues to mantle the gneissic core of the Rainy Lake Batholith. Outside the area of study, the Complex is predominantly dioritic in composition; diorite probably makes up 90-95% of the total volume of rock exposed. Within the study area,

however, two somewhat distinct rock suites are observed, dioritic and granodioritic. Both are strongly lineated to foliated and contain numerous mafic enclaves (Photos B, C, D). Some enclaves within the dioritic unit are up to one kilometer in length and contain remnant pillows (Blackburn, 1976a, p.13). The larger enclaves are oriented parallel to the hornblende lineation found within the rocks.

The diorite suite contains meladiorite, diorite, monzodiorite, quartz diorite and leucodiorite (oligoclasite). Volumetrically, diorite predominates. Essential mineralogy is hornblende (10-65%) and plagioclase (oligoclase to andesine, 35-90%). Minor phases include clinopyroxene, biotite, quartz, microcline, epidote, magnetite, chlorite and sphene.

The granodiorite suite contains quartz monzodiorite, granodiorite and microcline-albite syenite (Na-syenite). Essential mineralogy is oligoclase, microcline, quartz, and hornblende in all but the syenite, which contains only a trace of quartz and has albite as the plagioclase feldspar. Abundant minor and accessory minerals include biotite, epidote, sphene, opaques, apatite, hematite and muscovite. Microcline occurs primarily as aligned patch and stringlet perthite megacrysts up to 20 mm in length. Petrographic observations that suggest late growth for these megacrysts include:

1. aligned inclusions of altered plagioclase and unaltered plagioclase, each at different

orientations within the same microcline megacryst;

2. abundant inclusions of plagioclase, quartz, hornblende, and sphene;
3. apparent embayment and pseudomorphic replacement of plagioclase by perthite megacrysts;
4. growth of microcline megacrysts within mafic enclaves (Photo D).

Other rock types found within the Jackfish Lake Complex are quartz-plagioclase dikes, aplites, pegmatites and one occurrence of an albitite dike (Photo D).

Sutcliffe (1977) has discussed the structure of the Jackfish Lake Complex, and concluded that the Complex was emplaced by wedging upwards along the greenstone-gneiss interface, in agreement with this author's previous interpretation (Longstaffe, 1975; Longstaffe et al., 1977a), which was based upon lithological data.

Burditt Lake granodiorite

Only a brief description of the Burditt Lake pluton is given here as details are contained in a companion study (Birk, Ph.D. in preparation). The stock is composed of three lithologies: (1) the main phase, a muscovite-biotite, medium grained granodiorite, concentrated in the south lobe of the

stock; (2) microcline megacryst, hornblende-biotite granodiorite of the north lobe; (3) fine grained granodiorite and aplite, located throughout the stock. Sharply brecciated intrusive contacts with the metavolcanic rocks indicates high level emplacement for at least part of the pluton.

The microcline megacrysts of the north lobe have been attributed to autometasomatism (Birk and McNutt, 1976).

Geochronology

The age relationships between the various lithologies of the Burditt Lake - Lake Despair area are poorly known. The Burditt Lake stock, which intrudes the felsic metavolcanic rocks, has a Rb-Sr whole rock age of 2598±45 m.y. (Birk and McNutt, 1977). Birk (written comm.) has also obtained a survey isochron date of 2616±66 m.y. for the Footprint gneiss, Northwest Bay Complex and Jackfish Lake Complex. These dates are similar to others known for the District of Rainy River and related areas (Table 3-1).

Relative chronology

Field relationships show that quartz diorite and leucodiorite dikes of Jackfish Lake Complex aspect cut both the mafic metavolcanic rocks and the Footprint gneiss (Photo H).

Table 3-1 Selected geochronology, District of Rainy River and related areas

Age (My)	Method	$^{87}Sr/^{86}Sr$	Rock type and locality	Reference
2550	Rb-Sr wr		granite, near Rainy Lake	Hedge & Walthall, 1963
2730	U-Pb sphene		Saganaga tonalite, Ontario-Minnesota border, 120 mi. east Ft. Frances	Tilton & Grunenfelder, 1968
2750±30	U-Pb zircon		metasediments, volcanics and granites, near Rainy L.	Hart & Davis, 1969
2770±330	Rb-Sr wr	0.7010± 0.0038	volcanics, near Rainy L.	Hart & Davis, 1969
2690±110	Rb-Sr wr	0.7002± 0.0019	paragneiss and metasediments, near Rainy L.	Hart & Davis, 1969
2690±80	Rb-Sr wr	0.7008± 0.0013	metasediments, paragneiss, and volcanics, near Rainy L.	Hart & Davis, 1969
2520±100	Rb-Sr wr	0.7037± 0.0019	Bad Vermilion Bay tonalite, near Rainy Lake	Hart & Davis, 1969
2740±100	Rb-Sr wr	0.7006± 0.0040	Northern Lake gneiss, Ontario-Minnesota border, 120 mi. east Ft. Frances	Hanson et al., 1971
2710±560	Rb-Sr wr	0.7009± 0.0060	Saganaga tonalite, as above	Hanson et al., 1971
2690±480	Rb-Sr wr	0.7009± 0.0014	Icarus Pluton, as above	Hanson et al., 1971

Table 3-i/continued

Age (My)	Method	$^{87}Sr/^{86}Sr$	Rock type and locality	Reference
2700	U-Pb sphene		Icarus Pluton, as above	Catanzaro & Hanson, 1971
2750	U-Pb sphene		Saganaga tonalite, as above	Catanzaro & Hanson, 1971
2740	U-Pb sphene		Lynden syenite, as above	Catanzaro & Hanson 1971
2730	U-Pb sphene		Giants Range granite, as above	Catanzaro & Hanson 1971
2680	U-Pb sphene		Giants Range granite, as above	Catanzaro & Hanson 1971
2670±65	Rb-Sr wr		Giants Range quartz monzonite, as above	Prince & Hanson, 1972

A. Mafic amphibolite injected with quartz veins, both in 'lit-par-lit' and discordant fashions. The photograph was taken near the contact between the Jackfish Lake Complex and the mafic metavolcanic rocks, along the western shoreline of Lake Despair.

B. Jackfish Lake Complex diorite.

C. Small mafic enclave within Jackfish Lake Complex quartz diorite.

D. Jackfish Lake Complex granodiorite. The wider pegmatite cuts an earlier, coarser grained pegmatite as well as the granodiorite and associated feldspathized mafic enclaves.


C

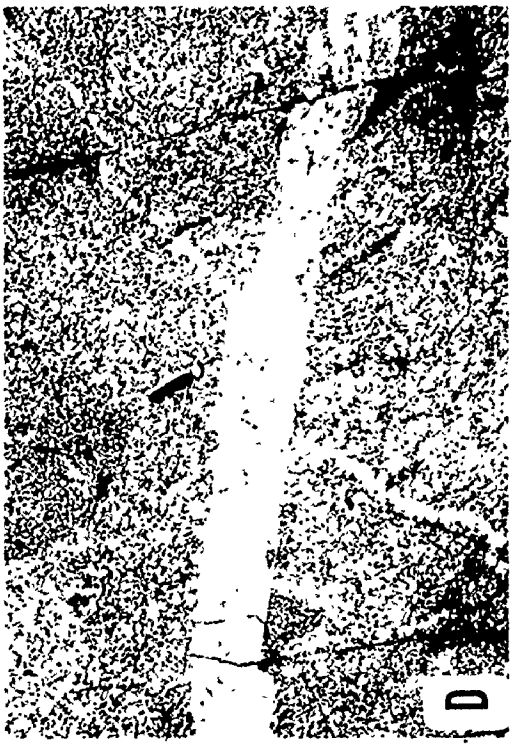
D


A

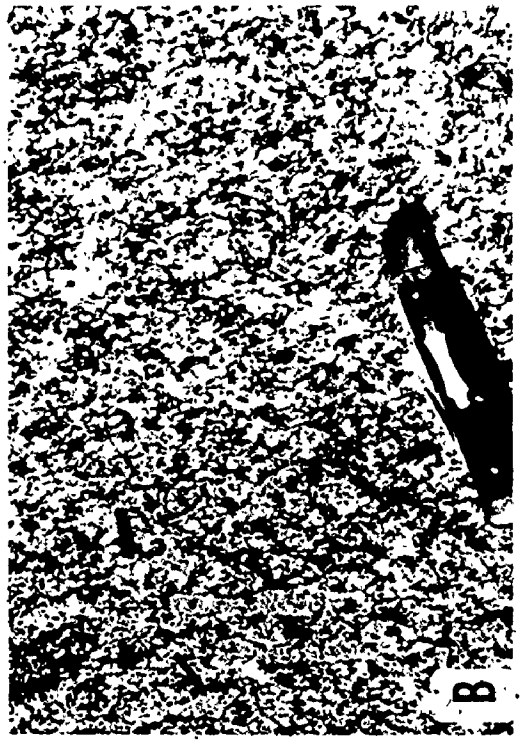
B

E. Migmatized mafic amphibolite enclave, Footprint gneiss

F. Migmatized mafic amphibolite enclave, more advanced development; Footprint gneiss

G. Deformed and migmatized mafic amphibolite enclave, Footprint gneiss

H. Contact breccia, Jackfish Lake Complex leucodiorite dike and the Footprint gneiss


G


H


E


F

I. Contact breccia, Footprint gneiss - Jackfish Lake Complex; vertical section

J. Highly flattened Footprint gneiss and migmatite

K. Footprint gneiss and migmatite

L. Footprint gneiss (probably unmigmatized)


K


L

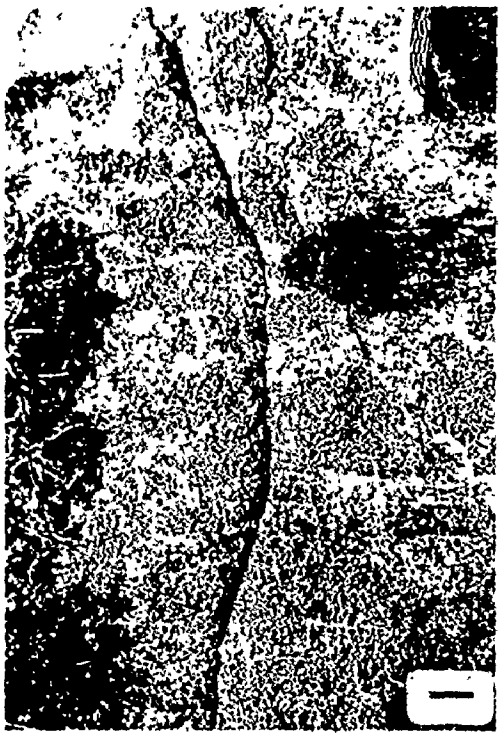
M

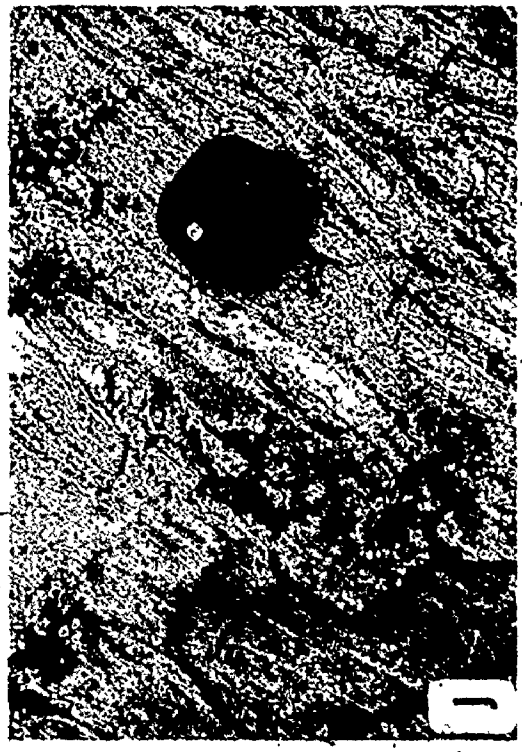
N

M. Footprint gneiss and migmatite. Note the totally melted portion of gneiss near the center of the photograph.

N. Northwest Bay Complex granodiorite.

O. Foliated Northwest Bay Complex granodiorite. The outcrop is cut by a Proterozoic diabase dike. The granodiorite also contains a boudinaged Archean mafic unit, possibly a dike.

P. Large boudinaged mafic enclave within the sheared Northwest Bay Complex granite.


O


P


M

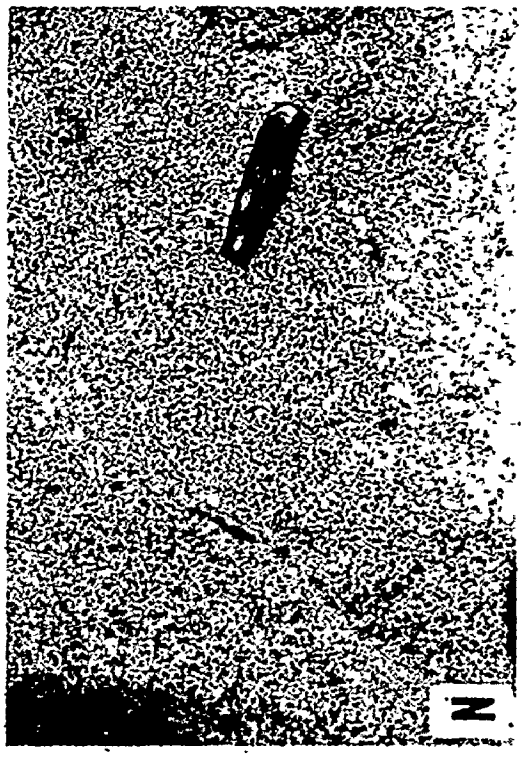
N

The Jackfish Lake Complex - Footprint gneiss contact is often marked by mafic breccias with tonalitic to dioritic matrices (Photo I). Elsewhere, the contact is gradational. Sutcliffe (1977) reports enclaves of gneiss within the Jackfish Lake Complex diorite. Thus, the field evidence suggests that the Jackfish Lake Complex and the Burditt Lake stock are the youngest major Archean lithologies in the area; the age relations between the Footprint gneiss, the Northwest Bay Complex and the metavolcanic rocks remain uncertain.

Finally, all of the rock units have been cut by Proterozoic diabase dikes (Photo O), which, in turn, have been fault offset.

III-3 COMPARATIVE GEOCHEMISTRY

For comparison of phaneritic and aphanitic rock types, all samples have been plotted as functions of normative quartz, plagioclase, orthoclase and feldspathoids (Figure 3-4), using the modified CIPW-Niggli equivalent cation norm of Shaw (1969). As mentioned, plutonic rock names have been assigned in accordance with I.U.G.S. nomenclature (Streckeisen, 1976) and aphanitic rocks after Irvine and Baragar (1971).

The geochemistry of each of these rock types will be discussed in the remaining sections of this chapter.

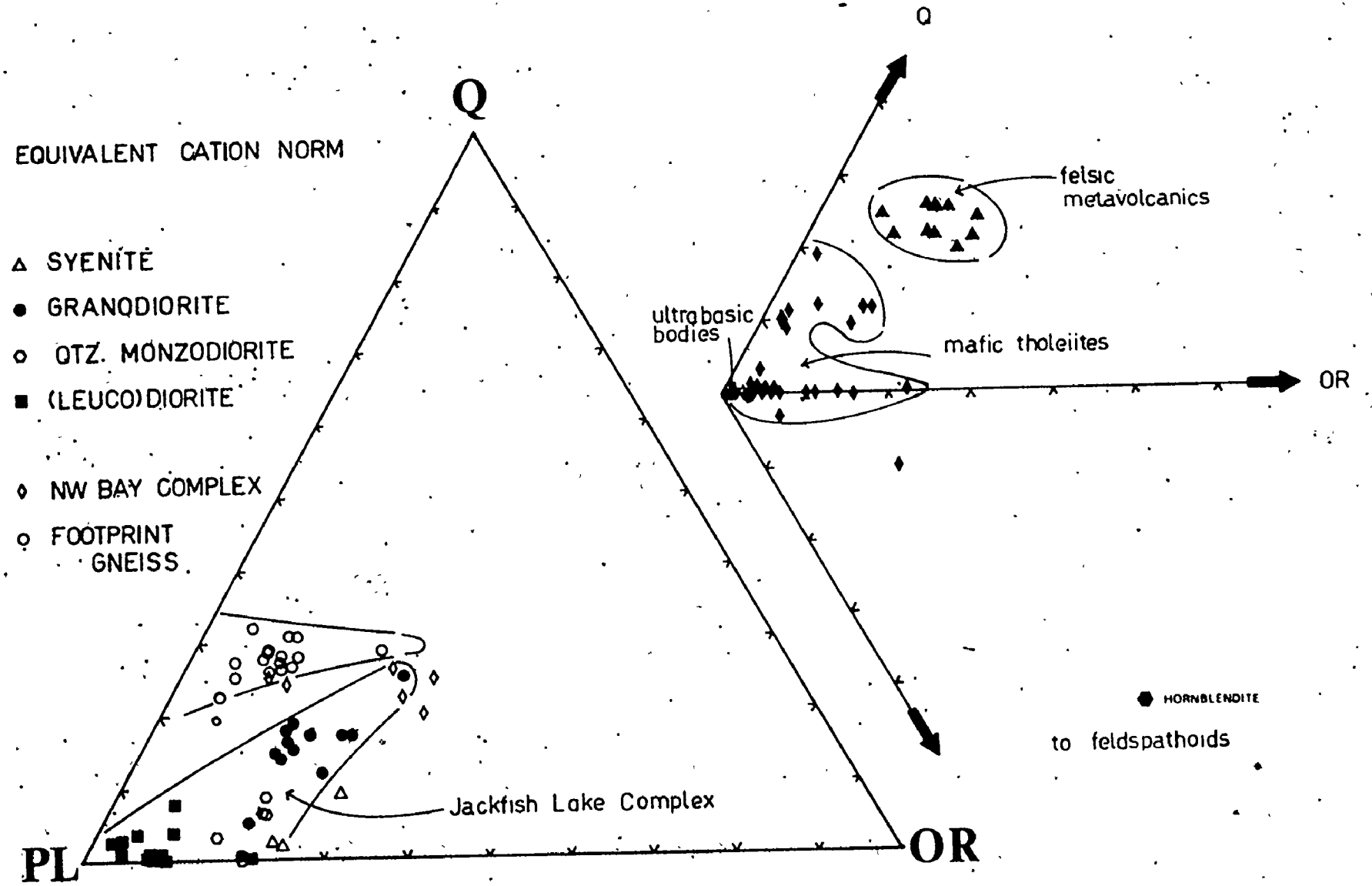

FIGURE 3-4 Normative quartz-plagioclase-orthoclase-feldspathoids diagram for the various lithologies from the Burditt Lake - Lake Despair area.

III-4 ISOTOPIC AND CHEMICAL ALTERATION OF BASALT - GENERAL CONSIDERATIONS

Chemical and isotopic alteration of the Burditt Lake - Lake Despair mafic metavolcanic rocks may have occurred during submarine weathering, hydrothermal activity, surface weathering and prograde metamorphism. All of these possible forms of alteration must be considered prior to any petrogenetic interpretation of the data. The purpose of this section is to summarize what is known about these phenomena.

Seawater alteration of basalt: oxygen isotope effects

Garlick and Dymond (1970) reported that the $\delta^{18}O$ values of submarine volcanic glass increased with age, and that the hydration of submarine basalt resulted in its enrichment in ^{18}O. Muehlenbachs and Clayton (1971, 1972a,b) recognized the effects of opposing processes upon the isotopic composition of submarine basalts. On one hand, the $\delta^{18}O$ values of submarine greenstones (2.8-6.8°/$_{oo}$; mean $\delta^{18}O$ = 5.2°/$_{oo}$) suggested interaction with seawater at 200-300°C. On the other hand, the $\delta^{18}O$ values of fresh submarine basalts lay in the same range as ocean island basalts (5.5-5.9°/$_{oo}$), but older, weathered samples were enriched in ^{18}O, a result of clay formation in cold seawater at a rate of 0.25°/$_{oo}$/million years.

Recent results for DSDP basalts (Pineau et al., 1973;

Lawrence et al., 1975; Muehlenbachs and Clayton, 1976; Muehlenbachs, 1976, 1977a,b; Gray et al., 1977; Friedrichsen and Hoernes, 1976) confirmed that most submarine basalts have experienced enrichment in ^{18}O, at least down to depths of 600 meters below the basalt-sediment interface; this alteration occurs at temperatures of 4 to 20°C. More deeply seated rocks have been depleted in ^{18}O, ($\delta^{18}O = 4.4 \pm 1.4‰$) due to seawater-rock interaction at 200-300°C. Similar results have been reported for ophiolites (Wenner and Taylor, 1973; Montigny et al., 1970; Spooner et al., 1974; Heaton and Sheppard, 1974; Magaritz and Taylor, 1974; 1976a). In these rocks, hydrothermal seawater circulation has affected oceanic crust at least to depths of two kilometers.

Seawater alteration of basalt: chemical effects.

Chemical modification accompanies seawater-basalt interaction. Hart (1969) and Philpotts et al. (1969) reported that seawater alteration had little effect upon the rare earth element (REE) and Sr concentrations of basalt, but caused significant enrichments in K, Rb, and Cs and depletions or enrichments in Ba. Contemporaneous and subsequent studies (Miyashiro et al., 1969; Thompson and Melson, 1970; Hart and Nalwalk, 1970; Hart, 1971, Dasch et al., 1973; Seitz and Hart, 1973; Hart et al., 1974; Frey et al., 1974; Fleet et al.,

1976; O'Nions and Pankhurst, 1976) showed that SiO_2, Al_2O_3, CaO, S, and Ga are lost and Fe_2O_3, MnO, K_2O, H_2O, Cl, B, Rb and Cs enriched during such alteration. $^{87}Sr/^{86}Sr$ also tends to increase. Erratic behaviour was reported for MgO, Na_2O, P_2O_5, Ba, Ni and Cu, whereas little or no change was observed in the abundances of TiO_2, Zr, Sr, V, Zn, Cr, Co, Y and Nb (Hart et al., 1974).

The behaviour of rare earth elements during the submarine alteration of basalts is an open question. Kay et al. (1970), Frey et al. (1968), Philpotts et al. (1969) and O'Nions and Pankhurst (1976) noted that REE patterns for submarine greenstones and amphibolites were similar to those of unaltered basalts from the same areas. Fleet et al. (1976) reported that altered DSDP leg 26 basalts had retained their primary rare earth abundances, except for a slight enrichment in La relative to Ce. On the other hand, Frey et al. (1974) found significant disturbances in the REE contents of leg 2 and 3 DSDP basalts; the alteration effects upon the REE contents of the crystalline material were smaller than observed for the coexisting palagonite, but the REE patterns had still shifted from LREE depleted to LREE enriched.

Prograde metamorphism: oxygen isotope effects

Prograde regional metamorphism is unlikely to have affected the oxygen isotopic composition of Archean basalts unless migmatization and/or the injection of material has occurred. Progressive dehydration reactions involving H_2O (rather than CO_2) do not greatly affect the isotopic composition of the metamorphosed rock (Taylor, 1970; Turi and Taylor, 1971a) unless the isotopic system has been open to an external reservoir. This generally does not occur until at least upper amphibolite facies of metamorphism (Shieh and Schwarcz, 1974; Fourcade and Javoy, 1973; Longstaffe et al., 1977c; see also Chapter IV).

Prograde metamorphism: chemical effects

Winkler (1976) states that prograde metamorphism is quasi-isochemical (loss only of volatiles), at least until the onset of anatexis. Some investigators of Archean rocks support this claim (Viljoen and Viljoen, 1969; Hallberg, 1970; Glikson, 1971, 1972; Pearce and Birkett, 1974; Hart et al., 1970; Jahn et al., 1974). Pearce and Birkett (1974), for example, showed that massive lava flows from the Abitibi granite-greenstone belt retain coherent trends that are indicative of igneous processes, in spite of wide variations in grain size and degree of hydration. Similar results have

been reported for young greenstones from Japan (Sawada and Kanmera, 1973).

Linearity of Rb-Sr whole rock isochrons has been used as evidence for the isochemical metamorphism of Archean rocks (Glikson, 1972, 1976a; Jahn et al., 1974). This argument is not valid, however, as there are numerous cases where statistically sound whole rock isochrons yield dates for units that are significantly younger than ages known for overlying strata or obviously intruding bodies (Arth and Hanson, 1975). On the other hand, lack of linearity is evidence for open system alteration (Jahn et al., 1974).

It may be true that the most ubiquitous alteration found in Archean metabasalts, the hydration of pyroxene, is isochemical, but element transfer between small domains during the formation of albite, epidote, prehnite and pumpellyite has almost certainly taken place, at least within localized domains (Jolly, 1974, 1975). It is this sort of chemical migration, on a much larger scale, that can cause 'spilitic degradation' of basalt (Smith, 1968; Vallence, 1973; Jolly and Smith, 1972).

The chemical changes that accompany the onset of anatexis and then granulite facies metamorphism cannot be ignored. Hovorka (1974), for example, showed that the migmatization of mafic volcanic rocks was accompanied by enrichment in K_2O,

Na_2O and SiO_2. However, Green et al. (1972) found no major modifications in the REE patterns or abundances between amphibolite and granulite facies dioritic-gabbroic rocks from Norway.

Retrograde metamorphism: chemical effects

Some studies (Heier and Thoresen, 1971; Green et al., 1972) report no significant chemical differences between completely retrograded and non-retrograded mafic (and acid) granulites. However, Drury (1974) noted that Lewisian mafic (and acid) granulites retrograded to amphibolite facies became enriched in K, Rb, Th and Pb, and depleted in Ba, Sr, Ca and P; retrogradation to greenschist facies resulted in further enrichment of K, Ba, La and Ce.

Summary statement

It is virtually impossible to separate and identify the effects of each of these alteration processes upon a particular Archean metabasalt; only surficial weathering can be avoided by careful selection of samples. However, inadequate as it is, I shall assume that metabasalt samples with low K and Rb contents have not been seriously affected by any of these types of alteration; the abundances of these elements

in these rocks probably would increase during even mild metasomatism or seawater alteration.

III-5 OXYGEN ISOTOPIC GEOCHEMISTRY OF THE BURDITT LAKE - LAKE DESPAIR MAFIC METAVOLCANIC ROCKS AND ENCLAVES

The purpose of this section is to discuss the oxygen isotope data obtained for mafic metavolcanic rocks and enclaves from the Burditt Lake - Lake Despair area, and to attempt to correlate this information with chemical parameters such as K, Rb, Ba and Sr, all of which can be used as indices of alteration.

$\delta^{18}O$ (rock), K, Rb, Ba, and Sr for these rocks are given in Table 3-2. Complete chemical analyses are listed in Appendix IV. Some $\delta^{18}O$ (mineral) data are reported in Table 3-3. A few samples from other study areas are included here; the discussion for the Burditt Lake - Lake Despair area is equally pertinent to them.

The rocks range in $\delta^{18}O$ from 4.4 to 9.2°/$_{oo}$, larger than observed for unaltered basalts (Figure 3-5; Taylor, 1968).

Table 3-2 Comparison of $\delta^{18}O$ whole rock and LIL element abundances in the mafic metavolcanic rocks

Group	Sa. #	$\delta^{18}O$ °/₀₀	K (wt.%)	Rb (ppm)	Ba (ppm)	Sr (ppm)
BURDITT LAKE - LAKE DESPAIR						
greenschist facies	B1	7.03	0.10	2	44	135
	B3	7.48	0.48	10	87	62
	B5	8.96	0.29	9	142	121
	B6	8.36	0.24	5	53	113
	B8	9.17	0.23	4	244	124
amphibolite facies:						
least altered	F19	5.52±0.15	0.20	3	74	76
	F27	8.11	0.19	5	85	66
	F115	7.53	0.25	7	68	102
altered	F44	5.69	1.14	41	280	305
	F49	5.95	0.76	41	139	182
	F116	4.37	0.87	53	105	138
large mafic enclaves	*D4	5.63±0.18	0.31	4	146	137
	*F134		0.42	4	175	208
	*F80	4.50±0.08	0.40	2	142	306
	*F145		0.51	3	161	184
	**F107	5.65	0.46	5	92	155
	**F15	6.38	0.51	4	89	139
	**F100	5.58	0.46	6	64	123
small mafic enclaves	*F22		1.62	79	580	1376
	*D6		2.67	71	2251	1435
	**F105		0.49	11	92	158
ultrabasic rocks	B2	5.34	0.02	2	16	5
	B4	6.39	0.01	1	19	7
	B7	6.76	0.01	<1	18	5

Table 3-2/continued

Group	Sa. #	$\delta^{18}O$ °/oo	K (wt.%)	Rb (ppm)	Ba (ppm)	Sr (ppm)
ultrabasic pods	**F59		0.99	33	476.	417
	**F89		3.64	202	1007	305
KIRKLAND LAKE						
greenschist facies mafic tuff	D43	9.01	1.51	50	229	147
ABRAM LAKE						
greenschist facies andesite	AR17	9.39	2.56	97	1326	1226
KENORA AREA						
mafic amphibolites	G835A	5.69	0.12	2	30	145
	G867A	4.81	0.38	3	46	105

*within Jackfish Lake Complex
**within Footprint Gneiss

Table 3-3 $\delta^{18}O$ mineral results, mafic amphibolites (‰)

Sample No.	Rock	Hornblende	Plagioclase	Locality
F19	5.52±0.15	4.23	4.92	Lake Despair
F49	5.95	3.77	6.28	Lake Despair
G835A	5.69	4.89		Kenora Area
G867A	4.81	4.72	7.46	Kenora Area

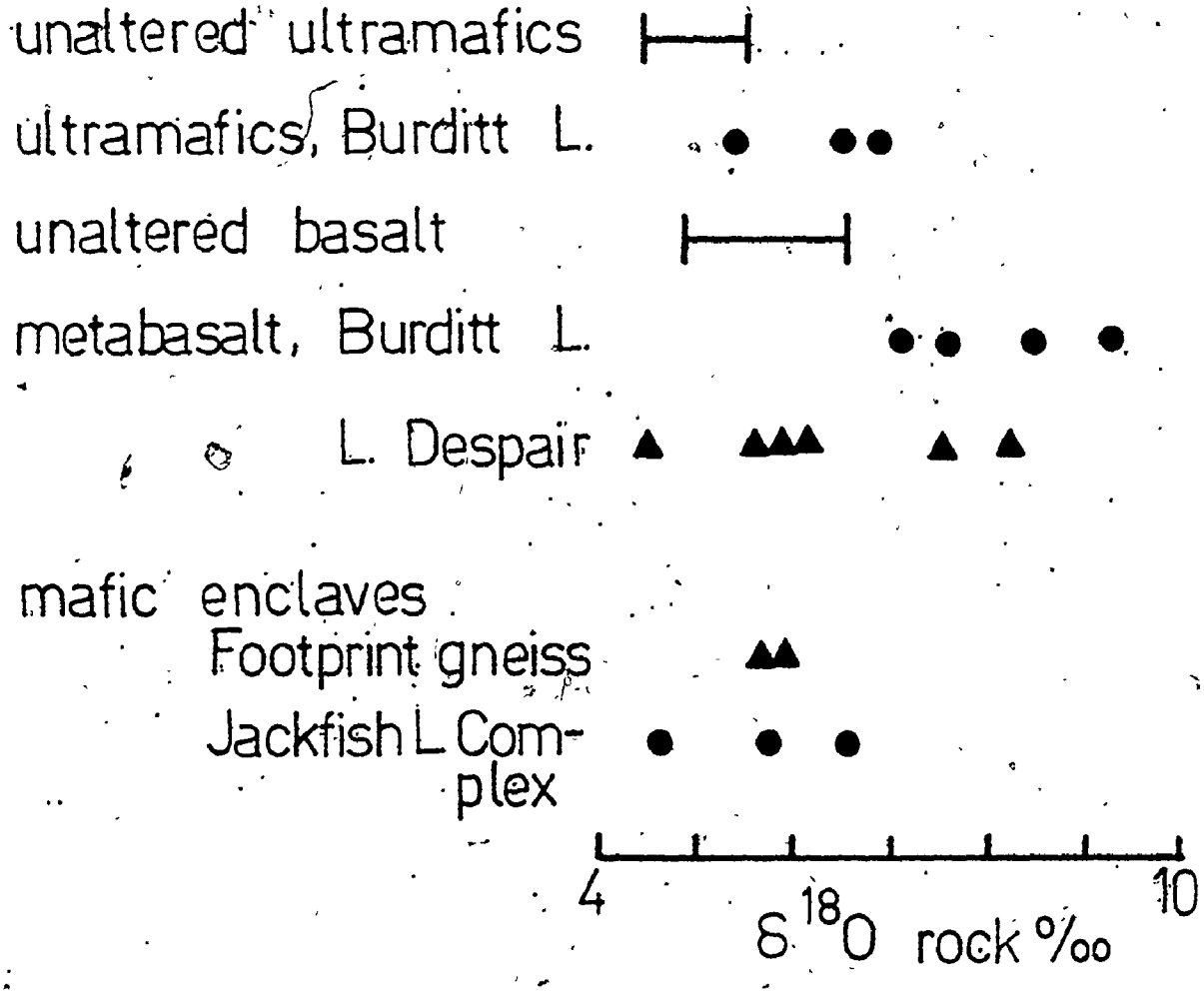

FIGURE 3-5 $\delta^{18}O$ rock results for mafic and ultramafic rocks from the Burditt Lake - Lake Despair area. The ranges shown for unaltered rocks are taken from Taylor (1968).

● greenschist facies

▲ amphibolite facies

Burditt Lake metabasalts, and associated ultramafic rocks

Systematic enrichment in ^{18}O has been observed for the greenschist facies metabasalts from Burditt Lake (B1, B3, B5, B6, B8); $\delta^{18}O$ values increase from 7.0°/$_{oo}$ at the northern end of Burditt Lake to 9.2°/$_{oo}$ near the Burditt Lake pluton, approximately three kilometers along strike. The $\delta^{18}O$ results for the ultramafic bodies found within the sequence (B2, B4, B7) echo this enrichment pattern. While this pattern might suggest magmatic water (from the stock) interaction with the mafic and ultramafic rocks, there are problems with such a hypothesis. Firstly, the stock derived fluids would have to interact with country rock over a radius of six kilometers, unless the pluton is oriented at a peculiar attitude. The normal limit of such interaction is about two kilometers for stocks similar in size to the Burditt Lake pluton (Turi and Taylor, 1971a,b). Secondly, a study of samples obtained across the felsic metavolcanic rocks, adjacent to the pluton, indicates that the magmatic water-rock interaction (at least in the felsic metavolcanic rocks) is limited to within 1700 meters of the contact (section III-7). Thirdly, except for the high K content of B3, there is little petrographic or chemical evidence to suggest that these rocks have been altered to a greater extent than others which exhibit 'normal' isotopic

compositions. Further investigation is therefore required before a completely satisfactory explanation of these data will be obtained.

Low ^{18}O metabasalts

Some of the analyzed mafic metavolcanic rocks have low $\delta^{18}O$ values (4.4-4.8‰, F116, F80, G867A). Barker et al. (1976b) reported $\delta^{18}O$ values of 4-7‰ (mean $\delta^{18}O = 4.9‰$) for seven seemingly unaltered Archean mafic amphibolites. If Archean basalts, for some petrogenetic reason, are depleted in ^{18}O relative to younger basalt, then the values observed may be primary, despite the somewhat high K, and/or Rb, Sr and Ba contents of these three samples. There are several irreconcilable problems with such a hypothesis. Only a very few examples of primary low ^{18}O basalts are known (Muehlenbachs et al., 1974; Muehlenbachs, 1977); on the other hand, submarine metamorphism is known to produce ^{18}O depletion in amphibolites, a process that can be, but not always is, accompanied by chemical alteration (section III-4). Such activity is probably the best explanation for our results.

Isotopically and chemically 'least altered' metabasalts

Some mafic amphibolites (but remarkably few, if this sampling is any indication) appear to have preserved both chemical and bulk isotopic compositions similar to unaltered basalt (F19, G835A). Even in these rocks, however, some isotopic disequilibrium appears to exist between minerals. For example, the plagioclase and hornblende of F19 preserve an isotopic temperature of 980°C, even though the hornblende is a metamorphic mineral. Other samples (F49, G867A) have more reasonable temperatures preserved by plagioclase-hornblende pairs (450-460°C) (Appendix I).

Other mafic amphibolites (F27, F115), although they appear chemically 'least altered', have high $\delta^{18}O$ values. However, they are located near the contact with the Jackfish Lake Complex and an ultramafic intrusion, respectively (Figure 3-3). The change in $\delta^{18}O$ may be related to small scale isotopic exchange with fluids from these plutonic rocks down to temperatures of about 450°C.

Isotopically and chemically 'altered' metabasalts and enclaves

Samples Du3 and Ar17 are chemically altered and have high $\delta^{18}O$ values; these data suggest that low temperature weathering has affected these rocks.

Some mafic amphibolites (F44, F49), which are enriched in K, Rb, Sr and Ba, have seemingly undisturbed oxygen isotopic compositions; any chemical alteration has left the oxygen isotope system apparently unaffected.

The preservation of 'primary' $\delta^{18}O$ values (5.6-6.4°/$_{oo}$) in the mafic enclaves (D4, F107, F15, F100) is probably, in part, fortuitous. Enclave D4 has been metamorphosed only to upper greenschist facies, and appears not to have chemically exchanged with the Jackfish Lake Complex (section III-6). Its $\delta^{18}O$ value may therefore be primary. However, if the enclave did isotopically re-equilibrate with its country rock at magmatic temperatures, its present value would not be much different, as the $\delta^{18}O$ of the surrounding diorite is only 6.4°/$_{oo}$ (F146). The remaining enclaves are located within the Footprint gneiss, and have been metamorphosed to amphibolite facies, and more or less migmatized (Photos E, F, G). Discussions in Chapter IV will show that migmatization is often accompanied by oxygen isotope re-equilibration down to $\delta^{18}O$ values of 6°/$_{oo}$, regardless of the pre-anatectic isotopic composition of the migmatized rock. For example, samples of migmatized Footprint tonalitic gneiss have $\delta^{18}O$ values as low as 5.9°/$_{oo}$. It may be worth noting that none of the enclaves have high $\delta^{18}O$ values, such as were found for other mafic metavolcanic rocks.

Conclusion

Isotopic alteration of Archean metabasalts is not necessarily accompanied by chemical alteration, and chemical alteration can occur without the isotopic systems having been subjected to open system exchange. Also, as with chemical data, 'unaltered' isotopic values may in fact reflect a complex series of events, rather than the preservation of a primary composition.

III-6 ELEMENTAL GEOCHEMISTRY OF THE MAFIC METAVOLCANIC ROCKS

Since $\delta^{18}O$ rock compositions have proven unsatisfactory for the detection of sample alteration or 'freshness', more usual, but more subjective tests for alteration have been applied to the mafic metavolcanic rocks. Samples exhibiting moderate to severe sericitization or saussuritization have been considered as altered; those samples with low LIL abundance levels and appearing relatively fresh in thin section have been considered 'least altered'.

The least-altered mafic metavolcanic rocks and large mafic enclaves are tholeiitic (Figure 3-6), and plot within the silica saturated and silica oversaturated fields of Yoder and Tilley (1962). Some very small enclaves are

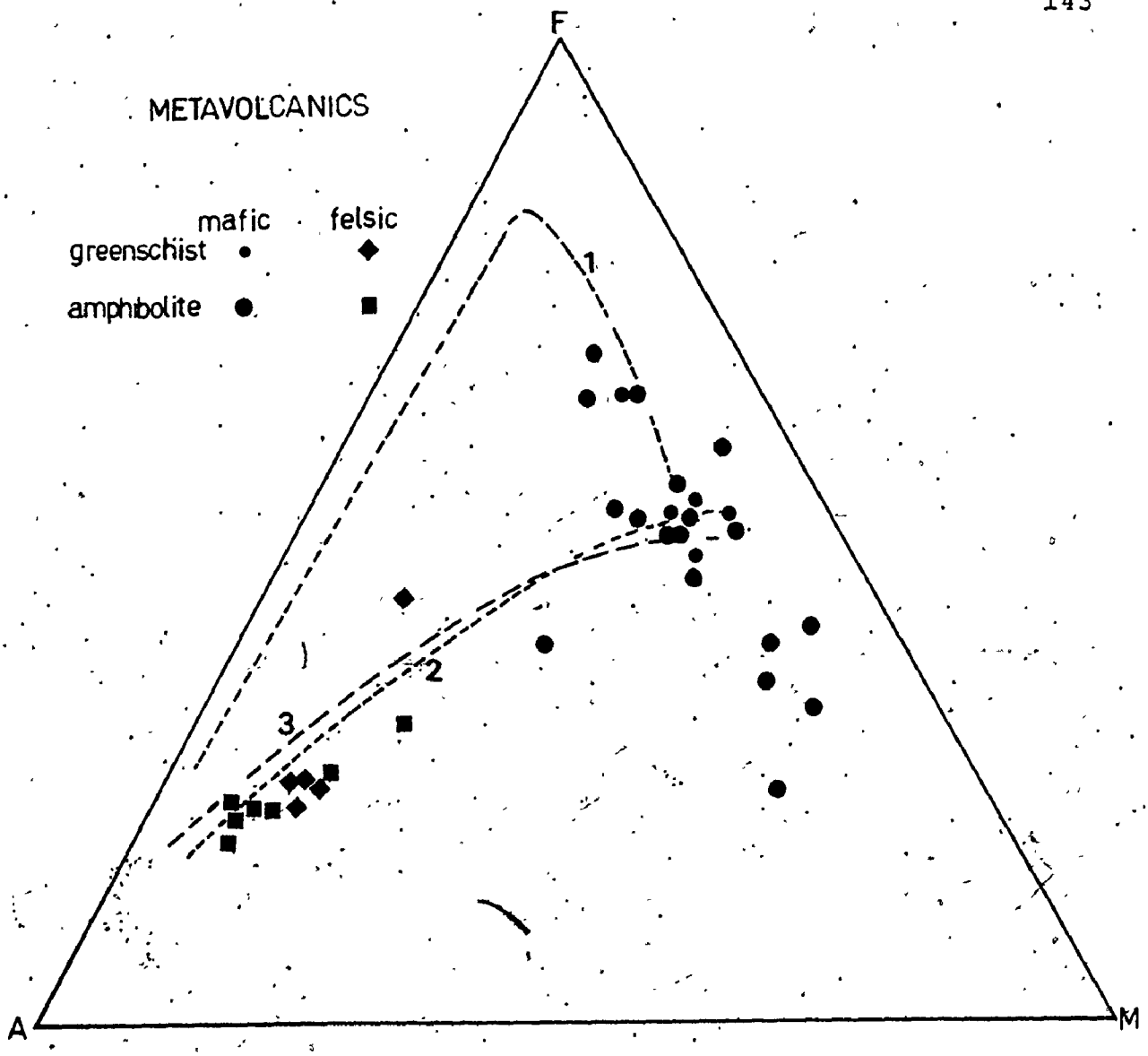

FIGURE 3-6 AFM diagram for the Burditt Lake - Lake Despair metavolcanic rocks.

1. Skaergaard tholeiitic trend
2. calc-alkaline Cascade volcanics trend
3. calc-alkaline Lower California Batholith trend

Trend lines taken from Carmichael et al. (1974).

$A = Na_2O + K_2O$

$F = FeO^t$

$M = MgO$

feldspathoid normative (Figure 3-4), but that is a function of chemical modification by their host magmas.

The average chemical composition of the 'least-altered' tholeiites is similar to other Archean mafic metavolcanic rocks (Table 3-4). The higher MgO contents of the greenschist facies Burditt Lake metavolcanic rocks may reflect their association with interlayered ultramafic bodies (Table 3-4, #1). Lower MgO contents for mafic metavolcanic rocks located elsewhere within the study area have been reported (Blackburn, 1976a; Table 3-4, #4).

There are major element chemical variations between the greenschist facies and amphibolite facies mafic metavolcanic rocks:

	greenschist facies		amphibolite facies	
	mean	range	mean	range
CaO wt.%	9.8	(8.7-10.7)	12.2	(10.3-13.4)
Na_2O	2.4	(1.5-3.1)	1.7	(0.9-2.2)
$Fe_2O_3{}^t$	12.7	(11.6-14.8)	10.4	(8.3-11.5)
TiO_2	0.9	(0.6-1.5)	0.6	(0.4-0.7)

Table 3-4 Chemical comparison, Archean tholeiites (least altered)

	1	2	3a	3b	4	5	6	7	8	9
SiO_2	52.95	52.74	49.46	49.56	53.75	51.40	52.21	52.30		51.07
TiO_2	0.92	0.56	1.33	0.87	1.03	1.41	1.05	0.98		1.02
Al_2O_3	14.27	14.85	15.02	15.45	14.99	14.03	15.66	15.09		14.99
FeO*	11.56	9.47	13.95	10.93	11.17	12.62	11.63	10.74		12.44
MnO	0.20	0.19	0.28	0.19	0.21	0.23	0.20			0.22
MgO	7.48	7.88	5.24	7.85	5.70	6.81	6.63	6.83		6.84
CaO	9.78	12.18	11.24	11.71	1.05	8.53	9.87	11.01		11.20
Na_2O	2.41	1.73	2.82	2.75	1.92	2.83	2.22	2.75		2.11
K_2O	0.33	0.26	0.48	0.54	0.12	0.30	0.34	0.18		0.11
P_2O_5	0.10	0.14	0.18	0.15	0.06	0.14	0.19	0.12		
Rb	6	5	3	5		5		9	5.90	
Sr	111	81	209	139	98	150	164	105	175	
Ba	114	76	156	82		70	105		70	
K/Rb	448	427	1356	880		481		430	360	
Sr/Ba	0.974	1.066	1.34	1.70		2.14	1.56		2.50	
Rb/Sr	0.054	0.062	0.014	0.036		0.033			0.034	
Ce	6	t	9	2						
Pb	4	4	7	4	10					
Zn	86	64	110	87	85					
Ni	92	90	89	120	105					
Zr	44	32	66	39						
Y	20	15	28	17						
Nb	t	t	t	t						

Notes for Table 3-4 Chemical comparison, Archean tholeiites (least altered)

* All analyses recalculated to 100%, anhydrous, total Fe as FeO

See Appendix IV for actual analyses

1. av. 5 greenschist facies metabasalts, Burditt Lake area (least altered)

2. av. 3 amphibolite facies metabasalts, Lake Despair area (least altered)

3a. av. 4 amphibolite facies enclaves (over 1000 m in length) from within the Jackfish Lake Complex

3b. av. 3 amphibolite facies enclaves (over 1000 m in length) from within the Footprint Gneiss

4. av. 4 metabasalts, Off Lake-Burditt Lake area; C. Blackburn (1972)

5. av. 5 tholeiites, Vermilion District; Arth and Hanson (1975)

6. average basalt of the Canadian Shield; Baragar and Goodwin (1969)

7. av. 337 basalts, Early Precambrian Eastern Goldfields; Hallberg and Williams (1972)

8. composite basalt from 3 Archean greenstone belts in the Canadian Shield; Hart et al. (1970)

9. average mafic metavolcanic, Wabigoon greenstone belt; Goodwin (1976 a)

The greenschist facies metavolcanics are usually quartz normative; the amphibolite facies representatives are predominantly olivine normative. The two units are also geographically distinct, the amphibolites overlying felsic schists, which, in turn, overlie or are interlayered with the greenschist facies metabasalts in the vicinity of Burditt Lake. It is likely that the chemical differences are primary, representing differences between flows or groups of flows.

The large mafic enclaves within the Jackfish Lake Complex occasionally retain pillow structures, and are volcanic in origin. Their chemistry is somewhat different from the other mafic metavolcanic rocks (Table 3-4, #3a); average values of SiO_2 and MgO are lower and TiO_2, MnO, FeO, P_2O_5, K_2O and Na_2O higher than the least altered greenschist facies or amphibolite facies mafic metavolcanics. Some of the differences could be the result of contamination by the host magma, but this process cannot account for all of the variations. For example, two small Jackfish Lake Complex enclaves (F22, D6), in various stages of digestion, are enriched in SiO_2, and depleted in TiO_2, FeO and MnO, a predictable result of chemical overprinting by the Jackfish Lake Complex magma. However, exactly opposite variations are observed for the large mafic enclaves. These perturbations are probably the result of primary compositional variations that are preserved best in the least altered,

large mafic enclaves.

Since the mafic enclaves within the Footprint gneiss are migmatized, a true estimate of their original composition is impossible. The few results obtained (Table 3-4, #3b; Appendix IV), however, are not notably enriched in K, Na and Sr, as would be expected for exchange with Footprint gneiss mobilisate.

Trace elements and tectonic setting

Many attempts have been made to compare the trace element geochemistry of Archean metabasalts to more modern analogues. Some limiting factors that inhibit such comparisons are the problems of element mobility, and the possibility of a somewhat unique mantle chemistry (Chapter I-2) during the Archean. Such problems not withstanding, some attempt to determine the tectonic environment of the Burditt Lake - Lake Despair mafic metavolcanic rocks can still be made.

The average values of Rb, Ba, and K/Rb of the metabasalts (Table 3-5) are similar to other Archean mafic metavolcanic rocks. Sr is low (and therefore Rb/Sr and Ba/Sr high), but it is still within the observed range for least altered Archean mafic metavolcanic rocks. Modern low K arc tholeiites are similar to all of these Archean metabasalts in K and Ba contents (Table 3-5), but the modern rocks

Table 3-5 LIL geochemistry - Archean mafic metavolcanics and modern island arc tholeiites

Ref.	K ppm	Rb ppm	Sr ppm	Ba ppm	K/Rb	Rb/Sr	Locality
1		13		90	490		Australia
2	1790	5	146	63	580	0.036	Minnesota
3	2106	6	175	70	351	0.034	Superior Province
4	2359	6	153	98	370	0.042	W. Australia & Canada
5	2490	5	150	70	481	0.033	Minnesota
6	2820		164	105			Canadian Shield
7	1500	9	105		430		W. Australia.
8	2740	6	111	114	448	0.054	Burditt Lake
9	2160	5	81	76	427	0.062	Lake Despair
10	2170	3	250	100	680	0.012	low K tholeiites

1. White et al. (1971)
2. Jahn et al. (1974)
3. Hart et al. (1970)
4. Jahn et al. (1974)
5. Arth and Hanson (1975)
6. Baragar and Goodwin (1969)
7. Hallberg and Williams (1972)
8. this work
9. this work
10. Jahn et al. (1974)

are somewhat lower in Rb and higher in Sr than the Archean rocks.

The immobile elements Ti, Zr, Y, Nb, REEs, and to a lesser extent, Sr, may be better suited to trace element tectonic classification schemes, since these elements are less affected by alteration than K, Rb and Ba (Cann, 1970). Smith and Smith (1976) analyzed many samples from an altered and metamorphosed basalt outcrop and found that diagrams or classification schemes using Ti, Zr, Y and P contained points that clustered closely together in spite of the mineralogical nature of the metamorphic domain involved (albitized basalt, prehnite-pumpellyite, epidote). Points plotted on diagrams using K and Sr showed distinct correlations with metamorphic mineralogy.

Pearce and Cann (1973) proposed a basalt classification based on three variation diagrams:

1. Ti-Zr (Figure 3-8); valid for metamorphosed basalts;
2. Ti/100-Zr-Y X 3 (Figure 3-7); valid for metamorphosed basalts;
3. Ti/100-Zr-Sr/2 (Figure 3-9); valid for unaltered basalts.

In addition, they stated that basalts with Y/Nb>3 were tholeiitic.

Y/Nb ratios are not accurately known for the samples

FIGURE 3-7 Ti-Zr-Y diagram for the Burditt Lake - Lake Despair area mafic metavolcanic rocks (after Pearce and Cann, 1973).

A. low K tholeiites (island arc environment)

B. ocean floor basalts (ridge environment) and the field of overlap for A and C

C. calc-alkali basalts (island arc environment)

D. ocean island and continental basalts (within plate environment)

\+ amphibolite facies metavolcanic rocks

● greenschist facies metavolcanic rocks

□ large mafic enclaves, Jackfish Lake Complex

△ large mafic enclaves, Footprint gneiss

FIGURE 3-8 Ti-Zr diagram for the Burditt Lake - Lake Despair area mafic metavolcanic rocks (after Pearce and Cann, 1973). Legend as in Figure 3-7.

A. low K tholeiites (island arc environment)

B. field of overlap for A, C and D

C. calc-alkali basalt (island arc environment)

D. ocean floor basalts (ridge environment)

1. Floyd and Winchester (1975) line for tholeiitic basalts

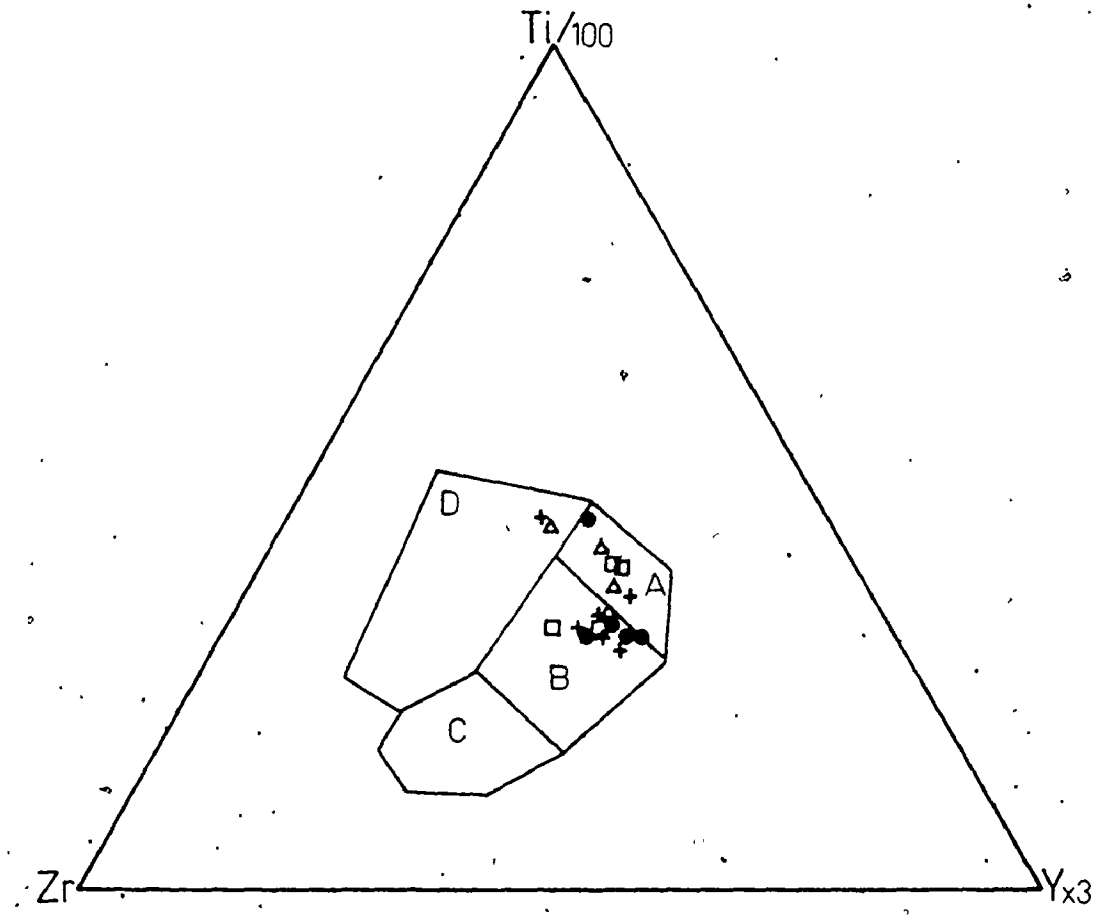
Ti/100
Zr
Y x3
A
B
C
D

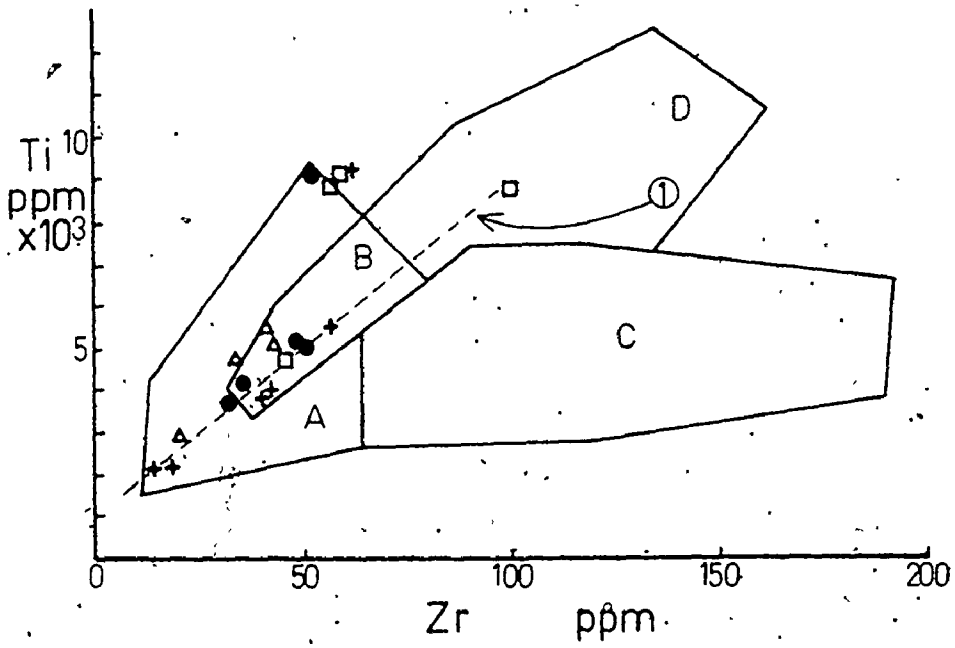
Ti ppm x10³
10
5
0
50
100
150
200
Zr ppm
A
B
C
D
1

FIGURE 3-9 Ti-Zr-Sr diagram for the Burditt Lake - Lake Despair area metavolcanic rocks (after Pearce and Cann, 1973). Legend as in Figure 3-7.

A. low K tholeiites (island arc environment)

B. calc-alkali basalts (island arc environment)

C. ocean floor basalts (ridge environment)

FIGURE 3-10 TiO_2-K_2O-P_2O_5 diagram for the Burditt Lake - Lake Despair area mafic metavolcanic rocks (after Pearce et al., 1975). Legend as in Figure 3-7. Some altered metabasalts not shown in Figures 3-7, 3-8 and 3-9 are included here: ⊕

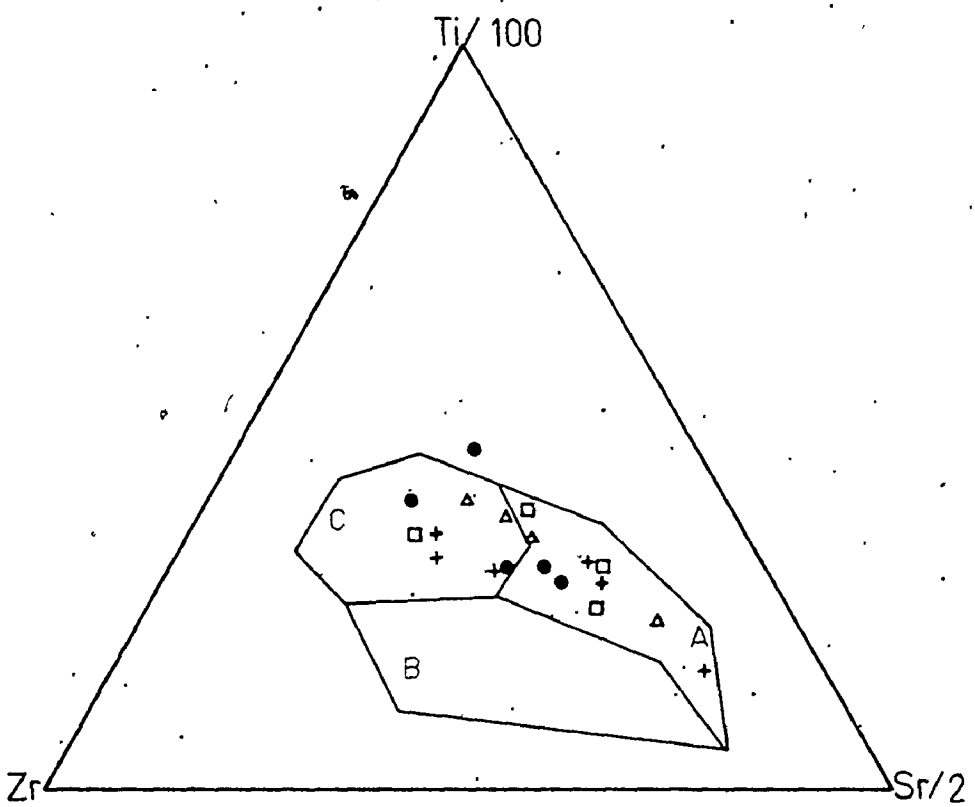
Ti/100
Zr
Sr/2
A
B
C

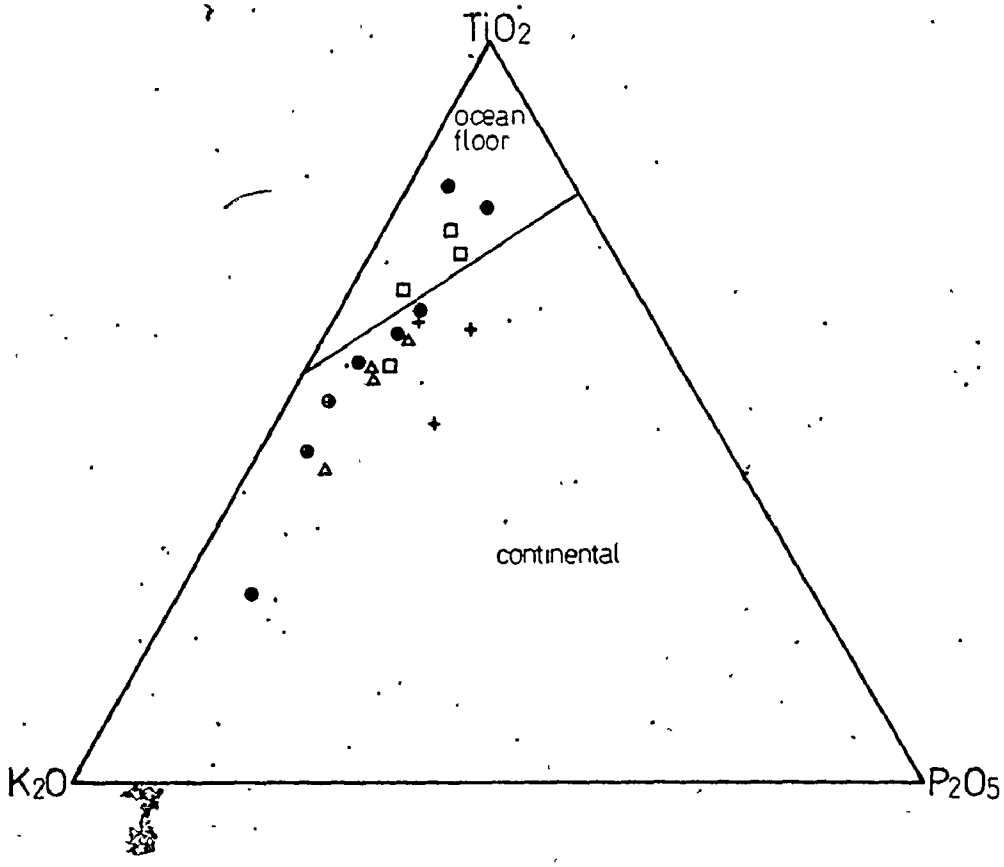
TiO2
ocean
floor
continental
K2O
P2O5

analyzed in this study as most of the Nb values were below detection limits (3 ppm). However, a minimum ratio of 6 can be assigned to these rocks, indicating a tholeiitic affinity. The precision and accuracy for the other elements is equal to that of Pearce and Cann (1973) (Appendix IV).

Figure 3-7 shows that most of the data points lie within the low K tholeiite field (A) or the field of overlap of low K tholeiites, ocean floor tholeiites, and calc-alkali basalts (B). Figure 3-8 indicates that many of the analyses lie within the field of low K arc tholeiites (A), but there are many that lie in the field of overlap (B). If Sr immobility is assumed, Figure 3-9 eliminates calc-alkali basalts.

These diagrams suggest that the Burditt Lake - Lake Despair metabasalts are most like modern low K arc tholeiites or ocean floor (ridge) tholeiites. Similar variation diagrams, proposed by Floyd and Winchester (1975), also indicate a tholeiitic origin for these mafic metavolcanic rocks (Figure 3-8).

Pearce et al. (1975) proposed to discriminate between oceanic and continental basalts by their K_2O, P_2O_5, and TiO_2 contents (Figure 3-10). The major drawback of such a scheme is the use of K_2O; potassium enrichment due to alteration will cause basalts of oceanic affinity to approach

'continental' compositions. Figure 3-10 shows that most of our samples do lie within the continental field, an observation also made for the Wabigoon greenstone belt in general by Pearce et al. (1975). I suspect that this trend towards the K_2O apex is indicative of at least some K_2O enrichment in most of our samples, including those believed to be least altered.

A final word of caution is in order. Lambert and Holland (1974) believe that Y levels in Archean basalts were lower than in modern basalts. If the Archean mantle contained different levels of elements such as Y than it does now, any classification based on such elements will reflect source conditions rather than tectonic environments.

Rare earth elements (REE)

Many authors have used REE data to identify tectonic environments for Archean metabasalts. Modern mid-ocean ridge basalts appear to be derived from a LIL and LREE depleted low velocity zone of the mantle (Schilling, 1971; Schilling and Bonatti, 1975). Jakes and Gill (1970) pointed out that island arc tholeiites also exhibit chondritic REE patterns, and frequently were more depleted in total REEs than ridge basalts (Figure 3-11). Subsequent studies (Jakes and White, 1972; Ewart and Bryan, 1972, 1973; Ewart et al.,

1973) established the geochemical nature of the arc tholeiite series more firmly, and also documented the change to more calc-alkali basaltic geochemistry with increasing maturity of the arc.

Based upon these modern patterns, arc tholeiite affinities have been suggested for the Norseman greenstones, Western Australia (White et al., 1971), for mafic metavolcanic rocks from Wyoming, Yellowknife and Swaziland (Condie and Baragar, 1974) and for the Vermilion greenstones of Minnesota (Jahn et al., 1974; Arth and Hanson, 1975). Similarity to ocean ridge basalts has been claimed for the Mafic Formation of the Midlands greenstones, and there are some indications that the Maliyama Formation of Rhodesia is of calc-alkaline tholeiite affinity (Condie and Harrison, 1976).

Results

Chondrite normalized REE abundances (Masuda, 1968) for the Burditt Lake - Lake Despair mafic metavolcanic rocks have been plotted versus atomic number (Figure 3-11); complete chemical analyses of the samples analyzed for REEs, along with some values for modern tholeiites are given in Table 3-6.

REE results for the least altered Burditt Lake meta-tholeiites (Table 3-6, #4,5) show the greatest similarity to the modern arc tholeiites (Table 3-6, #2; Figure 3-11). The

Table 3-6 Selected analyses: mafic metavolcanic rocks

		1	2	3	4	5	6	7	8
SiO_2	wt %	49.8	51.1	50.2	51.9	51.9	50.2	48.3	47.8
Al_2O_3		16.0	16.1	16.4	13.9	15.0	15.5	15.1	15.6
TiO_2		1.5	0.83	1.0	0.82	0.68	0.35	0.80	1.4
Fe_2O_3		10.0	11.8	11.3	11.7	11.6	8.26	11.2	14.6
MnO		-	-	-	0.19	0.20	0.16	0.18	0.35
MgO		7.50	6.10	6.30	6.87	8.05	9.68	8.77	4.31
CaO		11.2	10.8	10.7	10.0	10.7	12.4	11.3	11.1
Na_2O		2.75	1.96	3.00	2.82	1.53	2.16	2.98	3.02
K_2O		0.14	0.30	0.40	0.12	0.35	0.24	0.54	0.36
P_2O_5		-	-	-	0.13	0.10	0.14	0.15	0.24
LOI		-	-	-	2.89	3.31	1.40	1.33	1.05
Li	ppm	-	-	-	-	-	-	-	-
Rb		1	5	10	1.5	9	2.5	5	4
Sr		135	225	330	135	62	76	155	137
Ba		11	50	115	44	87	74	92	146
Pb		-	2	3	4	4	5	8	8
Th		-	-	-	0.70	t	0.61	t	1.6
Y		30	20	25	20	20	8	16	33
Nb		-	-	-	t	t	t	N.D.	4
Zr		85	60	100	50	36	15	33	101
Zn		-	-	-	44	74	41	81	89
Ni		100	25	25	58	85	93	64	89
Ta		-	-	-	0.41	0.27	0.59	0.56	0.77
Hf		-	-	-	3.5	5.7	7.9	5.3	4.3
Sc		-	-	-	25.6	22.1	22.8	30.0	36.9
La		3.9	3.3	10	4	2.2	1.6	2.3	9.9
Ce		12	6.7	19	10.1	6.8	3.8	6.5	20.6
Nd		-	-	-	5.4	3.2	3.4	4.1	13.2
Sm		3.9	2.2	4.0	1.9	1.6	0.75	1.7	3.5
Eu		1.4	0.76	1.3	0.68	0.51	0.28	0.60	1.2
Gd		-	-	-	-	-	-	-	-
Tb		1.2	0.40	0.80	0.45	0.46	0.32	0.42	0.75
Tm		-	-	-	0.30	0.33	0.26	0.29	0.45
Yb		4.0	1.9	2.7	2.0	2.1	0.81	2.1	3.8
Lu		0.40	0.30	0.30	0.33	0.29	0.13	0.25	0.53
Tl		-	-	-	-	-	-	-	-

Notes to Table 3-6 Selected analyses: mafic metavolcanic rocks

All analyses reported with $Fe^t = Fe_2O_3$, data not renormalized to 100%.

t = trace; N.D. = not detected

1. Modern rise tholeiite; Condie and Harrison (1976)
2. Modern arc tholeiite; Condie and Harrison (1976)
3. Modern calc-alkali tholeiite; Condie and Harrison (1976)
4. B1, greenschist facies metabasalt
5. B5, greenschist facies metabasalt
6. F19, amphibolite facies metabasalt
7. F107, amphibolite facies mafic enclave in Footprint gneiss
8. D4, greenschist facies mafic enclave in Jackfish Lake Complex diorite

similarity extends to Y, Ba, Zr and Ti. Ni values are more akin to those of modern ocean ridge tholeiites; high Ni seems to be a characteristic of almost all Archean metabasalts. The mafic enclave from the Footprint gneiss (Table 3-6, #7) also has REE abundances similar to modern arc tholeiites. All are low in Sc; this may reflect the presence of residual kyanite during the formation of these basalts (Gill, 1974).

The REE pattern of F19 (Lake Despair mafic amphibolite; Figure 3-11, #4) is peculiar. REE contents are low, and the pattern is not flat.

Jackfish Lake Complex mafic enclave D4 was analyzed because of its low metamorphic grade and its low Sr content (137 ppm), features that suggest only limited chemical modification of the rock by the surrounding Jackfish Lake Complex (Sr = 600-2700 ppm). The REE values of this enclave are almost identical to those observed for calc-alkali tholeiites (Figure 3-11; Table 3-6, #3,8). The comparison can be extended to include Na, K, Zr and Ba. The sample is also enriched in Th, Pb, Zn, Nb, Ta and Sc relative to the other metabasalts analyzed for REEs. Comparison of the REE content of the enclave with that of the nearby dioritic host rock (Table 3-20, F146) shows that enclave enrichment in La, Ce, Nd, Sm and Eu could be achieved by transfer of LREEs from the diorite. However, the HREEs and Th, Pb, Zn, Nb, Ta, Hf,

Sc, and Zr contents of the enclave are two to three times that of the host diorite. Also, if large scale chemical contamination has affected the enclave, why is its Rb content only 4 ppm, while the surrounding diorite contains close to 30 ppm, and why is its Sr content only 137 ppm, when the nearby diorite has 640 ppm?

REE modelling and basalt petrogenesis

It is possible that REEs cannot be used to distinguish the crustal environment in which Archean metabasalts have formed. Gill and Bridgwater (1976), for example, report that the Isua-type mafic dikes, intruded into granitic crust, have REE chemistry similar to ocean ridge basalts. These authors suggest that the REEs reflect the mantle melting regime or the melt differentiation path rather than tectonic setting.

The use of REE modelling, as a petrogenetic tool, accompanied the development of precise techniques for the measurement of REEs, the belief in the immobility of REEs during alteration, and the acquisition of data for REE partition coefficients (Higuchi and Nagasawa, 1969; Nagasawa, 1971; Cullers et al., 1973; Myson, 1976; Arth and Barker, 1976). The trace element modelling is usually performed using the Rayleigh fractionation law, and modal and non-modal

equilibrium partial melting relationships developed by Shaw (1970) and briefly summarized by Arth (1976a). More esoteric models involving volatiles, disequilibrium, incongruent melting, and other geologically realistic situations are available, but the present uncertainty in distribution coefficients, as well as the incomplete knowledge of mantle phase relationships and chemistry makes it difficult to separate real differences predicted by these models from spurious correlations.

Only the simple modal and non-modal equilibrium melting relationships summarized by Arth (1976a) will be used in this thesis. I fully realize that good model-data correspondence does not prove the operation of any particular process, but merely indicates its possibility. Batch melting will be assumed (the continuous equilibration of the liquid phase with a residual solid until the removal of the liquid). The equations for this process have been summarized by Arth (1976a);

(1) $C_L/C_o = 1 / (D_o + F(1 - P))$ Shaw (1970)

F = fraction of melting

C_o = initial trace element concentration of the solid

C_L = trace element concentration of the liquid

(2) D_o = bulk distribution coefficient

$= X_o{}^a K^{a-L} + X_o{}^b K^{b-L} + \ldots$

$X_o{}^a$ = weight fraction of phase a

K^{a-L} = solid-liquid distribution coefficient of a

(3) P = non-modal melting factor

$= p^a K^{a-L} + p^b K^{b-L} + \ldots$

p^a = fraction of liquid contributed by a during melting.

For modal melting $P = D_o$.

These equations will be used for all modelling of trace element data performed in this thesis.

REE models for the Lake Despair - Burditt Lake metabasalts

Most of the Burditt Lake metabasalts are quartz normative. Since there is a rough correlation between Ni and normative olivine in the analyzed metabasalts, the olivine or quartz normative nature of the least altered samples probably reflects the presence or absence of olivine in the rock prior to metamorphism.

Partial melting of anhydrous peridotite yields quartz normative melts only at pressures of less than 5 kb (Carmichael et al., 1974; Ringwood, 1975). If the mantle rock (or the hypothetical 'pyrolite' of Green and Ringwood, 1968) is hydrous, this pressure constraint no longer applies. Both low pressure (anhydrous) and higher pressure (hydrous) mantle mineralogies must therefore be considered in the REE modelling for the basalts.

Low pressure (anhydrous) models

Non-modal equilibrium batch melting models for 10, 25, and 35% melting of pyrolite (taken from Arth and Hanson, 1975) containing the REE concentrations equivalent to three times chondrites, are shown in Figure 3-12. The pyrolite mineralogy (olivine-orthopyroxene-clinopyroxene-plagioclase-quartz) is the normative composition of pyrolite at 0 to 5 kb.

High pressure (hydrous) models

30% to 60% melting models of spinel lherzolite (olivine-orthopyroxene-clinopyroxene-spinel) (taken from Condie and Harrison, 1976) are shown in Figure 3-12; this parent mineralogy is stable at pressures of 10 to 20 kb.

FIGURE 3-11 Chondrite normalized rare earth element results for the Burditt Lake - Lake Despair mafic metavolcanic rocks. The horizontal axis in this and subsequent REE diagrams is plotted in units of atomic number. The fields for modern ocean ridge and arc tholeiites are from Condie and Harrison (1976).

FIGURE 3-12 Chondrite normalized rare earth element melting model results for the Burditt Lake - Lake Despair mafic metavolcanic rocks.

A. 10% equilibrium non-modal melting of a parent pyrolite composed of 63% olivine, 15% orthopyroxene, 7% clinopyroxene and 10% plagioclase, as described by Arth and Hanson (1975).

B. 25% melting as described in A.

C. 35% melting as described in A.

D. 60% equilibrium non-modal melting of spinel lherzolite similar in chemical composition to the pyrolite described in A. Calculated after Condie and Harrison (1976).

E. 30% equilibrium non-modal melting of spinel lherzolite, as in D.

FIGURE 3-13 Chondrite normalized rare earth element model results for Jackfish Lake Complex mafic enclave D4.

F. Liquid remaining after 70% equilibrium bulk crystallization (50% plagioclase, 50% hornblende ± pyroxene) of a parent basaltic magma similar in chemical composition to the Burditt Lake metabasalts (B1, B5).

G. Liquid remaining after 70% equilibrium bulk crystallization of a parent magma (15% coesite, 50% clinopyroxene, 35% garnet) of similar chemical composition as F.

H. Liquid remaining after 70% equilibrium bulk crystallization (5% quartz, 25% hornblende, 45% clinopyroxene, 25% garnet) of a parent basaltic magma of similar chemical composition as F.

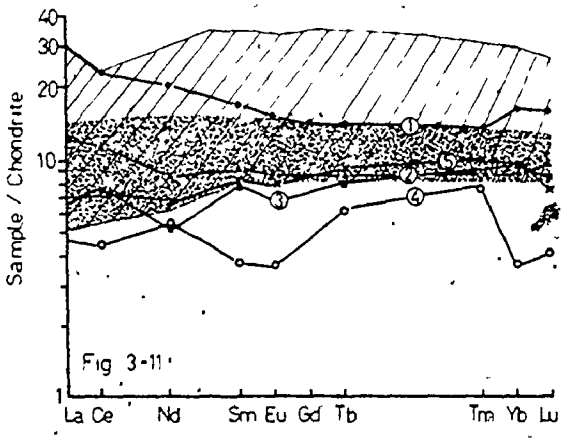

Fig 3-11

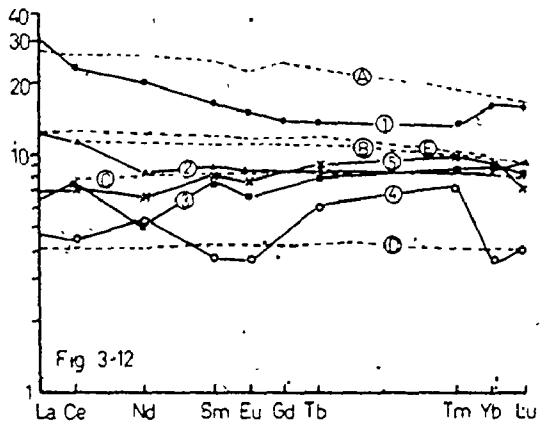

Fig 3-12

modern ocean ridge tholeiites

modern arc tholeiites

① D4 mafic enclave, JLC

② B1 Burditt Lake metabasalt

③ B5 Burditt Lake metabasalt

④ F19 mafic amphibolite

⑤ F107 mafic enclave, Footprint gneiss

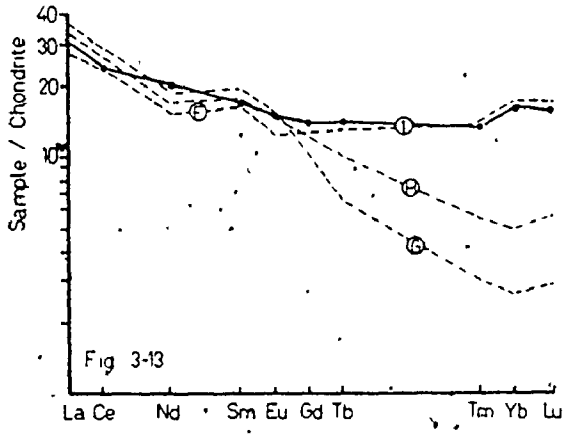

Fig 3-13

Conclusions

1. Models B, C and E (Figure 3-12) fall in the field of most arc tholeiites; Figure 3-12 also indicates that, except for Nd (for which analytical difficulties were experienced; Appendix V), the Burditt Lake greenschist facies metabasalts and the Footprint gneiss mafic enclave have REE patterns compatible with 30-40% partial melting of plagioclase pyrolite or spinel pyrolite (spinel lherzolite).
2. The REE pattern of amphibolite F19 was impossible to model; the possibility of analytical error cannot be ruled out.
3. The REE pattern of Jackfish Lake Complex enclave D4 was not adequately reproduced by any of these models.

REE model for the Jackfish Lake Complex mafic enclaves

Equilibrium bulk fractional crystallization models (Arth, 1976a) for enclave D4 are shown in Figure 3-13. 70% equilibrium bulk fractional crystallization of a magma with the chemical composition of the Burditt Lake metabasalts produces a REE pattern similar to that of D4 (Figure 3-13, F). Higher pressure models, which involve garnet-clinopyroxene mineralogies, can produce the required LREE characteristics, but the HREE values are too low.

There is some other evidence that indicates that D4 may be a low pressure differentiate of metabasalts similar to those in the Burditt Lake - Lake Despair area. The enclave has a higher $Fe_2O_3{}^t$ content (14.6%) and lower MgO (4.31%) than the other metabasalts; such Fe enrichment is characteristic of Skaergaard-type differentiation trends. One troublesome feature of this model is that D4 is lower in SiO_2 (47.8%) than other metabasalts from the area. However, Carmichael et al. (1974) note that Skaergaard-type differentiation can lead to silica depletion, at least up to 80% crystallization of the parent magma. Alternatively, the trace element content of this enclave may reflect contamination of the basalt magma especially if it passed through continental crust during its ascent.

Evolution of the basalts - some speculations

It would be philosophically unsatisfying to abandon the metabasalts without some attempt to model their origin on a grand scale.

The volcanic stratigraphy of the metabasaltic rocks of the Burditt Lake - Lake Despair area depends rather critically upon a few pillow determinations that suggest eastward facing tops (Blackburn, 1976a). If these are correct, however, the following model is at least compatible with the observed

geological and geochemical data. The model, however, is by no means unique!

1. The Burditt Lake quartz normative metabasalts formed at shallow depth (0-5 kb) by 30-40% partial melting of ultramafic rock. Their extrusion probably marked the initiation of island arc volcanism off-shore of the Rainy Lake gneiss (primitive sialic crust?).
2. Felsic pyroclastic volcanism accompanied and followed the first episode of mafic volcanism as the locus of magma formation moved laterally towards the sialic crust (Rainy Lake batholith).
3. Renewed mafic volcanism followed the felsic pyroclastic activity, but the magma genesis occurred at greater depths (5-20 kb) and resulted in the formation of olivine normative basalts. Plate movement culminated in the suturing of the island arc volcanics and the sialic crust (Rainy Lake batholith). This caused tectonic interleaving of the mafic metavolcanic and tonalitic rocks at the greenstone-gneiss contact, such as is represented by the Footprint gneiss migmatized mafic enclaves. The collision was also accompanied by regional greenschist facies metamorphism and contact amphibolite facies metamorphism at the junction.

4. High level differentiation of the olivine normative basaltic magma produced calc-alkali basalt which was extruded along the volcanic-gneiss suture. Alternatively, the olivine basalt extruded during and after the collision became contaminated and enriched in LREEs and other volatile elements by passage through continental crust present by that time on the one side of the suture.
5. The Jackfish Lake Complex was intruded at the basalt-gneiss interface, incorporating some of the calc-alkali basalt as enclaves. The intrusion caused further metamorphism of the amphibolites at its contacts, and also contributed to the migmatization of the Footprint gneiss.

One of the biggest problems with this model is that it assumes that the present position of the Jackfish Lake Complex mafic enclaves reflects their pre-intrusion location. Firmer evidence for this contention awaits additional field investigations.

III-7 GEOCHEMISTRY OF THE FELSIC METAVOLCANIC ROCKS AND THE BURDITT LAKE PLUTON

General geochemistry

The chemical composition of the felsic metavolcanic rocks, which occur interstratified with the metabasalts, is given in Appendix IV and summarized in Table 3-7. They are Na-dacites (Irvine and Baragar, 1971), although many of the more siliceous varieties would be considered rhyodacites by other classification schemes (Goodwin, 1967).

Blackburn (1976a) reports that such rocks occupy about one-third of the volcanic pile in the Burditt Lake - Lake Despair area. The rocks are chemically similar to other felsic metavolcanic rocks from the Wabigoon granite-greenstone belt (Table 3-7, #4-8) (Blackburn, 1976a; Goodwin, 1976a). The compositional gap that exists between the felsic and mafic metavolcanic rocks (Figure 3-6) appears to be real; other analysts (Birk, pers. comm.; Blackburn, 1976a) also have not reported samples that chemically resemble andesites. Two amphibolite facies silica-poor dacites (F119, F125; Table 3-7, #9) were sampled within the study area, but these rocks are not common.

Table 3-7 Average chemical results, siliceous rock types

	1	2	3	4	5	6	7	8	9
SiO_2	71.65	73.76	70.71	69.37	69.01	70.00	70.01	71.60	60.86
TiO_2	0.27	0.10	0.27	0.31	0.37	0.30	0.37	0.33	0.62
Al_2O_3	15.61	15.89	15.85	16.20	16.20	16.17	16.46	15.87	18.54
FeO*	1.91	0.68	2.03	2.33	2.71	2.51	2.77	2.60	5.02
MnO	0.03	0.03	0.03	0.03	0.05	0.07	0.04	0.06	0.13
MgO	0.82	0.30	0.89	1.12	1.28	1.20	1.70	1.33	1.00
CaO	2.94	1.93	2.88	3.18	3.04	2.50	2.47	2.47	6.44
Na_2O	5.12	4.27	5.22	4.91	5.06	5.34	4.43	4.49	4.51
K_2O	1.53	3.78	1.99	2.39	2.18	1.82	1.68	1.26	1.76
P_2O_5	0.12	0.06	0.14	0.15	0.10	0.09	0.07		0.32
Rb	42	90	55	47	45				39
Sr	555	461	708	571	506		313		1244
Ba	602	1173	617	513	451		367		760
Ce				17	15				56
Pb				5	5				10
Zn				41	46				88
Ni				t	t				14
Zr				85	98				114
Y				6	6				14
Nb				t	t				-
K/Rb	302	348	300	420	400				375
Sr/Ba	0.922	0.393	1.15	1.11	1.12		1.17		1.64
Rb/Sr	0.076	0.195	0.078	0.082	0.089				0.031

Notes for Table 3-7 Average chemical results, siliceous rock types

1. av. 14 Footprint Gneiss

2. representative granite gneiss, Footprint gneiss (F-110)

3. av. 2 analyses, Northwest Bay foliated to gneissic granodiorite

4. av. 6 amphibolite facies felsic metavolcanic schists

5. av. 4 Burditt Lake greenschist facies felsic tuffs

6. av. 8 Burditt Lake greenschist facies felsic tuffs (D. Birk, pers. comm.)

7. av. 4 Off Lake-Burditt Lake felsic tuffs (Blackburn, 1976a)

8. av. Wabigoon felsic metavolcanic rock (Goodwin, 1976a)

9. av. 2 amphibolite facies high Al dacites

* All analyses recalculated to 100% anhydrous, total Fe as FeO

t = trace

Major and minor element oxides in wt. %; trace elements in ppm

Oxygen isotope rock results, felsic metavolcanic rocks

The $\delta^{18}O$ rock values for the amphibolite facies felsic metavolcanic rocks range from 7.3 to 9.4°/$_{oo}$ (Table 2-7; Figure 3-14) and lie within the normal range of isotopically unaltered felsic metavolcanic rocks and least altered Archean felsic metavolcanic rocks (Figure 2-17). However, like the Burditt Lake metabasalts, the greenschist facies felsic metavolcanic rocks from the same area have somewhat anomalously high $\delta^{18}O$ values (8.0-11.4°/$_{oo}$). It is possible that at least some of the material mapped as felsic pyroclastics has been reworked; field evidence for the pyroclastic nature of these rocks is not overwhelming (Blackburn, 1976a, p.16-17); only their fragmental origin is indisputable. Clastic metasedimentary rocks with $\delta^{18}O$ of 8 to 13°/$_{oo}$ can occur interlayered with, or interfingering with primary tuffaceous material of lower $\delta^{18}O$ (Chapter II; Longstaffe and Schwarcz, 1977). What is more interesting is the progressive decrease in $\delta^{18}O$ of the felsic metavolcanic rocks as the Burditt Lake stock is approached (Figure 3-15; Figure 3-2); to properly interpret these results, this discussion must be diverted temporarily to consider the Burditt Lake pluton itself.

FIGURE 3-14 $\delta^{18}O$ rock results for felsic metavolcanic rocks from the Burditt Lake and Manomin Lake (Lake Despair) areas, and for the Burditt Lake granodiorite. The field for unaltered felsic volcanic rocks is from Taylor (1968).

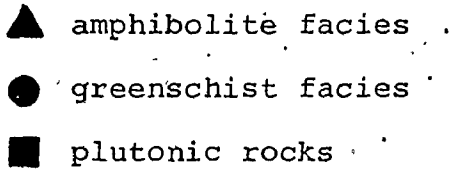

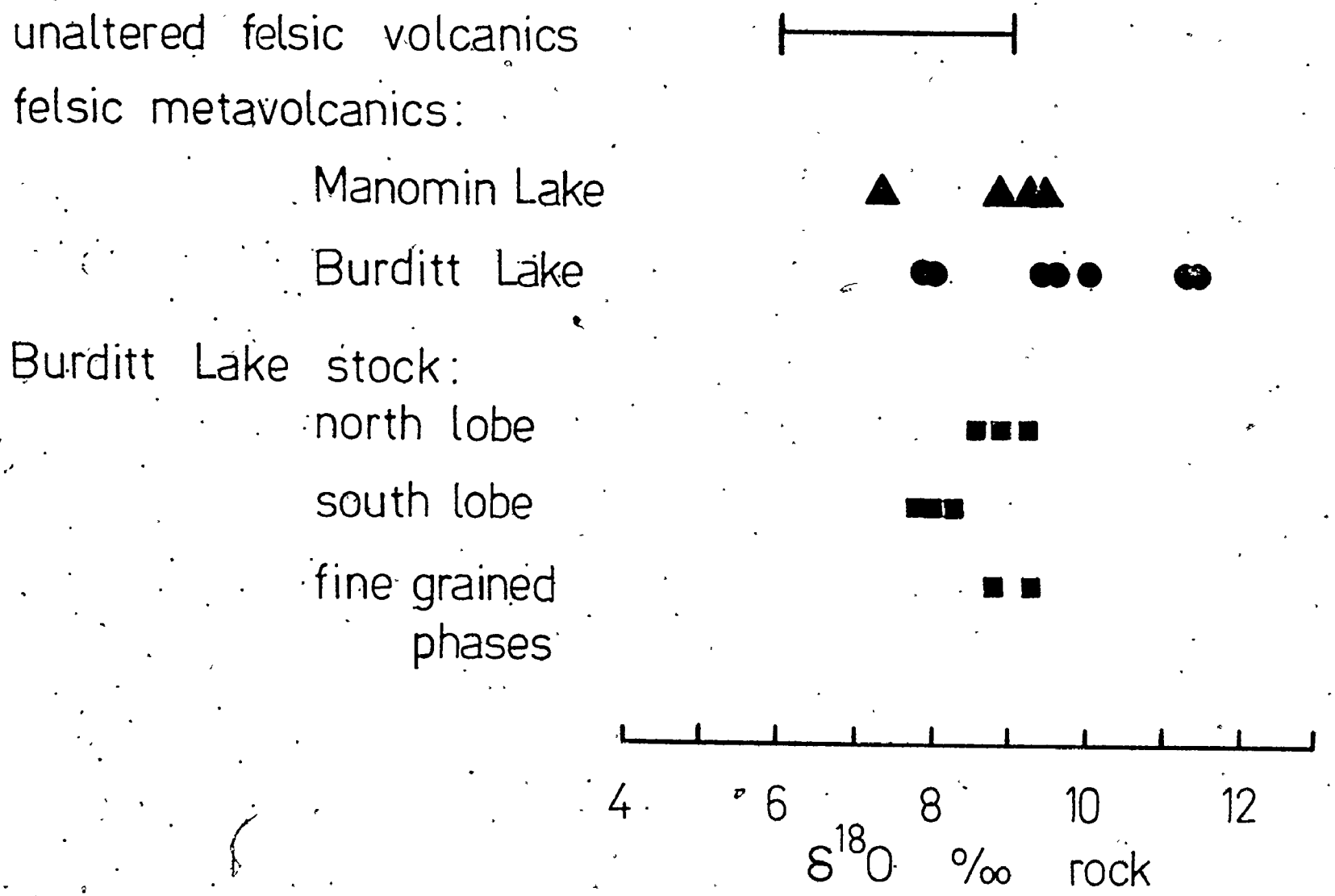
unaltered felsic volcanics
felsic metavolcanics:
Manomin Lake
Burditt Lake
Burditt Lake stock:
north lobe
south lobe
fine grained phases
4
6
8
10
12
δ18O ‰ rock

The oxygen isotope geochemistry of the Burditt Lake stock and associated greenschist facies felsic country rocks

The Burditt Lake pluton ranges in $\delta^{18}O$ from 7.8 to 9.3°/₀₀ (Table 3-8; Figure 3-14). The microcline megacryst bearing north lobe, as well as the aplitic and fine grained granodioritic phases, are about 1°/₀₀ enriched in $\delta^{18}O$ relative to the medium grained granodiorite of the north lobe.

Oxygen isotope data for a northwest-southeast traverse across the southern portion of the stock and its country rocks (Figure 3-15) showed that:

1. the medium grained granodiorite of the south lobe does not differ significantly in $\delta^{18}O$ from near its center to near its margin;
2. the felsic country rocks decrease in $\delta^{18}O$ from 11.4°/₀₀ 1700 meters from the granodiorite contact, to 7.9°/₀₀ within 25 meters of the contact; the latter value is identical to the 8.0°/₀₀ mean of the medium grained granodiorite.

Shieh and Taylor (1969) and Turi and Taylor (1971a,b) demonstrated that isotopic interaction between granitic plutons and their country rocks depends upon the attitude of the intrusive contact, and upon the temperature of the country rock prior to its intrusion; the metamorphic grade of the country rock can greatly affect its behaviour during

Table 3-8 $\delta^{18}O$ results, Burditt Lake Stock

Sample No. and Rock Type	$\delta^{18}O$ °/₀₀
South Lobe: medium-grained granodiorite	
G53	8.23
G56	8.34
442-10	7.76
441-2	8.04
North Lobe: microcline megacryst-bearing granodiorite	
G21	8.55
G22	8.91
G-78	8.84
Fine-grained granodiorite (G51)	9.27
Aplite (G8)	9.17

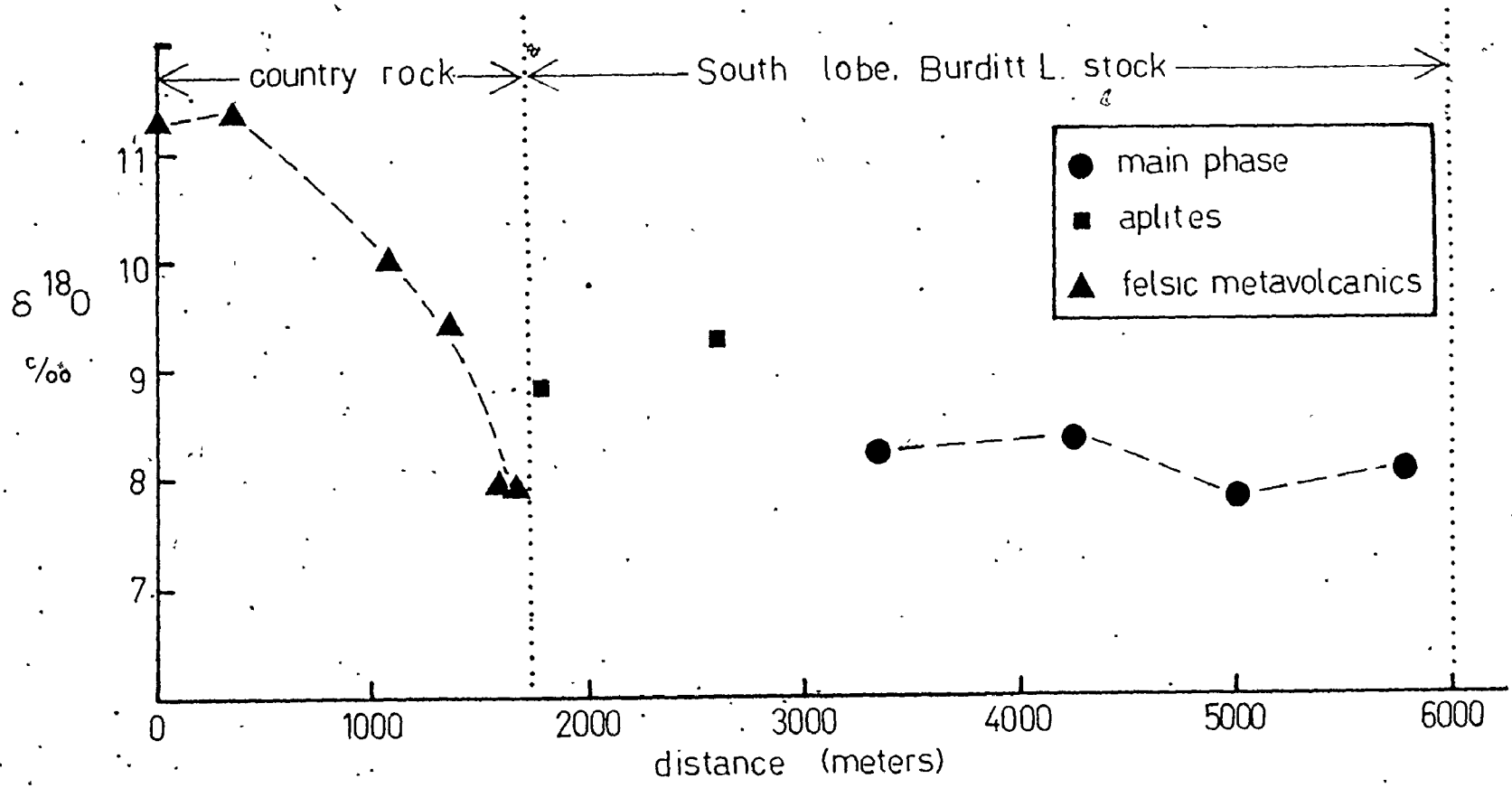

FIGURE 3-15 $\delta^{18}O$ rock results for the northwest-southeast traverse across the Burditt Lake stock and its felsic metavolcanic country rocks

oxygen isotopic exchange.

The Burditt Lake pluton was intruded into relatively dry (as compared to unmetamorphosed equivalents) country rocks, previously dehydrated during regional metamorphism. Turi and Taylor (1971a,b) showed that only such 'dry' country rocks exhibit isotopic depletion when intruded by plutons; even in these rocks, depletion occurs only in enclaves, or about roof zones of the plutons, areas where the country rocks are able to exchange with the magmatic fluids that are moving upwards through the pluton. As no fluids are moving from the country rocks into the pluton, the pluton's margin should remain isotopically unaltered, as is the case for the Burditt Lake stock.

Evidence for roof zone exposure of the Burditt Lake stock is difficult to obtain; sharply brecciated intrusive contacts, as well as the presence of fine grained granodioritic phases, might be interpreted to favour a high level of exposure. Archean post-kinematic plutons are generally thought to be exposed at high levels because of their textural variations (Ayres and Ermanovics, 1972, p.579). The presence of microcline megacrysts in the north lobe of the Burditt Lake stock, along with other deuteric features (Birk and McNutt, 1976), do indicate the presence of a water-rich fluid during the late stage development of the pluton.

The upward movement of magmatic water through the Burditt Lake pluton might also be responsible for the higher $\delta^{18}O$ of the microcline megacryst-bearing north lobe granodiorite and the fine grained phases, providing that these rocks are located near the top of the intrusion (Figure 3-16). Magmatic fluids in final isotopic equilibrium with the medium grained granodiorite ($\delta^{18}O = 8.0°/_{oo}$) at subsolidus temperatures of about 550°C would have a $\delta^{18}O$ composition of $7.7°/_{oo}$:

$$\Delta rock\text{-}H_2O = \frac{2.68\ (10^6)}{T^2} = 3.52;\ T \text{ in } °K$$

(Taylor, 1974)

Such subsolidus isotopic re-equilibration is a common feature of 'wet' granitic rocks (Bottinga and Javoy, 1975). If fluids of this composition further cooled to about 475°C during the autometasomatism of the north lobe rocks, and if the volume of the fluid was sufficient to control the isotopic composition of the rocks during isotopic exchange, then these granodiorites would attain $\delta^{18}O$ values of $9.0°/_{oo}$.

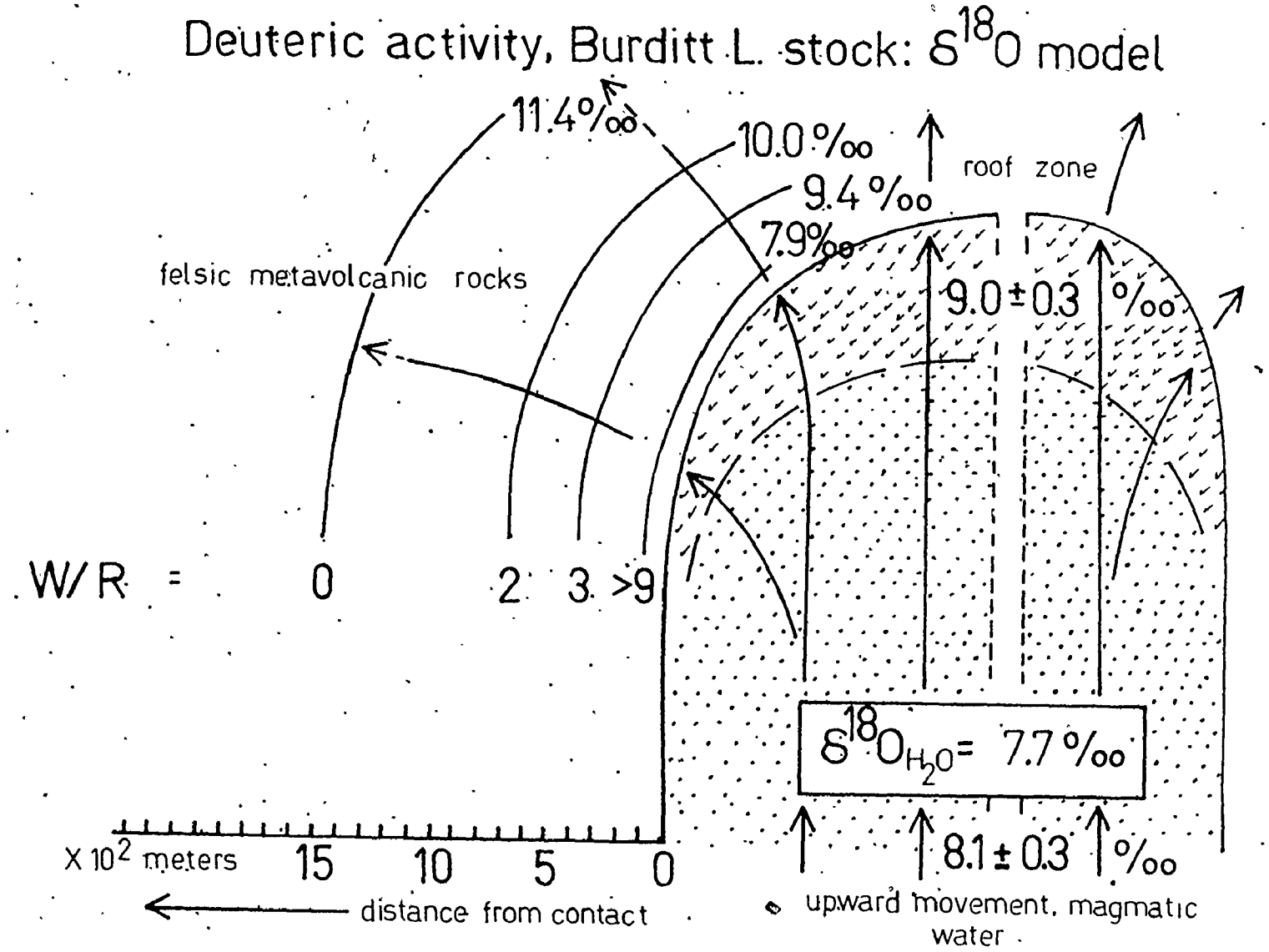

FIGURE 3-16 A model for magmatic water movement from the roof zone of the Burditt Lake stock into the surrounding felsic metavolcanic country rocks.

Water/rock ratios and the alteration of the contact zone country rocks

The volume of magmatic fluid (water) necessary to produce the observed ^{18}O depletion of the felsic country rocks can be estimated by calculations suggested by Taylor (1974, p.871-872). These equations are also given in Chapter IV-6. The calculations were performed assuming a slight temperature rise in the country rocks from ambient regional metamorphic temperatures to those expected near the contact with the Burditt Lake pluton. Also, two models have been used in the calculations: (1) the $\delta^{18}O$ of the magmatic fluid is kept constant; (2) the $\delta^{18}O$ of the fluid is permitted to increase (due to enrichment from the country rocks) according to the Rayleigh fractionation law. For both cases, water/rock (W/R) ratios of greater than two are required within 400 meters of the granodiorite contact:

Distance from contact (m)	$\delta^{18}O$ of rock °/₀₀	T°C of rock	W/R model 1	W/R model 2
25	7.87	450	>10	>10
50	7.92	450	>10	>10
400	9.42	425	2.4	3.0
650	10.01	400	1.2	1.8
1400	11.35	300-400	<0.1	0

Chemical alteration of the country rock in the contact zone would be expected to accompany fluid transfer on this scale. Figure 3-17 shows that the major and minor element composition of the felsic country rocks along the traverse (Figure 3-15) has been modified towards that of the medium grained granodiorite. Although not shown in Figure 3-17, the pattern is similar for Rb, Sr, Ba, Zr, and Y. Thin section study of the affected rocks shows them to be feldspathized (plagioclase blastesis); such a process is compatible with the chemical data. The correlation in the country rocks between Na_2O and $\delta^{18}O$ (Figure 3-18) emphasizes the importance of the somewhat saline magmatic fluids in the chemical and isotopic modification of the contact zone country rocks.

Oxygen isotope mineral results, Manomin Lake felsic schists

As previously mentioned, the amphibolite facies felsic metavolcanic rocks located near Manomin Lake (Figure 3-3) have $\delta^{18}O$ rock values (Table 2-7) similar to unaltered felsic volcanic rocks. Chemically, these rocks range in SiO_2 from 66-70%; some variation in Al_2O_3 (16-17%), Na_2O (4-5%) and K_2O (2-3%) also occurs. These chemical variations are reflected by the occurrence of muscovite and traces of garnet in some samples.

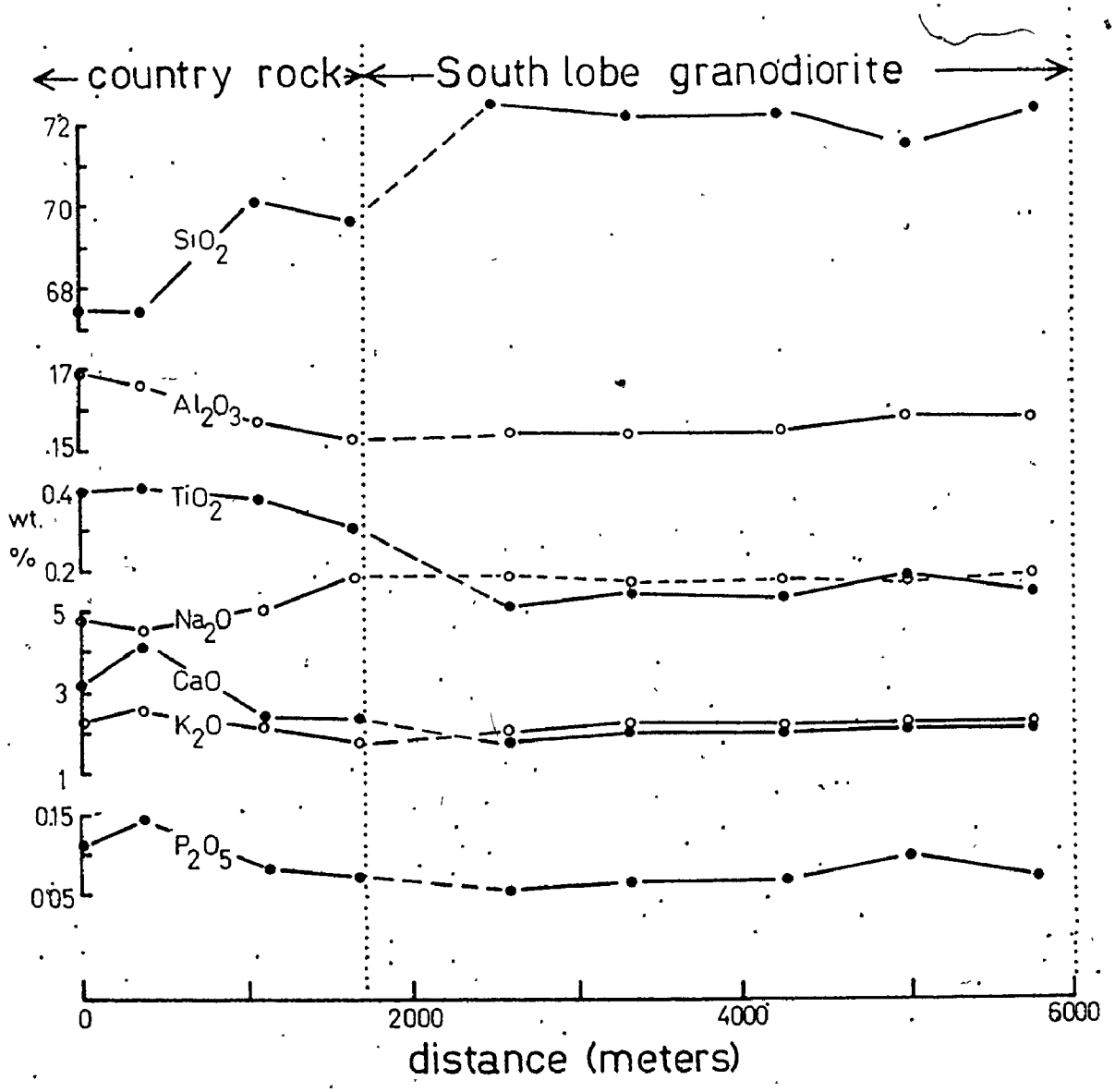

FIGURE 3-17 Chemical variation along the northwest-southeast traverse across the Burditt Lake stock and the associated felsic metavolcanic country rocks

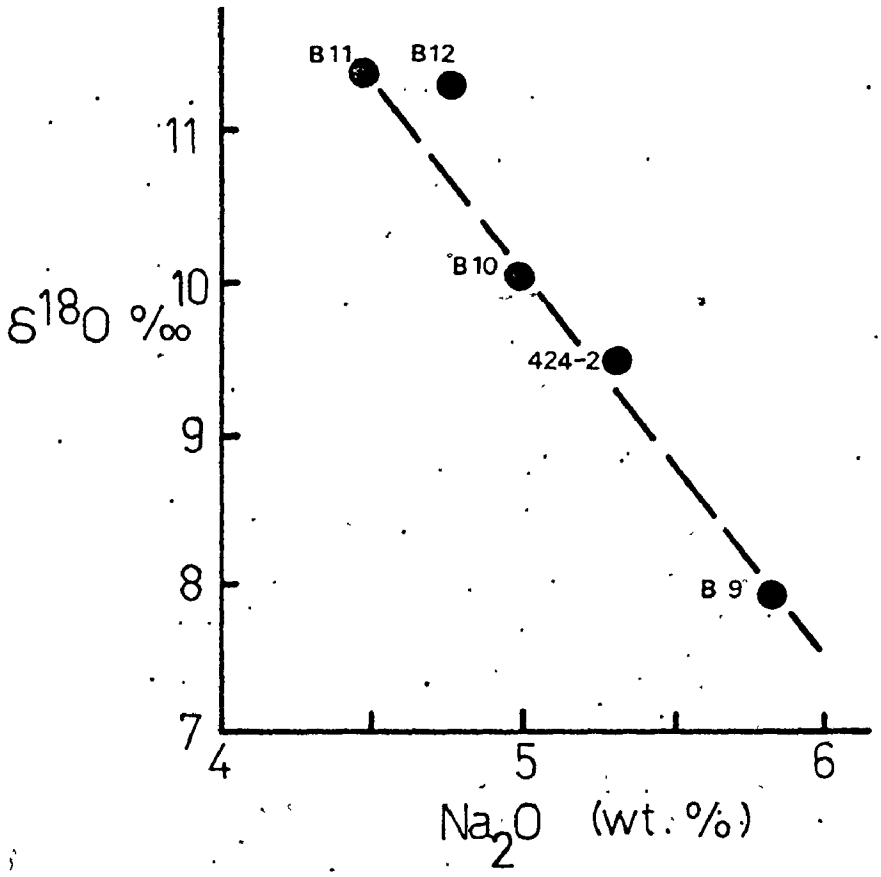

FIGURE 3-18 $\delta^{18}O$ rock versus Na_2O diagram for the altered felsic metavolcanic rocks surrounding the Burditt Lake stock

Two samples (F121, F124), which appear fresh in hand sample and thin section, were selected for more detailed isotopic and trace element studies. The chemical composition of these rocks is similar to that of the chemically least altered Burditt Lake greenschist facies felsic metavolcanic rocks (B11, B12; Table 3-9).

$\delta^{18}O$ results for quartz, microcline and biotite from F121 and F124 (Table 3-10) show that:

1. The microcline-biotite isotope fractionation, which should reflect metamorphic temperatures, is smaller for F121 (493°C), which is located one kilometer from the Rainy Lake batholith, than for F124 (426°C; temperature calculations are explained in Appendix I), which is three kilometers from the contact.
2. Quartz-biotite and microcline-biotite isotopic temperatures for F124 (404°, 426°C; Appendix I) indicate an approach to oxygen isotopic equilibrium in this sample; temperature concordance is not as good in sample F121 (413°, 493°C).

If the intrusion of the Jackfish Lake Complex was solely responsible for the metamorphism of the felsic schists, the most complete isotopic re-equilibration would be expected closest to the intrusive contact. However, if the felsic schists were first metamorphosed and isotopically re-equilibrated

Table 3-9 Some felsic metavolcanic rock analyses

		1	2	3	4
SiO_2	wt %	67.7	66.3	67.4	67.5
Al_2O_3		16.7	17.0	16.6	17.0
TiO_2		0.35	0.40	0.40	0.39
Fe_2O_3		2.85	3.36	3.02	3.02
MnO		0.03	0.04	0.05	0.05
MgO		1.42	1.84	1.26	1.65
CaO		2.79	3.81	4.19	3.20
Na_2O		4.93	3.97	4.49	4.79
K_2O		3.07	3.12	2.50	2.33
P_2O_5		0.15	0.17	0.14	0.11
LOI		N.D.	4.2	3.8	3.4
Li	ppm	N.D.	N.D.	N.D.	N.D.
Rb		58	60	54	46
Sr		878	437	554	515
Ba		664	497	381	399
Pb		7	7	6	5
Th		1.8	2.3	3	3
Y		5	6	6	8
Nb		t	t	t	3
Zr		89	82	102	116
Zn		48	61	43	57
Ni		7	14	6	t
Ta		3.1	2.2	N.D.	N.D.
Hf		2.9	3.0	N.D.	N.D.
Sc		10.5	14.1	N.D.	N.D.
La		12.9	13.7	N.D.	N.D.
Ce		26.7	31.3	19	23
Nd		10.3	12.2	N.D.	N.D.
Sm		2.1	2.1	N.D.	N.D.
Eu		0.56	0.73	N.D.	N.D.
Gd		N.D.	N.D.	N.D.	N.D.
Tb		0.29	0.33	N.D.	N.D.
Tm		0.09	0.10	N.D.	N.D.
Yb		<0.5	<0.5	N.D.	N.D.
Lu		0.07	0.10	N.D.	N.D.
Tl		N.D.	N.D.	N.D.	N.D.

Notes to Table 3-9 Some felsic metavolcanic rock analyses

Major elements normalized to 100% anhydrous; total Fe as Fe_2O_3

Major and minor elements by XRF; REE, Th, Hf, Ta, Sc by INNA; other trace elements by XRF.

N.D. = Not determined; t = trace

1. F121, Manomin Lake amphibolite facies felsic metavolcanic
2. F124, as in (1)
3. B11, Burditt Lake greenschist facies felsic metavolcanic
4. B12, as in (3)

Table 3-10 $\delta^{18}O$ mineral results, felsic schists

	quartz °/₀₀	microcline °/₀₀	biotite °/₀₀
F124	12.52±0.05 (2)	10.00±0.11 (2)	5.04±0.11 (2)
F121	11.79	8.59±0.00 (2)	4.56±0.31 (2)

Values in parentheses indicate number of individual analyses

during the emplacement of the Footprint gneiss, and then those felsic metavolcanic rocks closest to the greenstone-gneiss contact further disturbed during the subsequent intrusion of the Jackfish Lake Complex, the isotopic results can be explained. Microcline and biotite readily re-equilibrate isotopically; the higher temperature of F121 therefore probably reflects the effect of contact metamorphism superimposed upon the regional metamorphic grade. Quartz does not isotopically re-equilibrate as readily; thus, the quartz-biotite and microcline-biotite temperatures could conceivably become discordant during the two stages of metamorphism.

The origin of Archean 'tonalitic' rocks - general considerations

The purpose of this section is to discuss some of the chemical characteristics of Archean 'tonalitic' rocks. Many of the rock types in the Burditt Lake - Lake Despair area

(felsic metavolcanics, Jackfish Lake Complex, Northwest Bay Complex, Footprint gneiss) fall into this general grouping. Thus this discussion is pertinent not only to the felsic metavolcanic rocks but also to the other siliceous lithologies described in sections III-8 and III-9.

Two tonalite types have been defined by Barker and Arth (1976) and Barker et al. (1976a):

1. high Al (>15 wt. % Al_2O_3); moderate to low Rb, moderate to high Sr, moderately enriched LREE, depleted HREE, negligible Eu anomalies;
2. low Al (<15% Al_2O_3); low Rb and Sr, moderately enriched LREEs, flat HREE patterns, negative Eu anomalies.

They also concluded that large volumes of Archean tonalites fall into the first category, and suggested two mechanisms for their formation:

1. fractional crystallization of mafic liquids under hydrous conditions;
2. partial melting of parent rocks of basaltic composition (eclogite, quartz eclogite, mafic amphibolite); partial melting of a basaltic parent with little or no plagioclase as a residual phase can produce high Al tonalites.

Hanson and Goldich (1972) were among the first to recognize the importance of HREE depletion in Archean tonalites

and suggested, as an explanation for this feature, the presence of a garnet residue from the partial melting of quartz eclogite (quartz-orthopyroxene-clinopyroxene-garnet) at mantle depths.

Barker and Arth (1976) suggest that "models of genesis of trondhjemitic-tonalitic liquids involving quartz eclogite probably are not pertinent for Archean rocks" (p.599), citing the absence of eclogite and garnetiferous amphibolite in Archean gneisses to support the change in opinion from the previous year - "These quartz dioritic rocks display similar characteristics which ... are consistent with an origin by partial melting of quartz eclogite or amphibolite of Archean basalt composition at depths greater than 45 kilometers" (Arth and Hanson, 1975, p.355). According to Barker and Arth (1976), Archean geothermal gradients were too steep to intersect the eclogite field; 15 to 30% melting of the parent would occur before the pressures necessary for the formation of garnet (50-60 km) were achieved.

Arth and Barker (1976) reported a limited amount of phenocryst-dacite glass REE data for hornblende that suggests that hornblende is equally capable of concentrating HREEs during the formation of tonalites.

The controversy over the relative control of garnet and hornblende upon the REE patterns of Archean tonalites has fundamental implications for the pressure regimes in

which the basaltic parent of the tonalite is partially melted. Basaltic parent rocks can be assigned to two main mineralogic and pressure sensitive groupings:

1. the amphibolites: plagioclase + hornblende ± quartz ± clinopyroxene;
2. the eclogites: garnet + clinopyroxene ± coesite ± kyanite.

Transitions between the two can exist as well (e.g. hornblende bearing quartz eclogites). Workers too numerous to mention have studied the pressure and temperature stability regimes of such rocks. Recent summaries include those of Ringwood (1975), Carmichael et al. (1974), and Wyllie (1971). Recent advances in phase petrology not covered in these texts have been reported by Stern (1974), Stern et al. (1975) and Wyllie et al. (1976). The following summary is drawn from all of these sources.

Amphibole: Amphibole controls the fractionation and partial melting of hydrous basaltic rocks up to pressures of about 20 kb; the presence of water causes the crystallization field of plagioclase to be suppressed and that of amphibole extended (Yoder and Tilley, 1962). Such conditions might exist during partial melting of lower crust or sinking lithosphere (Ringwood, 1975). The first liquids produced by melting are silicic; for example, Holloway and Burnham (1972) report that the liquid coexisting with amphibole at 5 to 8 kb and 800 to 900°C ($P_{H_2O} > 0.5\ P_{total}$) is dacitic.

As temperature and degree of melting increase, the liquids become more mafic.

Garnet: At pressures greater than about 27 kb, and temperatures of 800 to 1000°C, amphibole is no longer stable and hydrous basaltic rocks introduced into the mantle are transformed to quartz eclogites. If the rocks are anhydrous, the transformation occurs at even lower pressures (Ringwood, 1975). Partial melting under anhydrous conditions at high pressures and temperatures yields liquids of andesitic composition as first melts. Under hydrous conditions, however, the first formed liquids are dacitic in composition up to about 35% melting. Ringwood (1975, p. 269) reports that siliceous liquids can be produced by partial melting of hydrous quartz eclogite at temperatures as low as 750°C ($P_{H_2O} = P_{total}$).

Fractional crystallization versus partial melting models

That fractional crystallization of wet basaltic magma can form tonalites is not denied. The Uusikaupunki-Kalanti (Finland) tonalites, for example, are part of a complete mafic to acid differentiation suite that follows a Na enrichment trend (Barker and Arth, 1976). However, partial melting models are preferred, at least for the Burditt Lake - Lake Despair felsic metavolcanics and the Footprint gneiss for two reasons:

1. Fractional crystallization at low pressures would result in plagioclase precipitation and the development of negative Eu anomalies;
2. Rocks of intermediate composition that are genetically and spatially related to these tonalites are absent.

Rare earth geochemistry and the origin of the felsic metavolcanic rocks

Like most Archean tonalites, the Burditt Lake - Lake Despair felsic metavolcanic rocks belong to the high Al category of Barker et al. (1976a):

	High Al tonalites (Barker et al., 1976a)	Burditt Lake - Lake Despair felsic metavolcanic rocks
Al_2O_3 (wt. %)	>15	15.2-17.0
Ce/Yb	>10	50-60
Sr (ppm)	>400	395-878
Rb (ppm)	<100	24-60
Eu anomaly	nil	nil

To help distinguish between eclogite and amphibolite melting models for these tonalites, two representative samples

(F121, F124) were analyzed for REEs (Figure 3-19; Table 3-9).

Any petrogenetic model for the felsic metavolcanic rocks must account for two features of the REE patterns:

1. the 30 to 40 X chondrite level enrichments in the LREEs, and the low HREE values;
2. the absence of Eu anomalies.

Three melting models, which hypothetically correspond to progressively higher pressure source regimes, were tested at equilibrium modal melting fractions of 1 to 40%:

Model 1 partial melting of amphibolite:

(a) 50% plagioclase, 50% hornblende (Figure 3-20a)

(b) 50% plagioclase, 25% hornblende, 25% clinopyroxene (Figure 3-20b)

Model 2 partial melting of hornblende bearing quartz eclogite:

30% clinopyroxene, 30% hornblende, 25% garnet, 15% quartz and kyanite (Figure 3-20c)

Model 3 partial melting of quartz eclogite:

(a) 55% clinopyroxene, 30% garnet, 15% coesite and kyanite (Figure 3-20d)

(b) 70% clinopyroxene, 15% garnet, 15% coesite and kyanite (Figure 3-20e)

(c) 80% clinopyroxene, 5% garnet, 15% coesite and kyanite (Figure 3-20f).

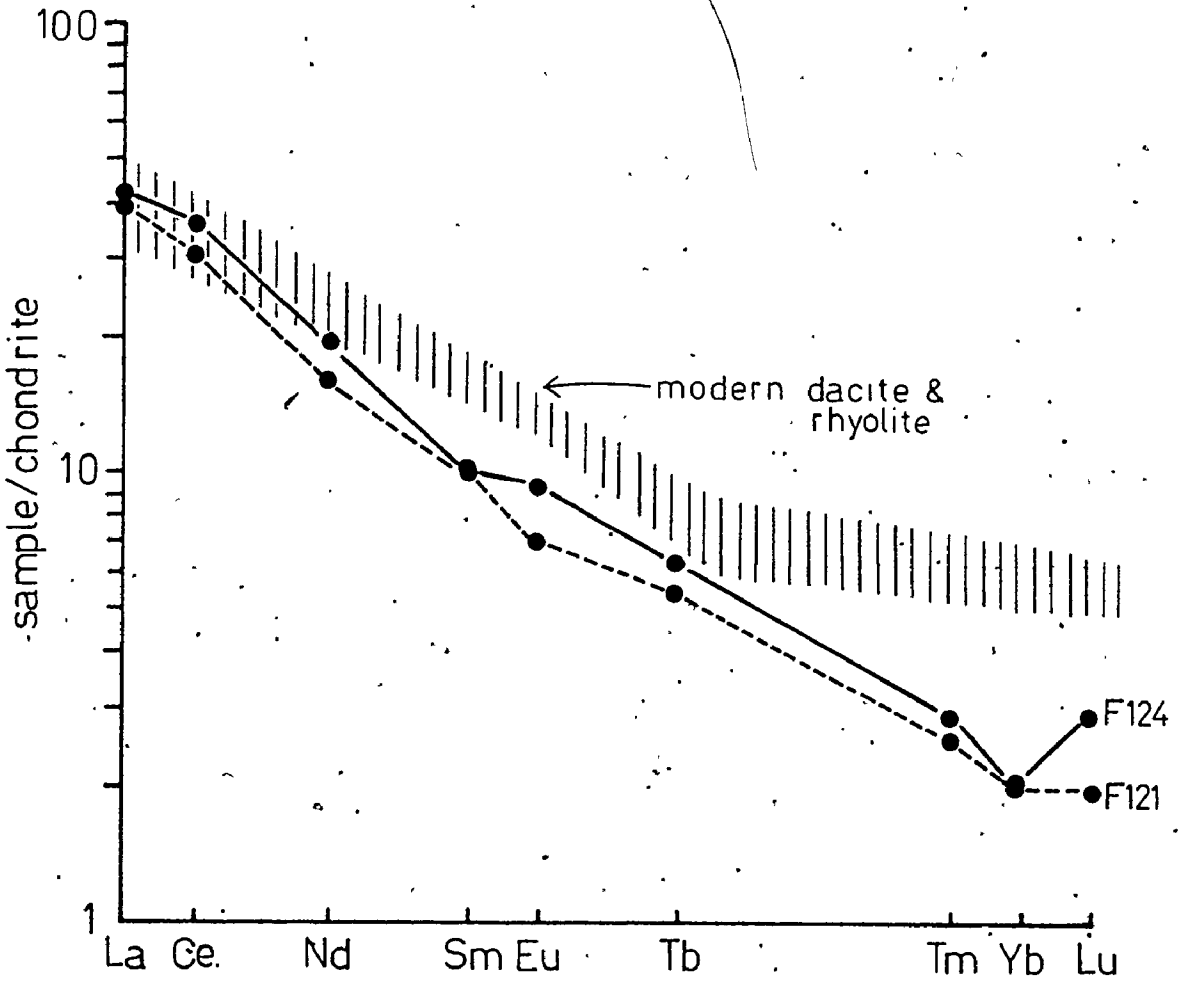

FIGURE 3-19 Chondrite normalized rare earth element results for the Manomin Lake felsic schists. The field for modern felsic volcanic rocks is taken from Condie and Harrison (1976)

The chemical composition of the parent basalt was taken to be that of the least altered Burditt Lake metabasalts (Table 3-6, #4,5); REE values for B1 and B5 were averaged.

Partition coefficients were taken from Arth and Hanson (1975), Arth (1976a) and Condie and Harrison (1976). Values for dacitic rocks have been used. Clinopyroxene D values for dacitic rocks were obtained by combining Arth's (1976a) values for basaltic and rhyolitic rocks. The theoretical REE patterns were calculated by programme MELT (written by this author) using the equations given in section III-6.

Figure 3-20 shows that:

1. Amphibolite melting models (1a and 1b) do not produce the observed REE pattern or abundances (Figure 3-20a,b); other amphibolite starting mineralogies were tested using both modal and non-modal melting models; equally poor results were obtained for these.
2. Hornblende bearing quartz eclogite (model 2) parent rocks can produce the appropriate REE pattern at 10-30% melting, but the absolute abundances are too low (Figure 3-20c).
3. The quartz eclogite models (Figure 3-20e,f,g) best fit the observed REE patterns and abundances; the HREE abundances, however, are very sensitive to the amount of residual garnet assigned by the calculation; 10% melting of model 3b quartz eclogite provides the

FIGURE 3-20 Chondrite normalized rare earth element modelling for the Manomin Lake felsic schists.

The stippled pattern shows the experimental results for F121 and F124 (Figure 3-19); the solid line shows model calculations for 1% melting, the long-dashed line for 10% melting, and the short-dashed line for 30% melting of a selected parent rock type. The chemical composition for the parent rock used in all models is that of the Burditt Lake metabasalt (B1, B5).

A. Model 1A: equilibrium modal melting of amphibolite (50% plagioclase, 50% hornblende)

B. Model 1B: equilibrium modal melting of amphibolite (25% clinopyroxene, 25% hornblende, 50% plagioclase)

C. Model 2: equilibrium modal melting of hornblende-bearing quartz eclogite (30% clinopyroxene, 30% hornblende, 25% garnet, 15% quartz + kyanite)

D. Model 3A: equilibrium modal melting of quartz eclogite (55% clinopyroxene, 30% garnet, 15% coesite + kyanite)

E. Model 3B: equilibrium modal melting of quartz eclogite (70% clinopyroxene, 15% garnet, 15% coesite + kyanite)

F. Model 3C: equilibrium modal melting of quartz eclogite (80% clinopyroxene, 5% garnet, 15% coesite + kyanite)

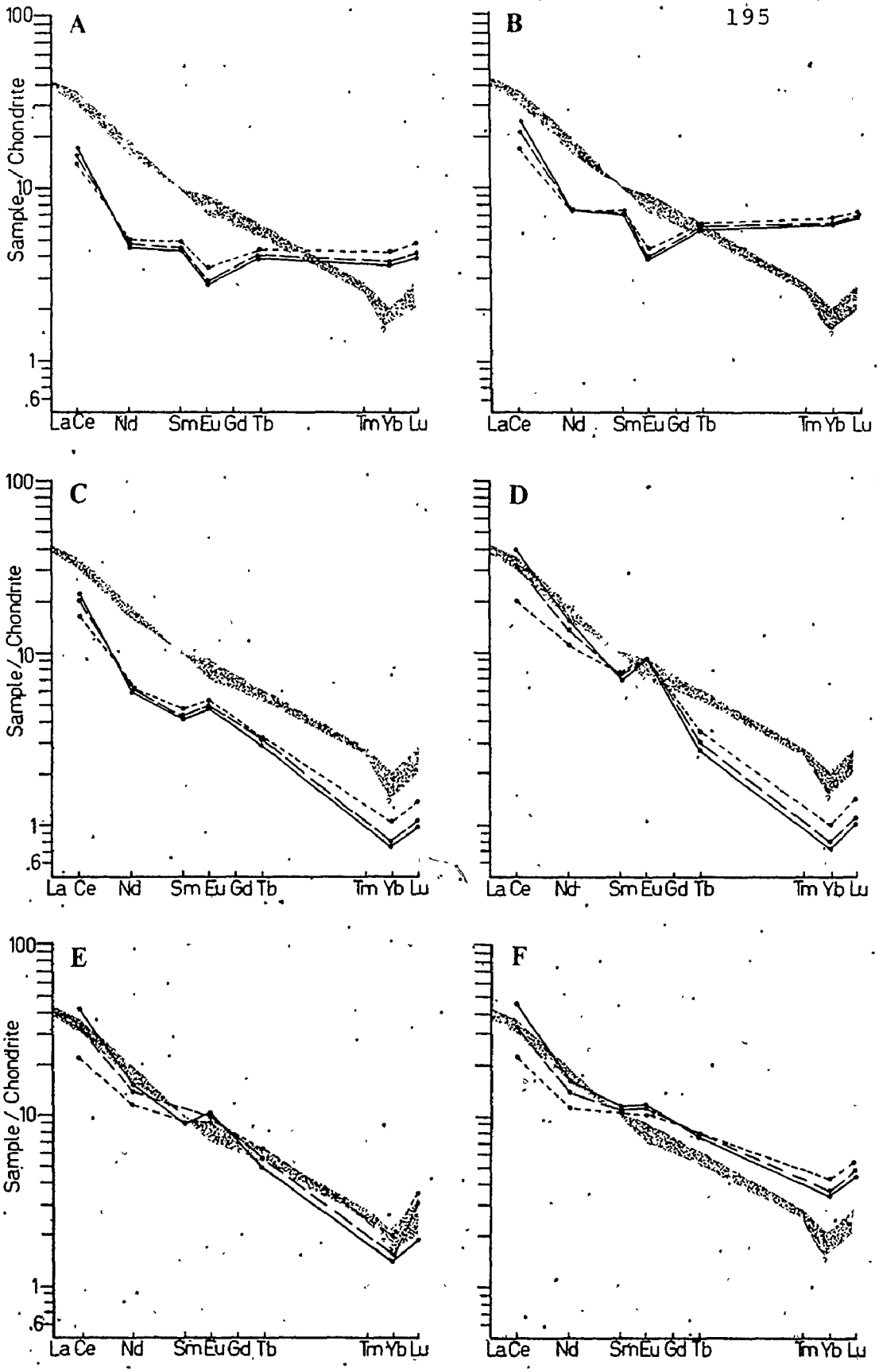
A
B
C
D
E
F
100
10
1
.6
Sample / Chondrite
La Ce Nd Sm Eu Gd Tb Tm Yb Lu

closest approximation to the REEs of the felsic metavolcanic rocks (Figure 3-20e).

Major element modelling

Other elements besides the REEs should be compatible with any melting model suggested by the above calculations. The starting mineralogy used in the rare earth model 3b, when combined with the postulated major element compositions of these theoretical mantle phases (Ringwood, 1975; Stern, 1974), yields a chemical composition similar to the Burditt Lake metabasalts (Table 3-11). However, the calculated Ca and Mg are too high, and Fe is too low. These anomalies would disappear if the hypothetical mantle pyroxene was ferro-augitic in composition. Unfortunately, the possible variation in the chemistry of mantle minerals is very large; until the compositional ranges of such phases are better constrained by experimental data, partial melting models based on major elements are difficult to formulate. Also, the partitioning of major elements during partial melting in the lower crust and upper mantle is not well understood. For these reasons quantitative major element modelling has been placed outside the scope of this thesis.

Table 3-11 Major element composition, quartz eclogite phases (theoretical)

Mode (%)	10.0	5.0	55.0	15.0	7.5	3.0	4.5		
	quartz	kyanite	aluminous clinopyroxene	jadeite*	garnet** almandine	garnet** grossular	garnet** pyrope	calculated composition	Burditt L. tholeiites
Ref.		1	2	3	4	5	6		
SiO_2	100.0	37.46	46.8	59.38	38.03	38.69	41.52	52.40	53.00
TiO_2		0.03	1.7	0.04		0.55		0.98	0.92
Al_2O_3		61.52	8.5	25.82	22.05	18.17	23.01	14.90	14.30
FeO			7.6		29.17	3.78	12.86	7.10	
Fe_2O_3		0.71		0.45	0.88	0.70	1.22	0.24	
FeO***									11.6
MgO		0.03	13.9	0.12	6.49	0.76	16.64	8.90	7.50
CaO		0.02	19.9	0.13	1.80	31.76	4.71	12.30	9.80
Na_2O		0.03	0.6	13.40				2.30	2.40

1. Deer, Howie and Zussman (1971), p.43
2. Ringwood (1975), p.260
3. Deer, Howie and Zussman (1971), p.107, #14
4. Deer, Howie and Zussman (1971), p.24, #1
5. Deer, Howie and Zussman (1971), p.24, #3
6. Deer, Howie and Zussman (1971), p.24, #6

* a jadeitic component is expected in mantle pyroxene (Wyllie et al., 1976)

** garnet composition ($Al_{50}Py_{30}Gr_{20}$) estimated from Stern (1974)

*** Total Fe as FeO

K, Rb, Sr and Ba modelling

The K, Rb, Sr, and Ba contents predicted by model 3b are compatible with the observed abundances of these elements in the felsic metavolcanic rocks (average values from Table 3-7, #4; Figure 3-21a). Agreement is not as good for the other models tested (Figure 3-21b).

Summary statement

The relationship between our simplistic equilibrium modal melting models and actual mantle melting conditions is that of liberal extrapolation. Modal melting of coesite, clinopyroxene, garnet and kyanite ($P_{total} = P_{H_2O}$ >27 kb) is petrologically unrealistic; under such conditions; all clinopyroxene melts before the beginning of melting of garnet and kyanite (Wyllie et al., 1976). In addition to the REE data that suggest the melting of some garnet, the Sc content of the felsic metavolcanics is two times higher than expected if only clinopyroxene (and garnet) were providing Sc to the melt. Gill (1974) suggests that Sc is preferentially incorporated into kyanite relative to both garnet and clinopyroxene. Partial melting of kyanite could therefore contribute to the higher Sc levels observed in the felsic metavolcanic rocks.

The only real constraints provided by the modelling

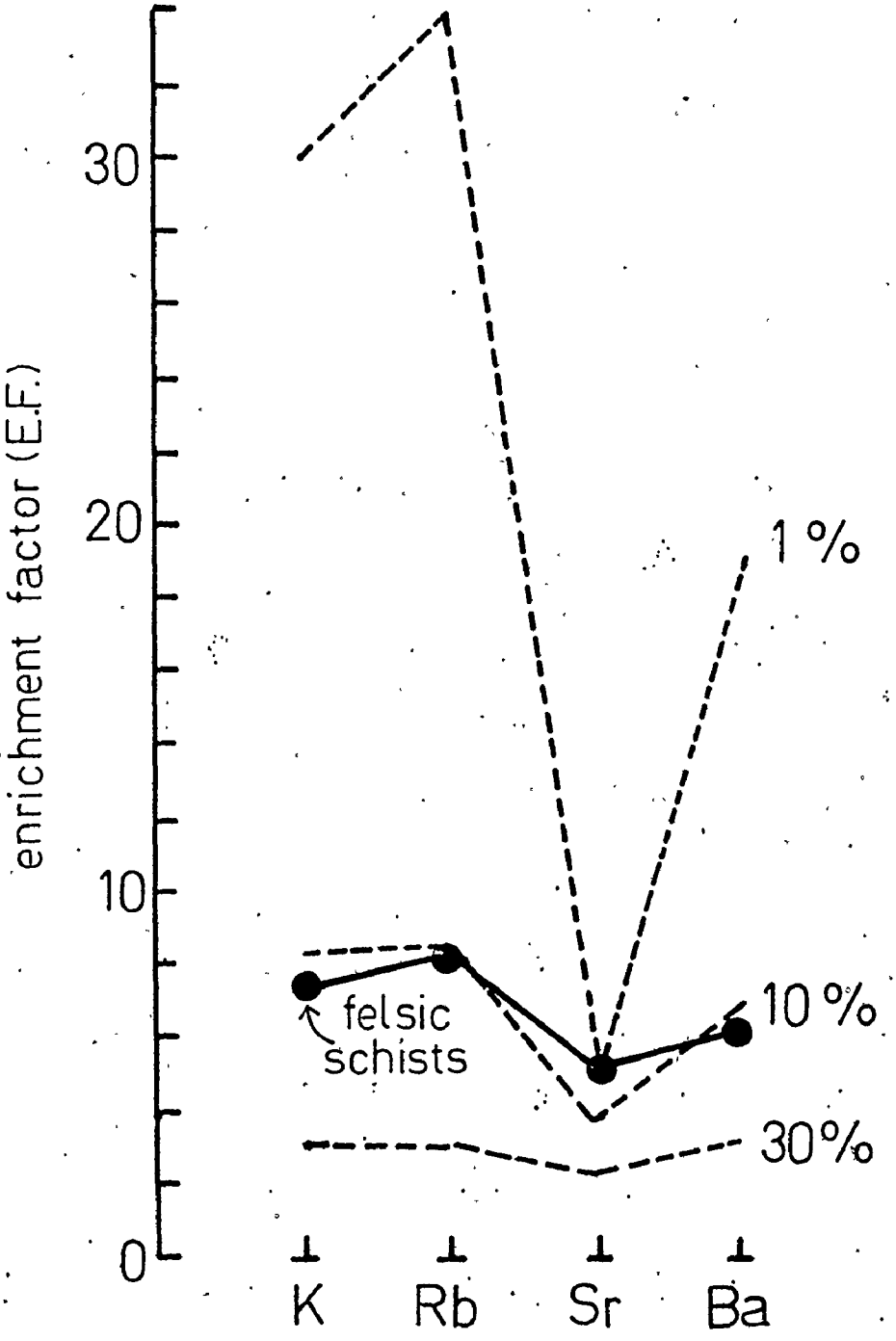

FIGURE 3-21a LIL element model for the Manomin Lake (Lake Despair) felsic schists. Dashed lines show the calculated factors for 1, 10 and 30% melting of the parent basalt described in the text as Model 3b.

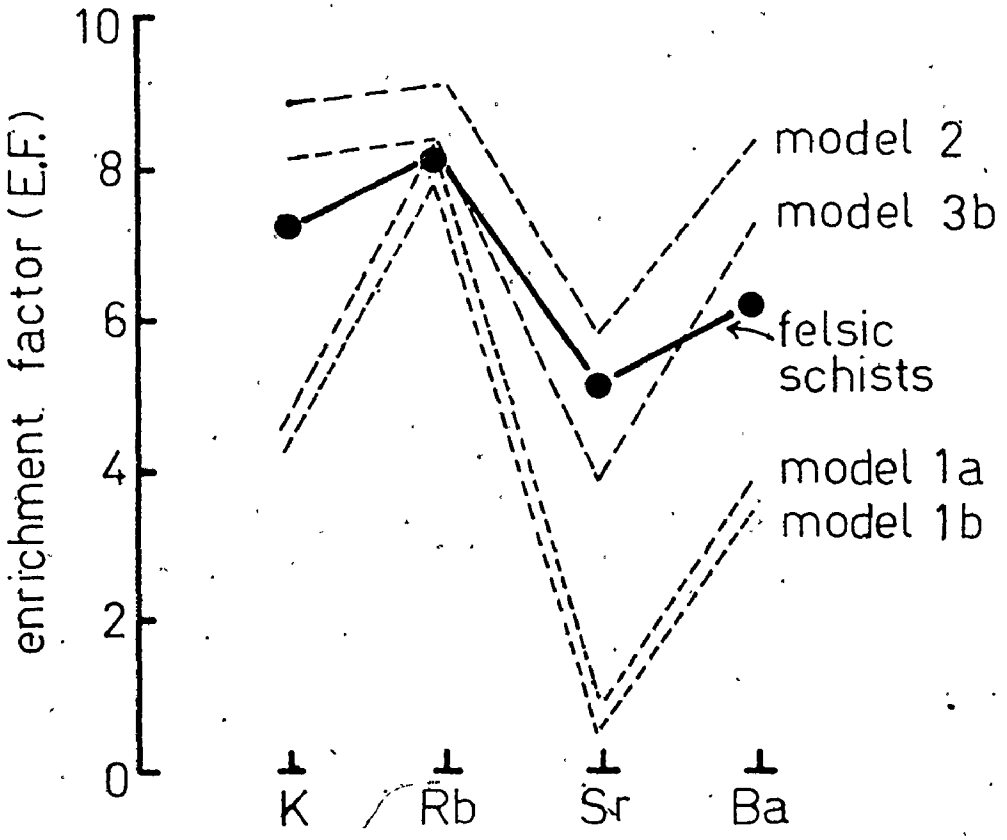

FIGURE 3-21b Comparison of LIL element models for the Manomin Lake (Lake Despair) felsic schists. Dashed lines show calculated results for 10% melting according to the models described in the text.

are that:

1. plagioclase is not a residual phase;
2. some garnet and clinopyroxene remain in the residue after melting.

Hornblende is NOT necessarily ruled out as a stable subsolidus phase.

According to Wyllie et al. (1976), quartz and hornblende enter the liquid at lower temperatures than clinopyroxene, garnet and kyanite during the partial melting of hornblende-bearing quartz eclogite under hydrous conditions at P_{total} of about 20 kb. The origin of the felsic metavolcanic rocks under such a pressure regime is most compatible an explanation of the facts as I understand them.

III-8 GEOCHEMISTRY OF THE JACKFISH LAKE COMPLEX

Introduction

The purpose of this section is to discuss the geochemistry of the Jackfish Lake Complex in terms of the differentiation, autometasomatic, and low temperature alteration processes that have affected its various lithologies (section III-2). Various aspects of the geochemistry discussed here have been previously reported (Longstaffe et al., 1976b, 1977a,b).

Chemical variation in the Jackfish Lake Complex is most pronounced in the Lake Despair area, a direct consequence of the lithological variation at this locality. For this reason, this portion of the Complex was selected for detailed study, rather than the dioritic rocks which dominate most of the unit. Those who have studied the diorites believe that the Jackfish Lake Complex was intruded in one episode, without differentiation; the variations in the Lake Despair area are dismissed as 'minor chemical drift' (Sutcliffe, pers. comm.). The following discussions will hopefully dispel this impression of simplicity.

Trondhjemitic affinities of the Jackfish Lake Complex

The average chemical composition of the major rock types in the Complex is given in Table 3-12; individual analyses are listed in Appendix IV.

As far as can be discerned, the various lithologies within the Complex have gradational contacts; their generalized spatial and volumetric relations are shown in Figure 3-22. The comparable chemical variation is shown in terms of normative mineralogy in Figure 3-4.

When plotted on an AFM diagram (Figure 3-23), the Jackfish Lake Complex rocks have a trend similar to, although somewhat lower in Fe than, calc-alkaline suites such as the Lower California batholith and the Cascade volcanics (Carmichael et al., 1974, p.568). According to the alkali-lime index (Peacock, 1931), all of the rocks are alkali-calcic to calc-alkali.

However, in spite of similarities to calc-alkaline rocks, the Jackfish Lake Complex also exhibits chemical characteristics that identify it as an example of the gabbro-trondhjemitic (Na-enriched) suite (Barker et al., 1976a) (Figure 3-24). Such suites have been previously recognized in Archean and Proterozoic rocks by Arth and Hanson (1975), Barker and Arth (1976) and Barker et al. (1976a).

Table 3-12 Average chemical analyses, Jackfish Lake Complex and similar rock types from the Vermilion District, northeastern Minnesota*

	1	2	3	4	5	6	7	8	9	10	11	12
SiO_2	56.16	56.09	53.19	62.79	68.98	59.09	71.60	63.61	59.83	57.25	59.54	61.09
Al_2O_3	16.35	13.94	16.10	18.51	15.50	17.83	14.90	17.73	19.54	19.17	15.58	16.67
TiO_2	0.68	0.76	0.83	0.35	0.24	0.54	0.28	0.36	0.38	0.65	0.62	0.60
FeO*	7.09	6.14	8.79	2.91	2.20	5.26	2.02	3.02	3.38	5.79	6.17	5.46
MnO	0.14	0.10	0.17	0.06	0.06	0.10	0.03	0.07	0.07	0.09	0.12	0.10
MgO	5.37	6.08	6.22	1.66	1.40	4.60	0.56	1.39	2.65	3.22	4.69	3.39
CaO	7.56	7.63	7.86	4.08	2.62	4.95	2.03	2.77	5.07	5.00	6.16	5.18
Na_2O	4.78	4.58	3.15	6.52	5.92	4.22	4.35	7.17	7.07	5.99	4.40	4.84
K_2O	1.54	4.08	3.69	2.94	2.97	3.11	4.13	3.65	1.11	2.64	2.45	2.39
P_2O_5	0.33	0.60		0.21	0.11	0.31	0.10	0.23	0.27	0.21	0.27	0.28
Rb	31	102	101	39	72	74		51	14	40	71	76
Sr	1355	1871	886	1810	1243	991		1941	2316	1465	1089	753
Ba	972	1725	1280	2338	1693	1071		1856	748	1928	1279	992
K/Rb	412	332	303	626	342	349		594	658	548	286	261
Sr/Ba	1.39	1.08	0.692	0.774	0.734	0.925		1.05	3.10	0.760	0.851	0.759
Rb/Sr	0.023	0.055	0.114	0.022	0.058	0.075		0.026	0.006	0.027	0.065	0.101

Notes for Table 3-12 Average chemical analyses, Jackfish Lake Complex and similar rock types from the Vermilion District, northeastern Minnesota

1. av. 7 monzodiorites and diorites, Jackfish Lake Complex (F146, F126, F84, F132, F131, F144, F82).
2. syenodiorite, Icarus Pluton; Arth and Hanson (1975).
3. syenodiorite, Vermilion Batholith; Arth and Hanson (1975).
4. quartz poor granodiorite, Jackfish Lake Complex.
5. granodiorite, Jackfish Lake Complex (F118).
6. quartz poor granodiorite, Icarus Pluton; Arth and Hanson (1975).
7. granodiorite, Vermilion Batholith; Arth and Hanson (1975).
8. av. 2 Jackfish Lake Complex syenites (F46, F28).
9. av. 3 Jackfish Lake Complex leucodiorites (F24, F94, F21).
10. av. 2 Farm Lake Na syenodiorites; Arth and Hanson (1975).
11. av. 3 quartz monzodiorites, Jackfish Lake Complex (F133, F135, F136).
12. quartz diorite, Giants Range; Arth and Hanson (1975).

* All analyses recalculated to 100%, anhydrous; total Fe as FeO.

Major and minor element oxides in wt. %; Rb, Sr and Ba in ppm.

FIGURE 3-22 Sketch map of the Jackfish Lake Complex, as observed in the Lake Despair area

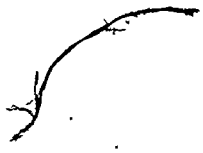

1. mostly diorite and monzodiorite, some meladiorite, quartz diorite and quartz monzodiorite
2. leucodiorite and leuco quartz diorite
3. microcline megacryst granodiorite
4. Na-syenite
5. Lake Despair mafic amphibolites and Manomin Lake felsic schists
6. Footprint gneiss and migmatite
7. Northwest Bay Complex granodiorite and granite

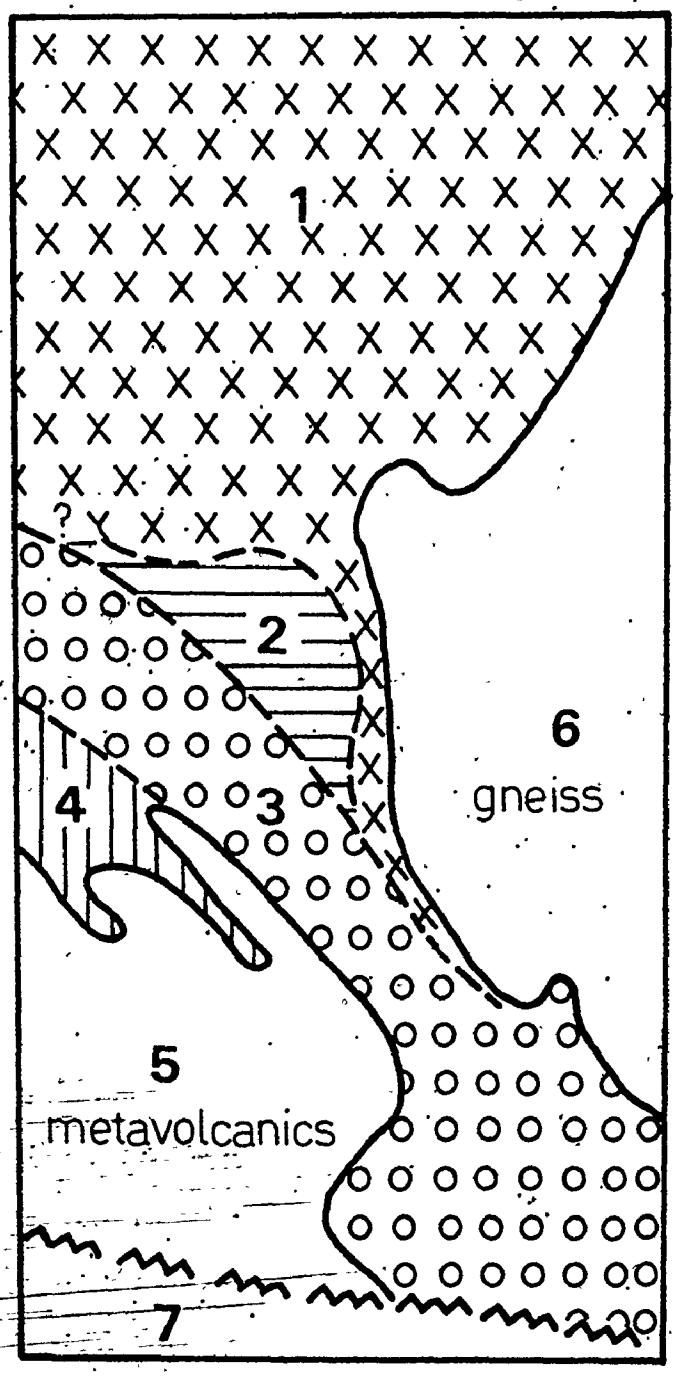
1
?
2
3
4
5
metavolcanics
6
gneiss
7
N
0 1
miles
0 1 2
km

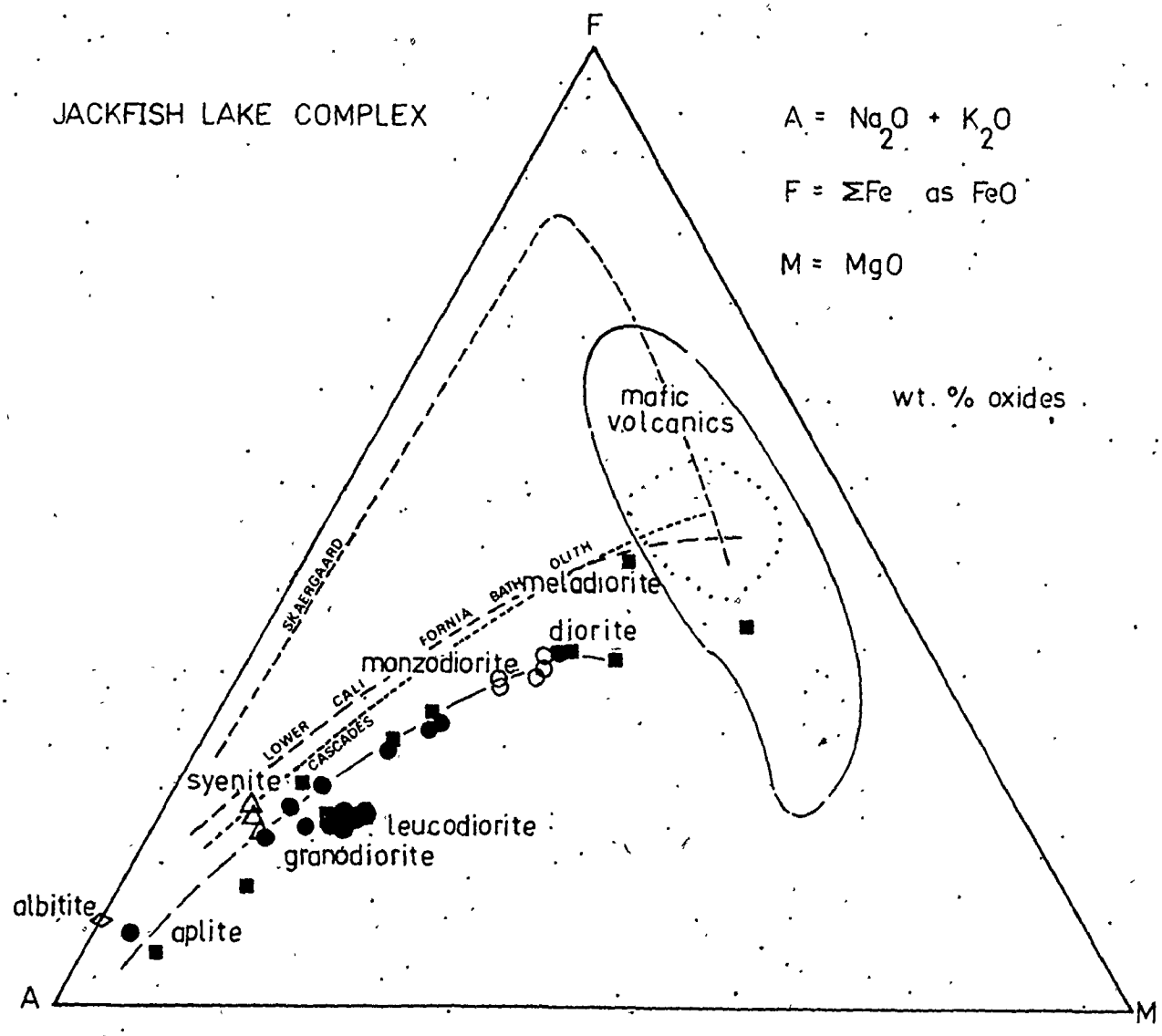

FIGURE 3-23 · AFM diagram for the Jackfish Lake Complex.

The mafic members of the Complex are less enriched in Fe than calc-alkaline rocks such as the Cascade metavolcanics or the Lower California batholith. Skaergaard, Cascade and Lower California batholith trends from Carmichael et al. (1974).

FIGURE 3-24 Na_2O-K_2O-CaO diagram for rocks from the Jackfish Lake Complex.

The calc-alkaline trend line is taken from Nockolds and Allen (1953); the gabbro-trondhjemite trend line is modified after Barker and Arth (1976).

+ (quartz) monzodiorite, granodiorite, Na-syenite, aplite
● meladiorite, (quartz) diorite, leuco (quartz) diorite, albitite

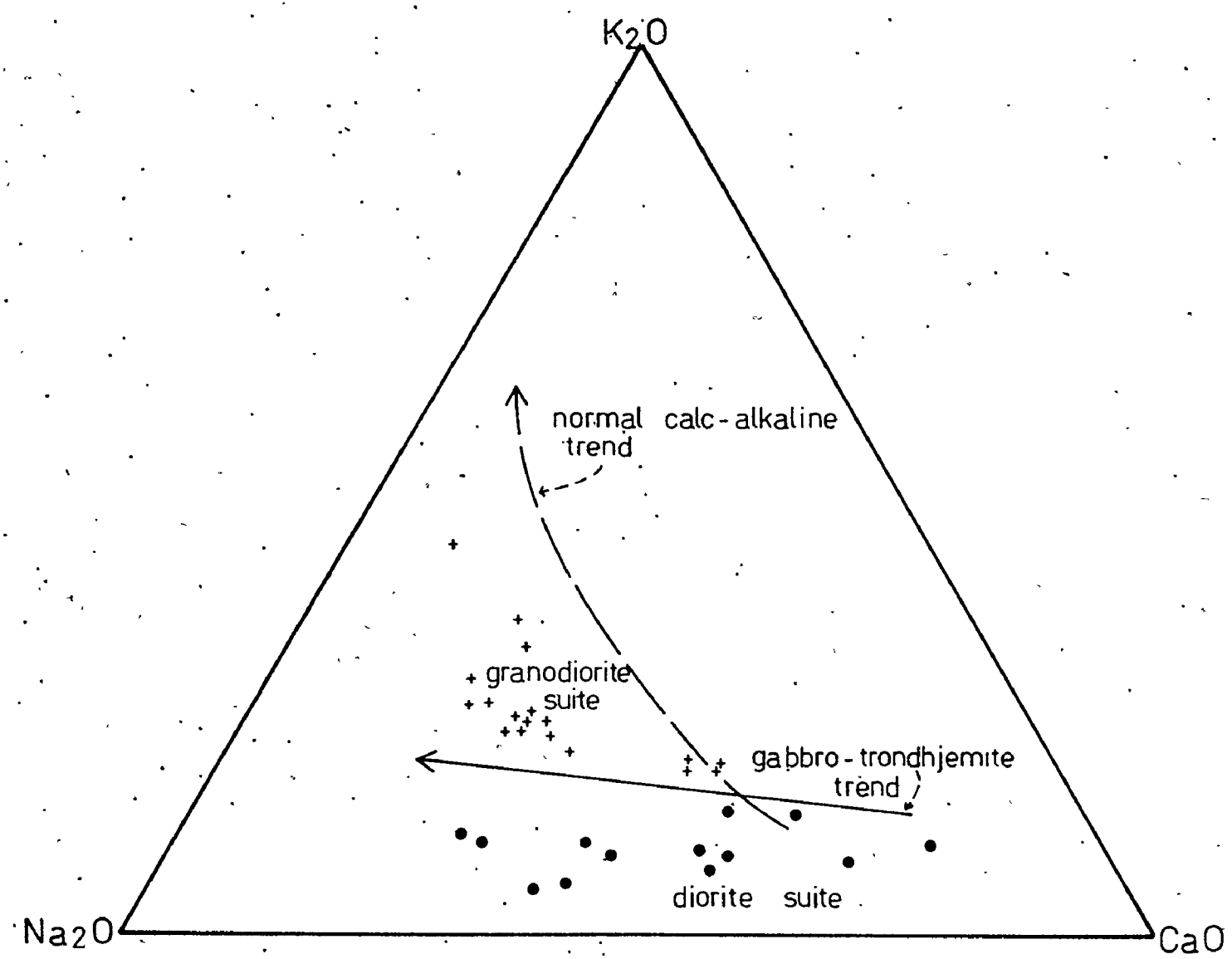
K_2O
normal calc-alkaline trend
granodiorite suite
gabbro-trondhjemite trend
diorite suite
Na_2O
CaO

The leucocratic members of the gabbro-trondhjemite suite in the Jackfish Lake Complex are the leucodiorites, leuco quartz diorites and Na syenites (Table 3-12, #8,9). Characteristic chemical features of these rocks are:

Al_2O_3	17-21%
Na_2O	5-9%
Na_2O/K_2O	2-12
Sr	>1500 ppm
Ba	>700 ppm; >1500 in Na syenite
K/Rb	>500
Rb/Sr	<0.03

Jackfish Lake Complex meladiorites, mafic enclaves and the possibility of hybridization

The presence of mafic enclaves within the Jackfish Lake Complex, in various states of digestion and/or feldspathization (Photos C and D; Appendix IV: D22, D6) indicates that mixing of mafic volcanic material with a tonalitic magma might be responsible for the production of the more mafic members of the trondhjemite suite. Hybridized tonalites have been described from nearby Atikwa Lake (Heimlich, 1971); Blackburn (1976a; p.25) refers to the Jackfish Lake Complex as a hybridized rock suite.

Didier (1973) suggests that hybrid granites and granodiorites generally contain pyroxene and/or brown-green to brown amphiboles (high in Ti and Fe); normally zoned plagioclases are surrounded by microcline. He also states that the development of large potassium feldspars (dents de cheval) within basic enclaves, aligned parallel to similar megacrysts in the granodiorite, is characteristic of hybrid granites and granodiorites which have assimilated basic enclaves. Hybridized diorites, according to Didier (op. cit.), commonly contain clinopyroxene cores surrounded by green-brown amphibole, or brown amphibole mantled by an amorphous green-brown amphibole. All of these petrographic features are well-developed in the Jackfish Lake Complex (Appendix III).

Some assimilation of mafic material can be observed in outcrop; amphibole-rich enclaves sometimes have very diffuse boundaries with the host diorite, such that near the boundary it is impossible to distinguish between amphibole derived from the enclave and amphibole crystallized from the plutonic magma. Petrographically, enclave derived amphiboles and amphiboles contained within the diorite are similar except for the more reacted appearance of the latter.

One of the major problems associated with any hypothesis

of large scale assimilation or hybridization is obtaining sufficient heat to fuse the mafic material (Bowen, 1922). Heat balance studies (Lazarenkov, 1962) show that granites can theoretically consume large volumes of mafic material, just as a result of the heat of crystallization. However, if such conditions do exist, enclaves located near the center of granitic bodies should not escape assimilation (Didier, 1973). Didier (op. cit.) suggests that the formation of melanocratic hybridized border zones around enclaves insulates the latter from further exchange with the magma; the Jackfish Lake Complex meladiorites occur in such border zones around mafic volcanic enclaves. However, it is unlikely that hybridization has been a major factor in the evolution of the Jackfish Lake Complex, as the following discussion will show.

Lutkov and Mogarovskiy (1973) concluded that element transfer associated with hybridization is governed by two processes:

1. change in concentration of an element due to assimilation of material of differing concentration;
2. diffusional transport of volatile elements into and out of the resulting magma.

If complete assimilation (by complete melting and recrystallization, by simple mixing of enclaves with magma,

or by mixing and partial melting) of mafic material has altered the chemistry of the Jackfish Lake Complex diorites, these processes should exert recognizable control upon the chemistry of the resulting hybrid rock.

F146 is a meladiorite which contains abundant clots of hornblende and clinopyroxene, and is located relatively near to a large mafic enclave; it should be one of the most likely candidates for a hybrid rock. To test the hybridization theory, two end member compositions were mathematically combined in the required proportions to produce the chemical composition of F146 (Table 3-20). The end member rock types are:

1. mafic metavolcanics (Table 3-4, #3a; Table 3-6, #8);
2. quartz diorite (F21, Table 3-20).

F21 was chosen as the magma end-member as it is relatively free of mafic enclaves, but has a relatively low differentiation index.

The results of these calculations (Table 3-13) show that most of the REEs, as well as K, Sc, Si, Y, and Zn are compatible with 20 to 40% assimilation of mafic metavolcanic material. Many other elements, however, require much higher percentages of assimilation, or cannot be modelled at all. This latter group includes both mobile and immobile elements. Variations of the end-member compositions, as

well as the meladiorite selected for comparison, were tested; even worse results were obtained for these calculations. In short, there is no satisfactory combination of mafic rocks and quartz dioritic rocks located within the study area that permit the formation of the meladiorites (or diorites) by hybridization mechanisms alone.

Table 3-13 Hybridization model for Jackfish Lake Complex diorites

Element	% assimilation	Element	% assimilation
Si	37	Pb	60
Al	92	Zn	17
Ti	not possible	Ni	not possible
Fe	46	Th	?
Mn	63	Y	35
Mg	not possible	Zr	not possible
Ca	58	Sc	26
Na	81	La	31
K	22	Ce	27
P	67	Sm	36
Rb	not possible	Eu	25
Sr	75	Tm	25
Ba	55	Yb	17
		Lu	25

Low temperature alteration processes affecting the Jackfish Lake Complex

The Jackfish Lake Complex is in fault contact with the granodioritic and granitic rocks of the Rainy Lake batholith in the vicinity of Northwest Bay (Figure 3-3). The Complex rocks located near the Northwest Bay Fault (Blackburn, 1976a) are visibly altered; plagioclase has altered to clays, sericite and epidote, and Fe staining gives the rocks a distinctive reddish hue. Microcline partially to completely replaces some plagioclase crystals. Some hornblende is altered to epidote, biotite and chlorite, and Fe-poor (leached) biotite is common (Appendix III).

The alteration of the mineral phases is reflected in their chemical composition; the chemical composition of plagioclase and biotite from altered granodiorite F37 (Table 3-14a) is contrasted with the range observed for the same minerals from unaltered granodiorite samples from the Complex in Table 3-14b. In particular, the altered plagioclase is much more calcic and the altered biotite has a much higher Mg/Fe ratio and K content and lower Rb, Li, and Ba than the unaltered equivalents.

The bulk chemical variations that occur along a north-south traverse from unaltered samples in the vicinity of Lake Despair (F118, F113, F3) to altered samples, as the

Table 3-14a Mineral analyses, altered granodiorite F37

	Li ppm	Na wt %	K wt %	Rb ppm	Tl ppm	Ca wt %	Sr ppm	Ba ppm	Mg wt %	Fe wt %
Rock	13	-	2.86	99	0.30	2.41	810	1535	3.20	-
Hornblende	8	0.81	0.78	12	0.15	8.68	227	140	7.04	11.33
Biotite	91	0.32	9.54	258	0.22	3.29	211	204	9.23	8.04
Plagioclase	-	2.90	0.22	10	0.52	4.50	672	2006	0.07	-
Microcline	1	-	12.59	291	0.74	0.04	811	4760	0.05	-

Analyses by atomic absorption analysis (P. Fung, analyst)

Fe by colorimetry (F. Longstaffe)

Table 3-14b Chemical comparison, altered and unaltered mineral phases

	Altered granodiorite (F37)	Unaltered granodiorites
PLAGIOCLASE		
Na/Ca	0.64	3.90
Sr	672 ppm	1319 - 1477 ppm
Ba	2006 ppm	1025 - 1513 ppm
Rb	10 ppm	24 - 26 ppm
K	0.22 wt %	1.18 - 1.70 wt %
BIOTITE		
Ba	204 ppm	738 - 866 ppm
Sr	211 ppm	50 - 93 ppm
Li	91 ppm	161 - 415 ppm
Rb	258 ppm	396 - 574 ppm
K	9.54 wt %	4.95 - 5.76 wt %
Mg	9.23 wt %	7.09 - 7.80 wt %
Fe	8.04 wt %	12.91 - 16.05 wt %

fault is approached (F40, F37, F67) are shown in Figures 3-25a,b. The possibility that at least part of such trends result from primary compositional differences can not be ruled out. For example, the decrease in SiO_2 from 67% (2400 meters from the fault) to 62% (220 meters from the fault) covers the range of silica contents found for unaltered Jackfish Lake Complex granodiorites (Table 3-12, #4,5). However, the LREE abundances of the altered sample F37 are higher than for unaltered quartz-rich granodiorite (F118) or quartz-poor quartz monzodiorites (F135), samples that bracket the major element compositional range of the altered granodiorites (Figure 3-26). Similarly, the K/Rb of the altered samples is lower (250-300) than most of the unaltered granodiorites.

Oxygen isotope analyses show that the altered rocks are anomalously low in $\delta^{18}O$ relative to the other Archean granitoids analyzed in this study (Figure 3-27; Table 3-15). The only similar analyses for Archean granitoids have been reported by Taylor and Magaritz (1975) and Barker et al. (1976b), and were attributed to low temperature interaction with meteoric water.

The $\delta^{18}O$ of the Jackfish Lake Complex samples decreases from 7.9°/$_{oo}$ 2300 meters from the fault, to 3.2°/$_{oo}$ within 220 meters of the shear zone (Figure 3-28). A number of

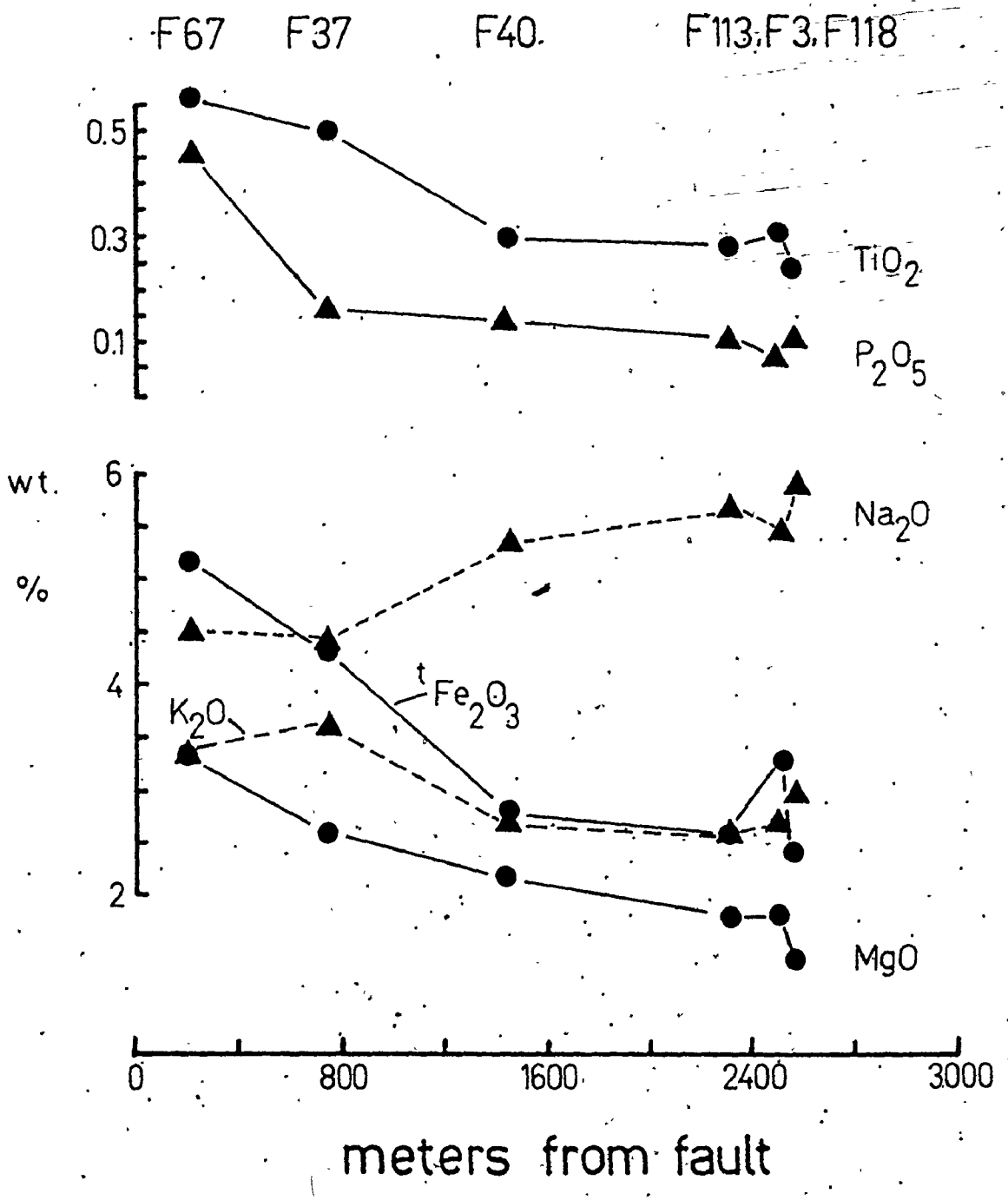

FIGURE 3-25a Major and minor element chemical variation of the Jackfish Lake Complex granodiorite along a traverse from the southern portion of Lake Despair to the Northwest Bay Fault (see Figure 3-3).

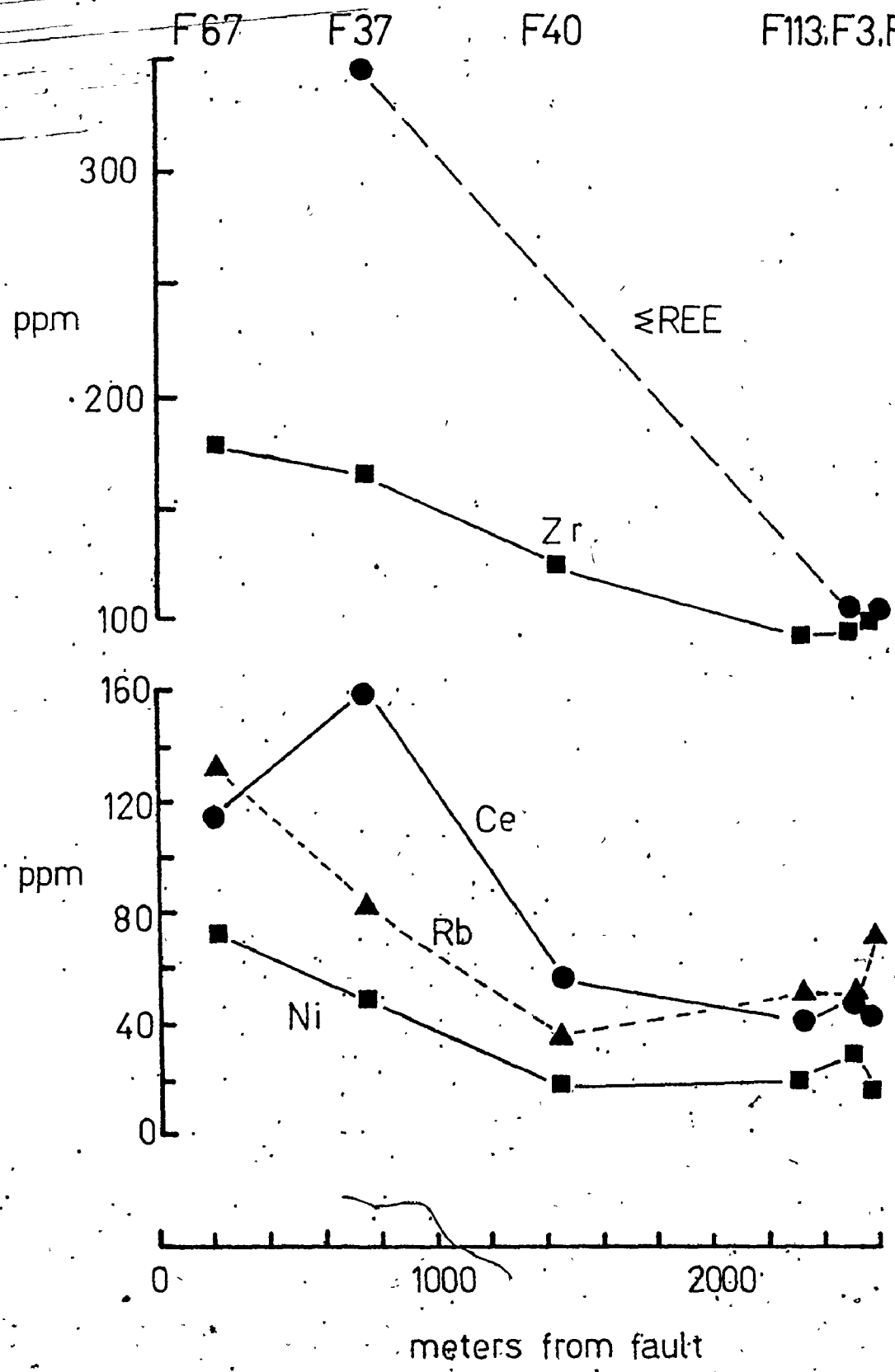

FIGURE 3-25b · Trace element variation of the Jackfish Lake Complex granodiorite along a north-south traverse from the southern portion of Lake Despair to the Northwest Bay Fault.

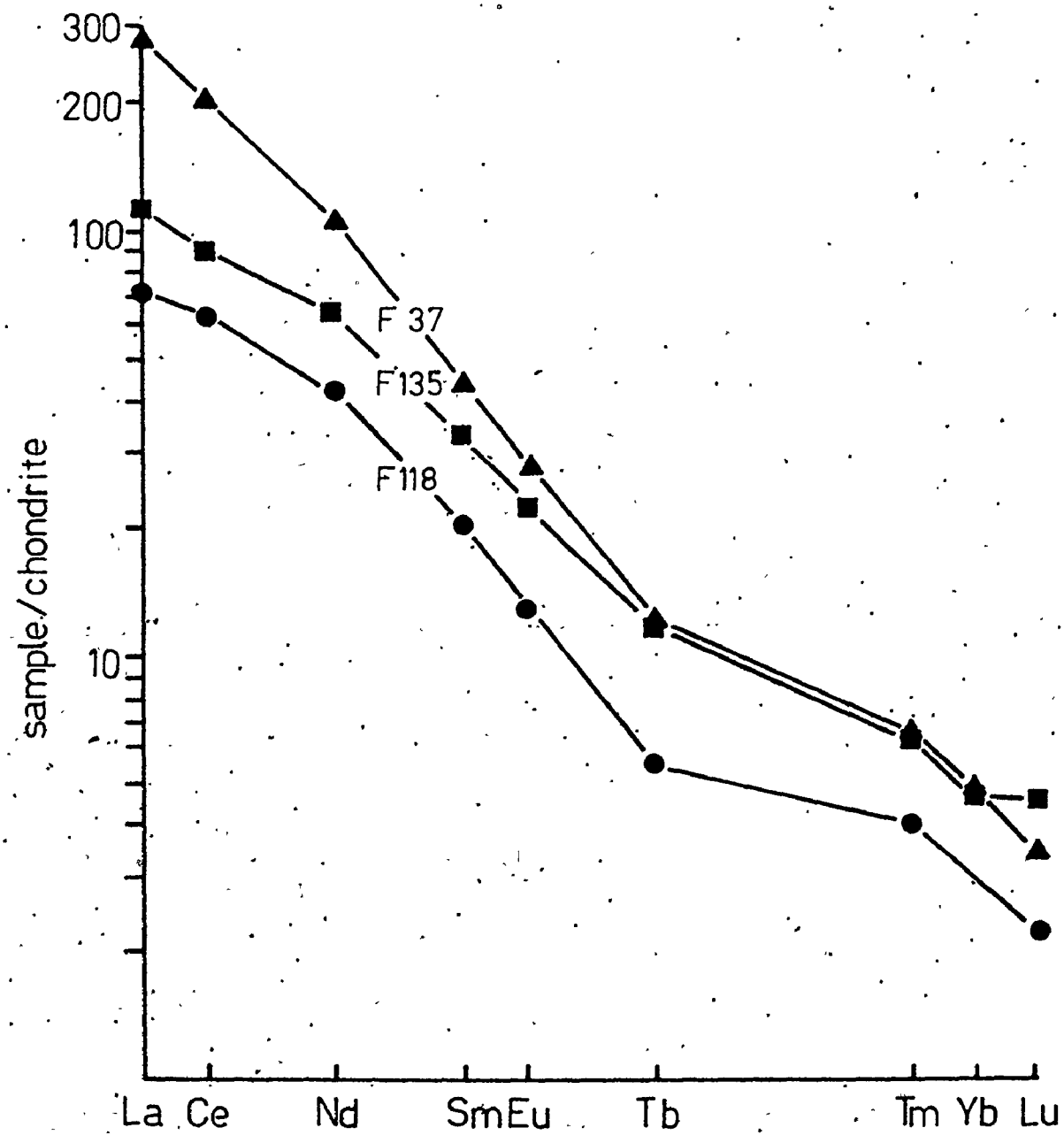

FIGURE 3-26 Chondrite normalized rare earth element patterns for the Jackfish Lake Complex altered granodiorite F37.

F37 altered granodiorite

F135 unaltered (quartz) monzodiorite

F118 SiO_2-rich granodiorite

FIGURE 3-27 Oxygen isotope results for Archean granitic rocks analyzed during this study.

The Burditt Lake stock, the Northwest Bay granodiorite, and the Jackfish Lake Complex rocks have probably not been significantly metamorphosed. The Dalles granodiorite and the Melick tonalite are at middle to upper amphibolite facies of metamorphism and are foliated to gneissic. Note the low $\delta^{18}O$ values of some of the Jackfish Lake Complex granodiorites.

▲ unaltered sample

● sample altered by meteoric water interaction

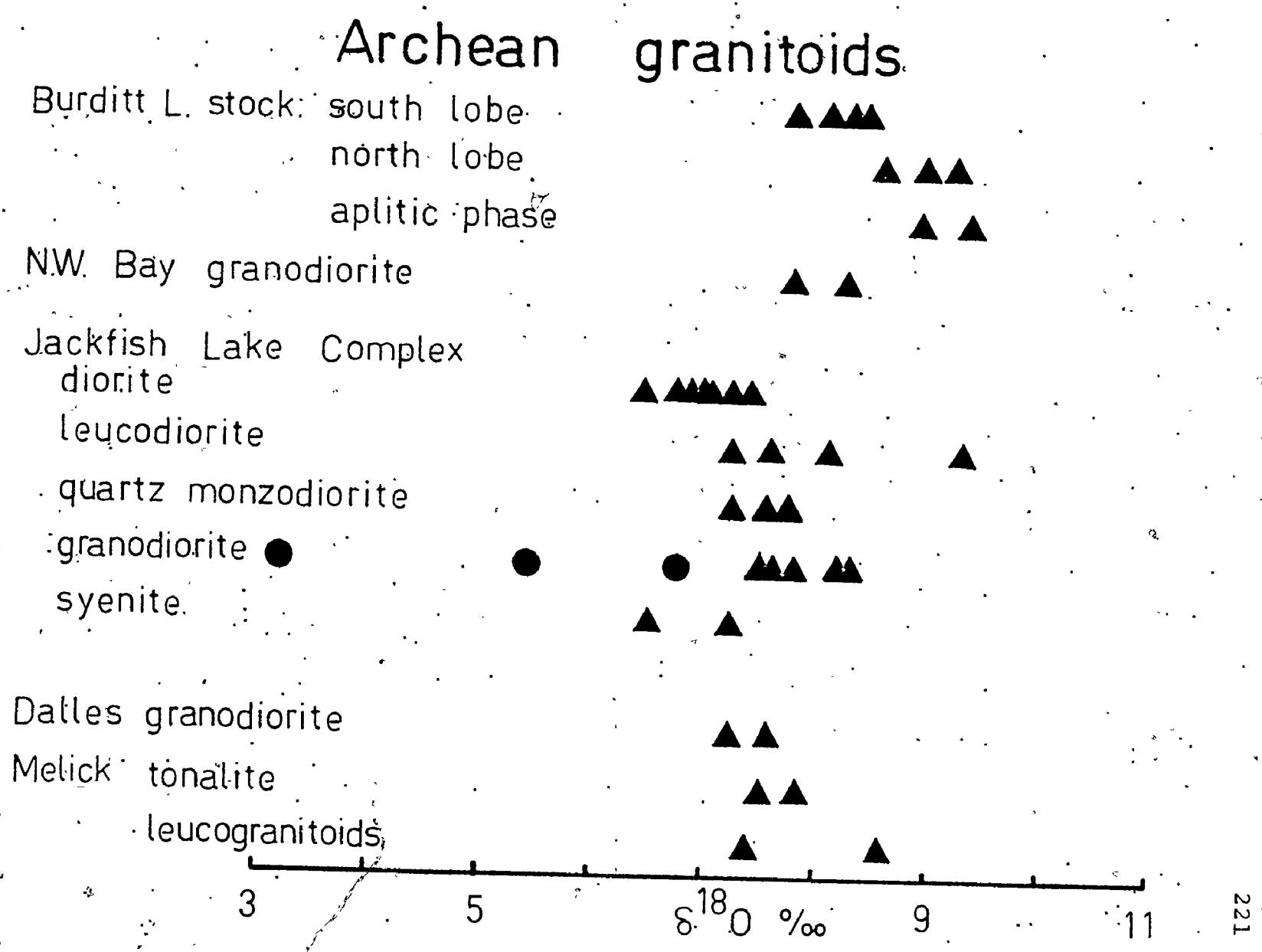
Archean granitoids
Burditt L. stock: south lobe
north lobe
aplitic phase
N.W. Bay granodiorite
Jackfish Lake Complex
diorite
leucodiorite
quartz monzodiorite
granodiorite
syenite
Dalles granodiorite
Melick tonalite
leucogranitoids
3
5
δ 18O ‰
9
11

Table 3-15 Oxygen isotope rock results, Jackfish Lake Complex

Rock type	Sample No.	$\delta^{18}O$ (‰)
meladiorite	F139	6.37
	F146	6.68
diorite	F84	6.99
	F21	6.86±0.17 (2)
	D8	6.96
	F131	7.19
	F144	7.33±0.06 (2)
leucodiorite	F94	7.54
	F24	8.08±0.16 (2)
qtz.-plag. dike	F23	9.23
(qtz.) monzodiorite	F135	7.54
	F82	7.72
	F133	7.26
granodiorite	F113	7.61
	F118	7.77
	F26	7.48
	D1	8.17
	F3	8.24
	F40	6.58*
	F37	5.41*
	F67	3.16*
Na syenite	F46	7.10
	F28	6.49
albite	F86	7.21

*altered by meteoric water interaction

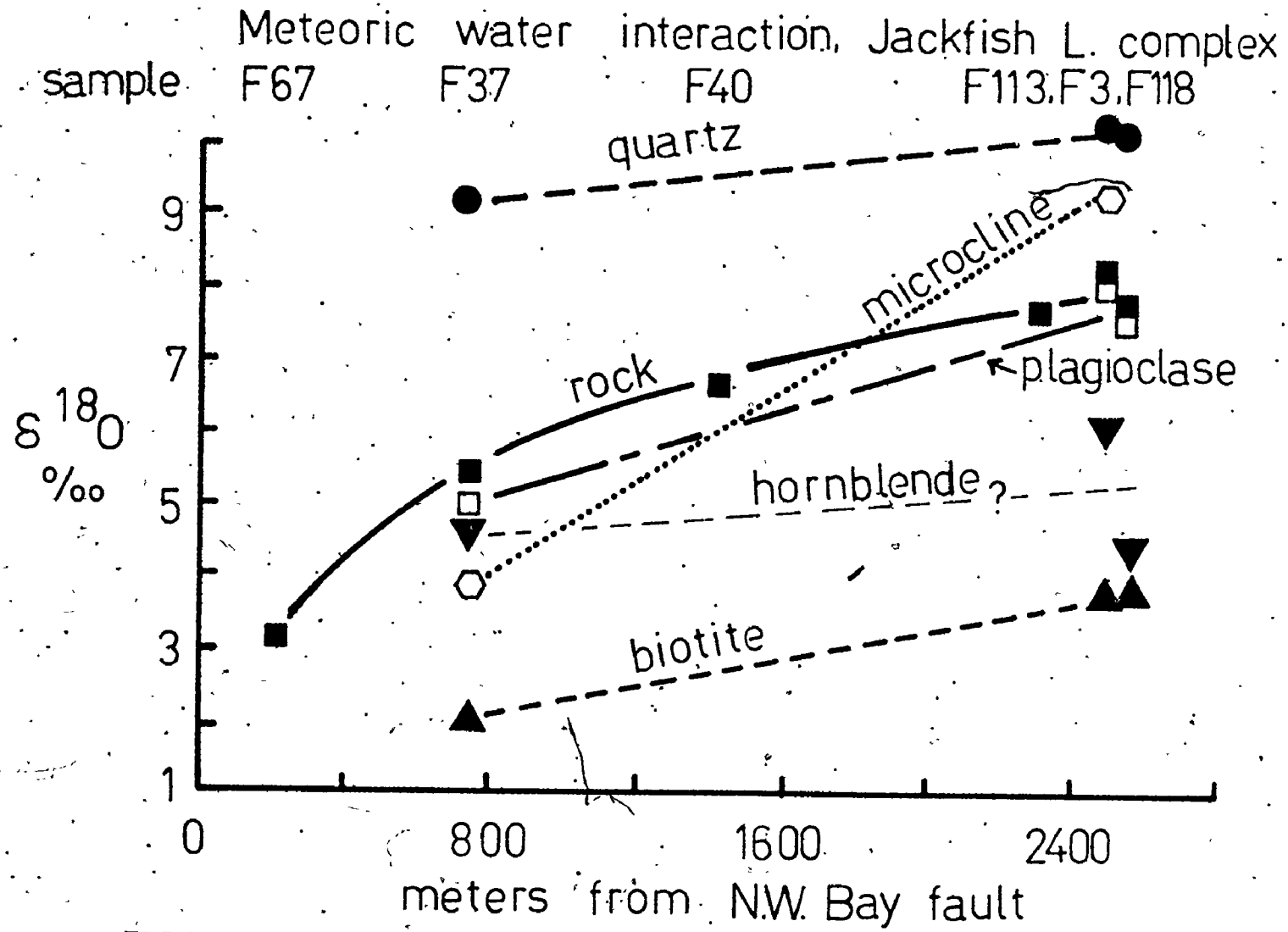

FIGURE 3-28 Oxygen isotope results for rocks and minerals from the Jackfish Lake Complex granodiorite located along a north-south traverse from the southern portion of Lake Despair to the Northwest Bay Fault.

isotopic characteristics suggest that these samples have undergone low temperature meteoric water-rock exchange:

1. The $\delta^{18}O$ values are distributed in the characteristic zonal pattern about the water source (the fault);
2. Except for low ^{18}O basalts from Iceland (Muehlenbachs et al., 1974) and some peculiar low ^{18}O uraninites (Muehlenbachs, pers. comm.), terrestrial rocks attain values as low as 3.2‰ only in low temperature water-rock interactions;
3. Minerals from altered granodiorite F37 are grossly out of isotopic equilibrium (Figure 3-28; Table 3-16). For example, microcline has a $\delta^{18}O$ value lower than coexisting hornblende; in unaltered rocks, the $\delta^{18}O$ of mineral phases increases in the order magnetite-biotite-hornblende-feldspar-quartz (Taylor, 1968).

If the microcline of F37 completely re-equilibrated with the fluid phase (and microcline does so readily; Magaritz and Taylor, 1976b), the oxygen isotopic composition of the fluid phase can be calculated for various temperatures using the experimentally calibrated alkali feldspar-H_2O curve of O'Neil and Taylor (1967); the results of such calculations are given below:

Table 3-16 $\delta^{18}O$ mineral data, Jackfish Lake Complex (°/₀₀)

Sample	quartz	microcline	plagioclase	hornblende	biotite	magnetite
F146 meladiorite			8.79±0.00	6.17±0.00	4.53	
F135 (qtz.) monzo-diorite	10.36	8.04	8.67±0.15	6.54	5.15±0.03	
F21 qtz. diorite		8.10±0.20	8.25	6.12±0.01	4.15±0.15	
F24 leuco qtz. diorite		7.83±0.22	8.08	5.42±0.01		
D1 qtz. poor granodiorite	10.51±0.01	7.61±0.36	7.51±0.13	5.37±0.22	4.24±0.15	
F3 granodiorite	10.16	9.17±0.23	8.14±0.01	6.01±0.11	3.70±0.22	
F26 granodiorite	10.41±0.10	9.12	7.29	6.35±0.10	5.70±0.18	0.56
F118 granodiorite	10.06	7.12±0.07	7.36±0.02	4.37±0.22	3.70±0.07	
F37 altered gran.	9.19±0.29	3.93±0.00	5.02±0.29	4.70	2.00±0.33	
F46 Na syenite		7.47±0.10	7.70±0.11	4.92		-1.89

Error shown is difference from mean of duplicate runs

T°C	$\delta^{18}O$ of fluid (‰)
600	3.5
400	-0.9
250	-3.3
200	-5.7
100	-13.6
20	-26.5

The actual exchange temperature can be estimated from the clay-chlorite-sericite assemblages in the altered granodiorites to be about 250°C or less (Winkler, 1976); thus the maximum $\delta^{18}O$ of the fluid should be about -3.3‰. Such compositions are characteristic of modern meteoric waters.

One interesting feature of this alteration pattern remains to be discussed; the $\delta^{18}O$ values of two samples of granitic to granodioritic Northwest Bay Complex located within 300 meters of the fault, but on its south side, are perfectly normal (Figure 3-27; Table 3-17). Quartz, microcline and biotite from granodiorite F31 are entirely in isotopic equilibrium (quartz-biotite and microcline-biotite oxygen isotope temperatures are both about 490°C; Appendix I). Also, petrographically, the rocks are unaltered.

The only conclusion that can be drawn from this curious

feature is that either the Northwest Bay Complex rocks were faulted into their present position after cessation of the meteoric water activity, or that they were faulted up from depths unaffected by near-surface meteoric water cells. Nonetheless, the fault itself seems to have served as a conduit for meteoric water.

Table 3-17 Oxygen isotope results, Northwest Bay Complex

	$\delta^{18}O‰$			
	quartz	microcline	biotite	rock
F129, granite	-	-	-	7.50±0.24 (3)
F31, granodiorite	9.65±0.22 (2)	8.40	3.92±0.16 (2)	-

Chemical variation of the diorite and granodiorite suites, Jackfish Lake Complex

Elimination of those rocks which underwent low temperature alteration (F67, F37, F35, F40) permits a clearer discussion of the chemical variations observed for the remaining Jackfish Lake Complex rocks. The purpose of this sections is to describe these variations, and indicate their dependence upon the amount and type of feldspar phase present in any particular sample.

A series of oxide versus Modified Larsen Index (MLI = 1/3 Si + K - Ca - Mg; Nockolds and Allen, 1953) variation diagrams (Figure 3-29a,b,c,d) illustrate the difference in chemical character between the 'diorite' and 'granodiorite' suites, the lithologies of which were described in section III-2. While such diagrams show some degree of spurious correlation due to (partially) closed array statistics (Chayes, 1964), the relationships displayed here are considered distinct enough to reflect the chemical evolution of these samples. The strong linearity of the CaO-MLI diagram (Figure 3-29a) could be produced by mixing (hybridization) but the remaining plots decry such an explanation; these results (Figure 3-29b,c,d) require the operation of some type of differentiation process.

One rock unit, the albite syenite, does not clearly fit into either the diorite or the granodiorite suite. Gradations to both leucodiorite and granodiorite compositions have been observed in outcrop and in chemical composition. The alkali content of the syenite is similar to that of the granodiorites; however, like the leucodiorites, the syenite contains little free quartz, and is lower than the granodiorites in SiO_2 (Table 3-12).

The differences between the chemistry of the diorite and granodiorite suites can also be illustrated by their K,

FIGURE 3-29 Modified Larsen Index diagrams for the Jackfish Lake Complex

■ meladiorite, (quartz) diorite, and leuco (quartz) diorite

○ (quartz) monzodiorite

● granodiorite

▲ Na-syenite

◆ albitite

⬢ aplite

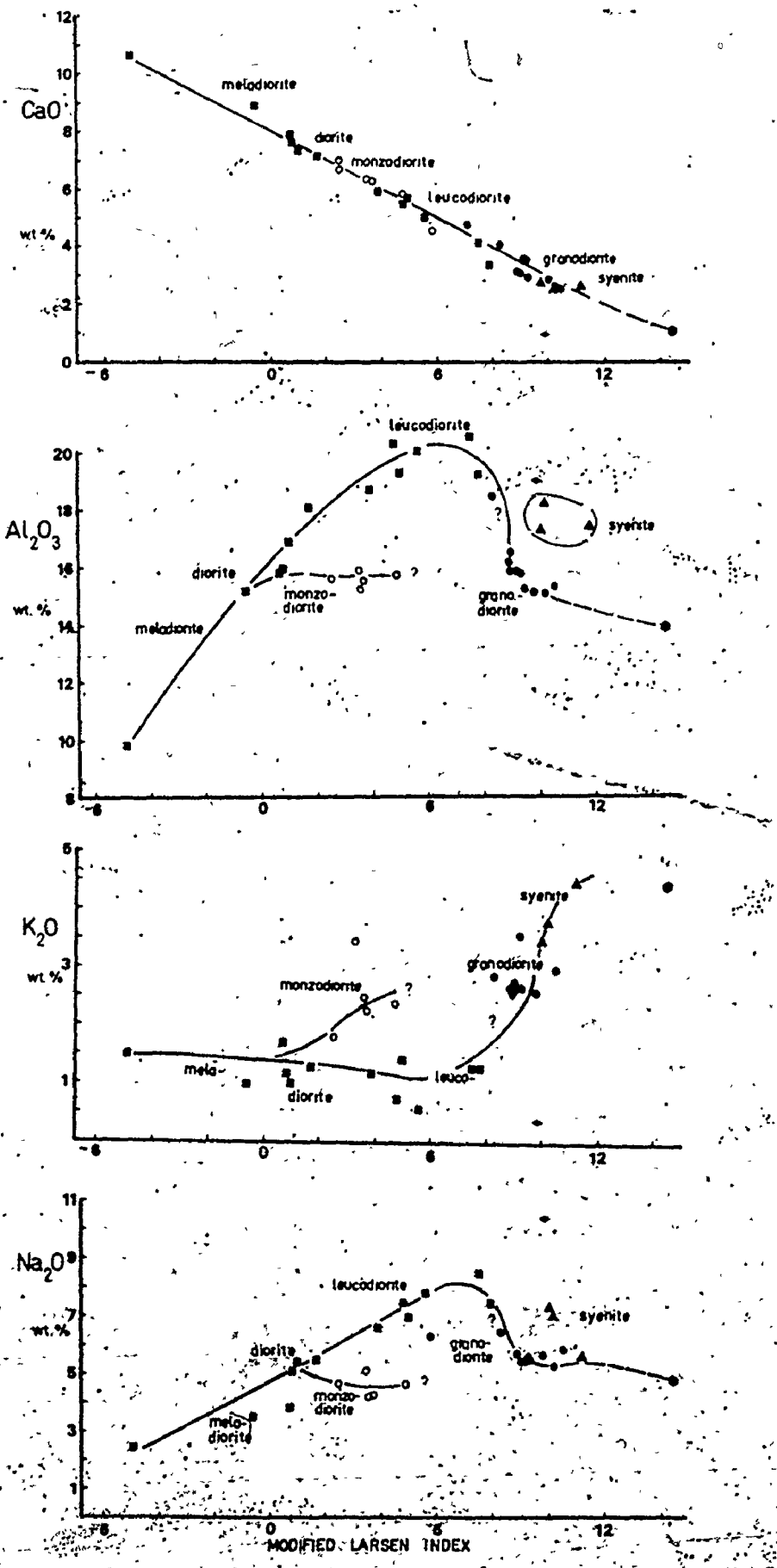
CaO
wt %
melodiorite
diorite
monzodiorite
leucodiorite
granodiorite
syenite
Al_2O_3
wt. %
leucodiorite
syenite
diorite
monzo-diorite
grano-diorite
melodiorite
K_2O
wt %
syenite
granodiorite
monzodiorite
mela-
leuco-
diorite
Na_2O
wt. %
leucodiorite
syenite
diorite
grano-diorite
monzo-diorite
melo-diorite
MODIFIED LARSEN INDEX

Ca, Rb, Sr and Ba systematics. The steady increase in Sr with decreasing Ca (Figure 3-30) observed for the diorite suite results from a decrease in the modal abundance of hornblende from about 70% to 10% and a corresponding increase in the amount of plagioclase. In addition, the actual Ca content of both the hornblende and the plagioclase decreases as the rocks become more leucocratic; the more sodic plagioclase is also richer in Sr (Table 3-18).

The more complex Ca-Sr pattern of the granodiorite suite is a function of the following factors:

1. the transition from monzodiorite to granodiorite is accompanied by a reduction in modal hornblende and a shift towards more Na-rich plagioclase; both cause a net reduction in Ca (Table 3-19);
2. the transition from monzodiorite to granodiorite is accompanied by an increase in quartz, which acts as a dilutant, causing both Ca and Sr abundances to decrease;
3. the variation in the Sr content of the granodiorite suite results from the wide fluctuation in the amount of plagioclase and microcline contained in individual samples. The very high Sr contents of the albite syenite results from the enrichment in feldspar that accompanied the disappearance of quartz, and from the

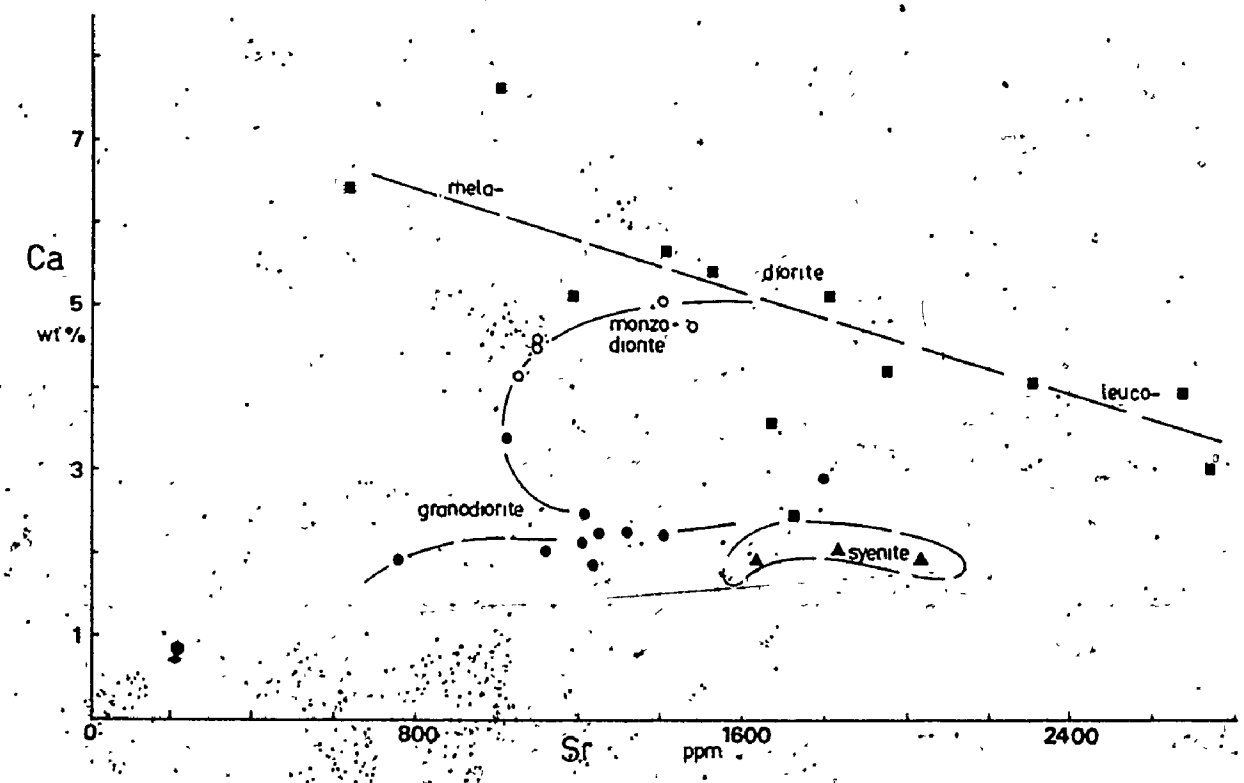

FIGURE 3-30 Ca versus Sr diagram for the Jackfish Lake Complex rocks. The legend is as in Figure 3-29.

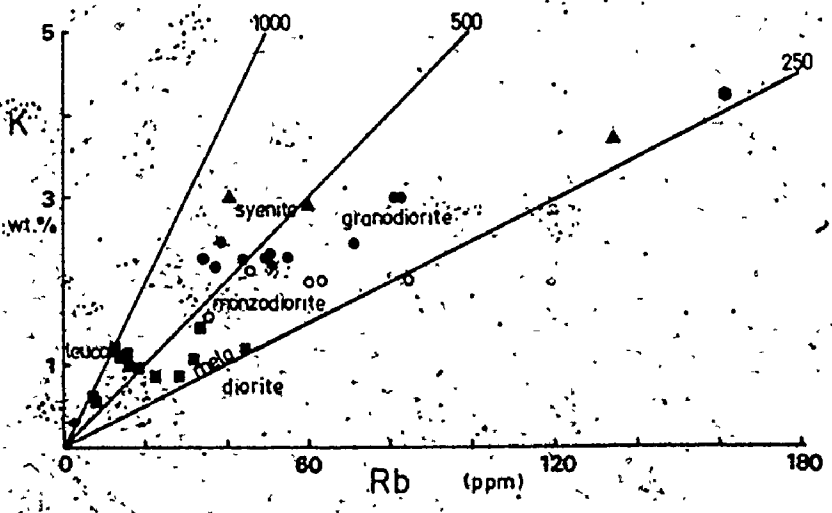

FIGURE 3-31 K versus Rb diagram for the Jackfish Lake Complex rocks. The legend is as in Figure 3-29.

Table 3-18 Mineral analyses, diorite suite

	Li ppm	Na wt %	K wt %	Rb ppm	Tl ppm	Ca wt %	Sr ppm	Ba ppm	Mg wt %	Fe wt %
F146										
diorite	25	2.82	0.79	29	0.20	5.89	730	488	3.52	-
hornblende	19	0.70	0.81	24	0.25	9.94	58	365	6.51	9.44
plagioclase	4	4.67	0.21	6	0.09	3.85	1402	480	0.05	-
F21										
qtz. diorite	27	5.15	0.91	21	0.15	3.92	1846	822	1.92	-
hornblende	46	0.88	0.60	16	0.19	8.29	328	318	4.84	11.10
biotite	354	0.40	4.49	254	2.02	2.28	103	1075	8.27	9.39
plagioclase	4	7.05	0.53	7	0.10	2.28	1994	686	0.04	-
F24										
qtz. leucodiorite	4	5.17	1.10	15	0.11	3.73	2270	747	1.53	-
hornblende	5	1.10	0.59	-	0.09	8.38	152	205	8.35	13.65
plagioclase	6	6.17	1.29	18	0.14	2.52	2153	904	0.03	-

Fe analyses by colorimetry; others by atomic absorption (P.C. Fung, analyst)

Table 3-19 Mineral analyses, granodiorite suite

	Li ppm	Na wt %	K wt %	Rb ppm	Tl ppm	Ca wt %	Sr ppm	Ba ppm	Mg wt %	Fe wt %
F135										
(qtz.) monzodiorite	23	-	2.07	79	0.43	4.43	1113	2440	5.10	-
hornblende	18	0.66	0.91	28	0.30	8.16	154	203	7.26	9.04
biotite	191	0.25	5.53	456	3.22	0.09	72	932	6.66	10.32
plagioclase	2	5.81	1.10	16	0.14	2.39	1341	1170	0.06	-
microcline	3	-	11.18	188	0.43	0.19	1110	6997	0.04	-
D1										
qtz. poor granodiorite	8	-	2.18	53	0.17	2.32	1332	1688	1.83	-
hornblende	10	0.87	0.76	12	0.21	8.91	221	198	6.63	12.07
biotite	161	0.27	5.76	434	2.24	0.15	50	810	7.09	12.91
microcline	2	-	11.82	187	0.42	0.07	747	5925	0.03	-
F3										
granodiorite	22	-	2.18	60	0.24	2.34	1242	1754	2.28	-
hornblende	18	0.84	0.65	-	0.13	9.27	602	155	6.69	11.05
biotite	415	0.39	4.95	396	2.32	0.21	92	738	7.80	14.01
plagioclase	6	6.24	1.70	26	0.20	1.60	1319	1513	0.03	-
microcline	1	-	9.93	222	0.51	0.13	1043	7304	0.03	-
F26										
granodiorite	18	-	2.90	100	0.33	1.91	788	1045	1.90	-
hornblende	27	0.86	0.82	27	0.36	8.30	186	105	7.30	11.05
microcline	2	-	11.69	318	0.85	0.65	433	3214	0.02	-

Table 3-19 /continued

	Li ppm	Na wt %	K wt %	Rb ppm	Tl ppm	Ca wt %	Sr ppm	Ba ppm	Mg wt %	Fe wt %
F118										
granodiorite	16	-	2.38	87	0.28	1.85	1194	1833	1.24	-
hornblende	14	0.98	0.84	10	0.21	8.80	89	191	6.58	11.52
biotite	332	0.36	5.60	574	3.52	0.16	93	866	7.48	16.05
plagioclase	5	6.15	1.18	24	0.24	1.54	1477	1025	0.01	-
microcline	2	-	11.13	309	0.75	0.05	740	5619	0.01	-
F46										
Na syenite	10	-	2.94	76	0.27	1.94	1745	1833	1.93	-
hornblende	54	0.92	0.51	-	0.21	8.89	278	167	7.74	11.98
plagioclase	4	8.11	3.88	4	0.14	0.50	1707	314	0.02	-
microcline	6	-	11.69	324	0.79	0.02	1872	5272	0.02	-

Fe by colorimetry; others by atomic absorption (R.C. Fung, analyst)

very high Sr contents of both the albite and the microcline (Table 3-19).

The K/Rb of the diorite suite increases from about 250 in the meladiorites to about 1000 in the leucodiorites; K contents remain relatively constant (0.8 to 1.0 wt. %) (Figure 3-31), reflecting the sympathetic variation in the K levels of the hornblende and plagioclase as the rocks become more leucocratic (Table 3-18). The K/Rb of both the hornblende and plagioclase also increase from about 340-350 to 700-1200 with decreasing colour index of the rocks.

K/Rb in the granodiorite suite varies from 400 to 800, except for one aplite sample and a syenite which has undergone high temperature metasomatism and alteration at the contact with the Footprint gneiss (F147). The monzodiorites generally have lower K/Rb than the granodiorites, a reflection of the greater abundance of hornblende in these rocks. The K/Rb of microcline also tends to decrease with increasing colour index; plagioclase, however, has a K/Rb of 500 to 1000 in these rocks, and controls, by its greater abundance, the observed K/Rb variations in the granodiorites and the syenites.

The uniform Ba content of the diorite suite (Figure 3-32) results from the antipathetic variation in Ba content and modal abundance of hornblende and plagioclase (Table 3-18), at least until the formation of the most leucocratic diorites.

FIGURE 3-32 Ba versus Sr diagram for the Jackfish Lake Complex

■ meladiorite, (quartz) diorite, and leuco (quartz) diorite

○ (quartz) monzodiorite

● granodiorite

△ Na-syenite

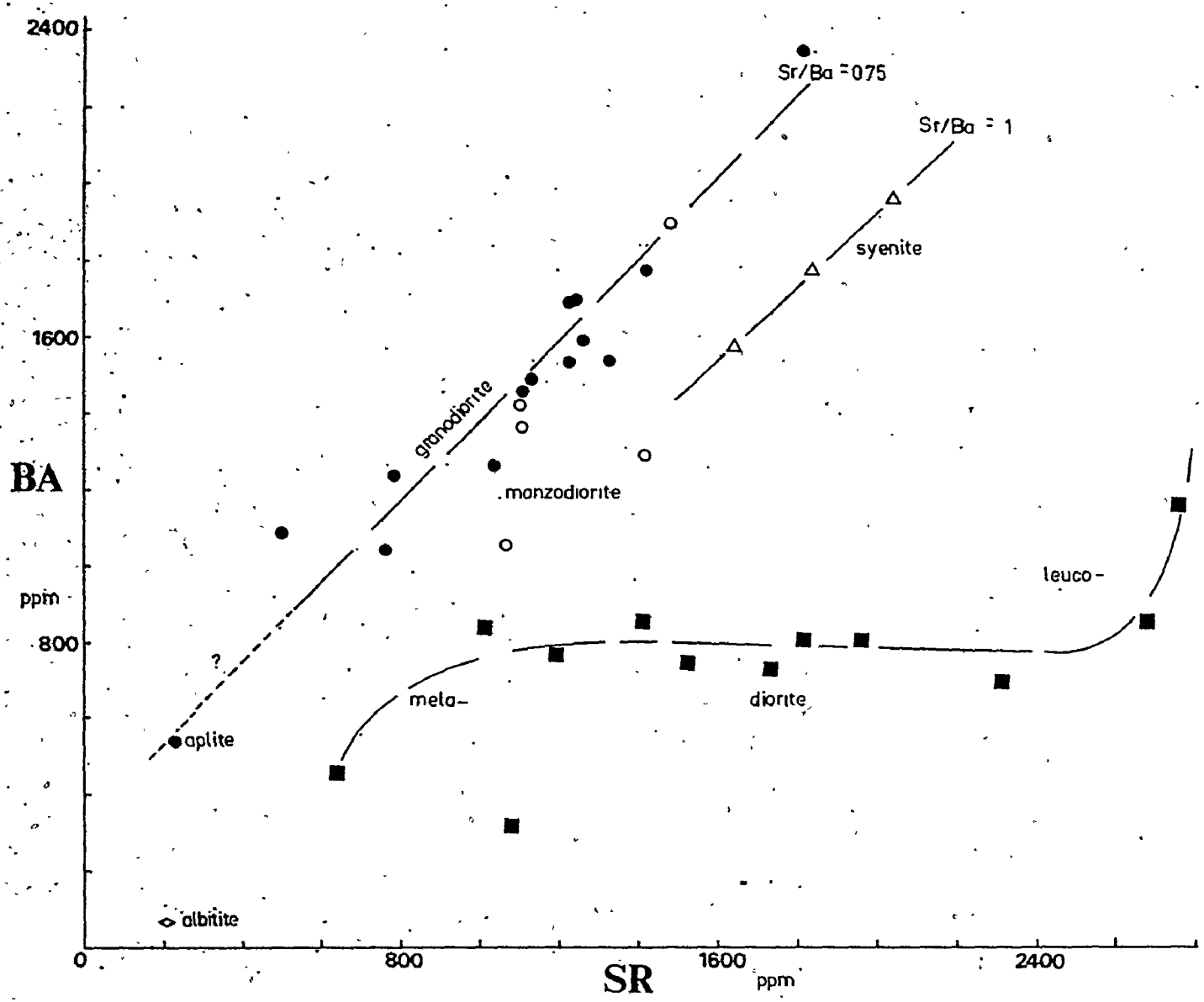
2400
1600
800
0
BA
ppm
SR
ppm
800
1600
2400
Sr/Ba =075
Sr/Ba = 1
syenite
granodiorite
monzodiorite
leuco-
meta-
diorite
aplite
albitite
?

Sr/Ba ratios increase, however, because the Sr/Ba of the plagioclase (2.4-3.0) is higher than that of the hornblende (0.2-1.0). The granodiorite suite, on the other hand, shows a positive correlation between Sr and Ba; the granodiorites have a relatively constant Sr/Ba of 0.75; the syenites are somewhat higher (1.0) and the monzodiorites and quartz monzodiorites vary between these two values. The lower Sr/Ba of the granodiorites reflect the low Sr/Ba of their microcline (0.1-0.2); microcline from the syenite has a somewhat higher Sr/Ba (0.4). The constant Sr/Ba arise from the mass balance of plagioclase (Sr/Ba of 0.8 to 5.5; modal abundance of 45-65%; Appendix III) and microcline (modal abundance of 10-20%).

The nature of the chemical variations in the unaltered Jackfish Lake Complex rocks should now be quite clear; the task of the remaining sections of this report is to evaluate its importance.

REE partial melting models for the origin of the Jackfish Lake Complex diorite

Introduction

Diorite and monzodiorite comprise the bulk of the Jackfish Lake Complex. Their origin, therefore is crucial

to an evolutionary model of the Complex. To aid the petrogenetic investigation, an unaltered, typical diorite (F146) was analyzed for REEs (Table 3-20; Figure 3-33), along with three other members of the diorite suite (F135, F21, F24). All of the diorites have strongly fractionated REE patterns, are depleted in HREEs, and have no Eu anomalies (Figure 3-33). In addition, the diorite, exemplified by F146, has the major element composition of some andesites and basaltic andesites (Table 3-21). The problems associated with the formation of the diorite magma, therefore, are, in some ways, analogous to the problem of the origin of andesite.

Ringwood (1975) concluded that the production of the calc-alkaline series requires pyroxene-plagioclase fractionation; amphibole fractionation or eclogite (garnet) fractionation, in order of increasing pressure. Low pressure plagioclase-pyroxene fractionation as a mode of origin for the diorites will not be considered, as the diorites lack Eu anomalies. Under somewhat hydrous conditions and P_{total} of 5 to 15 kb, the plagioclase crystallization field is suppressed, and hornblende and/or clinopyroxene fractionation control the evolution of intermediate liquids (Green, 1972; Eggler, 1972). Such conditions are pertinent to the partial melting of amphibolite of basaltic composition; low degrees of melting (<25%) produce dacitic liquids; larger melt fractions

Table 3-20 Selected analyses, diorite suite*

		diorite F146	qtz. diorite F21	leuco qtz. diorite F24
SiO_2	wt.%	54.62	58.25	60.21
Al_2O_3		15.18	18.72	19.35
TiO_2		0.49	0.54	0.33
Fe_2O_3		9.99	5.35	3.02
MnO		0.21	0.09	0.06
MgO		5.88	3.20	2.64
CaO		8.93	5.87	5.65
Na_2O		3.50	6.59	6.98
K_2O		1.00	1.15	1.44
P_2O_5		0.20	0.24	0.32
Li	ppm	25	27	4
Rb		29	19	14
Sr		639	1957	2310
Ba		451	806	690
Pb		9	12	11
Th		1.6	1.8	1.3
Y		17	11	5
Nb		t	t	t
Zr		31	170	49
Zn		91	77	34
Ni		90	43	30
Ta		0.4	0.7	0.7
Hf		1.2	5.0	2.4
Sc		22.5	18.0	16.1
La		26.0	33.1	17.9
Ce		59.2	73.7	46.2
Nd		23.8	34.5	21.9
Sm		5.5	6.63	4.86
Eu		1.65	1.73	1.39
Gd		t	t	t
Tb		0.718	0.484	0.389
Tm		0.201	0.150	0.133
Yb		1.44	0.940	0.617
Lu		0.242	0.126	0.085
Tl		0.20	0.15	0.11

Major elements normalized to 100%, anhydrous. Fe as Fe_2O_3.
REE, Th, Ta, Hf and Sc by INNA; all others by XRF.
t = trace

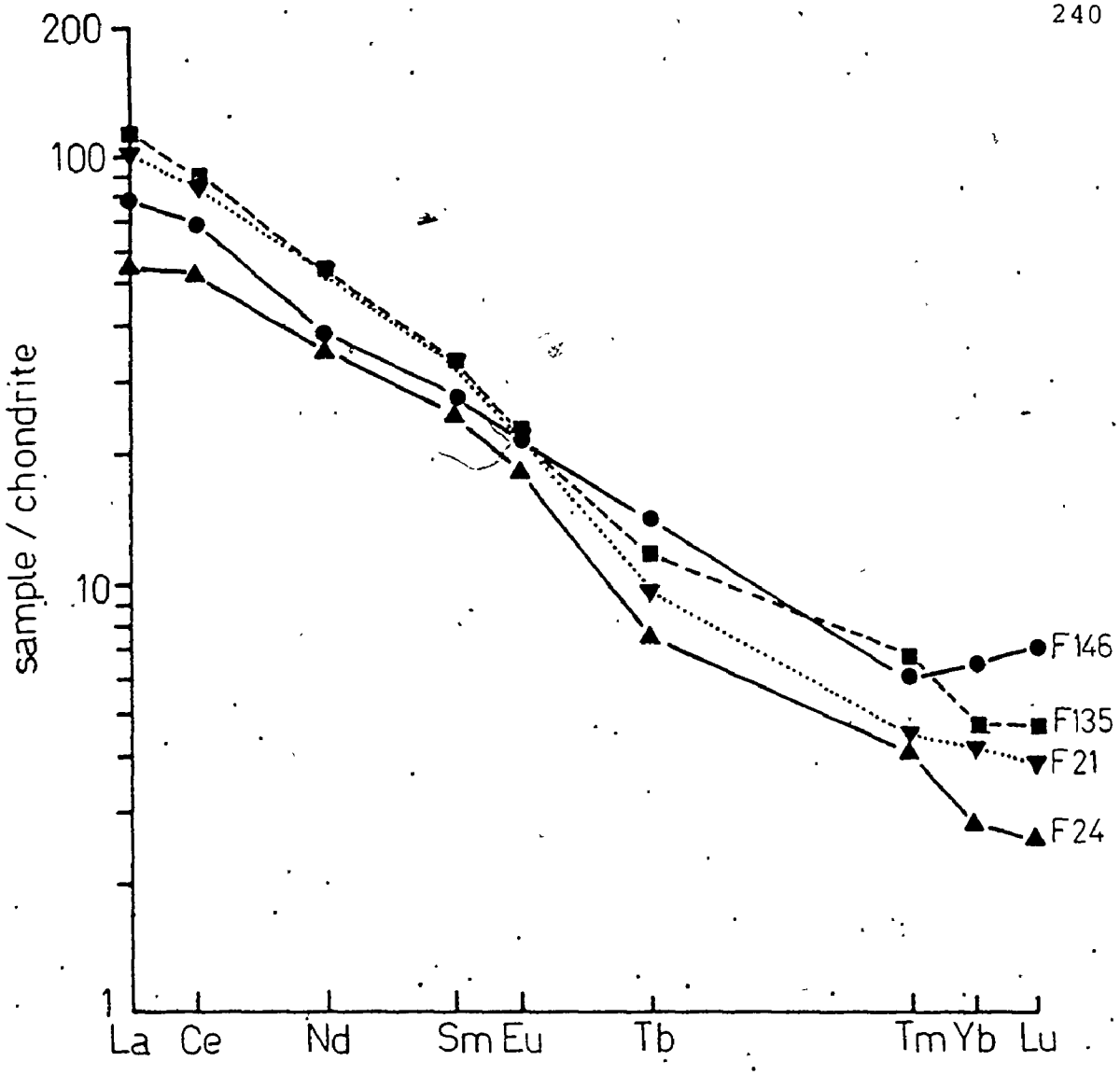

FIGURE 3-33 Chondrite normalized rare earth element results for the dioritic rocks from the Jackfish Lake Complex.

The pattern for the (quartz) monzodiorite (F135) is also shown as these rocks are similar to the diorites, except for the somewhat higher K content of the former group.

F146 diorite

F135 (quartz) monzodiorite

F21 quartz diorite

F24 leuco quartz diorite

Table 3-21 Comparison of Jackfish Lake Complex diorite and modern andesite

	1	2	3	4	5
SiO_2	56.16	55.76	57.16	56.35	55.93
Al_2O_3	16.35	16.55	17.37	17.04	15.47
TiO_2	0.68	0.80	0.64	0.77	0.75
FeO*	7.09	10.81	6.63	8.26	7.31
MnO	0.14	0.21	0.15	0.15	0.14
MgO	5.37	3.11	5.59	5.24	6.56
CaO	7.56	7.32	6.83	8.47	7.60
Na_2O	4.78	3.14	3.73	2.62	4.37
K_2O	1.54	1.94	1.66	1.01	2.27
P_2O_5	0.33	0.36	0.24	0.10	0.35

* Fe as FeO; all analyses recalculated to 100%, anhydrous

1. average of 7 diorites and monzodiorites, Jackfish Lake Complex

2. pyroxene-andesite lava, New Guinea. In Carmichael et al. (1974), p.537, #3.

3. hornblende-basaltic andesite, Solomon Islands. In Carmichael et al. (1974), p.544, #5.

4. andesite lava, New Zealand. In Carmichael et al. (1974), p.554, #2.

5. trachyandesite porphyry; northeastern Minnesota (Archean); Arth and Hanson (1975), p.331, #6.

result in melts of andesitic or dioritic composition. Partial melting of hydrous (high pressure) or anhydrous (low pressure) eclogite can also produce andesitic compositions. Ringwood (1975) notes that andesitic compositions lie in a thermal valley for partial melts of anhydrous quartz eclogite; first melts under hydrous conditions, however, are silicic. Stern and Wyllie (1973) have pointed out, however, that the liquids produced by the dry melting of eclogite need not necessarily evolve precisely along the calc-alkaline path; perhaps the gabbro-trondhjemite trend represents one of the possible divergences.

A fractional crystallization origin has not been considered for the Jackfish Lake diorites, although similar REE patterns to those observed could be produced by such a mechanism. The reason for this is geological; there are no gabbros exposed in the Jackfish Lake Complex.

Model 1: partial melting of amphibolite

Using the techniques described in sections III-6 and III-7, hypothetical REE patterns were calculated for partial melting of a parent rock similar in chemical composition to the Burditt Lake metabasalts, and compared with those measured for the Jackfish Lake Complex diorite. In this case, however, distribution coefficients measured for basaltic to andesitic

rocks (Arth and Hanson, 1975) were used, as the melt produced is dioritic in composition.

The results for a modal melt of 50% plagioclase and 50% hornblende (Figure 3-34a) do not reproduce the observed REE pattern. At 30% melting; that necessary to produce an andesitic liquid from a hydrous metabasalt, the agreement between predicted and observed REE patterns is at its poorest. Other modal and non-modal melting models, using various proportions of plagioclase and hornblende, came no closer to reproducing the desired REE pattern.

Other chemical data do not support an amphibolite model; according to Ringwood (1975) liquids produced by partial melting of amphibolite should have Na_2O/K_2O similar to the parent basalt, and be strongly depleted in Ni and TiO_2. Such is not the case:

	Burditt Lake metabasalt	Jackfish Lake Complex diorites
Na_2O/K_2O	7.3	3.1
TiO_2	0.92 wt.%	0.68 wt.%
Ni	92 ppm	90-110 ppm

FIGURE 3-34 Chondrite normalized rare earth element melting model results for the Jackfish Lake Complex diorite F146.

A. Model 1: equilibrium modal melting (1, 10 and 30%) of amphibolite, as described in the text.

B. Comparison of rare earth element results for the Jackfish Lake Complex diorite suite and similar rock types from the Archean Vermilion District of northeastern Minnesota.

1. Icarus pluton, syenodiorite
2. Vermilion batholith syenodiorite
3. Giants Range tonalite
4. Vermilion batholith granodiorite
5. trachy-andesite

The REE patterns for the Vermilion District rocks have been recalculated from the data of Arth and Hanson (1975, p.331-332), using the same partition coefficients and chondrite values as for the Jackfish Lake Complex. The stippled pattern represents the results for the Jackfish Lake Complex diorite suite.

C. Model 2: 10 and 30% equilibrium modal melting of quartz eclogite as described in Table 3-22.

D. Model 6ii: 5, 10, 15 and 30% equilibrium non-modal melting of eclogite (85% clinopyroxene, 15% garnet), with garnet and clinopyroxene entering the melt in equal proportions (Table 3-22).

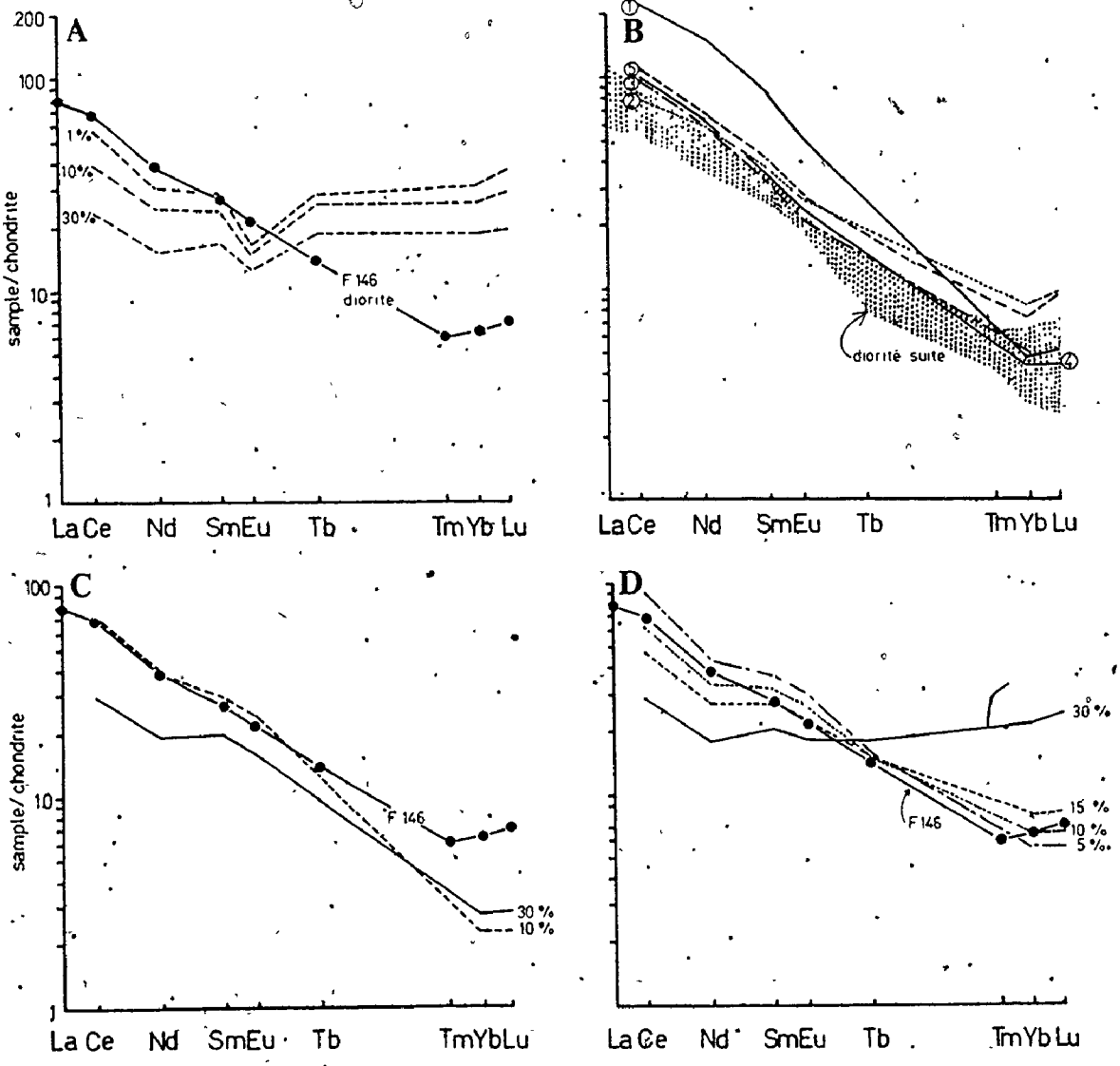
A
200
100
10
1
sample/chondrite
1%
10%
30%
F 146
diorite
La Ce Nd SmEu Tb TmYb Lu
B
1
2
3
4
diorite suite
La Ce Nd SmEu Tb TmYb Lu
C
100
10
1
sample/chondrite
F 146
30 %
10 %
La Ce Nd SmEu Tb TmYbLu
D
30 %
15 %
10 %
5 %
F 146
La Ce Nd SmEu Tb TmYb Lu

Modelling for Rb, Sr, and Ba, similar to that for the REEs, also failed to produce calculated results similar to those measured for the diorite.

Models 2 to 8, eclogite melting models

A close analogue for the Na-enriched rocks of the Jackfish Lake Complex is the alkali rocks of the Vermilion District, northeastern Minnesota (Arth and Hanson, 1975; Longstaffe et al., 1977a). Some chemical comparisons between the two areas are made in Table 3-12. The Jackfish Lake Complex (JLC) diorites and monzodiorites (1) are chemically and petrographically similar to rocks of the Icarus pluton (2) and the Vermilion batholith (3); the range in granodiorite composition observed in the Jackfish Lake Complex (4 and 5) is matched by that of the Icarus pluton (6) and the Vermilion batholith (7). JLC Na-syenites and Na-leucodiorites (8 and 9) are similar to Na syendiorites from the Farm Lake Facies of the Giants Range Batholith (10); the quartz diorites of the Giants Range Batholith (12) are not unlike the quartz monzodiorites of the Jackfish Lake Complex (11). However, most of the Jackfish Lake Complex rocks are somewhat higher in Na/K and lower in K than the Vermilion District analogues.

The chemical similarities between these rock types extends to REE patterns and concentrations (Figure 3-34b).

The origin proposed for the Vermilion District rocks involved partial melting and/or fractional crystallization of a mixed quartz eclogite-undersaturated eclogite parent (Arth and Hanson, 1975; Barker and Arth, 1976). Arth and Hanson (op. cit.) specifically propose that the high Na and Al rocks (which are most like the Jackfish Lake Complex) formed by partial melting of undersaturated eclogite. Such a parent composition allows low degrees of partial melting to produce melts of andesitic-alkali composition from hydrous mantle.

The various eclogite and quartz eclogite melting models tested in the attempt to reproduce the REE pattern of the Jackfish Lake Complex diorite (F146) are summarized in Table 3-22.

Model 2 (Figure 3-34c) shows that the eclogite model concept does produce the overall REE pattern and concentrations similar to those required, although in this particular example, the HREE depletion is three times greater than observed in the diorite (F146).

Using the mantle phase equilibria outlined by Stern et al. (1975) for the melting of gabbroic or basaltic rocks, non-modal melting models involving eclogite (Table 3-22, #3-8) were formulated. At pressures greater than 27 kb, the order of melting is coesite (750°C), kyanite (850°C), and then garnet and clinopyroxene, at the liquidus. This possibility,

Table 3-22 Eclogite melting models for Jackfish Lake diorite F146

Model	Parent mineralogy	Model type	Contribution to melt by parent phases
2	15% co + ky 50% cpx 35% ga	Modal melting	
3	5% co + ky 70% cpx 25% ga	Non-modal melting	all co and ky ga and cpx in equal proportions
4	5% qtz + ky 25% hb 45% cpx 25% cpx	Non-modal melting	all qtz and ky ga and hb in equal proportions all cpx in residue
5	5% qtz + ky 15% cpx 20% hb 60% ga	Non-modal melting	i. 35% hb, 50% ga, 15% qtz + ky ii. 10% hb, 75% ga, 15% qtz + ky iii. 20% hb, 65% ga, 15% qtz + ky iv. 30% hb, 55% ga, 15% qtz + ky v. 30% hb, 50% ga, 15% qtz + ky, 5% cpx vi. 25% hb, 50% ga, 15% qtz + ky, 10% cpx
6	85% cpx 15% ga	Non-modal melting	i. 65% cpx, 35% ga ii. 50% cpx, 50% ga iii. 35% cpx, 65% ga iv. 25% cpx, 75% ga v. 15% cpx, 85% ga
7	75% cpx 25% ga	Non-modal melting	i. 50% cpx, 50% ga ii. 25% cpx, 75% ga
8	5% co + ky 80% cpx 15% ga	Non-modal melting	all co and ky ga and cpx in equal proportions

co: coesite
ky: kyanite
qtz: quartz
cpx: clinopyroxene
hb: hornblende
ga: garnet

tested by model 3, produces a reasonable match for the LREEs of F146 at 10% melting, but 35% melting is required to produce the observed HREE pattern.

Model 4 (Table 3-22) tested the 20 kb phase relationships; at these pressures, hornblende, clinopyroxene, garnet, and kyanite can coexist as solidus phases and melt in the order quartz and kyanite (near the solidus), hornblende and garnet (near the liquidus) and clinopyroxene (at the liquidus). This model produced a REE pattern too depleted in LREEs at melt fractions greater than 5%, and too depleted in HREEs at melt fractions of less than 40%.

Model 5, designed to correspond to the 15 to 20 kb pressure regime, where phases melt in the order kyanite, quartz, garnet, hornblende and clinopyroxene, was equally inappropriate. For all variations attempted at 30% melting, there was little or no enrichment in LREEs; at lower degrees of melting (10%), the required LREE enrichment could be obtained, but only when accompanied by far greater depletion in the HREEs that is observed in the Jackfish Lake Complex diorite.

Model 6 most closely approximates the parent composition suggested by Arth and Hanson (1975) for the Vermilion District rocks. The observed REE pattern for diorite F146 corresponds reasonably well with the calculated pattern for

7 to 15% melting, according to model 6ii (Table 3-22; Figure 3-34d). The variation of the percentage of individual phases entering the melt (models 6i-6v) has little effect upon the LREE abundances; however, it critically affects the HREE contents. For example, the chondrite normalized calculated values for Lu varied from 5.8 to 9.3 as the percentage of garnet entering the melt was changed from 35 to 85%. That model 6ii fits the observed data best of all the variations attempted, is particularly gratifying, as Stern et al. (1975) showed that at pressures greater than 27 kb (to which the starting mineralogy of model 6 corresponds), garnet and clinopyroxene melt together at the liquidus, as is assumed in this model.

To test the sensitivity of model 6 to the proportions of garnet and clinopyroxene in the parent, similar calculations were performed for a lower clinopyroxene/garnet ratio in the parent (model 7; Table 3-22). For 10% melting, the calculated HREE values were 2 to 3 X below that required. Clearly, the clinopyroxene/garnet ratio of the parent eclogite exerts strong control upon the HREE distributions in the resulting melts. The high ratio required by the Jackfish Lake Complex diorite (greater than 5) may also explain the Na-rich nature of these diorites and the associated rocks; given that the clinopyroxene contains a jadeitic

component, high clinopyroxene/garnet ratios in the eclogite should cause Na enrichment in the melts, as long as the clinopyroxene and garnet enter the melt in at least equal proportions.

The final model (model 8; Table 3-22) contains a silica phase in the starting mineralogy; most of the diorites do contain some quartz (1 to 2%) and our assumed parent rock, the Burditt Lake metabasalt, is usually quartz normative. The REE patterns calculated for such a parent were virtually identical to those for model 6ii (Figure 3-34d).

The Rb, Sr and Ba enrichment factors calculated for models 1 to 8 also best fit models 6ii and 8 (Figure 3-35), although the results are not perfect.

Conclusion

The preceding discussion indicates that a quartz eclogite-eclogite source rock enriched in omphacitic clinopyroxene can be partially melted to produce the REE pattern observed for diorite F146 in a pressure regime where both garnet and clinopyroxene enter the melt in equal proportions (>27 kb, under hydrous conditions). If the melting has taken place under hydrous conditions, the major element composition of the diorite requires that the parent rock be slightly undersaturated in SiO_2, as low degrees of melting

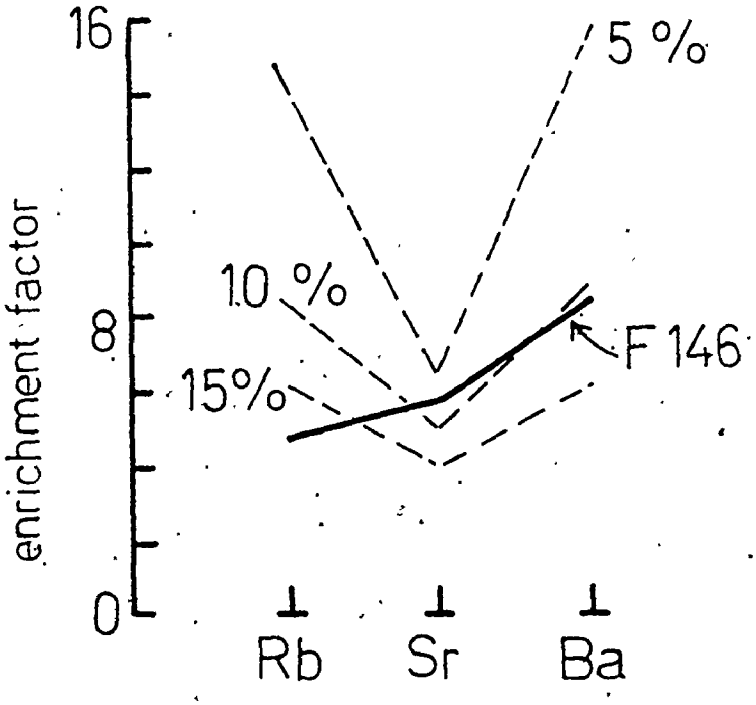

FIGURE 3-35 LIL element enrichment factors for the Jackfish Lake Complex diorite F146.

The Rb, Sr, and Ba enrichment factors were calculated for 5, 10 and 15% melting of eclogite (model 6ii, Table 3-22) or quartz eclogite (model 8, Table 3-22), using the chemical composition of the Burditt Lake metabasalts (Table 3-4, #1) as that of the hypothetical parent rock.

of silica saturated or slightly undersaturated eclogite in a hydrous mantle can produce 'andesitic-alkalic' melts (Arth and Hanson, 1975). Anhydrous partial melting of quartz eclogite to produce the diorite cannot be ruled out, however. Barker and Peterman (1974) suggested that the Archean mantle was dehydrated during the formation of the early Archean bimodal dacite-basalt suites, and that the onset of more calc-alkaline magmatism at about 2.7 b.y., reflected the completion of mantle dewatering. The Jackfish Lake Complex is about 2.6 b.y. and the last major intrusive episode in the Archean history of the Rainy Lake area (section III-2). Its formation, therefore, could demarcate the commencement of anhydrous mantle processes.

Origin of the Jackfish Lake Complex monzodiorites, leucodiorites, granodiorites and syenites

Introduction

The quartz monzodiorites (F135), quartz diorites (F21), leuco (quartz) diorites (F24) and granodiorites (F3, F118, D1, F26) (Tables 3-20, 3-23; Figures 3-33, 3-36) have REE abundances and patterns similar to the Complex diorite, although somewhat more depleted in HREEs. Some of the eclogite melting models discussed for the diorite accurately

Table 3-23 Selected analyses, granodiorite suite

		F135	D1	F3	F26	F118	F46	F37
SiO_2	wt %	58.48	66.37	66.85	67.60	68.80	63.60	65.69
Al_2O_3		15.25	16.20	15.92	15.05	15.46	17.21	15.13
TiO_2		0.68	0.32	0.31	0.32	0.24	0.39	0.50
Fe_2O_3		7.12	2.86	3.30	3.08	2.44	3.59	4.30
MnO		0.12	0.04	0.07	0.05	0.06	0.08	0.08
MgO		5.05	2.45	1.81	2.41	1.40	1.27	2.59
CaO		6.33	3.16	3.49	2.67	2.61	2.85	3.55
Na_2O		4.25	5.72	5.46	5.07	5.91	7.30	4.38
K_2O		2.45	2.73	2.73	3.61	2.96	3.47	3.62
P_2O_5		0.28	0.16	0.08	0.14	0.11	0.26	0.16
Li	ppm	23	8	22	18	16	10	13
Rb		64	45	50	83	72	60	82
Sr		1104	1325	1218	760	1243	1841	780
Ba		1430	1533	1692	1042	1693	1766	1235
Pb		12	15	16	23	17	23	15
Th		2.1	3.3	2.4	13	5.8	15	16
Y		13	8	9	12	6	10	14
Nb		t	t	t	3	3	t	4
Zr		50	133	98	138	103	342	167
Zn		85	47	51	52	41	61	55
Ni		86	21	29	24	16	20	49
Ta		0.6	1.7	2.8	3.2	2.9	0.7	2.5
Hf		2.3	4.4	3.4	4.5	3.7	10.8	5.0
Sc		20.8	11.0	11.4	11.7	10.0	12.9	12.2
La		37.7	29.0	20.7	41.9	23.6	64.7	91.6
Ce		78.2	68.4	48.0	80.8	54.4	118	174
Nd		33.1	24.3	21.0	30.1	26.1	37.3	66.1
Sm		6.69	4.83	3.82	5.70	4.09	9.11	8.83
Eu		1.72	1.21	1.05	1.07	0.997	1.74	1.94
Gd		t	t	6.90	2.40	3.87	t	t
Tb		0.620	0.334	0.451	0.365	0.284	0.238	0.626
Tm		0.221	0.119	0.119	0.126	0.139	0.163	0.227
Yb		1.06	0.595	t	t	t	1.14	t
Lu		0.155	0.092	0.097	0.139	0.075	0.173	0.114
Tl		0.43	0.17	0.24	0.33	0.28	0.27	0.30

Major elements normalized to 100%, anhydrous. Fe as Fe_2O_3.

REE, Th, Ta, Hf and Sc by INNA; others by XRF.

t = trace

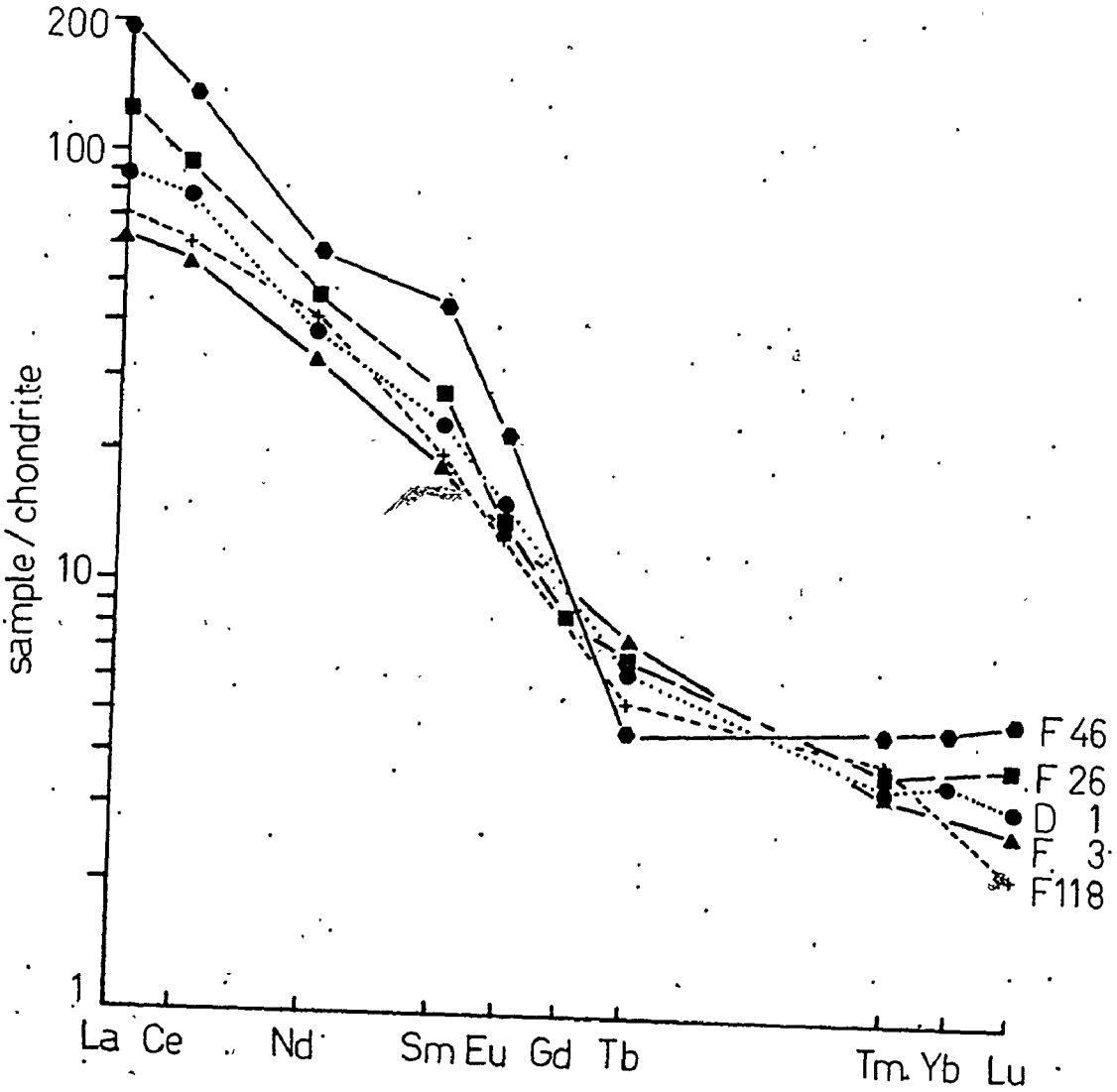

FIGURE 3-36 Chondrite normalized rare earth element patterns for the Jackfish Lake Complex granodiorite (F26, F3, F118, D1) and Na-syenite (F46).

reproduce the REE patterns observed for the leucodioritic (Figure 3-37a; Table 3-22, model 7) and granodioritic (Figure 3-37b; Table 3-22, model) rocks. However, these rocks form a very small proportion of the Jackfish Lake Complex; in addition, they form gradational contacts with each other. Thus, the formation of each of these rock types at great depths from heterogeneous mantle sources, followed by their emplacement within a very small area, seems unlikely.

Some aspects of the modelling support this conclusion; the LIL element distributions predicted by models 2 and 7 do not match those observed for the leucocratic members of the Complex (Figure 3-38), and the leuco quartz diorite (F24), which is among the volumetrically least important rock types, has LREE abundances that, according to such models, correspond to larger melting fractions than required for the diorite and monzodiorite (Figure 3-37a).

The spatial relationship between the leucocratic members of the Complex suggests, instead, that some sort of late stage fractional crystallization has modified the chemistry of portions of the dioritic magma, while still leaving unaffected the overall REE characteristics that are indicative of the source conditions involved in the formation of the parent dioritic magma.

FIGURE 3-37a Chondrite normalized rare earth element partial melting model for the Jackfish Lake Complex (quartz) monzodiorite, quartz diorite, and leuco quartz diorite. The solid line represents the model calculation for 10% melting of eclogite according to model 7 (Table 3-22). The vertical hatching shows the range of results for F135, F21 and F24.

FIGURE 3-37b Chondrite normalized rare earth element partial melting model for the Jackfish Lake Complex granodiorites. The solid line represents the model calculation for 10% melting of a quartz eclogite according to model 2 (Table 3-22). The vertical hatching shows the range of results for D1, F3, F26, and F118.

FIGURE 3-38 LIL element enrichment factor diagrams for the Jackfish Lake Complex leuco (quartz) diorite, granodiorite and Na-syenite. The Rb, Sr, and Ba values for the leuco (quartz) diorites are from Table 3-12, #9, those for the granodiorites from Table 3-23, and those for the Na-syenite from Table 3-12, #8. The parent rock compositions are those of the Burditt Lake metabasalt (Table 3-4, #1).

FIGURE 3-39 Modal hornblende content versus heavy rare earth element content (Tb, Tm, Yb, and Lu) for the Jackfish Lake Complex rocks.

fig 3-37a

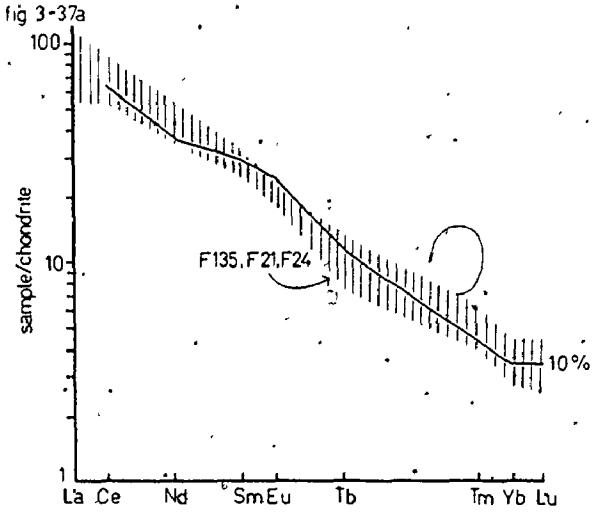

fig 3-37b

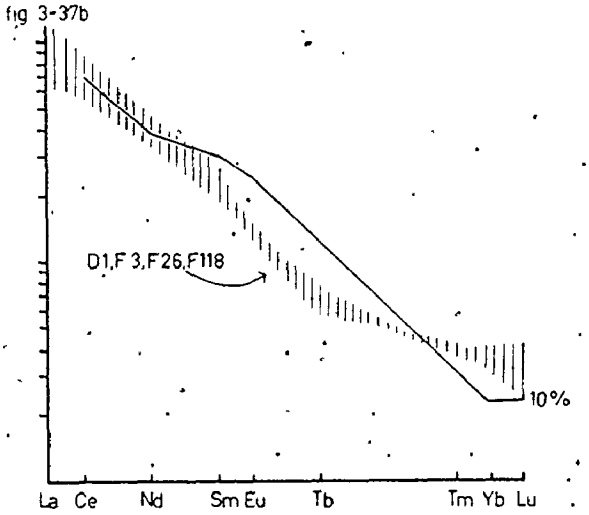

fig 3-38

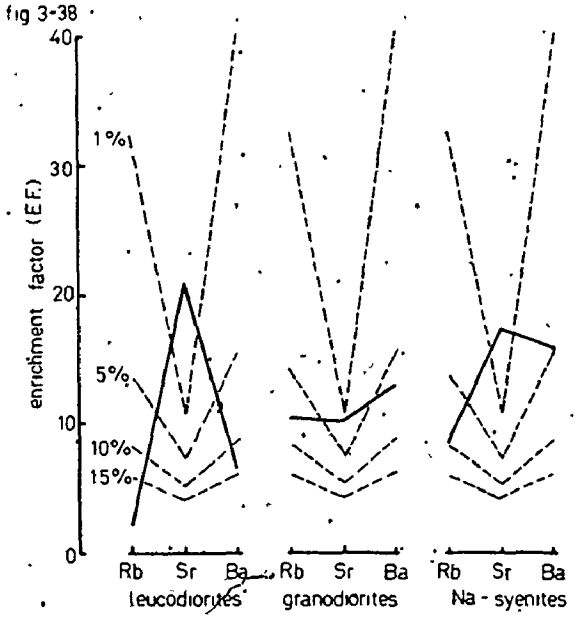

fig 3-39

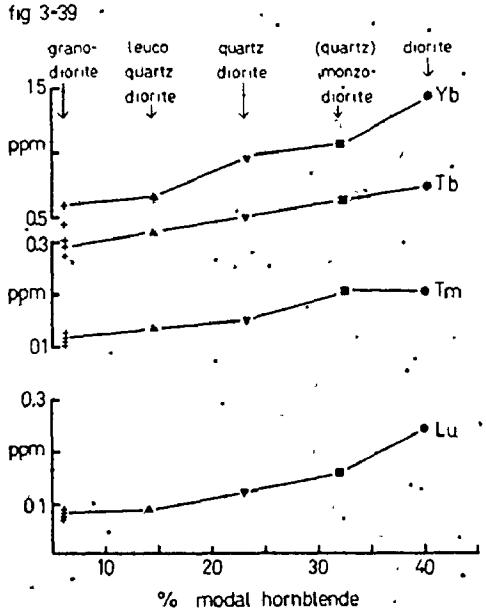

Hornblende fractionation and the diorite suite

The lithologic and chemical variation of the diorite suite from mela to leucodiorite can be explained by the process of hornblende fractionation.

1. The petrographic features of the Jackfish Lake Complex diorite are compatible with phenocryst-melt reactions during hornblende readsorption. Except for hornblende clots, which could have formed by crystal settling, the hornblende is ragged, has biotite rims, and is in a reaction relationship with the surrounding feldspar (Appendix III). The clots are less reacted, as would be expected, as they would be somewhat more insulated than discrete crystals from reaction with the surrounding felsic liquid.

2. There is a good correlation between Lu, Yb, Tm, and Tb and the modal abundance of hornblende contained in the dioritic suite (Figure 3-39). Arth and Barker (1976, p.597) showed that the precipitation of hornblende is capable of producing such HREE abundances in high Al tonalitic rocks.

3. The preferential incorporation of K and Rb into hornblende rather than plagioclase (Table 3-18), and the increasing K/Rb of the diorite suite as K and Rb contents decrease (Figure 3-31) are compatible with progressively smaller amounts of hornblende crystallization as the differentiation of the diorite suite progressed towards more

leucocratic compositions.

4. The increasing Sr and Sr/Ba ratio of the diorite suite (Figure 3-22) corresponds to the increasing importance of plagioclase as a liquidus phase; the liquid became more felsic because of impoverishment in mafic components attendant to the removal of hornblende.

5. The diorite suite has a 'J' type Ca/Y trend (Figure 3-40); according to Lambert and Holland (1974), this reflects that hornblende precipitation is a dominant control upon the differentiation of the suite.

6. The gradual decrease in LREE contents with increasing SiO_2 content (Figure 3-41) partially reflects the change in LREE partition coefficients from less than unity to greater than unity as the magma changes in composition from intermediate to leucocratic (Arth, 1976a).

Formation of microcline and the granodiorite suite

The granodiorite suite is chemically distinct from the diorite suite, primarily because of its higher content of K, Rb, Ba, Pb, Th, Zr, and Tl; its dominant member, granodiorite, is also characterized by the presence of large microcline megacrysts.

Progressive concentration of the alkalis into a

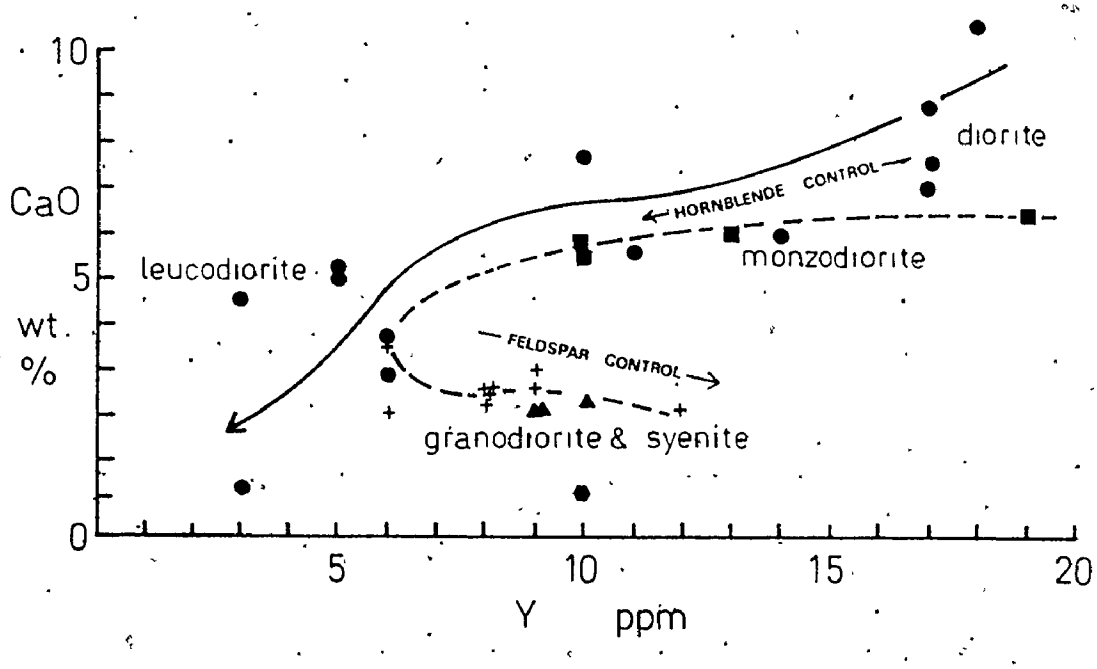

FIGURE 3-40 CaO versus Y diagram for the Jackfish Lake Complex

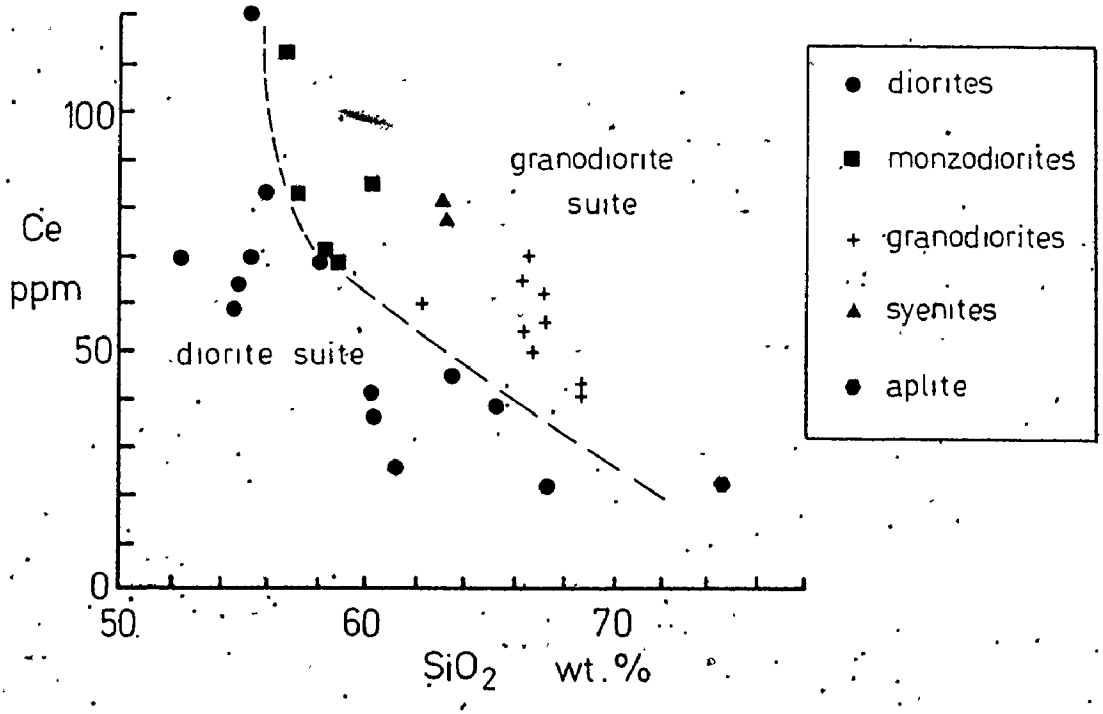

FIGURE 3-41 Ce versus SiO_2 diagram for the Jackfish Lake Complex

volatile-rich fluid phase during the formation of the diorite suite, and the subsequent formation of microcline megacrysts from this residual liquid during the crystallization of the granodiorite, can account for these features. Such a model implies that the granodiorites are a more fractionated continuation of the diorite suite, their formation marking the cessation of hornblende precipitation as the chief control on the evolution of the residual magma, and the beginning of extensive precipitation of feldspar (microcline and plagioclase) and quartz. This model can account for:

1. the relatively constant Sr/Ba of the granodiorite, a result of the crystallization of both plagioclase (high Sr/Ba) and microcline (low Sr/Ba) (Figure 3-32), and
2. the 'L' type Ca/Y trend of the granodiorite, which, according to Lambert and Holland (1974), is controlled by the precipitation of feldspar (Figure 3-40).

However, the granodiorite suite also includes much more mafic members, such as the monzodiorites and quartz monzodiorites, as well as the leucocratic Na-syenite. These rocks must also be explained if the concept of separate granodiorite and diorite suites is to be abandoned.

Feldspar structural states

Knowledge of the relative temperature and crystallization sequence of the feldspar phases (especially microcline) is requisite to understanding the evolution of the diorite and granodiorite rock suites. Accordingly, standard X-ray diffraction techniques were used to determine the feldspars' structural states. (131) and ($1\bar{3}1$) peaks (using Cu K_α radiation) were measured for plagioclase (Smith and Yoder, 1956); anorthite content was estimated from chemical analyses and optical determinations. The structural state of microcline was measured as the deviation from monoclinic structure (triclinicity = 12.5 [d(131) - d($1\bar{3}1$)] (Goldsmith and Laves, 1954b). All of the Jackfish Lake Complex microclines approach triclinic symmetry (Table 3-24); plagioclase separated from diorite and quartz diorite have high temperature structures; the granodiorite plagioclase mostly are in lower temperature states.

Goldsmith and Laves (1954a) reported that microcline cannot survive above 525°C under hydrothermal conditions; conversion to monoclinic orthoclase begins at 375°C (Steiger and Hart, 1967). Reversal of the transformation has been experimentally achieved only by the replacement of albite by potassium feldspar (Laves, 1951).

There are differing interpretations of the importance

Table 3-24 Feldspar structural states

Sample	Rock type	KF triclinicity	Plagioclase [20(131)-20(131)]
F146	diorite		2.35
F21	qtz. diorite	0.7174	2.10
F24	leuco qtz. diorite	0.8271	1.44
F135	(qtz.) monzodiorite	0.8276	1.52
D1	qtz. poor granodiorite	0.8413	1.83
F118	granodiorite	0.8576	1.41
F3	granodiorite	0.9238	1.42
F26	qtz. rich granodiorite	0.9455	1.10
F46	Na syenite	0.9144	1.08
F37	altered granodiorite	0.9263	1.81

of the monoclinic-triclinic transformation of alkali feldspars. Two end-member hypotheses are that:

1. microcline forms by diffusive transformation of pre-existing orthoclase during slow cooling, and is encouraged by the presence of volatiles (Mehnert, 1968; Goldsmith and Laves, 1954b);
2. microcline is formed directly at relatively low temperatures, providing that the time available for crystallization is sufficiently long; very rapid crystallization inhibits the necessary ordering of the Al-Si structure (Marmo, 1973).

The latter process may explain the high triclinicity of the microcline overgrowing plagioclase in the altered granodiorite F37, a rock which has undergone low temperature (250°C) alteration.

Interpretations of the importance of high and low temperature plagioclase structural states also vary. Marmo (1973) suggests that the ordering of sodic plagioclase requires geologic lengths of time; Mehnert (1968) suggests that the inversion from high to low temperature plagioclase states depends upon the cooling history of the rock, noting that more rapidly cooled plutons preserve more of their high temperature plagioclases.

The triclinicity and $[2\theta(131) - 2\theta(1\bar{3}1)]$ of plagioclase

have been plotted for coexisting microcline and plagioclase pairs from the Jackfish Lake Complex (Figure 3-42). Part of the variation in the latter parameter results from variation in the plagioclase An content; however, the difference in the 2 Θ values is large enough to reflect change in the structural quenching temperature. The correlation observed between the structural state for each microcline-plagioclase pair suggests that these parameters record the temperature at which Al-Si ordering was fixed, and this temperature is higher in the diorites and quartz diorites than in the granodiorites and syenites. If Mehnert's interpretation is correct, this is not a surprising result, given that transformation to lower temperature states is encouraged by the presence of volatiles.

If the triclinicity of microcline is some related function of temperature and volatile activity, some correlation should exist between triclinicity and oxygen isotope mineral fractionations involving microcline; such is the case (Figure 3-43). However, such a pattern cannot be found for plagioclase. This is not entirely unexpected; microcline isotopically re-equilibrates very readily during late-magmatic and post-magmatic deuteric activity; plagioclase is not as easily affected.

FIGURE 3-42 Potassium feldspar triclinicity versus the plagioclase intermediacy index for coexisting feldspar phases separated from some Jackfish Lake Complex rocks.

■ diorites, quartz diorites and leuco quartz diorites

● granodiorites

⬢ Na-syenites

▲ F37, altered granodiorite

FIGURE 3-43 Potassium feldspar triclinicity versus the potassium feldspar-hornblende oxygen isotope fractionation for some Jackfish Lake Complex rock types. The legend is as in Figure 3-42.

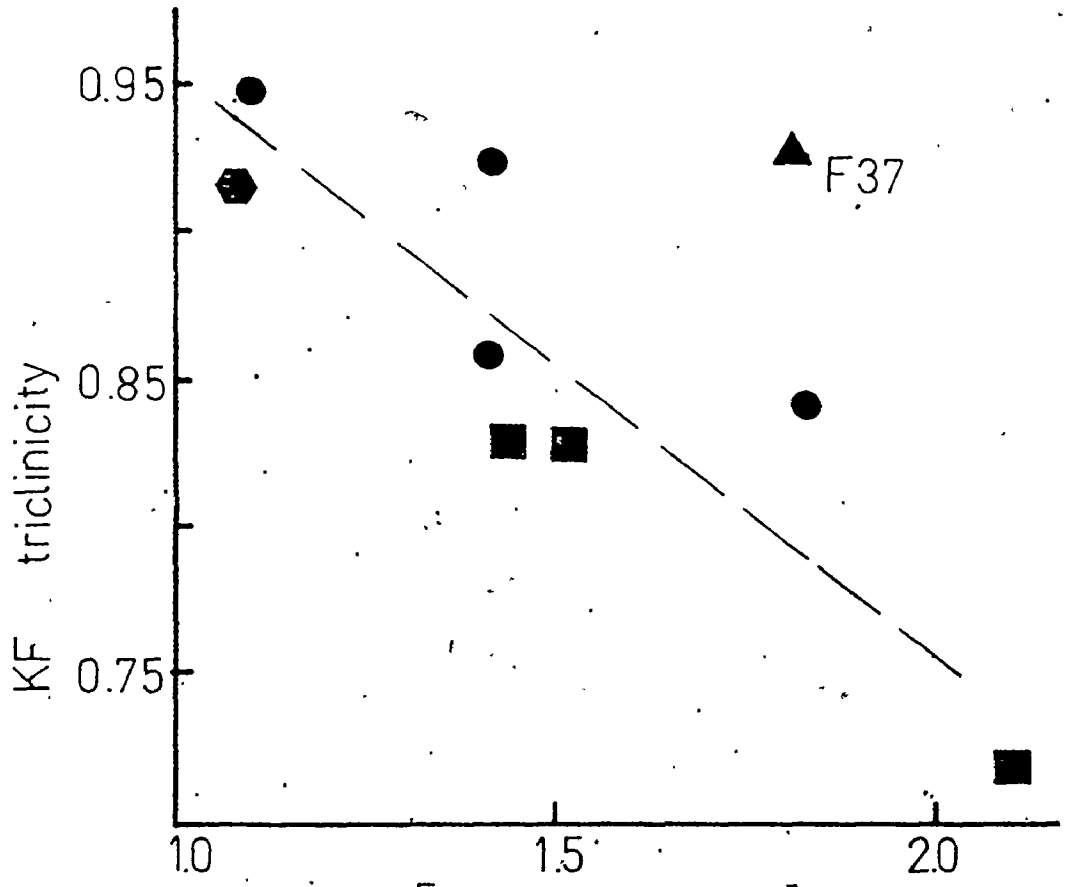
0.95
0.85
0.75
KF triclinicity
F37
1.0
1.5
2.0
[2θ(131) - 2θ(1$\bar{3}$1)] plagioclase

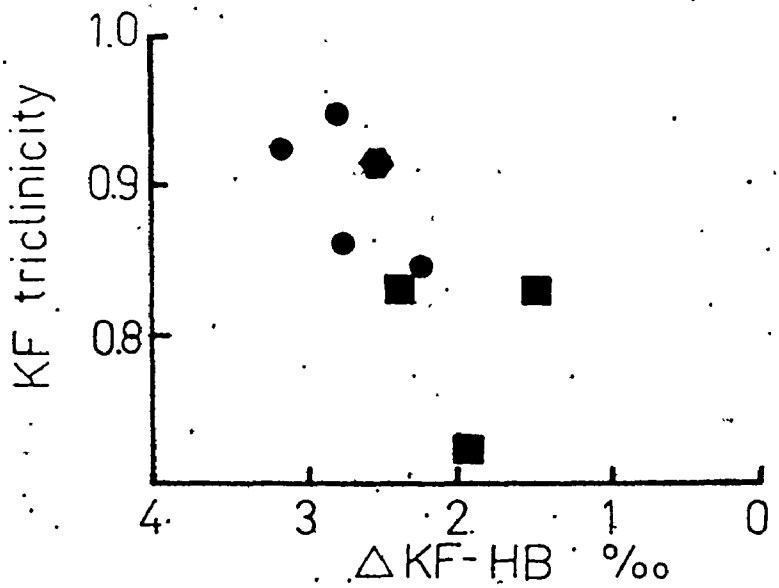
1.0
0.9
0.8
KF triclinicity
4
3
2
1
0
Δ KF-HB ‰

Late magmatic versus metasomatic origins of microcline

The fact that microcline from the Jackfish Lake Complex appears to have re-equilibrated to lower structural states during cooling and/or volatile activity suggests that this mineral is of magmatic rather than metasomatic origin. Other evidence supports this contention. Rb/Tl temperatures obtained from microcline/rock measurements range from 650°C in the monzodiorites and quartz monzodiorites to 530-570°C in the granodiorite and syenite (P. Fung, pers. comm.). Oxygen isotope temperatures for these rocks are similar, 620-700°C for the diorites, and 520-650°C for the granodiorites and syenites (Table A1-4a, Appendix I). These temperatures extend into subsolidus ranges, but are higher than expected for low temperature (300°C), metasomatic introduction of alkali feldspar, unrelated to the magmatism.

The trace element variations between interstitial microcline from the monzodiorites and from the granodiorites (megacrysts) are also those expected for progressive differentiation. Smith (1974) summarized the expected trace element behaviour of microcline and noted that:

1. Ba favours alkali feldspar relative to coexisting liquid and coexisting plagioclase;

2. Tl concentrates in liquids and late solutions; it prefers potassium feldspar relative to plagioclase;
3. Rb prefers potassium feldspar to plagioclase, and also concentrates in liquid relative to either feldspar;

These patterns, while not well developed, are present (Figure 3-44). Li and Sr are also partitioned into plagioclase relative to the coexisting microcline in any particular sample, as is expected if both had crystallized from the same magma, although not necessarily at exactly the same time (Tables 3-18 and 3-19).

The diorite and granodiorite 'suites' - a model for a common differentiation path

The X-ray diffraction, trace element and isotopic data indicate that the microcline, whether interstitial or as megacrysts, is of magmatic origin, and crystallized in a predictable petrogenetic sequence. Thus, the alkali enrichment of the monzodiorites and quartz monzodiorites cannot be explained by metasomatism of the spatially related diorite and quartz diorite (Figure 3-22), perhaps by the volatile-rich fluid phase assumed present during the crystallization of the granodiorites.

The monzodiorites and quartz monzodiorites range in

FIGURE 3-44 Rb, Tl and Ba content of microcline versus the microcline triclinicity for some Jackfish Lake Complex rock types.

See Table 3-24 for identification of individual rock types.

▲ Ba content of microcline versus its triclinicity

● Tl content of microcline versus its triclinicity

■ Rb content of microcline versus its triclinicity

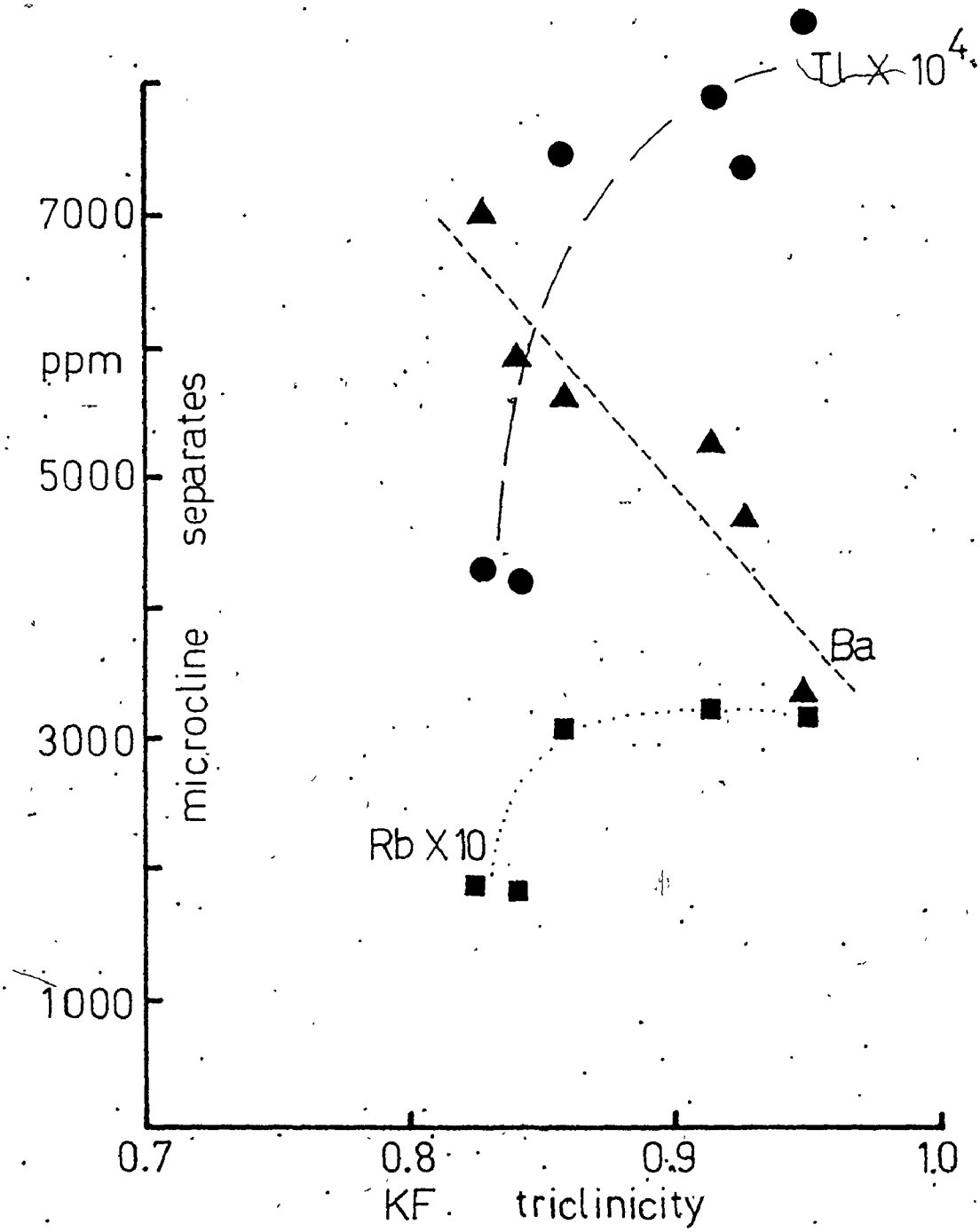
Tl X 10⁴
Ba
Rb X 10
7000
5000
3000
1000
ppm
microcline separates
0.7
0.8
0.9
1.0
KF triclinicity

SiO_2 from 56 to 60% and fit into a silica gap which occurs between the meladiorites and diorites (53-56%) and the leuco-diorites and leuco quartz diorites (58-61%). The grano-diorites complete the silica range of the Jackfish Lake Complex rocks (62-69%). This fact alone suggests the existence of a continuous differentiation sequence: meladiorite-diorite-monzodiorite-quartz monzodiorite and quartz diorite-leucodiorite and leuco quartz diorite-quartz poor granodiorite-granodiorite.

The early period of alkali enrichment responsible for the formation of the monzodiorites and quartz monzodiorites has also been described for a fractionally crystallized gabbro-trondhjemite suite from Finland (Barker and Arth, 1976, p.597). In these rocks, K, Rb and REEs increase in abundance until the remaining liquids contain near 60% SiO_2; alkali contents then decrease in the more differentiated rocks.

The processes responsible for such behaviour are not completely understood. However, one might speculate that the following factors are involved:

1. Initially water-undersaturated magmas, such as the Jackfish Lake Complex diorite, evolve a separate fluid phase during crystallization. At low water pressures, early in the differentiation, the alkalis cannot completely partition

into this as yet limited amount of fluid. Thus small amounts of interstitial microcline precipitate along with plagioclase and hornblende (Maaløe and Wyllie, 1975). As differentiation progresses, the fluid phase becomes volumetrically much more important and is capable of retaining most of the alkalis. The rocks crystallizing at this time are therefore depleted in the alkalis. Only at the final stages of crystallization are the alkalis released from the fluid phase to form the microcline megacrysts characteristic of the granodiorite.

2. The partition coefficients for K and Rb between hornblende and liquid favour incorporation of these elements into hornblende 10 to 30 times more for intermediate liquids than they do for hornblende-siliceous magma pairs.

The Na-syenite

The Na-syenite is spatially (Figure 3-22) and, in terms of its alkali content (Figure 3-29c,d), chemically related to the granodiorites. Its LIL, Pb, Th, Zr, Hf, Sc and Tl contents and plagioclase composition (An_5) (Table 3-23) suggest that the syenite represents the very last liquid, less H_2O, CO_2, etc., crystallized at the top of the Jackfish Lake Complex magma chamber. Its field position (Figure 3-22) is consistent with this interpretation; also, the Na-syenite, alone among the Jackfish Lake Complex rocks,

is highly jointed and fractured. Such dislocations would be expected at the top of a crystallizing magma chamber as a result of the escape of magma-related volatiles during the release of heat and pressure that accompanies the final stages of crystallization.

There are three peculiarities of the Na-syenite which require explanation:

1. the unit contains little or no quartz;
2. it contains anhedral microcline, not megacrysts;
3. it has higher HREE contents than the granodiorites (Table 3-23; Figure 3-36).

Krauskopf (1967, p.418) has suggested an explanation that could account for the first two features as well as the location of the syenite as the top of the Jackfish Lake Complex. He notes that if a granitic magma becomes particularly enriched in volatiles, those fluids can stream upwards through the magma carrying alkali-metal ions. The top of the magma body can therefore become enriched in Na and K, unaccompanied by enrichment in SiO_2; such syenites can even be nepheline bearing. In such a situation, simultaneous crystallization of albite and microcline would be expected, as is the case for the Jackfish Lake Complex Na-syenite.

The enrichment of the Na-syenite in HREEs relative to the granodiorites is more difficult to explain. However,

the Na-syenite does contain 25 to 30% more hornblende (8-10%) than the granodiorites (6-8%), a phase which preferentially incorporates HREEs. Also, the syenite is not diluted by 10 to 20% quartz, a phase which contains no HREEs. The very high LREE content of the Na-syenite, relative to the granodiorites, is also compatible with the absence of quartz and the high abundance of feldspar.

The question of Eu anomalies

Because plagioclase preferentially incorporates Eu^{+2} relative to Eu^{+3}, the crystallization of plagioclase during the formation of the Jackfish Lake Complex leucodiorites, granodiorites and syenites would tend to deplete the remaining melt in Eu. However, no statistically significant Eu anomalies are observed in these rocks (Figures 3-33, 3-36). However, other factors are also important in determining the distribution of Eu between plagioclase and magma; oxidation state is particularly crucial (Drake, 1975; Towell et al., 1965, 1969; Philpotts, 1970; Philpotts and Schnetzler, 1968). Under oxidizing conditions any potential Eu anomalies will be considerably moderated or removed altogether, even if phases capable of incorporating Eu^{+2} are available. Small volume residual melts and late magmatic fractions, such as are probably represented by the more leucocratic Jackfish

Lake Complex rocks, are generally highly oxidized (Towell et al., 1969). The hematite rims on magnetite grains within the Jackfish Lake Complex leucodiorites, leuco quartz diorites and granodiorites indicate the presence of oxidizing conditions in the magma at some stage. Thus, the absence of Eu anomalies is not particularly troublesome to our model.

Conclusions

The Jackfish Lake Complex monzodioritic to syenitic rocks developed along a single differentiation path by the fractional crystallization of a small portion of the dioritic magma (less than 5%). The precipitation of hornblende ($P_{total} < 20$ kb) controlled the suite's initial evolution, but the crystallization of feldspar, especially microcline, became more important during the formation of the more differentiated granodiorite and Na-syenite.

Somewhat low P_{H_2O} early during the differentiation is suggested by the formation of some monzodiorite and quartz monzodiorite. P_{O_2} and P_{H_2O} are required to be quite high during the end stages of crystallization in order to account for the microcline megacrysts present in the granodiorite, the absence of Eu anomalies, and the formation of a quartz-poor Na-syenite as the capping rock type.

The effect of differentiation upon the $\delta^{18}O$ values of the Jackfish Lake Complex

$\delta^{18}O$ rock results for the Jackfish Lake Complex range from 6.4 to 9.2°/$_{oo}$ (Table 3-15), and generally increase as the rocks become more leucocratic, as shown by the overall positive correlation between $\delta^{18}O$ and decreasing values of the solidification index (SI) of Kuno et al. (1957) (Figure 3-45). There is some important fine structure to this variation, however. The unaltered granodiorites ($\delta^{18}O$ = 7.5-8.2°/$_{oo}$) have $\delta^{18}O$ values that do not increase as rapidly with decreasing SI as do some of the more leucocratic members of the diorite suite, such as the volumetrically unimportant plagioclase-quartz dike (F23). The Na-syenite (F46) and related rocks (albitite dike F86, syenite-leucodiorite D8), which are among the most differentiated rocks, actually decrease in $\delta^{18}O$ (7.0-7.2°/$_{oo}$) relative to the granodiorites. A saussuritized syenite (F28) has a still lower $\delta^{18}O$ value (6.5°/$_{oo}$) but is probably the result of some alteration.

Positive correlations between $\delta^{18}O$ and differentiation indices have been documented by Taylor (1968) for numerous volcanic complexes. He notes, however, that since the oxygen isotope variation accompanying differentiation is a function of "magma composition, P_{H_2O}, oxygen fugacity, and

FIGURE 3-45 $\delta^{18}O$ versus the solidification index (SI) diagram for Jackfish Lake Complex rocks.

The $\delta^{18}O$ values for mineral phases are also shown and plotted at the SI value of the rock from which they were separated.

- ● quartz
- ⬡ microcline
- □ plagioclase
- ■ rock
- ▼ hornblende
- ▲ biotite

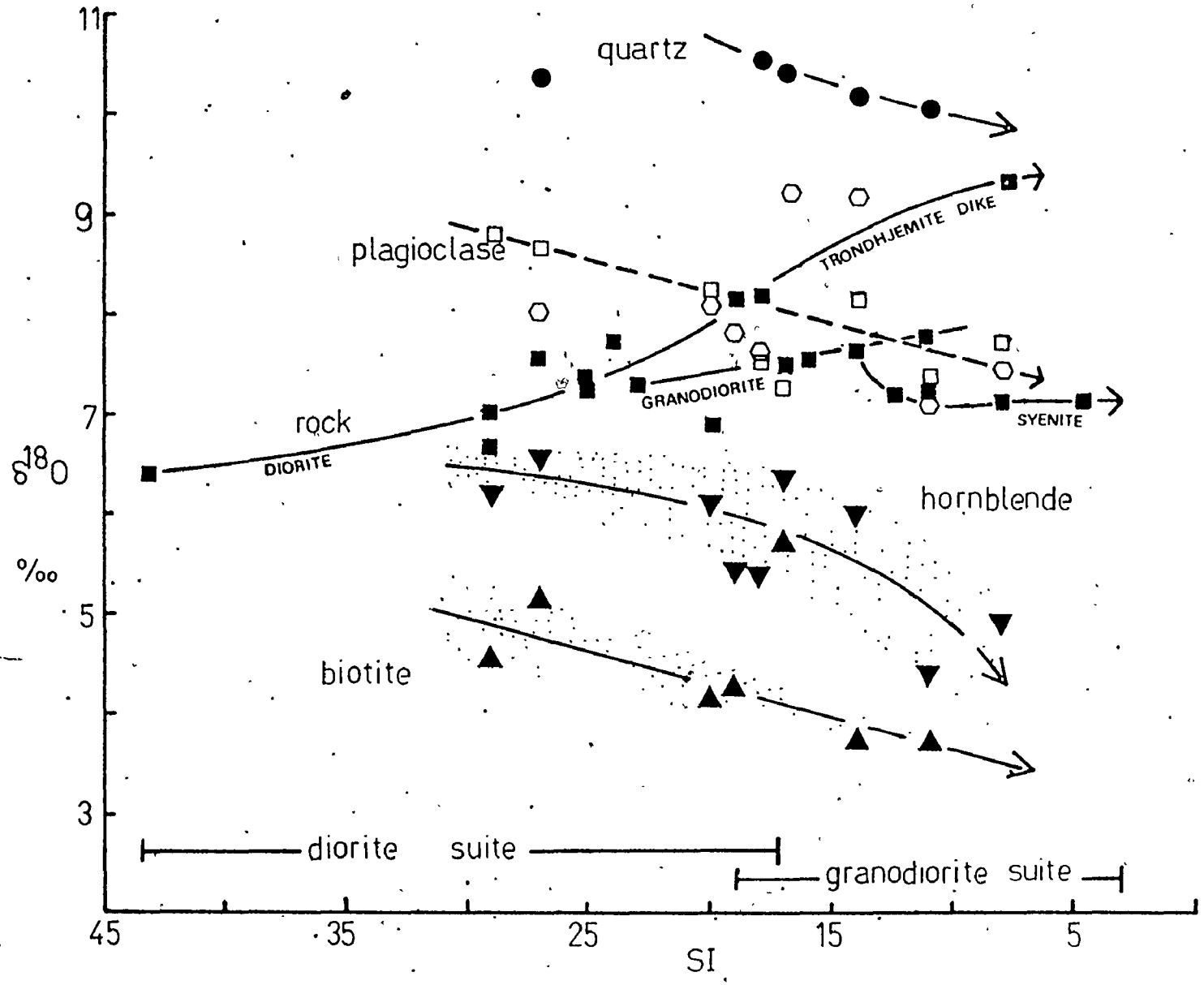
11
9
7
5
3
$\delta^{18}O$
‰
quartz
plagioclase
TRONDHJEMITE DIKE
GRANODIORITE
SYENITE
rock
DIORITE
hornblende
biotite
diorite suite
granodiorite suite
45
35
25
15
5
SI

melt viscosity" (Taylor, op. cit., p.32) the actual sense of variation in any particular case is difficult to predict theoretically. Any oxygen isotope modelling is also seriously restricted by the lack of accurate knowledge of mineral-magma fractionation factors at high temperatures. Nevertheless, some qualitative conclusions can be made.

Figure 3-45 shows that while $\delta^{18}O$ rock generally increases with decreasing SI, the $\delta^{18}O$ values of mineral phases (except microcline) decrease. The ^{18}O depletion becomes the most pronounced in the granodiorites and the syenite. If primary isotopic characteristics are still at least partially preserved in these mineral phases, this pattern suggests that the melt became impoverished in ^{18}O as differentiation progressed. Most of the mineral phases are not grossly out of isotopic equilibrium (Figure 3-46), although some of the calculated isotopic temperatures are discordant (Table A1-4a; Appendix I). In spite of such perturbations, I believe that the decreasing $\delta^{18}O$ values of quartz, plagioclase, hornblende, and biotite reflect a primary trend. Previous discussions showed that the precipitation of first hornblende and then feldspar controlled the chemical evolution of the Jackfish Lake Complex rocks; such activity can explain the behaviour of the oxygen isotopes. The precipitation of hornblende ($\delta^{18}O$ of about 5‰)

during the crystallization of the meladiorites and diorite would enrich the remaining melt in ^{18}O. However, when large proportions of ^{18}O-rich minerals such as quartz and feldspar begin to crystallize, the remaining liquid becomes depleted in ^{18}O, providing that the system is isotopically closed to oxygen. Thus, in the Jackfish Lake Complex, the cessation of hornblende fractionation and the beginning of feldspar crystallization was accompanied by a change in the oxygen isotope bulk solid-magma fractionation factor from greater than unity to less than unity.

The low $\delta^{18}O$ values of the Na-syenite and related rocks can be explained by this model. If these rocks represent the last residual liquids, they should have the lowest $\delta^{18}O$ values of those rocks dominated by the crystallization of feldspar, rather than hornblende.

Deuteric activity and oxygen isotopes

The preservation of primary trends in the rock oxygen isotope data suggests that any redistribution of ^{18}O between coexisting mineral phases has occurred within a closed isotopic system. Regional metamorphism has not noticeably affected the Jackfish Lake Complex; the low ^{18}O biotites characteristic of Archean metagranitic terrains (Chapter IV) are not present here. However, some process

must be invoked to explain the somewhat discordant isotopic temperatures (Figure 3-46; Table A1-4a). The most reasonable explanation is isotopic exchange during the autometasomatic activity that accompanied the formation of the microcline megacrysts. Isotopic exchange to subsolidus temperatures has been recognized by Bottinga and Javoy (1975) as the prime cause of disequilibrium and low isotopic temperatures in hydrous, plutonic rocks.

Some comments on the oxygen isotopic composition of eclogite

Most ultramafic rocks have $\delta^{18}O$ values of 5 to 7‰ (Taylor, 1968), suggesting that the upper mantle is fairly uniform in its oxygen isotopic composition. However, Garlick et al. (1971) reported anomalous $\delta^{18}O$ values (2 to 8‰) for eclogite inclusions from South African kimberlites; these they believed were the result of fractional crystallization at high pressures within the mantle. The kimberlite eclogites poor in ^{18}O were interpreted as residual liquids and those enriched in ^{18}O were explained as crystal cumulates. Garlick et al. (op. cit.) suggested that at eclogitic pressures, the crystal-melt fractionations became larger, and reversed direction. Clayton et al. (1975), however, reported only negligible pressure effects on solid-water

FIGURE 3-46 Oxygen isotope concordancy diagrams for the Jackfish Lake Complex.

The temperatures are given in °C.

▲ granodiorite suite

● diorite suite

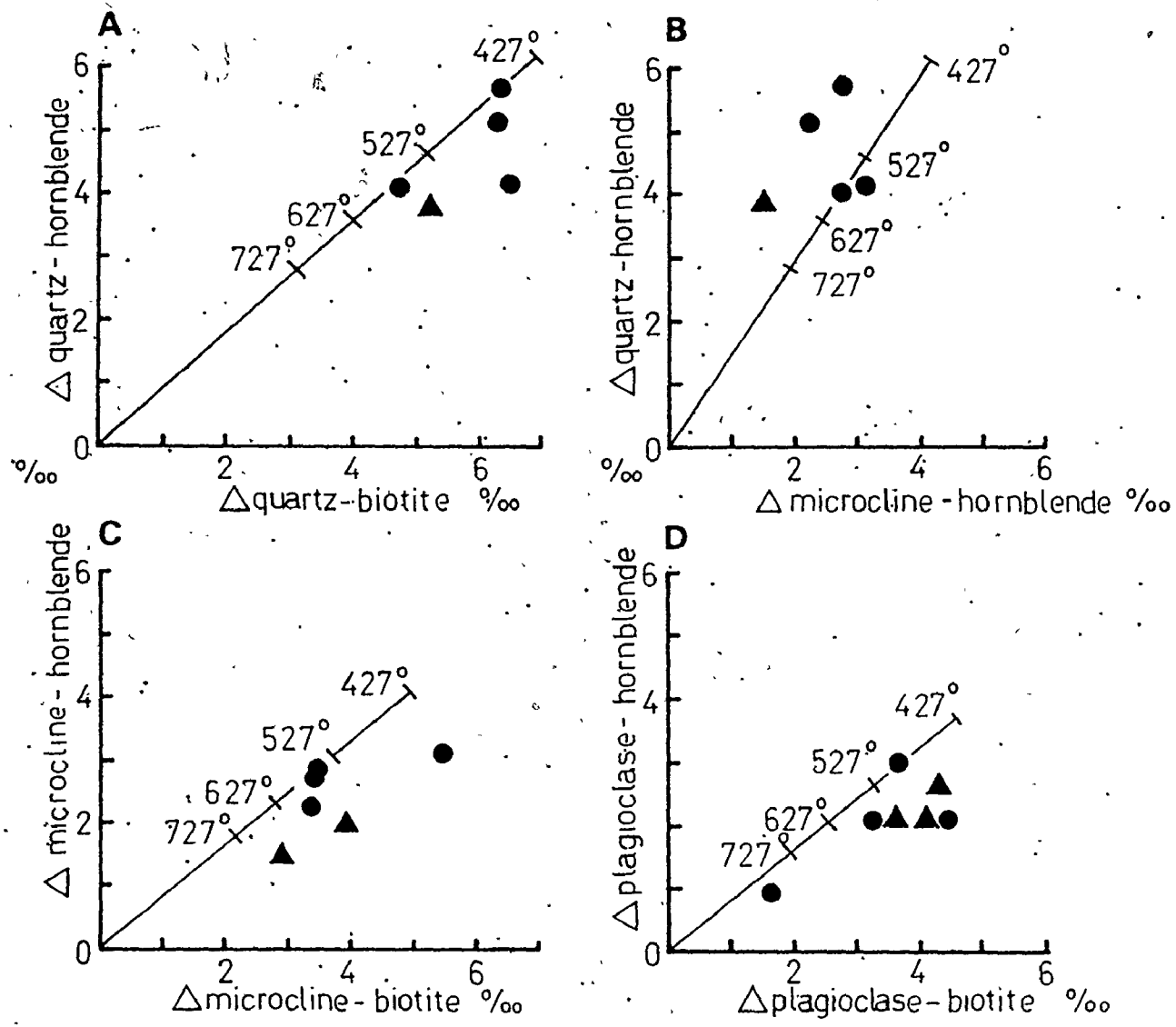
A
B
C
D
427°
527°
627°
727°
Δ quartz - hornblende ‰
Δ quartz-biotite ‰
Δ quartz-hornblende ‰
Δ microcline - hornblende ‰
Δ microcline - hornblende
Δ microcline - biotite ‰
Δ plagioclase - hornblende
Δ plagioclase - biotite ‰
0
2
4
6

fractionation factors.

The Jackfish Lake Complex diorite, which I believe to have formed by partial melting of eclogite at high pressure has $\delta^{18}O$ values of 6.4 to 7.3°/$_{oo}$ (mean $\delta^{18}O$ = 6.9°/$_{oo}$), within the range observed for most andesites (5.4-7.5°/$_{oo}$; mean $\delta^{18}O$ = 6.2°/$_{oo}$; Taylor, 1968, p.36). Such compositions may have been attained in at least two ways:

1. If the basaltic rock which subsequently was converted to quartz eclogite or eclogite had been enriched in ^{18}O during submarine processes, its initial isotopic composition may have been changed and enriched to about 7°/$_{oo}$, such as is observed for the least altered Burditt Lake metabasalts. Its partial melting at high pressure, with little or no solid-melt fractionation, would then produce a dioritic melt of the required oxygen isotope composition.

2. Taylor (1968) notes that most plutonic rocks have higher $\delta^{18}O$ values than their volcanic equivalents because plutonic differentiation occurs at lower temperatures and/or plutonic rocks have greater opportunity to assimilate or exchange with isotopically heavier crust during their emplacement. Thus, partial melting of eclogite of normal basaltic composition (6°/$_{oo}$) could produce a dioritic magma which subsequently became enriched by 1°/$_{oo}$ during plutonism.

There is no evidence, however, to suggest that somewhat unique high pressure isotopic fractionation occurs during the formation of quartz eclogites and the production of dioritic-dacitic melts and clinopyroxene-garnet eclogitic residues.

How then can the variability in the observed oxygen isotopic compositions of the eclogites be explained? Firstly, post-formation low temperature alteration, which has produced other eclogites with $\delta^{18}O$ values of 1.5 to 10.5°/$_{oo}$ (Vogel and Garlick, 1970) is difficult to completely rule out. There is another possible but less likely mechanism; in section III-4, the wide variety in isotopic composition of submarine basalt was pointed out. If these rocks are transformed to eclogites during subduction (in an isotopically closed system), a corresponding variety in eclogite isotopic compositions would be expected. If this is the case, it is unwise to use the isotopic compositions of most eclogites to infer anything about the isotopic composition of the mantle.

The petrogenesis of the Jackfish Lake Complex: a summary

The geology and geochemistry of the Jackfish Lake Complex is compatible with the following model:

1. Partial melting at high pressure of hydrous eclogite or anhydrous quartz eclogite, enriched in omphacitic pyroxene,

produced a dioritic magma.

2. This magma was emplaced along the Rainy Lake batholith-metavolcanic interface.

3. Most of the magma crystallized in place to form a diorite of similar chemical composition to the magma except for loss of volatiles.

4. A small volume of residual magma differentiated along a 'trondhjemitic' path to form a progressive sequence of quartz monzodiorite and quartz diorite-leuco (quartz) diorite-Na granodiorite-Na syenite; these occur upwards in the magma chamber, with the Na-syenite at the top. The first portion of the sequence was controlled by the precipitation of hornblende; the latter portion, which contains rocks with somewhat more K than usual for trondhjemitic differentiation trends, was controlled by the crystallization of feldspar, especially microcline, as the coexisting fluid phase became oversaturated in alkalis.

5. Deuteric activity continued to subsolidus temperatures, causing some isotopic re-equilibration of mineral phases, especially microcline; the effects were most pronounced in the granodiorites.

6. Meteoric water activity, associated with faulting in the vicinity of Northwest Bay, caused chemical and isotopic alteration of some of the granodiorites and quartz monzodiorites at some time after the cessation of magmatic and

late-magmatic processes in the Jackfish Lake Complex, but before the emplacement of the Northwest Bay Complex at its present position.

III-9 GEOCHEMISTRY OF THE FOOTPRINT GNEISS

Introduction

The Footprint gneiss is a marginal portion of a relatively widespread unit that comprises most of the interior of the Rainy Lake batholith (Manitou Dome). It is chemically similar to other biotite tonalitic to granodioritic rocks that occur within the study area, such as the Northwest Bay Complex foliated granodiorite, and the Burditt Lake - Manomin Lake felsic metavolcanic rocks (Table 3-7, #1,3,4,5). However, the gneiss is, on average, enriched in SiO_2 and depleted in K_2O relative to these latter two units, a variation reflected in the gneiss' higher normative quartz and lower normative K-feldspar contents (Figure 3-4).

The gneiss is a high Al tonalite (Barker and Arth, 1976):

1. Al_2O_3 15.0-16.3 wt. %
2. Sr 42-711 ppm
3. Rb 24-78 ppm

4. Ce/Lu >100

5. no or only small Eu anomalies

The Footprint gneiss is similar in major and minor element composition to other Archean tonalitic gneisses (Table 3-25). However, there is considerably more variation in the LIL element contents between the different gneisses. Hurst et al. (1975) suspect that the Uivak and Amitsoq gneisses (Tables 3-25, #9,11) "represent a dominantly tonalitic intrusive suite of rocks which have gained variable amounts of K and Rb, and lost Ba and Sr during a period of regional metamorphism and possibly partial melting and should thus be regarded as migmatites rather than a purely igneous suite which has undergone isochemical metamorphism" (p.399). Barton (1975), on the other hand, suggests that the LIL element distribution in the Hebron gneiss (Table 3-25, #8) reflects derivation from pre-existing sialic crust, or else anomalous mantle.

Chemical effects of metamorphism on the Footprint gneiss

The purpose of this section is to determine whether the geochemistry of the Footprint gneiss has been seriously modified by metamorphism.

There are some obviously altered portions of the gneiss that can be mentioned first and eliminated from further

Table 3-25 Chemical comparison of the Footprint gneiss with other Precambrian siliceous rock types

	1	2	3	4	5	6	7	8	9	10	11
SiO_2 wt%	71.65	67.07	69.64	74.04	70.74	71.19	71.11	71.57	69.38	71.40	70.73
TiO_2	0.27	0.19	0.26	0.18	0.29	0.28	0.28	0.26	0.40	0.26	0.32
Al_2O_3	15.61	18.04	16.71	13.65	16.19	16.56	15.72	15.30	16.08	14.98	15.46
Fe_2O_3			0.72	0.74	0.79		0.64	2.04*	2.56*	0.67	2.56*
FeO	1.91*	1.65*	1.57	2.53	1.43	1.10*	1.47			2.03	
MnO	0.03	0.03	0.03	0.10	0.07	0.06	0.03	0.03	0.03	0.03	0.04
MgO	0.82	1.76	0.86	0.71	0.66	0.88	1.13	0.69	0.95	0.72	0.83
CaO	2.94	4.03	3.45	1.92	2.28	3.43	3.18	2.45	2.63	2.31	2.85
Na_2O	5.12	5.88	5.46	4.05	4.86	4.75	5.24	5.06	5.34	4.48	4.58
K_2O	1.53	1.26	1.15	2.02	2.60	1.73	1.13	2.53	2.50	3.04	2.52
P_2O_5	0.12	0.09	0.15	0.06	0.09	0.02	0.08	0.09	0.13	0.07	0.12
Rb ppm	42	32	28	45	76	16.4	31	86	100	91	100
Sr	555	657	500	217	547	509	588	351	570	381	273
Ba	602	519	300	180	855	382	202	503	310	806	361
K/Rb	302	317	360	387	299	865	291	243	205	275	205
Sr/Ba	0.922	1.27	1.67	1.21	0.81	1.33	2.91	0.698	1.84	0.473	0.756
Rb/Sr	0.076	0.048	0.056	0.368	0.207	0.032	0.053	0.245	0.175	0.239	0.366

Notes to Table 3-25 Chemical comparison of the Footprint gneiss with other Precambrian siliceous rock types

All analyses recalculated to 100%, anhydrous.

* Total Fe.

1. Average 14 Footprint gneiss.
2. Early Precambrian dacite, Vermilion District; Arth and Hanson (1975).
3. Average 3 Archean Northern Light gneiss; Goldich et al. (1972).
4. Average 9 Proterozoic Twilight gneiss; Barker et al. (1976a).
5. Average 9 Proterozoic Kroenke granodiorite; Barker et al. (1976a).
6. Klamath Mt. trondhjemite (Mesozoic); Arth and Hanson (1975), in Lanphere et al. (1968).
7. Average 3 Ancient tonalites, Swaziland, Barberton Mountain Land; Glikson (1976a).
8. Average 8 Hebron (3.6 b.y.) gneiss, Labrador; Barton (1975).
9. Average 10 Uivak gneiss (3.6 b.y.), Labrador; Hurst et al. (1975).
10. Average 3 Morton gneiss, Minnesota; Goldich et al. (1970).
11. Average 12 Amitsoq gneiss, Greenland (3.7 b.y.); Hurst et al. (1975).

discussion. Samples F12 and F12-1 (Appendix IV) are located at the sheared contact between the gneiss and the Jackfish Lake Complex diorite (Figure 3-3). The gneiss and the diorite have been tectonically interleaved; this mixing is reflected in the chemistry of the resulting rocks (low Si and Rb, high Ti, Al, Fe, Mn, Mg, Ca, P, Sr, Ni, Zr, and Y relative to uncontaminated gneiss). Gneiss samples F53 and F54, which occur adjacent to a large Jackfish Lake Complex quartz diorite dike, have developed abundant epidote (Appendix III) due to contact metamorphism accompanying the dike's intrusion.

The Footprint gneiss is deformed (Photos K and L), contains migmatized mafic amphibolite enclaves (Photos E, F, and G), and has locally developed stromatic, phlebitic and ptygmatic migmatite structures. These features suggest that the rocks have undergone metamorphism to middle to upper amphibolite facies, a conclusion that cannot be arrived at from the relatively uninformative plagioclase-quartz-microcline-biotite-magnetite mineralogy of the gneiss.

A quantitative division between gneiss and migmatite cannot be made on the basis of outcrop evidence. However, in the apparently migmatized zones, partial melting, metamorphic differentiation and/or injection have produced quartz-microcline enriched leucosomes that occur in 1-5 cm wide bands, concordantly interlayered with narrower (0.5-2.0 cm)

biotite-rich melanosomes and quartz-plagioclase-biotite-microcline paleosomes; the amount of leucosome can be used to estimate the extent of migmatization. The unmigmatized gneiss is also laminated, but the layering is less well defined. Unlike the migmatite, the contacts between layers are diffuse. The increase in grain size and the distinct layering that occurs as the gneiss is transformed to migmatite is characteristic of other Archean tonalitic gneiss and migmatite complexes (Kays, 1976).

The gneiss and migmatite do not appear to have been depleted in elements such as Li, K, Rb, Th and Pb, such as frequently accompanies high pressure migmatization and granulite facies metamorphism (Heier and Thoresen, 1971; Sighinolfi, 1971; Heier, 1973; Drury, 1974). For example, the concentrations of these elements in the granodioritic portions of the gneiss (F73) are similar to those observed for the lower grade Northwest Bay Complex granodiorite (F31), also from the Rainy Lake batholith (Table 3-26). Depletion in LIL elements during high grade metamorphism is usually accompanied by an increase in K/Rb to greater than 500 (Heier and Thoresen, 1971; Heier, 1973; Drury, 1974; Lewis and Spooner, 1973). The K/Rb of the Footprint gneiss is only 300, similar to that of the Northwest Bay Complex granodiorite (Table 3-7; Figure 3-47b). However, K/Ba ratios of

Table 3-26 Selected analyses; Footprint Gneiss and Northwest Bay Complex

		F10[1]	F152[1]	F150[2]	F73[3]	F31[4]
SiO_2	wt %	70.45	71.10	70.43	71.94	70.83
Al_2O_3		15.89	15.63	15.77	15.66	15.57
TiO_2		0.35	0.26	0.31	0.22	0.27
Fe_2O_3		2.35	2.17	2.68	1.62	2.33
MnO		0.03	0.03	0.03	0.03	0.02
MgO		1.11	1.12	0.96	0.61	0.87
CaO		2.98	3.27	3.24	2.63	2.86
Na_2O		5.24	5.40	5.02	5.15	5.32
K_2O		1.47	0.91	1.40	2.07	1.81
P_2O_5		0.12	0.11	0.17	0.08	0.13
LOI						
Li	ppm	23	-	16	14	-
Rb		38	25	30	47	44
Sr		633	691	638	496	714
Ba		516	423	622	675	580
Pb		6	6	8	9	10
Th		3.8	6.2	5.5	1.6	1.9
Y		6	2	7	3	5
Nb		3	t	t	t	t
Zr		139	125	120	103	92
Zn		58	33	61	37	54
Ni		t	t	t	t	6
Ta		2.9	3.4	1.5	1.0	2.4
Hf		4.0	4.3	4.0	3.0	3.7
Sc		12.1	12.9	14.8	7.2	9.3
La		20.4	30.2	34.5	9.78	9.94
Ce		48.3	63.4	70.0	21.7	26.1
Nd		18.1	20.6	30.5	6.18	12.1
Sm		2.93	2.92	4.66	1.11	2.16
Eu		0.647	0.542	1.02	0.416	0.597
Gd		-	-	-	-	-
Tb		0.809	0.233	0.323	0.184	0.332
Tm		0.085	0.044	0.092	0.062	0.103
Yb		-	-	-	-	-
La		0.062	0.028	0.079	0.029	0.057
Tl		0.25	-	0.25	0.29	-

Major elements normalized to 100%, anhydrous; total Fe as Fe_2O_3. REE, Th, Ta, Hf and Sc by INNA; Li and Tl by AAS; others by XRF.

[1] trondhjemitic gneiss; [2] tonalitic gneiss; [3] granodioritic gneiss; [4] foliated granodiorite (NWB Complex)

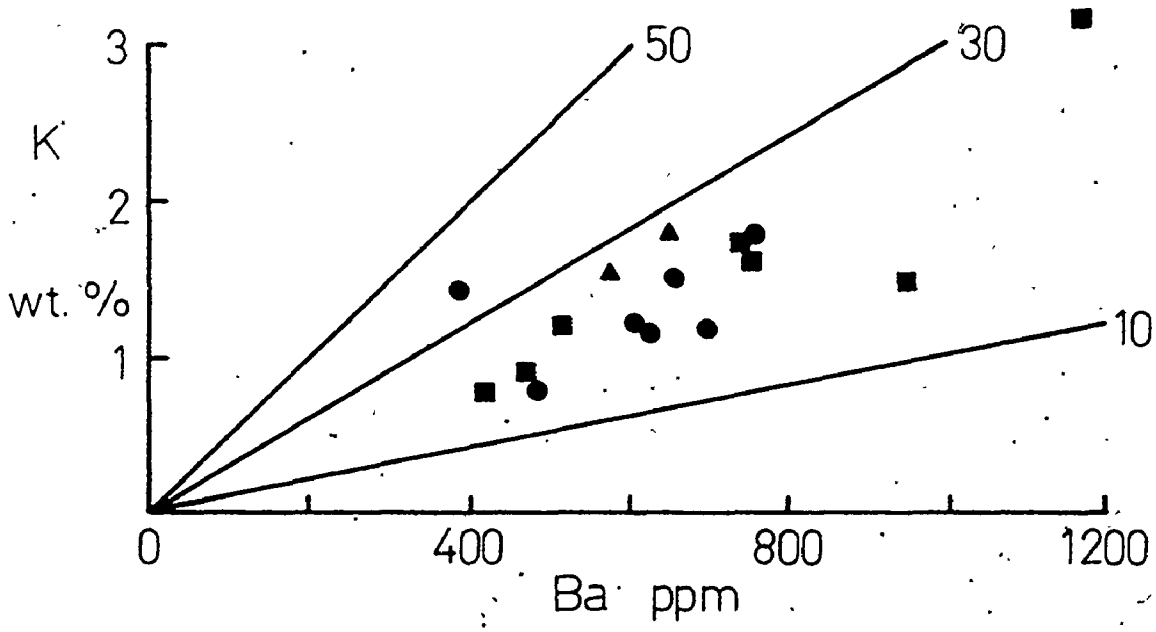

FIGURE 3-47a K versus Ba diagram for the Footprint gneiss and migmatite

● migmatized gneiss

■ unmigmatized gneiss

▲ Northwest Bay Complex granodiorite

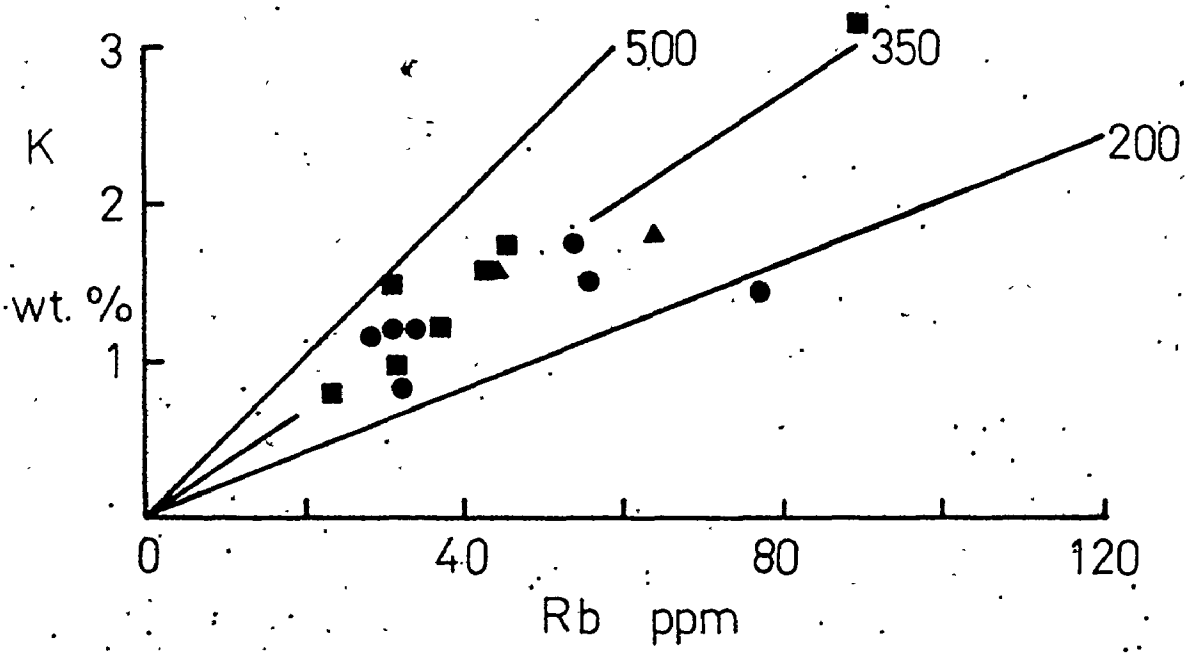

FIGURE 3-47b K versus Rb diagram for the Footprint gneiss and migmatite

Legend as in Figure 3-47a

depleted rocks are usually less than 30 (Heier and Thoresen, 1971), as is observed for the Footprint gneiss and the Northwest Bay Complex granodiorite (Figure 3-47a); the usefulness of such criteria in detecting element mobility is therefore suspect.

The most compelling evidence for isochemical metamorphism of the Footprint gneiss is that there are few consistent chemical differences between 'migmatized' and 'unmigmatized' varieties, at least on the 40 kg hand specimen scale. The Ti-Zr distribution (Figure 3-48), for example, is as expected for a suite of cogenetic rocks.

REEs and the origin of the Footprint gneiss

As it is generally accepted that the REEs are among the least mobile of elements during prograde metamorphism, they should be the most useful for petrogenetic interpretations.

The REE patterns for the Footprint gneiss are more fractionated than those of the other tonalitic to granodioritic rocks located within the Lake Despair - Burditt Lake study area (Figure 3-49); REE abundances vary considerably. The Ce content, for example, ranges from 11 to 65 ppm (Appendix IV, XRF Ce data). The tonalitic and trondhjemitic gneiss samples have small negative Eu anomalies ($Eu/Eu^* = 0.7$ to 0.9); the granodioritic gneiss has a small positive Eu anomaly

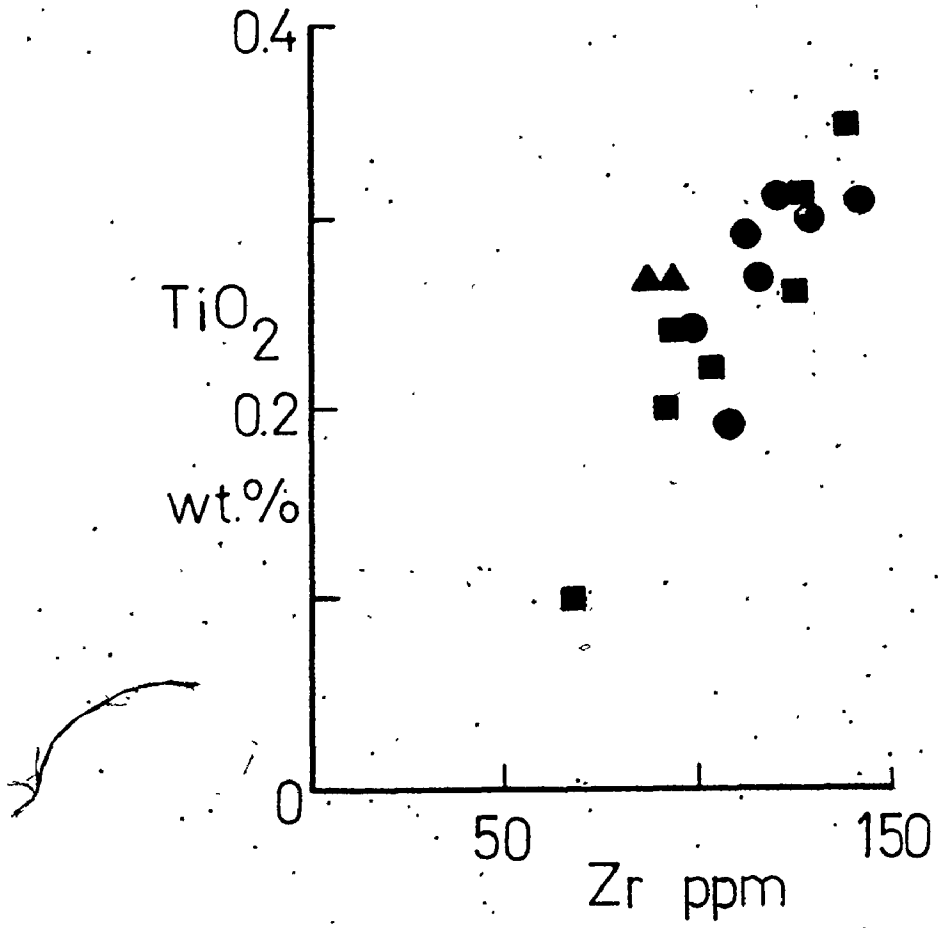

FIGURE 3-48 TiO_2 versus Zr diagram for the Footprint gneiss and migmatite.
Legend as in Figure 3-47a.

FIGURE 3-49 Chondrite normalized rare earth patterns for the Footprint gneiss

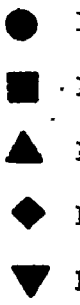

- F150 tonalitic gneiss
- F152 trondhjemitic gneiss
- F10 trondhjemitic gneiss
- F73 granodioritic gneiss
- F31 Northwest Bay Complex granodiorite

FIGURE 3-50 Melting model for the tonalitic to trondhjemitic protolith of the Footprint gneiss.

The hypothetical parent rock is assumed to have rare earth element concentrations similar to Jackfish Lake Complex mafic enclave D4, that is, enriched in light rare earth elements (calc-alkali basalt). The solid, dashed and dotted lines show the results of calculations for 1, 10, 30 and 40% melting of a quartz eclogite parent rock (55% clinopyroxene, 30% garnet, 15% coesite ± kyanite) of this chemical composition. The hatching shows the field for the Footprint tonalitic to trondhjemitic gneisses.

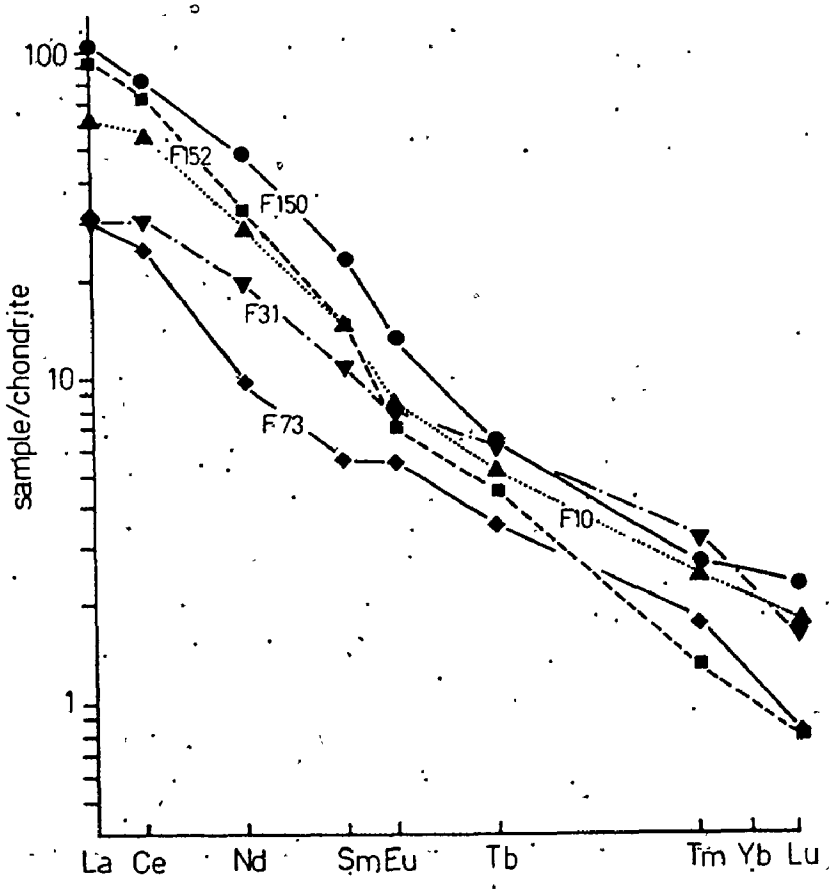
100
10
1
sample/chondrite
F152
F150
F31
F73
F10
La Ce Nd Sm Eu Tb Tm Yb Lu

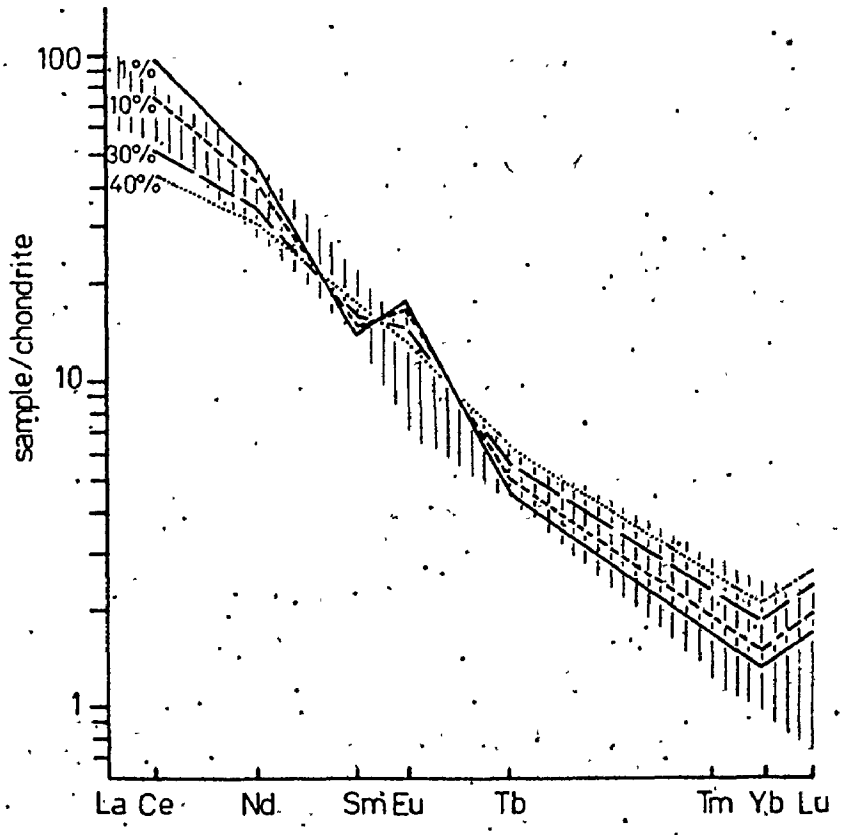
100
10
1
sample/chondrite
1%
10%
30%
40%
La Ce Nd Sm Eu Tb Tm Yb Lu

(Eu/Eu* = 1.2) (Table 3-26).

Previous discussions (sections III-6, III-7) concerning the origin of tonalites, and the interpretation of REE data apply equally well to the Footprint gneiss and the Northwest Bay Complex granodiorite. The REE pattern of the Northwest Bay Complex granodiorite, for example, can be reproduced by 10% melting of a quartz eclogite, as described for the felsic metavolcanic rocks (section III-6; model 3b; Figure 3-20e). The similarity between the LIL element concentration of the granodiorite and the felsic metavolcanic rocks strengthens the comparison (Table 3-7, #3,4).

The more fractionated REE patterns of the tonalitic and trondhjemitic gneiss, as compared to the felsic metavolcanics and the Northwest Bay Complex granodiorite, require some modification of the quartz eclogite model, however. Some tonalitic rocks from other areas are also enriched in LREEs and/or have highly fractionated REE patterns. These include dacite and tonalitic gneiss from the Archean Vermilion District (Table 3-25, #2,3), the Proterozoic Kroenke granodiorite (Table 3-25, #5) and some albite porphyries from the Barberton Mountain Land (Glikson, 1976a, p.1269).

Moderate degrees of melting of quartz eclogite have been suggested as a possible origin for all of these units. The melting models shown in Figures 3-20c and 3-20d can match

the HREE concentration of the Footprint gneiss, for example, at melt fractions of about 10%. However, these same models require much smaller (<1%) melt fractions to reproduce the high LREE abundances of some of the Footprint gneiss samples and the Vermilion District and South African samples. Glikson (1976a) noted that the highly fractionated REE patterns of the Barberton Mountain Land porphyries require not only a sizeable garnet fraction in the eclogite residue, but also an initially LREE-enriched source rock.

REE patterns calculated for partial melting of a LREE-enriched quartz eclogite (similar in composition to the Jackfish Lake Complex mafic enclave D4) fit the observed pattern of the trondhjemitic to tonalitic portions of the Footprint gneiss almost perfectly for melt fractions of 10 to 30% (Figure 3-50). Only the calculated Eu values deviate from the observed REE trend; this is probably only a function of the uncertainty in the D of garnet (Arth and Barker, 1976).

The higher SiO_2 and lower Al_2O_3, TiO_2, $Fe_2O_3{}^t$, MgO, and CaO of the Footprint gneiss relative to the felsic metavolcanic rocks suggest that, in addition to formation from a LREE-enriched source rock, more garnet remained in the residue during the melting that formed the Footprint gneiss magma than did during the production of the felsic metavolcanics.

This may reflect: (1) different initial garnet/clinopyroxene ratios in the source rock; (2) different proportions of garnet and clinopyroxene entering the melt phases, or (3) different degrees of partial melting.

The maximum degree of partial melting for the Footprint gneiss and the felsic metavolcanics can be estimated from LIL element concentrations, using the equation of Shaw (1970):

$$\text{degree of partial melting } \alpha\ 1/\text{E.F.} = \frac{\text{amount of } \underline{e} \text{ in melt}}{\text{amount of } \underline{e} \text{ in parent}},$$

where $\underline{e}$ can be K, Rb, Sr or Ba in this particular calculation. Using the Jackfish Lake Complex mafic enclave D4 as typical of the parent rock composition of the Footprint gneiss, and the Burditt Lake tholeiites as parent for the felsic metavolcanic rocks, such calculations suggest a somewhat larger degree of melting for the gneiss (20-25%) than for the felsic metavolcanic rocks (15-20%).

The interpretation of the small Eu anomalies observed in the Footprint gneiss (Figure 3-49) is difficult and equivocal. Negative Eu anomalies are generally associated with plagioclase fractionation; high level fractionation during crystallization may have produced the anomalies in the tonalitic to trondhjemitic gneisses. The small positive Eu anomaly of the granodioritic gneiss may reflect the

precipitation of potassium feldspar near the end stages of the proposed high level differentiation.

Possible sedimentary origins for the Footprint gneiss

In developing the quartz eclogite model for the Footprint gneiss, an igneous parentage has been assumed; the possibility of a sedimentary origin will now be considered.

Formation of the Footprint gneiss by direct metamorphism of a pre-existing clastic metasedimentary sequence is highly unlikely. A Dennen and Moore (1971) type plot for the Footprint gneiss and the Pakwash gneiss (Figure 3-51) shows that, in contrast to the Pakwash paragneiss, the Footprint gneiss lies along the igneous trend, outside the field for mature sediments. Oxygen isotope data for the Footprint gneiss (Table 4-2) also rule out clastic metasedimentary rocks as the protolith; $\delta^{18}O$ rock results range from 5.9 to 8.9°/$_{oo}$; unmigmatized portions of the gneiss have $\delta^{18}O$ values of 7.5-7.8°/$_{oo}$. These values are too low for Archean clastic metasedimentary rocks (8-13°/$_{oo}$; Chapter II).

Production of the Footprint gneiss by partial melting of greywacke is also unlikely:

1. Greywackes, including those analyzed in this study, contain too much K to have produced the Footprint gneiss by partial melting (Tables 3-27, 2-3), unless they are

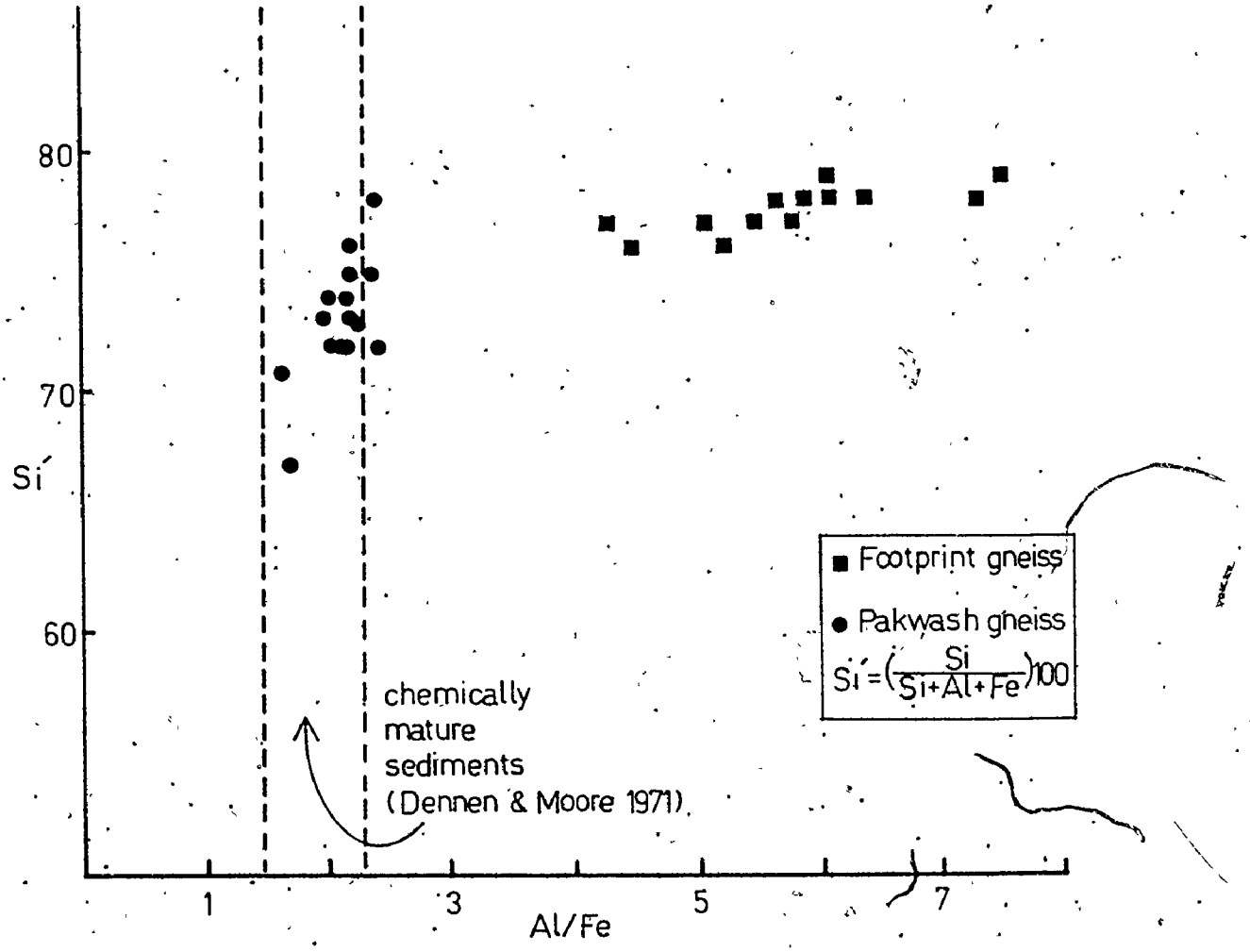

FIGURE 3-5.1 Normalized Si (Si') versus Al/Fe diagram for the Footprint and Pakwash gneisses.

Table 3-27 Chemical comparison, Footprint Gneiss and some Archean metagreywackes

	1	2	3	4	5
SiO_2*	71.50	65.81	68.65	67.05	68.28
Al_2O_3	15.58	15.04	13.68	13.70	16.06
TiO_2	0.27	0.55	0.46	0.63	0.43
Fe_2O_3**	2.12	5.28	5.85	6.25	3.79
MnO	0.03	0.08	0.09	0.09	0.05
MgO	0.82	2.88	3.00	3.78	1.42
CaO	2.93	4.35	2.26	2.62	3.96
Na_2O	5.11	3.67	4.39	4.32	4.07
K_2O	1.53	2.16	1.53	1.47	1.84
P_2O_5	0.12	0.18	0.09	0.09	0.10
Rb	42	71	37	43	32

* Analyses not normalized to 100%

**Total Fe as Fe_2O_3

1. Average 14 Footprint gneisses
2. Average 6 Uphill Lake Fm. metagreywackes, Upper Manitou Lake
3. Average 4 Moshor Bay Fm. metagreywackes, Upper Manitou Lake
4. Average 8 Kirkland Lake metagreywackes
5. Average 14 Kakagi Lake metagreywackes

predominantly of mafic origin (Table 2-4);

2. The volume of greywacke necessary to form the Rainy Lake gneiss by partial melting would need to be extremely large;

3. Partial melting of greywacke at crustal depths should produce melts enriched in ^{18}O relative to granitic rocks derived from non-crustal sources (greater than 8°/$_{oo}$ for granitoids derived from Archean clastic metasedimentary rocks). Pegmatites formed by partial melting of the Pakwash paragneiss, for example, have $\delta^{18}O$ values of about 10°/$_{oo}$ (Chapter IV). On the other hand, metagreywackes tectonically transported to the base of the crust, where the required temperatures for melting and the production of tonalitic liquids could be achieved, might re-equilibrate with mafic rocks and attain $\delta^{18}O$ values near that of basalt (6°/$_{oo}$). The $\delta^{18}O$ values of unmigmatized portions of the Footprint gneiss are instead similar to lower grade Archean plutonic granodiorites, such as the Burditt Lake stock, the Northwest Bay Complex and Jackfish Lake Complex examples (~7.5 °/$_{oo}$).

Conclusions and speculations

The geochemical data suggest that the Footprint gneiss formed by 20 to 25% melting of a quartz eclogite enriched in LREEs and other elements such as Th, Pb, Zr, and Hf

(Table 3-26). The data also indicate that more garnet remained in the residue during the formation of melt for the gneiss' protolith than did during the formation of the melt for the felsic metavolcanic rocks, also located within the study area. At high pressure (>27 kb) and water-saturated conditions, an increase in P_{total} causes clinopyroxene to enter the melt at lower temperatures than garnet (Wyllie et al., 1976). Thus the tonalitic magma which formed the protolith of the gneiss may have originated at higher pressure (greater depth) than that involved in the formation of the felsic metavolcanic rocks. Some higher level differentiation may have caused the variation in chemical composition of the gneiss from tonalitic to granodioritic; the bulk of the gneiss, however, is tonalitic.

Two-thirds of the Rainy Lake batholith (most of its interior) is composed of gneiss; if the chemistry of the Footprint gneiss is representative of this gneiss, the following speculations are warranted:

1. The true age of the batholith's gneissic interior is unknown; it may therefore be remobilized, old (>3 b.y.) sialic basement;

2. The postulated LREE-enriched source rock is possible only if the chemical composition of quartz eclogite in the mantle is variable; this could arise in at least three ways:

(i) the gneiss formed by melting of transformed primitive basalt which had not yet been depleted in LREEs and volatile elements by repeated cycling through the mantle, accompanied by episodes of partial melting;

(ii) the felsic magma formed by partial melting of subducted calc-alkali basalt, similar to that preserved as enclaves in the Jackfish Lake Complex;

(iii) the felsic magma was derived by partial melting of quartz eclogitic material located at greater depths in the mantle than that involved in the formation of the felsic metavolcanic rocks; because of its greater depth, the source rock had not yet been depleted in LREEs and volatiles or undergone previous episodes of melting.

The existing data does not permit a clear choice between these alternatives.

A final comment concerning a possible genetic relationship between the source rocks of the Footprint gneiss and the Jackfish Lake Complex diorite is appropriate. Partial melting of the quartz eclogite involved in the formation of the protolith of the gneiss would leave behind a clinopyroxene-garnet residue, undersaturated in SiO_2, and enriched in HREEs.

The Jackfish Lake Complex diorite, which was intruded as the last major phase of the batholith along the gneiss-metavolcanic interface, has a major element composition compatible with the partial remelting of such a SiO_2-undersaturated eclogite residue, and is 4 to 10 times enriched in HREEs relative to the gneiss. Its LREE content is similar to that of the gneiss, but that does not rule out remelting of the eclogite residue as LREEs are preferentially incorporated into dioritic liquids relative to tonalitic liquids (Arth and Hanson, 1975; Arth, 1976a), thus offsetting any depletion in LREEs that accompanied the first period of melting. Because of its refractory nature, the eclogite probably would undergo the second period of melting only under hydrous conditions.

However, it must be emphasized that there is no real proof of a genetic relationship between the hypothetical mantle source rocks involved in the formation of the Jackfish Lake Complex and the Footprint gneiss.

CHAPTER IV

THE OXYGEN ISOTOPE GEOCHEMISTRY OF ARCHEAN GNEISSES

IV-1 INTRODUCTION

The purpose of Chapter IV is to interpret the oxygen isotope geochemistry of Archean gneisses in light of the isotopic data obtained for least-metamorphosed granitoids, greenschist facies clastic metasedimentary rocks, and greenschist to amphibolite facies metavolcanic rocks, also from Archean terrains (Chapters II and III).

Archean gneissic terrains are known to include older meta-igneous sialic crustal material as well as younger supracrustal granitic, metavolcanic and volcaniclastic metasedimentary rocks. It may be possible to use the oxygen isotope data, along with other criteria, to recognize this variation in protolith rock types.

Previous analyses of orthogneisses (meta-igneous) and paragneisses (metasedimentary) illustrate some of the potential problems that can accompany such an application of isotopic data. For example, Fourcade and Javoy (1973)

and Shieh and Schwarcz (1974) have reported $\delta^{18}O$ values of 5 to 9‰ for upper amphibolite to granulite facies paragneisses, lower than would be expected, given their provenance. In order to understand such variations, and, in general, to be able to discuss oxygen isotopic variations in Archean gneisses, the following questions require answers:

1. What is the range of $\delta^{18}O$ values in Archean gneisses?
2. To what extent are the $\delta^{18}O$ values of Archean gneisses a function of :
   (i) differentiation at high temperature;
   (ii) detrital processes;
   (iii) regional metamorphism;
   (iv) large scale, high temperature isotopic exchange with low ^{18}O reservoirs;
   (v) isotopic exchange with meteoric or seawater?
3. Are Archean gneisses in oxygen isotopic equilibrium? What is the significance of oxygen isotopic temperatures of gneisses and associated metamorphosed granitic rocks?

Our discussion will be focused upon four gneisses:

(a) the Footprint gneiss, Lake Despair area, an example of an Archean gneiss from within a granite-greenstone belt (orthogneiss);

(b) the Cedar Lake - Clay Lake and Jaffrey-Melick gneisses, two examples of gneisses and metamorphosed granitoids

from within the predominantly plutonic southern portion of the English River gneiss belt (orthogneiss);

(c) the Pakwash gneiss, a banded paragneiss and migmatite associated with a supracrustal sequence in the northern portion of the English River gneiss belt.

The locations of these areas are shown in Figure 2-1a,b.

IV-2 OXYGEN ISOTOPE RESULTS FOR ARCHEAN GRANITOIDS - A REVIEW OF THE LITERATURE

$\delta^{18}O$ values for five granitic composites from the Superior Province ranged in $\delta^{18}O$ from 7.6 to 8.6°/$_{oo}$ for rock types varying from high level massive leucocratic granites to deep-seated, strongly foliated granitic gneisses and migmatites (Shieh and Schwarcz, 1977). These values fall within the range for most granitic rocks.

Viswanathan (1974a,b) reported $\delta^{18}O$ results for quartz separated from various members of the 2.7 b.y. Giants Range batholith, previously discussed in Chapter III-8. $\delta^{18}O$ values of 9.2 to 9.6°/$_{oo}$ were observed for four 'magmatic' granodiorites and granites; four granitoids believed by Viswanathan to have been formed by granitization of a sedimentary parent had $\delta^{18}O$ values of 10.8 to 11.4°/$_{oo}$, about 1 to 2°/$_{oo}$ lower than the presumed clastic metasedimentary

parent. Five migmatitic gneisses, also from the area, had $\delta^{18}O$ quartz values of 8.8 to 9.9‰. Viswanathan (1974a) estimated oxygen isotopic rock compositions for these samples (7.9 to 9.6‰ for the granitic rocks, 7.6 to 8.5‰ for the migmatitic gneisses), but such estimates are not very reliable.

Wilson and Green (1971), in a companion study to an investigation of the Proterozoic Musgraves Range basic granulites (Wilson et al., 1970), measured $\delta^{18}O$ values for quartz, plagioclase, phlogopite, pyroxene, ilmenite, magnetite and spinel separated from the Archean sapphirine-bearing basic granulites of Western Australia. Concordant isotopic temperatures for individual samples ranged from 575°C for a pyroxene granulite, to 695°C for an enderbite (all temperatures about 70°C lower than obtained from the equations of Bottinga and Javoy, 1975), and indicated a close approach to oxygen isotopic equilibrium. Since all of the rocks had experienced the same grade of metamorphism, Wilson and Green (1971) suggested that retrograde isotopic exchange and depletion during the waning stages of metamorphism, by means of autometasomatic fluids, had affected these samples to varying degrees. The absence of retrogression in the enderbite was attributed to the anhydrous nature of its mineral phases, which, therefore, preserved an isotopic temperature equivalent to the culmination of metamorphism. $\delta^{18}O$ rock

values for the granites and gneisses were about 8.3°/$_{oo}$, but the tonalites and mafic granodiorites had lower values (6.9-7.0°/$_{oo}$; Figure 4-1). The $\delta^{18}O$ rock values of the granulites (Fourcade and Javoy, 1973) (5.5-7.8°/$_{oo}$), in spite of their pelitic to granitic compositions, are lower than most plutonic granitoids (Figure 4-1) and far removed from the values for paragneisses described by Garlick and Epstein (1967). The oxygen isotope mineral data for the granulites, which are composed of interlayered charnockitic gneisses, garnet paragneisses, quartzites and leucocratic, pegmatitic gneisses, most of detrital origin, reflect bulk depletion in ^{18}O, although most phases approach isotopic equilibrium (Table 4-1).

Table 4-1 Oxygen isotope mineral data for the In Ouzzal granulites (Fourcade and Javoy, 1973)

	$\delta^{18}O$°/$_{oo}$	anomalous results
quartz	7.48 - 9.56	1.58
plagioclase	8.12	
biotite	3.02 - 5.21	
amphibole		-2:23
clinopyroxene	4.14 - 5.85	
orthopyroxene	4.79 - 5.23	
garnet	4.73 - 6.13	
magnetite	-0.25 - 1.36	

Fourcade and Javoy (1973) suggested that two factors contributed to the low ^{18}O values of the granulites:

1. their very high metamorphic grade;
2. their very old age (3.3 b.y.).

Two models, based upon these factors, were developed to account for the ^{18}O depletion:

Model 1: The granulites isotopically exchanged with upper mantle rocks during high grade metamorphism. The deep crustal position of the In Ouzzal granulites facilitated exchange with the lower crust and/or upper mantle. However, the absence of large scale partial melting, and the presence of high and concordant oxygen isotope temperatures suggests that the exchange medium was not water; CO_2, outgassing from the mantle, is a viable alternative.

Model 2: The sedimentary protolith of the granulites was derived from acid rocks of isotopic composition near that of basalt; such compositions could be attained during differentiation from basalt at high temperatures. The erosion of the acid rocks and the subsequent sedimentary processes occurred too rapidly to alter the isotopic composition of the detritus.

Shieh and Schwarcz (1974) analyzed two groups of Grenville rocks; group A contained upper amphibolite to granulite facies migmatites, paragneisses and concordantly emplaced

granitic gneiss and ranged in $\delta^{18}O$ from 5.0 to 8.9°/$_{oo}$; group B was composed of lower grade metasedimentary rocks and high level granitic plutons that ranged in $\delta^{18}O$ from 9 to 17°/$_{oo}$. These data led Shieh and Schwarcz (op. cit.) to propose large scale oxygen isotopic exchange with a mafic reservoir in the lower crust or upper mantle during migmatization, leading to the lower isotopic values in the group A rocks. These results therefore support the concept that high grade metamorphism can cause ^{18}O depletion.

Barker et al. (1976a,b) reported $\delta^{18}O$ values for Proterozoic and Archean trondhjemites and their metamorphosed equivalents. The $\delta^{18}O$ values of apparently undisturbed (unaltered) samples ranged from 4.9 to 8.6°/$_{oo}$ (recalculated to SMOW = 0°/$_{oo}$, rather than 0.3°/$_{oo}$, as used by Barker et al., 1976b). The average $\delta^{18}O$ value of these rocks is somewhat lower than observed for most plutonic granitoids (Figure 4-1). Specifically, tonalitic gneisses from Swaziland have $\delta^{18}O$ values of 5.8 to 7.7°/$_{oo}$; whereas related veined gneisses, injected with K-rich pegmatoidal material, have higher values. Barker and his coworkers have proposed high temperature origins for trondhjemitic and tonalitic Archean rocks by partial melting of hydrous primitive basalt, and suggest that $\delta^{18}O$ values of 5 to 7°/$_{oo}$, such as are observed in the Swaziland tonalitic gneisses, support such an interpretation.

Thus, Barker et al. (1976b) favour the second model of Fourcade and Javoy (1973). However, the former workers were unable to distinguish between partial melting and fractional crystallization processes on the basis of oxygen isotopic data. Also, the somewhat higher values observed for the Archean tonalitic gneisses from Wyoming (Figure 4-1) remain unexplained by them.

Taylor and Magaritz (1975) have analyzed Archean tonalitic rocks from southern Africa, and found that the average $\delta^{18}O$ value for Swaziland tonalites was 7.3°/$_{oo}$, still lower than observed for most plutonic granitoids. They suggested that such oxygen isotope values reflect differentiation from mafic material, much in the same manner that similar low ^{18}O tonalites of younger age such as the San Jose and Bonsall tonalites have formed from mafic rocks such as the San Marcos gabbro with little or no change in $\delta^{18}O$ during differentiation. The somewhat higher values of the migmatitic gneiss (Figure 4-1), which is roughly equivalent to Barker et al.'s veined gneiss, were attributed to the possible partial melting of a parent metasedimentary rock. Some younger (2.9 b.y.) granitic rocks showed ^{18}O depletions that appear to be the result of interaction with meteoric water.

Perry et al. (1976) have reported $\delta^{18}O$ results for tonalitic to granodioritic gneisses from Greenland that are similar in isotopic composition to most plutonic granitoids

FIGURE 4-1 Oxygen isotope results taken from the literature for Archean granitic and gneissic rocks

(a) Taylor (1968)

(b) Fourcade and Javoy (1973)

(c) Barker et al. (1976b)

(d) Taylor and Magaritz (1975)

(e) Perry et al. (1976)

FIGURE 4-2 Oxygen isotope results for Archean gneisses analyzed during this study.

The range and mean values for greenschist and lower metamorphic grade clastic metasedimentary, metavolcanic and plutonic rocks also analyzed are shown as well.

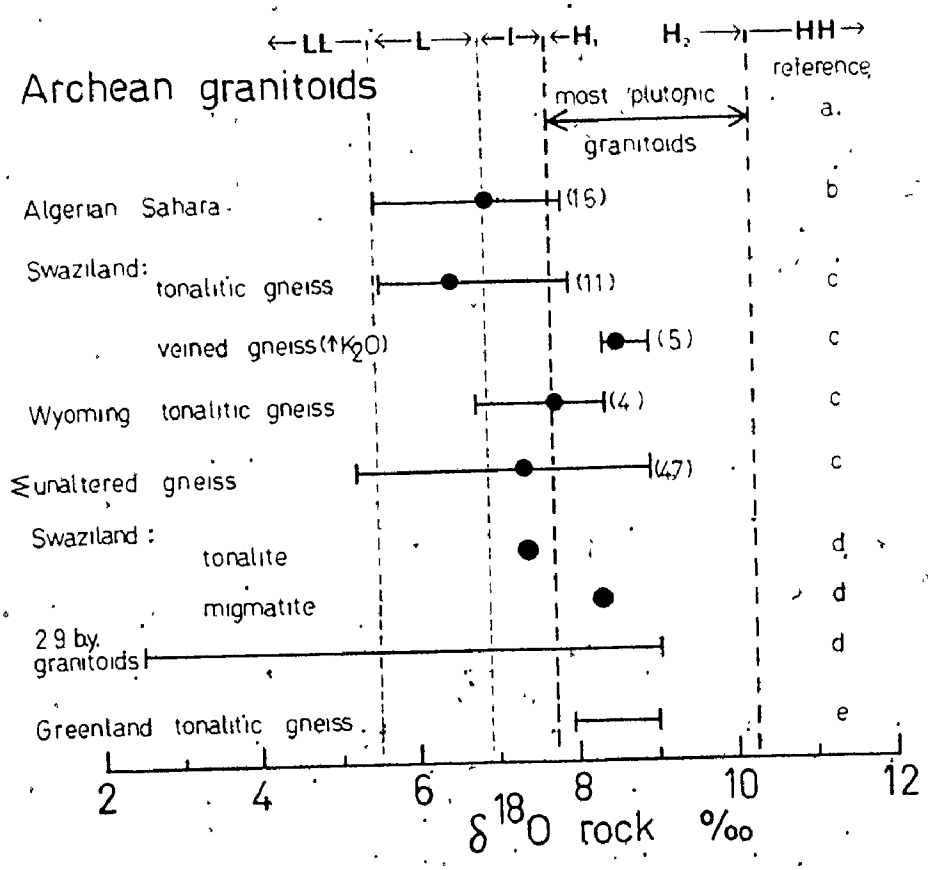
←LL— ←L→ ←I→ ←H₁ H₂→ —HH→
reference
Archean granitoids
most plutonic granitoids
a.
Algerian Sahara
(16)
b
Swaziland: tonalitic gneiss
(11)
c
veined gneiss (↑K₂O)
(5)
c
Wyoming tonalitic gneiss
(4)
c
≷unaltered gneiss
(47)
c
Swaziland :
tonalite
d
migmatite
d
29 by. granitoids
d
Greenland tonalitic gneiss
e
2
4
6
8
10
12
δ 18O rock ‰

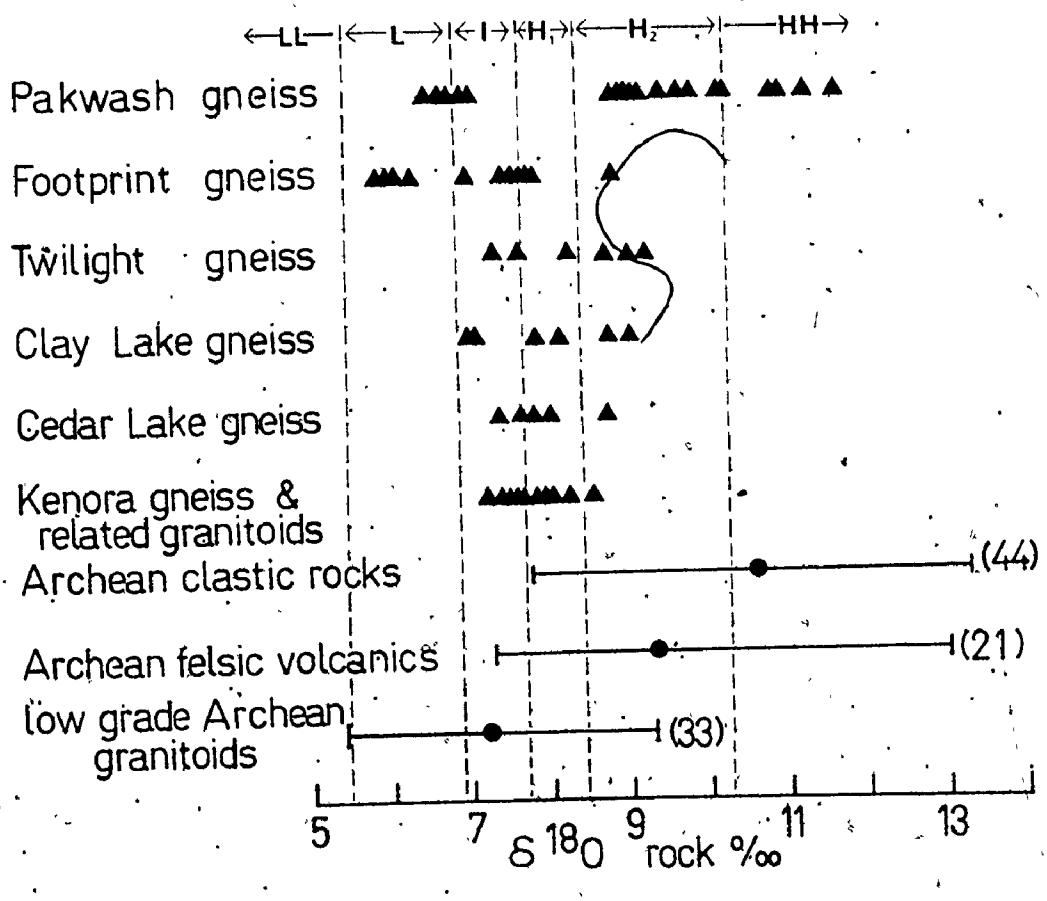
←LL— ←L→ ←I→ ←H₁ H₂→ —HH→
Pakwash gneiss
Footprint gneiss
Twilight gneiss
Clay Lake gneiss
Cedar Lake gneiss
Kenora gneiss & related granitoids
Archean clastic rocks
(44)
Archean felsic volcanics
(21)
low grade Archean granitoids
(33)
5
7
9
11
13
δ 18O rock ‰

(Figure 4-1). Tonalitic gneisses bordering the Isua Supracrustal belt ranged in $\delta^{18}O$ from 7.9 to 8.4°/$_{oo}$ for the 'inner' gneiss, to 8.4 to 9.0°/$_{oo}$ for the 'outer' gneiss. Longstaffe et al. (1977c) suggested that these higher values may reflect a previous crustal history for these rocks. Perry et al. (in press), however, suggest that basaltic parent rocks were enriched in ^{18}O by low temperature submarine weathering and alteration in the Archean oceans. These rocks were then buried (subducted?) and partially melted (in an isotopically closed system) in the manner described by Arth and Hanson (1975) to produce acid rocks with $\delta^{18}O$ values within the plutonic range.

One additional analysis, published by Taylor (1968), will prove useful in our consideration of the Pakwash paragneiss; the nearby Dome granite has a $\delta^{18}O$ value of 11.2°/$_{oo}$. Using sulphur isotopes, Shima et al. (1963) showed this granite to be of sedimentary origin.

IV-3 OXYGEN ISOTOPE RESULTS FOR ARCHEAN GNEISSES FROM NORTHWESTERN ONTARIO

The $\delta^{18}O$ rock results for over 50 Archean gneisses examined during this study are shown in Figure 4-2 and listed in Table 4-2. Some of these results have been reported

Table 4-2. $\delta^{18}O$ rock results, Archean gneisses, northwestern Ontario

Locality	$\delta^{18}O$°/$_{oo}$	Rock type
LAKE DESPAIR, WABIGOON GRANITE-GREENSTONE BELT		
Footprint Gneiss		
F110	8.85	granitic gneiss
F103	7.79	tonalitic gneiss
F10	7.59	trondhjemitic gneiss
F73	7.72	granodioritic gneiss
F152	7.45	trondhjemitic gneiss
F98	7.57	granodioritic gneiss
F99	7.00±0.16 (2)	tonalitic gneiss
F150	6.31	quartz dioritic gneiss
F7	6.09	tonalitic gneiss
F151	6.05	trondhjemitic gneiss
F149	5.93	granodioritic gneiss
CEDAR LAKE-CLAY LAKE, SOUTHERN PORTION, ENGLISH RIVER GNEISS BELT		
1. Twilight Gneiss		
309	7.33±0.32 (2)	granulite facies paragneiss
377	8.29±0.09 (2)	granulite facies paragneiss
535	8.73	granulite facies paragneiss
378	7.63	granulite facies paragneiss (?)
448	9.03	granulite facies paragneiss (?)
538	9.25	granulite facies paragneiss (?)
2. Clay Lake Gneiss		
513A	7.02	granulite facies enderbite
433	7.06	granulite facies enderbite
553	7.87	granulite facies enderbite
516	9.03	granulite facies alaskite
458	8.15	granulite facies alaskite
367	8.76	granulite facies alaskite

Table 4-2 /continued

3. Cedar Lake Gneiss		
432	8.72	amphibolite facies granitoid gneiss
24	7.37	amphibolite facies granitoid gneiss
62	7.63	amphibolite facies granitoid gneiss
350	8.01	amphibolite facies granitoid gneiss
560	7.81	amphibolite facies granitoid gneiss
KENORA AREA: MELICK GNEISS & ASSOCIATED GRANITOIDS, SOUTHERN PORTION, ENGLISH RIVER GNEISS BELT		
G106B	7.59	biotite tonalitic gneiss
G110A	7.39	leucogranitoid associated with tonalitic gneiss
G350A	7.96	biotite tonalitic gneiss
G350B	8.02	granitic pegmatoid gneiss
G886	8.26	granitic pegmatoid gneiss
G715	7.51	Melick tonalite
G596A	7.85	Melick tonalite
G135	7.54	Dalles grey granodiorite
G145	7.26	Dalles pink granite
G835B	8.56	leucogranitoid associated with amphibolite
G867A	4.81	amphibolite
G835A	5.69	amphibolite
PAKWASH LAKE, NORTHERN PORTION, ENGLISH RIVER GNEISS BELT		
L37	8.97	plagioclase-quartz-biotite-garnet layered metagreywacke
P178	10.95	plagioclase-quartz-biotite-layered metagreywacke
P249A	9.18	plagioclase-quartz-biotite-garnet layered metagreywacke

Table 4-2 /continued

P61A	11.31	plagioclase-quartz-biotite-garnet layered metagreywacke
P164	9.04	plagioclase-quartz-biotite-garnet layered metagreywacke
P205B	9.83	plagioclase-quartz-biotite-garnet layered metagreywacke
P202A	11.69	plagioclase-quartz-biotite-garnet layered metagreywacke
P306A	10.93	plagioclase-quartz-biotite-garnet layered metagreywacke
P1097	8.83	plagioclase-quartz-biotite-garnet layered metagreywacke (?)
P52B	10.21	plagioclase-quartz-biotite-garnet layered metagreywacke
P181	9.11	plagioclase-quartz-biotite-garnet layered metagreywacke
P80	10.23	plagioclase-quartz-biotite-garnet layered metagreywacke
L42	9.46	plagioclase-quartz-biotite-garnet layered metagreywacke
L40	6.75	migmatized metagreywacke, bulk sample
L44A	6.99	migmatized metagreywacke
L44B	6.53	white, mobilisate-depleted migmatized metagreywacke
L43	7.68	white mobilisate (qtz-plag-microcline-musc-bio)
L45B	6.99	migmatized metagreywacke (bulk sample)
L45A	9.70	garnetiferous metapelite
L41	10.0*	pink pegmatite dike, qtz-microcline-plag-musc-bio

* Estimated from mineral $\delta^{18}O$ and modal data

The following persons provided samples:

Cedar Lake-Clay Lake area: C. Westerman
Kenora area : C. Gower
Pakwash Lake (P-series samples) : G. Bea

previously (Longstaffe et al., 1976a,b, 1977a,b; Longstaffe and Schwarcz, 1977). The $\delta^{18}O$ values of the gneisses range from 5.9 to 11.7°/$_{oo}$. Those believed to be of igneous origin include the Footprint gneiss (5.93-8.85°/$_{oo}$), the Clay Lake gneiss (7.02-9.03°/$_{oo}$), the Cedar Lake gneiss (7.37-8.72°/$_{oo}$), and the Kenora gneiss and related foliated to gneissic granitoids (7.26-7.85°/$_{oo}$). Those bodies believed to be of sedimentary origin include the Pakwash gneiss (6.53-11.69°/$_{oo}$) and the Twilight gneiss (7.33-9.25°/$_{oo}$).

The $\delta^{18}O$ values of these gneisses can be compared with the results for least-metamorphosed granitoids from the Lake Despair - Burditt Lake area as well as with the metavolcanic and clastic metasedimentary rocks (Figure 4-2). The field observed for most of the gneisses is similar to that of the low grade granitoids, but the data for the Pakwash gneiss overlap the isotopic range observed for the low grade supracrustal rocks.

Four general observations can be made concerning the oxygen isotope rock data for the gneisses, as well as the least-metamorphosed granitic rocks (Figures 4-2 and 3-27):

1. Most of the analyses for the Footprint gneiss, the Kenora gneissic rocks, the Clay Lake enderbites (Table 4-2), and the plutonic Jackfish Lake Complex fall within the L to H_1 groups of Taylor (1968),

unlike most younger granitic rocks from batholithic and orogenic complexes, which are concentrated in the H_2 group (Taylor, 1968). Many of the Archean gneisses discussed in section IV-2 also lie within this L to H_1 field. According to Taylor (1968), most modern examples of I-type (intermediate grouping between L and H_1) granitoids occur in minor intrusive bodies or are of a hypersolvus nature. Turi and Taylor (1971a) have noted, however, that some mafic enclave bearing granodiorites, such as the Domenigoni Valley granodiorite, Southern California Batholith, have low $\delta^{18}O$ values (7.7‰) because of large scale exchange and/or mixing and assimilation of underlying gabbro, or because of differentiation from a gabbroic melt with little or no change in $\delta^{18}O$.

2. $\delta^{18}O$ results in the LL-L range include some diorites and granodiorites from the Jackfish Lake Complex, and groups of samples from the Footprint and Pakwash gneisses. The low diorite values are expected, given the chemical composition of these rocks (section III-8); the low ^{18}O granodiorites have already been shown to be altered by meteoric water interaction. The processes involved in the formation of the low ^{18}O values of the gneisses will be discussed in the remainder of this chapter.

3. Archean granitoids intruded into known pre-existing sialic crust, such as the Burditt Lake pluton, or believed formed from pre-existing supracrustal sequences (Pakwash paragneiss), have $\delta^{18}O$ values in the H_1-HH range (Figure 3-27, Figure 4-2). The Twilight gneiss, however, and portions of the Pakwash gneiss, in spite of their supposed supracrustal origin, have lower $\delta^{18}O$ values.
4. Many leucogranitoid veins and dikes contained within the gneisses or mafic amphibolites have high $\delta^{18}O$ values (H_1-HH group; F110, 516, 458, 367, L41, F23, G835B), although some exceptions are present (L43, G110A).

Let us now examine some of the possible influences upon the oxygen isotopic composition of Archean gneisses and associated granitic rocks, and attempt to determine the relative importance of each of these factors in shaping the final isotopic composition of the rock.

IV-4a ISOTOPIC EXCHANGE OF GNEISSES WITH METEORIC WATER

Taylor and his coworkers (Taylor, 1968, 1971, 1973, 1974, 1976; Taylor and Forester, 1971; Forester and Taylor, 1972; Magaritz and Taylor, 1976a,b; Sheppard and Taylor, 1974; Sheppard et al., 1969, 1971) have documented the depletion of

^{18}O and D in granitic rocks by the interaction with heated ground waters. Such effects are common in Mesozoic and Tertiary intrusions, particularly around epizonal stocks. The effects are most pronounced in areas where the intruded country rocks are highly jointed, permeable, volcanic rocks which permit the free flow of water. The characteristics of such ^{18}O depleted rocks have been outlined in summary form by Taylor (1974); these criteria have already been discussed in our explanation of the low ^{18}O Jackfish Lake Complex granodiorites (section III-8) and need not be repeated here.

A recent oxygen and hydrogen isotope study of the Coast Range batholith, British Columbia (Magaritz and Taylor, 1976b) indicated the presence of enormous meteoric water circulatory systems that extend to depths of at least three kilometers. Thus, meteoric-hydrothermal activity can affect the $\delta^{18}O$ values of granitic rocks on a regional scale. However, the deep-seated gneisses within the Coast Range batholith retained normal $\delta^{18}O$ values; only the δD values of sericite showed the effects of exchange with low ^{18}O fluids; coexisting biotites had igneous $\delta^{18}O$ and δD values. Taylor (1976) has concluded that meteoric water circulatory systems have been established in most batholiths; however, he also points out that the bulk of batholithic rocks are undisturbed by such processes, except perhaps for the D/H ratios of the

hydrous minerals.

Because of metamorphic recrystallization, petrographic data is of little use in the detection of meteoric water-hydrothermal activity that may have affected Archean gneisses prior to their metamorphism. However, a number of other factors suggest that such activity has not affected the gneisses examined in this study:

1. The $\delta^{18}O$ rock values for the chemically similar meta-igneous English River belt gneisses (Cedar Lake - Clay Lake and Kenora areas) are in the same range, although the localities are over 100 km apart. A similar comparison can be made for the Footprint gneiss, Lake Despair area, which is located over 100 km south of the other two units and occurs in a tectonically different geological subprovince (Wabigoon granite-greenstone belt) (Figure 2-1a,b). This comparison can be extended to include many of the other Archean gneisses discussed in section IV-2 that occur in entirely different Archean shield areas, thousands of kilometers distant. This uniformity of $\delta^{18}O$ values is not compatible with the zonal depletion patterns usually associated with meteoric water activity; also, none of the Archean gneisses examined in this study have $\delta^{18}O$ values of less than 5.9°/$_{oo}$,

in contrast with the larger depletions expected from meteoric water interaction.

2. While estimates of the level of emplacement of Archean meta-igneous gneisses vary with the prevailing theories of Archean thermal gradients and crustal evolution, minimum depths of 5 to 15 km are generally conceded. If meteoric water-related isotopic alteration has occurred, it seems likely that only the upper 5 to 7 km will have been seriously affected (Magaritz and Taylor, 1976b); these are precisely the rocks which stand the greatest chance of being eroded following uplift, since their formation 2.7 to 3.7 b.y. ago. It is not surprising that the only previously documented cases of meteoric-hydrothermal depletion in Archean granitoids have been documented for high level, late to postkinematic granites and granophyres (Taylor and Magaritz, 1975). Recall that the meteoric water-rock interaction observed in the Lake Despair area (section III-8) also occurred in the high level, late stage Jackfish Lake Complex granodiorites, not in the juxtaposed Northwest Bay foliated granodiorite.
3. It is very unlikely that meteoric water has affected the gneisses since their metamorphism; almost all of the mineral phases analyzed (Tables 4-3, 4-7, 4-8)

are approximately in isotopic equilibrium, with quartz, feldspar, amphibole, epidote, biotite, and magnetite occurring in the order normally found in unaltered plutonic rocks.

Wenner and Taylor (1976) recently suggested that, at very low temperatures (50-200°C) meteoric water circulation could cause enrichment in ^{18}O, especially of alkali feldspars. The operation of such a process is not indicated by any of our data, and will not be considered further.

IV-4b THE ISOTOPIC COMPOSITION OF THE ARCHEAN OCEAN

The unstable nature of the Archean crust, and the varying possibilities for the generation of Archean granitic rocks, makes it impossible to exclude, *a priori*, the possibility that seawater may have percolated through the gneisses at some time in their history, and caused a depletion in ^{18}O. However, before such a hypothesis can be properly evaluated, we must make some judgement upon the $\delta^{18}O$ value of Archean seawater. The isotopic composition of the Archean hydrosphere is a matter of some controversy; in the preceding comments on meteoric water activity the tacit assumption was made that such activity was controlled by an ocean reservoir of $\delta^{18}O$ equal

to 0°/$_{oo}$. We shall attempt to justify that assumption here.

Since 1951, two schools of thought have developed concerning the $\delta^{18}O$ of the oceans throughout geological time. One group (Weber, 1965; Perry, 1967; Dontsova, 1970; Dontsova et al., 1972; Perry and Tan, 1972; Chase and Perry, 1972; Perry et al., 1977) proposes that Archean oceans were depleted in ^{18}O and have become isotopically enriched with time. The second school proposes that the $\delta^{18}O$ value of ocean water has remained constant (Muehlenbachs, 1971; Taylor and Magaritz, 1975; Knauth and Epstein, 1976; Muehlenbachs and Clayton, 1976).

Perry and Tan (1972) discovered that the highest $\delta^{18}O$ values of Archean cherts and carbonates, believed on textural grounds to be unaltered, were about 17°/$_{oo}$ lower than observed for recently precipitated SiO_2 and carbonates, and therefore suggested that the oceans have become enriched in ^{18}O by about 15 to 17°/$_{oo}$ since the Archean.

Classical interpretations for the wide range in $\delta^{18}O$ of cherts and carbonates, and their apparent time dependence involve the progressive lowering of primary $\delta^{18}O$ values by exchange with meteoric water during diagenesis, hydrothermal alteration, and metamorphism (Clayton and Epstein, 1958; Engel et al., 1958; Degens and Epstein, 1962; James and Clayton, 1962; Keith and Weber, 1964; Taylor and Coleman, 1968).

Epstein and his coworkers have recently challenged the views of both the depletionists and the alterationists. Knauth and Epstein (1975) showed that deep sea cherts of mid-Eocene age ranged in $\delta^{18}O$ by several per mil strictly as a function of formation temperature. A detailed study by Kolodny and Epstein (1976) of Jurassic to Miocene DSDP cherts demonstrated that the most ^{18}O rich-cherts reflected the ocean bottom temperatures during chert formation and that further diagenesis led to ^{18}O depletion. Knauth and Epstein (1976) showed that the data for Precambrian cherts can be accounted for by surface temperatures of 70°C at 3.0 b.y. and 52°C at 1.3 b.y., within the liberal 0 to 146°C range suggested by Oskvarek and Perry (1976).

Other more indirect evidence also suggests that the $\delta^{18}O$ of the ocean has been constant throughout geological time. Muehlenbachs (1971) and Muehlenbachs and Clayton (1976) calculated the net transfer in ^{18}O for the seawater-rock cycle to be near zero. Taylor and Magaritz (1975) suggested that early Precambrian surface waters were similar to Phanerozoic waters because the $\delta^{18}O$ and δD values of Archean granitoids which had undergone meteoric water-rock interaction (section IV-2) were similar to Phanerozoic examples. Wenner and Taylor (1976) have made similar arguments for altered Proterozoic granitoids.

In summary, the bulk of the evidence supports the contention that Archean seawater had an oxygen isotopic composition near to $0°/_{oo}$.

IV-4c ISOTOPIC EXCHANGE OF GNEISSES WITH SEAWATER

Seawater-rock interaction ($0°/_{oo}$) at hydrothermal temperatures (section III-4) could produce the lower $\delta^{18}O$ values observed in the Archean gneisses, providing that seawater was able to gain access to the gneisses or their protoliths. This could occur if (a) the granitoids were overlain by submarine volcanics during subsidence and volcanism subsequent to plutonism, or (b) if the granitoids were tectonically emplaced into oceanic crust (during the initial formation of sialic crust - Glikson's (1972) "island nuclei of sodic granite") at sufficiently high levels (less than 5 km). Granitic rocks thus affected could have very similar isotopic compositions despite their geographically wide distribution. However, the seawater-rock interaction hypothesis, as a general explanation for the somewhat lower $\delta^{18}O$ of Archean granitoids, founders on two points: (1) the depth of emplacement for those granitoids of igneous or meta-igneous origin was probably greater than 5 km; (2) there is little chemical data that suggests interaction of the

granitoids with large quantities of saline fluids.

It seems unlikely, therefore, that seawater interaction with the gneisses or their protoliths has produced the observed $\delta^{18}O$ values.

IV-5 THE EFFECT OF REGIONAL METAMORPHISM UPON THE OXYGEN ISOTOPE COMPOSITION OF SILICEOUS ROCKS - A REVIEW OF THE LITERATURE

The purpose of this section is to determine the effect of high grade regional metamorphism upon the final isotopic composition of gneisses.

The effects of regional metamorphism upon oxygen isotope systems do not manifest themselves in any particularly well-known or predictable fashion. Cretaceous granites from the Ryoke metamorphic belt of Japan (Matsuhisa et al., 1972; Honma and Sakai, 1976) and some meta-anorthosites from the Adirondack Mountains (Taylor, 1970) seem to be enriched in ^{18}O. Many pelitic metasediments become depleted in ^{18}O with increasing metamorphic grade, such as observed for the metapelites surrounding the migmatite dome at Naxos (Rye et al., 1976) and for the progressively metamorphosed suite of phyllites, schists and migmatites from the Yenisey Ridge, Ukraine (Dontsova and Milovskiy, 1967).

Migmatization appears to be important in the $\delta^{18}O$

depletion of many pelitic and granitic rocks. As previously mentioned in section IV-2, upper amphibolite to granulite facies migmatites, paragneisses and granitic gneisses from the Grenville have much lower $\delta^{18}O$ values than found for the lower grade equivalents from the same area (Shieh and Schwarcz, 1974). Paleozoic Inner Schieferhulle pelites range in $\delta^{18}O$ from 15 to 20°/$_{oo}$, while their metamorphosed and migmatized Inner Schieferhulle equivalents have much lower $\delta^{18}O$ values (5-12°/$_{oo}$; Hoernes and Friedrichsen, 1974). Many other examples of ^{18}O depletion accompanying the metamorphism of metasedimentary rocks have been reported (Black, 1974; Dontsova, 1970; Shieh and Taylor, 1969; Taylor and Coleman, 1968).

However, not all metasediments which undergo regional metamorphism experience depletion in ^{18}O. Garlick and Epstein (1967) concluded that there was no definite trend in $\delta^{18}O$ with regional metamorphic grade, although, in specific areas, a decrease in $\delta^{18}O$ was observed. Calcareous and pelitic metamorphic rocks from New England have $\delta^{18}O$ values inherited from their protoliths, although mineral fractionations decrease with increasing metamorphic grade (Schwarcz et al., 1970). Andalusite-sillimanite-cordierite pelitic schists from the Domenigoni Valley, Southern California, have $\delta^{18}O$ values of 19-20°/$_{oo}$, which, if anything, are higher than unmetamorphosed

pelites (Turi and Taylor, 1971a).

The varied oxygen isotope behaviour of metamorphosed silicate rocks is largely a function of the degree of isotopic re-equilibration during metamorphism, the nature of the exchange medium, and the size and isotopic composition of the exchange reservoir.

Dimensions of oxygen isotope equilibrium

Taylor et al. (1963) showed that kyanite grade pelitic schists had identical $\delta^{18}O$ values and mineral fractionations over a 200 meter area. Similar results were reported for metasediments and metabasalts collected over a 25 meter area, at Wards Creek, California (Taylor and Coleman, 1968). It was suggested that such results represented re-equilibration during recrystallization within a narrow temperature range. Sharma et al. (1965), on the other hand, explained extremely uniform $\delta^{18}O$ values of mineral phases from Quebec iron-formation, which were collected over an area of several kilometers, as being primary. Anderson (1967) observed isotopic disequilibrium on the kilometer, meter and centimeter scale during his examination of a variety of rock groups. His results showed that, in general, oxygen isotope equilibrium was attained and preserved only over dimensions of a few millimeters to centimeters, and varied with mineral grain

size and the amount of exchange required for equilibration. Others have since shown that large scale (kilometer) complete re-equilibration of metamorphic rocks is a rare phenomenon, whereas partial re-equilibration is commonplace (Epstein and Taylor, 1967).

Nature of the isotopic exchange medium

Three mediums are generally considered capable of facilitating large scale oxygen isotopic exchange during metamorphism: H_2O, CO_2, and silicate melts. Mobile pore fluids derived by dehydration reactions provide a convenient and reasonable (if often unproven) exchange fluid, and have been invoked by many authors to explain oxygen isotope mobility between interbedded metasedimentary units, high ^{18}O country rocks and granitic rocks/magmas, and mafic enclaves and silicic host rocks (Matsuhisa et al., 1972; Taylor, 1968, 1970; Black, 1974; Taylor and Coleman, 1968; Honma and Sakai, 1976; Taylor et al., 1963). Sheppard and Schwarcz (1970) and Taylor (1968) have demonstrated that decarbonation of limestones and dolomites produces (at 500-700°C) a CO_2-rich fluid which is about 5-7‰ heavier in ^{18}O than the Ca-silicates left behind. During such activity, the fluid acts not only as the exchange medium, but also as the ^{18}O reservoir.

The behaviour of oxygen isotopes during dehydration reactions involving water is quite different. Shieh and Taylor (1969) showed that $\delta^{18}O$ values remained constant across contact metamorphic aureoles, in systems where homogenization of the oxygen isotopes is confined to centimeter scales. $\delta^{18}O$ rock values were either equal to, or up to 4‰ higher than the coexisting waters, as calculated from mineral assemblages. These studies confirmed, as earlier suggested by Garlick and Epstein (1967), that H_2O dehydration reactions do not have a significant effect upon the rocks from which the water is extracted. The low volumes of these fluids necessitate that their isotopic compositions be controlled, in a closed system, by the rocks with which they are in contact.

The association of low ^{18}O rocks with the development of migmatites, and the preservation of original isotopic patterns in its absence, caused Shieh and Schwarcz (1974) to suggest that extensive oxygen isotope exchange with an external reservoir is greatly facilitated by the presence of a silicate melt. Shieh et al. (1976) have also proposed that physical admixing of high ^{18}O granitic mobilisate can cause enrichment of the affected host.

Nature of the oxygen isotope reservoirs

The nature of the oxygen isotope reservoirs involved during regional metamorphism is not well understood. The problem can be approached in terms of system size:

1. small scale closed system re-equilibration;
2. large scale 'balanced' system re-equilibration;
3. large scale open system exchange and re-equilibration.

The first case involves small scale isotopic re-equilibration between mineral phases to $\delta^{18}O$ values indicative of the metamorphic thermal regime by means of H_2O, but without any net transfer of ^{18}O into or out of the system. The second case represents open system movement of oxygen isotopes, but in a manner in which ^{18}O is conserved in a recognizable fashion. Such is the case when plutonic rocks of low $\delta^{18}O$ are intruded into country rocks of high $\delta^{18}O$. The country rock acts as an ^{18}O reservoir, the plutonic rocks as an ^{18}O acceptor, and the pore fluids as the exchange medium. It is generally proposed that such solutions move upwards through the plutonic bodies along fractures provided by tectonism, and exchange at the high temperatures associated with the regional metamorphism (Taylor, 1970). Direct exchange of fluids with magma has been proposed (Taylor, 1970; Honma and Sakai, 1976), but the convective processes necessary

for isotopic exchange are more difficult to maintain in a liquid than in a solid. Nevertheless, the isotopic homogeneity of the ^{18}O rich monzonites from the Loon Lake pluton (Shieh et al., 1976), as opposed to its isotopically heterogeneous quartz monzonite rim, is compatible with CO_2-magma exchange.

The third case is the most difficult to comprehend. Nevertheless, isotopic exchange with undefined or poorly defined external reservoirs may be the only explanation for the results from the Grenville (Shieh and Schwarcz, 1974), from Naxos (Rye et al., 1976), from the Inner Schieferhulle (Hoernes and Friedrichsen, 1974), and from In Ouzzal (Fourcade and Javoy, 1973). All require low ^{18}O fluids from depth. A similar explanation could account for many of the Archean gneisses and granitoids analyzed in this study, especially the low ^{18}O groups of the Footprint and Pakwash gneisses (Figure 4-2).

IV-6 OXYGEN ISOTOPE GEOCHEMISTRY OF THE FOOTPRINT GNEISS

The purpose of this section is to describe the behaviour of oxygen isotopes in the middle to upper amphibolite facies Footprint orthogneiss. $\delta^{18}O$ rock data for this unit lie within the L to H_1 groups of Taylor (1968); $\delta^{18}O$ mineral data

is given in Table 4-3 and illustrated in Figure 4-3.

While few, if any, chemical differences were observed between migmatized and unmigmatized varieties of the Footprint gneiss, there is a distinct difference in their oxygen isotope compositions. Migmatized samples (F99, F150, F7, F151, F149) have $\delta^{18}O$ rock values of 5.9 to 7.0‰, the range suggested by Barker et al. (1976b) as diagnostic of differentiation from basalt at high temperatures; the least altered or unmigmatized gneiss has $\delta^{18}O$ rock values of 7.5 to 7.8‰, still low ('I' type) relative to modern granitoids, but higher than can be attributed to high temperature differentiation of a basaltic parent (Figure 4-2).

Figure 4-3 shows that individual mineral phases have undergone an overall depletion in $\delta^{18}O$ that parallels the change observed in $\delta^{18}O$ rock composition, although there is some scatter in the data, especially for biotite and microcline. The depleted samples, however, are not grossly out of isotopic equilibrium. Complete re-equilibration, nevertheless, has not been achieved. While most of the quartz-biotite and feldspar-biotite oxygen isotope temperatures approach concordancy, the quartz-magnetite temperatures are clearly higher than those obtained from other mineral pairs, and all measured temperatures are lower than expected for high grade metamorphic conditions (Figure 4-4, Table A1-4A).

Table 4-3 Oxygen isotope mineral results, Footprint Gneiss

	$\delta^{18}O$‰				
	quartz	microcline	epidote	biotite	magnetite
F110	10.59±0.10	7.99±0.17	5.74	2.52±0.08	0.18±0.29
F73	10.64±0.10	6.63±0.13		2.50±0.26	
F98	9.76±0.17	7.08±0.27	3.91±0.10	1.36±0.12	0.00±0.07
F103	9.65±0.12	7.57±0.25[2]	4.66±0.16	2.04±0.25	0.24±0.49
F10	9.74±0.15	7.65±0.11	4.45±0.01	2.34	
F152	8.86	8.14		4.49	
F99[1]	8.84±0.12	8.55		1.69±0.09	
F150[1]	8.66±0.03	5.59±0.02	3.63	0.20±0.23	0.61
F7[1]	8.97±0.02	6.65		2.70	
F151[1]	9.62±0.25	7.30±0.20	2.87	2.18	-1.81±0.10
F149[1]	8.86±0.00	7.05±0.10	4.59	1.89±0.03	-0.09±0.02

[1] 'migmatized'

[2] plagioclase (An_{24})

Errors given as deviation from mean of duplicate analyses

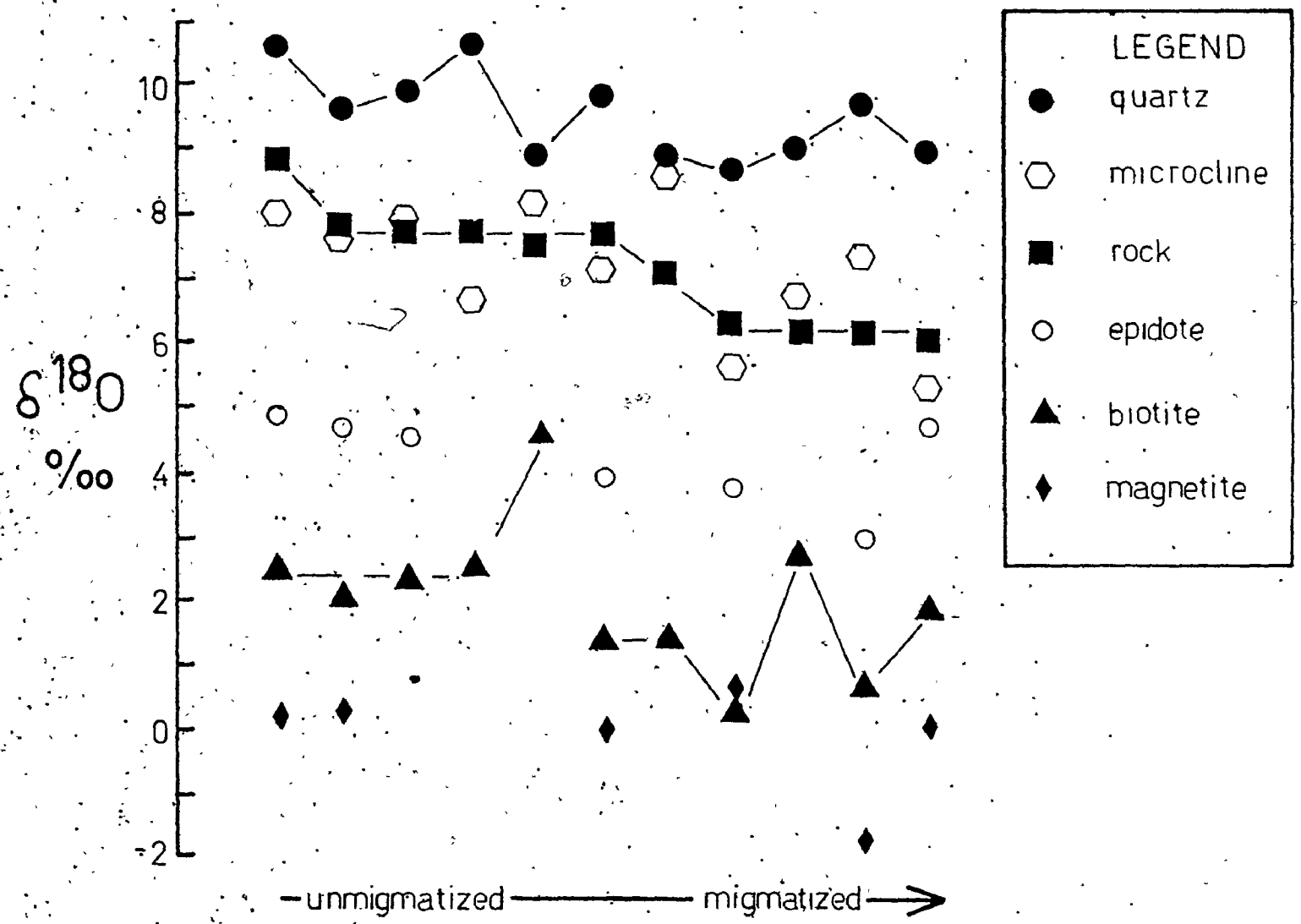

FIGURE 4-3 $\delta^{18}O$ mineral and rock results for the Footprint gneiss. The $\delta^{18}O$ values of migmatized samples are lower than for chemically similar unmigmatized specimens.

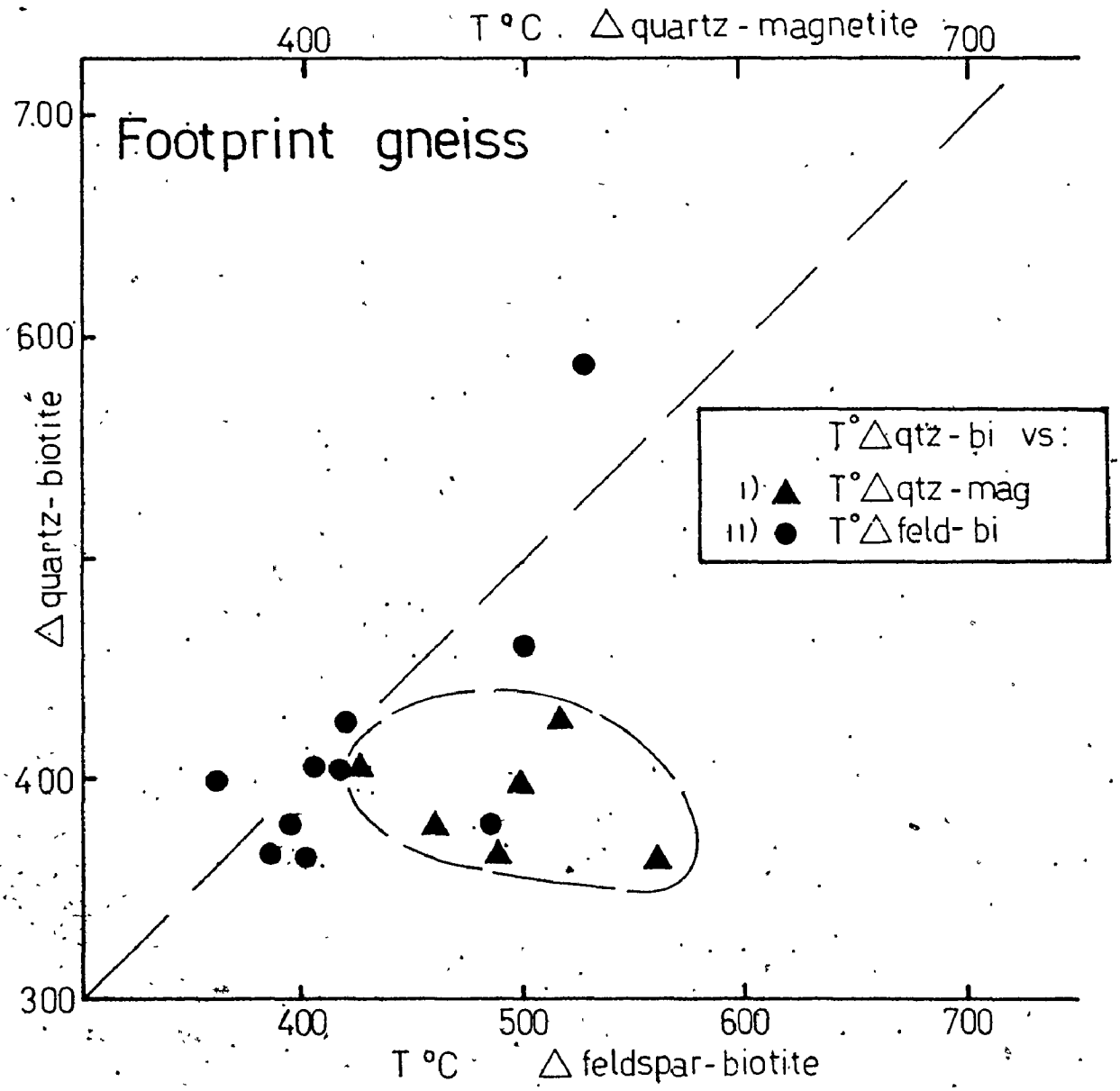

FIGURE 4-4

Oxygen isotope concordancy diagram for the mineral phases from the Footprint gneiss:

The temperatures are given in °C and have been calculated from the indicated mineral pair fractionations using the equations of Bottinga and Javoy (1975)

Such temperatures probably reflect retrograde or external exchange that has affected different minerals differently. Rb/Tl microcline/rock geothermometry also gives low temperatures (500-570°C; Table 4-4; P. Fung, pers. comm.) for these gneisses, similar to those measured from oxygen isotope quartz-magnetite fractionations. Perhaps notably, the migmatized samples have lower Rb/Tl temperatures than unmigmatized gneiss samples.

Microcline

No systematic correlations between oxygen isotope composition, mineral chemistry and triclinicity have been observed for microcline from the Footprint gneiss. The most triclinic microcline, however, does occur at the contact with the Jackfish Lake Complex (F149; Table 4-4). Also, there is a general decrease in Ba and an increase in Rb content of microcline which accompanies the transition from quartz dioritic to granodioritic gneiss (Table 4-5; Figure 4-5). Such a pattern supports the suggestion (section III-9) that the chemical variation in the Footprint gneiss is primary.

Epidote

The isotopic behaviour of epidote in the gneiss is somewhat of a puzzle. It occurs as a metamorphic mineral, mostly

Table 4-4 Footprint gneiss microcline triclinicity and Rb/Tl geothermometry

	microcline triclinicity	T°C (Rb/Tl)*
F150**	0.9001	510
F151**	0.8135	500
F98	0.8913	530
F73	0.9401	570
F110	0.8869	530
F149**	0.9500	-

*P. Fung, analyst; calibration of Rb/Tl geothermometer by P. Fung (Ph.D. thesis, in prep., McMaster Univ.)

**migmatized

Table 4-5 - Mineral analyses for the Footprint gneiss

	Li ppm	Na wt %	K wt %	Rb ppm	Tl ppm	Ca wt %	Sr ppm	Ba ppm	Mg wt %	Fe wt %
F98										
granodioritic gneiss	15	-	1.50	37	0.08	1.97	488	1062	0.62	-
biotite	230	0.27	2.83	148	1.22	1.84	51	743	6.18	13.6
microcline	2	-	9.07	166	0.31	0.27	358	5288	0.03	-
plagioclase	4	4.53	1.47	20	0.18	2.02	660	1164	0.04	-
F151*										
trondhjemitic gneiss	13	-	1.07	38	-	0.16	537	726	0.64	-
biotite	215	0.23	7.23	430	2.97	0.17	-	1520	5.25	17.6
microcline	1	-	9.73	159	0.18	0.26	430	7440	0.01	-
plagioclase	1	3.91	0.41	8	0.08	2.06	647	552	0.01	-
F73										
granodioritic gneiss	14	3.74	1.40	48	0.29	1.79	470	634	0.29	-
biotite	188	0.11	6.87	505	1.91	0.14	6	596	5.63	16.1
microcline	3	1.27	8.73	198	0.82	0.39	408	4059	0.02	-
F150*										
quartz dioritic gneiss	16	2.52	0.75	34	0.25	1.41	582	551	0.32	-
biotite	188	0.14	4.84	262	1.59	0.50	56	1101	5.16	16.7
microcline	2	1.67	12.68	88	0.57	0.56	601	7785	0.02	-
plagioclase	1	4.61	0.39	9	0.12	1.92	843	422	0.02	-
F149*										
granodioritic gneiss	16	3.84	1.10	33	0.25	1.98	540	527	0.41	-
biotite	213	0.17	6.78	368	2.60	0.39	-	1214	5.74	-
plagioclase	2	3.77	0.58	8	0.13	2.54	822	566	0.03	-

Table 4-5 /continued

	Li ppm	Na wt %	K wt %	Rb ppm	Tl ppm	Ca wt %	Sr ppm	Ba ppm	Mg wt %	Fe wt %
F103										
tonalitic gneiss	14	4.14	0.95	34	0.32	2.04	617	433	0.47	-
biotite	172	0.16	5.93	355	1.43	0.15	12	1327	5.87	13.7
F10										
trondhjemitic gneiss	23	3.95	1.13	42	0.25	1.99	556	477	0.44	-
biotite	252	0.20	4.69	254	1.38	0.15	11	858	5.74	11.4
F110										
granitic gneiss	13	-	3.08	114	0.34	1.41	431	1275	0.29	-
biotite	522	0.14	7.78	680	4.96	0.23	-	744	5.40	12.1
microcline	2	-	10.81	339	0.84	0.11	373	4760	0.01	-
plagioclase	11	5.13	1.79	39	0.27	2.09	607	839	0.01	-

* migmatized

Analyses by AAS (P. Fung, analyst)

FIGURE 4-5 Trace element content of microcline (Sr, Rb, Ba) from the Footprint gneiss versus the Modified Larsen Index value for the associated rock

1. quartz dioritic gneiss
2. trondhjemitic gneiss
3. trondhjemitic → granodioritic gneiss
4. granodioritic gneiss
5. granitic gneiss

FIGURE 4-6 Oxygen isotope mineral fractionations for the Footprint gneiss that involve epidote

● migmatized gneiss

■ unmigmatized gneiss

Figure 4-5

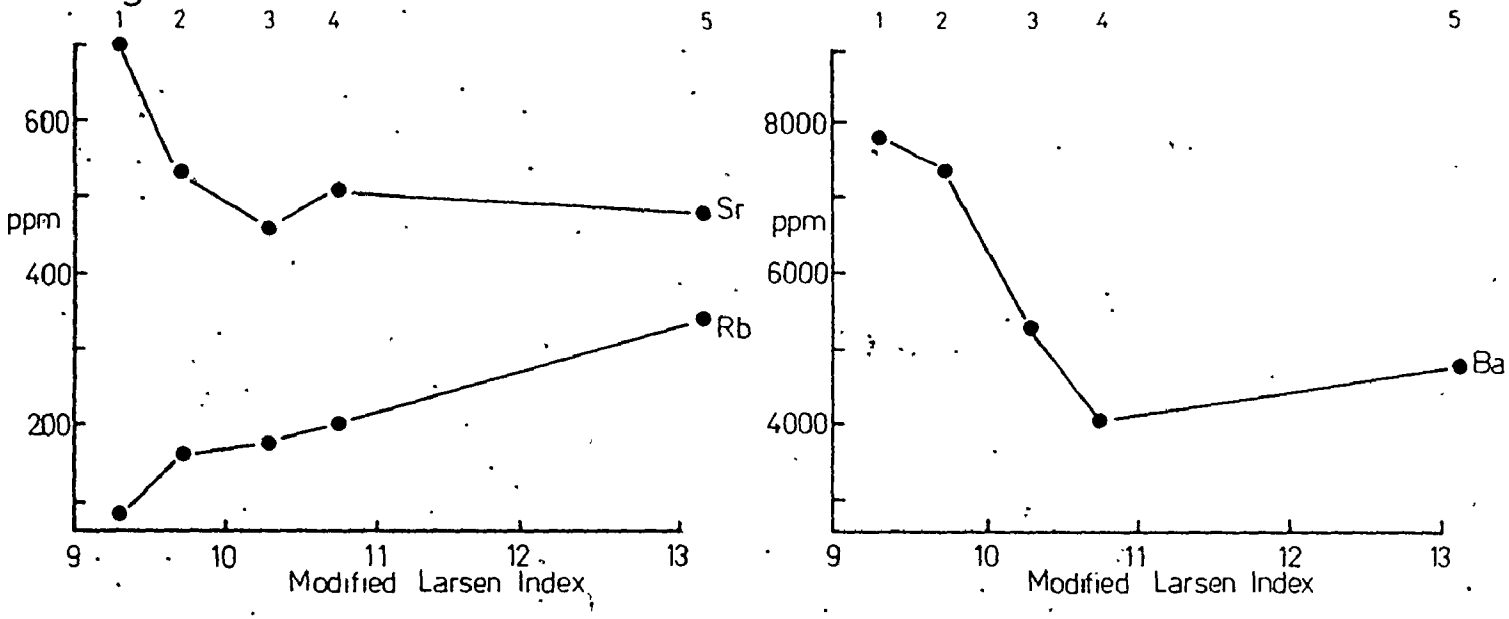

Figure 4-6

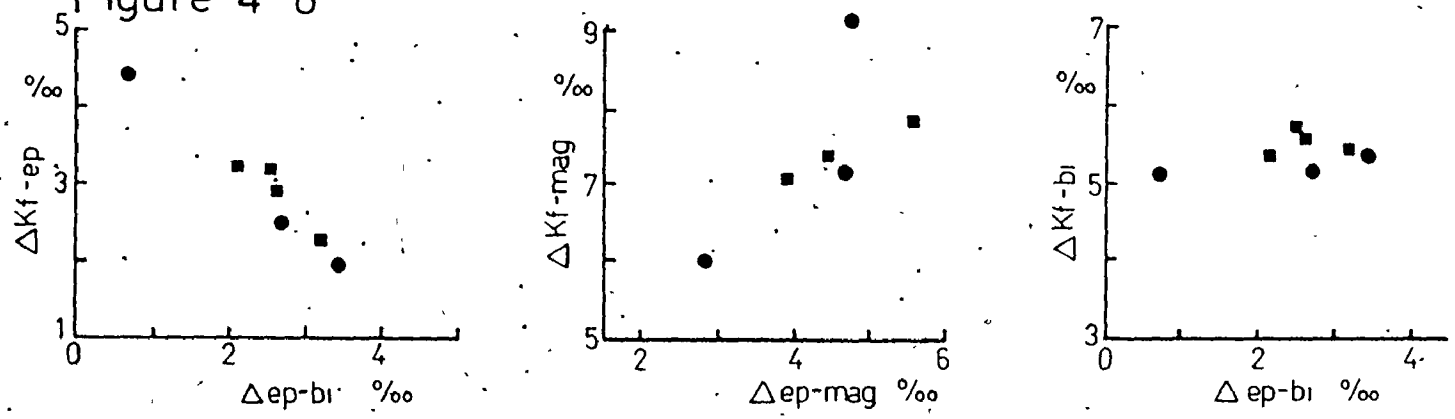

in association with biotite (Appendix III). The $\delta^{18}O$ of epidote tends to decrease along with the $\delta^{18}O$ rock value, but some samples, located closest to the contacts with the Jackfish Lake Complex (migmatized and unmigmatized), have high (4.6-5.7‰) $\delta^{18}O$ epidote values. Also, while microcline-biotite fractionations remain relatively constant (Figure 4-6c), microcline-epidote and epidote-biotite fractionations are inversely correlated (Figure 4-6a) and microcline-magnetite and epidote-magnetite (as well as quartz-magnetite and epidote-magnetite) fractionations show a slight positive correlation (Figure 4-6b). Microcline and biotite are more susceptible to isotopic exchange than magnetite, and, to a lesser extent, quartz (Bottinga and Javoy, 1975; O'Neil et al., 1977); the mixed SiO_4 tetrahedral and AlO_6-$AlO_4(OH)_2$ chain structure of epidote is also probably more resistant to isotopic exchange than microcline or biotite. Thus, the patterns observed in Figure 4-6a,b,c could be produced if epidote, magnetite and quartz retain higher temperature isotopic memories than microcline or biotite.

Biotite

The $\delta^{18}O$ compositions of Footprint gneiss biotite, and biotite from Archean gneisses in general, are of particular

interest because of their depletion in ^{18}O relative to less metamorphosed granitoids of all ages (Figure 4-7; Table 4-6). Biotites from the unmigmatized portions of the Footprint gneiss and the Kenora area gneisses are 2 to 3‰ lower in ^{18}O than Archean and younger granitic rocks. Migmatized samples of Footprint gneiss have still lower $\delta^{18}O$ values.

Many of the low ^{18}O analyses reported in the literature have been attributed to interaction with meteoric water (Table 4-6; Grimstad granite, Coast Ranges batholith, Hiroshima granite). The low $\delta^{18}O$ of the Myoken pluton biotite is associated with magmatic quartz-biotite temperatures. The variation of $\delta^{18}O$ in biotites in the Domenigoni granodiorite is explained by post-solidification, closed system isotopic exchange; according to Turi and Taylor (1971a), the low modal abundance of biotite in this granodiorite causes it to be most affected by any increase in the quartz-biotite isotopic fractionation. Low oxygen isotope quartz-biotite temperatures for the Loon Lake pluton can be attributed to similar processes (Shieh et al., 1976). Hoernes and Friedrichsen (1974) have attributed the low ^{18}O of biotites from Paleozoic prasinites (metagranites) to greenschist facies metamorphism at 420-440°C.

Garlick and Epstein (1967) recognized that biotite usually undergoes isotopic re-equilibration during retrogradation,

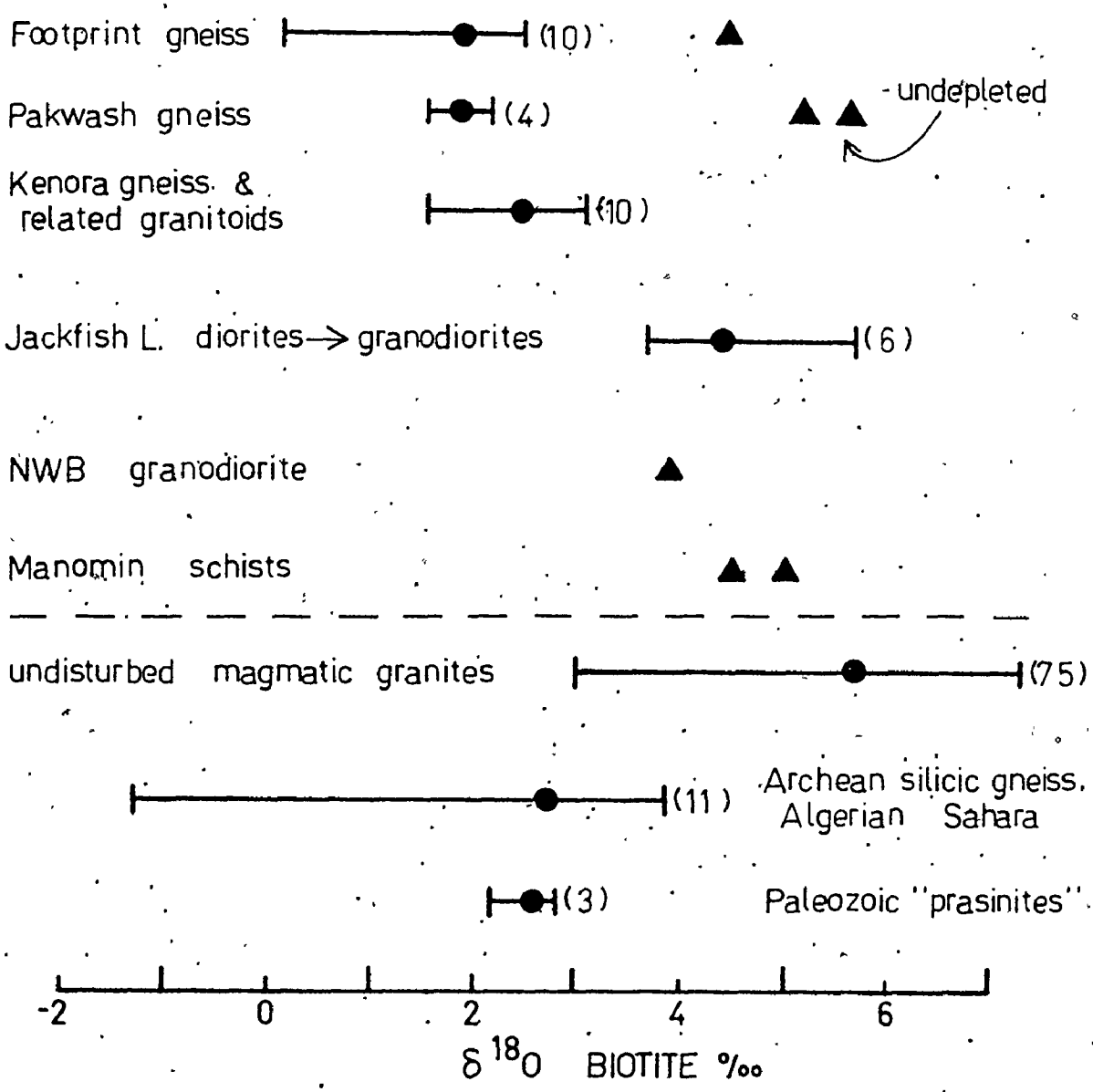

FIGURE 4-7 $\delta^{18}O$ values for biotite.

Those samples plotted below the horizontal dashed line have been compiled from the literature (Table 4-6)

Table 4-6 Oxygen isotope composition of biotite in silicic rocks

Locality	Range °/₀₀	Mean	No. of samples	Reference
Footprint gneiss	0.20-2.52	1.94	10	
Kenora area gneiss and related granitoids	1.59-3.12	2.50	10	
'depleted' Pakwash gneiss	1.63-2.17	1.92	3	
'altered' Pakwash metasediment		2.30	1	
Pakwash white mobilisate		2.10	1	
altered JLC granodiorite		2.00	1	
JLC diorite to granodiorite	3.70-5.70	4.45	6	
'undepleted' Pakwash gneiss	5.20-5.57	5.39	2	
Pakwash pink pegmatite		6.69	1	
NWB granodiorite		3.92	1	
Manomin felsic schists	4.56-5.04	4.80	2	
Pakwash metasandstone		5.11	1	
'anomalous' Footprint gneiss		4.49	1	
Hiroshima and Ryoke granites	4.5 -7.0			Honma & Sakai (1976)
granites-granodiorites	4.3 -6.6	5.3	4	Taylor (1970)
In Ouzzal granulites	3.02-5.21			Fourcade & Javoy (1973)
Nosean granite	3.5 -5.6	5.0	4	Matsuhisa et al. (1973)
Yakutat Bay granitoids	3.2 -7.6	5.1	9	Magaritz & Taylor (1976c)
Tauern Hole:				
metagranitoids	3.3 -6.9	4.6	16	Hoernes & Friedrichsen (1974)
migmatitic gneiss	3.5 -3.9	3.7	3	"
hornblende gneiss		5.3	1	"
felsic volcanics	3.8 -7.8	6.8	6	Bottinga and Javoy (1975)
granitoids	4.4 -9.7	5.6	23	"
gneisses	3.9 -8.1	6.5	10	"
Grimstad granite	1.3 -5.7	3.2	8	Friedrichsen (1971)
Myoken pluton		2.3	1	Matsuhisa et al. (1973a)
Coast Ranges batholith:				
zone II		2.0	1	Magaritz & Taylor (1976b)
zone III	1.5 -2.8	2.3	3	"

Table 4-6 /continued

Locality	Range °/₀₀	Mean	no. of samples	Reference
Reading gneiss		2.5	1	Garlick & Epstein (1967)
Hiroshima granite (HS8)		1.5	1	Honma and Sakai (1976)
Domenigoni granodiorite (G19)	2.6-4.0			Turi and Taylor (1971a)
gneiss (H4)		1.3	1	Hoernes & Friedrichsen (1974)
prasinites	2.2-2.8	2.6	3	"
Archean granitoids	-1.25-3.91	2.75	11	Fourcade (1972)
Grenville migmatite (G4B)		2.6	1	Shieh & Schwarcz (1974)
Grenville gneiss (G19)		2.37	1	"

obliterating the initial isotopic fractionations established at the peak of metamorphism. Bottinga and Javoy (1975) noted that rocks formed at less than 700°C (igneous or metamorphic) usually end up with discordant isotopic temperatures, as equilibrium is not frozen into each mineral phase at the same temperature. Since meteoric water interaction has already been ruled out for these gneisses, variation in the isotopic quenching temperature of mineral phases during metamorphism or autometasomatism is probably responsible for the oxygen isotope composition of the biotite.

Biotite from the Jackfish Lake Complex occurs as a deuteric phase, and, in keeping with its autometasomatic origin, the isotopic temperatures calculated for mineral pairs involving biotite are generally lower than for those pairs which do not involve biotite (Table A1-4A). However, the lowest $\delta^{18}O$ values of these biotites are still higher than found for the gneisses. The oxygen isotope quartz-biotite temperatures preserved in the gneisses and schists are also lower than those preserved in the Jackfish Lake Complex plutonic rocks:

	Range	Mean T°C
Footprint gneiss	365-460°C	400 (10)
Kenora area gneiss	357-431°C	404 (10)
Manomin schists	404-413°C	409 (2)
Pakwash gneiss	376-550°C	430 (6)
Jackfish Lake Complex	440-530°C	500 (5)

Such temperatures have probably resulted from isotopic exchange during retrograde metamorphism down to greenschist facies following the culmination of metamorphism in the amphibolite facies. Because of its hydrous nature, and ease of exchange, biotite probably continued to exchange to lower temperatures than other phases such as quartz, plagioclase and magnetite (O'Neil et al., 1977). It remains unclear, however, why biotite from regionally metamorphosed rocks should isotopically re-equilibrate to lower temperatures than biotite formed during the autometasomatism of plutonic rocks. Grain size may be one possible explanation; the gneisses are much finer grained than the Jackfish Lake Complex granodiorites. The smaller grain size of biotite from the gneiss may encourage isotopic exchange to lower temperatures.

Low ^{18}O Footprint gneiss samples, and the hypothesis of open system isotopic exchange during migmatization

While isotopic re-equilibration during the waning stages of metamorphism can account for the somewhat discordant and low oxygen isotope temperatures of the Footprint gneiss and the generation of low ^{18}O biotites, the low $\delta^{18}O$ values of the migmatized portions of the Footprint gneiss (5.9-7.0‰) relative to unmigmatized portions of equivalent

chemical compositions (7.5-7.8°/$_{oo}$) must still be explained.

A reasonable explanation for this phenomenon is that the gneiss isotopically re-equilibrated at high temperatures with a large mafic (or ultramafic) reservoir, perhaps underlying mafic rocks, by means of fluids present during migmatization.

The equations given by Taylor (1974) to model water/rock interactions (W/R) during meteoric-hydrothermal activity can be used to semi-quantitatively model reservoir/rock ratios (equilibrated via a fluid phase) at various temperatures for given reservoir starting compositions. Given that

(1) $$\frac{W}{R} = \frac{\delta^{18}O\ (rock_f) - \delta^{18}O\ (rock_i)}{\delta^{18}O\ (H_2O_i) - (\delta^{18}O\ (rock_f) - \Delta)}$$ Taylor (1974)

(2) $$\Delta = \delta^{18}O\ (rock_f) - \delta^{18}O\ (H_2O_f);$$ Taylor (1974)

(3) $$\Delta = \frac{2.68\ (10^6)}{T^2} - 3.53;\quad T \text{ in } °K;$$ O'Neil and Taylor (1969) (best suited to tonalites)

where $\delta^{18}O\ (rock_f)$ = final isotopic composition of the rock

$\delta^{18}O\ (rock_i)$ = initial isotopic composition of the rock

and assuming that

(i) $\delta^{18}O$ rock = $\delta^{18}O$ plagioclase.

(ii) $\delta^{18}O_{H_2O_i}$ = initial isotopic composition of the water in exchange equilibrium with the rock,

then hypothetical curves of $\delta^{18}O_{H_2O_i}$ versus W/R can be calculated for a given Δ and temperature. Such a plot for the Footprint gneiss is given in Figure 4-8; Δ for the Footprint gneiss is the difference between average $\delta^{18}O$ values of the migmatized and unmigmatized gneiss samples, and is 1.5°/$_{oo}$.

For reservoir compositions of about 6°/$_{oo}$ (Figure 4-8) to be responsible for the depletion in ^{18}O, temperatures of greater than 650°C are required, and the volume of oxygen in the reservoir must be greater than 2 times that in the gneisses (W/R > 2). The temperature requirement is compatible with that required to begin melting in rocks of tonalitic composition, and the specified W/R ratio suggests that the volume of the reservoir (mafic or ultramafic rocks from the lower crust or upper mantle) is large compared to the volume of the gneisses.

While this hypothesis of ^{18}O depletion during migmatization appears likely, a primary origin for the low ^{18}O of the gneisses (partial melting of mafic rocks at high temperature to form the protolith of the gneiss and preservation of the low $\delta^{18}O$ values during slow cooling and crystallization) cannot be ruled out on the basis of this data alone; data to be presented for the Pakwash paragneiss, however, will help eliminate this latter possibility.

FIGURE 4-8 $\delta^{18}O_{H_2O_i}$ versus W/R diagram for the Pakwash and Footprint gneisses.
The $\delta^{18}O_{H_2O_i}$ values represent possible isotopic compositions of hypothetical oxygen isotope reservoirs. The W/R (water/rock) ratio reflects the relative size of the oxygen isotope reservoir (which controls the isotopic composition of the exchange fluid) to that of the rocks being depleted in ^{18}O.
Note that the isotopic depletions for both the Footprint and Pakwash gneisses require $\delta^{18}O_{H_2O_i}$ values of about 6‰, at W/R > 2, given that this process occurs at high (migmatitic) temperatures (>650°C). The Pakwash gneisses are further discussed in section IV-9.

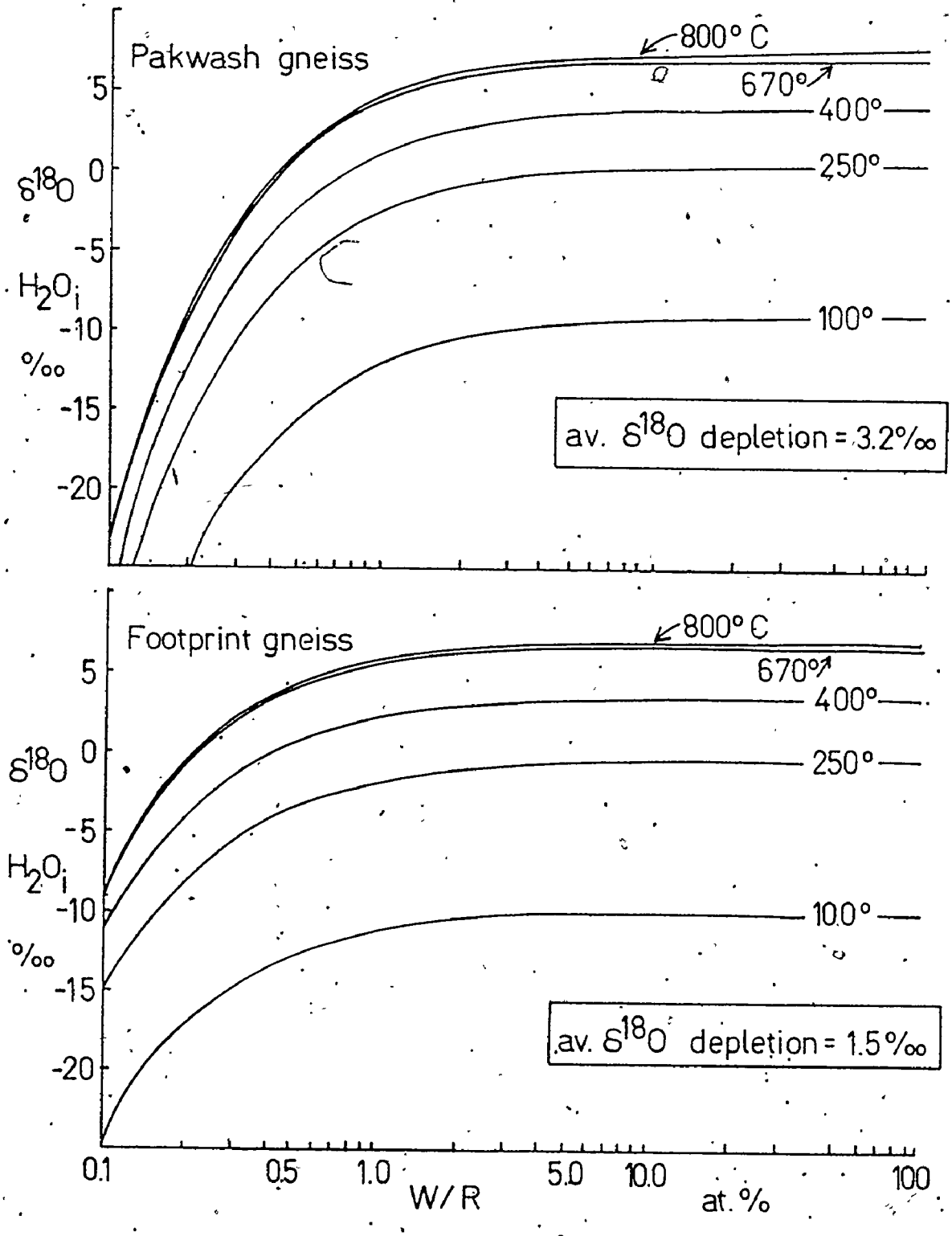
Pakwash gneiss
800° C
670°
400°
250°
100°
$\delta^{18}O_{H_2O_i}$ ‰
5
0
-5
-10
-15
-20
av. $\delta^{18}O$ depletion = 3.2‰
Footprint gneiss
800° C
670°
400°
250°
100°
$\delta^{18}O_{H_2O_i}$ ‰
5
0
-5
-10
-15
-20
av. $\delta^{18}O$ depletion = 1.5‰
0.1
0.5
1.0
W/R
5.0
10.0
at. %
100

IV-7 OXYGEN ISOTOPE GEOCHEMISTRY OF THE KENORA AREA: THE MELICK GNEISS AND RELATED GRANITOIDS

Introduction

The Melick gneiss and related granitoids are contained within a 100 square kilometer area located about 10 km north of Kenora, Ontario (Figure 2-1). The geology and geochemistry of this area have been studied by Gower (1975, 1976; Ph.D. in prep.) and Gower and Clifford (1977). The following details have been drawn from these sources.

The Melick gneiss and related granitoids are located within the predominantly meta-igneous southern portion of the English River gneiss belt (Beakhouse, 1975). The Melick gneiss itself can be subdivided into three major components, granitic pegmatoid gneiss, tonalitic gneiss (including associated leucogranitoids), and amphibolite; these can occur in separate mappable units, but also are commonly intimately interleaved with each other (Gower, 1975, 1976). The granitic pegmatoid gneiss (samples G350B, G886; see Table 4-2 for $\delta^{18}O$ rock of these and subsequent sample numbers) occurs in bands, patches and lenses which vary in width from millimeters to several meters. The rocks contain alkali feldspar megacrysts up to 10 cm in diameter which are enveloped by a coarse grained quartzo-feldspathic matrix.

Gower (1975) interprets these rocks as injection pegmatites. The biotite tonalite gneiss, of average grain size 1 to 2 mm (G106B, G350A), together with the associated leucogranitoids of tonalitic composition (G110A; average grain size of 3 to 4 mm), form a major portion of the Melick gneiss. These rocks vary from well laminated to foliated; lamina width varies from about 2 to several centimeters. The biotite tonalite gneiss commonly contains magnetite and epidote as accessory minerals and also grades into hornblende biotite tonalitic gneiss (G350A) in some localities. In some areas the biotite tonalitic gneiss also contains garnet. The leucogranitoids generally occur in continuous, concordant bands composed almost entirely of quartz and plagioclase, although epidote, biotite, hornblende and sometimes garnet do occur. Gower (1975) regards the biotite tonalite gneiss as one of the earliest, most deformed rocks in the area, and also suggests that the associated leucogranitoids have formed by partial melting of the biotite tonalitic gneiss. The fine grained amphibolite (G867A, G835A) shows subtle banding due to variations in grain size and mafic content, as well as layering resulting from the presence of leuco-tonalite veins, mafic veneers and calcic pods and lenses. In addition, there are irregular blobs of quartz-plagioclase leucogranitoids (G835B) which are completely enclosed by the

amphibolite. Gower (1975) interprets these amphibolites as part of a mafic extrusive sequence which has been subsequently injected by leucogranitoid material. The blob-like leucogranitoids, however, may represent in situ partial melts.

The Melick tonalite (G715, G596A) is a medium to coarse grained granitoid, which, while chemically and mineralogically similar to the Melick gneiss (Figure 4-9), is usually foliated rather than gneissic. Gower (1975) interprets this unit as an originally coarse grained intrusion emplaced into what is now the Melick gneiss.

The Dalles intrusion is composed of moderately foliated, medium grained grey to pink granodiorite (G135), which contains biotite, magnetite and epidote as mafic phases. Medium grained, pink granitic rocks, believed by Gower to be a differentiate of the main phase granodiorite, also occur within the intrusion (G145). The Dalles granodiorite was subsequently intruded by several episodes of tonalitic and pegmatitic dikes, some of which suffered subsequent deformation.

Gower and Clifford (1977) have defined two metamorphic episodes in the Kenora area. The first (M_1) reached uppermost amphibolite facies, under P-T conditions estimated from mineral assemblages of 5.25 kb and 650°C ± 40. The second (M_2) appears to have been retrograde, and to have

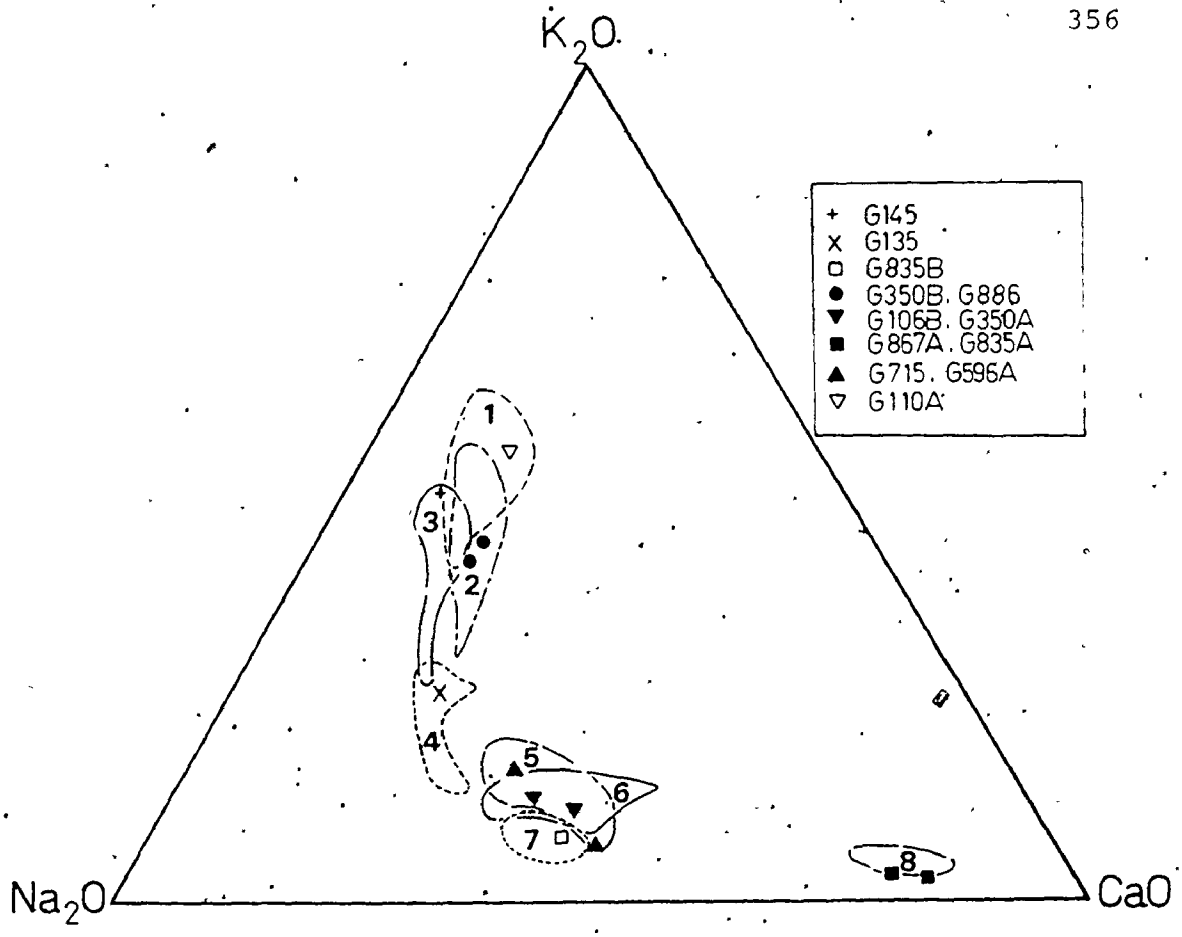

FIGURE 4-9 K_2O-Na_2O-CaO diagram for the Kenora area gneisses and related granitic rocks. The chemical data was provided by C. Gower (written communication). Names are those of Gower.

1. Leucogranitoids associated with the Melick biotite tonalitic gneiss
2. Melick granitic pegmatoid gneiss
3. Dalles pink granite
4. Dalles grey granodiorite
5. Melick tonalite
6. Melick biotite tonalitic gneiss
7. Leucogranitoid associated with the Melick amphibolite
8. Melick amphibolite

occurred under greenschist facies conditions at about 400°C ± 50.

Some of the chemical variation between the rocks of the Kenora area are summarized in Figure 4-9.

Oxygen isotope results

$\delta^{18}O$ results for representative samples of the Melick gneiss and associated metamorphosed plutonic rocks are given in Table 4-2 and shown in Figure 4-2. The location of these samples is given in Gower (1977). As previously noted, the results lie within the I to H_1 groups of Taylor, somewhat lower than most Phanerozoic granitoids (Figure 4-1), but similar to isotopically undepleted lower grade Archean granitoids, as well as unmigmatized portions of the chemically similar Footprint gneiss (Figure 4-2). There are no anomalously high $\delta^{18}O$ values that could indicate a sedimentary or altered metavolcanic protolith, nor are there any 'L' group values that might suggest differentiation at very high temperatures from a mafic source or $\delta^{18}O$ depletion during high grade metamorphism. The close grouping of $\delta^{18}O$ values in the I to H_1 group is most compatible with a plutonic protolith, derived from, or thoroughly equilibrated with a more mafic, less differentiated source than Phanerozoic granitoids.

In general, the coarser grained pegmatoidal material (G350B, G886 and G835B) have higher $\delta^{18}O$ rock values (8.0-8.6°/$_{oo}$) than the finer grained gneisses and metamorphosed granitoids (7.3-8.0°/$_{oo}$). This may reflect the presence of abundant volatiles in the pegmatoids, which promoted oxygen isotope exchange with the country rocks to quite low temperatures, thus causing the quartz and feldspar from the coarse grained pegmatoids to be enriched in ^{18}O.

The finer grained leucogranitoid (G110A), associated with the biotite tonalite gneiss, is chemically similar to the granitic pegmatoid gneiss (Figure 4-9), but has a lower $\delta^{18}O$ rock value (7.4°/$_{oo}$); even the Melick gneiss, from which it has probably formed by partial melting, has higher $\delta^{18}O$ values (7.6-8.0°/$_{oo}$). The Dalles granite (G145; $\delta^{18}O$ of 7.3°/$_{oo}$) is likewise depleted in ^{18}O relative to the granodiorite from which it was presumably differentiated (G135; $\delta^{18}O$ of 7.5°/$_{oo}$). Depletion of ^{18}O can occur in late stage differentiates if the magma was previously impoverished in ^{18}O-rich minerals such as quartz and feldspar, such as described in section III-8 for the Jackfish Lake Complex Na-syenite. Alternatively, post-formation isotopic exchange may have affected these samples; both G110A and G145 contain about 30% microcline (much more than the other analyzed samples), and the microcline from these rocks is low in ^{18}O.

$\delta^{18}O$ mineral results for the Kenora area rocks are given in Table 4-7 and illustrated in Figure 4-10. The results of oxygen isotope geothermometry are given in Table A1-4B and shown in Figure 4-11. Quartz-biotite temperatures range from 360 to 435°C (average of 405°C), similar to Gower and Clifford's (1977) estimate for the M_2 greenschist facies metamorphism. There are no consistent differences between the quartz-biotite temperatures obtained for the Melick gneiss and for the metamorphosed Dalles and Melick intrusions. As mentioned earlier, these temperatures are similar to the quartz-biotite values obtained for the Footprint gneiss, and probably reflect the isotopic quenching of (primarily) biotite near the low temperature end of the retrograde greenschist facies metamorphism. As such, the significance of the quartz-biotite temperature values becomes much less meaningful, as the quartz and biotite are not in mutual isotopic equilibrium.

Quartz-magnetite temperatures were obtained only for the metamorphosed Dalles and Melick intrusions; these temperatures are significantly higher (550-660°C) than the quartz-biotite temperatures (Figure 4-11), a feature also observed for the Footprint gneiss. The quartz-magnetite temperatures are similar to those estimated by Gower and Clifford (1977) for the M_1 metamorphism. Since magnetite is much more

Table 4-7 Oxygen isotope mineral results, Kenora area

	$\delta^{18}O‰$				
	quartz	microcline	hornblende	biotite	magnetite
G106B	10.13±0.25			2.73±0.06	
G110A	10.29±0.08	6.97±0.07		1.59	
G350A	10.50±0.10		5.18±0.12	3.09	
G350B	9.65±0.10	8.42		2.29	
G886	10.46±0.06	7.63		2.20±0.06	
G715	9.94			2.24	3.26
G596A	9.31±0.09	7.54±0.03		2.70±0.25	1.71±0.06
G135	9.73±0.03	7.07		2.70±0.03	1.53±0.19
G145	9.70±0.10	7.07		2.29	3.33
G835B	9.96±0.14			3.12	

Errors given as deviation from mean of duplicate analyses

FIGURE 4-10 $\delta^{18}O$ results for the Kenora area gneisses and related rocks

FIGURE 4-11 Oxygen isotope geothermometry for the Kenora area gneisses and related rocks.

The dashed line represents theoretical temperature concordancy for the plotted mineral pairs. The isotopic temperatures have been calculated from the respective mineral-pair oxygen isotope fractionations by using the equations of Bottinga and Javoy (1975).

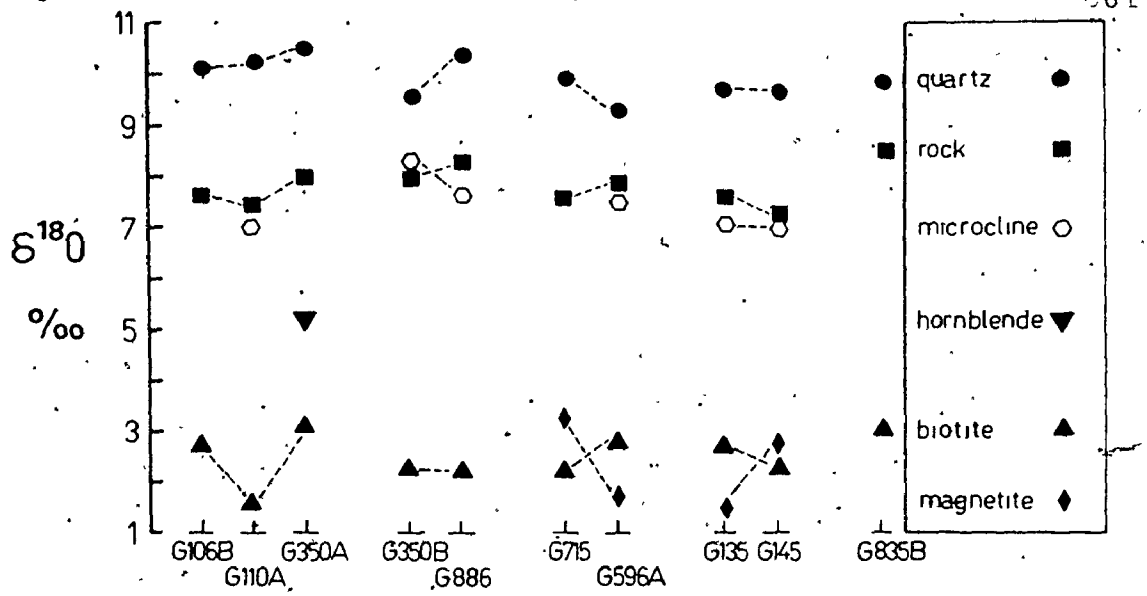
11
9
7
5
3
1
δ18O
‰
quartz
rock
microcline
hornblende
biotite
magnetite
G106B
G110A
G350A
G350B
G886
G715
G596A
G135
G145
G835B

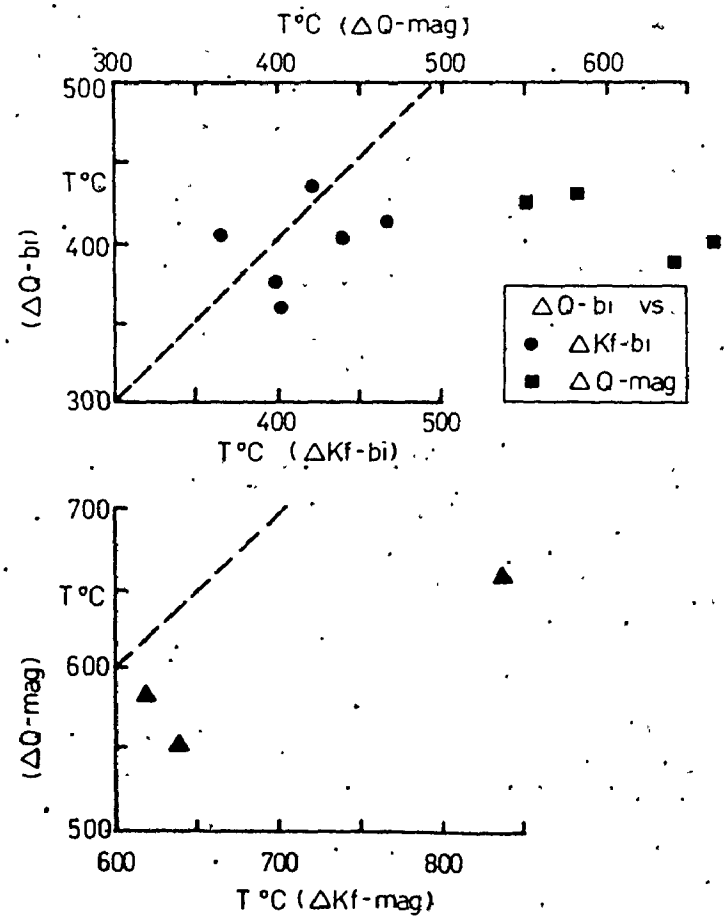
T°C (ΔQ-mag)
300
400
500
600
T°C
(ΔQ-bi)
ΔQ-bi vs.
ΔKf-bi
ΔQ-mag
T°C (ΔKf-bi)
700
T°C
(ΔQ-mag)
800
T°C (ΔKf-mag)

resistant to isotopic exchange than biotite, the quartz-magnetite temperatures probably reflect rock temperatures existing shortly after the culmination of amphibolite facies metamorphism, thus providing a minimum temperature estimate of the M_1 episode.

This hierarchy of isotopic quenching "temperatures" following the culmination of metamorphism can explain other isotopic features of these granitoids. Firstly, the quartz-hornblende "temperature" determined for G350A (475°C), as well as the plagioclase-hornblende "temperature" obtained for amphibolite G867A (455°C) lie between "temperatures" preserved using biotite and magnetite. Hornblende does appear to isotopically exchange less readily than biotite (see section III-8., Figure 3-28), but, because of the presence of an 'OH' radical, is more susceptible to isotopic modification than magnetite. Thus, progressively lower apparent isotopic "temperatures" should be preserved in quartz-magnetite, quartz-amphibole and quartz-biotite pairs during retrograde metamorphism. This is probably also the case during deuteric activity; quartz-hornblende apparent "temperatures" for the Jackfish Lake Complex granodiorite are generally higher than quartz-biotite "temperatures" (Table A1-4A; Figure 3-46). Secondly, the reversal in position of magnetite and biotite in the $\delta^{18}O$ series in

samples G715, G145, and Footprint gneiss F150 (Figure 4-10, Figure 4-3) can be explained by continuous isotopic exchange of the biotite to a much lower temperature than the magnetite. The relatively normal quartz-magnetite fractionation, on the other hand, shows that the isotopic composition of quartz has probably not changed much during the retrogradation episode.

While the quartz-biotite "temperatures" preserved in the Kenora area rocks are very similar to those from the Footprint gneiss, quartz-magnetite temperatures (mean of 610°C) from the former area are higher than observed for the latter (mean of 490°C). This suggests that the culmination of metamorphism occurred at a higher temperature in the Kenora area; alternatively, there may have been a longer period of retrograde metamorphism (slower cooling) in the Footprint gneiss, which allowed greater re-equilibration of the magnetite. A third possibility is a variation in grain size; magnetite from the Footprint gneiss is finer grained than that of the Melick and Dalles metaplutonic rocks; this would facilitate greater amounts of isotopic exchange in the finer grained material.

Isotopic behaviour of microcline

Microcline is out of isotopic equilibrium with many of the other mineral phases in the Kenora rocks, an observation also valid for the Footprint gneiss. Microcline-biotite "temperatures" are higher (415°C for both the Kenora area and the Footprint gneiss) than the quartz-biotite "temperatures" from the respective areas; microcline-magnetite "temperatures" are likewise higher than the respective quartz-magnetite temperatures (see Tables A1-4A,B; Figures 4-11 and 4-4). This results from the somewhat low $\delta^{18}O$ values of microcline in these rocks. $\delta^{18}O$ values for microcline separated from G110A, G135 and G145 are 6.97, 7.07 and 7.07°/$_{oo}$, respectively; values as low as 6.63°/$_{oo}$ are found for microclines from the Footprint gneiss in unmigmatized samples.

Any explanation for the low ^{18}O microclines requires exchange with a low ^{18}O reservoir at temperatures low enough not to affect biotite (less than 400°C), and on a scale small enough so as not to greatly deplete the bulk $\delta^{18}O$ composition of the rock. The process must also be selective, as not all samples are affected. Magaritz and Taylor (1976b) note that microcline is the most susceptible to meteoric-hydrothermal alteration of all the major rock forming minerals; such activity at low temperatures (250-350°C) and at very low water/rock ratios (much less than 0.01) could be responsible

for the depletion of the microcline, without being the cause of the overall large scale depletions in ^{18}O. However, the $\delta^{18}O$ values of the microcline are very uniform, unlike that expected if meteoric water interaction had been involved. Perhaps, instead, especially in the case of the very late differentiates, the microcline was precipitated late from a residual fluid already depleted in ^{18}O by the previous crystallization of quartz and plagioclase. None of these explanations is very satisfactory, and further investigations are required.

IV-8 OXYGEN ISOTOPE GEOCHEMISTRY OF THE CEDAR LAKE - CLAY LAKE AREA

Introduction

The Cedar Lake - Clay Lake area occupies about 270 square kilometers about 30 km northwest of Vermilion Bay, Ontario, and straddles highway 105 (latitude 50°10'N; longitude 93°15'N; NTS 52K, SW; Figure 2-1). The area lies within the predominantly plutonic southern portion of the English River gneiss belt. Westerman (1973, 1975, 1977) has recently completed a geological and geochemical study of the area; the Ontario Division of Mines has also conducted recent mapping in the area, the results of which are summarized

in Breaks and Bond (1977) and Breaks et al. (1975). The geological details outlined here have been drawn from the work of Westerman (1977).

Westerman has defined three major units of interest to us, the amphibolite facies Cedar Lake gneiss, the granulite facies Clay Lake gneiss, and the granulite facies Twilight gneiss.

The Cedar Lake gneiss (samples 432, 24, 62, 350, 560; Table 4-2) is an interlaminated assemblage of deformed granitic to amphibolitic rocks which have undergone at least three stages of deformation. Westerman suggests that the most likely protolith for the felsic portions of the gneiss (which were analyzed in this study) is an intrusive granitoid. It ranges in SiO_2 from 70 to 75 wt. % and has Al_2O_3 contents of less than 15 wt. % (13.8-14.8 wt. %); these rocks follow a normal calc-alkaline differentiation trend (Figure 4-12). Westerman regards the Cedar Lake gneiss as a basement unit, which either intruded through a mafic metavolcanic cover or else was reactivated during metamorphism and deformation and subsequently tectonically interleaved with a mafic metavolcanic cover.

The Clay Lake gneiss is a calc-alkaline suite of granitoid intrusive rocks which ranges in composition from biotite tonalite to leucocratic alaskitic granite (Figure 4-12).

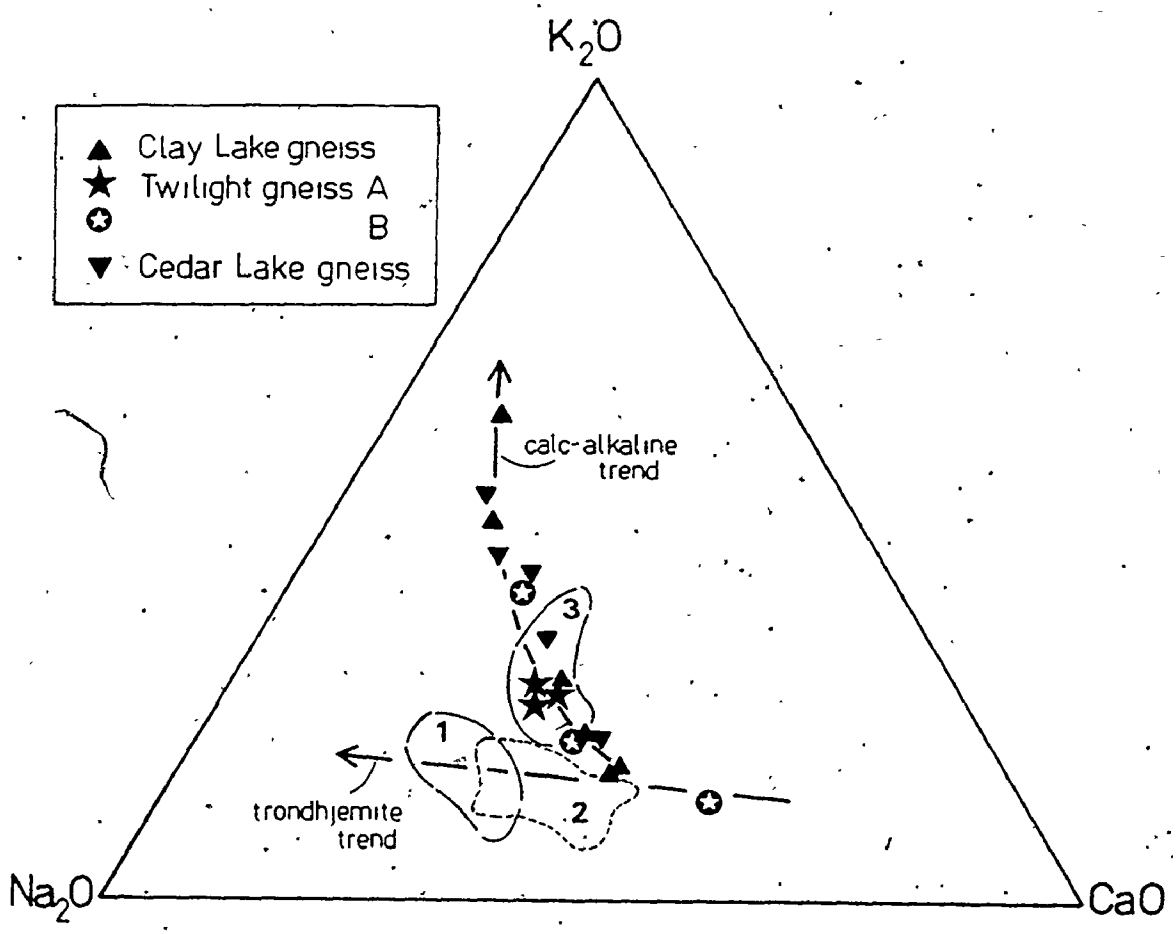

FIGURE 4-12 K_2O-Na_2O-CaO diagram for the Cedar Lake - Clay Lake area. The chemical data was provided by C. Westerman (written communication).

1. Footprint gneiss and migmatite
2. Melick gneiss (Kenora area)
3. Pakwash gneiss

It intruded the Cedar Lake gneiss prior to the third period of deformation, and was subsequently metamorphosed to granulite facies. The rocks produced include enderbites (513A, 433, 553) that contain retrograde biotite in addition to hypersthene and magnetite (SiO_2 of 66-69 wt. %; Al_2O_3 of 15.7-16.1 wt.%) and garnetiferous alaskites (SiO_2 of 70-74 wt. %; Al_2O_3 of 14.4-15.4 wt. %). Westerman suggests that the present concordance of the chemically different units resulted from either emplacement as sheets during the waning stages of the second deformational episode, or by strong flattening accompanying the third period of deformation.

The Twilight gneiss has been subdivided into two groups; group A samples (309, 377, 535) are believed derived from a predominantly clastic metasedimentary protolith similar to that of the paragneisses from the northern portion of the English River gneiss belt; group B rocks are coarser grained, more massive and less voluminous than group A, and Westerman suggests ash fall tuff or fine grained pyroclastic debris, possibly reworked by sedimentary processes, as their most likely protolith.

Chemically, the group A Twilight gneisses are similar to the Pakwash gneisses (Figure 4-12; section IV-9; SiO_2: 62-65 wt. %; Al_2O_3: 15.9-16.8 wt. %). A Dennen and Moore plot (Figure 4-13) shows that the Cedar Lake gneiss, the Clay

FIGURE 4-13 Normalized Si versus Al/Fe diagram for some Archean gneisses.

The field for chemically mature clastic sediments is from Dennen and Moore (1971).

→ indicates Al/Fe > 10

FIGURE 4-14 Discriminant Function (D.F.) versus $\delta^{18}O$ diagram for some Archean gneisses.

The discriminant function is from Shaw (1972). The legend is as in Figure 4-13. L43 is an anatectic pegmatoid derived from partial melting of the Pakwash gneiss metagreywacke or metapelite layers.

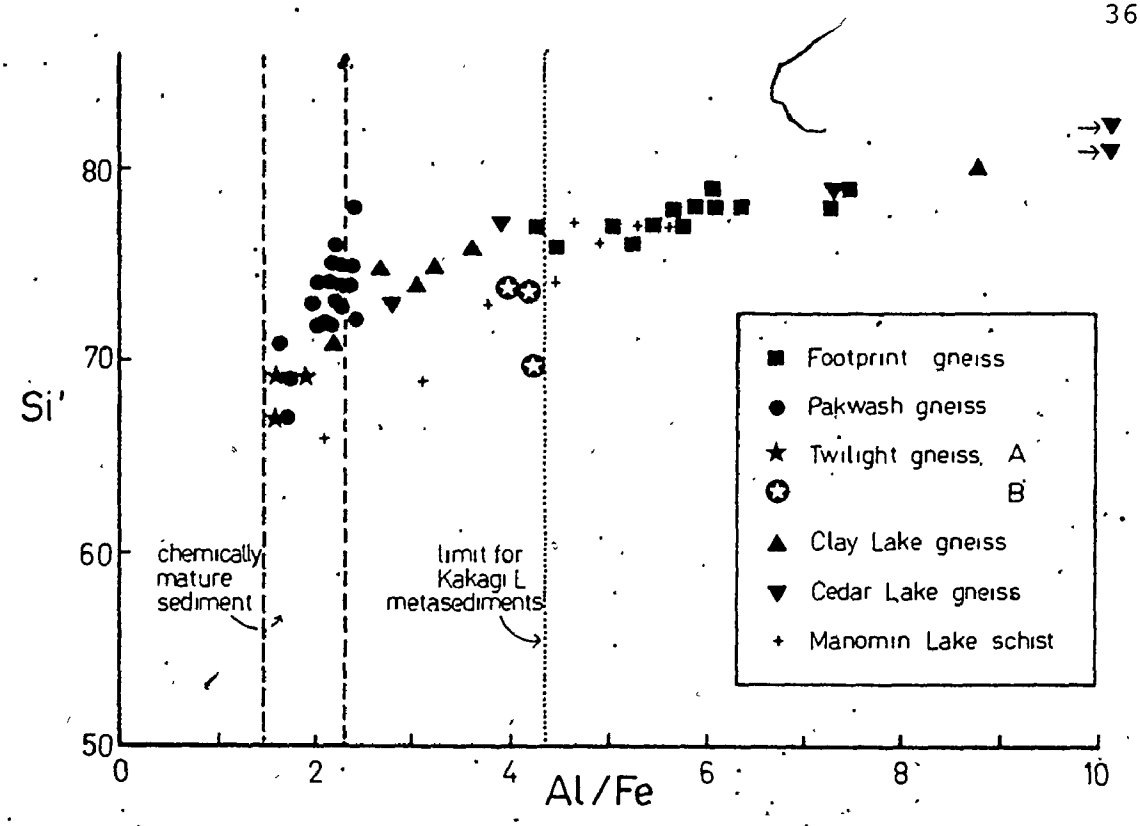
80
70
60
50
Si'
0
2
4
6
8
10
Al/Fe
chemically mature sediment
limit for Kakagi L metasediments
Footprint gneiss
Pakwash gneiss
Twilight gneiss, A
B
Clay Lake gneiss
Cedar Lake gneiss
Manomin Lake schist

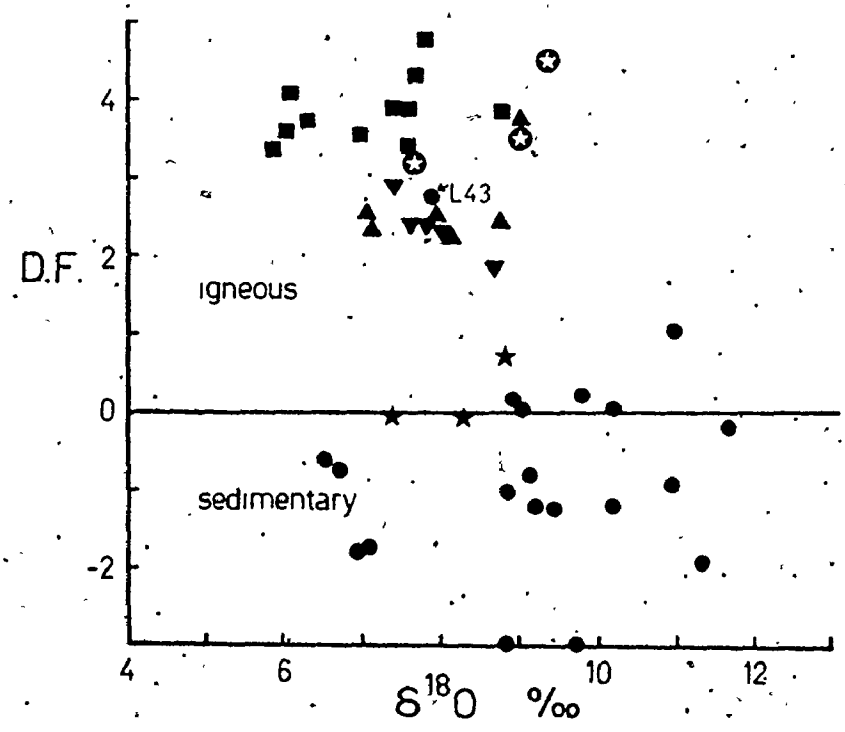
4
2
0
-2
D.F.
igneous
sedimentary
L43
4
6
10
12
δ18O ‰

Lake gneiss, the group B Twilight gneiss, as well as the Footprint gneiss and most of the Burditt Lake felsic metavolcanics, plot outside the field of chemically mature clastic metasediments. The Kenora area granitoids (not shown in Figure 4-13) also lie outside this field. The only gneisses contained within this field are the Twilight A group and Pakwash rocks.

The group B Twilight gneisses (378, 448, 538) are more siliceous than group A (SiO_2: 64-68 wt. %; Al_2O_3: 16.6-19.0 wt. %), and do not fall within the sedimentary field on Figure 4-13. They do lie within the limits found for the very immature Kakagi Lake metagreywackes (Figure 2-7a), although so also do the Clay Lake and some of the Cedar Lake gneisses. The interlayered nature of the group A and B Twilight gneiss, as well as their gradational boundaries with each other, tends to suggest a supracrustal origin for the group B rocks.

The discriminant function of Shaw (1972) groups the Twilight A gneisses together with the Pakwash gneiss, separately from the Footprint, Clay Lake, Cedar Lake, or B group Twilight gneisses (Figure 4-14). These latter rocks have highly positive igneous discriminant function values. The dioritic rocks of the Jackfish Lake Complex, which overlap the sedimentary field on the Dennen and Moore diagram

(Figure 2-7b), also have positive D.F. values (0.6-11.5; mean of 5.4); clearly, Shaw's discriminant function does not suffer from the same flaw as that of Dennen and Moore. However, very immature clastic metasedimentary rocks can have D.F. values greater than 0 (Figure 2-21). Thus, while the sedimentary protolith of the group A Twilight gneiss is confirmed by these tests, the meta-igneous or metasedimentary nature of the group B supracrustal rocks remains uncertain.

According to Westerman, the Twilight gneisses postdate the Clay Lake and Cedar Lake gneisses, but underwent severe flattening early in their history. They were than metamorphosed (but not migmatized) to granulite facies. Since the Twilight gneiss is presently at a lower structural level than the Cedar Lake or Clay Lake gneisses, Westerman suggests that subhorizontal thrusting, or recumbent nappe formation, depressed the southern portion of the Cedar Lake - Clay Lake area (which contains the Twilight and Clay Lake gneisses) into higher temperature and pressure regimes, thus causing much of the late deformation, as well as the granulite facies metamorphism.

Oxygen isotope results

The $\delta^{18}O$ rock results for the Cedar Lake - Clay Lake area are given in Table 4-2 and shown in Figures 4-2 and 4-15.

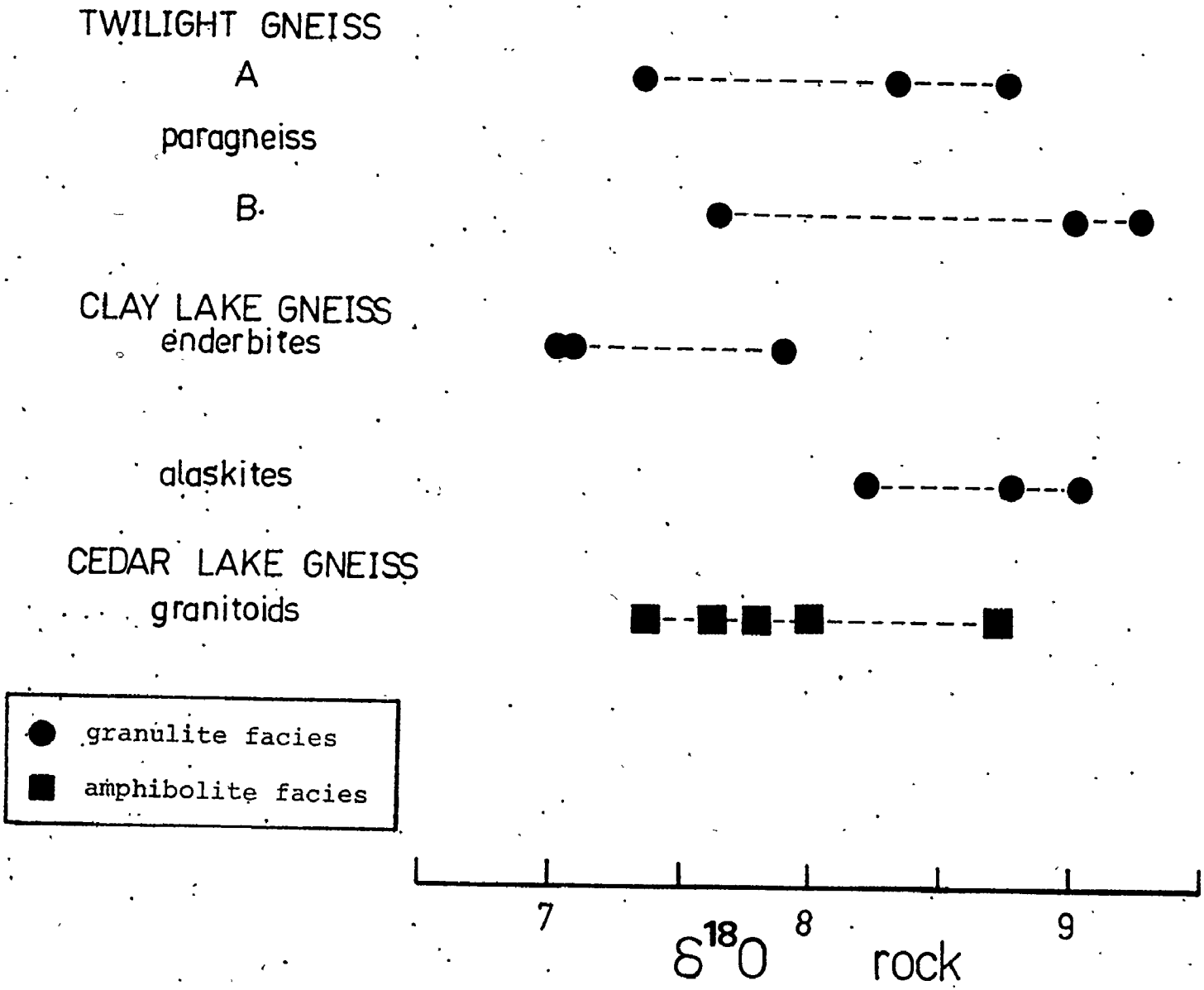

FIGURE 4-15 $\delta^{18}O$ rock values for gneisses from the Cedar Lake - Clay Lake area.

All units have $\delta^{18}O$ values between 7.0 and 9.3°/$_{oo}$, similar to the other isotopically undepleted Archean granitoids and meta-igneous gneisses analyzed in this study (Figure 4-2). Sample locations are given in Westerman (1977).

The granulite facies Clay Lake enderbites are about 1°/$_{oo}$ lower in $\delta^{18}O$ than the interlayered alaskites (Figure 4-15). This probably reflects primary compositional differences between the two units.

The granulite facies Twilight gneiss groups A and B show similar ranges in $\delta^{18}O$ (Figure 4-15). If group A was derived from chemically mature clastic metasedimentary rocks, they have been depleted in $\delta^{18}O$ by 1 to 3°/$_{oo}$. They certainly have lower $\delta^{18}O$ values than most of the chemically similar Pakwash gneiss samples (Figure 4-14; Figure 4-2). The group B gneisses have $\delta^{18}O$ values which are compatible with both a felsic metavolcanic origin and an immature clastic metasedimentary protolith. However, if the group A gneisses have been isotopically depleted, the intimately interlayered, granulite facies group B gneisses should have also been depleted by about 1 to 3°/$_{oo}$ from their protolith compositions. It is more likely that both have re-equilibrated during granulite facies metamorphism with some reservoir, but that the group B gneisses were already in equilibrium with this hypothetical unit before the exchange began. This implies

that the isotopic composition of the reservoir was about 7-9°/$_{oo}$.

It is unlikely that the Twilight gneiss re-equilibrated with a mafic reservoir, such as basalt, as no isotopic values less than 7.0°/$_{oo}$ were measured. This is in contrast to the behaviour of migmatized portions of the Footprint and Pakwash gneisses, which have samples in the $\delta^{18}O$ range of 6.0 to 6.5°/$_{oo}$. An alternative and mechanistically simpler explanation for the smaller depletion observed for the Twilight 'A' group gneiss is that the sedimentary gneiss (mean $\delta^{18}O$ of 8.4°/$_{oo}$; range of 7.3-9.3°/$_{oo}$) underwent isotopic exchange with the surrounding volumetrically more important meta-igneous rocks in the area (mean $\delta^{18}O$ of 8.0°/$_{oo}$) during amphibolite and granulite facies metamorphism. Westerman notes that the granulitic rocks are not depleted in LIL elements; chemical and isotopic exchange of the granulite facies metasedimentary gneisses with material of similar LIL element concentration (tonalites) is compatible with this observation.

There is an important point to be made here concerning the use of oxygen isotopes in protolith determinations for gneissic rocks. Comparison of whole rock isotopic compositions from the middle amphibolite facies Pakwash paragneiss (undepleted portions: 8.8-11.7°/$_{oo}$) with the amphibolite

to granulite facies Twilight gneiss (7.3-9.2°/$_{oo}$) shows that at metamorphic grades higher than middle amphibolite facies, Archean metasedimentary gneisses may have $\delta^{18}O$ rock compositions similar to Archean orthogneisses, and are therefore no longer isotopically recognizable as metasedimentary rocks (Figure 4-2; Longstaffe and Schwarcz, 1977).

IV-9 OXYGEN ISOTOPE GEOCHEMISTRY OF THE PAKWASH GNEISS

Introduction

The Pakwash gneiss is located near Pakwash Lake, about 45 km southeast of Red Lake, Ontario (Figure 2-1), within the northern metasedimentary portion of the English River gneiss belt. The presence of migmatized metasedimentary rocks in this area has been long recognized (Dyer, 1933). A number of recent investigations (Dwibidi, 1966; McRitchie and Weber, 1971; McRitchie, 1971; Fruend and Turnock, 1971; Breaks et al., 1974, 1975; Beakhouse, 1974a,b, 1975, 1976, 1977; Breaks and Bond, 1977) have been concerned with the relationship of these rocks to the Uchi granite-greenstone belt to the north, and the meta-igneous rocks of the southern portion of the English River gneiss belt.

The Pakwash gneisses are composed of plagioclase,

quartz, biotite, garnet, and sometimes muscovite, sillimanite, magnetite and cordierite. Variations in biotite and garnet contents help to define a primary layering (average thickness: 5-30 cm) which Beakhouse (1974b) interprets as an interlayered sequence of metagreywacke, shaley metagreywacke and lesser amounts of meta-argillite. Most sedimentary structures are not well preserved. However, Beakhouse (1977) notes that bedding, as defined by mineralogic and textural variations, is continuous, and that slump structures, graded bedding, and small scale cross-laminations have been observed. He regards the Pakwash gneisses as part of a major sedimentary basin with most of the detritus deposited as turbidites.

Sediment source

Beakhouse (1974b, 1975) feels that some of the detritus was derived from synchronous Uchi belt mafic to felsic volcanism, but also stresses the importance of a component derived from acid rocks, such as an uplifted Winnipeg River batholithic belt to the south, or surfacing granodioritic plutons to the north. Breaks and Bond (1977) also believe that Uchi belt volcanism and English River gneiss belt sedimentation were contemporaneous; in some areas, they have observed a continuous transition from Uchi metavolcanics to the English River metasedimentary gneisses.

Certain trace element parameters support the hypothesis of a mixed source for the metagreywacke paleosome of the Pakwash gneiss. Breaks and Bond (1977) reported high average Cr (177 ppm), V (77 ppm), and Ni (37 ppm) contents for these rocks that are indicative of a significant mafic component in the sediment detritus. Beakhouse (pers. comm.) also reports high Ni contents in the metagreywacke layers of the gneiss. One Ni determination for the metagreywacke paleosome performed in this study (L37; 54 ppm) also supports such an interpretation.

The Uchi belt metadacites from the Pakwash Lake area (and elsewhere) are much lower in Ni (L32, L35; 11-18 ppm) than the metagreywacke layers of the Pakwash gneiss. The metadacites may, however, be the source of the felsic component in the metagreywacke paleosome (Table 4-8); the Pakwash paragneiss metagreywacke layers are relatively enriched in Rb, Sr, Ba, Ce and Zr.

Table 4-8 Trace element contents of the Pakwash gneiss metagreywacke layers and related rock types from the Uchi belt

	Pakwash gneiss		Uchi granite-greenstone belt	
	amphibolite facies		greenschist facies	
	metagreywacke	metapelite	metagreywacke	metadacite
Rb	74-109	105	77	80-84
Sr	255-399	196	369	396-475
Ba	220-620	326	654	438-560
Zr	103-169	118	127	136-158
Ce	34-68	36	44	53-78
No. of analyses	6	1	1	2

Metamorphism and partial melting

The Pakwash gneiss has been metamorphosed to middle to upper amphibolite facies, and has been migmatized and partially melted. The amount of mobilisate varies, but averages about 15% (Beakhouse, 1977). Krogh et al. (1975) have dated the migmatization episode at 2.68 ± 0.20 b.y.

Breaks and Bond (1977) have classified these metasedimentary gneisses and migmatites into four groups; in order of increasing degree of migmatization these are:

	leucosome/paleosome
1. protometatexite	<0.1
2. metatexite	0.1-0.6
3. inhomogeneous diatexite	0.6-0.9
4. diatexite	>0.9

The protometatexite contains mobilisate (leucosome) which is confined to lenses and pods in pelitic layers. Most of the 'P' series samples (see Table 4-2) fit into this group. The metatexites, which, on outcrop scale are the most common migmatite type, are characterized by stromatic banding caused by the interlayering of metagreywacke paleosome with the now continuous mobilisate (leucosome). Some leucosome is also injected discordantly into the paleosome. Samples

L40, L44A, L44B, L45A and L45B fit into this group (Table 4-2). The inhomogeneous and homogeneous diatexites represent progressively higher degrees of partial melting, to the extent that the migmatitic banding is destroyed. These have not been analyzed in this study, but further investigations are underway.

Both the pelitic and greywacke layers of the gneiss may act as paleosomes (Breaks and Bond, 1977), but the latter is much more common than the former, and has been concentrated upon in this study. Major element compositions of the two paleosomes, as well as the mobilisate, are given in Table 4-9. The results obtained from this and other studies are reasonably similar, given the wide range in chemical composition between individual samples and the small number of samples analyzed. The major element chemistry of the metagreywacke paleosome is not dissimilar to that of the Archean metagreywackes discussed in Chapter II (Figure 4-16), or the Uchi granite-greenstone belt metadacites (Table 4-9, #8), located just north of the Pakwash gneiss. The metagreywacke paleosome lies within the field of chemically mature metasediments (Figure 4-4) and has discriminant function values of near to or less than zero (Shaw, 1972; Figure 4-14).

The mobilisate (leucosome) varies from medium grained to pegmatoidal, is leucocratic and generally white (L43),

Table 4-9 Major element composition, Pakwash gneiss

	1	1a	2	3	4	5	6	7	8
SiO_2	69.3	67.9	67.9	67.1	60.3	59.2	72.3	67.5	67.2
Al_2O_3	14.8	15.0	15.3	16.1	17.2	19.6	15.8	14.5	15.3
TiO_2	0.52	0.49	0.60	0.90	0.71	0.85	0.04	0.52	0.51
Fe_2O_3*	5.27	5.31	5.53	5.68	12.3	9.20	0.67	5.29	4.45
MnO	0.05	0.09	0.09	0.08	0.18	0.08	0.03	0.08	0.12
MgO	2.15	2.16	2.29	2.69	3.44	3.79	0.35	2.77	1.61
CaO	2.50	2.82	3.07	3.27	1.73	1.31	1.10	3.30	3.78
Na_2O	3.26	4.06	3.15	2.23	1.92	2.08	2.61	4.11	4.57
K_2O	2.05	2.08	1.88	1.83	2.12	3.86	6.94	1.75	2.37
P_2O_5	0.10	0.06	0.16	0.12	0.11	0.12	0.17	0.12	0.12

* Total Fe as Fe_2O_3; all analyses recalculated to 100%, anhydrous.

1. Average 6 metagreywacke layers, Pakwash gneiss (L37, L40, L42, L44B, L45B, L45C), this study

1a. Greenschist facies metagreywacke (L30); Pakwash Lake; Uchi greenstone belt

2. Average 11 metagreywacke layers, Pakwash gneiss (Beakhouse, pers. comm.; sample numbers given in Table).

3. Average 21 greywacke paleosome, northern portion of English River gneiss belt (Breaks and Bond, 1977)

4. Pelitic paleosome (L45A), Pakwash gneiss

5. Average 15 pelitic paleosome, northern portion of English River gneiss belt (Breaks and Bond, 1977)

6. White pegmatoid mobilisate, Pakwash gneiss (L43)

7. Weight average of 32 greenschist facies metagreywackes from Upper Manitou Lake, Kirkland Lake and Kakagi Lake

8. Average 2 metadacites, Pakwash Lake, Uchi Lake greenstone belt (L32, L35)

FIGURE 4-16 Mesonorm plot for the Pakwash gneiss and greenschist facies metagreywackes.

Some of the chemical data for the Pakwash gneisses were provided by Beakhouse (written communication).

+ Pakwash gneiss metagreywacke layer

▲ Pakwash gneiss metapelite layer

■ Pakwash gneiss leucosome (white mobilisate)

● Archean greenschist facies metagreywackes analyzed during this study

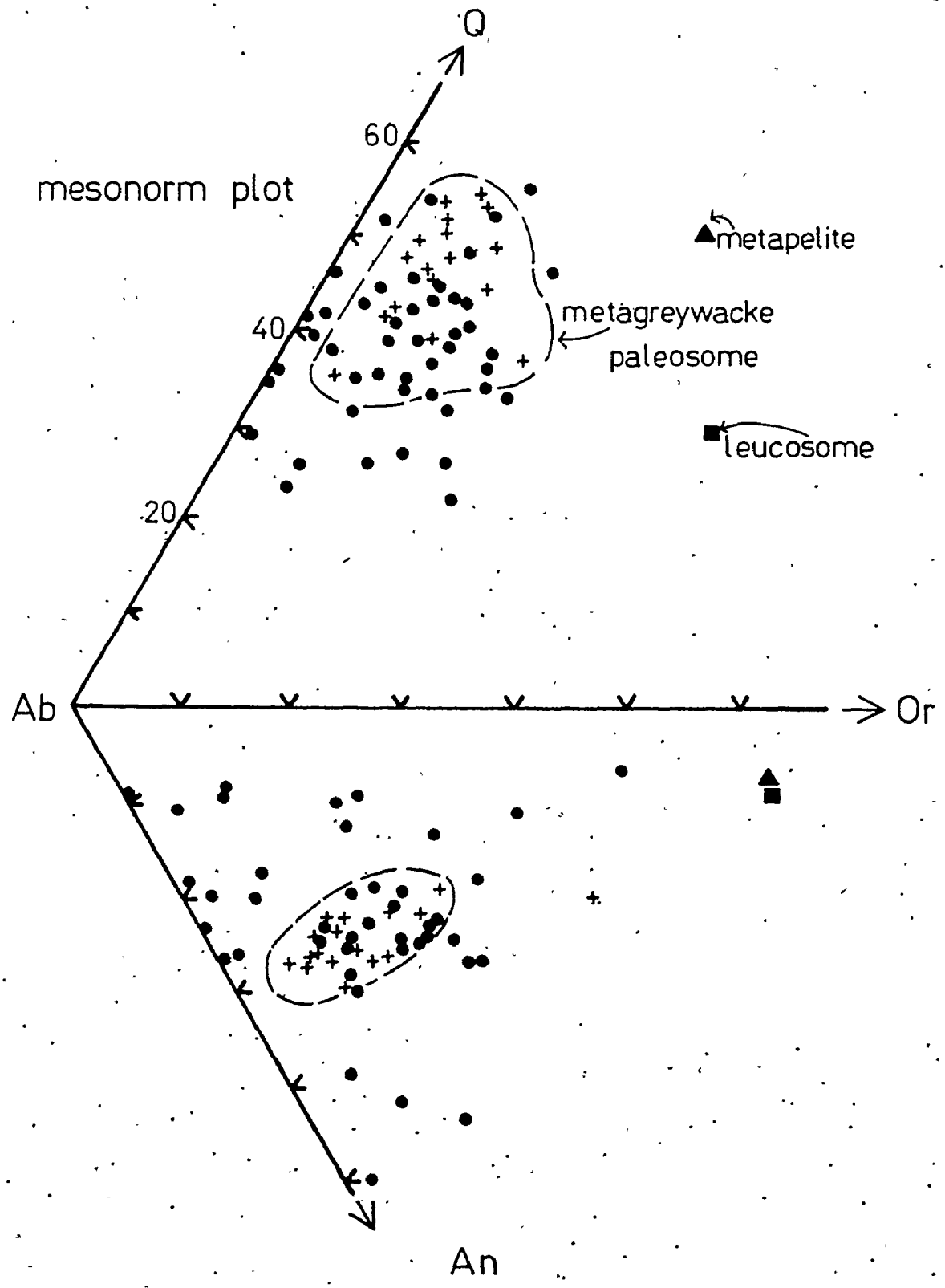
Q
60
40
20
mesonorm plot
metapelite
metagreywacke
paleosome
leucosome
Ab
Or
An

although some pink varieties do occur (L41). Most of the mobilisate is granitic in composition, but all gradations to trondhjemitic chemistry exist (Breaks and Bond, 1977). Breaks and Bond (1977) suggest that partial melting of the pelitic paleosome may produce the strongly potassic mobilisate, whereas the more sodic varieties could be derived from the metagreywacke paleosome. A notable characteristic of the mobilisate (white or pink) is that it contains garnet.

The melanosome is composed mostly of biotite-rich veneers, located between the paleosome and leucosome; these have not been analyzed in this study.

$\delta^{18}O$ rock results

The $\delta^{18}O$ rock results for the metagreywacke paleosome of the Pakwash gneiss range from 6.5 to 11.7°/$_{oo}$ (Table 4-2; Figure 4-2). Most of the results lie within the 'H_2-HH' group of Taylor (1968); five results, however, fall within the 'L to I' category. Those in the H_2-HH group (8.8-11.7°/$_{oo}$; mean of 10.1°/$_{oo}$) represent the highest $\delta^{18}O$ rock values reported to date for Archean gneisses. Such values are similar to Archean clastic metasedimentary rocks (Figure 4-2), and thus support such an origin, although an altered metavolcanic protolith cannot be ruled out on the basis of the isotopic evidence alone.

Those samples in the 'L to I' group have $\delta^{18}O$ values in the range appropriate to both high temperature primary processes (Barker et al., 1976b) and high temperature metamorphic processes (Fourcade and Javoy, 1973; Shieh and Schwarcz, 1974).

Both the low ^{18}O and high ^{18}O rock groups are similar in chemistry and have D.F. values near to or less than zero (Figure 4-14); all samples also lie within the field of chemically mature sediments (Figure 4-13) and would therefore be expected to initially have had high $\delta^{18}O$ values, similar to the Mosher Bay metaturbidites and the Kirkland Lake metasandstones (Figures 2-17, 2-18, 2-20). What has caused the difference in the isotopic composition between the two groups?

The 'H_2-HH' group rocks are protometatexites (Breaks and Bond, 1977); the metagreywacke layers have not been migmatized. The 'L-I' group rocks are metatexites; the metagreywacke paleosome of these rocks is much more intimately associated with mobilisate (melted) material than the group with high $\delta^{18}O$ values. Thus, as was the case for the Footprint gneiss, low $\delta^{18}O$ values (6-7‰) appear to be associated with migmatization and the development of a silicate melt; the exchange process must therefore occur at temperatures of at least 650°C for rocks of greywacke and pelite composition (Winkler, 1976).

$\delta^{18}O$ mineral results

The oxygen isotope mineral results for the Pakwash gneiss are given in Table 4-10 and illustrated in Figure 4-17. Except for the (unexplained) $\delta^{18}O$ quartz value of L37, the two samples of unmigmatized metagreywacke paleosome (L42, L37) have much higher $\delta^{18}O$ mineral values than comparable minerals from the more highly migmatized metatexites (L40, L44A, L44B). The white leucosome material (L43), which is associated with the metatexites, has $\delta^{18}O$ mineral values similar to the migmatized metagreywackes.

Oxygen isotope geothermometry

Oxygen isotope temperature determinations for the Pakwash rocks are given in Table A1-4A, and illustrated in Figure 4-18. Four samples (L40, L41, L42, and L43) approach isotopic equilibrium; L44A and L37 do not. Of the samples in or near isotopic equilibrium, the highest quartz-biotite and feldspar-biotite temperatures are preserved in the pink pegmatite (L41; 545°C) and the unmigmatized metagreywacke paleosome (L42; 460°C). The isotopic temperatures of the white mobilisate (L43; 405°C) and the migmatized metagreywacke (L40; 380°C) are considerably lower. The quartz-muscovite temperature of the pink pegmatite (L41; 605°C)

Table 4-10 Oxygen isotope mineral results for Pakwash gneiss and associated pegmatoids

	$\delta^{18}O°/_{oo}$				
	quartz	microcline	plagioclase	muscovite	biotite
L41[1]	11.79±0.05	10.02±0.01		9.54	6.69±0.07
L42	11.81±0.07	10.02±0.08			5.57±0.17
L37	10.05		9.32±0.07 An_{20}		5.20
L40[3]	9.30±0.03		7.28±0.01 An_{20}		1.63±0.19
L44B[3]	9.22±0.06				1.95±0.26
L44A[3]	10.33±0.02	6.52±0.13			2.17±0.19
L43[2]	10.11±0.02	7.09±0.25		5.59	2.10±0.37

Errors given as deviation from mean of duplicate analyses

[1] discordant pink pegmatite

[2] white mobilisate pegmatoid

[3] migmatized

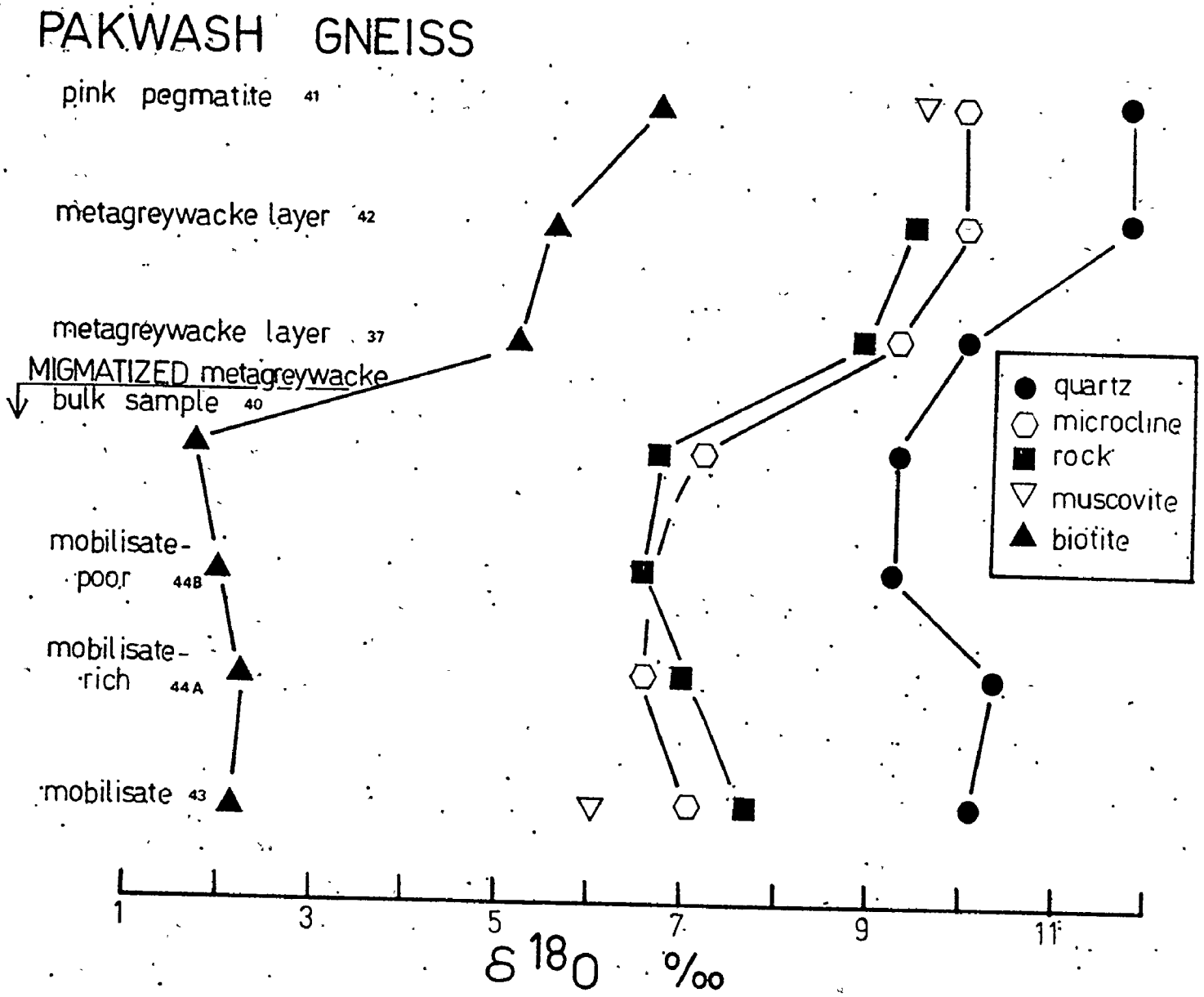

FIGURE 4-17 Oxygen isotope results for the Pakwash gneiss and associated pegmatoids

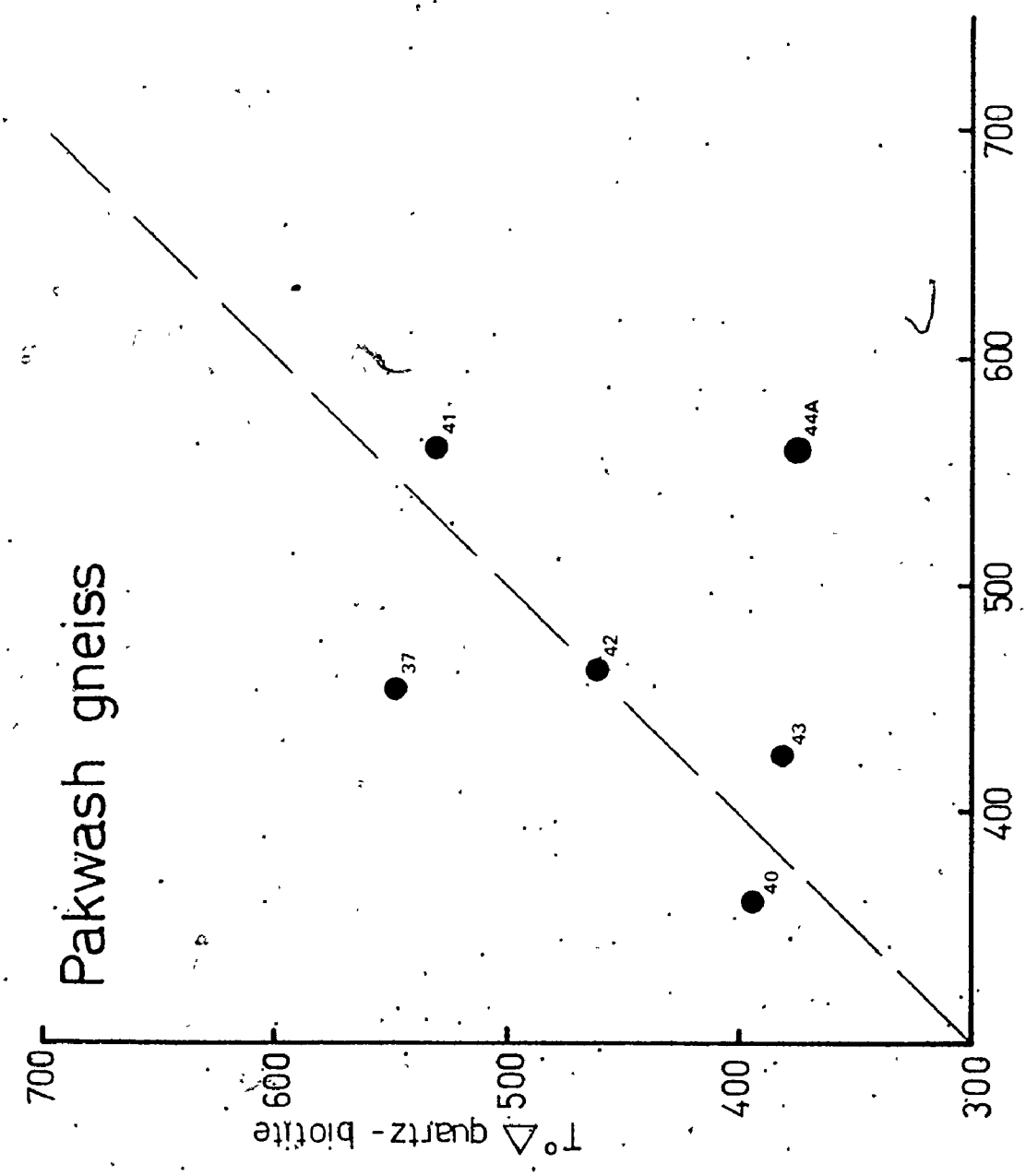

FIGURE 4-18 Oxygen isotope concordancy diagram for the Pakwash gneiss and associated pegmatoids

is also higher than that measured for the white mobilisate (L43; 410°C).

The quartz-biotite and feldspar-biotite temperatures preserved in the unmigmatized metagreywackes are about 50 to 100°C lower than suggested by the middle amphibolite facies mineral assemblages of these rocks; thus some retrograde isotopic exchange has undoubtedly taken place. These isotopic temperatures are higher, however, than preserved in the Footprint or Kenora gneisses, perhaps because of more rapid cooling (shallower depth of burial?) or less efficient isotopic exchange (less volatiles?). The migmatized metagreywackes and the associated while mobilisate, on the other hand, besides their low $\delta^{18}O$ values, also have lower quartz-biotite and feldspar-biotite temperatures. Both partial melting and isotopic re-equilibration with an isotopic reservoir are facilitated by the presence of a fluid phase; perhaps remnants of such fluid allowed isotopic re-equilibration of mineral phases to continue to lower temperatures, long after the open system isotopic exchange that occurred during migmatization had been completed.

Nature of the low ^{18}O reservoir

The nature of the isotopic exchange reservoir which produced the ^{18}O depletion in the migmatized portions of the

Pakwash gneiss can be estimated in the same manner as for the Footprint gneiss (section IV-6). The average depletion in $\delta^{18}O$, or Δ, for the Pakwash gneiss is 3.2°/$_{oo}$; a reasonable estimate of the exchange temperature is 670°C. A plot of $\delta^{18}O_{H_2O_i}$ versus W/R (Figure 4-19) shows that at W/R ratios of greater than unity, the $\delta^{18}O$ value of the proposed reservoir should be about 5-7°/$_{oo}$, similar to basaltic rocks. From comparison of Figures 4-8 and 4-19, it is apparent that only at W/R ratios of greater than 1-2 can two rock types of as dissimilar initial isotopic composition as the Footprint orthogneiss and the Pakwash paragneiss be isotopically depleted to produce final isotopic compositions of 5.9 to 7.0°/$_{oo}$. Moreover, if this exchange is related to migmatization, it must occur at a temperature of near 670°C. It follows, therefore, that the isotopic composition of the reservoir was 5-7°/$_{oo}$ for both the Footprint and Pakwash gneisses.

The only common rock type with such a range of $\delta^{18}O$ values is basalt. I suggest, therefore, that the gneisses are re-equilibrated during partial melting with fluids whose isotopic composition is controlled by (underlying?) mafic rocks.

FIGURE 4-19 $\delta^{18}O_{H_2O_i}$ versus W/R diagram for the Pakwash and Footprint gneisses.

The $\delta^{18}O_{H_2O_i}$ values represent possible isotopic compositions of hypothetical oxygen isotope reservoirs. The W/R (water/rock) ratio reflects the relative size of the oxygen isotope reservoir (which controls the isotopic composition of the exchange fluid) to that of the rocks being depleted in ^{18}O. Note that the isotopic depletions for both the Footprint and Pakwash gneisses require $\delta^{18}O_{H_2O_i}$ values of about 6‰, at W/R > 2, given that this process occurs at high (migmatitic) temperatures (>650°C).

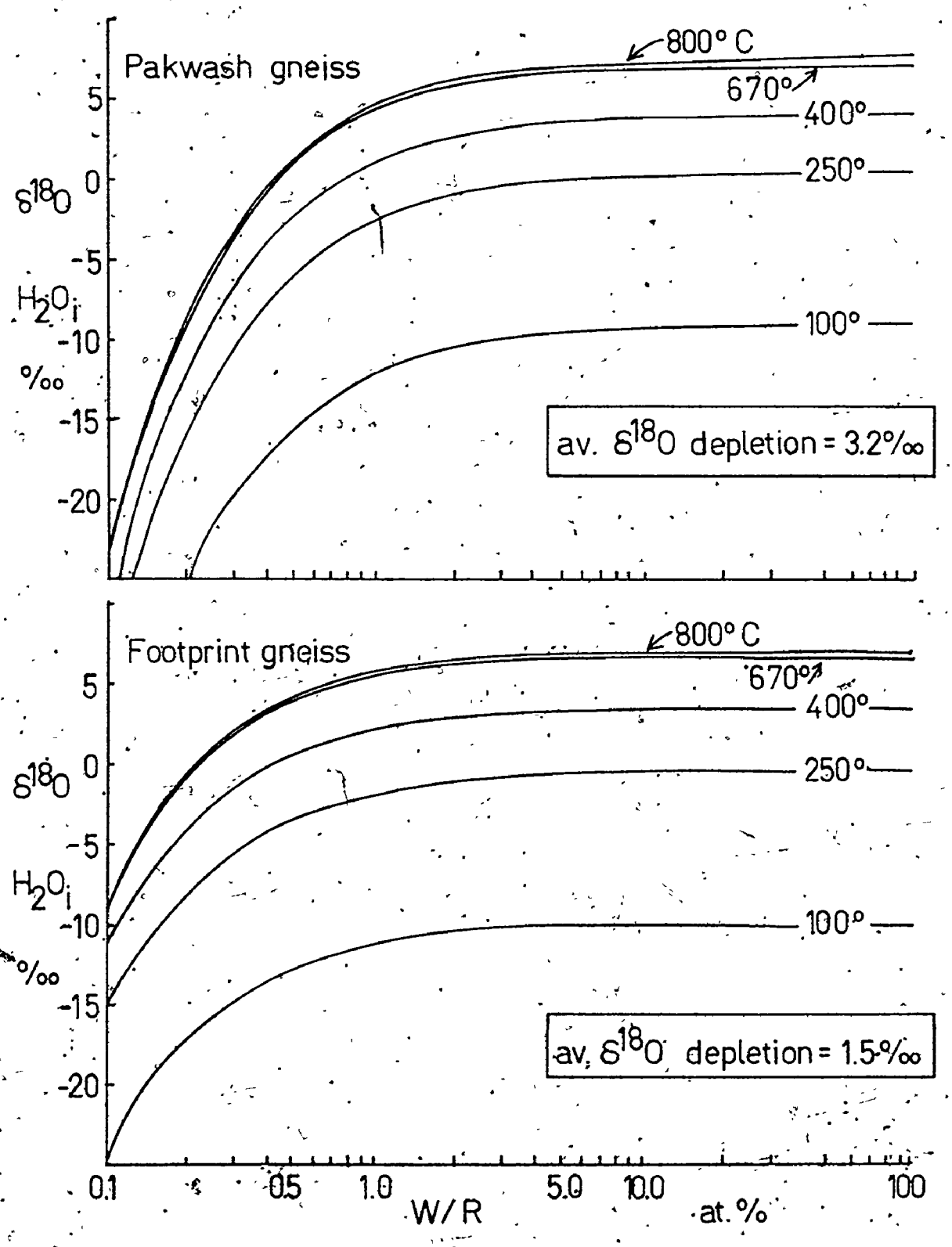
Pakwash gneiss
800° C
670°
400°
250°
100°
$\delta^{18}O_{H_2O_i}$ ‰
5
0
-5
-10
-15
-20
av. $\delta^{18}O$ depletion = 3.2‰
Footprint gneiss
800° C
670°
400°
250°
100°
$\delta^{18}O_{H_2O_i}$ ‰
av. $\delta^{18}O$ depletion = 1.5‰
0.1
0.5
1.0
5.0
10.0
100
W/R
at.%

The pernicious problem of the pink pegmatite (L41)

The high $\delta^{18}O$ mineral values of the pink pegmatite, which discordantly intrudes the low ^{18}O paragneiss, suggest that this rock was formed by partial melting of isotopically undepleted Pakwash metagreywacke or metapelite, and subsequently intruded into the metatexites after the episode of ^{18}O depletion. A metapelite sample (L45A), taken at the contact with the pink pegmatite, also has a high $\delta^{18}O$ value ($9.7°/_{oo}$), although it is located within the low ^{18}O group of rocks. Isotopic exchange with the pink pegmatite is probably responsible for this result.

Why the episode of melting involved in the formation of the pink pegmatite did not result in ^{18}O depletion is unclear. The only suggestion that I can offer is that isotopically undepleted Pakwash gneiss was partially melted after the major period of migmatization at a much higher crustal level than that involved in the formation of the metatexites. Because it was formed at shallow depths, the resulting melt was not able to equilibrate with deeper-seated low ^{18}O rocks.

IV-10 SUMMARY AND CONCLUSIONS

Some answers to the questions posed at the beginning of this chapter can now be provided;

1. $\delta^{18}O$ values for Archean gneisses from northwestern Ontario range from 5.9 to 11.7°/$_{oo}$.
2. Differentiation of tonalitic to granitic melts at high temperature from primitive mafic crust is not responsible for the $\delta^{18}O$ values of those gneisses analyzed in this study that lie between 5.9 and 7.0°/$_{oo}$.
3. Detrital processes can cause ^{18}O enrichment of the protolith of an Archean gneiss which is not necessarily subsequently lost during metamorphism.
4. Regional metamorphism up to pre-anatectic temperatures (or middle amphibolite facies) does not notably deplete the gneisses in ^{18}O, if comparison with the oxygen isotopic composition of low grade Archean granitoids of similar chemical composition is any guide. Similarly, the mean $\delta^{18}O$ value of greenschist facies Archean metagreywackes (10.6°/$_{oo}$) is not statistically different from that of the unmigmatized metagreywacke layers of the Pakwash gneiss.
5. Large scale open system isotopic exchange with low ^{18}O rocks (6°/$_{oo}$) appears to accompany migmatization.

Such a process implies access to lower crustal or upper mantle depths, and the resulting isotopic compositions suggest that the low ^{18}O reservoir is basaltic or ultramafic in composition.

6. The granulite facies metamorphism of the Twilight group A gneiss, although unaccompanied by large scale partial melting, also seems to have resulted in isotopic depletion. The depletion is about 1 to 2‰, and probably has resulted from the closed system isotopic re-equilibration of the paragneiss with the surrounding, volumetrically more important meta-igneous rocks.
7. Isotopic exchange with meteoric or seawater is not a regionally important process in Archean gneisses. Local occurrences are also unlikely because of the reasonably deep tectonic level represented by most meta-igneous Archean gneisses.
8. Many Archean gneisses, including those which have been depleted in ^{18}O, approach internal oxygen isotope equilibrium, but do not preserve strictly concordant oxygen isotope temperatures. Quartz-magnetite temperatures are frozen in at temperatures somewhat below the culmination of amphibolite facies metamorphism; quartz-biotite temperatures invariably reflect retrograde greenschist facies metamorphism (400-450°C)

during which the low ^{18}O character of biotite is created. Variations in the isotopic fixing temperature of biotite may reflect differing cooling rates during retrograde metamorphism, or may be a function of grain size or residual fluid content.

9. The generally low (I to H_1) oxygen isotope values of Archean gneisses and many less-metamorphosed Archean plutonic granitoids probably reflect a difference in their formation relative to Phanerozoic batholithic rocks of similar major element chemical composition, which have $\delta^{18}O$ values in the H_1-H_2 group. The lower $\delta^{18}O$ results probably indicate that:

   (i) the $\delta^{18}O$ values that should be inherited from the partial melting of basaltic rocks have not been overprinted by isotopic exchange with ^{18}O-enriched rocks during the emplacement of the tonalites and granodiorites, and

   (ii) (subducted) pre-existing ^{18}O-enriched crustal material was not a component of the parent rock from which the magmas for the tonalitic to granodioritic rocks were generated.

   Both of these features reinforce earlier suggestions that the I to H_1 group rocks were NEW (juvenile) additions to a then relatively small volume of Archean continental crust.

10. Archean sialic rocks which have $\delta^{18}O$ values in the H_1-H_2 group probably did not form under the same conditions as the I-H_1 group. The higher $\delta^{18}O$ values of the Burditt Lake stock, for example, may be the result of either formation from a somewhat ^{18}O-enriched source rock such as immature metagreywacke, or isotopic exchange during emplacement with ^{18}O-rich pre-existing sialic rocks. Its post-tectonic, high level intrusive nature is compatible with both interpretations. The average $\delta^{18}O$ value (8.0°/$_{oo}$) of the Cedar Lake - Clay Lake gneisses may reflect ^{18}O enrichment accompanying isotopic re-equilibration with the Twilight group A paragneiss. On the other hand, the higher $\delta^{18}O$ values of the Cedar Lake - Clay Lake gneisses (0.5°/$_{oo}$ higher than the Footprint or Kenora gneisses) may be related to the calc-alkaline differentiation trend shown by these rocks, unlike the gabbro-trondhjemite evolutionary path observed for the I to H_1 group Footprint and Kenora gneisses, as well as the Jackfish Lake Complex (Figure 4-12).

CHAPTER V

CONCLUSIONS

"To believe with certainty
we must begin to doubt".

Stanislaus

There can be no sweeping pronouncement or wild cachinnation to announce the end of a survey study such as this. However, some points already summarized at the ends of Chapters II, III, and IV are worthy of repetition.

V-1 ARCHEAN CLASTIC METASEDIMENTARY ROCKS AND ASSOCIATED FELSIC METAVOLCANICS

1. The clastic metasedimentary rocks analyzed in this study have chemical compositions which indicate that their detritus has been derived from predominantly felsic source terrains, and that the rocks have been formed in a eugeosynclinal environment.

2. Some samples show no recognizable chemical or isotopic effects of residence in a sedimentary environment. Others,

which are designated as 'chemically mature', have Al/Fe, Na_2O/K_2O and CaO/Na_2O ratios, discriminant function values (D.F.) and oxygen isotope compositions that indicate chemical and isotopic modification during sedimentary processes. The $\delta^{18}O$ values of the analyzed Archean clastic metasedimentary rocks range from 8.0 to 13.3°/$_{oo}$ and tend to increase as the sediment becomes more mature. These chemical and isotopic features can be useful in the identification of mature sedimentary protoliths in Archean gneisses.

3. Archean felsic metavolcanic rocks have $\delta^{18}O$ values similar to Archean clastic metasedimentary rocks; the range extends to values higher than normally observed in felsic volcanics because of low temperature alteration processes.

V-2 GEOCHEMISTRY OF THE BURDITT LAKE - LAKE DESPAIR AREA

Mafic metavolcanic rocks

(a) The trace element contents of the Burditt Lake metabasalts most closely correspond to those of modern arc tholeiites.

(b) REE patterns for the Burditt Lake metabasalts and mafic enclaves from the Footprint gneiss are compatible with formation of the units by 30 to 40% melting of a hypothetical ultrabasic rock such as plagioclase-bearing or spinel-bearing pyrolite.

(c) The $\delta^{18}O$ values of the Burditt Lake - Lake Despair metabasalts (4.4-9.2°/$_{oo}$) reflect a variety of alteration processes, none of which can be consistently correlated with chemical parameters that also indicate some type of alteration.

Felsic metavolcanic rocks

(a) The felsic metavolcanic rocks were probably formed by a low degree of partial melting of hydrous quartz eclogite, similar in chemical composition to the Burditt Lake metabasalts.

(b) Burditt Lake felsic metavolcanic rocks located within 1700 meters of the Burditt Lake pluton have been chemically altered and depleted in ^{18}O by up to 3.5°/$_{oo}$ during exchange with stock-derived magmatic waters.

Jackfish Lake Complex

(a) Partial melting of hydrous eclogite or anhydrous quartz eclogite at high pressures was probably responsible for the formation of the Na-enriched Jackfish Lake Complex dioritic magma. This magma was subsequently emplaced at a higher level along the contact between the Footprint gneiss and the Burditt Lake - Lake Despair metavolcanics, where most of it crystallized to form a Na-diorite.

(b) Some residual magma and fluids differentiated to form progressively smaller volumes of quartz monzodiorite, quartz diorite, leuco quartz diorite, Na granodiorite and Na-syenite. This evolution was first controlled by the precipitation of hornblende and then by feldspar crystallization, especially microcline. $\delta^{18}O$ rock values for the suite (6.4-9.2°/$_{oo}$), as well as oxygen isotope mineral data, show that the isotopic composition of the residual melt is controlled strictly by the crystallization sequence of the mineral phases.

(c) Low temperature meteoric water-rock interaction associated with faulting has caused isotopic and chemical alteration of some of the Complex granodiorites and quartz monzodiorites.

Footprint gneiss

(a) The Footprint gneiss probably formed by 20-25% melting of a LREE-enriched quartz eclogite.

(b) The metamorphism and migmatization of the Footprint gneiss appears to have been quasi-isochemical, but its oxygen isotope composition is depleted from about 7.5 to 6.0°/$_{oo}$ during migmatization.

Crustal evolution of the Burditt Lake - Lake Despair area

The geochemistry of the Burditt Lake - Lake Despair area is compatible with a model which involves the formation

of a tonalitic protocontinent (Footprint gneiss) by melting of relatively unfractionated upper mantle rocks and the development of a near-shore island arc, responsible for bimodal basalt-dacite volcanism. The subsequent intrusion of the Jackfish Lake Complex at the interface between the two may record (1) the beginning of anhydrous melting conditions in the mantle; which favour the production of intermediate liquids by partial melting of quartz eclogite, (2) a later influx of heat and volatiles capable of melting a stagnant, quartz undersaturated eclogite residue remaining from the formation of the Footprint gneiss, or (3) the partial melting of a completely different volume of eclogitic rocks genetically unrelated to those previously underlying this portion of the Archean crust.

V-3 THE OXYGEN ISOTOPE GEOCHEMISTRY OF ARCHEAN GNEISSES AND GRANITIC ROCKS

1. The $\delta^{18}O$ values of Archean gneisses from northwestern Ontario range from 5.9 to 11.7°/$_{oo}$.

2. Up to middle amphibolite facies of metamorphism, Archean gneisses have $\delta^{18}O$ values that reflect the nature of their protolith(s).

3. Large scale open system isotopic exchange with low ^{18}O rocks (6°/$_{oo}$), possibly underlying basalt, occurs during migmatization; probably because the presence of melt and fluid phases facilitates isotopic exchange with rocks at depth.

4. Quartz-magnetite oxygen isotope temperatures for the gneisses are frozen in at temperatures somewhat below the culmination of amphibolite facies metamorphism. Quartz-biotite temperatures in the gneisses reflect further isotopic exchange, mostly of the biotite, to lower temperatures (400-450°C). This results in the formation of biotites with low $\delta^{18}O$ compositions (<3°/$_{oo}$).

5. Many Archean gneisses and granitoids have $\delta^{18}O$ values of about 7.5°/$_{oo}$, lower than the 8 to 10°/$_{oo}$ range common in Phanerozoic batholiths, and yet show no signs of any post-protolith formation alteration or depletion in ^{18}O. This suggests that these Archean rocks have formed from less differentiated source rocks, relative to the Phanerozoic batholiths, in keeping with the other geochemical evidence for more primitive origins for Archean tonalitic rocks.

V-4 SUGGESTIONS FOR FUTURE STUDIES

1. A detailed oxygen isotope study of minerals from modern sediments would help establish more clearly the relative effects of provenance, diagenesis, and weathering upon the isotopic composition of lithified clastic (meta)sedimentary rocks.

2. An oxygen isotope study of Paleozoic and younger volcanogenic greywackes would determine whether the low ^{18}O nature of Archean metagreywackes is a function of provenance or geologic age.

3. Detailed Rb/Sr and U/Pb geochronology of the various units in the Lake Despair-Burditt Lake area, as well as the English River gneiss belt, are requisite to the proper formulation of a crustal evolution model of these areas. I predict that the Footprint gneiss could turn out to be older than 2.7 b.y., if the proper techniques are used.

4. D/H studies of mineral separates would help confirm and expand the magmatic and meteoric water interaction hypotheses proposed here for the Burditt Lake stock and surrounding country rocks, and the Northwest Bay Fault and associated granodiorites and quartz monzodiorites.

5. More detailed mapping and geochemical sampling of the Burditt Lake - Lake Despair mafic metavolcanic rocks would establish more clearly the stratigraphic and chemical evolution

of this greenstone pile.

6. Detailed geochemical studies of the interior of the Rainy Lake batholith are required to support, modify, or refute interpretations made here concerning the origin of the batholith based upon the data available for the Footprint gneiss.

7. An oxygen isotope study of a detailed section of gneiss and migmatite, such as the Pakwash gneiss (where the isotopic differences between altered and unaltered samples are large), accompanied by D/H measurements, could more closely establish where and when the ^{18}O depletion begins during migmatization, as well as the nature of the exchange fluid involved in the process.

REFERENCES

ABBEY, S. (1973). Studies in "standard samples" of silicate rocks and minerals. Part 3, 1973 extension and revision of "usable" values. Geol. Surv. Can., Paper 73-36, 25p.

ABBEY, S. (1975). Studies in "standard samples" of silicate rocks and minerals. Part 4, 1974 edition of "usable" values. Geol. Surv. Can., Paper 74-41, 23p.

ANDERSON, A.T. (1967). The dimensions of oxygen isotopic equilibrium attainment during prograde metamorphism. Jour. Geol., 75, 323-332.

ANDERSON, A.T., CLAYTON, R.N. and MAYEDA, T.K. (1971). Oxygen isotope thermometry of mafic igneous rocks. Jour. Geol., 79, 715-729.

ANHAEUSSER, C.R. (1971). Cyclic volcanicity and sedimentation in the evolutionary development of Archaean greenstone belts of shield areas. Spec. Pub. 3, Geol. Soc. Australia, 57-70.

ANHAEUSSER, C.R. (1973). The evolution of the early Precambrian crust of southern Africa. Phil. Trans. R. Soc. Lond. A 273, 359-388.

ANHAEUSSER, C.R., MASON, R., VILJOEN, M.J. and VILJOEN, R.P. (1969). A reappraisal of some aspects of Precambrian shield geology. Geol. Soc. Amer. Bull., 80, 2175-2200.

ARTH, J.G. (1976a). Behaviour of trace elements during magmatic processes - a summary of theoretical models and their applications. Jour. Research, U.S. Geol. Survey, 4, 41-47.

ARTH, J.G. (1976b). A model for the origin of the Early Precambrian greenstone-granite complex of Northeastern Minnesota. In The Early History of the Earth (ed. B.F. Windley), Wiley and Sons, Ltd., 299-302.

ARTH, J.G. and BARKER, F. (1976). Rare-earth partitioning between hornblende and dacitic liquid and implications for the genesis of trondhjemitic-tonalitic magmas. Geology, 4, 534-536.

ARTH, J.G. and HANSON, G.N. (1972). Quartz diorites derived by partial melting of eclogite or amphibolite at mantle depths. Contr. Mineral. and Petrol., 37, 161-174.

ARTH, J.G. and HANSON, G.N. (1975). Geochemistry and origin of the early Precambrian crust of northeastern Minnesota. Geochim. Cosmochim. Acta, 39, 325-362.

AYRES, L.D. (1969). Early Precambrian metasandstone from Lake Superior Park, Ontario, Canada, and implications for the origin of the Superior Province. Geol. Soc. Amer., Abs. with Programs for 1969, Part 7, 5.

AYRES, L.D. and ERMANOVICS, I.F. (1972). Granitic plutons. In Variations in Tectonic Styles in Canada (eds. R.A. Price and R.J.W. Douglas), Geol. Assoc. Can., Spec. Paper 11, 575-589.

BAILEY, E.H., IRWIN, W.P. and JONES, D.L. (1964). Franciscan and related rocks, and their significance in the geology of western California. California Div. Mines, Geol. Bull. 183, 177p.

BARAGAR, W.R.A. and GOODWIN, A.M. (1969). Andesites and Archean volcanism on the Canadian shield. Oregon Dept. Geology and Mineral Industries Bull., 65, 121-142.

BARAGAR, W.R.A. and McGLYNN, J.C. (1976). Early Archean basement in Canadian shield: a review of the evidence. Geol. Surv. Can., Paper 76-14, 21p.

BARKER, F. and ARTH, J.G. (1976). Generation of trondhjemitic-tonalitic liquids and Archean bimodal trondhjemite-basalt suites. Geology, 4, 596-600.

BARKER, F., ARTH, J.G., PETERMAN, Z.E. and FRIEDMAN, I. (1976a). The 1.7-1.8 b.y. old trondhjemites of southwestern Colorado and northern New Mexico: Geochemistry and depths of genesis. Geol. Soc. Amer. Bull., 87, 189-198.

BARKER, F., FRIEDMAN, I., HUNTER, D.R. and GLEASON, J.D. (1976b). Oxygen isotopes of some trondhjemites, siliceous gneisses, and associated mafic rocks. Precambrian Res., 3, 547-557.

BARKER, F. and PETERMAN, Z.E. (1974). Bimodal tholeiitic-dacitic magmatism and the Early Precambrian crust, Precambrian Res., 1, 1-12.

BARTON, J.M., Jr. (1975). Rb-Sr isotopic characteristics and chemistry of the 3.6-b.y. Hebron gneiss, Labrador. Earth Planet. Sci. Lett., 27, 427-435.

BASTIN, E.S. (1909). Chemical composition as a criterion in identifying metamorphosed sediments. Jour. Geol., 17, 445-472.

BEAKHOUSE, G.P. (1974a). A preliminary appraisal of the geology and geophysics of the English River gneiss belt. Centre for Precambrian Studies 1974 Ann. Rept., Part 2, 233-239.

BEAKHOUSE, G.P. (1974b). Geology of the Pakwash Lake area, northwestern Ontario. Centre for Precambrian Studies, Univ. Manitoba, 1974 Ann. Rept., Part 2.

BEAKHOUSE, G.P. (1975). The English River subprovince. Centre for Precambrian Studies, Univ. Manitoba, 1975 Ann. Rept., 51-66.

BEAKHOUSE, G.P. (1976). A reappraisal of the western portion of the English River subprovince, northwestern Ontario and southeastern Manitoba. Proc. 22nd Meeting on Lake Superior Geology, May 1976, p.8.

BEAKHOUSE, G.P. (1977). A subdivision of the western English River subprovince. Can. Jour. Earth Sci., 14, 1481-1489.

BECKER, R.H. and CLAYTON, R.N. (1976). Oxygen isotope study of a Precambrian banded iron-formation, Hamersley Range, Western Australia. Geochim. Cosmochim. Acta, 40, 1153-1165.

BECKINSALE, R.D. and DURHAM, J.J. (1974). Progress Report 1970-1973, the Natural Environment Research Council Pub. Series C, No. 13, Great Britain.

BECK, R.T. and JOLLY, W.T. (1975). Archean greywackes: petrology and lithogenesis. 1975 Geotraverse Conference Report, No. 35, 10p.

BIGELEISEN, J. and MAYER, M.G. (1947). Calculation of equilibrium constants for isotopic exchange reactions. Jour. Chem. Physics, 15, 261-267.

BIRK, D. and McNUTT, R.H. (1976). Autometasomatism as a mechanism of differentiation in Archean granitoid diapirs (abstr.). Abs. with Programs for 1976, Geol. Assoc. Can., 1, 74.

BIRK, D. and McNUTT, R.H. (1977). Rb/Sr isochrons for Archean granitoid plutons within the Wabigoon greenstone belt, northwestern Ontario: a preliminary evaluation. In Report of Activities, Part A, Geol. Surv. Can., Paper 77-1A, rep. 33.

BLACK, P.M. (1974). Oxygen isotope study of metamorphic rocks from the Ouegoa District, New Caledonia. Contrib. Mineral. and Petrol., 47, 197-206.

BLACKBURN, C.E. (1972). Off-Lake - Burditt Lake area (eastern part), District of Rainy River. Ont. Dept. Mines and Northern Affairs, Prelim. Map P.742, Geol. Ser., Scale 1 inch to 1/2 mile.

BLACKBURN, C.E. (1976a). Geology of the Off Lake - Burditt Lake area, District of Rainy River. Ontario Div. Mines, GR 140, 62p. Accompanied by Map 2325, Scale 1 inch to 1 mile (1:63360).

BLACKBURN, C.E. (1976b). Geology of the Lower Manitou - Uphill Lakes area, District of Kenora. Ont. Div. Mines, GR 142, 81p.

BLACKBURN, C.E. (1976c). Boyer Lake area, District of Kenora. Ont. Div. Mines, Prelim. Map P 1187, Geol. Ser., Scale 1 inch to 1/4 mile (1:15840), Geology, 1975.

BLACKBURN, C.E. (1976d). Meggisi Lake area, District of Kenora. Ont. Div. Mines, Prelim. Map, P 1188, Geol. Ser., Scale 1 inch to 1.4 mile (1:15840), Geology, 1975.

BLATT, H., MIDDLETON, G.V. and MURRAY, R. (1972). Origin of Sedimentary Rocks. Prentice-Hall, Inc., N.J., 634p.

BLATTNER, P. (1975). Oxygen isotopic compositions of fissure-grown quartz, adularia and calcite from Broadlands geothermal field, New Zealand, with an appendix on quartz-K-feldspar-calcite-muscovite oxygen isotope geothermometers. Amer. Jour. Sci., 275, 785-800.

BLATTNER, P. and BIRD, G.W. (1974). Oxygen isotope fractionation between quartz and K-feldspar at 600°C. Earth Planet. Sci. Lett., 23, 21-27.

BLISS, N.W. (1969). Thermal convection in the Archean crust? Nature, 222, 972-975.

BOTTINGA, Y. and JAVOY, M. (1973). Comments on oxygen isotope geothermometry. Earth Planet. Sci. Lett., 20, 250-265.

BOTTINGA, Y. and JAVOY, M. (1975). Oxygen isotope partitioning among the minerals in igneous and metamorphic rocks. Rev. Geophys. Space Phys., 12, 403-418.

BOWEN, N.L. (1922). The behaviour of inclusions in igneous magmas. Jour. Geol., 30, 513-570.

BREAKS, F.W. and BOND, W.D. (1977). Manifestations of recent reconnaissance investigation in the English River subprovince. 1977 Geotraverse Conference Report No. 27, 170-211.

BREAKS, F.W., BOND, W.D., HARRIS, N. and WESTERMAN, C. (1975). Operation Kenora-Ear Falls, District of Kenora. Summary of Field Work 1975. Ont. Div. Mines, M.P. 63, 19-33.

BREAKS, F.W., BOND, W.D., WILLIAMS, G.H. and GOWER, C. (1974). Operation Kenora-Sydney Lake, District of Kenora. Ont. Dept. Mines, Summary of Field Work 1974, 17-36.

BRIDGWATER, D.J. and FYFE, W.S. (1974). The pre 3 b.y. crust: fact - fiction - fantasy. Geoscience Can., 1, 7-11.

BRIDGWATER, D.J., WATSON, J. and WINDLEY, B.F. (1973). The Archean craton of the North Atlantic region. Phil. Trans. R. Soc. Lond., A 273, 493-512.

BURKE, K., DEWEY, J.F. and KIDD, W.S.F. (1976). Dominance of horizontal movements, arc and microcontinental collisions during the later permobile regime. In The Early History of the Earth (ed. B.F. Windley), Wiley and Sons, Ltd., 113-130.

BURWASH, E.M. (1933). Geology of the Kakagi Lake area. Ont. Dept. Mines Rept. 42, Part 4, 41-92. Accompanied by May 42b, 1 inch to 1 mile.

CAHEN, L. and SNELLING, N.J. (1966). The Geochronology of Equatorial Africa. North Holland Pub. Co.

CAMERON, E.M. and BAUMANN, A. (1972). Carbonate sedimentation during the Archean. Chem. Geol., 10, 17-30.

CANN, J.R. (1970). Rb, Sr, Y, Zr and Nb in some ocean floor basaltic rocks. Earth Planet. Sci. Lett., 10, 7-11.

CARMICHAEL, I.S.E., TURNER, F.J. and VERHOOGEN, J. (1974). Igneous Petrology, McGraw-Hill Book Co., N.Y., 739p.

CATANZARO, E.J. and HANSON, G.N. (1971). U-Pb ages for sphene from Early Precambrian igneous rocks in northwestern Minnesota - northwestern Ontario. Can. Jour. Earth Sci., 8, 1319-1324.

CERLING, T.E., BIGGS, D.L., VONDRA, C.F. and SVEC, H.J. (1975). Use of oxygen isotope ratios in correlation of tuffs, East Rudolf basin, Northern Kenya. Earth Planet. Sci. Lett., 25, 291-296.

CHAPPELL, B.W. (1986). Volcanic greywackes from the Upper Devonian Baldwin Formations, Tamworth-Banaba District, New South Wales. Jour. Geol. Soc. Australia, 15, 87-102.

CHASE, C.G. and PERRY, E.C., Jr. (1972). The oceans: growth and oxygen isotope evolution. Science, 177, 992-994.

CHAYES, F. (1964). Variance-covariance relations in some published Harker diagrams of volcanic suites. Jour. Petrol., 5, 219-237.

CLAYTON, R.N. and EPSTEIN, S. (1958). The relationships between O^{18}/O^{16} ratios in coexisting quartz carbonate and iron oxides from various geologic deposits. Jour. Geol., 66, 352-373.

CLAYTON, R.N., GOLDSMITH, J.R., KAREL, K.J., MAYEDA, T. and NEWTON, R.C. (1975). Limits on the effect of pressure on isotopic fractionation. Geochim. Cosmochim. Acta, 39, 1197-1201.

CLAYTON, R.N. and MAYEDA, T.K. (1963). The use of bromine pentafluoride in the extraction of oxygen from oxides and silicates for isotopic analysis. Geochim. Cosmochim. Acta, 27, 43-52.

CLAYTON, R.N., O'NEIL, J.R. and MAYEDA, T.K. (1972a). Oxygen isotope exchange between quartz and water. Jour. Geophys. Res., 77, 3057-3067.

CLAYTON, R.N., REX, R.W., SYERS, J.K. and JACKSON, M.L. (1972b). Oxygen isotope abundance in quartz from Pacific pelagic sediments. Jour. Geophys. Res., 77, 3907-3915.

CONDIE, K.C. (1967). Geochemistry of early Precambrian greywackes from Wyoming. Geochim. Cosmochim. Acta, 31, 2135-2149.

CONDIE, K.C. (1973). Archean magmatism and crustal thickening. Geol. Soc. Amer. Bull., 84, 2981-2992.

CONDIE, K.C. (1976). Trace element models for the origin of Archean volcanic rocks. In The Early History of the Earth (ed. B.F. Windley), Wiley and Sons, Ltd., 419-424.

CONDIE, K.C. and BARAGAR, W.R.A. (1974). Rare-earth element distribution in volcanic rocks from Archean greenstone belts. Contr. Mineral. and Petrol., 45, 237-246.

CONDIE, K.C. and HARRISON, N.M. (1976). Geochemistry of the Archean Bulawayan group, Midlands greenstone belt, Rhodesia. Precambrian Res., 3, 253-271.

CONDIE, K.C., MACKE, J.E. and REIMER, T.O. (1970). Petrology and geochemistry of Early Precambrian greywackes from the Fig Tree Group, South Africa. Geol. Soc. Amer. Bull., 81, 2759-2776.

CONDIE, K.C. and POTTS, M.J. (1969). Calc-alkaline volcanism and the thickness of the early Precambrian crust in North America. Can. Jour. Earth Sci., 6, 1179-1184.

CONDIE, K.C. and SNANSIENG, S. (1971). Petrology and geochemistry of the Duzel (Ordovician) and Gazelle (Silurian) Formations, northern California. Jour. Sed. Petrology, 41, 741-751.

COOKE, D.L. and MOORHOUSE, W.W. (1969). Timiskaming volcanism in the Kirkland Lake area, Ontario, Canada. Can. Jour. Earth Sci., 6, 117-132.

COOMBS, D.S. (1954). The nature and alteration of some Triassic sediments from Southland, New Zealand. Trans. R. Soc. New Zealand, 82, 65-109.

COOMBS, D.S., ELLIS, A.J., FYFE, W.S. and TAYLOR, A.M. (1959). The zeolite facies, with comments on the interpretation of hydrothermal synthesis. Geochim. Cosmochim. Acta, 17, 53-107.

COWARD, M.P., GRAHAM, R.H., JAMES, P.R. and WAKEFIELD, J. (1973). A structural interpretation of the northern margin of the Limpopo orogenic belt, southern Africa. Phil. Trans. R. Soc. Lond., A 273, 487-491.

CRAIG, H. (1957). Isotopic standards for carbon and oxygen and correction factors for mass-spectrometric analysis of carbon dioxide. Geochim. Cosmochim. Acta, 12, 133-149.

CRAIG, H. (1961). Standard for reporting concentrations of deuterium and oxygen-18 in natural waters. Science, 133, 1833-1834.

CUDDY, G. (1971). Structural geology of the Kakagi Lake area. Unpub. M.Sc. Thesis, McMaster Univ., Hamilton, Canada.

CULLERS, R.L., MEDARIS, L.G. and HASKIN, L.A. (1973). Experimental studies of the distribution of rare earths as trace elements among silicate minerals and liquids and water. Geochim. Cosmochim. Acta, 37, 1499-1512.

DASCH, E.J., HEDGE, C.E. and DYMOND, J. (1973). Effect of seawater interaction on strontium isotope composition of deep-sea basalts. Earth Planet. Sci. Lett., 19, 177-183.

DAVIES, J.C. and MORIN, J.A. (1972). Cedartree Lake area, District of Kenora. Ont. Dept. Mines and Northern Affairs, Prelim. Map P 731. Geol. Ser., Scale 1 inch to 1/4 mile. Geology 1971.

DEER, W.A., HOWIE, R.A. and ZUSSMAN, J. (1971). An Introduction to the Rock-Forming Minerals (2nd impression). Longman Group, Ltd., 528p.

DEGENS, E.T. and EPSTEIN, S. (1962). Relations between O^{18}/O^{16} ratios in coexisting carbonates, cherts and diatomites. Bull. Am. Assoc. Petroleum Geologists, 46, 534-542.

DE LAETER, J.R. and ABERCROMBIE, I.D. (1970). Mass spectrometric isotope dilution analysis of rubidium and strontium in standard rocks. Earth Planet. Sci. Lett., 9, 327-330.

DENNEN, W.H. and MOORE, B.R. (1971). Chemical definition of mature detrital sedimentary rocks. Nat. Phys. Science, 234, 127-128.

DICKINSON, W.R. and LUTH, W.C. (1971). A model for plate tectonic evolution of mantle layers. Science, 74, 400-404.

DIDIER, J. (1973). Granites and Their Enclaves. Elsevier Scientific Pub. Co., Amsterdam, 393p.

DONALDSON, J.A. and JACKSON, G.D. (1965). Archaean sedimentary rocks of North Spirit Lake area, northwestern Ontario. Can. Jour. Earth Sci., 2, 622-647.

DONTSOVA, Ye.I. (1970). Oxygen isotope exchange in rock-forming processes. Geochem. Int., 624-635; trans from Geokhimiya, 8, 903-916.

DONTSOVA, Ye.I., MIGDISOV, A.A. and RONOV, A.B. (1972). On the causes of variation of oxygen isotopic composition in the carbonate strata of the sedimentary column. Geochem. Int., 9, 885-891; trans. from Geokhimiya, 11, 1317-1324.

DONTSOVA, Ye.I. and MILOVSKIY, A.V. (1967). Oxygen isotopes in granitization. Geochem. Int., 4, 537-544.

DRAKE, M.J. (1975). The oxidation state of europium as an indicator of oxygen fugacity. Geochim. Cosmochim. Acta, 39, 55-64.

DRURY, S.A. (1974). Chemical changes during retrogressive metamorphism of Lewisian granulite facies rocks from Coll and Tiree. Scott. Jour. Geol., 10, 237-256.

DWIBIDI, K. (1966). Petrology of the English River gneissic belt, northwestern Ontario. Unpub. Ph.D. Thesis, Univ. Manitoba.

DYER, W.S. (1933). Geology of the Pashkokogan-Misehkow area. Ont. Dept. Mines, 42, Pt. 6, 1-20 (published 1934).

EADE, K.E. and FAHRIG, W.F. (1971). Geochemical evolutionary trends of continental plates - a preliminary study of the Canadian shield. Geol. Surv. Can., Bull. 179, 51p.

EDWARDS, A.B. (1950). The petrology of the Cretaceous greywackes of the Puraii Valley, Papua. Proc. R. Soc. Vict., 60, 163-171.

EDWARDS, G.R. and LORSONG, J. (1976). Pipestone Lake area (southern half), Districts of Rainy River and Kenora. Ont. Div. Mines, Prelim. Map P 1103, Geol. Ser.

EDWARDS, G.R. and SUTCLIFFE, R.H. (1977). Straw Lake area, Districts of Kenora and Rainy River. Ont. Div. Mines, Prelim. Map (to be released), Geology 1976.

EGGLER, D.H. (1972). Water-saturated and undersaturated melting relations in a Paricutin andesite and an estimate of water content in the natural magma. Contr. Mineral. and Petrol., 34, 261-271.

ENGEL, A.E.J., CLAYTON, R.N. and EPSTEIN, S. (1958). Variations in isotopic composition of oxygen and carbon in Leadville limestone (Mississippian, Colorado) and in its hydrothermal and metamorphic phases. Jour. Geol., 66, 374-393.

ENGEL, A.E.J. and ENGEL, C.G. (1953). Grenville series in the northwest Adirondack Mountains, New York. Geol. Soc. Amer. Bull., 64, 1013-1097.

ENGEL, A.E.J., ITSON, S.P., ENGEL, C.G., STICKNEY, D.M. and CRAY, E.J. (1974). Crustal evolution and global tectonics: a petrogenic view. Geol. Soc. Amer. Bull., 85, 843-858.

EPSTEIN, S. and TAYLOR, H.P., Jr. (1967). Variation of O^{18}/O^{16} in minerals and rocks. In Researches in Geochemistry (ed. P.H. Abelson), Wiley and Sons, N.Y., 29-62.

ERIKSSON, K.A. (1977). Tidal deposits from the Archaean Moodies Group, Barberton Mountain Land, South Africa. Sed. Geol., 18, 257-281.

ESKOLA, P.E. (1948). On the problem of mantled gneiss domes. Quat. Jour. Geol. Soc. Lond., 104, 461-476.

ESLINGER, E.V. and SAVIN, S.M. (1973). Oxygen isotope geothermometry of the burial metamorphic rocks of the Precambrian Belt Supergroup, Glacier National Park, Montana. Geol. Soc. Amer. Bull., 84, 2549-2560.

EWART, A. and BRYAN, W.B. (1972). Petrography and geochemistry of the igneous rocks from Eua, Tongan Islands. Geol. Soc. Amer. Bull., 83, 3281-3298.

EWART, A. and BRYAN, W.B. (1973). The petrology and geochemistry of the Tongan islands. In The Western Pacific: Island Arcs, Marginal Seas, Geochemistry (ed. P.J. Coleman), Univ. Western Australia Press.

EWART, A.E., BRYAN, W.B. and GILL, J.B. (1973). Mineralogy and geochemistry of the younger volcanic islands of Tonga, S.W. Pacific. Jour. Petrol., 14, 429-465.

FLANAGAN, F.J. (1973). 1972 values for international geochemical reference samples. Geochim. Cosmochim. Acta, 37, 1189-1200.

FLANAGAN, F.J. (1976). Descriptions and analyses of eight new U.S.G.S. rock standards. U.S. Geol. Surv. Prof. Pap. 840, 192p.

FLEET, A.J., HENDERSON, P. and KEMPE, D.R.C. (1976). Rare earth element and related chemistry of some drilled southern Indian Ocean basalts and volcanogenic sediments. Jour. Geophys. Res., 81, 4257-4268.

FLOYD, P.A. and WINCHESTER, J.A. (1975). Magma type and tectonic setting discrimination using immobile elements. Earth Planet. Sci. Lett., 27, 211-218.

FOLK, R.L. (1968). Petrology of Sedimentary Rocks. Hemphill's Book Store, Austin, Texas; 170p.

FORESTER, R.W. and TAYLOR, H.P., Jr. (1972). Oxygen and hydrogen isotope data on the interaction of meteoric ground waters with a gabbro-diorite stock, San Juan Mountains, Colorado. XXIV Int. Geol. Congress, Sec. 10, 254-263.

FOURCADE, S. (1972). Etude des fractionnements isotopiques $^{18}O/^{16}O$ dans quelques series metamorphiques et massifs granitiques precambriens de l'Ahagaar algerien. These 3eme cycle, 102pp., Univ. Paris VI.

FOURCADE, S. and JAVOY, M. (1973). Rapports $^{18}O/^{16}O$ dans les roches du vieux socle catazonal d'In Ouzzal (Sahara algerien). Contrib. Mineral. and Petrol., 42, 235-244.

FRANCOEUR, D. (1972). Study of diabase dikes in the Rainy River District, Ontario. Unpub. B.Sc. Thesis, Univ. Ottawa, 77p.

FRASER, N.H.C. (1943). Geology of the Whitefish Bay area, Lake of the Woods. Ont. Dept. Mines, Rept. 52, Part 4, 17p. Accompanied by Map 52C, 1 inch to 1 mile.

FREY, F.A., BRYAN, W.B. and THOMPSON, G. (1974). Atlantic Ocean floor: geochemistry and petrology of basalts from Legs 2 and 3 of the Deep-Sea Drilling Project. Jour. Geophys. Res., 79, 5507-5527.

FREY, F.A., HASKIN, M.A., POETZ, J. and HASKIN, L.A. (1968). Rare earth abundances in some basic rocks. Jour. Geophys. Res., 73, 6085-6098.

FRIEDMAN, I. and GLEASON, J.D. (1973). A new silicate inter-comparison standard for ^{18}O analysis. Earth Planet. Sci. Lett., 18, 124.

FRIEDRICHSEN, H. (1971). Oxygen isotope fractionation between coexisting minerals of the Grimstad granite. Neues. Jahrb. Mineral. Monatsh, 26-33.

FRIEDRICHSEN, H. and HOERNES, S. (1976). Oxygen isotope studies on oceanic basalts of Leg 37 (abstr.). EOS Trans. Amer. Geophys. Union, 57, 413.

FRUEND, H.H. and TURNOCK, A.C. (1971). Petrology of the paragneiss at Quesnel Lake, Manitoba. Manitoba Mines Branch, Pub. 71-1, 227-234.

FYFE, W.S. (1973). The granulite facies, partial melting and the Archean crust. Phil. Trans. R. Soc. Lond., A 273, 457-461.

GARLICK, G.D. and DYMOND, J.D. (1970). Oxygen isotope exchange between volcanic material and ocean water. Geol. Soc. Amer. Bull., 81, 2137-2142.

GARLICK, G.D. and EPSTEIN, S. (1967). Oxygen isotope ratios in coexisting minerals of regionally metamorphosed rocks. Geochim. Cosmochim. Acta, 31, 181-214.

GARLICK, G.D., MACGREGOR, I.D. and VOGEL, D.E. (1971). Oxygen isotope ratios in eclogites from kimberlites. Science, 172, 1025-1027.

GARRELS, R.M. and MACKENZIE, F.T. (1969). Sedimentary rock types: relative proportions as a function of geological time. Science, 163, 570-571.

GARRELS, R.M. and MACKENZIE, F.T. (1971). Evolution of Sedimentary Rocks: A Geochemical Approach. Norton, N.Y., 397p.

GARRELS, R.M., MACKENZIE, F.T. and SIEVER, R. (1971). Sedimentary cycling in relation to the history of the continents and oceans. In The Nature of the Solid Earth (ed. E.C. Robertson). McGraw-Hill, N.Y., 93-121.

GARY, M., McAFEE, R., Jr. and WOLF, C.L. (eds.) (1972). Glossary of Geology. Amer. Geol. Inst., Washington, D.C., 805p.

GILL, J.B. (1974). Role of underthrust oceanic crust in the genesis of a Fijian calc-alkaline suite. Contrib. Mineral. and Petrol., 43, 29-45.

GILL, R.C.O. and BRIDGWATER, D. (1976). The Ameralik dykes of West Greenland, the earliest known basaltic rocks intruding stable continental crust. Earth Planet. Sci. Lett., 29, 276-282.

GLIKSON, A.Y. (1971). Primitive Archean element distribution patterns: chemical evidence and geotectonic significance. Earth Planet. Sci. Lett., 12, 309-320.

GLIKSON, A.Y. (1972). Early Precambrian evidence of a primitive ocean crust and island nuclei of sodic granite. Geol. Soc. Amer. Bull., 83, 3323-3344.

GLIKSON, A.Y. (1976a). Trace element geochemistry and origin of early Precambrian acid igneous series, Barberton Mountain Land, Transvaal. Geochim. Cosmochim. Acta, 40, 1261-1280.

GLIKSON, A.Y. (1976b). Earliest Precambrian ultramafic-mafic volcanic rocks: ancient oceanic crust or relic terrestrial maria? Geology 4, 201-205.

GLUSKOTER, H.J. (1964). Orthoclase distribution and authigenesis in the Franciscan Formation of a portion of western Marin County, California. Jour. Sed. Petrology, 34, 335-343.

GOLDICH, S.S., HANSON, G.N., HALLFORD, C.R. and MUDREY, M.G., Jr. (1972). Early Precambrian rocks in the Saganaga Lake - Northern Light Lake area, Minnesota-Ontario. Part I. Petrology and structure. Geol. Soc. Amer. Mem. 135, 151-177.

GOLDICH, S.S. and HEDGE, C.E. (1974). 3,800 Myr granitic gneiss in southwestern Minnesota. Nature, 252, 467-468.

GOLDICH, S.S., HEDGE, C.E. and STERN, T.W. (1970). Age of the Morton and Montevideo gneiss and related rocks, southwestern Minnesota. Geol. Soc. Amer. Bull., 81, 3671-3696.

GOLDSMITH, J.R. and LAVES, F. (1954a). The microcline-sanidine stability reactions. Geochim. Cosmochim. Acta, 5, 1-19.

GOLDSMITH, J.R. and LAVES, F. (1954b). Potassium feldspars structurally intermediate between microcline and sanidine. Geochim. Cosmochim. Acta, 6, 100-118.

GOODWIN, A.M. (1965). Preliminary report on volcanism and mineralization in the Lake of the Woods - Manitou Lake - Wabigoon region of northwestern Ontario. Ont. Dept. Mines, Prelim. Rept. 1665-2, 63p. Accompanied by Map. 1 inch to 4 miles.

GOODWIN, A.M. (1967). Volcanic studies in the Birch-Uchi Lakes area of Ontario. Ont. Dept. Mines, Misc. Paper 6.

GOODWIN, A.M. (1968a). Evolution of the Canadian shield. Geol. Assoc. Can. Proc., 19, 1-13.

GOODWIN, A.M. (1968b). Archean protocontinental growth and the early crustal history of the Canadian shield. XXIII Int. Geol. Congress, 1, 69-89.

GOODWIN, A.M. (1972). The Superior Province. In Variations in Tectonic Styles in Canada (eds. R.A. Price and R.J.W. Douglas). Geol. Assoc. Canada, Spec. Paper 11, 527-624.

GOODWIN, A.M. (1973). Archean iron formations and tectonic basins of the Canadian shield. Econ. Geol., 68, 915-933.

GOODWIN, A.M. (1974). Precambrian belts, plumes, and shield development. Amer. Jour. Sci., 274, 987-1028.

GOODWIN, A.M. (1976a). Lithologic and major element compositions, Superior geotraverse. Proc. 1976 Geotraverse Conference, 7-12.

GOODWIN, A.M. (1976b). Giant impacting and the development of the continental crust. In The Early History of the Earth (ed. B.F. Windley), Wiley and Sons, 77-95.

GOWER, C.F. (1975). The geology and tectonic evolution of the English River gneiss belt in the Jaffray-Melick area, near Kenora, northwest Ontario. Unpub. Tech. Memo 75-8, Dept. Geology, McMaster Univ., Hamilton, Canada.

GOWER, C.F. (1976). The geology of gneissic rocks in the Kenora district, English River gneiss belt. Proc. 22nd Meeting, Inst. on Lake Superior Geology, May 1976, 24.

GOWER, C.F. and CLIFFORD, P.M. (1977). Metamorphism in the English River Subprovince near Kenora, northwest Ontario. Proc. 23rd Meeting, Inst. on Lake Superior Geology, May 1977, 19.

GRAY, J., CUMMING, G.L. and LAMBERT, R.St.J. (1977). Oxygen and strontium isotopic compositions and thorium and uranium contents of basalts from DSDP 37 cores. In Initial Reports of the Deep-Sea Drilling Project, 37, U.S. Government Printing Office, Washington, D.C., 607-609.

GREEN, D.H. (1972). Archean greenstone belts may include terrestrial equivalents of lunar maria? Earth Planet. Sci. Lett., 15, 263-270.

GREEN, D.H. (1974). Genesis of Archean peridotitic magmas and constraints on Archean geothermal gradients and tectonics. Geology, 3, 15-18.

GREEN, T.H. (1972). Crystallization of calc-alkaline andesite under controlled high-pressure conditions. Contrib. Mineral. and Petrol., 34, 150-166.

GREEN, T.H., BRUNFELT, A.O. and HEIER, K.S. (1972). Rare-earth element distribution and K/Rb ratios in granulites, mangerites and anorthosites, Lofoten-Vesteraalen, Norway. Geochim. Cosmochim. Acta, 36, 241-257.

GREEN, T.H. and RINGWOOD, A.E. (1968). Genesis of the calc-alkaline igneous rock suite. Contrib. Mineral. and Petrol., 18, 105-162.

HALLBERG, J.A. (1970). The petrology and geochemistry of metamorphosed Archean basic volcanic rocks between Coolgardie and Norseman, Western Australia. Ph.D. Thesis, Univ. Western Australia, Nedlands, W.A.

HALLBERG, J.A. and WILLIAMS, D.A.C. (1972). Archaean mafic and ultramafic rock associations in the eastern Goldfields Region, Western Australia. Earth Planet. Sci. Lett., 15, 191-200.

HANSON, G.N. and GOLDICH, S.S. (1972). Early Precambrian rocks in the Saganaga Lake - Northern Light Lake area, Minnesota-Ontario, Part II: petrogenesis. Geol. Soc. Amer., Mem, 135, 179-192.

HANSON, G.N., GOLDICH, S.S., ARTH, J.G. and YARDLEY, D.H. (1971). Age of the Early Precambrian rocks of the Saganaga Lake - Northern Light Lake area, Ontario - Minnesota. Can. Jour. Earth Sci., 8, 1110-1124.

HART, R.A. (1973). A model for chemical exchange in the basalt-seawater system of oceanic layer II. Can. Jour. Earth. Sci., 10, 799-816.

HART, S.R. (1969). K, Rb, Cs contents and K/Rb, K/Cs ratios of fresh and altered submarine basalts. Earth Planet. Sci. Lett., 6, 295-303.

HART, S.R. (1971). K, Rb, Cs, Sr and Ba contents and Sr isotope ratios of ocean floor basalts. Phil. Trans. R. Soc. Lond., A 268, 573-587.

HART, S.R., BROOKS, C., KROGH, R.E., DAVIS, G.L. and NAVA, D. (1970). Ancient and modern volcanic rocks: a trace element model. Earth Planet. Sci. Lett., 10, 17-28.

HART, S.R. and DAVIS, G.L. (1969). Zircon U-Pb and whole rock Rb-Sr ages and early crustal development near Rainy Lake, Ontario. Geol. Soc. Amer. Bull., 80, 595-616.

HART, S.R., ERLANK, A.J. and KABLE, E.J.D. (1974). Sea floor basalt alteration: some chemical and Sr isotopic effects. Contrib. Mineral. and Petrol., 44, 219-230.

HART, S.R. and NALWALK, A.J. (1970). K, Rb, Cs and Sr relationships in submarine basalts from the Puerto Rico Trench. Geochim. Cosmochim. Acta, 34, 145-155.

HEATON, T.H.E. and SHEPPARD, S.M.F. (1974). Hydrogen and oxygen isotope evidence for the origins of the fluids during the metamorphism of oceanic crust (Troodos complex, Cyprus) (abstr.). N. Atl. Treaty Organ. Advan. Study Inst., Nancy, France.

HEDGE, C.E. and WALTHALL, F.G. (1963). Radiogenic strontium 87 as an index of geological processes. Science, 140, 1214-1217.

HEIER, K.S. (1973). Geochemistry of granulite facies rocks and problems of their origin. Phil. Trans. R. Soc. Lond., A 273, 429-442.

HEIER, K.S. and THORESEN, K. (1971). Geochemistry of high grade metamorphic rocks, Lofoten-Vesteraalen, North Norway. Geochim. Cosmochim. Acta, 35, 89-99.

HEIMLICH, R.A. (1971). Greenstone assimilation by tonalitic magma, Atikwa Lake. Geol. Mag., 108, 1-12.

HENDERSON, J.B. (1972). Sedimentology of Archean turbidites at Yellowknife, Northwest Territories. Can. Jour. Earth Sci., 9, 882-902.

HENDERSON, J.B. (1975). Sedimentology of the Archean Yellowknife Supergroup at Yellowknife, District of Mackenzie. Geol. Surv. Can. Bull. 246, 62p.

HEWITT, D.F. (1963). The Timiskaming series of the Kirkland Lake area. Can. Mineral., 7, 497-523.

HIGUCHI, H. and NAGASAWA, H. (1969). Partition of trace elements between rock-forming minerals and the host volcanic rocks. Earth Planet. Sci. Lett., 7, 281-287.

HOERNES, S. and FRIEDRICHSEN, H. (1974). Oxygen isotope studies on metamorphic rocks of the Western Hohe Tauern area (Austria). Schweiz. Mineral. Petrogr. Mitt., 54, 769-788.

HOLLOWAY, J.R. and BURNHAM, C.W. (1972). Melting relations of basalt with equilibrium water pressure less than total pressure. Jour. Petrol., 13, 1-29.

HONMA, H. and SAKAI, H. (1976). Zonal distribution of oxygen isotope ratios in the Hiroshima granite complex, southwest Japan. Lithos, 9, 173-178.

HOVORKA, D. (1974). Amphibolites of migmatite areas, West Carpathian Mountains. Chem. Erde, XXXIII, 222-233.

HURST, R.W., BRIDGWATER, D., COLLERSON, K.D. and WETHERILL, G.W. (1975). 3600 m.y. Rb-Sr ages from very early Archean gneisses from Saglek Bay, Labrador. Earth Planet. Sci. Lett., 27, 393-403.

HYDE, R.S. and WALKER, R.G. (1977). Sedimentary environments and the evolution of the Archean greenstone belt in the Kirkland Lake area, Ontario. Geol. Surv. Can., Paper 77-1A, 185-190.

IRVINE, T.N. and BARAGAR, W.R.A. (1971). A guide to the chemical classification of the common volcanic rocks. Can. Jour. Earth Sci., 8, 523-548.

IUGS SUBCOMMISSION ON THE SYSTEMATICS OF IGNEOUS ROCKS (1973). Classification and nomenclature of plutonic rocks, recommendations. N. Jahrb. Miner. Mh., 149-164.

JAHN, B.M., SHIH, C.Y. and MURTHY, V.R. (1974). Trace element geochemistry of Archean volcanic rocks. Geochim. Cosmochim. Acta, 38, 611-627.

JAKES, P. and GILL, J. (1970). Rare earth elements and the island arc tholeiitic series. Earth Planet. Sci. Lett., 9, 17-28.

JAKES, P. and WHITE, A.J.R. (1970). K/Rb ratios of rocks from island arcs. Geochim. Cosmochim. Acta, 34, 849-858.

JAMES, H.L. and CLAYTON, R.N. (1962). Oxygen isotope fractionation in metamorphosed iron formations of the Lake Superior region and in other iron-rich rocks. Geol. Soc. Amer., Buddington Vol., 217-239.

JENKINS, R. and DE VRIES, J.L. (1972). Practical X-ray Spectrometry. 2nd edition, 2nd impression, Philips, Eindhoven, 200p.

JOLLY, W.T. (1974). Regional metamorphic zonation as an aid in study of Archean terrains: Abitibi region, Ontario. Can. Mineral., 12, 499-508.

JOLLY, W.T. (1975). Subdivision of the Archean lavas of the Abitibi area, Canada, from Fe-Mg-Ni-Cr relations. Earth Planet. Sci. Lett., 27, 200-210.

JOLLY, W.T. and SMITH, R.E. (1972). Degradation and metamorphic differentiation of the Keweenawan tholeiitic lavas of northern Michigan, U.S.A. Jour. Petrol., 13, 273-309.

KAY, R., HUBBARD, N.J. and GAST, P.W. (1970). Chemical characteristics and origin of oceanic ridge volcanic rocks. Jour. Geophys. Res., 75, 1585-1613.

KAYE, L. (1974). Crow Lake area, District of Kenora, Ont. Dept. Mines, Prelim. Maps, 920-921, Geol. Ser., Scale 1/4 mile to 1 inch.

KAYS, M.A. (1976). Comparative geochemistry of migmatized, interlayered quartzo-feldspathic and pelitic gneisses: a contribution from rocks of southern Finland and northeastern Saskatchewan. Precambrian Res., 3, 433-462.

KEITH, M.L. and WEBER, J.N. (1964). Carbon and oxygen isotope composition of selected limestones and fossils. Geochim. Cosmochim. Acta, 28, 1787-1816.

KNAUTH, L.P. and EPSTEIN, S. (1975). Hydrogen and oxygen isotope ratios in silica from the Joides Deep Sea Drilling Project. Earth Planet. Sci. Lett., 25, 1-10.

KNAUTH, L.P. and EPSTEIN, S. (1976). Hydrogen and oxygen isotope ratios in nodular bedded cherts. Geochim. Cosmochim. Acta, 40, 1095-1108.

KOLJONEN, T. and ROSENBERG, R.T. (1974). Rare earth elements in granitic rocks. Lithos, 7, 249-261.

KOLODNY, J. and EPSTEIN, S. (1976). Stable isotope geochemistry of deep sea cherts. Geochim. Cosmochim. Acta, 40, 1195-1209.

KRAUSKOPF, K.B. (1967). Introduction to Geochemistry. McGraw-Hill, Inc., N.Y., 721p.

KROGH, T.E., DAVIS, G.L., HARRIS, N.B.W. and ERMANOVICS, I.F. (1975). Isotopic ages in the eastern Lac Seul region of the English River gneiss belt. Carnegie Inst. Washington Year Book 74, 623-625.

KUNO, H., YAMASAKA, K., IIDA, C. and NAGASHIMA, K. (1957). Differentiation of Hawaiian magmas. Jap. Jour. Geol. Geography, 28, 179-218.

KWONG, Y.-T.J. (1975). Distribution of gold in an Archean greenstone belt as exemplified by the Kakagi Lake area, northwestern Ontario. Unpub. M.Sc. Thesis, McMaster Univ., Hamilton, Canada, 82p.

LAMBERT, I.B. and HEIER, K.S. (1967). The vertical distribution of uranium, thorium and potassium in the continental crust. Geochim. Cosmochim. Acta, 31, 377-390.

LAMBERT, R. St. J. (1976). Archean thermal regimes, crustal and upper mantle temperatures, and a progressive evolutionary model for the earth. In The Early History of the Earth (ed. B.F. Windley), Wiley and Sons, Ltd., 363-376.

LAMBERT, R. St. J., CHAMBERLAIN, V.E. and HOLLAND, J.G. (1976). The geochemistry of Archean rocks. In The Early History of the Earth (ed. B.F. Windley), Wiley and Sons, Ltd., 377-388.

LAMBERT, R. St. J. and HOLLAND, J.G. (1974). Yttrium geochemistry applied to petrogenesis utilizing calcium-yttrium relationships in minerals and rocks. Geochim. Cosmochim. Acta, 38, 1393-1414.

LANGFORD, F.F. and MORIN, J.A. (1976). The development of the Superior Province of northwestern Ontario by merging island arcs. Amer. Jour. Sci., 276, 1023-1034.

LANPHERE, M.A., IRWIN, N.P. and HOTZ, P.W. (1968). Isotopic age of the Nevadan Orogeny and older plutonic and metamorphic events in the Klamath Mountains, California. Geol. Soc. Amer. Bull., 79, 1027-1052.

LAVES, F. (1951): Artificial preparation of microcline. Jour. Geol., 59, 511-512.

LAWRENCE, J.R., GIESKES, J.M. and BROECKER, W.S. (1975). Oxygen isotope and cation composition of DSDP pore waters and the alteration of Layer II basalts. Earth Planet. Sci. Lett., 27, 1-10.

LAWSON, A.C. (1888). Report on the geology of the Rainy Lake region. Geol. Surv. Can., Ann. Rep., 3, Part 1, 1F-182F.

LAZARENKOV, V.G. (1962). On the process of normal hybridization. Zap. Vses., Mineral. Obschch. (1), 50-66 (in Russian), from Didier (1973) Granites and Their Enclaves, Elsevier, Amsterdam, 393p.

LEWIS, J.D. and SPOONER, C.M. (1973). K/Rb ratios in Precambrian granulite terrains. Geochim. Cosmochim. Acta, 37, 1111-1118.

LIPMAN, P.W. and FRIEDMAN, I. (1975). Interaction of meteoric water with magma: an oxygen-isotope study of ash-flow sheets from southern Nevada. Geol. Soc. Amer. Bull., 86, 695-702.

LONGSTAFFE, F.J. (1973). The petrology and geochemistry of Bijou Point. Unpub. B.Sc. Thesis, Univ. Windsor, Windsor, Canada, 65p.

LONGSTAFFE, F.J. (1975). A proposal for an oxygen and strontium isotope study of the Archean crustal evolution of a granite-greenstone area and gneissic belt terrain in northwestern Ontario. Unpub. Research Proposal, McMaster Univ., Hamilton, Canada, 52p.

LONGSTAFFE, F.J., McNUTT, R.H. and SCHWARCZ, H.P. (1976a). Whole rock oxygen isotope results for Archean clastic metasediments. Abst. Program, 1976 Ann. Meetings, Geol. Assoc. Can., 1, 46.

LONGSTAFFE, F.J., McNUTT, R.H. and SCHWARCZ, H.P. (1976b). Geochemistry of the Lake Despair area, northwestern Ontario. Abst. Program, 1976 Ann. Meetings, Geol. Assoc. Can., 1, 48.

LONGSTAFFE, F.J., McNUTT, R.H. and SCHWARCZ, H.P. (1977a). Geochemistry of the Archean Lake Despair area, a preliminary report. Geol. Surv. Can., Paper 77-1A, 169-178.

LONGSTAFFE, F.J., McNUTT, R.H. and SCHWARCZ, H.P. (1977b). $^{18}O/^{16}O$ results for Archean plutonic rocks, Lake Despair area, northwestern Ontario. Proc. 23rd Meeting, Inst. on Lake Superior Geology, May 1977, 24.

LONGSTAFFE, F.J., McNUTT, R.H. and SCHWARCZ, H.P. (1977c). $^{18}O/^{16}O$ in Archean gneisses: primary and metamorphic variations (abstr.). Abst. Program, 1977 Ann. Meetings, Geol. Assoc. Can., 2, 33.

LONGSTAFFE, F.J. and SCHWARCZ, H.P. (1977). $^{18}O/^{16}O$ of Archean clastic metasedimentary rocks: a petrogenetic indicator for Archean gneisses? Geochim. Cosmochim. Acta, 41, 1303-1312.

LUTKOV, V.S. and MOGAROVSKIY, V.V. (1973). Geochemistry of hybridism in granitoids (illustrated by the Pamirs). Geochem. Int., 1199-1208; trans. from Geokhimiya, 11, 1627-1635.

MAALØE, S. and WYLLIE, P.J. (1975). Water content of a granite magma deduced from the sequence of crystallization determined experimentally with water-undersaturated conditions. Contrib. Mineral. and Petrol., 52, 175-191.

MACGREGOR, A.M. (1951). Some milestones in the Precambrian of southern Rhodesia. Geol. Soc. S. Africa Proc., 54, 27-71.

MAGARITZ, M. and TAYLOR, H.P., Jr. (1974). Oxygen and hydrogen isotope studies of serpentinization in the Troodos ophiolite complex, Cyprus. Earth Planet. Sci. Lett., 23, 8-14.

MAGARITZ, M. and TAYLOR, H.P., Jr. (1976a). Oxygen, hydrogen and carbon isotope studies of the Franciscan Formation, Coast Ranges, California. Geochim. Cosmochim. Acta, 40, 215-234.

MAGARITZ, M. and TAYLOR, H.P., Jr. (1976b). $^{18}O/^{16}O$ and D/H studies along a 500 km traverse across the Coast Range batholith and its country rocks, central British Columbia. Can. Jour. Earth Sci., 13, 1514-1536.

MAGARITZ, M. and TAYLOR, H.P., Jr. (1976c). Isotopic evidence for meteoric-hydrothermal alteration of plutonic igneous rocks in the Yakutat Bay and Skagway areas, Alaska. Earth Planet. Sci. Lett., 30, 179-190.

MARCHAND, M. (1973). Determination of Rb, Sr and Rb/Sr by XRF. Unpub. Tech. Memo 73-2, Dept. Geology, McMaster Univ., Hamilton, Canada.

MARCHAND, M. (1976). A geochemical and geochronologic investigation of meteorite impact melts at Mistastin Lake, Labrador and Sudbury, Ontario. Unpub. Ph.D. Thesis, McMaster Univ., Hamilton, Canada, 142p.

MARMO, V. (1973). Granite Petrology and the Granite Problem. Elsevier, Amsterdam, 244p.

MASON, R. (1973). The Limpopo mobile belt - southern Africa. Phil. Trans. R. Soc. Lond., A 273, 463-485.

MASUDA, A. (1968). Geochemistry of lanthanides in basalts of central Japan. Earth Planet. Sci. Lett., 4, 284-292.

MATSUHISA, Y. (1974). $^{18}O/^{16}O$ ratios of NBS-28 and some silicate reference samples. Geochem. Jour., 8, 103-107.

MATSUHISA, Y., GOLDSMITH, J.R. and CLAYTON, R.N. (1976). Oxygen isotopic fractionation in the system quartz-albite-anorthite-water. GSA Abstracts with Programs, 8, 999.

MATSUHISA, Y., HONMA, H., MATSUBAYA, O. and SAKAI, H. (1972). Oxygen isotopic study of the Cretaceous granitic rocks in Japan. Contrib. Mineral. and Petrol., 37, 65-74.

MATSUHISA, Y., TAINOSHO, Y. and MATSUBAYA, O. (1973). Oxygen isotope study of the Ibaragi granitic complex, Osaka, southwest Japan. Geochem. Jour., 7, 201-213.

MATTIAT, B. (1960). Beitrag zur Petrographie der Oberharzer Kulmgrauwacke. Contrib. Mineral. and Petrol., 7, 242-280.

McELHINNEY, M.W., BRIDEN, J.C., JONES, D.L. and BROCK, A. (1968). Geological and geophysical implications of paleomagnetic results from Africa. Rev. Geophys., 6, 201-237.

McRITCHIE, W.D. (1971). Geology of the Wanipigou-Winnipeg Rivers region, southeastern Manitoba. Manitoba Mines Branch, Pub. 71-1, Map 71-1/1.

McRITCHIE, W.D. and WEBER, N. (1971). Metamorphism and deformation in the Manigotagan gneissic belt, southeastern Manitoba. Manitoba Mines Branch, Pub. 71-1, 235-284.

MEHNERT, K.R. (1968). Migmatites and the Origin of Granitic Rocks. Elsevier, Amsterdam, 393p.

MIDDLETON, G.V. (1960). Chemical composition of sandstone. Geol. Soc. Amer. Bull., 71, 1011-1025.

MIDDLETON, G.V. (1972). Albite of secondary origin in Charny Sandstones, Quebec. Jour. Sed. Petrol., 42, 341-349.

MIYASHIRO, A., SHIDO, F. and EWING, M. (1969). Diversity and origin of abyssal tholeiite from the mid-Atlantic ridge near 24° and 30° north latitude. Contrib. Mineral. and Petrol., 23, 38-52.

MONTIGNY, R., JAVOY, M. and ALLEGRE, C.J. (1970). Sr^{87}/Sr^{86}, K/Rb and O^{18}/O^{16} ratios in the Pinde ophiolite complex, Greece (abstr.). Geol. Soc. Amer. Bull., Abstr. with Programs, 2, 627-628.

MOORBATH, S. (1976). Age and isotopic constraints for the evolution of Archean crust. In The Early History of the Earth (ed. B.F. Windley), Wiley and Sons, Ltd., 351-360.

MOORE, B.R. and DENNEN, W.H. (1970). A geochemical trend in silicon-aluminum-iron ratios and the classification of clastic sediments. Jour. Sed. Petrol., 40, 1147-1152.

MUEHLENBACHS, K. (1971). Oxygen isotope studies of rocks from mid-ocean ridges. Ph.D. Thesis, Univ. Chicago, Chicago.

MUEHLENBACHS, K. (1976). Oxygen-isotope geochemistry of DSDP Leg 34 basalts. In Initial Reports of the Deep-Sea Drilling Project, 34, U.S. Government Printing Office, Washington, D.C., 337-340.

MUEHLENBACHS, K. (1977a). Oxygen isotope geochemistry of rocks from DSDP Leg 37. Can. Jour. Earth Sci., 14, 771-776.

MUEHLENBACHS, K. (1977b). Oxygen-isotope geochemistry of DSDP Leg 37 rocks. In Initial Reports of the Deep-Sea Drilling Project, 37, U.S. Government Printing Office, Washington, D.C., 617-619.

MUEHLENBACHS, K., ANDERSON, A.T. and SIGVALDASON, G.E. (1974). Low-O^{18} basalts from Iceland. Geochim. Cosmochim. Acta, 38, 577-588.

MUEHLENBACHS, K. and CLAYTON, R.N. (1971). Oxygen isotope ratios of submarine diorites and their constituent minerals. Can. Jour. Earth Sci., 8, 1591-1595.

MUEHLENBACHS, K. and CLAYTON, R.N. (1972a). Oxygen isotope studies of fresh and weathered submarine basalts. Can. Jour. Earth Sci., 9, 172-184.

MUEHLENBACHS, K. and CLAYTON, R.N. (1972b). Oxygen isotope geochemistry of submarine greenstones. Can. Jour. Earth Sci., 9, 471-478.

MUEHLENBACHS, K. and CLAYTON, R.N. (1976). Oxygen isotope composition of the oceanic crust and its bearing on seawater. Jour. Geophys. Res., 81, 4365-4369.

MYSON, B. (1976). Partitioning of samarium and nickel between olivine, orthopyroxene, and liquid; preliminary data at 20 kbar and 1025°C. Earth Planet. Sci. Lett., 31, 1-7.

NAGASAWA, H. (1971). Partitioning of Eu and Sr between coexisting plagioclase and K-feldspar. Earth Planet. Sci. Lett., 13, 139-144.

NANCE, W.B. and TAYLOR, S.R. (1977). Rare earth element patterns and crustal evolution. II. Archean sedimentary rocks from Kalgoorlie, Australia. Geochim. Cosmochim. Acta, 41, 225-231.

NANZ, R.H. (1953). Chemical composition of pre-Cambrian slates with notes on the geochemical evolution of lutites. Jour. Geol., 61, 51-64.

NAQVI, S.M. and HUSSAIN, S.M. (1972). Petrochemistry of early Precambrian metasediments from the central part of the Chitaldrug schist belt, Mysore, India. Chem. Geol., 10, 109-135.

NOCKOLDS, S.R. and ALLEN, R. (1953). The geochemistry of some igneous rock series. Geochim. Cosmochim. Acta, 4, 105-142.

NORRISH, K. and CHAPPEL, R.W. (1967). X-ray fluorescence spectrography. In Physical Methods in Determinative Mineralogy (ed. J. Zussman), Academic Press, London, 161-214.

OJAKANGAS, R.W. (1972). Archean volcanogenic graywackes of the Vermilion District, northeastern Minnesota. Geol. Soc. Amer. Bull., 83, 429-442.

ONDRICK, C.W. and GRIFFITHS, J.G. (1969). Frequency distribution of elements in Rensselaer graywacke, Troy, New York. Geol. Soc. Amer. Bull., 80, 509-518.

O'NEIL, J.R., ADAMI, L.H. and EPSTEIN, S. (1975). Revised value for the O^{18} fractionation between CO_2 and H_2O at 25°C. Jour. Research, U.S. Geol. Survey, 3, 623-624.

O'NEIL, J.R. and CLAYTON, R.N. (1964). Oxygen isotope geothermometry. In Isotopic and Cosmic Chemistry (Urey Volume) (eds. H. Craig, S.L. Miller and G.J. Wasserburg), North-Holland, 157-168.

O'NEIL, J.R. and EPSTEIN, S. (1966). A method for oxygen isotopic analysis of milligram quantities of water and some of its applications. Jour. Geophys. Rés., 71, 4955-4961.

O'NEIL, J.R., SHAW, S.E. and FLOOD, R.H. (1977). Oxygen and hydrogen isotope compositions as indicators of granite genesis in the New England batholith, Australia. Contrib. Mineral. and Petrol., 62, 313-328.

O'NEIL, J.R. and TAYLOR, H.P., Jr. (1967). The oxygen isotope and cation exchange chemistry of feldspars. Amer. Mineral., 52, 1414-1437.

O'NEIL, J.R. and TAYLOR, H.P., Jr. (1969). Oxygen isotope fractionation between muscovite and water. Jour. Geophys. Res., 74, 6012-6222.

O'NIONS, R.K. and PANKHURST, R.J. (1976). Sr isotope and rare earth element geochemistry of DSDP Leg 37 basalts. Earth Planet. Sci. Lett., 31, 255-261.

OSKVAREK, J.D. and PERRY, E.C., Jr. (1976). Temperature limits on the early Archaean ocean from oxygen isotope variations in the Isua supracrustal sequence, West Greenland. Nature, 259, 192-194.

OXFORD ISOTOPE GEOLOGY LABORATORY and McGREGOR, V.R. (1971). Isotopic dating of very Early Precambrian amphibolite facies gneisses from the Godthaab District, West Greenland. Earth Planet. Sci. Lett., 12, 245-259.

PEACOCK, M.A. (1931). Classification of igneous rock series. Jour. Geol., 39, 54-67.

PEARCE, J.A. and CANN, J.R. (1973). Tectonic setting of basic volcanic rocks determined using trace element analyses. Earth Planet. Sci. Lett., 19, 290-300.

PEARCE, T.H. (1968). A contribution to the theory of variation diagrams. Contrib. Mineral. and Petrol., 19, 142-157.

PEARCE, T.H. and BIRKETT, T.C. (1974). Archean metavolcanic rocks from Thackeray township, Ontario. Can. Mineral., 12, 509-519.

PEARCE, T.H., GORMAN, B.E. and BIRKETT, T.C. (1975). The TiO_2-K_2O-P_2O_5 diagram: a method of discriminating between oceanic and non-oceanic basalts. Earth Planet. Sci. Lett., 24, 419-426.

PEELING, G.R. (1974). Petrography and geochemistry of sedimentary rocks of the Yellowknife Supergroup (Archean) Slave Province, Northwest Territories. Unpub. M.Sc. Thesis, Carleton Univ., Ottawa, Canada.

PERRY, E.C. Jr. (1967). The oxygen isotope chemistry of ancient cherts. Earth Planet. Sci. Lett., 3, 62-66, errata p.496.

PERRY, E.C., Jr., AHMAD, S.N., READ, D.L. and SWULIUS, T.M. (1976). Oxygen and carbon isotope geochemistry of the 3.7 AE Isua supracrustal belt, West Greenland (abstr.). Geol. Soc. Amer. Abstr. with Programs 8, 1047-1048.

PERRY, E.C., Jr., AHMAD, S.N. and SWULIUS, T.M. (1977). The oxygen isotope composition of 3800 m.y. old metamorphosed chert and iron formation from Isukasia, West Greenland. Jour. Petrol. (in press).

PERRY, E.C., Jr. and TAN, F.C. (1972). Significance of oxygen and carbon isotope variations in Early Precambrian cherts and carbonate rocks of southern Africa. Geol. Soc. Amer. Bull., 83, 647-664.

PETTIJOHN, F.J. (1943). Archaean sedimentation. Geol. Soc. Amer. Bull., 54, 925-972.

PETTIJOHN, F.J. (1957). Sedimentary Rocks (2nd ed.), Harper and Row, 718p.

PETTIJOHN, F.J. (1963). Data of geochemistry. Chapter S: Chemical composition of sandstones - excluding carbonate and volcanic sands. U.S. Geol. Surv. Prof. Paper 440-S, 19p.

PETTIJOHN, F.J. and BASTRON, H. (1959). Chemical compositions of argillites of the Cobalt Series (Precambrian) and the problems of soda-rich sediments. Geol. Soc. Amer. Bull., 70, 593-599.

PETTIJOHN, F.J., POTTER, P.E. and SIEVER, R. (1973). Sand and Sandstones. Springer-Verlag, N.Y., 618p.

PHILPOTTS, J.A. (1970). Redox estimation from a calculation of Eu^{2+} and Eu^{3+} concentrations in natural phases. Earth Planet. Sci. Lett., 9, 257-268.

PHILPOTTS, J.A. and SCHNETZLER, C.C. (1968). Europium anomalies and the genesis of basalt. Chem. Geol., 3, 5-13.

PHILPOTTS, J.A., SCHNETZLER, C.C. and HART, S.R. (1969). Submarine basalts: some K, Rb, Sr, Ba, rare-earth, H_2O and CO_2 data bearing on their alteration, modification by plagioclase, and possible source materials. Earth Planet. Sci. Lett., 7, 293-299.

PINEAU, F., JAVOY, M., HAWKINS, J.W. and CRAIG, H. (1976). Oxygen isotope variations in marginal basin and ocean-ridge basalts. Earth Planet. Sci. Lett., 28, 299-307.

PRINCE, L.A. and HANSON, G.N. (1972). Rb-Sr isochron ages for the Giants Range granite, northeastern Minnesota. Geol. Soc. Amer. Mem. 135, 217-225.

RAMBERG, H. (1967). Gravity deformation and the earth's crust as studied by centrifuged models. Academic Press, London.

RAMSAY, C.R. (1973). Controls of biotite zone mineral chemistry in Archaean metasediments near Yellowknife, Northwest Territories, Canada. Jour. Petrol., 14, 467-488.

RAMSAY, J.G. (1963). Structural investigations in the Barberton Mountain Land, eastern Transvaal. Trans. Geol. Soc. S. Africa, 66, 353-398.

RAY, S. (1970). The plutonic concept. Jour. Geol. Soc. India, 11, 54-60.

REED, J.J. (1957). Petrology of the Lower Mesozoic rocks of the Wellington district. Bull. Geol. Surv. New Zealand, 57p.

REILLY, G.A. and SHAW, D.M. (1967). An estimate of the composition of part of the Canadian Shield in northwestern Ontario. Can. Jour. Earth Sci., 4, 725-739.

REIMER, T.O. (1972). Diagenetic reactions in Early Precambrian graywackes of the Barberton Mountain Land (South Africa). Sediment. Geol., 7, 263-282.

RIDLER, R.H. (1965). Petrographic study of a Crow Lake ultrabasic sill, Keewatin volcanic belt, northwestern Ontario. Unpub. M.Sc. Thesis, Univ. Toronto, Toronto, Canada.

RIDLER, R.H. (1969). The relationship of mineralization to volcanic stratigraphy in the Kirkland Lake area, Ontario. Unpub. Ph.D. Thesis, Univ. Wisconsin.

RIDLER, R.H. (1970). Relationship of mineralization to volcanic stratigraphy in the Kirkland-Larder Lakes area, Ontario. Geol. Assoc. Can. Proc., 21, 33-42.

RIDLER, R.H. (1976). Stratigraphic keys to the gold metallogeny of the Abitibi Belt. Can. Mineral. Jour., 97, 2-8.

RINGWOOD, A.E. (1975). Composition and Petrology of the Earth's Mantle. McGraw-Hill, Inc., N.Y., 618p.

ROBERTSON, D.K. (1973). A model discussing the early history of the earth based on a study of lead isotope ratios from veins in some Archean cratons of Africa. Geochim. Cosmochim. Acta, 37, 2099-2124.

ROGERS, J.J.W. (1966). Geochemical significance of source rocks of some greywackes from Western Oregon and Washington. Texas Jour. Sci., 18, 5-20.

ROGERS, J.W., CONDIE, K.C. and MAHAN, S. (1969). Significance of thorium, uranium and potassium in some early Precambrian graywackes from Wyoming and Minnesota. Chem. Geol., 5, 207-213.

ROGERS, J.J.W. and DONNELLY, T.W. (1966). Radiometric evidence for the origin of eugeosynclinal materials. Tulane Studies Geol., 4, 133-140.

ROGERS, J.J.W. and RICHARDSON, K.A. (1964). Thorium and uranium contents of some sandstones. Geochim. Cosmochim. Acta, 28, 2005-2011.

RONOV, A.B. (1972). Evolution of rock composition and geochemical processes in the sedimentary shell of the earth. Sedimentology, 19, 157-172.

ROUTTI, J.T. (1969). SAMPO, A Fortran IV program for computer analysis of gamma spectra from Ge(Li) detectors, and for other spectra with peaks. Lawrence Radiation Lab. Report UCRL 19452, 33p.

RYE, R.O., SCHUILING, R.D., RYE, D.M. and JANSEN, J.B.H. (1976). Carbon, hydrogen and oxygen isotope studies of the regional metamorphic complex at Naxos, Greece. Geochim. Cosmochim. Acta, 40, 1031-1049.

SAGGERSON, E.P. and OWEN, L.M. (1969). Geol. Soc. S. Africa, Spec. Pub. 2.

SAVIN, S. and EPSTEIN, S. (1970a). The oxygen and hydrogen isotope geochemistry of clay minerals. Geochim. Cosmochim. Acta, 34, 25-42.

SAVIN, S. and EPSTEIN, S. (1970b). The oxygen isotopic compositions of coarse grained sedimentary rocks and minerals. Geochim. Cosmochim. Acta, 34, 323-329.

SAVIN, S. and EPSTEIN, S. (1970c). The oxygen and hydrogen isotope geochemistry of ocean sediments and shales. Geochim. Cosmochim. Acta, 34, 43-63.

SAWADA, K. and KANMORA, K. (1973). Greenstones from the Sorachi and Hidaka Groups of the Hidaka Mountains, Hokkaido. Mem. Nat. Sci. Mus. Tokyo, 6, 147-161.

SCHILLING, J.-G. (1971). Sea-floor evolution: rare-earth evidence. Phil. Trans. R. Soc. Lond., A 268, 663-706.

SCHILLING, J.-G. and BONATTI, E. (1975). East Pacific Ridge (2°S-19°S) versus Nazca intraplate volcanism: rare-earth evidence. Earth Planet. Sci. Lett., 25, 93-102.

SCHWARCZ, H.P. (1966). Chemical and mineralogic variations in an arkosic quartzite during progressive regional metamorphism. Geol. Soc. Amer. Bull., 77, 509-532.

SCHWARCZ, H.P. (1971). Conversion of mass spectrometric data for C, O, S. Unpub. Tech. Memo 71-7, Dept. Geology, McMaster Univ., Hamilton, Canada.

SCHWARCZ, H.P., CLAYTON, R.N. and MAYEDA, T. (1970). Oxygen isotopic studies of calcareous and pelitic metamorphic rocks, New England. Geol. Soc. Amer. Bull., 81, 2299-2316.

SEITZ, M.G. and HART, S.R. (1973). Uranium and boron distributions in some oceanic ultramafic rocks. Earth Planet. Sci. Lett., 7, 293-299.

SHACKLETON, R.M. (1973). Problems of the evolution of the continental crust. Phil. Trans. R. Soc. Lond., A 273, 317-320.

SHARMA, T., MUELLER, R.F. and CLAYTON, R.N. (1965). $^{18}O/^{16}O$ ratios of minerals from the iron formations of Quebec. Jour. Geol., 73, 664-667.

SHAW, D.M. (1969). Evaluation of Data. In Handbook of Geochemistry, Chapter 11, Vol. 1, 324-375, Springer-Verlag.

SHAW, D.M. (1970). Trace element fractionation during anatexis. Geochim. Cosmochim. Acta, 34, 237-243.

SHAW, D.M. (1972). The origin of the Apsley gneiss, Ontario. Can. Jour. Earth Sci., 9, 18-35.

SHAW, D.M. (1976). Development of the early continental crust. Part 2. Prearchean, protoarchean and later eras. In The Early History of the Earth (ed. B.F. Windley), Wiley and Sons, London, 33-53.

SHEPPARD, S.M.F., NIELSEN, R.L. and TAYLOR, H.P., Jr. (1969). Oxygen and hydrogen isotope ratios of clay minerals from porphyry copper deposits. Econ. Geol., 64, 755-777.

SHEPPARD, S.M.F., NIELSEN, R.L. and TAYLOR, H.P., Jr. (1971). Hydrogen and oxygen isotope ratios in minerals from porphyry copper deposits. Econ. Geol., 66, 515-542.

SHEPPARD, S.M.F. and SCHWARCZ, H.P. (1970). Fractionation of carbon and oxygen isotopes and magnesium between metamorphic calcite and dolomite. Contrib. Mineral. and Petrol., 26, 161-198.

SHEPPARD, S.M.F. and TAYLOR, H.P., Jr. (1974). Hydrogen and oxygen isotope evidence for the origins of water in the Boulder batholith and the Butte ore deposits, Montana. Econ. Geol., 69, 926-946.

SHIEH, Y.N. (1972). Instructions for the operation of the bromine pentafluoride line. Unpub. Tech. Memo 72-5, Dept. Geology, McMaster Univ., Hamilton, Canada.

SHIEH, Y.N. and SCHWARCZ, H.P. (1974). Oxygen isotope studies of granite and migmatite, Grenville province of Ontario, Canada. Geochim. Cosmochim. Acta, 38, 21-45.

SHIEH, Y.N. and SCHWARCZ, H.P. (1977). An estimate of the oxygen isotope composition of a large segment of the Canadian shield in northwestern Ontario. Can. Jour. Earth Sci., 14, 927-931.

SHIEH, Y.N., SCHWARCZ, H.P. and SHAW, D.M. (1976). An oxygen isotope study of the Loon Lake Pluton and the Apsley Gneiss, Ontario. Contrib. Mineral. and Petrol., 54, 1-16.

SHIEH, Y.N. and TAYLOR, H.P., Jr. (1969). Oxygen and hydrogen isotope studies of contact metamorphism in the Santa Rosa Range, Nevada, and other areas. Contrib. Mineral. and Petrol., 20, 306-356.

SHIMA, M., GROSS, W.H. and THODE, H.G. (1963). Sulfur isotope abundances in basic sills, differentiated granites and meteorites. Jour. Geophys. Res., 68, 2835-2847.

SIGHINOLFI, G.P. (1971). Investigations into deep crustal levels: fractionating effects and geochemical trends related to high-grade metamorphism. Geochim. Cosmochim. Acta, 35, 1005-1021.

SILVERMAN, S.R. (1951). The isotope geology of oxygen. Geochim. Cosmochim. Acta, 2, 26-42.

SINHA, A.K. (1976). Tectonic significance of Th/U ratios from Archean basalts. Chem. Geol., 18, 215-225.

SMITH, D.R., McNUTT, R.H. and CLIFFORD, P.M. (1973). Nature and origin of sialic pyroclastic rocks at Kakagi Lake, northwestern Ontario. Can. Jour. Earth Sci., 10, 538-550.

SMITH, J.R. and YODER, H.S. (1956). Variations in X-ray powder diffraction patterns of plagioclase feldspar. Amer. Mineral., 41, 632-647.

SMITH, J.V. (1974). Feldspar Minerals. 2: Chemical and Textural Properties. Springer-Verlag, N.Y., 690p.

SMITH, R.E. (1968). Redistribution of major elements in the alteration of some basic lavas during burial metamorphism. Jour. Petrol., 9, 191-219.

SMITH, R.E. and SMITH, S.E. (1976). Comments on the use of Ti, Zr, Y, Sr, K, P and Nb in classification of basaltic magmas. Earth Planet. Sci. Lett., 32, 114-120.

SPOONER, E.T.C., BECKINSALE, R.D., FYFE, W.S. and SMEWING, J.D. (1974). O^{18} enriched ophiolitic metabasic rocks from E. Liguria (Italy), Pindos (Greece), and Troodos (Cyprus). Contrib. Mineral. and Petrol., 47, 41-62.

STEIGER, R.H. and HART, S.R. (1967). The microcline-orthoclase transition within a contact aureole. Amer. Mineral., 52, 87-116.

STERN, C.R. (1974). Melting products of olivine tholeiite basalt in subduction zones. Geology, 2, 227-230.

STERN, C.R., HUANG, W.-L. and WYLLIE, P.J. (1975). Basalt-andesite-rhyolite-H_2O: crystallization intervals with excess H_2O and H_2O- undersaturated liquidus surfaces to 35 kilobars, with implications for magma genesis. Earth Planet. Sci. Lett., 28, 189-196.

STERN, C.R. and WYLLIE, P.J. (1973). Melting relations of basalt-andesite-rhyolite-H_2O and a pelagic red clay at 30 kbar. Contrib. Mineral. and Petrol., 42, 313-323.

STRECKEISEN, A. (1976). To each plutonic rock its proper name. Earth-Sci. Reviews, 12, 1-33.

STUCKLESS, J.S. and O'NEIL, J.R. (1973). Petrogenesis of the Superstition - Superior volcanic area as inferred by strontium and oxygen-isotope studies. Geol. Soc. Amer. Bull., 84, 1987-1997.

SUTCLIFFE, R.H. (1977). Geology and emplacement of the Jackfish Lake Pluton, a major intrusion in the Rainy Lake Dome. Univ. Toronto Geotraverse Conf. Report, 146-154.

SUTTON, J. (1976). Tectonic relationships in the Archaean. In The Early History of the Earth (ed. B.F. Windley), Wiley and Sons, Ltd., London, 99-104.

TALBOT, C.J. (1968). Thermal convection in the Archean crust? Nature, 220, 552-556.

TALBOT, C.J. (1973). A plate tectonic model for the Archean crust. Phil. Trans. R. Soc. Lond., A 273, 413-427.

TARNEY, J., DALZIEL, I.W.D. and DE WIT, M.J. (1976). Marginal basin 'Rochas Verdes' Complex from S. Chile: a model for Archaean greenstone belt formation. In The Early History of the Earth (ed. B.F. Windley), Wiley and Sons, Ltd., London, 131-146.

TAYLOR, H.P., Jr. (1968). The oxygen isotope geochemistry of igneous rocks. Contrib. Mineral. and Petrol., 19, 1-71.

TAYLOR, H.P., Jr. (1970). Oxygen isotope studies of anorthosites, with particular reference to the origin of bodies in the Adirondack mountains, New York. In Origin of Anorthosites, N.Y. State Museum and Sci. Serv. Mem. 18, 111-134.

TAYLOR, H.P., Jr. (1971). Oxygen isotope evidence for large-scale interaction between meteoric ground waters and Tertiary granodiorite intrusions, Western Cascade Range, Oregon. Jour. Geophys. Res., 76, 7855-7874.

TAYLOR, H.P., Jr. (1973). O^{18}/O^{16} evidence for meteoric-hydrothermal alteration and ore deposition in the Tonopah, Comstock Lode and Goldfield mining districts, Nevada. Econ. Geol., 68, 747-764.

TAYLOR, H.P., Jr. (1974). The application of oxygen and hydrogen isotope studies to problems of hydrothermal alteration and ore deposition. Econ. Geol., 69, 843-883.

TAYLOR, H.P., Jr. (1976). Water-rock interactions and the origin of H_2O in granitic batholiths (abstr.). William Smith Lecture, Geological Society Newsletter, 5, 14-15.

TAYLOR, H.P., Jr., ALBEE, A.L. and EPSTEIN, S. (1963). $^{18}O/^{16}O$ ratios of coexisting minerals in three assemblages of kyanite-zone pelitic schist. Jour. Geol., 71, 513-522.

TAYLOR, H.P., Jr. and COLEMAN, R.G. (1968). $^{18}O/^{16}O$ ratios of coexisting minerals in glaucophane-bearing metamorphic rocks. Geol. Soc. Amer. Bull., 79, 1727-1756.

TAYLOR, H.P., Jr. and EPSTEIN, S. (1962). Relationships between O^{18}/O^{16} ratio in coexisting minerals of igneous and metamorphic rocks. Parts 1 and 2. Geol. Soc. Amer. Bull., 73, 461-480; 675-694.

TAYLOR, H.P., Jr. and FORESTER, R.W. (1971). Low ^{18}O igneous rocks from the intrusive complexes of Skye, Mull and Ardnamurchan, Western Scotland. Jour. Petrol., 12, 465-497.

TAYLOR, H.P., Jr. and MAGARITZ, M. (1975). Oxygen and hydrogen isotope studies of 2.6-3.4 b.y. old granites from the Barberton Mountain Land, Swaziland, and the Rhodesian craton, south Africa. Abst. Program, Geol. Soc. Amer., 7, 1293.

TEAL, P.R. and WALKER, R.G. (1977). Stratigraphy and sedimentology of the Archean Manitou Group, northwestern Ontario. Geol. Surv. Can. Paper 77-1A, 181-184.

THOMPSON, G. and MELSON, W.G. (1970). Boron contents of serpentinites and metabasalts in the oceanic crust: implications for the boron cycle in the oceans. Earth Planet. Sci. Lett., 8, 61-65.

THOMSON, J.E. (1946). The Keewatin-Timiskaming unconformity in the Kirkland Lake district. Trans. R. Soc. Can., ser. 3, 40, 113-124.

TILTON, G.R. and GRUNENFELDER, M. (1968). Sphene, uranium-lead ages. Science, 159, 1458-1461.

TOWELL, D.G., SPIRN, R.V. and WINCHESTER, J.W. (1969). Europium anomalies and the genesis of basalt: a discussion. Chem. Geol., 4, 461-465.

TOWELL, D.G., WINCHESTER, J.W. and SPIRN, R.V. (1965). Rare-earth distributions in some rocks and associated minerals of the batholith of southern California. Jour. Geophys. Res., 70, 3485-3496.

TURI, B. and TAYLOR, H.P., Jr. (1971a). An oxygen and hydrogen isotope study of a granodiorite pluton from the Southern California batholith. Geochim. Cosmochim. Acta, 35, 383-406.

TURI, B. and TAYLOR, H.P., Jr. (1971b). O^{18}/O^{16} ratios of the Johnny Lyon granodiorite and Texas Canyon quartz monzonite plutons, Arizona, and their contact aureoles. Contrib. Mineral. and Petrol., 32, 138-146.

TURNER, C.C. (1972). Archaean sedimentation: alluvial fan and turbidite deposits, Little Vermilion Lake, northwestern Ontario. Unpub. M.Sc. Thesis, McMaster Univ., Hamilton, Canada, 211p.

TURNER, C.C. and WALKER, R.G. (1973). Sedimentology, stratigraphy and crustal evolution of the Archean greenstone belt near Sioux Lookout, Ontario. Can. Jour. Earth Sci., 10, 817-845.

UREY, H.C. (1947). The thermodynamic properties of isotopic substances. Jour. Chem. Soc., 562-581.

VALLANCE, T.G. (1973). Spilitic degradation of a tholeiitic basalt. Jour. Petrol., 15, 79-96.

VEIZER, J. (1973). Sedimentation in geologic history: recycling vs. evolution or recycling with evolution. Contrib. Mineral. and Petrol., 38, 261-278.

VILJOEN, M.J. and VILJOEN, R.P. (1969). The geology and geochemistry of the lower ultramafic unit of the Onverwacht Group and a proposed new class of igneous rocks. Geol. Soc. S. Africa Spec. Publ. 2, 55-85.

VINE, J.D. and TOURTELOT, E.B. (1973). Geochemistry of Lower Eocene sandstones in the Rocky Mountain region. U.S. Geol. Surv. Prof. Paper 789, 36p.

VISWANATHAN, S. (1974a). Oxygen isotope studies of Early Precambrian granitic rocks from the Giants Range batholith, northeastern Minnesota, U.S.A. Lithos, 7, 29-34.

VISWANATHAN, S. (1974b). Oxygen isotope ratios of quartz in granitic rocks of magmatic and metasomatic origins. Indian Jour. Earth Sci., 1, 12-21.

VOGEL, D.E. and GARLICK, G.D. (1970). Oxygen isotope ratios in metamorphosed eclogites. Contrib. Mineral. and Petrol., 28, 183-191.

WALKER, R.G. and PETTIJOHN, F.J. (1971). Archaean sedimentation: analysis of the Minnitaki basin, northwestern Ontario, Canada. Geol. Soc. Amer. Bull., 82, 2099-2130.

WEBER, J.N. (1965). Evolution of the oceans and the origin of fine-grained dolomites. Nature, 207, 930-933.

WENNER, D.B. and TAYLOR, H.P., Jr. (1971). Temperatures of serpentinization of ultramafic rocks based on O^{18}/O^{16} fractionation between coexisting serpentine and magnetite. Contrib. Mineral. and Petrol., 32, 165-185.

WENNER, D.B. and TAYLOR, H.P., Jr. (1973). Oxygen and hydrogen isotope studies of the serpentinization of ultramafic rocks in oceanic environments and continental ophiolite complexes. Amer. Jour. Sci., 273, 207-239.

WENNER, D.B. and TAYLOR, H.P., Jr. (1976). Oxygen and hydrogen isotope studies of a Precambrian granite-rhyolite terrane, St. Francois Mountains, southeastern Missouri. Geol. Soc. Amer. Bull., 87, 1587-1598.

WESTERMAN, C.J. (1973). Geologic investigations in the English River gneissic belt, N.W. Ontario (NTS 52-K). A progress report, 1973. Unpub. Tech. Memo 73-6, McMaster Univ., Hamilton, Canada.

WESTERMAN, C. (1975). Tectonic evolution of the Archean English River gneissic belt at Cedar Lake, N.W. Ontario (NTS 52-K). Unpub. Progress Rept., Dept. Geology, McMaster Univ., Hamilton, Canada.

WESTERMAN, C.J. (1977). Unpub. Ph.D. Thesis, to be completed 1977, McMaster Univ., Hamilton, Canada.

WHETTEN, J.T., KELLEY, J.-C. and HANSON, L.G. (1969). Characteristics of Columbia river sediment and sediment transport. Jour. Sed. Petrol., 39, 1149-1166.

WHITE, A.J.R., JAKES, P. and CHRISTIE, D.M. (1971). Composition of greenstones and the hypothesis of sea-floor spreading in the Archean. Geol. Soc. Australia, Spec. Publ. 3, 47-56.

WILDEMAN, T.R. and HASKIN, L.A. (1973). Rare earths in Precambrian sediments. Geochim. Cosmochim. Acta, 37, 419-438.

WILLIS, J.P., FESQ, H.W., KABLE, E.J.D. and BERG, G.W. (1969). The determination of barium in rocks by X-ray fluorescence spectrometry. Can. Spectr., 14, 150-163.

WILSON, A.F. and GREEN, D.C. (1971). The use of oxygen isotopes for geothermometry of Proterozoic and Archean granulites. Geol. Soc. Australia, Spec. Pub. 3, 389-400.

WILSON, A.F., GREEN, D.C. and DAVIDSON, L.R. (1970). The use of oxygen isotope geothermometry on the granulites and related intrusives, Musgrave Ranges, central Australia. Contrib. Mineral. and Petrol., 27, 166-178.

WILSON, H.D.B. (1973). Archean volcanic belts, Kakagi Lake and Stormy Lake sections. 1973 Ann. Rept., Univ. Manitoba, 74-84.

WILSON, H.D.B., MORRICE, M.G. and ZIEHLKE, D.V. (1974). Archean continents. Geoscience Canada, 1, 12-20.

WINDLEY, B.F. (1973). Crustal development in the Precambrian. Phil. Trans. R. Soc. Lond., A 273, 321-341.

WINDLEY, B.F. (1976). New tectonic models for the evolution of Archaean continents and oceans. In The Early History of the Earth (ed. B.F. Windley), Wiley and Sons, Ltd., London, 105-112.

WINDLEY, B.F. and SMITH, J.V. (1976). Archaean high grade complexes and modern continental margins. Nature, 260, 671-675.

WINKLER, H.F.G. (1976). Petrogenesis of Metamorphic Rocks (4th ed.), Springer-Verlag, N.Y., 334p.

WOLFF, M. (1977). Geochemistry of the Kakagi Lake area. Unpub. M.Sc. Thesis, McMaster Univ., Hamilton, Canada.

WOLLENBERG, H.A., SMITH, A.R. and BAILEY, E.H. (1967). Radioactivity of Upper Mesozoic graywackes in the northern Coast Ranges, California. Jour. Geophys. Res., 72, 4139-4150.

WYLLIE, P.J. (1971). The Dynamic Earth. Wiley and Sons, N.Y., 416p.

WYLLIE, P.J., HUANG, W.-L., STERN, C.R. and MAALØE, S. (1976). Granitic magmas: possible and impossible sources, water contents, and crystallization sequences. Can. Jour. Earth Sci., 13, 1007-1019.

YEH, H.-W. and SAVIN, S.M. (1977). The mechanism of burial metamorphism of argillaceous sediments. 3. Oxygen isotopic evidence. Geol. Soc. Amer. Bull. (in press).

YODER, H.S. and TILLEY, C.E. (1962). Origin of basaltic magmas, an experimental study of natural and synthetic rock systems. Jour. Petrol., 3, 342-532.

YOUNG, G.M. (1969). Geochemistry of early Proterozoic tillites and argillites of the Gowganda formations, Ontario, Canada. Geochim. Cosmochim. Acta, 33, 483-492.

APPENDIX I

OXYGEN ISOTOPE ACCURACY AND PRECISION, AND GEOTHERMOMETRY

1. ACCURACY AND PRECISION

Oxygen isotope analyses were performed on 12 mg rock and mineral samples ground to 200-300 mesh. Mineral purity was estimated by optical techniques to be greater than 97%, except for magnetite (> 90%). Oxygen extractions were performed using BrF_5 (Clayton and Mayeda, 1963; see Appendix II). O_2 was converted to CO_2 by reaction with a hot graphite rod (Taylor and Epstein, 1962). Mass spectrometric analyses of CO_2 were performed using a 90° sector, 6 inch radius, dual collecting Nier-type mass spectrometer. Stoichiometric yields are difficult to estimate for rock samples; measured yields generally compared within ±4% of theoretical yields calculated from major element compositions. Yields obtained for mineral samples were usually 100% ± 2 to 3. $\delta^{18}O$ mineral results for samples outside that range were generally discarded.

The experimental results are reported in the usual δ (del) notation relative to Standard Mean Ocean Water (SMOW) (Craig, 1961):

$$\delta \text{ (per mil)} = \left[\frac{R(\text{sample}) - R(\text{standard})}{R(\text{standard})} \right] \times 1000;$$

where $R = {}^{18}O/{}^{16}O$.

$\delta^{18}O$ results were calculated relative to an internal calcite standard (GCS), which has been calibrated relative to NBS 20 assuming $\delta^{18}O$ of NBS-20 = -4.14‰ on the PDB scale, $\delta^{18}O_{CO_2}$

of PDB = 0.22‰ relative to SMOW (Craig, 1957, 1961) and that the ^{18}O fractionation factor between CO_2 and H_2O at 25°C is equal to 1.0412 (O'Neil et al., 1975).

Conversion from $\delta^{46}CO_2$ (GCS) to $\delta^{18}O$ (SMOW) was made following Schwarcz (1971), but using a formula similar to that calculated by Fallick (pers. comm.), based upon more recent machine characteristics:

$$\delta^{18}O \text{ (SMOW)} = 1.02979 \cdot \delta^{46}CO_2 + 29.01$$

where $\delta^{13}C$ (GCS) of the carbon conversion rod equals -24.5‰ (Schwarcz, 1971).

Final $\delta^{18}O$ results were adjusted to the mean $\delta^{18}O$ value of a second internal standard (8.7‰; 135 determinations on our mass spectrometer; 8.67‰ on a Micromass 30.2, analysis courtesy of B. Coker, Canada Center for Inland Waters, Burlington, Ontario), which was run every hour along with each batch of 4 to 6 samples. This correction was necessary to account for a small linear time-dependent kinetic isotope fractionation which resulted from the gas flow through the mass spectrometer capillaries into the spectrometer analyzer tube. The average depletion observed was 0.069‰ per hour (range 0.037-0.085‰ per hour for 25 determinations).

A summary of the accuracy and precision of the oxygen isotope data presented in this study is given in Table A1-1a,b; individual results are given in Table A1-2a,b. The results of this study for standards OQQ (Oliver Quarry Quartz) and RQ (Rose Quartz) are virtually identical to those reported by other workers (Table A1-1a). Results for silica sand standard NBS-28 lie at the low end of the range reported by others for this standard (9.0 to 10.0°/$_{oo}$), but near the value obtained recently by other laboratories (9.0-9.5°/$_{oo}$). Our value for SBQ-1 (Snowbird Quartz) is somewhat peculiar. One vial gives a consistent $\delta^{18}O$ result of 15.7°/$_{oo}$, about 0.5°/$_{oo}$ lower than the generally accepted value of 16.2°/$_{oo}$; a second vial (SBQ-2), however, gives more reasonable results. The cause of this variation remains uncertain.

The reproducibility for unknowns is summarized in Table A1-1b. The largest errors occur, not unexpectedly, in the rock powder samples. Of the mineral samples, biotite has the largest error, probably because of the ease of alteration of the relatively loosely bonded OH radical. Nevertheless, the overall reproducibility of duplicates is quite satisfactory (±0.09°/$_{oo}$, 1σ).

Table A1-1a Accuracy and precision of $\delta^{18}O$ results (‰)

Standard	$\bar{x}$	1σ	S^2	2σ	Literature values
NBS 28 (45)	9.17	0.21	0.05	0.43	9.0[a], 9.5[b], 10.0[c], 9.2[d], 9.1[e], 9.4[f]
OQQ (12)	9.99	0.16	0.02	0.31	9.9[g], 9.9[g]
RQ (9)	8.45	0.13	0.02	0.27	8.45[h]
SBQ-1 (6)	15.71	0.07	0.01	0.14	16.2[h]
SBQ-2 (2)	16.35				16.2[h]

Values in parentheses indicate number of individual analyses

a. Lipman and Friedman (1975)

b. Matsuhisa (1974)

c. Friedman and Gleason (1973)

d. Coplen, from Olson, private communications (1975)

e. Olson, private communications (1975)

f. Kerridge, private communications (1977)

g. Shieh and Schwarcz (1974)

h. Beckinsale and Durham (1974), in Progress Report 1970-1973, the Natural Environment Research Council Publications Series C, #13, Great Britain.

Table A1-1b Precision on duplicate analyses of unknowns

Unknown		Mean of duplicate differences (±) °/₀₀	1σ	s^2 °/₀₀	2σ
Rock	(17)	0.17	0.10	0.01	0.19
Quartz	(37)	0.10	0.08	0.01	0.17
Microcline	(20)	0.12	0.08	0.01	0.17
Plagioclase	(11)	0.09	0.07	0.01	0.15
Epidote	(3)	0.09	0.06	-	0.12
Hornblende	(8)	0.10	0.08	0.007	0.16
Magnetite	(6)	0.12	0.09	0.008	0.18
Biotite	(27)	0.15	0.08	0.007	0.17
Total	(129)	0.12	0.09	0.008	0.18

Values in parentheses indicate number of pairs

Table A1-2a $\delta^{18}O$ results for standards

$\delta^{18}O$ °/₀₀	Yield (μmoles O_2/mg)	$\delta^{18}O$ °/₀₀	Yield (μmoles O_2/mg)
NBS 28			
DATA COLLECTED NOV. 1974-NOV. 1976			
9.02	16.9	9.32	16.7
9.11	16.9	9.21	16.5
9.22	16.7	9.14	16.7
9.33	16.7	9.21	16.6
9.51	16.5	9.28	16.8
9.04	16.9	9.25	17.1
8.72	16.6	9.23	17.0
8.94	16.6	9.39	16.7
8.79	16.6	9.34	16.6
8.81	16.5	9.12	17.1
8.99	16.6	9.22	16.8
9.03	17.0	9.34	16.4
9.01	16.7	9.08	16.5
9.04	17.0	9.51	16.5
9.65	16.7	8.97	16.6
9.01	16.9	9.24	16.7
9.42	16.4	9.32	17.1
8.93	16.6	9.16	16.4
8.79	16.4	9.27	16.8
9.47	16.6	9.02	17.0
9.52	16.7	9.12	17.1
9.24	16.5	9.13	17.0
9.23	16.7		

$\delta^{18}O$ °/₀₀	Yield (μmoles O_2/mg)	$\delta^{18}O$ °/₀₀	Yield (μmoles O_2/mg)
NBS 28			
RESULTS FOR INCORRECT YIELDS			
8.42	18.9	8.6	17.7
9.47	18.1	10.36	15.9
8.36	17.6	9.75	15.0
9.87	17.4	12.39	15.1
7.08	19.7	10.37	16.0
OLIVER QUARRY QUARTZ (OQQ)			
10.20	16.9	10.03	16.5
10.01	16.4	9.79	16.6
9.82	16.8	9.62	16.6
10.04	17.0	9.89	16.9
10.05	16.7	10.15	16.5
10.11	16.8	10.12	16.4
ROSE QUARTZ (RQ)			
8.59	16.5	8.57	16.6
8.28	16.7	8.42	16.7
8.53	16.7	8.55	17.1
8.44	16.4	8.45	16.6
8.22	16.7		
SNOWBIRD QUARTZ (SBQ)			
SBQ-1		SBQ-2	
15.78	16.6	16.33	16.7
15.62	16.9	16.37	16.9
15.72	16.9		
15.56	16.8		
15.72	16.5		
15.83	17.1		

Table A1-2b Duplicate differences of unknowns (‰)

ROCK SAMPLES (17)

± 0.07	± 0.17	± 0.09	± 0.28
.13	.18	.13	.05
.38	.15	.07	
.10	.31	.18	
.16	.32	.08	

QUARTZ (37)

± 0.12	± 0.12	± 0.11	± 0.05	± 0.06
.10	.17	.22	.25	
.01	.02	.02	.08	
.29	.00	.03	.03	
.25	.27	.07	.10	
.10	.30	.05	.10	
.15	.08	.06	.09	
.10	.03	.02	.14	
.03	.00	.02	.10	

MICROCLINE (20)

± 0.23	± 0.00	± 0.02	± 0.25
.20	.20	.27	.11
.10	.17	.08	.00
.22	.11	.01	.07
.07	.13	.13	.03

PLAGIOCLASE (11)

± 0.15	± 0.02	± 0.25	± 0.16
.01	.13	.10	.01
.11	.01	.07	

Table A1-2b (continued)

EPIDOTE (3)			
± 0.01	± 0.16	± 0.10	
HORNBLENDE (8)			
± 0.11	± 0.01	± 0.01	± 0.22
.10	.01	.22	.12
BIOTITE (27)			
± 0.22	± 0.25	± 0.19	± 0.09
.18	.26	.17	.31
.03	.23	.07	.06
.15	.12	.19	.03
.15	.03	.26	.25
.07	.10	.16	.02
.08	.18	.25	
MAGNETITE (6)			
± 0.10	± 0.07	± 0.19	
.29	.02	.06	

Values in parentheses indicate number of pairs

2. OXYGEN ISOTOPE GEOTHERMOMETRY

The oxygen isotope fractionation factor, α, for two minerals A and B can be expressed as

$$\alpha_{AB} = (^{18}O/^{16}O)_A / (^{18}O/^{16}O)_B .$$

This expression is related to δ by

$$\ln\alpha_{AB} = \ln\left(1 + \frac{\delta_A}{1000}\right) - \ln\left(1 + \frac{\delta_B}{1000}\right)$$

where

$$\delta(‰) = \frac{R(\text{sample}) - R(\text{standard})}{R(\text{standard})} \times 1000; \quad R = \frac{^{18}O}{^{16}O},$$

and

$$1000 \ln\alpha_{AB} \simeq \delta_A - \delta_B = \Delta_{AB} \quad \text{for } |\Delta| < 10.$$

Urey (1947) and Bigeleisen and Mayer (1947) were among the first to show that

$$\alpha \equiv K$$

if only one atom is exchanged. K is the equilibrium constant for an isotopic exchange reaction such as

$$H_2{}^{18}O + 1/2\ C\ {}^{16}O_2 \rightleftharpoons H_2{}^{16}O + 1/2\ C\ {}^{18}O_2$$

which involves only one set of exchangeable atoms in each compound. Urey and Bigeleisen and Mayer also recognized that

$$\ln K \alpha \frac{1}{T^2}, \qquad T \text{ in } °K$$

over a wide temperature range, and is independent of pressure effects.

Some experimentally calibrated oxygen isotope geothermometers of importance to this work include magnetite-H_2O (O'Neil and Clayton, 1964), alkali feldspar-H_2O and anorthite-H_2O (O'Neil and Taylor, 1967), muscovite-H_2O (O'Neil and Taylor, 1969), quartz-H_2O (Clayton et al., 1972a; Matsuhisa et al., 1976) and quartz-K-feldspar (Blattner, 1975).

Blattner used a somewhat different approach to the determination of α. He directly measured the oxygen isotope fractionation between fissure grown quartz, adularia, and calcite. The mineral samples were obtained from a geothermal (hot-spring) locality where direct measurements of temperature (250°C), pressure and solution chemistry were possible. Blattner and Bird (1974) equilibrated quartz and K-feldspar in a common fluid at 600°C and analyzed them as a mineral pair to obtain α. These two measurements of α were then combined to give a temperature relationship. Because the equation is based only on two points, its usefulness is somewhat limited. However, the analytical approach does avoid some of the problems encountered in experimental determination of α that involve isotopic measurement of an intermediate fluid phase.

A large number of empirical oxygen isotope geothermometers have been constructed, primarily by Taylor and his co-workers (Taylor and Coleman, 1968; Shieh and Taylor, 1969; Taylor, 1968; Wenner and Taylor, 1971). These geothermometers are calibrated to give reasonable temperatures for rocks believed to be in isotopic equilibrium. One of the most useful relationships of this sort is

$$\Delta \text{ quartz-biotite} = 0.59 \, \Delta \text{ quartz-magnetite}$$ (Taylor, 1968).

Another approach to the calibration of oxygen isotope geothermometers has been made by Bottinga and Javoy (1973, 1975). They combined theoretical calculations with the available experimental data for α and integrated this information with that available for natural rock assemblages to produce a series of geothermometric equations.

The geothermometers produced by these various techniques often give significantly different temperatures for the same mineral-pair fractionation. Table A1-3a illustrates such variation for the quartz-magnetite pairs analyzed in this study. Below 500°C, the results of different calculations agree; at higher temperatures, however, some serious discrepancies arise. Similar data for quartz-muscovite pairs (Table A1-3b) record the same difficulty. However, plagioclase-magnetite oxygen isotope temperatures (Table A1-3c), calculated by different methods, do agree, at least over the 400-500°C range observed

for the samples analyzed in this study.

Quartz-feldspar pairs are of less value to the geothermometry in this study, as the measured fractionations are small relative to the analytical error (±0.20°/$_{oo}$).

Of these equations, those developed by Bottinga and Javoy (1973, 1975) are the most useful, and have been employed throughout the text of the thesis, unless otherwise noted. These equations give geologically reasonable temperatures, and have the added advantage of allowing comparison of isotopic temperatures for a given sample from a number of different mineral-pair fractionations. The concordance of such temperatures provides a good estimate of the degree of oxygen isotope equilibrium present in any particular sample. However, there is one drawback; the theoretical basis for the Bottinga and Javoy (1975) equations is valid only at temperatures near or above 500°C. However, at least for the temperature range 350-500°C, reasonable temperatures are obtained, and these agree with most other semi-empirical estimates. Rye et al. (1976) have had similar success in applying these equations to temperatures as low as 350°C.

Table A1-4a and A1-4b list the isotopic temperatures for all samples analyzed in this study, calculated according to the method of Bottinga and Javoy (1975). A separate column also gives the quartz-biotite temperatures as calculated according to Taylor (1968); comparison between the two quartz-biotite temperatures is generally very good.

Table A1-3a Comparison of quartz-magnetite oxygen isotope geothermometers (T °C)

Sample No.	1	2	3	4
F110	470±10*	460±10	435±5	435±5
F103	530±15	495±10	470±10	510±10
F98	505±15	480±10	455±10	490±10
F150	645±20	560±10	535±10	615±10
F151	415±10	425±5	400±5	400±5
F149	565±15	515±10	490±10	545±10
G135	630±20	550±10	525±10	600±10
G715	830±35	640±15	635±15	775±20
G145	890±40	660±15	665±20	825±20
G596A	695±20	585±15	565±15	660±15
F26	500±10	480±10	455±10	455±10

*errors calculated for ±0.2 °/oo analytical variation

1. Taylor and Coleman (1968):

   (a) $1000 \ln_{\alpha} Q\text{-musc} = 1.16 + \frac{1.19(10^6)}{T^2}$; T in °K

   (b) $\Delta Q\text{-mag} = \Delta Q\text{-musc}/0.32$

   (c) $1000 \ln_{\alpha} Q\text{-}H_2O = \frac{3.57(10^6)}{T^2} - 2.73$; Taylor (1974)

   (d) $1000 \ln_{\alpha} \text{musc-}H_2O = \frac{2.38(10^6)}{T^2} - 3.89$; O'Neil & Taylor (1969)

2. Bottinga and Javoy (1975)

Table A1-3a/continued

3. Shieh and Schwarcz (1974):

(a) $1000 \ln_{\alpha} Q\text{-}H_2O = \frac{3.38(10^6)}{T^2} - 3.40$; T in °K

for T (°C) of 200-500°; Clayton et al. (1972a)

(b) $1000 \ln_{\alpha} Q\text{-}H_2O = \frac{2.51(10^6)}{T^2} - 1.96$; T in °K

for T (°C) of 500-750°; Clayton et al. (1972a)

(c) $1000 \ln_{\alpha} mag\text{-}H_2O = -3.41 - \frac{1.81(10^6)}{T^2}$; T in °K;

O'Neil and Clayton (1964) and Anderson et al. (1971)

4. As in (3), except the high temperature quartz-H_2O equation is replaced by

$1000 \ln_{\alpha} Q\text{-}H_2O \approx -0.20 + \frac{2.01(10^6)}{T^2}$; T in °K

at T (°C) of 500-700°C; calculated from the data of Matsuhisa et al. (1976).

Table A1-3b Comparison of quartz-muscovite oxygen isotope geothermometers (T °C)

Sample No.	1	2	3
L41	770±85*	885±105	605±30
L43	360±20	400±20	410±15

*errors calculated assuming ±0.2°/°° analytical variation

1. Taylor and Coleman (1968): as given in Table

2. Blattner (1975):

$$1000 \ln_{\alpha} \text{Q-musc} = 1.30 + \frac{1.27(10^6)}{T^2} \; ; \quad T \text{ in } °K$$

3. Bottinga and Javoy (1975):

$$1000 \ln_{\alpha} \text{Q-musc} = -0.60 + \frac{2.2(10^6)}{T^2} \; ; \quad T \text{ in } °K$$

Table A1-3c Comparison of plagioclase-magnetite oxygen isotope geothermometers (T °C)

Sample No.	1	2	3
F103	495±15*	520±15	505±15
F2	540±15	560±15	550±15
F46	415±10	410±10	420±10

*errors calculated for ±0.2‰ analytical variation

1. Bottinga and Javoy (1975)

2. Taylor (1968):

$$\Delta_{plag-mag} = \frac{3.38(10^6)}{T^2} + 3.40; \quad T \text{ in } °K$$

assumes plagioclase composition to be An_{45}

3. Anderson et al. (1971)

$$\Delta_{plag-mag} = \frac{(4.72 - 1.19\beta)10^6}{T^2}; \quad T \text{ in } °K$$

$\beta \equiv$ mole fraction of An

Table A1-4a Oxygen isotope geothermometry for the Lake Despair area (°C)

	ΔQ-kF	ΔQ-Pl	ΔQ-hb	ΔQ-bi	ΔQ-mag	ΔkF-hb	ΔkF-bi	ΔkF-mag	ΔPl-hb	ΔPl-bi	ΔPl-mag	ΔQ-bi*
FELSIC SCHISTS												
F124	355			405			425					365
F124	285			415			495					380
MAFIC AMPHIBOLITES												
F49									465			
F19									985			
FOOTPRINT GNEISS												
F110	345			380	460		395	495				345
F103		565		395	500					360	495	360
F10	415			405			405					370
F73	225			380			485					340
F152	900			590			525					580
F98	335			365	480		385	535				330
F99	1575			415			330					380
F150	295			365	560		400	690				330
F7	380			460			500					425
F151	380			405	425		415	435				370
F149	465			425	515		420	530				390
NORTHWEST BAY COMPLEX												
F31	615			490			495					460

Table A1-4a/continued

	ΔQ-kF	ΔQ-Pl	ΔQ-hb	ΔQ-bi	ΔQ-mag	ΔkF-hb	ΔkF-bi	ΔkF-mag	ΔPl-hb	ΔPl-bi	ΔPl-mag	ΔQ-bi*
JACKFISH LAKE COMPLEX												
F146									515	425		
F21						705	500		625	455		
F24						625			540			
F135	380	575	600	525		825	610		615	500		495
F118	305	370	450	455		570	550		510	505		420
F3	725	470	570	440		520	395		640	440		415
F37	160	280	540	415		-	635		1455	540		380
F26	600	325	575	560	480	575	550	460	1005	810	540	540
D1	310	390	490	460		655	555		635	510		425
F46						600		430	550		415	

Calculated using equations of Bottinga and Javoy (1975)

* Taylor (1968): $\Delta qtz\text{-}bi = 0.59\ \Delta qtz\text{-}mag$

Table A1-4b Oxygen isotope geothermometry for the Pakwash Lake and Kenora areas (°C)

	ΔQ-kF	ΔQ-Pl	ΔQ-hb	ΔQ-bi	ΔQ-mag	ΔkF-bi	ΔkF-mag	ΔPl-hb	ΔPl-bi	ΔQ-musc	ΔkF-musc	ΔQ-bi*
PAKWASH PARAGNEISS												
L37		1000		550					455			525
L40		490		395					360			360
L42	470			460		460						430
L41	475			530		560				605	795	505
L44B				410								375
L44A	235			375		560						340
L43	300			380		425				410	575	345
PAKWASH METASEDIMENTS												
L33		415		430					510			395
L30				520								495
KENORA AREA												
G106B				410								370
G110A	270			360		400						320
G135	340			420	550	470	640					390
G350A			475	410								370
G350B	625			410		365						370
G145	340			410	660	440	835					370
G715				395	640							360
G596A	475			435	585	420	615					410
G835B				430								400
G886	220			370		400						335
G867A								455				
G835A								610				

Calculated using equations of Bottinga and Javoy (1975)

* Taylor (1968): $\Delta qtz\text{-}bi = 0.59\ \Delta qtz\text{-}mag$

APPENDIX II

OPERATION OF THE BROMINE PENTAFLUORIDE LINE

1. INTRODUCTION AND PRINCIPLE

The purpose of the bromine pentafluoride (BrF_5) line is to extract O_2 quantitatively from silicates and oxides for mass spectrometric analysis of the $^{18}O/^{16}O$ ratios. In the feldspar-BrF_5 reaction, for example, the following takes place:

$$KAlSiO_3 + 8BrF_5 \rightarrow KF + AlF_3 + 3SiF_4 + 4O_2 + 8BrF_3$$

All of the products except O_2 are condensed in liquid nitrogen traps: the O_2 diffuses through the traps, is converted to CO_2 gas, and is then ready to be introduced into the mass spectrometer.

An oxygen extraction method needs to meet certain criteria in order to produce accurate results:

1. There must be no oxygen from any other source than the specimen being analyzed.
2. There must be no isotopic exchange between the sample, the apparatus, and associated reagents.
3. The oxygen extraction from the sample must be quantitative or else involve no isotopic fractionation.

A modified version of Clayton and Mayeda's (1963) procedure is described here. This report updates and modifies an earlier technical memorandum on the same subject by Shieh (1972).

2. CONSTRUCTION

The BrF_5 line is shown schematically in Figure A2-1. It can be divided into the following sections:

Metal line: This portion of the line is used to handle the corrosive BrF_5. It is made of Inconel except for areas where flexibility is necessary, in which case copper tubing is employed. Whitey valves are used to isolate various sections of the line. Three Kel-F tubes are used, KF-1 and KF-2 to store and distill BrF_5, and KF-3 to store condensible reaction products. The metal and glass lines are connected by a Kovar-Pyrex seal.

Glass line: This is composed of a $O_2 \rightarrow CO_2$ conversion tube, a mercury manometer for measuring yields of CO_2, a thermocouple vacuum gauge for measuring the $O_2 \rightarrow CO_2$ conversion, and a high vacuum Veeco gauge for use during leak detection operations. High vacuum is achieved by a mercury diffusion pump backed by a mechanical pump.

Waste Disposal System: At the end of the metal line there is a detachable glass U-tube (U-5) for the disposal of condensible wastes. This system is connected to a rough pump which transfers any potentially toxic noncondensible gases directly into a fume hood.

Nickel Reaction Vessels: The six gun-bored nickel reaction vessels are attached to a manifold by detachable flanges. The flanges are sealed by Teflon gaskets. A water-cooled copper-vinyl tubing system protects the gaskets from overheating (when the furnaces are in place) and from freezing (when the reaction vessels are immersed in liquid nitrogen).

Furnaces: Six resistance heated furnaces with individual temperature controls are used to heat the reaction vessels.

Dry Box: (not shown) The dry box is used to remove moisture from the samples and to avoid the introduction of moisture into the reaction vessels during sample loading. The air is dried by P_2O_5 and molecular sieves, and the air is circulated by a small fan. A system is also available whereby the air in the box can be exchanged for dry nitrogen gas. The nitrogen gas is passed at a moderate rate through a dry ice, carbon tetrachloride and chloroform water trap prior to its entry into the dry box. Flow rates of five to seven cubic feet per hour allow the nitrogen to diffuse sufficiently slowly through the water trap, and still exchange completely with the air in the dry box within three hours. A small hot plate, controlled by a variac, is located in the dry box. Samples are placed on this and heated at 100°C for about two hours (25 on the variac) prior to their loading into the reaction vessels.

Others: Face mask, rubber gloves, bucket of sand.

3. OPERATING PROCEDURES

I. Cleaning of the reaction vessels

1. Fill traps U-1, U-2, and U-3 with liquid nitrogen.
2. Evacuate the reaction vessels through the roughage pump.
3. Turn on the cold water which runs through the copper-vinyl tubing below the flanges of the reaction vessels.
4. Freeze out about 1000 micromoles of BrF_5 into each reaction vessel, one at a time. This can be accomplished by expanding the reagent on the portion of the metal line defined by V-3, V-4, V-6, V-7 to a reading of 24 on the pressure guage (Figure A2-2).
5. Place the furnaces on the reaction vessels and heat at 600°C for 5 to 6 hours. See Table A2-1 for variac settings.
6. Turn off the furnaces and remove them from the reaction vessels. Let the reaction vessels cool to room temperature.
7. Blow air through the copper-vinyl tubing until dry.
8. Empty the reaction vessels, one at a time, by transferring the BrF_5 and other products to the waste trap (KF-3). A liquid nitrogen trap should be placed on KF-3 and U-5 prior to this operation. When the reaction products have condensed in KF-3 to a point where no further decrease in pressure is noted on the pressure gauge, pump the remaining products through U-5 and the roughage pump until the pressure gauge reads 30. Close V-9 and V-10.

9. Closing V-7, open the reaction vessels to high vacuum through the mercury diffusion pump for about one hour. Check that traps U-1, U-2, and U-3 are filled with liquid nitrogen.
10. Close the valves on the reaction vessels; close V-4, V-5, and V-6; open V-7; remove the vinyl tubing; detach the manifold from the metal vacuum line. Place a plastic wrap securely over the exposed upper flange of the metal line to prevent excessive adsorption of moisture at this opening.
11. Dispose of the reagent in U-5 as described in Part V, Steps 4 and 5.

II. Sample loading in the dry box

1. Open the dry box and make sure that sufficient P_2O_5 is in the evaporating dishes and that freshly dried molecular sieves are in the container over the fan.
2. Load the manifold into the dry box and place the samples (about 12 milligrams of powder each) together in a petri dish onto the hot plate.
3. Close and seal the dry box with vinyl tape. Turn on the fan (a variac setting of 80 is adequate). Leave the samples overnight.

4. First thing in the morning, turn on the hot plate for 2 hours, as earlier described. If the humidity has not fallen near zero (less than or equal to 6 on the hygrometer), exchange the air in the dry box for dried nitrogen gas.
5. When the hygrometer reads near zero, detach in turn each vessel from the manifold and dump out gently any solid products of the previous reaction. Check to see if the teflon gaskets have been baked, that is, turned yellowish-brown. If so, replace the gasket carefully. Load the sample to the bottom of the reaction vessel and attach it back to the manifold securely. Turn off the fan.
6. Return the manifold to the metal line, and reseal the dry box.
7. Slowly evacuate the air in the metal line through the roughage pump. Make sure that U-1, U-2, U-3, and U-5 are filled with liquid nitrogen.
8. Expand 1000 micromoles of BrF_5 into the section of the metal line that has been exposed to the air (V-3, V-4, V-8, V-9, and the reaction vessel valves closed, and V-6 and V-7 open). Leave for about 5 to 8 minutes.
9. Transfer the BrF_5 etc., to KF-3 and then pump on the metal line through U-5 and the roughage pump until all traces of the BrF_5 have been removed. Slowly evacuate the dry air from the reaction vessels by gently cracking open each of the reaction vessel valves, pumping through

the roughage pump.

10. Closing V-7, S-3 and S-5, and opening V-4 and V-5, open the reaction vessels to the mercury diffusion pump, making sure that U-1, U-2 and U-3 are filled with liquid nitrogen.
11. Connect up the copper-vinyl tubing system to the cool water and heat the reaction vessels for 3 to 5 hours at 200-300°C while open to high vacuum.

III. Fluorination of samples

1. Shut off and remove the furnaces; allow the reaction vessels to cool to room temperature. Close V-5, V-4 and reaction vessel valves.
2. Immerse the reaction vessel in liquid nitrogen and freeze down approximately 5 times the stoichiometric amount of BrF_5 required for the reaction into each reaction vessel.

   Sample calculation:

   for quartz: $1SiO_2 + 2BrF_5 \rightarrow 1SiF_4 + 1O_2 + 2BrF_3$

   From 0.018 grams SiO_2, 300 micromoles of O_2 are theoretically released. Therefore, the reaction requires 600 micromoles of BrF_5. Therefore, a 5 times stoichiometric excess of reagent would be 3000 micromoles. Thus for this reaction, 3000 micromoles of BrF_5 would be

used, measured out as described earlier.

3. Pump away any non-condensible gases through U-5 and close the reaction vessel valve. Repeat this procedure for each reaction vessel. When all of the vessels have been fluorinated, and all of the reaction vessel valves are closed, evacuate the remainder of the metal line (with V-4 and V-5 closed) through the roughage pump to remove any traces of BrF_5. IT IS IMPORTANT TO REALIZE AT ALL TIMES THAT BrF_5 SHOULD NEVER BE LET INTO THE GLASS PORTION OF THE LINE.
4. Place the furnaces on the reaction vessels and heat to 550-600°C (Table A2-1). For rock, magnetite, olivine, garnet, and alumino-silicate samples, increase the temperature to 600°C. Reaction times vary from 8 to 15 hours.

IV. Separation of O_2 and conversion of O_2 to CO_2

1. Switch off and remove the furnaces, and allow them to cool to room temperature.
2. Switch on the thermocouple gauge, and note its position. Outgas glowly the carbon rod in the CO_2 conversion tube by heating it to "orange-red" temperatures at short intervals (on two minutes, off one minute) until the thermocouple gauge registers hard vacuum while the carbon

rod is on. Close S-3 and S-5.

3. Fill U-1, U-2 and U-3 with liquid nitrogen. Open the metal line to high vacuum (by closing V-7, and opening V-4 and V-5) for 30 minutes.
4. Close S-2, S-6 and S-7. Place the sample vessel on the line; open S-6 and evacuate it. Heat the vessel with the hot air gun for a few minutes.
5. Immerse the first reaction vessel in liquid nitrogen; isolate the CO_2 conversion tube from the mercury diffusion pump (it should already be in this configuration); open S-3 and note the position on the thermocouple gauge. Put a dewar on the conversion tube and fill with N_2 (l).
6. Slowly open the valve on the nickel reaction gessel part way and allow the oxygen to diffuse slowly through U-1, U-2 and U-3 to the CO_2 conversion tube. Close S-1 so as to store some O_2.
7. Turn on the graphite filament in the CO_2 conversion tube. Slowly increase the variac setting (to about 65 to 80) until the filament is orange-red. Keep the liquid nitrogen trap on the conversion tube full at all times. The oxygen combines with carbon to form CO_2 which condenses on the inner wall of the conversion tube. If the temperature of the filament is too high, CO will form; this shows up as a failure of pressure to drop to zero on the thermocouple gauge. It then becomes

necessary to reduce the filament temperature immediately and to introduce some of the saved O_2 in order to convert this non-condensible CO to condensible CO_2. The conversion of O_2 to CO_2 must be carried to completion to avoid the large isotopic fractionations that accompany the earlier formed CO_2.

8. After the oxygen is completely converted to CO_2 (as shown on the thermocouple gauge), close the nickel reaction vessel valve, and open the system to high vacuum in order to pump away any non-condensible gases. This non-condensible fraction should be very small.
9. Isolate the section of the glass line containing the CO_2 conversion chamber and the cold finger by closing S-3, S-4, S-6, and the sample tube stopcock. Transfer the CO_2 to the cold finger, and warm the conversion tube with warm water. Warm the carbon filament by passing a small voltage through it.
10. After a few minutes, open S-4 and check to see that all the CO_2 has frozen down into the cold finger, and pump away any non-condensible gas.
11. Close S-7; warm the cold finger and measure the yield of CO_2 on the right arm of the manometer (Figure A2-3). The yield should be within 100 ± 2% of the calculated value. Transfer the CO_2 into the sample tube; close the sample tube; close S-5; remove the sample tube and go to step 4. It is wise to check that all portions

of the glass line are free of any trace of the last sample before proceding to the next sample (i.e. pump on the glass line for a few minutes).

NOTE: the manometer has a pinhole leak which has been patched with cellulose acetate cement. Do not flame this tube or attempt to clean its outside with acetone, etc.

V. Disposal of excessive reagent and gaseous reaction products

1. Turn off the cold water in the copper-vinyl tubing and blow air through the tubing.
2. Closing V-4, V-5 and V-7, open the first nickel reaction vessel and record the reading on the pressure gauge. Transfer the reaction products to KF-3 (and through U-5 filled with liquid nitrogen if all of the material does not condense in KF-3). Repeat this for each reaction vessel.
3. The amount of excess reagent can then be calculated from Figure A2-2 by multiplying the pressure gauge reading in micromoles by 1.81.
4. Close V-8; don the safety shield and the safety gloves. Make sure U-5 is filled. Shut off the roughage pump; open and then close S-10 carefully and remove U-5 from

the line, keeping it immersed in liquid nitrogen at all times. Transfer the U tube in this fashion into the fumehood. Remove the U tube from the liquid nitrogen and fasten it to a retort stand. Close the fume hood.

5. Replace U-5 with another detachable U tube, using only miniscule amounts of grease on the connecting rubber "O" rings, and evacuate the line through the roughage pump.
6. When the level of waste reagent in KF-3 rises above one centimeter, transfer the waste to U-5 and repeat steps 4 and 5.

VI. Loading of BrF_5 into KF-1 and KF-2

BrF_5 is contained in a commercial cylinder attached to the metal line by a length of copper tubing. From time to time it is necessary to load KF-1 and KF-2 with the reagent. This procedure is not difficult, but because of the potentially hazardous nature of BrF_5, it should be carried out with care.

1. Pump out to the main valve on the BrF_5 cylinder with the roughage pump. The needle valve on the cylinder is open at this stage.
2. Still pumping, place liquid nitrogen on KF-1 to a depth of one inch.

3. Close the needle valve.
4. Open the main valve carefully.
5. Close off valve V-7 to the roughage pump.
6. Crack open the needle valve and observe the pressure rise on the pressure gauge.
7. Let the flow proceed for 2 to 3 minutes and then shut the needle valve. The pressure should drop slowly on the pressure gauge as the BrF_5 diffuses through the other non-condensible gases and freezes down in KF-1.
8. When the pressure drop levels out, open valve V-7 to the roughage pump and pump for 10 to 15 seconds until the gauge goes to vacuum.
9. Close valve V-7 to the roughage pump and go to step 6, unless sufficient reagent has been collected (in which case, go to step 10). Raise the level of liquid nitrogen on KF-1 an additional inch.

   NOTE: With each cycle the amount of non-condensible gas will be less. As the amount decreases, the BrF_5 transfers will become more efficient.
10. When sufficient BrF_5 has been collected, close the main valve on the cylinder carefully.
11. Open the needle valve and freeze out the remaining BrF_5 into KF-1. When the pressure gauge stabilizes, pump away the non-condensible gas.
12. Close the needle valve.

13. Distill the BrF_5 by freezing it from KF-1 to KF-2.

VII. Line maintenance

1. Check regularly for any leaks in the BrF_5 line.
2. The reaction vessels should be gently polished with steel wool when the metal fluoride coating on the inner wall becomes too thick.
3. The graphite filament should be replaced after combustion of every twelfth sample. The carbon rod should be thinned at its centre by polishing with steel wool. A small drill is available for making the connection sockets in the rod. The conversion tube should also be cleaned at this time.
4. The stopcocks on the line should be regreased when they become stiff.

VIII. Safety precautions

BrF_5 is an extremely dangerous chemical. It reacts violently with water, acetone, and hydrocarbons, including grease. It etches glass at room temperature.

The recommended treatment for the toxic effect of bromine and its related compounds is as follows:

1. If bromine vapour has been inhaled, cautious inhalation of ammonia is suggested, with artificial respiration and oxygen when necessary.
2. Splashes should be immediately washed off the skin and a paste of sodium bicarbonate or phenol glycerine applied, followed by an emolient dressing.
3. In any event, any contact with the reagent should be regarded as serious and immediate medical treatment sought.

The following suggestions (Shieh, 1972) will help prevent accidents:

1. Do not operate the BrF_5 line if there is a leak.
2. Never use a flame or a spark near the BrF_5 traps.
3. Transfer BrF_5 slowly.
4. Never allow water to condense in the BrF_5 traps as BrF_5 and water react violently.
5. The laboratory bench should be kept clear of all flammable materials.
6. Always wear the face mask and gloves (over elbow type) when disposing of BrF_5 and any other gaseous reaction products.
7. Use sand to extinguish any fire resulting from BrF_5.
8. Never work alone with BrF_5!

IX Line modifications performed during this study

1. Venting of roughage pump, and replacement of both fore-pumps.
2. Addition of VEECO high-vacuum detection guages.
3. Replacement of nickel reaction vessels with gun-bored vessels.
4. Replacement of Whitey valves.
5. Temperature profiling of reaction vessels.
6. Introduction of dry N_2 gas-flow into the dry box.
7. Full-range variac control for CO_2 conversion chamber.

FIGURE A2-1 Schematic of the BrF_5 line

V: Whitey valve number referred to in the text

S: Stopcock number referred to in the text

1. Furnace temperature controls
2. Furnaces
3. Water line inlet
4. Water line outlet
5. To rough pump (mechanical) and fume hood
6. Vacuum gauge
7. Veeco ionization tube
8. Veeco ionization vacuum gauge
9. CO_2 conversion tube and carbon rod
10. Carbon rod variac control
11. Thermocouple vacuum gauge
12. Thermocouple vacuum tube
13. Glass (Pyrex) sample tube
14. Cold finger
15. Mercury manometer
16. To mercury diffusion and mechanical fore-pumps

Diagram modified from Shieh (1972)

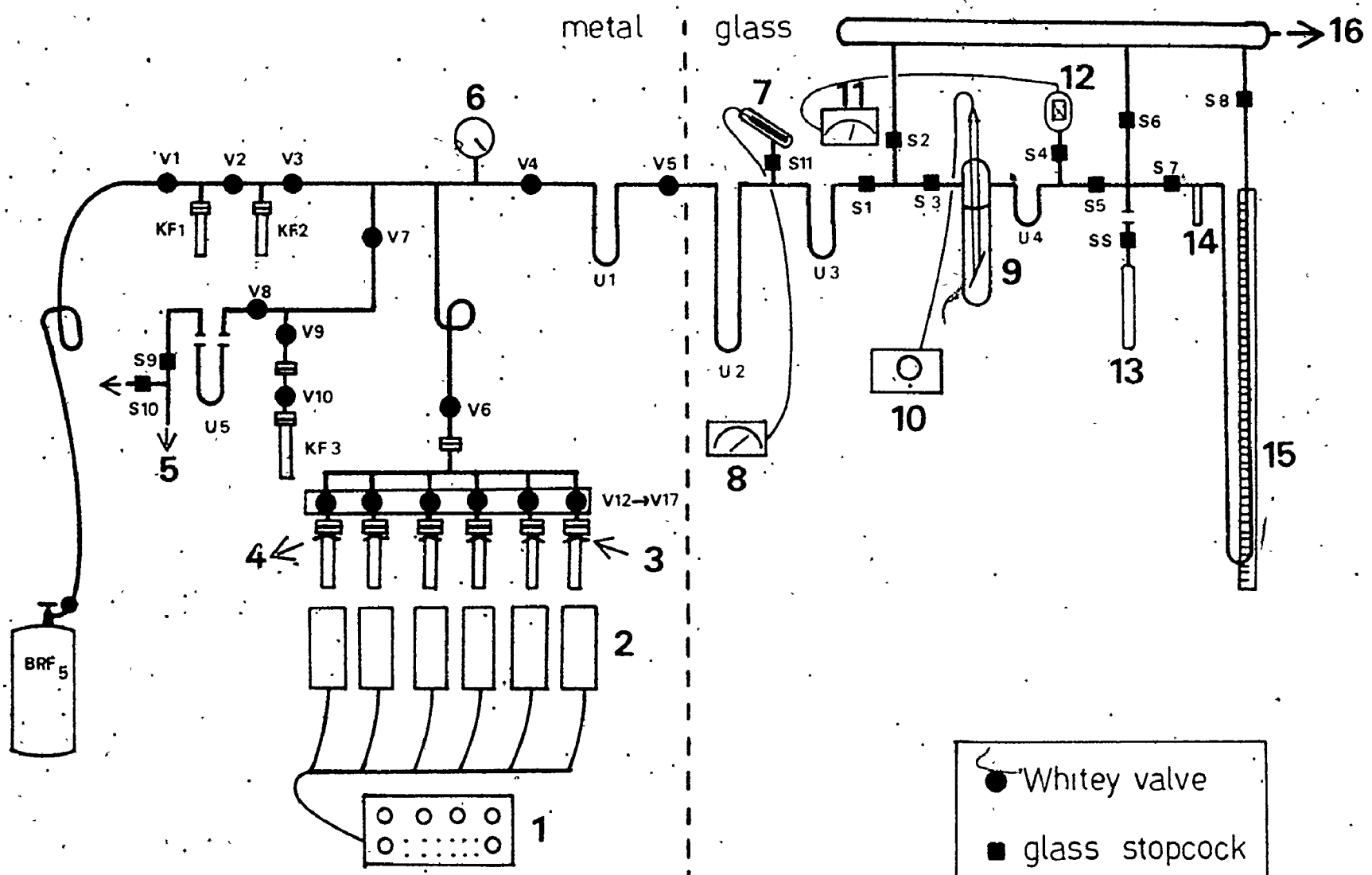
metal
glass
16
6
7
11
12
S8
V1
V2
V3
V4
V5
S11
S2
S6
S4
S7
KF1
KF2
V7
U1
S1
S3
U4
S5
14
V8
U3
9
SS
V9
S9
S10
U5
V10
U2
13
15
V6
KF3
10
V12→V17
4
3
8
5
2
BrF5
1
Whitey valve
glass stopcock

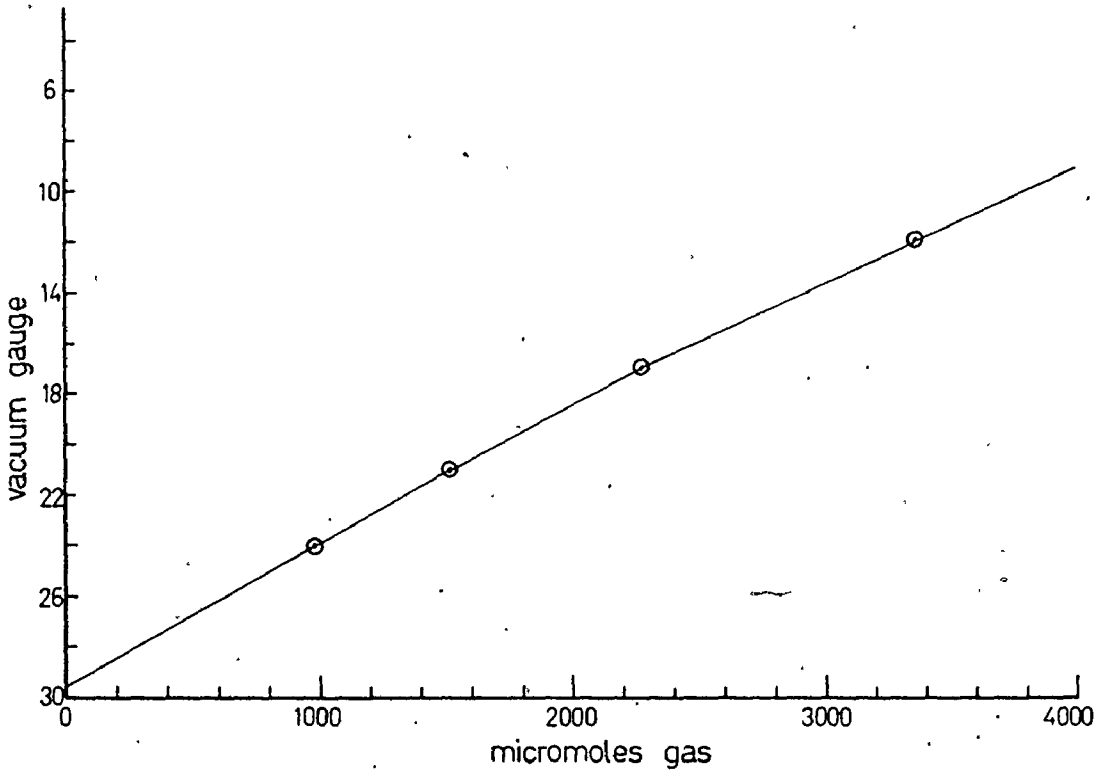

FIGURE A2-2 BrF_5 gas calibration graph

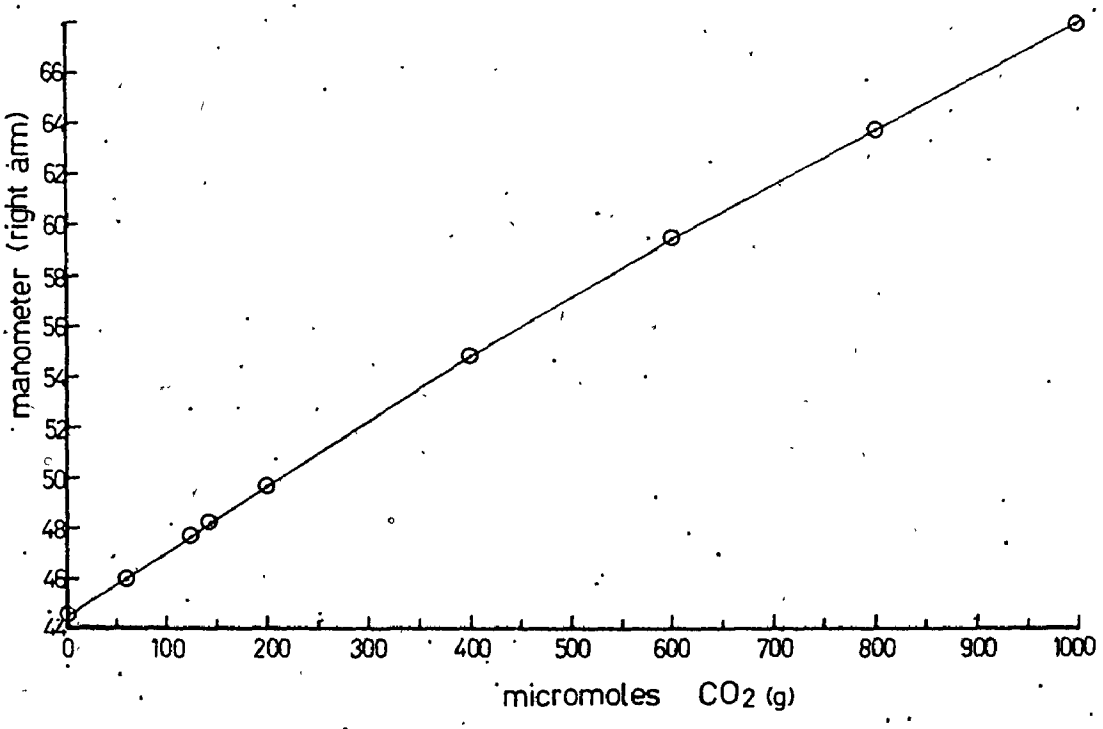

FIGURE A2-3 Manometer calibration graph for CO_2 gas

Table A2-1 Temperature calibration of furnaces (°C), March 29, 1976

vessel →	17			16			15			14			13			12		
variac →	70	76	80	65	70	75	58	63	67	65	70	75	65	72	77	64	70	74
Distance from vessel base (inches)																		
BASE	363	422	435	355	393	595	447	494	520	338	337	368	374	435	494	405	445	484
1	443	502	488	423	466	640	483	537	570	428	372	476	438	520	569	454	542	549
2	483	553	555	466	518	645	488	555	587	463	455	515	476	550	603	493	576	609
3	503	553	581	498	537	645	507	548	590	483	431	554	493	564	609	509	585	624
4	495	553	581	506	527	645	498	548	574	485	507	565	495	564	609	511	581	624
5	492	553	569	503	509	645	469	525	543	476	499	558	478	539	593	498	555	609
6	468	553	527	468	447	555	419	469	480	448	476	537	445	528	534	476	509	533
7		532	457		328	470	330		379	395		485	420	471	460	450	492	426
8		388				363			327	304			337			395		
9		344														320		

APPENDIX III

PETROGRAPHY OF THE BURDITT LAKE - LAKE DESPAIR AREA

1. INTRODUCTION

The purpose of this appendix is to summarize the petrographic data obtained from a study of over 100 thin sections of various rock types from the Burditt Lake - Lake Despair area. Modal data for the rocks of plutonic aspect are given in Table A3-1, and summarized in Figures A3-2 and A3-3. The IUGS (1972) classification of rock names has been used.

2. JACKFISH LAKE COMPLEX

Aside from a number of interesting but volumetrically unimportant bodies, the Jackfish Lake complex can be divided into three major petrographic units:

A. hornblende leucodiorite, quartz diorite, quartz monzodiorite, monzodiorite, diorite and meladiorite;

B. microcline megacryst-bearing biotite-hornblende granodiorite and quartz monzodiorite;

C. hornblende albite-microcline syenite.

Other units of interest include plagioclase dikes, quartz diorite dikes, albitite dikes, aplites, and pegmatites.

A. Hornblende leucodiorite to meladiorite group

The essential mineralogy of this suite is anhedral to subhedral plagioclase and subhedral to euhedral hornblende. Variation in the modal mafic colour index from 20 to 70, as well as the presence or absence of quartz and microcline in minor amounts distinguish the various rock types within the group. Accessory, relic and alteration minerals are augite, epidote, chlorite, magnetite, pyrite, sericite, sphene, apatite, clays, hematite and stilpnomelane. The rocks are salt and pepper coloured, some with a pinkish tinge due to alteration. They are holocrystalline, medium to coarse grained, hypidiomorphic, sometimes porphyritic, and strongly lineated to foliated. Mafic lensoid xenoliths ranging in length from less than one centimeter to greater than one hundred metres are ubiquitous; more mafic members of the group also contain irregular mafic clots.

Oligoclase (An_{22}-An_{29}) is the most common plagioclase, although andesine (An_{33}) is found in the more mafic samples. Plagioclase forms between 23 and 69% of the rocks. Most crystals are anhedral with an average grain size of 1-3 mm; some samples also contain subhedral lath-shaped phenocrysts up to 6 mm long. Crystals are generally untwinned, although albite, Carlsbad and pericline twins are observed, albeit in a poor state of preservation. Some twin traces are bent. Other grains show indistinct normal zoning, and have Na-rich

growth rims. Rounded and altered plagioclase cores, frequently myrmekitic, are often surrounded by microcline. In most of the samples, plagioclase forms an interlocking matrix, but some of the more mafic varieties also contain plagioclase poikilitically included in hornblende.

While some samples contain fresh plagioclase, saussuritization is the rule, with incipient to total alteration observed, often within the same thin section. The most severe alteration occurs within crystal cores, along twin planes and at plagioclase-hornblende crystal boundaries. Alteration products include epidote, clays, sericite, magnetite and calcite. Epidote most often replaces plagioclase that is in contact with a corroded amphibole. The alteration can be summed up as follows:

plagioclase → clays + epidote + sericite ± magnetite.

Amphibole occurs in two habits: (1) subhedral, corroded, poorly terminated, lath-like, simple twinned, well cleaved, poikilitic and pleochroic (green-brown) hornblende that varies from one to six mm in length, and contains abundant inclusions of apatite, magnetite and plagioclase; (2) anhedral uralitic amphibole that contains occasional inclusions of chloritized biotite, and is pleochroic (light green-dark green). The amphiboles comprise 22-63% of the rock. Clots of amphibole up to 10 mm in diameter have been observed, as well as

amphibolite enclaves, which are composed of over 80% amphibole which is much less reacted than the discrete hornblende crystals.

The reaction relationships shown by the amphiboles are varied. They include:

1. augite → hornblende → uralitic amphibole → chloritic biotite

This paragenesis, found in its entirety only occasionally, consists of a prismatic augite core up to 6 mm long surrounded by a poikilitic hornblende (occasionally this stage is absent), which, in a similar fashion, alters to uralitic amphibole. The uralite, in turn, is rimmed by chloritic biotite.

2. hornblende → biotite + sphene

Sphene is found as euhedral crystals up to 1 mm in length, separating biotite and hornblende. The hornblende often contains wormy plagioclase inclusions at or near its edge, and the augite may include bits of biotite, microcline, and plagioclase. Opaques (probably magnetite) are often located at the augite-hornblende interface, suggesting that:

3. augite → hornblende + magnetite

Other major parageneses and possible reactions observed are:

4. hornblende → uralitic amphibole + biotite + epidote
   chlorite

In this assemblage, hornblende is in reaction relationship

with the uralitic amphibole, both of which are surrounded by biotite; many of the biotite flakes are terminated by subhedral grains of epidote.

5. hornblende - sphene - magnetite

Subhedral sphene and magnetite appear to be exsolved from hornblende, especially along cleavages.

6. hornblende - plagioclase - epidote - sericite

These minerals are involved in a reaction which occurs at the intergranular boundary between plagioclase and hornblende. An intimate mixture of sericite and epidote is formed as a result of the interaction.

7. hornblende - epidote - biotite - magnetite - chlorite - sericite

In this assemblage, ragged biotite flakes, many terminating in granular epidote, replace the hornblende surfaces; other hornblendes are altered to mixtures of sericite-epidote-chlorite within and at the margins of the amphibole crystal. Magnetite is sometimes developed at the amphibole margin. In cases of extreme alteration, a mixture of radiating chlorite, epidote and clinozoisite pseudomorphically replaces the hornblende.

Quartz contents vary from 0-5%, the grains being anhedral and less than 3 mm in diameter.

Microcline occurs in amounts varying from traces to 14%, with the higher abundances occurring in samples laced by small

feldspar veinlets. The crystals range in size from less than 1 mm to 5.5 mm in a few tabular porphyroblasts. Gridiron twinning is well developed. Most microcline occurs as an interstitial phase, or as an exsolution product within plagioclase.

Some samples (i.e. D8) (which are located in transition zones between leucodiorite, syenite, and granodiorite) contain large amounts of irregularly shaped, patch and stringlet microcline perthite megacrysts having abundant plagioclase and hornblende inclusions.

Biotite can also occur as a primary mineral phase, as well as a deuteric alteration product. It forms between 0.5-15% of the rock. The flakes are stubby, ragged, and contain apatite and opaques as inclusions. Crystal length varies from 0.2-5.0 mm.

Magnetite is a common phase in the reactions involving hornblende, but only occurs in trace amounts. Discrete grains are rimmed by hematite.

The leucodiorite (oligoclasite) can be distinguished from the other rocks of the Jackfish Lake complex by its high content of oligoclase (70-83%) and its concomitant low colour index (13-16%). The essential mineralogy is oligoclase (An_{22}-An_{23}) and hornblende. Quartz and microcline vary systematically and sympathetically from 0.5-7% and 0.5-8%, respectively. Accessory and alteration phases are epidote,

sphene, apatite, biotite, chlorite, sericite, magnetite, and zircon. The rock texture is holocrystalline, medium to coarse grained, porphyritic, hypidiomorphic. Hornblende defines a strong lineation. Small amphibolite lenses are common xenoliths.

Plagioclase occurs in two generations: the first is subhedral, tabular, and ranges in length from 2-9 mm; the second is anhedral, rounded and averages 1-3 mm in diameter. Many of the rounded grains are surrounded by microcline; some of the larger grains are antiperthitic. Both generations of plagioclase are, for the most part, untwinned, although albite and Carlsbad twins are present, often with deformed twin traces. Alteration of the plagioclase, especially in the larger phenocrysts, is common and takes the form:

plagioclase → clays + epidote + sericite.

Microcline occurs interstitially, especially in proximity to hornblende grains. Quartz, when present, occurs as small anhedral grains.

Hornblende occurs as in the other dioritic rocks.

B. Hornblende granodiorite and quartz monzodiorite (microcline megacryst-bearing)

The granodiorites and quartz monzodiorites of this group contain numerous subhedral to euhedral coarse grained microcline

perthite megacrysts; these rocks also contain much more quartz than any others from the Jackfish Lake complex.

Quartz occurs in three habits: (1) elongated recrystallized grains 1-5 mm in length; (2) a fine grained recrystallized mosaic surrounding microcline megacrysts; (3) myrmekite.

Plagioclase occurs in two forms, as megacrysts up to 10 mm in length, and as grains in the matrix, averaging 2-3 mm in diameter. Twinning occurs according to the albite, Carlsbad, and pericline laws, and twin lamellae are often sawtooth in shape and/or bent. Untwinned crystals are common. Alteration to clays, white mica (sericite) and epidote varies in severity. Fe staining and hematite can be detected on some crystal faces. Plagioclase composition varies from An_{14} to An_{17}; no consistent compositional differences were detected between the megacryst and matrix plagioclase.

Microcline occurs primarily as patch and stringlet perthite megacrysts up to 20 mm in length; the megacrysts are subhedral to euhedral and aligned roughly parallel to the hornblende foliation. Some megacrysts have been deformed into ovoid shapes. The perthites contain inclusions of plagioclase, quartz, hornblende, sphene, opaques, other perthites, and apatite. Parallel alignment of twinned, unaltered plagioclase inclusions has been observed in one megacryst, which also contains aligned, altered and untwinned plagioclase inclusions oriented in a different direction. The microcline megacrysts embay the matrix plagioclase and quartz, forming a ragged

reaction boundary. Myrmekite is localized at this boundary. Pseudomorphic replacement of individual plagioclase grains by microcline also can be observed.

Interstitial microcline occurs in the matrix (1-2 mm).

The predominant mafic mineral is hornblende (2-4 mm in length). It occurs as corroded and fractured anhedral to subhedral laths and tablets, and contains inclusions of opaques, sphene, and apatite. Association with, and alteration to epidote, biotite, sphene, and magnetite is ubiquitous.

Summary of texture

The granodiorites and quartz monzodiorites are holocrystalline, medium to coarse grained, hypidiomorphic, porphyritic, and nematoblastic.

Nature of the microcline perthite megacrysts

Petrographic evidence for the later growth of the microcline perthites includes:

i. parallel inclusions of altered plagioclase and parallel inclusions of unaltered plagioclase at a different orientation within the same megacryst (i.e. two different crystals replaced);

ii. abundant inclusions of plagioclase and hornblende;

iii. embayment of matrix plagioclase and quartz by the perthite;

iv. pseudomorphic replacement of plagioclase crystals by microcline.

C. Na-syenite

This highly jointed and fractured pink and black rock is medium grained and has a strong hornblende lineation. Its mafic colour index is about 10. Essential mineralogy is albite (An_6; 69-71%), microcline (18-19%) and hornblende (8-9%). Alteration and accessory minerals are quartz, biotite, epidote, augite, apatite, magnetite, sphene and chlorite.

The albite is anhedral, fresh, and has well developed albite and Carlsbad twins. Average grain size is 1 mm. Occasional oligoclase cores are found within large albite crystals.

Microcline occurs as an interstitial anhedral phase with an average grain size of 0.5 mm.

Hornblende (light green-dark green pleochroic scheme) occurs as corroded anhedral to subhedral laths and granular aggregates up to 4 mm in length; its average grain size is 2 mm. Some crystals contain granular clinopyroxene cores. Inclusions contained within hornblende crystals include apatite, magnetite and sphene.

Biotite, when present, occurs both as discrete flakes up to 4 mm in length and as an alteration product rimming

hornblende. Individual flakes often terminate in granular epidote.

D. Albitite dike (F86)

This rock is fine to medium grained, pink, sugary, and has a colour index of less than one. It has an allotriomorphic-granular texture. The essential mineralogy is albite, a phase which comprises more than 95% of the rock. All of the grains are anhedral, 0.5-1.0 mm in diameter, and form an interlocking mosaic. Some crystals are untwinned, but albite twinning, including bent and offset twin traces, is common. Most grains show only minor surface alteration.

Epidote occurs as granular aggregates up to 0.5 mm in diameter; these aggregates often surround cubic magnetite.

Trace amounts of quartz and microcline occur interstitially.

E. Quartz diorite dikes (F54, F55, F126)

These dikes cut both the felsic metavolcanic rocks and the Footprint gneiss. The dikes vary widely in their composition; those associated with the Footprint gneiss contain irregular, elongated, recrystallized quartz eyes up to 10 mm in length; other dikes, cutting the metavolcanic rocks, are

more mafic, and contain basic enclaves.

The essential mineralogy of the dikes is oligoclase (An_{24}-An_{33}; 43-68%), quartz (3-16%), and hornblende (8-26%). Alteration and accessory minerals include biotite, clays, epidote, clinozoisite, muscovite, chlorite, allanite, apatite and magnetite.

Much of the oligoclase is altered, especially in crystal cores where felted masses of sericite, clinozoisite, epidote and clays are located. Sericite and epidote are developed on crystal faces parallel to cleavage. Albite, Carlsbad and pericline twinning is present but poorly preserved. Faint, normal concentric zoning is common. Apatite, hornblende, and magnetite are found as inclusions in the plagioclase; bleb-like quartz is found embaying the plagioclase and the plagioclase similarly embays some hornblende grains. The average plagioclase grain size is 1-2 mm.

Hornblende occurs as anhedral to subhedral grains (average grain size of 2 mm), and contains inclusions of biotite, epidote, magnetite and pleochroic zircon. Some hornblende crystals are altered to chloritized biotite and epidote.

Quartz occurs as 1-2 mm unstrained anhedral grains, as well as in the xenocrysts already mentioned. Microcline is interstitially dispersed around plagioclase cores, as well as exsolved from plagioclase (antiperthites).

F. Quartz-plagioclase dikes (F23)

Quartz-plagioclase dikes cut the Jackfish Lake complex leucodiorites and quartz diorites, as well as the adjacent metavolcanic rocks. These dikes contain two grain sizes of plagioclase: 2-8 mm antiperthitic grains, and smaller (0.2-0.5 mm) grains in a recrystallized mosaic matrix. The large grains show indistinct concentric zoning, are poorly twinned, irregular in shape, and are altered to clays, sericite and epidote, especially at their cores. The smaller grains are unaltered, twinned, and have a composition of An_{13}.

Hornblende (1-3 mm in length), if fractured and corroded, contains abundant apatite and sphene. The sphene occurs in clusters and trains of small euhedral grains, often encircling plagioclase crystals. Microcline occurs interstitially, and also in antiperthite. Quartz occurs in the matrix as small rounded grains.

G. Pegmatite veins and dikes

Medium to coarse grained pink pegmatites are commonly found cross-cutting the Jackfish Lake complex. These are composed of quartz (7-15%), plagioclase (75-85%), and microcline (3-15%) with traces of sphene, epidote, and hematite iron staining. The plagioclase is highly saussuritized and appears

in places to have been partially replaced by microcline. Quartz and microcline are anhedral to subhedral and quite fresh. Sphene is developed at the pegmatite-host rock contacts.

3. THE FOOTPRINT GNEISS

The Footprint gneiss is a relatively monotonous fine to medium grained, well-banded, finely-banded leucocratic biotite tonalitic to granodioritic gneiss and migmatite. It contains thin (less than 1 mm) bands of biotite, thicker (2-5 mm) bands of fine to medium grained grey quartzo-feldspathic material, and occasional lenses, pods and bands of coarser grained pink quartzo-feldspathic material. Feldspar megacrysts up to 10 mm in length are present. Essential mineralogy is quartz (18-28%), oligoclase (An_{24}-An_{27}; 51-71%), microcline (1-16%), and biotite (4-12%). Alteration and accessory minerals are muscovite, epidote and/or clinozoisite, magnetite, apatite, sphene, pyrite, and clays.

The oligoclase is anhedral, with an average grain size of 0.5-2.0 mm. Composite grains are common. Occasional subhedral perthitic porphyroblasts up to 4 mm in length are found, as well as wormy mats of plagioclase associated with muscovite. Myrmekite, surrounded by microcline, is common, as are perthitic grains and grains that appear to be overgrown

by microcline. Carlsbad, albite and pericline twinning are present but poorly preserved. Bent twin traces are common. The odd grain shows faint normal concentric zoning. Alteration to clays, epidote and muscovite is strongest in the plagioclase cores, but large percentage of the plagioclase is quite fresh.

Quartz occurs as anhedral grains elongated parallel to gneissosity. These grains average 0.2-2.0 mm in length; with some quartz eyes reaching 5 mm in length. Round quartz grains are also present. The quartz forms an interlocking mosaic together with plagioclase. Quartz is also found as pseudo-graphic intergrowths in microcline, and as rounded and myrmekitic inclusions in plagioclase.

Most microcline occurs as an interstitial phase with an average grain size of 0.25-1.0 mm. Small biotite inclusions are infrequently present. Gridiron twinning is well-developed. Some porphyroblasts up to 4 mm in length exist, overgrowing quartz and plagioclase crystals.

Biotite exists as subhedral stubby to acicular flakes about 0.25-2.0 mm in length. The flakes are in subparallel alignment, some being bent around quartz and feldspar grains. Inclusions of apatite are common. A common paragenesis is epidote, biotite, muscovite, magnetite and sphene, and is displayed in reactions such as:

biotite + epidote + sphene

where biotite flakes terminate in granular or crystalline epidote and have sphene crystals growing at the biotite crystal edges, or within the epidote. Some biotite is also intergrown with muscovite, radiating about an epidote core. Some biotite is mantled by flakes of muscovite.

Occasionally complete to partial alteration of amphibole xenocrysts to granular epidote and biotite can be observed near contacts with the Jackfish Lake complex.

Pyrite cores are sometimes present within discrete magnetite grains.

Hydrothermal alteration of the Footprint gneiss is present in the vicinity of the quartz diorite dike intrusions. The gneiss is fine grained, highly deformed, and porphyroblastic. The plagioclase is andesine (An_{37}), and occurs as rounded 0.5-1.0 mm grains and larger (up to 3 mm) megacrysts. Twinning is poorly preserved. There are abundant inclusions of magnetite in the plagioclase, much of which is corroded and partially replaced by epidote. Some plagioclase crystals have soda-rich rims which are free of inclusions. Quartz is rounded and unstrained, with the occasional porphyroblast up to 2 mm in diameter being present. Biotite is chloritized or replaced by epidote. The granular epidote is very abundant (see sample number F53) (15-16%).

4. THE NORTHWEST BAY COMPLEX

The Northwest Bay complex can be divided into three distinct rock types:

A. biotite-muscovite monzogranite to syenogranite;

B. foliated biotite leucogranodiorite;

C. pegmatite dikes

A. Biotite monzogranites and syenogranites (F33, F66, F129)

These are medium grained, equigranular to mildly foliated, pink, allotriomorphic to hypidiomorphic granitic rocks. Essential mineralogy is quartz (19-29%), oligoclase (An_{12-15}; 43-47%), microcline (19-31%), biotite (1-4%) and muscovite (0.5-3%). Accessory and alteration minerals are epidote, magnetite, sphene, apatite, and chlorite.

The oligoclase is anhedral to subhedral, with an average grain size of 1 mm. Some larger crystals up to 3 mm have been observed. In the foliated samples, the crystals are rounded, but the equigranular specimens are mostly composed of lath-shaped, poorly terminated crystals. Albite, Carlsbad and pericline twins are well preserved in unfoliated samples; preservation is poorer in foliated members. In the more strongly foliated rocks, bent twin traces are common. Myrmekite, surrounded by microcline, is ubiquitous. Alteration,

concentrated in plagioclase cores, is common, but crystal edges can be completely free from alteration.

Quartz is anhedral, and has an average grain size of 2 mm; crystals up to 5 mm in diameter have been observed. Some grains show undulose extinction. Boundaries with plagioclase are sutured; with microcline, they are ragged. Iron staining is present along fractures within certain grains.

Microcline has an average grain size of 1-3 mm; it occurs interstitially, and is moderately to well twinned. It contains abundant, rounded quartz inclusions, many of which are strung out in bead-like chains.

Biotite occurs as subhedral, aligned, ragged flakes about 0.5-1.5 mm in length. It occurs in association with epidote and magnetite.

B. Foliated biotite leucogranodiorite (F31)

This phaneritic, holocrystalline rock type is fine to medium grained, grey, and foliated to gneissic. It contains abundant concordant and discordant pink pegmatoid veinlets, as well as agmatitic mafic clots. Essential mineralogy is quartz (22%), oligoclase (An_{22}; 58%), microcline (10%), and biotite (5%). Accessory and alteration minerals are epidote, muscovite, sphene, magnetite, apatite and hematite.

The average grain size of the oligoclase is 0.5-1.0 mm

and the grains are rounded and anhedral.

Quartz has an average grain size of 1 mm, is anhedral, and somewhat strained. Microcline occurs as interstitial grains up to 3 mm in diameter, in which quartz is a common inclusion, especially at the edges of microcline crystals, where fine granular rims of quartz, oligoclase and microcline are found.

Biotite occurs as ragged flakes of average grain size 0.5 mm in association with clots of granular epidote (containing apatite inclusions) up to 1.0 mm in length. Biotite is also found in matted complexes of biotite, muscovite, magnetite and epidote.

Magnetite cubes often have a halo of rusty red material, probably hematite.

C. Pegmatite dikes (F32, F65)

Concordantly and discordantly intruded pink pegmatites occur throughout the Northwest Bay complex; the larger dikes are mineralogically zoned. Many of the dikes contain agmatized amphibolite enclaves. The dikes contain quartz (10-20%), oligoclase (10-16%), microcline (60-80%), epidote, muscovite, chlorite, biotite, magnetite and some calcite. Grain size is highly variable.

The plagioclase is anhedral, poorly twinned and altered to sericite, epidote, magnetite and chlorite assemblages.

The microcline occurs as euhedral crystals, as an interstitial phase, and as a replacement product of plagioclase. It is well twinned, and contains abundant inclusions of quartz, often in bead-like trains. Quartz-microcline crystal boundaries are often separated by a thin veneer of muscovite, magnetite and hematite.

5. FELSIC METAVOLCANIC ROCKS - AMPHIBOLITE GRADE (F121, F122, F123, F124)

The amphibolite grade felsic metavolcanic rocks are now recognizable as quartz-feldspar-mica schists, with some lensoid bodies suggestive of smeared tuffaceous (lapilli) material. The rocks are light grey, holocrystalline, fine to medium grained, porphyroblastic, and occasionally poikiloblastic. Essential mineralogy is quartz (13-26%), oligoclase (An_{24}-An_{25}; 43-64%), microcline (2-11%), biotite (5-11%), epidote (1-7%), and muscovite (0.5-14%). Accessory and alteration minerals are apatite, magnetite, sphene and calcite.

The oligoclase is subhedral to anhedral, generally untwinned, and has an average grain size of 0.25 to 1.0 mm; some albite, Carlsbad, and pericline twinning is present. Alteration to sericite, clays and epidote is present, especially in the crystal cores and on larger (over 1 mm)

grains. Some crystals are bordered by secondary growth rims which include muscovite; others are embayed by microcline.

Quartz occurs as anhedral, rounded grains about 0.25 mm in diameter and as elliptical, somewhat strained 'quartz eye' phenoblasts up to 5 mm in length. These phenoblasts contain occasional minute inclusions of plagioclase, magnetite and chlorite.

Microcline occurs interstitially, and surrounds myrmekitic plagioclase; it also replaces some plagioclase crystals.

Biotite occurs as aligned ragged flakes which vary in length from less than 0.2 mm to 1 mm. It contains apatite and sphene as inclusions. Biotite commonly occurs in felted masses along with epidote, muscovite, magnetite and sphene.

Magnetite can be anhedral or cubic and occurs rimmed by epidote and/or chlorite. Furthermore, chloritized biotite grains can contain exsolved magnetite.

Muscovite can also be found as discrete subhedral flakes or as needle-shaped individuals within a radiating aggregate of white mica, often centered on an epidote grain. Some samples contain poorly terminated muscovite flakes up to 2.5 mm in length; such crystals approach equidimensional shapes and are clearly porphyroblastic, overgrowing quartz and plagioclase grains.

6. LOW GRADE FELSIC METAVOLCANIC ROCKS, BURDITT LAKE AREA

These rocks have been described by Blackburn (1976a) as dominantly fragmental and of pyroclastic origin (bedded and graded tuffs have been observed). They include a wide and heterogeneous range in fragment sizes. In thin section, quartz and plagioclase grains (0.5-15 mm) lie in a fine grained matrix of quartz, feldspar, chlorite, clays, radiating aggregates of white mica, opaques, and calcite. Calcite also occurs as secondary veinlets.

The large quartz grains, probably relic primary quartz crystals, are angular to rounded and recrystallized. They have been embayed by a fine grained mosaic of quartz and plagioclase. The plagioclase grains are generally altered and recrystallized, but often have euhedral outlines.

7. METABASALTS AND ASSOCIATED MAFIC ROCKS

A. Mafic amphibolites

The lineated to foliated mafic amphibolites vary in grain size from less than 0.2 mm to samples with hornblende and plagioclase crystals about 3 mm in length, sitting in a fine grained matrix. The hornblende is anhedral to subhedral, well-cleaved, twinned, and reasonably fresh; it contains inclusions of opaques, apatite and sphene as well as relic cores of

clinopyroxene. Plagioclase is anhedral to subhedral; albite, Carlsbad and pericline twins are observed in varying states of preservation. Incipient alteration to clays and epidote exists in all samples; those located near ultramafic intrusions are the most severely altered.

Small elongated quartz crystals occur in some samples, and are surrounded by hornblende coarser than typical for the sample. Elliptically shaped intermediate fragments (plagioclase and hornblende) up to 10 mm in length are found in other samples.

Opaques (mostly magnetite) are very common in the matrix, and in sub-phenocryst size fractions; highly altered rocks contain leucoxene replacing these opaques.

The matrix is composed of plagioclase, clays, epidote, brown micas, and opaques. Pods and fracture fillings of calcite are common, as are small amounts of calcite in the matrix.

B. Migmatized amphibolites and enclaves

A variety of migmatized mafic amphibolites occur at the contacts with the Jackfish Lake Complex and included within the Footprint gneiss. These rocks are foliated to gneissic and contain leucocratic veins and pods. Greenish-grey fine to medium grained bands, layers, and streaks of amphibolite

alternate with lit-par-lit injected bands and pods of smeared felsic material which is generally coarser grained than the amphibolite.

Plagioclase varies from 20-60% and is in the oligoclase to andesine compositional range. Average grain size is 1-3 mm, with some porphyroblasts up to 5 mm. Albite, Carlsbad, and pericline twinning is preserved in some grains; others have been partially to totally replaced by alteration to clays and epidote. Bent cleavage traces accompany elongation of the grains parallel to the lineation. Some crystals embay and are embayed by hornblende. Such areas contain large grains of epidote, abundant clays and fine grained sericite.

The hornblende is comprised of elongated, corroded, subhedral, columnar crystals averaging 2-3 mm in length. Inclusions of plagioclase, apatite, magnetite and sphene are present; sieve texture is well developed in some crystals. Edges and tips of hornblende crystals are usually altered to epidote; other grains are altered to biotite and epidote along twin seams. Crystals may be partially to totally altered to a lusterless green chloritic amphibole, and, at their edges, to chlorite.

Quartz occurs as anhedral, sutured, interlocking elliptical pods up to 4 mm long, concentrated in the coarser, more leucocratic bands.

Biotite is most common as subhedral, poorly terminated,

aligned flakes up to 2 mm in length. Their tips and edges are often mantled by granular epidote. Chloritization is common.

Rare samples contain discrete subhedral crystals of clinozoisite up to 0.5 mm in length. These appear to replace plagioclase and hornblende. Granular epidote can be found within the same thin section.

C. Jackfish Lake complex mafic enclaves

The large mafic enclaves contained within the Jackfish Lake complex are at a somewhat lower grade (upper greenschist facies - lowermost amphibolite facies) relative to those found in the Footprint gneiss or the mafic metavolcanic rocks located at the contact with the Jackfish Lake complex. Some of the enclaves have preserved, albeit deformed, pillow structures. The enclaves are fine to medium grained, some showing indistinct compositional banding. The predominant amphibole is hornblende (less than 0.5-3 mm); it occurs in subhedral laths and blades, some of which have been rounded. Relic pyroxene cores, often altered partially to epidote, are common. Much of the hornblende exists in reaction relationship with overgrowing granular epidote, chloritic biotite, and cubic opaques. Some of the finer grained samples appear to contain actinolitic amphibole. Plagioclase is twinned (with

sawtooth lamellae very common) according to albite, Carlsbad and pericline twin laws, and generally free of alteration.

8. ULTRAMAFIC BODIES, BURDITT LAKE AND SOUTH BAY, LAKE DESPAIR

The presence of ultramafic rocks in South Bay has been recognized since the work of Lawson; those in the Burditt Lake area were first recognized by Blackburn (1972) and other bodies were found in this study. It is most likely that they are all part of cumulate peridotite sills within the mafic volcanic pile.

The rocks are fine grained and dark grey but weather tan. They are composed almost entirely of serpentine pseudomorphs after olivine (90-95%). One sample (F114) contains small amounts of only partially altered olivine; all others have been completely replaced by granular serpentine at crystal cores and radiating fibrous serpentine towards the crystal boundaries. Opaques are ubiquitous (1-4%), often growing raggedly, parallel to crystal faces. The pseudomorphs have brownish alteration rims, probably of hastingsite. The alteration of the olivine has probably been:

olivine + antigorite + magnetite + hastingsite.

Orthopyroxene and clinopyroxene are also present in largely serpentinized states (1-5%). Irregular veinlets and

patches of secondary calcite permeate the samples (1-4%).

9. PROTEROZOIC DIABASE DIKES

These are fine grained, grey, microporphyritic rocks composed of clinopyroxene, orthopyroxene and plagioclase microphenocrysts set in a fine grained felted groundmass of plagioclase, opaques and mafics. They have been studied by Francoeur (1972), and will not be considered further.

FIGURE A3-1 Quartz-alkali feldspar-plagioclase diagram for the rocks from the Burditt Lake - Lake Despair area. Tonalites containing less than 10% mafics are referred to as trondhjemites (Strecheisen, 1976).

FIGURE A3-2 Quartz-feldspar-mafics diagram for the rocks from the Burditt Lake - Lake Despair area

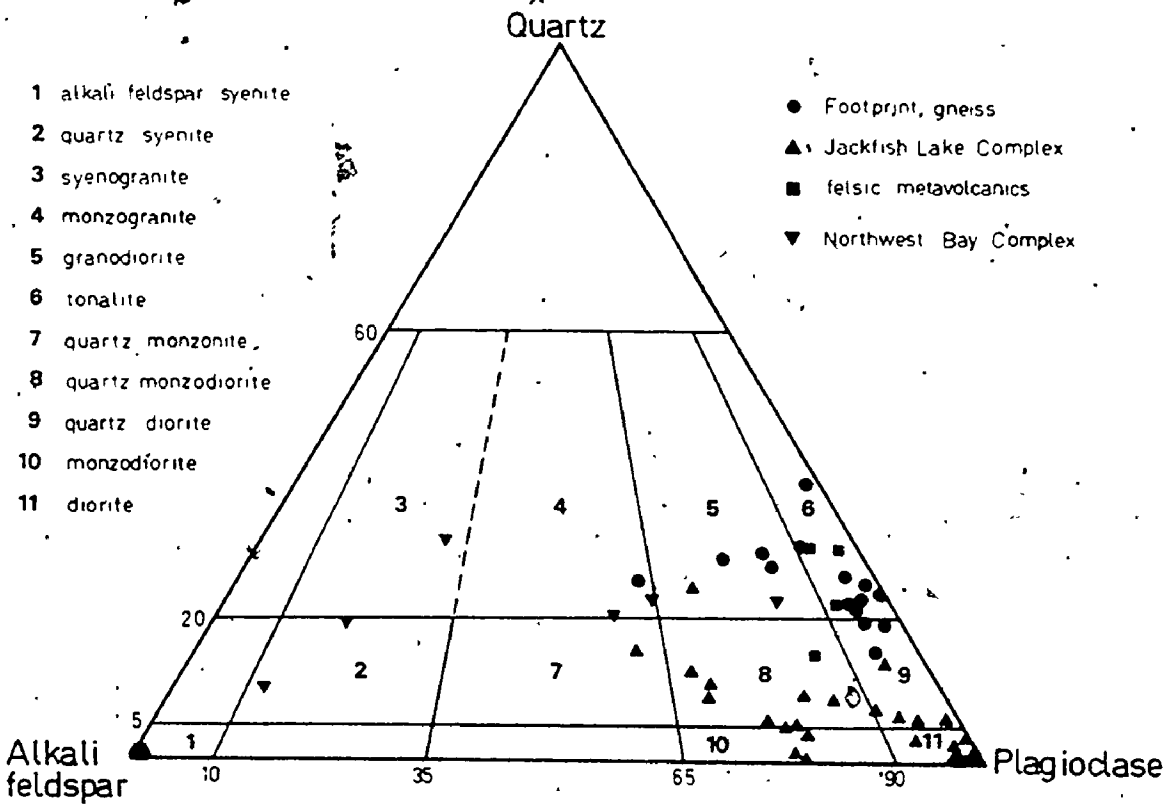
Quartz
1 alkali feldspar syenite
2 quartz syenite
3 syenogranite
4 monzogranite
5 granodiorite
6 tonalite
7 quartz monzonite
8 quartz monzodiorite
9 quartz diorite
10 monzodiorite
11 diorite
Footprint, gneiss
Jackfish Lake Complex
felsic metavolcanics
Northwest Bay Complex
60
20
5
Alkali feldspar
Plagioclase
10
35
65
90

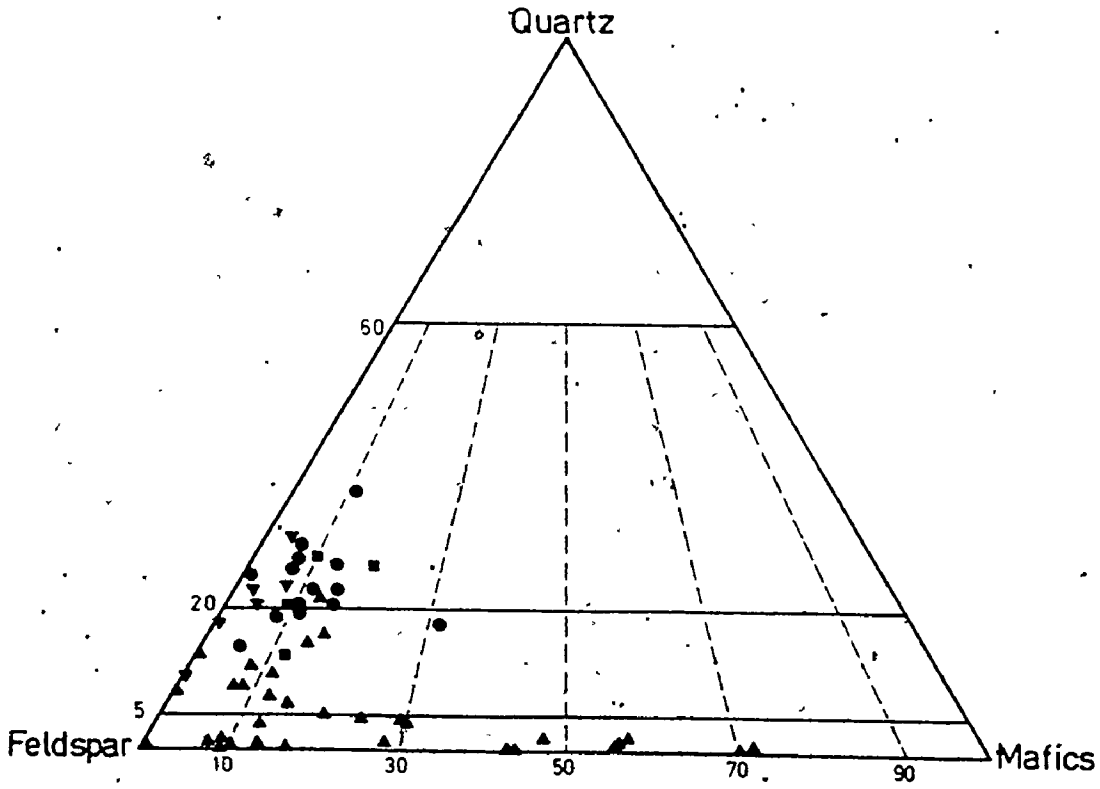
Quartz
60
20
5
Feldspar
Mafics
10
30
50
70
90

Table A3-1 Modal analyses for the Lake Despair area

	Burditt Lake low grade mafic metavolcanic rocks		Lake Despair amphibolite facies mafic metavolcanic rocks			
			least altered		altered	
	B1	B5	F19	F115	F49	F116
Quartz	0.0	3.0	0.0	0.6	0.0	0.9
Plagioclase	0.0	0.0	26.0	19.6	2.5	25.0
Albite	0.0	0.0	0.0	0.0	0.0	0.0
Microcline	0.0	0.0	0.0	0.0	0.0	0.0
Biotite	0.0	0.0	0.0	0.0	0.0	0.0
Chlorite	0.0	0.0	0.0	0.6	0.0	0.0
Hornblende	30.0	65.0	72.2	77.2	70.3	72.5
Epidote	0.0	0.0	1.6	0.6	0.0	0.1
Sphene	0.0	0.0	t	0.0	0.0	0.0
Opaques	0.0	2.0	0.2	1.4	t	1.5
Apatite	0.0	0.0	t	0.0	t	0.0
W. Mica	0.0	0.0	0.0	0.0	0.0	0.0
Hematite	0.0	0.0	0.0	0.0	0.0	0.0
Clinopyroxene	20.0	0.0	0.0	0.0	0.0	0.0
Allanite	0.0	0.0	0.0	0.0	0.0	0.0
Zircon	0.0	0.0	0.0	0.0	0.0	0.0
Calcite	0.0	0.0	0.0	0.0	0.0	0.0
Tourmaline	0.0	0.0	0.0	0.0	0.0	0.0
Matrix	50.0	30.0	0.0	0.0	27.1	0.0
Leuxocene	0.0	0.0	0.0	0.0	0.0	0.0
Orthopyroxene	0.0	0.0	0.0	0.0	0.0	0.0
Stilpnomelane	0.0	0.0	0.0	0.0	0.0	0.0
Plag. Comp.			An_{58}		An_{62}	An_{43}

	Large mafic enclaves within the Jackfish Lake Complex			Footprint Gneiss		
				mafic enclaves		ultramafic enclaves
	F80	F145	F134	F105	F13	F59
Quartz	0.0	0.0	0.0	1.1	0.0	t
Plagioclase	26.6	17.5	35.4	38.9	20.3	4.6
Albite	0.0	0.0	0.0	0.0	0.0	0.0
Microcline	0.1	0.0	0.0	0.9	0.0	0.0
Biotite	0.0	0.0	0.4	0.2	2.4	10.8
Chlorite	0.1	0.0	0.0	1.5	0.0	3.4
Hornblende	71.3	73.9	47.9	50.2	75.3	80.2
Epidote	0.0	6.5	13.0	7.2	1.3	0.0
Sphene	0.1	0.2	0.0	0.2	0.4	0.0
Opaques	1.7	1.4	1.8	t	0.0	0.9
Apatite	t	0.0	t	0.0	0.4	0.2
W. Mica	0.0	0.0	0.0	0.0	0.0	0.0
Hematite	0.0	0.0	0.0	0.0	0.0	t
Clinopyroxene	0.0	0.0	1.1	0.0	0.0	0.0
Allanite	0.0	0.0	0.0	0.0	0.0	0.0
Zircon	0.0	0.0	0.0	0.0	0.0	0.0
Calcite	0.0	0.0	0.0	0.0	0.0	0.0
Tourmaline	0.0	0.0	0.0	0.0	0.0	0.0
Matrix	0.0	0.0	0.0	0.0	0.0	0.0
Leuxocene	0.0	0.5	0.0	0.0	0.0	0.0
Orthopyroxene	0.0	0.0	0.4	0.0	0:0	0.0
Stilpnomelane	0.0	0.0	0.0	0.0	0.0	0.0
Plag. Comp.	An_{41}	An_{52}		An_{49}	An_{27}	An_{30}

	Lake Despair felsic schists				Northwest Bay Complex granodiorites and granites			
	F124	F121	F123	F122	F31	F129	F66	F33
Quartz	20.7	13.1	25.4	18.8	22.1	21.4	19.3	28.5
Plagioclase	43.7	64.0	58.5	62.2	57.9	47.0	43.6	43.8
Albite	0.0	0.0	0.0	0.0	0.0	0.0	0.0	0.0
Microcline	3.9	10.8	2.1	4.5	9.8	25.8	30.9	19.7
Biotite	11.0	10.1	5.7	6.9	4.8	1.9	3.3	2.7
Chlorite	0.0	0.0	0.5	0.0	0.0	0.0	0.0	0.0
Hornblende	0.0	0.0	0.0	0.0	0.0	0.0	0.0	0.0
Epidote	6.9	1.4	6.8	5.3	3.8	1.3	1.7	3.7
Sphene	t	0.2	0.2	0.0	0.3	t	t	0.0
Opaques	0.2	t	0.2	0.5	0.3	t	0.3	t
Apatite	0.2	t	0.2	0.0	0.2	0.0	0.0	t
W. Mica	13.2	0.6	0.6	1.9	0.5	2.6	0.9	1.7
Hematite	0.0	t	0.0	0.0	0.2	0.0	0.0	t
Clinopyroxene	0.0	0.0	0.0	0.0	0.0	0.0	0.0	0.0
Allanite	0.0	0.0	0.0	0.0	0.0	0.0	0.0	0.0
Zircon	0.0	0.0	0.0	0.0	0.0	0.0	0.0	0.0
Calcite	0.3	0.0	0.0	0.0	0.0	0.0	0.0	0.0
Tourmaline	0.0	0.0	0.0	0.0	0.0	0.0	0.0	0.0
Matrix	0.0	0.0	0.0	0.0	0.0	0.0	0.0	0.0
Leuxocene	0.0	0.0	0.0	0.0	0.0	0.0	0.0	0.0
Orthopyroxene	0.0	0.0	0.0	0.0	0.0	0.0	0.0	0.0
Stilpnomelane	0.0	0.0	0.0	0.0	0.0	0.0	0.0	0.0
Plag. Comp.	An_{25}	An_{24}	An_{24}	An_{24}	An_{22}	An_{15}	An_{12}	An_{28}

	Northwest Bay Complex		
	pink pegmatites		mafic enclaves
	F65	F32A	F32B
Quartz	10.8	17.8	0.0
Plagioclase	10.5	15.6	0.0
Albite	0.0	0.0	0.0
Microcline	78.2	65.0	0.0
Biotite	t	0.0	0.0
Chlorite	t	0.3	0.0
Hornblende	0.0	0.0	95.9
Epidote	t	1.3	3.2
Sphene	0.0	0.0	0.5
Opaques	t	t	0.0
Apatite	0.0	0.0	0.5
W. Mica	0.5	0.0	0.0
Hematite	t	t	0.0
Clinopyroxene	0.0	0.0	0.0
Allanite	0.0	0.0	0.0
Zircon	0.0	0.0	0.0
Calcite	0.0	t	0.0
Tourmaline	0.0	0.0	0.0
Matrix	0.0	0.0	0.0
Leuxocene	0.0	0.0	0.0
Orthopyroxene	0.0	0.0	0.0
Stilpnomelane	0.0	0.0	0.0
Plag. Comp.	An_{16}		

Footprint Gneiss

	F103	F10	F7	F5	F8	F72
Quartz	19.6	27.6	22.0	20.1	18.6	26.5
Plagioclase	62.2	57.5	60.5	62.9	65.1	51.8
Albite	0.0	0.0	0.0	0.0	0.0	0.0
Microcline	2.0	5.6	2.7	6.6	3.8	15.5
Biotite	12.1	4.3	11.5	8.2	8.6	4.8
Chlorite	0.0	0.0	0.0	0.0	0.0	0.0
Hornblende	0.0	0.0	0.0	0.0	0.0	0.0
Epidote	3.3	2.0	1.9	9.5	2.7	0.6
Sphene	0.3	0.0	0.0	0.0	0.5	0.2
Opaques	t	0.2	t	t	0.0	0.3
Apatite	0.0	0.0	t	0.0	0.5	0.0
W. Mica	0.5	2.8	1.4	1.3	0.2	0.3
Hematite	t	t	0.0	0.0	0.0	0.0
Clinopyroxene	0.0	0.0	0.0	0.0	0.0	0.0
Allanite	0.0	0.0	0.0	0.0	0.0	0.0
Zircon	0.0	0.0	0.0	0.0	0.0	0.0
Calcite	0.0	0.0	0.0	0.0	0.0	0.0
Tourmaline	0.0	0.0	0.0	0.0	0.0	0.0
Matrix	0.0	0.0	0.0	0.0	0.0	0.0
Leuxocene	0.0	0.0	0.0	0.0	0.0	0.0
Orthopyroxene	0.0	0.0	0.0	0.0	0.0	0.0
Stilpnomelane	0.0	0.0	0.0	0.0	0.0	0.0
Plag. Comp.	An_{24}	An_{24}	An_{24}	An_{24}	An_{24}	An_{25}

	Footprint Gneiss				
	F73	F151	F149	F152	F150
Quartz	25.1	22.6	25.7	20.0	18.2
Plagioclase	57.3	66.5	52.7	65.9	70.4
Albite	0.0	0.0	0.0	0.0	0.0
Microcline	10.7	1.4	9.9	3.5	3.8
Biotite	5.1	8.4	9.1	8.1	6.5
Chlorite	0.0	0.0	0.0	0.0	0.0
Hornblende	0.0	0.0	0.0	0.0	0.0
Epidote	1.0	0.5	1.2	0.9	0.9
Sphene	0.0	0.2	0.0	0.2	0.1
Opaques	t	0.2	0.8	t	0.2
Apatite	0.0	0.2	0.0	0.0	0.0
W. Mica	0.8	0.0	0.0	1.4	0.0
Hematite	t	t	t	0.0	0.0
Clinopyroxene	0.0	0.0	0.0	0.0	0.0
Allanite	0.0	0.0	0.0	0.0	0.0
Zircon	0.0	0.0	0.0	0.0	0.0
Calcite	0.0	0.0	0.0	0.0	0.0
Tourmaline	0.0	0.0	t	0.0	0.0
Matrix	0.0	0.0	0.0	0.0	0.0
Leuxocene	0.0	0.0	0.0	0.0	0.0
Orthopyroxene	0.0	0.0	0.0	0.0	0.0
Stilpnomelane	0.0	0.0	0.0	0.0	0.0
Plag. Comp.	An_{27}	An_{24}		An_{21}	An_{25}

	Contact metamorphosed Footprint gneiss		Sheared & contaminated Footprint gneiss	Dikes within Footprint gneiss		
				felsic dikes & pegmatites		metadiabase dike
	F53	F54	F11	F9	F101	F75
Quartz	12.5	16.2	17.3	24.5	35.6	0.0
Plagioclase	63.9	68.1	54.9	45.4	54.8	15.6
Albite	0.0	0.0	0.0	0.0	0.0	0.0
Microcline	4.0	t	0.5	26.8	1.0	0.0
Biotite	3.6	4.4	3.9	0.8	6.9	0.0
Chlorite	0.0	t	0.0	0.0	0.0	1.0
Hornblende	0.0	8.6	22.3	0.0	0.0	81.2
Epidote	15.9	2.0	1.1	1.1	1.0	2.0
Sphene	0.0	0.0	0.0	0.0	0.0	0.0
Opaques	t	0.3	0.2	t	0.2	0.2
Apatite	0.0	0.2	t	0.0	0.0	t
W. Mica	0.0	0.2	0.0	1.4	0.5	t
Hematite	0.0	0.0	0.0	0.0	t	t
Clinopyroxene	0.0	0.0	0.0	0.0	0.0	0.0
Allanite	0.0	0.2	0.0	0.0	0.0	0.0
Zircon	0.0	0.0	0.0	0.0	0.0	0.0
Calcite	0.0	0.0	0.0	0.0	0.0	0.0
Tourmaline	0.0	0.0	0.0	0.0	0.0	0.0
Matrix	0.0	0.0	0.0	0.0	0.0	0.0
Leuxocene	0.0	0.0	0.0	0.0	0.0	0.0
Orthopyroxene	0.0	0.0	0.0	0.0	0.0	0.0
Stilpnomelane	0.0	0.0	0.0	0.0	0.0	0.0
Plag. Comp.	An_{37}	An_{23}	An_{27}	An_{24}	An_{30}	

Jackfish Lake Complex

diorites and leucodiorites

	F142B	F143B	F139	F146	F126	F84
Quartz	0.0	0.2	0.9	1.7	3.4	0.3
Plagioclase	28.8	43.0	25.9	50.8	50.2	42.9
Albite	0.0	0.0	0.0	0.0	0.0	0.0
Microcline	0.0	0.0	1.7	0.2	0.7	1.8
Biotite	0.7	1.0	14.1	5.9	5.8	0.6
Chlorite	0.0	0.0	0.0	0.8	7.5	2.3
Hornblende	63.1	50.5	48.6	39.9	25.2	39.5
Epidote	0.0	0.2	0.2	0.3	8.5	2.0
Sphene	0.4	0.2	0.9	0.0	0.0	0.1
Opaques	0.0	t	0.3	0.2	t	t
Apatite	0.6	0.2	0.7	0.3	0.5	0.4
W. Mica	0.0	0.0	t	0.0	0.2	0.0
Hematite	0.0	0.0	0.0	0.0	0.0	0.0
Clinopyroxene	6.5	4.6	7.8	0.0	0.0	0.1
Allanite	0.0	0.0	0.0	0.0	0.0	0.0
Zircon	0.0	0.0	0.0	0.0	0.0	0.0
Calcite	0.0	0.0	0.0	0.0	0.0	0.0
Tourmaline	0.0	0.0	0.0	0.0	0.0	0.0
Matrix	0.0	0.0	0.0	0.0	0.0	0.0
Leuxocene	0.0	0.0	0.0	0.0	0.0	0.0
Orthopyroxene	0.0	0.0	0.0	0.0	0.0	0.0
Stilpnomelane	0.0	0.0	0.0	0.0	0.0	0.0
Plag. Comp.	An_{23}	An_{23}	An_{29}	An_{33}	An_{24}	An_{23}

	Jackfish Lake Complex diorites and leucodiorites				
	F132	F131	F21	F94	F95
Quartz	0.5	1.0	4.4	0.6	0.9
Plagioclase	52.4	68.8	67.8	78.8	82.9
Albite	0.0	0.0	0.0	0.0	0.0
Microcline	1.5	0.0	3.4	1.9	0.6
Biotite	0.8	5.8	0.1	0.2	0.2
Chlorite	0.8	0.0	t	0.5	0.0
Hornblende	42.3	22.0	22.7	15.9	13.1
Epidote	0.6	2.4	0.0	1.9	2.0
Sphene	0.0	0.0	0.3	0.0	0.2
Opaques	0.2	t	0.0	t	t
Apatite	0.2	t	0.1	0.2	0.3
W. Mica	0.3	0.0	0.0	0.2	t
Hematite	0.0	0.0	0.0	0.0	0.0
Clinopyroxene	0.0	0.0	0.6	0.0	t
Allanite	0.0	0.0	0.0	0.0	0.0
Zircon	0.0	0.0	t	0.0	t
Calcite	0.0	0.0	t	0.0	0.0
Tourmaline	0.0	0.0	0.0	0.0	0.0
Matrix	0.0	0.0	0.0	0.0	0.0
Leuxocene	0.0	0.0	0.0	0.0	0.0
Orthopyroxene	0.0	0.0	0.0	0.0	0.0
Stilpnomelane	0.6	0.0	0.0	0.0	0.0
Plag. Comp.	An_{25}	An_{22}		An_{22}	An_{23}

Jackfish Lake Complex
diorites and leucodiorites

	F24	F70	F23	D8	F86
Quartz	6.6	1.8	1.2	5.9	0.6
Plagioclase	71.8	89.5	89.4	73.1	0.0
Albite	0.0	0.0	0.0	0.0	95.6
Microcline	7.6	0.4	1.7	14.5	0.9
Biotite	0.0	2.7	0.0	0.5	0.0
Chlorite	0.0	0.0	0.0	0.0	0.0
Hornblende	14.0	4.2	5.8	5.7	0.0
Epidote	0.3	1.0	0.2	0.3	2.6
Sphene	0.3	0.3	1.6	0.0	0.0
Opaques	0.0	t	0.0	0.0	0.4
Apatite	0.3	0.1	t	0.0	0.0
W. Mica	0.0	0.0	0.0	0.0	0.0
Hematite	0.0	0.0	0.0	0.0	t
Clinopyroxene	0.0	0.0	0.0	0.0	0.0
Allanite	0.0	0.0	0.0	0.0	0.0
Zircon	0.0	0.0	0.0	0.0	0.0
Calcite	0.0	0.0	0.0	0.0	0.0
Tourmaline	0.0	0.0	0.0	0.0	0.0
Matrix	0.0	0.0	0.0	0.0	0.0
Leuxocene	0.0	0.0	0.0	0.0	0.0
Orthopyroxene	0.0	0.0	0.0	0.0	0.0
Stilpnomelane	0.0	0.0	0.0	0.0	0.0
Plag. Comp.			An_{13}		An_1

Jackfish Lake Complex

	(quartz) monzodiorites			Na syenites		
	F144	F135	F133	F28	F47	F147
Quartz	3.8	4.7	6.4	1.0	0.4	8.8
Plagioclase	52.5	40.3	58.0	0.0	0.0	68.1
Albite	0.0	0.0	0.0	69.2	70.3	0.0
Microcline	13.2	7.8	4.4	18.8	18.2	14.7
Biotite	2.6	11.5	3.7	1.2	0.0	0.0
Chlorite	1.8	0.6	0.0	t	0.0	0.3
Hornblende	25.3	31.6	23.4	8.8	8.5	5.8
Epidote	0.2	2.9	2.9	0.3	1.9	1.8
Sphene	0.0	0.0	0.3	t	0.0	0.0
Opaques	t	t	t	0.2	0.7	0.6
Apatite	0.2	0.3	0.0	0.2	0.0	t
W. Mica	0.5	0.0	0.3	0.0	0.0	0.0
Hematite	0.0	0.0	0.0	0.0	0.0	0.0
Clinopyroxene	0.0	0.5	0.5	0.3	0.0	0.0
Allanite	0.0	0.0	0.0	0.0	0.0	0.0
Zircon	0.0	0.0	0.0	0.0	0.0	0.0
Calcite	0.0	0.0	0.0	0.0	0.0	0.0
Tourmaline	0.0	0.0	0.0	0.0	0.0	0.0
Matrix	0.0	0.0	0.0	0.0	0.0	0.0
Leuxocene	0.0	0.0	0.0	0.0	0.0	0.0
Orthopyroxene	0.0	0.0	0.0	0.0	0.0	0.0
Stilpnomelane	0.0	0.0	0.0	0.0	0.0	0.0
Plag. Comp.	An_{28}	An_{24}	An_{23}	An_{6}	An_{7}	An_{25}

Jackfish Lake Complex.

	granodiorites					pegmatites		
	D1	D3	F37	F40	F113	F26	F142A	F143A
Quartz	11.8	4.2	13.4	9.6	10.4	20.8	13.8	8.6
Plagioclase	55.2	65.5	48.3	62.8	63.1	46.6	81.5	78.0
Albite	0.0	0.0	0.0	0.0	0.0	0.0	0.0	0.0
Microcline	24.2	12.0	18.8	18.4	16.5	18.9	4.7	13.3
Biotite	1.4	4.6	0.0	1.1	1.6	3.8	0.0	0.0
Chlorite	0.0	0.0	7.0	0.0	0.0	0.0	0.0	0.0
Hornblende	5.8	11.3	8.3	4.3	6.9	6.4	0.0	0.0
Epidote	1.4	2.4	4.2	3.8	1.3	3.3	0.0	t
Sphene	0.2	t	t	t	0.2	0.1	0.0	0.1
Opaques	t	t	t	t	t	0.1	0.0	0.0
Apatite	t	t	t	t	t	t	0.0	0.0
W. Mica	t	t	t	t	t	t	0.0	0.0
Hematite	t	t	t	t	t	t	0.0	t
Clinopyroxene	0.0	0.0	0.0	0.0	0.0	0.0	0.0	0.0
Allanite	0.0	0.0	0.0	0.0	0.0	0.0	0.0	0.0
Zircon	0.0	0.0	0.0	0.0	0.0	0.0	0.0	0.0
Calcite	0.0	0.0	0.0	0.0	0.0	0.0	0.0	0.0
Tourmaline	0.0	0.0	0.0	0.0	0.0	0.0	0.0	0.0
Matrix	0.0	0.0	0.0	0.0	0.0	0.0	0.0	0.0
Leuxocene	0.0	0.0	0.0	0.0	0.0	0.0	0.0	0.0
Orthopyroxene	0.0	0.0	0.0	0.0	0.0	0.0	0.0	0.0
Stilpnomelane	0.0	0.0	0.0	0.0	0.0	0.0	0.0	0.0
Plag. Comp.	An_{14}	An_{18}		An_{14}		An_{14}	Olig	Olig

APPENDIX IV

X-RAY FLUORESCENCE SPECTROGRAPHY, TECHNIQUE AND RESULTS

1. TECHNIQUE

Major and minor element analyses were performed by X-ray fluorescence spectrography, using a Phillips PW1450 automatic sequential machine. Ten to twenty kilogram samples were crushed, homogenized and then split so that a representative 200-300 g sample could be further pulverized to 200-300 mesh in a tungsten carbide Spex shatterbox and mill. 2.000 g of this pulverized sample were then thoroughly mixed with 4.000 g of lithium tetraborate (dry) and fused in a carbon crucible at 1100°C for one hour. The resulting glass beads were then recrushed in a Spex tungsten carbide rotor mill and 5 g of the powder pressed into a pellet together with a boric acid backing, in the manner described by Marchand (1973). These pellets were then analyzed by routine XRF procedures, as described in Norrish and Chappel (1967), Longstaffe (1973) and Westerman (1977); raw counts were corrected for background, and matrix effects (programme of B. Gunn, University of Montreal) and compared against single standards of appropriate composition by means of Fortran programme XRFFUS.

Trace element analyses were performed on powder pellets produced in the manner described by Marchand (1973) and Longstaffe (1973). One modification of both techniques was the use of large samples (5 g). The analytical procedures involved four separate routines: (1) Rb-Sr; (2) Ba-Ce; (3) Rb-Sr-Y-Zr-Nb, and (4) U-Th-Rb-Pb-Zn-Ni. Only Rb and Sr

results from routine (1) were incorporated into the thesis material. The XRF analytical technique for Ba-Ce was developed by Longstaffe and the corresponding Fortran IV data processing package prepared by C. Westerman (1977). Willis et al. (1969) noted the potential of the analytical technique employed for Ba. The techniques for routines (2), (3) and (4) were adapted to the McMaster machine and CDC 6400 computer by M. Marchand (1976). The work of Marchand has laid the foundation for most of the XRF trace element geochemistry presently conducted at McMaster. Copies of the necessary Fortran data processing programmes are available from R.H. McNutt (Department of Geology, McMaster University) and contain the necessary imput instructions.

All of the XRF analytical parameters used in this study for trace element analysis were prepared by this author, and are listed in Tables A4-1 to A4-4. However, these settings may vary somewhat depending upon machine operation and should be used only as guidelines. Actual analytical conditions should be tested by each operator, if high quality data is to be obtained. Detailed interpretation of the listed parameters is contained in the operator's manual, McMaster X-Ray Fluorescence Laboratory, Department of Geology, McMaster University.

Table A4-1 Rb-Sr analytical methods

Radiation:	Mo
X-ray generator:	90 KV, 25 mA
PHA settings:	lower level - 250 V; window - 750 V
Vacuum:	optional
Analytical lines:	Rb - $K\alpha_{1,2}$
	Sr - $K\alpha_{1,2}$

Parameters: (to be punched into the PW1450 for analysis control)

Molycompton Peak:	1021211 6600305	Rb background:	1025771 6600305
Sr background:	1024311 6600305	Rb peak:	1026531 6600305
Sr peak:	1025071 6600305		

Table A4-2 Ba-Ce analytical methods

Radiation:	Mo
X-ray generator:	50 KV, 50 mA
PHA settings:	lower level - 200 V; window - 450 V
Vacuum:	yes
Analytical lines:	Ba L β_1
	Ce L β_1

Parameters:

Ba background:	4180501 1000303	Ce background:	4174471 1000303
Ba peak:	4179181 1000306	Ce peak:	4171681 1000306
Ba background:	4178151 1000303	Ce background:	4170681 1000303

Table A4-3 Rb-Sr-Y-Zr-Nb analytical methods

Radiation:	W		
X-ray generator:	50 KV, 25 mA		
PHA settings:	lower level - 250 V;	window - 750 V	
Vacuum:	no		
Analytical lines:	Nb $K\alpha_{1,2}$	Sr	$K\alpha_{1,2}$
	Zr $K\alpha_{1,2}$	Rb	$K\alpha_{1,2}$
	Y $K\alpha_{1,2}$	Rb	$K\alpha_{1,2}$

Parameters:

Nb peak:	7121311 6000305	Y peak:	7123731 6000305
Nb background:	7122151 6000305	Y background:	7124421 6000305
Zr peak:	7122491 6000305	Sr peak:	7125101 6000305
Zr background:	7123131 6000305	Rb peak:	7126581 6000305

Table A4-4 U-Rb-Th-Pb-Zn-Ni analytical methods

Radiation:	Mo		
X-ray generator:	90 KV, 25 mA		
PHA settings:	lower level - 150 V;	window - 400 V	
Vacuum:	no		
Analytical lines:	U $L\alpha_{1,2}$	Zn	$K\alpha_{1,2}$
	Rb $K\alpha_{1,2}$	Cu	$K\alpha_{1,2}$
	Th $L\alpha_{1,2}$	Ni	$K\alpha_{1,2}$
	Pb $K\alpha_{1,2}$		

Parameters:

Table A4-4 /continued

Molycompton peak:	6021201 6000305	background:	6028931 6000305
background:	6024261 6000305	background:	6040701 6000305
U peak:	6026071 6000305	Zn peak:	6041731 6000305
Rb peak:	6026541 6000305	Cu peak:	6044961 6000305
Th peak:	6027401 6000305	Ni peak:	6048611 6000305
Pb peak:	6028191 6000305	background:	6049671 6000305

2. MAJOR ELEMENT RESULTS

Accuracy and precision data for standards are given in Table A4-5. Primary standards analyzed were:

GSP-1	U.S.G.S. standard granodiorite
GA	C.R.P.G. standard granite
BCR-1	U.S.G.S. standard basalt
W-1	U.S.G.S. standard diabase

Other samples analyzed included:

JG-1	Geological Survey of Japan standard granodiorite
JB-1	Geological Survey of Japan standard basalt
DR-N	C.R.P.G. standard diorite
AGV-1	U.S.G.S. standard andesite
DTS-1	U.S.G.S. standard dunite
NIM-G	National Institute of Metallurgy standard granite
NIM-D	National Institute of Metallurgy standard dunite

The accepted values listed in Table A4-5 are from Abbey (1973, 1975). Agreement between these results and those reported in this study is very good. Only MgO at levels below 1.0 wt. % tends to be somewhat low, although results for NIM-G and GA are quite satisfactory.

Table A4-6 gives replicate results for 5 fusion preparations of the same powder, and therefore should give a representative

estimate of our total experimental error. The coefficient of variation is less than 3% for all elements except MnO and P_2O_5, which occur only in very small amounts. The error observed for those samples prepared in duplicate (Table A4-7) is not much different from that given in Table A4-6 for the 5 replicate analyses.

3. TRACE ELEMENT RESULTS

Accuracy and precision data for those trace elements analyzed by X-ray fluorescence are given in Tables A4-8a to A4-8k. Accepted values are taken from Abbey (1975) and Flanagan (1973). Detection limits for each element are also given; detection limit is defined after Jenkins and de Vries (1972) as the "concentration which gives a net count rate equivalent to $2\sqrt{2}$ times the standard deviation of the background count rate for the 95% confidence limit".

Results for all trace elements except U, Nb and Th are quite acceptable. The U results, however, were neither precise nor accurate, and have been discarded; the Nb data are precise enough (c = 8-14%) but are also consistently low by about 33% below 15 ppm and about 16% below 30 ppm; only at abundance levels of about 90 ppm are reasonable results obtained. Most of the Nb results reported in this study must therefore be considered as semi-quantitative (and probably low) estimates

of the true values. The Th values are consistently high at low concentrations.

The reproducibility of separate powder preparations of the same sample is given in Table A4-9. The coefficient of variation varies from 0.06 to 16.0%, with the correspondingly higher c values occurring for those elements at abundances near the sensitivity of the technique.

All unknowns were analyzed at least twice; no differences outside the ranges given in Table A4-9 were observed.

Table A4-5 Accuracy and reproducibility of standards (wt %)

	Accepted value (Abbey, 1975)	This study (5 analyses) mean	range
GSP-1			
SiO_2	67.31	67.34	67.14-67.56
Al_2O_3	15.19	14.99	14.83-15.22
Fe_2O_3 t	4.33	4.35	4.32-4.37
MgO	0.96	0.81	0.73-0.90
CaO	2.02	2.04	2.02-2.05
Na_2O	2.80	2.83	2.77-2.94
K_2O	5.53	5.46	5.39-5.54
TiO_2	0.66	0.67	0.66-0.69
MnO	0.04	0.05	0.04-0.06
P_2O_5	0.28	0.28	0.27-0.29
GA			
SiO_2	69.96	69.96	69.75-70.18
Al_2O_3	14.51	14.82	14.54-14.95
Fe_2O_3 t	2.86	2.84	2.81-2.86
MgO	0.95	1.03	0.92-1.11
CaO	2.45	2.43	2.42-2.46
Na_2O	3.55	3.49	3.39-3.57
K_2O	4.03	4.07	4.01-4.11
TiO_2	0.38	0.37	0.36-0.38
MnO	0.09	0.07	0.06-0.09
P_2O_5	0.12	0.14	0.12-0.15

Table A4-5 /continued

	Accepted value (Abbey, 1975)	This study (5 analyses) mean	range
BCR-1			
SiO_2	54.85	54.55	54.20-54.91
Al_2O_3	13.68	13.63	13.56-13.67
Fe_2O_3 t	13.52	13.31	13.15-13.54
MgO	3.49	3.43	3.40-3.49
CaO	6.98	7.03	6.97-7.07
Na_2O	3.29	3.24	3.20-3.30
K_2O	1.68	1.69	1.66-1.72
TiO_2	2.22	2.21	2.19-2.22
MnO	0.19	0.18	0.18-0.19
P_2O_5	0.33	0.33	0.33-0.34
W-1		8 analyses	
SiO_2	52.72	52.68	51.76-53.47
Al_2O_3	14.87	14.84	14.70-15.00
Fe_2O_3 t	11.11	11.05	10.25-11.40
MgO	6.63	6.80	6.67-6.92
CaO	10.98	10.40	10.06-11.01
Na_2O	2.15	2.13	2.09-2.20
K_2O	0.64	0.64	0.62-0.65
TiO_2	1.07	1.08	1.07-1.11
MnO	0.17	0.17	0.17-0.19
P_2O_5	0.14	0.14	0.13-0.15

Table A4-5/continued Single analysis results for standards

	Accepted value	This study		Accepted value	This study
JG-1			JB-1		
SiO_2	72.31	72.27		52.49	52.34
Al_2O_3	14.25	14.23		14.66	14.62
Fe_2O_3 t	2.21	2.20		9.08	8.91
MgO	0.76	0.60		7.80	8.06
CaO	2.15	2.17		9.31	9.01
Na_2O	3.37	3.35		2.80	2.77
K_2O	3.92	3.91		1.42	1.44
TiO_2	0.25	0.26		1.37	1.33
MnO	0.06	0.06		0.16	0.16
P_2O_5	0.09	0.10		0.26	0.30
DRN			AGV-1		
SiO_2	52.88	53.16		59.72	60.08
Al_2O_3	17.56	17.63		17.22	17.45
Fe_2O_3 t	9.69	9.17		6.84	6.91
MgO	4.47	4.31		1.55	1.29
CaO	7.09	7.32		5.00	5.15
Na_2O	3.00	3.05		4.31	4.25
K_2O	1.73	1.72		2.93	2.93
TiO_2	1.10	1.11		1.05	1.05
MnO	0.21	0.21		0.10	0.10
P_2O_5	0.25	0.22		0.50	0.49

Table A4-5 /continued

	Accepted value	This study		Accepted value	This study
NIM-G			DTS-1		
SiO_2	75.73	75.40		40.68	40.99
Al_2O_3	12.13	12.77		0.29	0.30
Fe_2O_3 t	1.96	2.10		8.60	8.68
MgO	0.05 (?)	0.10		49.83	49.99
CaO	0.77	0.81		0.15	0.14
Na_2O	3.36	3.55		0.01	-
K_2O	5.04	5.19		-	-
TiO_2	0.09	0.09		0.01	0.01
MnO	0.02	0.03		0.11	0.11
P_2O_5	0.02	0.02		-	-
NIM-D					
SiO_2	38.97	38.85			
Al_2O_3	0.26	0.45			
Fe_2O_3 t	16.99	17.12			
MgO	43.68	44.12			
CaO	0.26	0.24			
Na_2O	0.06 (?)	-			
K_2O	0.02	-			
TiO_2	0.02	-			
MnO	0.21	0.16			
P_2O_5	0.03	-			

Table A4-6 Replicate pellets of same sample (5)

	wt % mean	range	1σ	σ (%)
SiO_2	70.66	70.52-70.73	0.11	0.16
$Al_2O_{3_t}$	14.81	14.76-14.90	0.06	0.41
Fe_2O_3	4.72	4.69-4.74	0.020	0.42
MgO	2.15	2.13-2.16	0.011	0.51
CaO	2.24	2.21-2.26	0.019	0.85
Na_2O	2.76	2.64-2.85	0.081	2.93
K_2O	2.05	2.04-2.07	0.013	0.63
TiO_2	0.41	0.41-0.42	0.0055	1.34
MnO	0.04	0.03-0.04	0.0045	11.3
P_2O_5	0.17	0.16-0.18	0.0084	4.94

Table A4-7 1σ error* for duplicate pellets (11 pairs)

SiO_2	0.05
$Al_2O_{3_t}$	0.01
Fe_2O_3	0.02
MgO	0.04
CaO	0.01
Na_2O	0.02
K_2O	0.01
TiO_2	0.006
MnO	0.005
P_2O_5	0.008

* 1σ mean of duplicate differences

Table A4-8a Standard results for Rb (ppm)

Standard	Accepted value*	This study mean	range	1σ	C(%)	No. of analyses
G2[1]	170	169	168-172	1.4	0.81	6
AGV1[1]	67	67	67-68	0.50	0.75	4
GSP1[1]	250	257	254-261	2.4	0.94	5
W1[1]	21	21	19-22	1.2	5.6	6
BCR1[1]	47	47	46-48	0.63	1.3	6
GH	390	358				1
BR	45	45	44-46	0.69	1.5	7
JB1	40	41				1
DR-N	75	75	74-76	1.3	1.7	6
GA	175	174	172-176	3.2	1.8	6
JG1	185	179				1
NIMS	560	560	559-561	0.71	0.13	5

* Abbey (1975)

[1] Standard also used on calibration curve

Detection limit = 1 ppm

Table A4-8b Standard results for Sr (ppm)

Standard	Accepted value*	This study				No. of analyses
		mean	range	1σ	C(%)	
NBS70[1]	65[2]	65				1
G2[1]	480	472	470-473	0.98	0.21	5
GSP1[1]	230	236				1
AGV1[1]	650	655	653-659	2.3	0.36	3
W1[1]	190	192				1
BCR1[1]	330	332				1
GH	10	9	9-10	1.2	12.4	6
BR	1350	1320	1301-1322	8.7	0.66	5
JB1	440	445	440-450	3.7	0.83	5
DR-N	400	396	393-400	2.7	0.69	5
GA	300	299	296-302	2.4	0.80	5
JG1	185	185	183-187	1.8	0.95	5
NIMS	76	68				1
NIMP	32	38				1
NIMG	12	13	12-15	1.3	9.9	5

[1] Standard also used on calibration curve

[2] De Laeter and Abercrombie (1970)

Detection limit = 3 ppm

*Abbey (1975)

Table A4-8c Standard results for Ba (ppm)

Standard	Accepted value 1	2	This study mean	range	1σ	C(%)	No. of analyses
W1[a]	160	160	167	162-174	6.1	3.7	3
BCR1[a]	675	680	681	657-709	19.5	2.9	5
AGV1[a]	1208	1200	1203	1196-1209	6.5	0.5	3
G2[a]	1870	1850	1844	1833-1852	8.3	0.4	6
NIMS		2400	2460	2449-2477	8.6	0.4	4
GSP1	1300	1300	1336	1325-1346	9.2	0.7	5
NIMG		210	211	208-214	2.0	1.0	6
BR		1050	1088	1076-1108	12.3	1.1	5
NIMD		20 ?	15	14-17	1.3	8.3	6

1. Flanagan (1976); 2. Abbey (1975)
a. Also used on calibration curve
Detection limit = 5 ppm

Table A4-8d Standard results for Ce (ppm)

Standard	Accepted value 1	2	This study mean	range	1σ	C(%)	No. of analyses
W1[a]	23	23	21	19-24	2.5	11.7	5
BCR1[a]	53.9	54	57	53-61	4.1	7.1	5
AGV1[a]	63	63	67	65-68	1.5	2.3	5
G2[a]	150	150	158	156-162	2.6	1.7	6
NIMS		12 ?	12	9-14	2.6	22.3	7
NIMG		200 ?	198	195-199	1.7	0.9	5

1. Flanagan (1973); 2. Abbey (1975)
a. Also used on calibration curve
Detection limit = 2 ppm

Table A4-8e Standard results for Zr (ppm)

Standard	Accepted value 1	2	This study mean	range	1σ	C(%)	No. of analyses
AGV1	225	220	220	219-221	0.9	0.4	5
W1	105	105	89	86-91	2.1	2.4	5
G2	300	300	303	301-308	2.8	0.9	5
GSP1	500	500	539	529-554	10.1	1.9	5
BCR1	190	185	183	180-186	2.8	1.5	5
BR		240	231	228-234	2.8	1.2	5

Detection limit = 3 ppm

Table A4-8f Standard results for Y (ppm)

Standard	Accepted value 1	2	This study mean	range	1σ	C(%)	No. of analyses
AGV1	21.3	26	24	21-26	1.9	7.8	5
W1	25	25	23	21-24	1.4	6.0	5
G2	12	12	13	12-14	0.9	7.3	5
GSP1	30.4	32	30	27-32	2.1	7.0	5
BCR1	37.1	46	38	36-40	1.6	4.3	5
BR		27 ?	28	27-30	1.4	5.0	5

Detection limit = 4 ppm

Table A4-8g Standard results for Nb (ppm)

Standard	Accepted value 1	2	This study mean	range	1σ	C(%)	No. of analyses
AGV1	15	15	10	8-12	1.4	13.8	5
W1	9.5	9.5?	6	5-7	0.7	10.8	5
G2	13.5	14	8	6-8	1.1	14.2	5
GSP1	29	29	24	20-26	2.4	10.0	5
BCR1	13.5	14	9	8-10	1.1	12.6	5
BR		90	87	75-91	7.0	8.1	5

Detection limit = 2 ppm

1. Flanagan (1973)
2. Abbey (1975)

Table A4-8h Standard results for Th (ppm)

Standard	Accepted value 1	2	This study mean	range	1σ	C(%)	No. of analyses
BCR1	6.0	6.4	8.9	7.4-9.9	0.92	10.4	8
AGV1	6.41	6.0	8.3	7.4-9.8	0.78	9.4	9
W1	2.42	2.4	4.4	2.7-5.7	1.1	24.4	9
G2	24.2	24	29	27-31	1.0	3.6	8
NIMG		57	55	54-56	1.4	2.5	8
BR		?	13	13-14	0.5	3.7	8
JG1		13	16				1
JB1		?	14				1

Detection limit = 2 ppm
1. Flanagan (1973)
2. Abbey (1975)

Table A4-8i Standard results for Pb (ppm)

Standard	Accepted value 1	2	This study mean	range	1σ	C(%)	No. of analyses
BCR1	17.6	15	19	17-20	0.9	4.6	8
AGV1	35.1	36	39	38-40	0.5	1.3	9
W1	7.8	8	10	8-11	1.1	11.7	9
G2	31.2	29	33	31-35	1.4	4.1	8
NIMG		35	36	35-37	0.7	1.8	8
JG1		24	26				1
GA		26	26				1

Detection limit = 3 ppm
1. Flanagan (1973)
2. Abbey (1975)

Table A4-8j Standard results for Zn (ppm)

Standard	Accepted value 1	2	This study mean	range	1σ	C(%)	No. of analyses
AGV1	84	84	81	77-84	2.8	3.4	10
W1	86	86	80	77-85	3.0	3.8	10
G2	85	85	82	79-84	2.1	2.6	9
NIMG		60 ?	44	43-44	0.5	1.2	9
GSP1	98	98	96	95-98	2.2	2.3	9
BR		160	148	138-155	5.9	4.0	9
JG1		36	39	38-39			2
JB1		83	80	79-80			2

Detection limit = 2 ppm
1. Flanagan (1973)
2. Abbey (1975)

Table A4-8k Standard results for Ni (ppm)

Standard	Accepted value 1	2	This study mean	range	1σ	C(%)	No. of analyses
BCR1	15.8	16	14	10-18	3.5	22.0	8
AGV1	18.5	17	15	12-17	1.6	10.9	9
W1	76	78	72	69-75	2.4	3.3	10
G2	5.1	6	5.4	3.6-7.9	2.0	37.7	8
T1		13 ?	15	12-18	2.7	17.5	8
GA		7	8				1

Detection limit = 6 ppm
1. Flanagan (1973)
2. Abbey (1975)

Table A4-9 5 replicate pellets from same powder (ppm)

	Mean	Range	1σ	C(%)
Rb	23.9	23.8-24.1	0.257	1.07
Sr	765.6	765-766	0.469	0.06
Ba	516.2	511-519	4.15	0.80
Pb	7.0	6-8	0.707	10.10
Zn	56.4	55-58	1.14	2.02
Ni	20.4	19-22	1.14	5.59
Th	2.8	2-3	0.447	16.0
Ce	46.4	45-49	1.67	3.61
Y	9.4	9-10	0.548	5.83
Nb	?	below detection limit		
Zr	143.0	141-144	1.22	0.86

Sample F12: migmatized and sheared Footprint gneiss

TABLE A4-10 X-ray fluorescence major, minor and trace element results.

All major and minor element oxide results have been normalized to 100% on an anhydrous basis. Total iron is given as Fe_2O_3.

LOI: loss on ignition
T: trace
ND: not detected

MAJOR AND MINOR ELEMENT OXIDE RESULTS FOR THE KIRKLAND LAKE AREA

BRAIDED RIVER FACIES METASANDSTONES

SAMPLE	SIO2	AL2O3	TIO2	FE2O3	MNO	MGO	CAO	NA2O	K2O	P2O5	LOI
CH 7	63.62	14.17	.64	6.88	.14	3.96	4.39	5.22	.89	.10	6.13
EL 3	63.87	13.24	.78	7.97	.11	5.05	3.82	3.43	1.61	.11	4.68
RP 4	64.86	15.36	.75	5.80	.08	3.72	2.28	5.40	1.68	.07	4.55
CK 2	64.95	15.14	.74	7.66	.06	4.52	.83	4.48	1.53	.08	4.59
LS 1	65.63	13.77	.68	7.31	.10	3.82	3.01	4.75	.84	.10	5.60
LL 8	67.73	13.46	.57	5.99	.10	3.77	2.87	4.40	1.06	.06	3.94
IL 3	70.90	13.10	.52	4.64	.07	2.65	2.01	3.69	2.31	.12	4.29
ME 2	74.88	11.35	.39	3.79	.05	2.72	1.74	3.17	1.83	.10	4.53

TURBIDITE FACIES META-ARGILLITES

SAMPLE	SIO2	AL2O3	TIO2	FE2O3	MNO	MGO	CAO	NA2O	K2O	P2O5	LOI
LL 4	58.49	20.90	.87	7.94	.10	3.85	1.01	3.52	3.15	.16	4.46
BEAR	66.73	16.29	.62	6.59	.05	3.17	1.04	2.01	3.23	.27	4.51

MAFIC METATUFF

SAMPLE	SIO2	AL2O3	TIO2	FE2O3	MNO	MGO	CAO	NA2O	K2O	P2O5	LOI
OU 3	47.99	14.94	1.09	16.75	.17	6.90	8.72	1.53	1.82	.08	14.18

METATRACHYTE

SAMPLE	SIO2	AL2O3	TIO2	FE2O3	MNO	MGO	CAO	NA2O	K2O	P2O5	LOI
HL 5	52.07	13.92	1.02	10.64	.17	3.86	8.18	2.50	7.04	.60	12.29

TRACE ELEMENT RESULTS FOR THE KIRKLAND LAKE AREA

BRAIDED RIVER FACIES METASANDSTONES

SAMPLE	RB	SR	BA	PB	ZN	NI	TH	CE	NB	ZR	Y
CH 7	18	537	748	11	80	118	6	54	ND	100	16
EL 3	36	435	599	7	89	139	5	47	ND	112	18
RP 4	42	164	368	8	107	78	4	37	5	124	25
CK 2	54	186	288	7	73	104	9	67	4	161	22
LS 1	33	399	447	11	94	93	6	50	5	121	15
LL 8	24	441	285	6	80	180	3	28	ND	81	17
IL 3	83	172	591	8	42	65	9	61	5	122	15
ME 2	52	190	544	23	40	48	4	28	7	84	13

TURBIDITE FACIES META-ARGILLITES

SAMPLE	RB	SR	BA	PB	ZN	NI	TH	CE	NB	ZR	Y
LL 4	100	223	743					60	9	145	24
BEAR	97	159	858					59	11	166	18

MAFIC METATUFF

SAMPLE	RB	SR	BA	PB	ZN	NI	TH	CE	NB	ZR	Y
OU 3	50	147	229					18	3	43	16

METATRACHYTE

SAMPLE	RB	SR	BA	PB	ZN	NI	TH	CE	NB	ZR	Y
HL 5	312	2136	2740	18	111	81	24	316	ND	312	35

MAJOR AND MINOR ELEMENT OXIDE RESULTS FOR THE KAKAGI LAKE AREA

METASANDSTONES

SAMPLE	SIO2	AL2O3	TIO2	FE2O3	MNO	MGO	CAO	NA2O	K2O	P2O5	LOI
JK 169	65.01	16.31	.62	5.97	.07	2.16	5.64	2.96	1.15	.12	4.47
JK 174	65.15	16.92	.54	4.84	.06	1.63	5.95	3.31	1.40	.17	2.54
JK 29	65.19	16.52	.50	3.97	.05	1.21	6.12	4.18	2.17	.08	6.31
JK 173	66.97	15.66	.51	5.24	.06	1.90	4.92	2.41	2.14	.19	5.71
JK 28	66.98	16.64	.43	3.51	.05	1.20	4.54	4.73	1.85	.08	3.70
JK 176	67.30	16.57	.50	4.03	.06	1.47	5.00	3.63	1.28	.14	2.58
JK 196	67.71	16.98	.44	2.92	.05	1.42	3.51	4.74	2.13	.09	1.46
JK 252	68.37	15.66	.52	4.62	.05	1.67	3.17	4.75	.88	.11	2.10
JK 238	68.80	17.07	.34	2.77	.04	.98	3.48	4.72	1.72	.07	2.13
JK 4	69.89	16.67	.34	2.75	.04	1.11	2.61	5.85	1.49	.06	1.56
JK 6	69.43	16.36	.36	3.11	.04	1.31	3.15	4.09	2.07	.08	1.86
JK 8	70.76	15.29	.34	3.32	.05	1.15	2.60	4.16	2.25	.09	2.20
JK 5	76.09	12.76	.29	2.24	.05	.90	1.37	4.19	2.11	.05	1.60

META-ARGILLITE

SAMPLE	SIO2	AL2O3	TIO2	FE2O3	MNO	MGO	CAO	NA2O	K2O	P2O5	LOI
JK 769	68.92	15.45	.39	3.49	.06	1.76	3.34	3.32	3.09	.18	1.96

TRACE ELEMENT RESULTS FOR THE KAKAGI LAKE AREA

METASANDSTONE

SAMPLE	RB	SR	BA	PB	ZN	NI	TH	CE	NB	ZR	Y
JK 169	22	540	281					9	T	67	10
JK 174	26	417	321					37	4	113	10
JK 29	39	556	411					15	5	84	7
JK 173	35	337	254					52	T	106	9
JK 28	28	616	370					21	T	87	7
JK 176	29	473	308					36	3	106	9
JK 196	53	658	552					27	T	89	5
JK 252	22	303	247					29	T	123	10
JK 238	30	498	412					19	5	92	6
JK 4	27	383	290					22	4	85	6
JK 6	37	508	547					22	T	112	5
JK 8	34	421	522					23	5	104	6
JK 5	39	329	539					16	9	103	4

META-ARGILLITE

SAMPLE	RB	SR	BA	PB	ZN	NI	TH	CE	NB	ZR	Y
JK 768	87	381	585					53	6	125	9

MAJOR AND MINOR ELEMENT OXIDE RESULTS FOR THE SIOUX LOOKOUT AREA

METASANDSTONES

SAMPLE	SIO2	AL2O3	TIO2	FE2O3	MNO	MGO	CAO	NA2O	K2O	P2O5	LOI
GW 19	71.09	15.32	.33	2.52	.05	1.06	3.38	3.85	2.28	.11	2.79
AR 30	68.12	15.37	.50	5.48	.09	2.46	2.12	4.20	1.59	.06	3.75
AR 12	75.61	13.63	.17	1.69	.04	.31	1.13	4.98	2.41	.02	1.87

TRACE ELEMENT RESULTS FOR THE SIOUX LOOKOUT AREA

METASANDSTONES

SAMPLE	RB	SR	BA	PB	ZN	NI	TH	CE	NB	ZR	Y
GW 19	72	1248	740	15	49	8	4	28	ND	95	4
AR 30	52	343	416	11	73	45	9	49	3	130	15
AR 12	59	357	845	8	16	T	4	20	T	57	5

MAJOR AND MINOR ELEMENT OXIDE RESULTS FOR THE UPPER MANITOU LAKE AREA

CANE LAKE FORMATION FELSIC METAVOLCANIC ROCKS

SAMPLE	SIO2	AL203	TIO2	FE203	MNO	MGO	CAO	NA2O	K2O	P2O5	LOI
T 10	61.93	13.85	.47	13.89	.14	3.07	2.97	3.24	1.05	.16	4.86
OT 17	65.06	15.27	.54	7.03	.09	2.36	3.24	3.88	2.44	.10	
T 119	65.50	15.95	.58	5.35	.06	3.22	3.16	3.36	2.60	.22	2.54
T 25	66.17	15.96	.41	3.92	.07	2.26	3.90	4.46	2.76	.09	2.08
T 214	68.37	16.43	.51	3.85	.04	1.38	2.04	4.66	2.49	.23	1.27

UPHILL LAKE FORMATION FELSIC METAVOLCANIC AND ALLUVIAL FAN FACIES CLASTIC METASEDIMENTARY ROCKS

SAMPLE	SIO2	AL203	TIO2	FE203	MNO	MGO	CAO	NA2O	K2O	P2O5	LOI
OT 21	65.19	15.95	.53	4.83	.08	2.48	3.94	4.23	2.67	.10	2.84
T 9	66.32	15.56	.50	3.98	.08	2.86	4.31	4.29	2.99	.12	3.69
OT 2	65.87	16.55	.49	4.03	.05	2.49	3.87	4.27	2.20	.19	3.05
OT 4	68.67	16.12	.42	3.25	.05	1.80	3.19	4.74	1.64	.13	3.67

UPHILL LAKE FORMATION BRAIDED RIVER FACIES CLASTIC METASEDIMENTARY ROCKS

SAMPLE	SIO2	AL203	TIO2	FE203	MNO	MGO	CAO	NA2O	K2O	P2O5	LOI
T 109	61.25	14.05	.75	8.70	.13	4.10	5.95	2.99	1.75	.32	2.64
OT 6	63.73	13.73	.63	8.17	.15	3.96	5.13	3.07	1.34	.09	1.65
T 32	66.27	15.74	.63	4.53	.06	2.50	3.25	4.28	2.51	.21	3.92
OT 25	71.17	14.58	.36	3.09	.06	2.29	2.00	2.80	3.59	.15	3.90

RUSH BAY MEMBER FELSIC METAVOLCANIC ROCKS AND META-ARGILLITES

SAMPLE	SIO2	AL203	TIO2	FE203	MNO	MGO	CAO	NA2O	K2O	P2O5	LOI
T 220	64.40	17.68	.72	6.35	.07	3.11	1.98	2.87	2.62	.26	3.33
T 222	70.79	14.85	.48	4.13	.05	2.31	2.07	2.67	2.53	.14	2.89

MOSHER BAY FORMATION TURBIDITE FACIES METASANDSTONES

SAMPLE	SIO2	AL203	TIO2	FE203	MNO	MGO	CAO	NA2O	K2O	P2O5	LOI
S 2	66.81	13.92	.46	6.06	.10	3.74	2.67	4.76	1.42	.07	2.95
S 5	67.99	13.68	.45	6.10	.10	2.94	2.46	4.17	2.05	.06	4.42
OT 5	69.31	12.56	.46	5.98	.10	3.13	3.04	4.38	.92	.12	2.41
T 42	70.52	14.56	.46	5.27	.05	2.19	.90	4.23	1.72	.09	2.45

MOSHER BAY FORMATION TURBIDITE FACIES METASILTSTONES AND META-ARGILLITES

SAMPLE	SIO2	AL203	TIO2	FE203	MNO	MGO	CAO	NA2O	K2O	P2O5	LOI
T 152	57.97	23.09	.92	8.44	.07	1.86	.66	3.09	3.83	.09	5.30
T 38	63.88	17.86	.61	6.70	.09	2.66	1.43	3.72	2.97	.07	3.75
T 104	64.87	17.38	.69	7.01	.08	2.66	1.10	4.66	1.54	.08	4.23

TRACE ELEMENT RESULTS FOR THE UPPER MANITOU LAKE AREA

CANE LAKE FORMATION FELSIC METAVOLCANIC ROCKS

SAMPLE	RB	SR	BA	PB	ZN	NI	TH	CE	NB	ZR	Y
T 10	32	564	597					60	T	125	16
OT 17	76	465	497	16	96	102	9	63	T	127	14
T 119	83	668	858					79	T	156	11
T 25	80	739	914	15	59	46	9	67	NO	140	11
T 214	57	555	1385					92	8	146	8

UPHILL LAKE FORMATION FELSIC METAVOLCANIC AND ALLUVIAL FAN FACIES CLASTIC METASEDIMENTARY ROCKS

SAMPLE	RB	SR	BA	PB	ZN	NI	TH	CE	NB	ZR	Y
OT 21	74	657	849	17	67	63	9	62	T	141	10
T 9	71	878	1158	20	68	59	11	88	T	145	10
OT 2	47	911	948					86	4	153	11
OT 4	38	613	541					53	7	109	8

UPHILL LAKE FORMATION BRAIDED RIVER FACIES CLASTIC METASEDIMENTARY ROCKS

SAMPLE	RB	SR	BA	PB	ZN	NI	TH	CE	NB	ZR	Y
T 109	61	463	611	15	90	105	13	77	3	146	21
OT 6	40	360	333	12	106	96	8	47	T	100	16
T 32	74	698	718					100	8	193	14
OT 25	109	490	951	17	51	38	14	71	5	144	8

RUSH BAY MEMBER FELSIC METAVOLCANIC ROCKS AND META-ARGILLITES

SAMPLE	RB	SR	BA	PB	ZN	NI	TH	CE	NB	ZR	Y
T 220	75	438	735					99	9	192	19
T 222	69	454	734					63	7	124	11

MOSHER BAY FORMATION TURBIDITE FACIES METASANDSTONES

SAMPLE	RB	SR	BA	PB	ZN	NI	TH	CE	NB	ZR	Y
S 2	23	255	404	10	63	111	8	42	3	102	8
S 5	40	248	637	17	69	66	11	42	5	124	15
OT 5	28	299	327	12	60	38	10	54	6	135	10
T 42	36	292	474					59	7	139	15

MOSHER BAY FORMATION TURBIDITE FACIES METASILTSTONES AND META-ARGILLITES

SAMPLE	RB	SR	BA	PB	ZN	NI	TH	CE	NB	ZR	Y
T 152	129	221	1026	8	81	65	10	47	6	155	22
T 38	98	305	674	12	85	67	10	50	6	116	18
T 104	56	292	485	11	105	71	11	56	5	149	21

MAJOR AND MINOR ELEMENT OXIDE RESULTS FOR THE PAKWASH LAKE AREA

GREENSCHIST FACIES METASANDSTONES

SAMPLE	SIO2	AL2O3	TIO2	FE2O3	MNO	MGO	CAO	NA2O	K2O	P2O5	LOI
L 30	67.89	15.04	.49	5.31	.09	2.16	2.82	4.06	2.08	.06	1.70
L 33	62.71	14.89	.74	8.07	.12	2.31	5.51	3.46	1.95	.26	2.54

GREENSCHIST FACIES FELSIC METAVOLCANIC ROCKS

SAMPLE	SIO2	AL2O3	TIO2	FE2O3	MNO	MGO	CAO	NA2O	K2O	P2O5	LOI
L 32	64.77	15.71	.63	5.85	.18	1.77	4.98	4.20	1.77	.13	
L 35	69.56	14.91	.38	3.04	.06	1.44	2.59	4.93	2.97	.11	

MIDDLE AMPHIBOLITE FACIES METAGREYWACKE LAYERS FROM THE PAKWASH GNEISS

SAMPLE	SIO2	AL2O3	TIO2	FE2O3	MNO	MGO	CAO	NA2O	K2O	P2O5	LOI
L 37	64.20	16.09	.65	6.81	.10	2.90	2.97	3.55	2.61	.06	
L 40	69.47	14.77	.57	5.34	.04	2.06	2.56	3.22	1.87	.11	
L 42	73.61	12.92	.46	4.11	.03	1.65	2.05	3.07	2.06	.05	
L 44B	68.52	15.00	.55	5.72	.04	2.20	2.45	3.30	2.13	.09	
L 44A	74.62	13.16	.22	2.66	.06	1.37	1.08	1.63	4.90	.29	
L 45B1	70.59	14.76	.41	4.71	.04	2.15	2.25	2.85	2.06	.17	
L 45B2	70.73	14.81	.41	4.74	.04	2.16	2.26	2.64	2.84	.16	
L 45C1	69.56	15.04	.48	4.93	.04	1.95	2.73	3.54	1.59	.14	
L 45C2	69.43	15.08	.49	4.92	.04	1.92	2.75	3.64	1.61	.13	
L 45D1	69.33	17.83	.20	1.92	.03	.82	3.73	4.98	1.06	.10	
L 45D2	69.68	17.51	.21	1.96	.04	.85	3.67	4.94	1.84	.09	

MIDDLE AMPHIBOLITE FACIES METAPELITE LAYER FROM THE PAKWASH GNEISS

SAMPLE	SIO2	AL2O3	TIO2	FE2O3	MNO	MGO	CAO	NA2O	K2O	P2O5	LOI
L 45A	60.28	17.23	.71	12.28	.18	3.44	1.73	1.92	2.12	.11	

WHITE MOBILISATE (LEUCOSOME) FROM THE PAKWASH GNEISS

SAMPLE	SIO2	AL2O3	TIO2	FE2O3	MNO	MGO	CAO	NA2O	K2O	P2O5	LOI
L 43	72.32	15.76	.04	.67	.03	.35	1.10	2.61	6.94	.17	

TRACE ELEMENT RESULTS FOR THE PAKWASH LAKE AREA

GREENSCHIST FACIES METASANDSTONES

SAMPLE	RB	SR	BA	PB	ZN	NI	TH	CE	NB	ZR	Y
L 30	77	369	654	27	67	48	11	44	4	127	16
L 33	60	322	716	14	87	71	10	44	7	138	18

GREENSCHIST FACIES FELSIC METAVOLCANIC ROCKS

SAMPLE	RB	SR	BA	PB	ZN	NI	TH	CE	NB	ZR	Y
L 32	80	475	438	12	72	18	10	78	7	158	13
L 35	84	396	560	10	45	11	11	53	4	136	8

MIDDLE AMPHIBOLITE FACIES METAGREYWACKE LAYERS FROM THE PAKWASH GNEISS

SAMPLE	RB	SR	BA	PB	ZN	NI	TH	CE	NB	ZR	Y
L 37	109	399	620	19	90	54	16	68	4	165	21
L 40	92	295	220					56	9	142	12
L 42	84	278	411					46	12	169	8
L 44B	108	286	243					48	11	147	12
L 44A	123	263	1562					20	3	74	12
L 45B1	93	255	311					34	8	103	12
L 45B2	91	252	303					33	9	104	13
L 45C1	74	307	234					34	12	117	10
L 45C2	73	307	236					34	13	122	10
L 45D1	36	449	190					16	5	55	T
L 45D2	36	444	208					7	7	56	T

MIDDLE AMPHIBOLITE FACIES METAPELITE LAYER FROM THE PAKWASH GNEISS

SAMPLE	RB	SR	BA	PB	ZN	NI	TH	CE	NB	ZR	Y
L 45A	105	193	326					36	11	118	20

WHITE MOBILISATE (LEUCOSOME) FROM THE PAKWASH GNEISS

SAMPLE	RB	SR	BA	PB	ZN	NI	TH	CE	NB	ZR	Y
L 43	129	407	2650					9	T	62	5

MAJOR AND MINOR ELEMENT OXIDE RESULTS FOR MAFIC METAVOLCANIC ROCKS, BURDITT LAKE-LAKE DESPAIR AREA

GREENSCHIST FACIES MAFIC METAVOLCANIC ROCKS FROM THE BURDITT LAKE AREA

SAMPLE	SIO2	AL2O3	TIO2	FE2O3	MNO	MGO	CAO	NA2O	K2O	P2O5	LOI
B 1	52.71	14.10	.83	11.86	.19	6.98	10.20	2.87	.12	.13	2.89
B 3	53.51	13.31	.87	12.63	.18	7.94	8.73	1.96	.58	.09	3.04
B 5	51.84	14.95	.68	11.61	.20	8.05	10.69	1.53	.35	.10	3.31
B 6	52.00	14.92	1.54	14.77	.18	4.86	8.95	2.40	.29	.09	1.79
B 8	51.31	13.17	.62	12.39	.25	9.09	9.69	3.12	.28	.09	2.65

AMPHIBOLITE FACIES METAVOLCANIC ROCKS FROM THE LAKE DESPAIR AREA

SAMPLE	SIO2	AL2O3	TIO2	FE2O3	MNO	MGO	CAO	NA2O	K2O	P2O5	LOI
F 19	50.66	15.67	.35	8.34	.17	9.77	12.47	2.18	.24	.14	1.40
F 27	52.94	13.93	.65	11.38	.19	6.26	13.37	.87	.23	.18	1.67
F 115	52.96	14.48	.67	11.51	.21	7.37	10.31	2.08	.30	.11	1.30
F 44	50.73	14.36	1.56	12.82	.17	6.29	9.56	2.99	1.37	.14	1.95
F 49	50.70	15.14	.35	7.92	.18	10.59	11.92	2.14	.92	.13	2.26
F 116	53.16	13.99	.93	12.34	.22	6.48	9.65	2.05	1.05	.13	1.64

LARGE MAFIC ENCLAVES FROM THE JACKFISH LAKE COMPLEX

SAMPLE	SIO2	AL2O3	TIO2	FE2O3	MNO	MGO	CAO	NA2O	K2O	P2O5	LOI
F 80	47.81	14.33	1.47	16.83	.23	5.84	10.56	2.42	.36	.17	1.01
F 145	47.30	14.56	1.52	18.02	.31	4.19	10.76	2.54	.61	.16	0.79
D 4	48.34	15.76	1.46	14.83	.35	4.36	11.21	3.06	.37	.24	1.05
F 134	51.34	14.50	.79	11.40	.24	6.24	11.75	3.10	.58	.13	0.91

LARGE MAFIC ENCLAVES FROM THE FOOTPRINT GNEISS

SAMPLE	SIO2	AL2O3	TIO2	FE2O3	MNO	MGO	CAO	NA2O	K2O	P2O5	LOI
F 107	48.62	15.18	.81	11.26	.18	8.84	11.40	3.01	.55	.15	1.33
F 100	48.98	14.90	.85	13.13	.20	7.04	12.00	2.23	.56	.12	1.44
F 15	49.27	15.70	.92	11.62	.19	7.41	11.31	2.93	.48	.17	1.33

SMALL MAFIC ENCLAVES FROM THE JACKFISH LAKE COMPLEX

SAMPLE	SIO2	AL2O3	TIO2	FE2O3	MNO	MGO	CAO	NA2O	K2O	P2O5	LOI
F 22	52.46	16.12	.85	9.48	.14	6.39	6.82	5.41	1.95	.38	2.07
D 6	58.38	17.37	.43	5.95	.11	3.19	5.09	5.85	3.22	.41	1.65

SMALL MAFIC ENCLAVES FROM THE FOOTPRINT GNEISS

SAMPLE	SIO2	AL2O3	TIO2	FE2O3	MNO	MGO	CAO	NA2O	K2O	P2O5	LOI
F 105	48.78	19.17	.50	9.55	.15	6.22	12.94	1.99	.59	.11	3.67

ULTRAMAFIC ROCKS, BURDITT LAKE AREA

SAMPLE	SIO2	AL2O3	TIO2	FE2O3	MNO	MGO	CAO	NA2O	K2O	P2O5	LOI
B 2	42.37	1.74	.09	11.11	.13	43.71	.24	.62	.02	0.00	15.52
B 4	42.47	2.15	.10	10.88	.13	42.21	1.50	.57	.01	0.00	15.70
B 7	42.73	3.12	.14	11.27	.15	41.14	.85	.61	.01	0.00	13.86

ULTRAMAFIC ENCLAVES FROM THE FOOTPRINT GNEISS

SAMPLE	SIO2	AL2O3	TIO2	FE2O3	MNO	MGO	CAO	NA2O	K2O	P2O5	LOI
F 59	49.05	10.63	.44	10.03	.17	16.04	10.11	2.14	1.19	.20	1.99
F 89	47.49	10.61	.77	7.47	.13	16.29	11.54	1.13	4.39	.17	2.39

PROTEROZOIC DIABASE DIKES

SAMPLE	SIO2	AL2O3	TIO2	FE2O3	MNO	MGO	CAO	NA2O	K2O	P2O5	LOI
F 140	49.35	15.84	2.09	14.91	.20	4.31	9.41	2.58	1.17	.14	
F 141	49.09	7.91	.95	12.33	.21	14.52	12.53	1.60	.61	.24	

TRACE ELEMENT RESULTS FOR MAFIC METAVOLCANIC ROCKS , BURDITT LAKE-LAKE DESPAIR AREA

GREENSCHIST FACIES MAFIC METAVOLCANIC ROCKS FROM THE BURDITT LAKE AREA

SAMPLE	RB	SR	BA	PB	ZN	NI	TH	CE	NB	ZR	Y
B 1	1.5	135	44	4	44	58	4	8	2	50	20
B 3	9.5	62	87	4	71	31	T	10	4	49	25
B 5	9.0	121	142	4	74	85	3	ND	T	36	20
B 6	5.0	113	53	5	161	86	3	6	3	52	22
B A	3.6	124	244	5	79	202	3	5	T	32	15

AMPHIBOLITE FACIES METAVOLCANIC ROCKS FROM THE LAKE DESPAIR AREA

SAMPLE	RB	SP	BA	PB	ZN	NI	TH	CE	NB	ZR	Y
F 19	2.5	76	74	5	41	93	3	ND	T	15	8
F 27	4.7	66	85	9	75	81	4	2	T	40	20
F 115	6.6	102	68	T	77	94	3	T	T	42	16
F 44	41.1	304	280	7	127	79	5	22	T	62	19
F 49	41.0	182	139	5	42	101	T	9	T	18	8
F 116	52.8	138	185	4	197	49	3	6	3	57	25

LARGE MAFIC ENCLAVES FROM THE JACKFISH LAKE COMPLEX

SAMPLE	RB	SP	BA	PB	ZN	NI	TH	CE	NB	ZR	Y
F 80	1.5	306	142	7	110	64	3	12	2	57	29
F 145	3.0	184	161	8	145	72	4	12	2	59	30
D 4	3.9	137	146	8	89	64	4	14	4	101	33
F 134	3.7	208	175	7	97	54	4	10	T	46	20

LARGE MAFIC ENCLAVES FROM THE FOOTPRINT GNEISS

SAMPLE	RB	SP	BA	PB	ZN	NI	TH	CE	NB	ZR	Y
F 107	5.0	155	92	8	81	164	3	6	ND	33	16
F 100	6.0	123	54	7	92	88	T	T	T	43	20
F 15	4.3	139	89	5	87	108	T	T	ND	42	16

SMALL MAFIC ENCLAVES FROM THE JACKFISH LAKE COMPLEX

SAMPLE	RB	SR	BA	PB	ZN	NI	TH	CE	NB	ZR	Y
F 22	79.3	1376	580	12	161	95	3	80	T	197	16
D 6	71.2	1435	2251	17	92	48	8	139	ND	211	11

SMALL MAFIC ENCLAVES FROM THE FOOTPRINT GNEISS

SAMPLE	RB	SP	BA	PB	ZN	NI	TH	CE	NB	ZR	Y
F 105	11.5	158	92	5	62	105	T	8	T	21	11

ULTRAMAFIC ROCKS, BURDITT LAKE AREA

SAMPLE	RB	SP	BA	PB	ZN	NI	TH	CE	NB	ZR	Y
B 2	1.5	5	16	T	37	2445	T	ND	T	5	3
B 4	1.0	7	19	T	33	2408	T	ND	3	5	4
B 7	T	5	18	T	31	2254	T	ND	3	4	4

ULTRAMAFIC ENCLAVES FROM THE FOOTPRINT GNEISS

SAMPLE	RB	SR	BA	PB	ZN	NI	TH	CE	NB	ZR	Y
F 59	32.8	417	476	8	65	557	4	22	2	48	11
F 49	202.4	305	1007	5	59	451	9	75	T	106	15

PROTEROZOIC DIABASE DIKES

SAMPLE	RB	SP	BA	PB	ZN	NI	TH	CE	NB	ZR	Y
F 140	52.1	357	170	8	122	54	3	27	4	105	35
F 141	12.4	530	393	6	96	230	3	87	3	57	21

MAJOR AND MINOR ELEMENT OXIDE RESULTS FOR FELSIC METAVOLCANIC ROCKS, BURDITT LAKE-LAKE DESPAIR AREA

GREENSCHIST FACIES FELSIC METAVOLCANIC ROCKS FROM THE BURDITT LAKE AREA

SAMPLE	SIO2	AL2O3	TIO2	FE2O3	MNO	MGO	CAO	NA2O	K2O	P2O5	LOI
B 9	69.56	15.23	.31	3.33	.05	1.59	2.32	5.83	1.70	.07	1.61
B 10	70.14	15.65	.37	2.63	.05	1.56	2.38	5.01	2.14	.08	2.28
B 11	67.37	16.60	.40	3.02	.05	1.26	4.19	4.49	2.50	.14	3.75
B 12	67.50	16.96	.39	3.02	.05	1.65	3.20	4.79	2.33	.11	3.40

AMPHIBOLITE FACIES FELSIC SCHISTS FROM THE MANOMIN LAKE AREA

SAMPLE	SIO2	AL2O3	TIO2	FE2O3	MNO	MGO	CAO	NA2O	K2O	P2O5	LOI
F 124	66.30	16.98	.40	3.36	.04	1.84	3.81	3.97	3.12	.17	4.16
F 121	67.68	16.73	.35	2.85	.03	1.42	2.79	4.93	3.07	.15	
F 120	69.85	15.48	.24	2.08	.03	.95	3.70	4.44	3.07	.16	
F 123	70.34	15.86	.27	2.24	.03	.80	3.50	5.12	1.69	.15	3.52
F 45	70.37	16.10	.30	2.47	.02	.71	2.79	5.04	2.08	.13	1.10
F 122	70.67	15.82	.27	2.51	.02	1.02	2.49	5.87	1.22	.12	

AMPHIBOLITE FACIES INTERMEDIATE METAVOLCANIC ROCKS FROM THE MANOMIN LAKE AREA

SAMPLE	SIO2	AL2O3	TIO2	FE2O3	MNO	MGO	CAO	NA2O	K2O	P2O5	LOI
F 119	59.40	18.30	.74	6.60	.16	1.49	7.39	3.84	1.75	.32	1.11
F 125	61.79	18.42	.50	4.51	.09	2.08	5.42	5.13	1.75	.31	

TRACE ELEMENT RESULTS FOR FELSIC METAVOLCANIC ROCKS, BURDITT LAKE-LAKE DESPAIR AREA

GREENSCHIST FACIES FELSIC METAVOLCANIC ROCKS FROM THE BURDITT LAKE AREA

SAMPLE	RB	SR	BA	PB	ZN	NI	TH	CE	NB	ZR	Y
B 9	37.6	548	435	5	41	T	2	14	2	87	5
B 10	41.1	407	591	4	43	9	2	4	ND	86	5
B 11	54.2	554	381	6	43	6	3	19	T	102	6
B 12	46.1	515	399	5	57	T	3	23	3	116	8

AMPHIBOLITE FACIES FELSIC SCHISTS FROM THE MANOMIN LAKE AREA

SAMPLE	RB	SR	BA	PB	ZN	NI	TH	CE	NB	ZR	Y
F 124	60.1	437	497	7	61	14	3	24	T	82	6
F 121	57.5	878	664	7	48	7	T	16	2	89	5
F 120	55.3	395	589	4	26	T	T	10	2	90	7
F 123	42.5	527	495	7	43	7	T	17	2	80	6
F 45	44.8	550	405	T	28	T	T	18	2	84	6
F 122	24.0	638	428	6	41	6	T	15	T	85	4

AMPHIBOLITE FACIES INTERMEDIATE METAVOLCANIC ROCKS FROM THE MANOMIN LAKE AREA

SAMPLE	RB	SR	BA	PB	ZN	NI	TH	CE	NB	ZR	Y
F 119	37.9	1408	741	11	116	10	4	55	ND	108	18
F 125	40.6	1080	779	9	60	17	4	57	ND	117	9

MAJOR AND MINOR ELEMENT OXIDE RESULTS FOR THE FOOTPRINT GNEISS, BURDITT LAKE-LAKE DESPAIR AREA

TONALITIC TO GRANITIC GNEISS

SAMPLE	SIO2	AL2O3	TIO2	FE2O3	MNO	MGO	CAO	NA2O	K2O	P2O5	LOI
F 103	70.20	16.27	.31	2.35	.02	.75	3.24	5.61	1.09	.17	
F 150	70.43	15.77	.31	2.68	.03	.96	3.24	5.02	1.40	.17	
F 10	70.45	15.89	.35	2.35	.03	1.11	2.98	5.24	1.47	.12	
F 7	70.80	16.07	.31	2.10	.02	.77	2.97	5.07	1.72	.18	
F 152	71.10	15.63	.26	2.17	.03	1.12	3.27	5.40	.91	.11	
F 149	71.11	15.32	.30	2.69	.04	1.06	2.90	5.05	1.43	.11	
F 5	71.55	15.69	.29	2.00	.02	.67	2.83	5.02	1.81	.13	
F 8	71.72	15.60	.27	1.85	.02	.68	2.76	4.88	2.10	.13	
F 151	71.81	15.39	.24	2.03	.03	.94	2.97	5.07	1.42	.09	
F 73	71.94	15.66	.22	1.62	.03	.61	2.63	5.15	2.07	.08	
F 98	72.45	15.28	.24	1.89	.02	.64	2.87	4.73	1.76	.12	
F 76	73.18	14.79	.20	1.81	.02	.62	2.51	4.85	1.91	.11	
F 99	73.56	15.04	.19	1.52	.02	.57	2.92	5.13	.96	.09	
F 110	73.71	15.07	.10	.76	.03	.30	1.93	4.27	3.78	.06	

ALTERED AND/OR CONTAMINATED GNEISS

SAMPLE	SIO2	AL2O3	TIO2	FE2O3	MNO	MGO	CAO	NA2O	K2O	P2O5	LOI
F 53	70.35	16.10	.32	2.41	.03	.82	2.91	5.24	1.70	.13	
F 54	67.38	16.19	.51	3.51	.03	2.03	3.90	5.33	.90	.22	
F 12	65.09	16.39	.55	4.83	.07	1.86	4.95	5.08	.98	.20	
F 12-1	64.11	16.87	.57	4.92	.04	2.11	4.94	5.11	1.07	.26	

TRACE ELEMENT RESULTS FOR THE FOOTPRINT GNEISS, BURDITT LAKE-LAKE DESPAIR AREA

TONALITIC TO GRANITIC GNEISS

SAMPLE	RB	SR	BA	PB	ZN	NI	TH	CE	NB	ZR	Y
F 103	32.3	711	474	5	54	T	2	11	2	126	2
F 150	30.1	638	622	8	61	T	6	65	2	120	7
F 10	38.2	633	516	6	55	T	4	41	3	139	6
F 7	28.2	475	392	9	54	T	3	15	4	141	3
F 152	24.8	691	423	6	33	T	7	49	T	125	2
F 149	32.3	536	613	8	60	T	4	16	5	129	4
F 5	57.9	523	660	8	65	T	3	11	2	113	4
F 8	54.9	583	762	9	47	T	4	28	ND	116	3
F 151	34.0	534	658	8	43	T	4	42	ND	99	3
F 73	46.9	496	675	9	37	T	T	21	T	103	3
F 98	32.0	530	958	9	34	T	3	21	4	93	3
F 76	44.4	421	678	9	35	T	3	21	2	91	5
F 99	33.4	562	491	7	28	NT	4	25	3	107	2
F 110	90.2	461	1173	17	19	T	3	16	2	69	3

ALTERED AND/OR CONTAMINATED GNEISS

SAMPLE	RB	SR	BA	PB	ZN	NI	TH	CE	NB	ZR	Y
F 53	45.5	432	586	8	54	T	3	34	2	105	2
F 54	26.3	692	314	6	53	T	4	34	ND	189	4
F 12	23.9	766	511	7	58	21	3	45	2	143	10
F 12-1	24.0	766	521	7	56	19	3	49	T	144	9

MAJOR AND MINOR ELEMENT OXIDE RESULTS FOR THE JACKFISH LAKE COMPLEX, BURDITT LAKE-LAKE DESPAIR AREA

MELADIORITES, (QUARTZ) DIORITES, AND LEUCO (QUARTZ) DIORITES

SAMPLE	SIO2	AL203	TIO2	FE203	MNO	MGO	CAO	NA2O	K2O	P2O5	LOI
F139	52.52	9.83	.77	10.91	.19	11.01	10.62	2.44	1.48	.24	
F146	54.62	15.18	.49	9.99	.21	5.83	8.93	3.50	1.00	.20	
F131	54.92	18.07	.72	7.16	.11	4.73	7.14	5.49	1.33	.31	
F132	55.14	16.94	.68	7.72	.13	5.35	7.27	5.45	.98	.32	
F84	55.46	16.02	.75	7.76	.13	5.63	7.56	5.09	1.18	.41	
F126	55.94	15.81	.66	7.43	.12	6.24	7.91	3.79	1.73	.37	
F21	58.25	18.72	.54	5.35	.09	3.20	5.87	6.59	1.15	.24	
F24	60.21	19.35	.33	3.02	.06	2.64	5.65	6.98	1.44	.32	
F94	60.37	20.33	.25	2.86	.06	2.07	5.52	7.54	.74	.25	
F70	61.10	20.03	.44	3.29	.05	1.46	5.03	7.76	.63	.22	
F23	63.74	20.52	.22	.67	.04	.76	4.21	8.52	1.27	.06	
D8	65.32	19.16	.18	1.59	.03	1.42	3.40	7.54	1.27	.09	
F86	67.36	19.03	.31	1.01	.03	.44	.98	10.38	.39	.07	

(QUARTZ) MONZODIORITES

SAMPLE	SIO2	AL203	TIO2	FE203	MNO	MGO	CAO	NA2O	K2O	P2O5	LOI
F144	57.14	15.62	.69	7.66	.14	4.81	7.03	4.70	1.86	.34	
F42	56.87	15.92	.68	6.99	.13	4.67	6.66	5.14	2.61	.35	
F135	58.46	15.25	.68	7.12	.12	5.05	6.33	4.25	2.45	.28	
F136	58.72	15.45	.62	6.89	.12	4.96	6.24	4.30	2.42	.27	
F35	58.78	16.39	.66	6.08	.14	3.92	4.64	6.31	2.75	.33	
F133	60.19	15.72	.55	6.43	.12	3.97	5.78	4.57	2.43	.25	

GRANODIORITES

SAMPLE	SIO2	AL203	TIO2	FE203	MNO	MGO	CAO	NA2O	K2O	P2O5	LOI
F67	62.38	15.54	.56	5.14	.09	3.26	4.75	4.50	3.32	.48	
D2	62.59	18.45	.35	3.23	.06	1.65	4.07	6.45	2.93	.21	
F37	65.69	15.13	.50	4.30	.08	2.59	3.55	4.38	3.62	.16	
D1	66.37	16.20	.32	2.86	.04	2.45	3.16	5.72	2.73	.16	
D3	66.49	16.54	.30	2.79	.04	2.28	3.10	5.72	2.60	.14	
D7	66.74	15.89	.30	2.92	.05	2.56	3.12	5.47	2.80	.16	
F3	66.85	15.92	.31	3.30	.07	1.80	3.49	5.46	2.73	.08	
F40	67.35	15.89	.30	2.78	.04	2.15	2.98	5.61	2.72	.14	
F26	67.60	15.05	.32	3.08	.05	2.41	2.67	5.07	3.61	.14	
F118	68.80	15.46	.24	2.44	.06	1.40	2.61	5.91	2.96	.11	
F113	68.92	15.07	.28	2.59	.06	1.79	2.83	5.73	2.63	.11	

APLITE

SAMPLE	SIO2	AL203	TIO2	FE203	MNO	MGO	CAO	NA2O	K2O	P2O5	LOI
D5	74.71	13.96	.10	1.03	.05	0.00	1.13	4.92	4.52	.01	

SYENITE

SAMPLE	SIO2	AL203	TIO2	FE203	MNO	MGO	CAO	NA2O	K2O	P2O5	LOI
F28	63.23	18.14	0.32	3.09	0.05	1.50	2.67	7.00	3.81	0.19	
F46	63.60	17.21	.39	3.59	.08	1.27	2.85	7.30	3.47	.26	
F147	64.79	17.41	.37	3.18	.06	1.23	2.66	5.64	4.50	.17	

TRACE ELEMENT RESULTS FOR THE JACKFISH LAKE COMPLEX, BURDITT LAKE-LAKE DESPAIR AREA

MELADIORITES, (QUARTZ) DIORITES, AND LEUCO (QUARTZ) DIORITES

SAMPLE	RB	SR	BA	PB	ZN	NI	TH	CE	NB	ZR	Y
F139	45.0	1009	839	8	109	187	3	69	T	36	18
F146	28.5	639	451	9	91	98	3	58	T	31	17
F131	32.0	1816	798	10	90	61	3	63	ND	192	14
F132	23.1	1191	769	9	85	62	2	70	T	95	17
F84	15.9	1529	743	13	104	69	6	123	T	154	17
F126	34.1	1413	851	12	77	108	8	83	2	53	10
F21	19.2	1957	886	12	77	43	T	68	ND	170	11
F24	13.5	2310	690	11	34	38	T	41	ND	49	5
F94	8.1	2681	748	11	36	22	T	36	ND	82	5
F70	7.9	1077	313	8	45	17	2	25	ND	205	3
F23	14.4	2759	1156	14	6	7	T	44	ND	ND	6
D8	16.5	1727	723	13	24	6	T	38	ND	72	6
F86	3.4	215	60	T	5	n	2	21	4	157	3

(QUARTZ) MONZODIORITES

SAMPLE	RB	SR	BA	PB	ZN	NI	TH	CE	NB	ZR	Y
F144	35.9	1412	1285	12	93	48	3	84	T	75	17
F82	46.0	1462	1909	15	90	62	6	113	2	145	19
F135	64.4	1104	1430	12	85	86	4	71	T	50	13
F136	61.5	1104	1361	13	85	89	4	69	ND	50	10
F35	55.4	581	1082	9	70	82	12	143	7	196	17
F133	85.8	1060	1046	19	74	46	15	85	T	93	10

GRANODIORITES

SAMPLE	RB	SR	BA	PB	ZN	NI	TH	CE	NB	ZR	Y
F67	130.2	1030	1264	20	68	77	13	117	5	171	16
D2	36.5	1810	2338	16	50	24	2	60	ND	119	6
F37	81.4	780	1235	15	55	49	18	159	4	167	14
D1	44.9	1325	1533	15	47	21	4	65	T	133	8
D3	37.2	1411	1771	15	50	17	3	54	T	114	8
D7	50.9	1256	1586	18	42	26	3	70	T	108	9
F3	49.5	1218	1692	16	51	29	2	49	T	98	9
F40	34.9	1217	1524	17	41	15	4	56	T	125	8
F26	82.7	760	1040	23	52	24	14	66	3	138	12
F118	71.7	1243	1693	17	41	16	5	44	3	103	6
F113	51.5	1126	1367	17	39	19	4	41	2	94	8

APLITE

SAMPLE	RB	SR	BA	PB	ZN	NI	TH	CE	NB	ZR	Y
D5	162.6	221	544	41	22	7	17	22	18	133	10

SYENITE

SAMPLE	RB	SR	BA	PB	ZN	NI	TH	CE	NB	ZR	Y
F28	41.3	2041	1945	21	49	28	5	82	T	79	9
F46	60.2	1441	1766	23	61	28	7	78	T	342	10
F147	135.2	1639	1578	28	50	21	12	97	3	195	9

MAJOR AND MINOR ELEMENT OXIDE RESULTS FOR THE NORTHWEST BAY COMPLEX, DESPAIR AREA

FOLIATED GRANODIORITE

SAMPLE	SIO2	AL2O3	TIO2	FE2O3	MNO	MGO	CAO	NA2O	K2O	P2O5	LOI
F 29	70.28	16.08	.27	2.18	.82	.93	2.88	5.17	2.15	.14	
F 31	70.63	15.57	.27	2.33	.02	.87	2.86	5.32	1.81	.13	

GRANITE

SAMPLE	SIO2	AL2O3	TIO2	FE2O3	MNO	MGO	CAO	NA2O	K2O	P2O5	LOI
F 129	71.36	15.33	.26	1.91	.03	.66	1.26	4.05	5.06	.08	
F 66	72.38	14.77	.18	1.56	.85	.01	1.41	4.92	4.68	.05	

PEGMATITES

SAMPLE	SIO2	AL2O3	TIO2	FE2O3	MNO	MGO	CAO	NA2O	K2O	P2O5	LOI
F 34	72.98	15.63	.01	.26	.04	.12	.26	5.28	5.58	.01	
F 130	73.66	14.82	.10	.70	.02	.29	1.26	4.63	4.28	.04	

TRACE ELEMENT RESULTS FOR THE NORTHWEST BAY COMPLEX, BURDITT LAKE-LAKE DESPAIR AREA

FOLIATED GRANODIORITE

SAMPLE	RB	SR	BA	PB	ZN	NI	TH	CE	NB	ZR	Y
F 29	65.0	782	654	12	50	8	3	23	2	88	7
F 31	44.2	714	580	10	54	6	3	24	2	92	5

GRANITE

SAMPLE	RB	SR	BA	PB	ZN	NI	TH	CE	NB	ZR	Y
F 129	222.9	437	1299	27	39	9	32	108	6	214	5
F 66	157.0	332	981	25	36	7	18	31	6	123	4

PEGMATITES

SAMPLE	RB	SR	BA	PB	ZN	NI	TH	CE	NB	ZR	Y
F 34	1941.1	67	82	17	39	82	9	5	76	2	16
F 130	82.6	481	878	22	11	7	11	27	9	73	5

APPENDIX V

INSTRUMENTAL NON-DESTRUCTIVE NEUTRON ACTIVATION ANALYSIS

REEs, Th, Ta, Hf and Sc were analyzed by instrumental non-destructive neutron activation (INNA) techniques, using the method introduced into the McMaster laboratory by Dr. D.K. Paul during the spring of 1976.

Powdered rock samples and standards (BCR-1, GSP-1), each weighing about 200 mg, were irradiated at the McMaster University Reactor Centre in a neutron flux of about 1.5 megawatts for 3 hours. After a one week cooling period, each sample was counted for 10 hours, using a high resolution lithium-drifted germanium detector (Ortec detector, resolution of 2 KeV, peak/background ratio of 15:1 for 0.66 MeV). Data reduction was by means of the peak stripping and peak fitting programme 'SAMPO' (Routti, 1969).

PRECISION AND ACCURACY

Reproducibility for La, Ce, Nd, Sm, Eu, Yb, Th, Ba, Hf, and Sc, as determined for duplicate analyses of GSP-1, is better than ±5%; for Tm and Lu, it is ±6%; for Tb and Ta, it is ±15% (Table A5-1).

Accuracy is more difficult to evaluate as the actual abundances of the REEs and Hf are not well known for GSP-1. La, Ce, Sm, Eu, Th, and Ba lie within ±10% of the Abbey (1975) value; Tb and Ta lie within ±15%, and values for Yb, Lu, and Hf are within ±20% of the values reported by Abbey. Nd and

Table A5-1 Instrumental non-destructive neutron activation analyses (INNA) for GSP1 (ppm)

	Abbey (1975)	This study	
La	200 (?)	185	193
Ce	390 (?)	422	423
Nd	190 (?)	231	242
Sm	27 (?)	26	27
Eu	2.4 (?)	2.2	2.4
Tb	1.3	1.3	1.0
Tm	-	0.72	0.81
Yb	2.5	2.2	2.0
Lu	0.23	0.26	0.29
Th	105	109	120
Ta	1.0	1.3	1.0
Ba	1300	1215	1210
Hf	13 (?)	15	16
Sc	8	11	11

Values followed by (?) based on 5 to 9 analyses

Sc results are biased towards high values, if those reported by Abbey are correct.

Table A5-2 Distribution coefficients used in model calculations

I. BASALTIC AND ANDESITIC ROCKS

	diopside	augite	hornblende	plagioclase	garnet
Ce	0.07	0.15	0.20	0.12	0.028
Nd	0.12	0.31	0.33	0.081	0.068
Sm	0.18	0.50	0.52	0.067	0.29
Eu	0.18	0.51	0.59	0.34	0.49
Tb	0.3	0.3	0.3	0.1	5
Yb	0.16	0.62	0.49	0.067	11.5
Lu	0.13	0.56	0.43	0.060	11.9
K	0.011	0.038	0.96	0.17	0.015
Rb	0.015	0.031	0.29	0.071	0.042
Sr	0.12	0.12	0.46	1.83	0.012
Ba	0.013	0.26	0.42	0.23	0.023

II. DACITIC ROCKS

	garnet	plagioclase	hornblende
Ce	0.35	0.24	0.899
Nd	0.53	0.17	2.80
Sm	2.66	0.13	3.99
Eu	1.50	2.11	3.44
Rb	10*	0.13*	
Yb	39.9	0.077	4.89
Lu	29.6	0.062	4.53
K	0.020	0.263	
Rb	0.0085	0.048	
Sr	0.015	2.84	
Ba	0.017	0.36	

III. RHYOLITIC ROCKS

	clinopyroxene	amphibole
Ce	0.50	1.52
Nd	1.11	4.26
Sm	1.67	7.77
Eu	1.56	5.14
Rb	1.5	8
Yb	1.58	8.38
Lu	1.54	5:5
K	0.037	0.081
Rb	0.032	0.014
Sr	0.516	0.022
Ba	0.131	0.044

All values from Arth (1976a), except for Tb, which is taken from Condie and Harrison (1976)

*Average of values for mafic and felsic rocks